

# CELLULAR DORMANCY: STATE DETERMINATION AND PLASTICITY

EDITED BY: Guang Yao, Alexis Ruth Barr and Jyotsna Dhawan  
PUBLISHED IN: Frontiers in Cell and Developmental Biology



# frontiers

## Frontiers eBook Copyright Statement

The copyright in the text of individual articles in this eBook is the property of their respective authors or their respective institutions or funders. The copyright in graphics and images within each article may be subject to copyright of other parties. In both cases this is subject to a license granted to Frontiers.

The compilation of articles constituting this eBook is the property of Frontiers.

Each article within this eBook, and the eBook itself, are published under the most recent version of the Creative Commons CC-BY licence.

The version current at the date of publication of this eBook is CC-BY 4.0. If the CC-BY licence is updated, the licence granted by Frontiers is automatically updated to the new version.

When exercising any right under the CC-BY licence, Frontiers must be attributed as the original publisher of the article or eBook, as applicable.

Authors have the responsibility of ensuring that any graphics or other materials which are the property of others may be included in the CC-BY licence, but this should be checked before relying on the CC-BY licence to reproduce those materials. Any copyright notices relating to those materials must be complied with.

Copyright and source acknowledgement notices may not be removed and must be displayed in any copy, derivative work or partial copy which includes the elements in question.

All copyright, and all rights therein, are protected by national and international copyright laws. The above represents a summary only. For further information please read Frontiers' Conditions for Website Use and Copyright Statement, and the applicable CC-BY licence.

ISSN 1664-8714

ISBN 978-2-88976-972-8

DOI 10.3389/978-2-88976-972-8

## About Frontiers

Frontiers is more than just an open-access publisher of scholarly articles: it is a pioneering approach to the world of academia, radically improving the way scholarly research is managed. The grand vision of Frontiers is a world where all people have an equal opportunity to seek, share and generate knowledge. Frontiers provides immediate and permanent online open access to all its publications, but this alone is not enough to realize our grand goals.

## Frontiers Journal Series

The Frontiers Journal Series is a multi-tier and interdisciplinary set of open-access, online journals, promising a paradigm shift from the current review, selection and dissemination processes in academic publishing. All Frontiers journals are driven by researchers for researchers; therefore, they constitute a service to the scholarly community. At the same time, the Frontiers Journal Series operates on a revolutionary invention, the tiered publishing system, initially addressing specific communities of scholars, and gradually climbing up to broader public understanding, thus serving the interests of the lay society, too.

## Dedication to Quality

Each Frontiers article is a landmark of the highest quality, thanks to genuinely collaborative interactions between authors and review editors, who include some of the world's best academicians. Research must be certified by peers before entering a stream of knowledge that may eventually reach the public - and shape society; therefore, Frontiers only applies the most rigorous and unbiased reviews.

Frontiers revolutionizes research publishing by freely delivering the most outstanding research, evaluated with no bias from both the academic and social point of view. By applying the most advanced information technologies, Frontiers is catapulting scholarly publishing into a new generation.

## What are Frontiers Research Topics?

Frontiers Research Topics are very popular trademarks of the Frontiers Journals Series: they are collections of at least ten articles, all centered on a particular subject. With their unique mix of varied contributions from Original Research to Review Articles, Frontiers Research Topics unify the most influential researchers, the latest key findings and historical advances in a hot research area! Find out more on how to host your own Frontiers Research Topic or contribute to one as an author by contacting the Frontiers Editorial Office: [frontiersin.org/about/contact](https://frontiersin.org/about/contact)

# CELLULAR DORMANCY: STATE DETERMINATION AND PLASTICITY

Topic Editors:

**Guang Yao**, University of Arizona, United States

**Alexis Ruth Barr**, London Institute of Medical Sciences, Medical Research Council, United Kingdom

**Jyotsna Dhawan**, Centre for Cellular & Molecular Biology (CCMB), India

**Citation:** Yao, G., Barr, A. R., Dhawan, J., eds. (2022). Cellular Dormancy: State Determination and Plasticity. Lausanne: Frontiers Media SA.  
doi: 10.3389/978-2-88976-972-8

# Table of Contents

- 04 Editorial: Cellular dormancy—State determination and plasticity**  
Guang Yao, Jyotsna Dhawan and Alexis R. Barr
- 07 Calcium State-Dependent Regulation of Epithelial Cell Quiescence by Stanniocalcin 1a**  
Shuang Li, Chengdong Liu, Allison Goldstein, Yi Xin, Caihuan Ke and Cunming Duan
- 20 Cell Cycle Re-entry in the Nervous System: From Polyploidy to Neurodegeneration**  
Shyama Nandakumar, Emily Rozich and Laura Buttitta
- 33 Pan-Cancer Survey of Tumor Mass Dormancy and Underlying Mutational Processes**  
Anna Julia Wiecek, Daniel Hadar Jacobson, Wojciech Lason and Maria Secrier
- 52 Cell Cycle Commitment and the Origins of Cell Cycle Variability**  
Robert F. Brooks
- 72 Molecular Regulation of Paused Pluripotency in Early Mammalian Embryos and Stem Cells**  
Vera A. van der Weijden and Aydan Bulut-Karslioglu
- 88 Cell Cycle Entry Control in Naïve and Memory CD8<sup>+</sup> T Cells**  
David A. Lewis and Tony Ly
- 98 Quiescence Through the Prism of Evolution**  
Bertrand Daignan-Fornier, Damien Laporte and Isabelle Sagot
- 105 Is There a Histone Code for Cellular Quiescence?**  
Kenya Bonitto, Kirthana Sarathy, Kaiser Atai, Mithun Mitra and Hilary A. Collier
- 139 Monitoring Spontaneous Quiescence and Asynchronous Proliferation-Quiescence Decisions in Prostate Cancer Cells**  
Ajai J. Pulianmackal, Dan Sun, Kenji Yumoto, Zhengda Li, Yu-Chih Chen, Meha V. Patel, Yu Wang, Euisik Yoon, Alexander Pearson, Qiong Yang, Russell Taichman, Frank C. Cackowski and Laura A. Buttitta
- 153 Why Senescent Cells Are Resistant to Apoptosis: An Insight for Senolytic Development**  
Li Hu, Huiqin Li, Meiting Zi, Wen Li, Jing Liu, Yang Yang, Daohong Zhou, Qing-Peng Kong, Yunxia Zhang and Yonghan He
- 170 Extracellular Fluid Flow Induces Shallow Quiescence Through Physical and Biochemical Cues**  
Bi Liu, Xia Wang, Linan Jiang, Jianhua Xu, Yitshak Zohar and Guang Yao





## OPEN ACCESS

EDITED AND REVIEWED BY  
Philipp Kaldis,  
Lund University, Lund, Sweden

## \*CORRESPONDENCE

Guang Yao,  
guangyao@arizona.edu  
Jyotsna Dhawan,  
jdhawan@ccmb.res.in  
Alexis R. Barr,  
a.barr@lms.mrc.ac.uk

## SPECIALTY SECTION

This article was submitted to Cell Growth and Division, a section of the journal Frontiers in Cell and Developmental Biology

RECEIVED 01 July 2022

ACCEPTED 08 July 2022

PUBLISHED 04 August 2022

## CITATION

Yao G, Dhawan J and Barr AR (2022),  
Editorial: Cellular dormancy—State  
determination and plasticity.  
*Front. Cell Dev. Biol.* 10:984347.  
doi: 10.3389/fcell.2022.984347

## COPYRIGHT

© 2022 Yao, Dhawan and Barr. This is an open-access article distributed under the terms of the [Creative Commons Attribution License \(CC BY\)](https://creativecommons.org/licenses/by/4.0/). The use, distribution or reproduction in other forums is permitted, provided the original author(s) and the copyright owner(s) are credited and that the original publication in this journal is cited, in accordance with accepted academic practice. No use, distribution or reproduction is permitted which does not comply with these terms.

# Editorial: Cellular dormancy—State determination and plasticity

Guang Yao<sup>1\*</sup>, Jyotsna Dhawan<sup>2\*</sup> and Alexis R. Barr<sup>3\*</sup>

<sup>1</sup>Department of Molecular and Cellular Biology, Tucson, AZ, United States, <sup>2</sup>Centre for Cellular & Molecular Biology (CCMB), Hyderabad, Andhra Pradesh, India, <sup>3</sup>MRC London Institute of Medical Sciences (LMS), London, England, United Kingdom

## KEYWORDS

cellular dormancy, quiescence, senescence, heterogeneity, plasticity

## Editorial on the Research Topic

### Cellular Dormancy -State Determination and Plasticity

## Introduction

Most cells in the adult human body are non-dividing. Among these dormant cells, many are postmitotic and permanently out of the cell cycle (e.g., terminally differentiated and senescent cells), while a small sub-population, namely quiescent cells (such as adult stem and progenitor cells), can re-enter the cell cycle and divide in response to physiological cues. The balance between cell proliferation and dormancy plays critical roles in tissue homeostasis, repair, regeneration, and development. Pathological changes in cellular dormancy can lead to a wide range of hyper- or hypo-proliferation diseases, including cancer, fibrosis, autoimmunity, anemia, and aging.

Cellular dormancy exhibits significant heterogeneity and plasticity. Like sleep that has shallow and deep stages, dormancy appears to have different depths that are inversely correlated with the likelihood of cell cycle re-entry upon stimulation (Coller et al., 2006; Rodgers et al., 2014; Kwon et al., 2017). We lack a fundamental understanding of what determines and shapes cellular dormancy states: What cellular activities control dormancy entry, maintenance, and exit? What physiological signals regulate cell dormancy in different tissues and organs? Can we manipulate dormant states to improve human health, e.g., against aging and cancer?

This Research Topic includes original research and review articles that address the fascinating and complex states of cell dormancy in both human and model organisms. Three broad themes are collectively addressed:

## Dormancy entry, maintenance, and exit

The proliferative cycle can be described by four consecutive phases: G1, S (DNA synthesis), G2, and M (Mitosis). Dormant cells sit outside of this proliferative cycle, with quiescent cells still retaining proliferative potential but senescent and terminally differentiated cells losing it. While the field has studied and revealed a lot about the successive cell cycle phase transitions, we have much to learn regarding how cells enter, maintain and, in the case of quiescent cells, exit, dormant states.

The review by [Brookes](#) describes advances in our understanding of how cells exit quiescence back into the proliferative cell cycle. The time taken for cells to exit quiescence is highly variable and this review integrates and discusses a flurry of recent single-cell imaging studies that have started to change the way we think about how cells exit dormancy.

It has been tempting to speculate that epigenetic mechanisms may play an important role in the control of cell dormancy, but the specifics have been hard to pin down. The review by [Bonitto et al.](#) discussed the histone code hypothesis enabling reversible arrest. Given the technical advances, and new appreciation of cooperative nuclear events, understanding chromatin conformational dynamics is likely to help elucidate the control of transitions into and out of dormancy.

It is becoming clear that the signalling pathways coordinating dormancy entry and exit differ between cell and tissue types. Here, two review articles highlight these differences in two systems: in CD8<sup>+</sup> T-cells by [Lewis and Ly](#) and in the nervous system by [Nandakumar et al.](#) We anticipate that this will be a burgeoning field in the coming years where we try to understand the commonalities, but also the key cell type-specific differences. This could have important implications for our understanding for how dysregulated cell cycle components contribute to tissue-specific tumours. On the subject of cancer, to round up this set of articles, a research article by [Pulianmackal et al.](#) investigates asynchronous proliferation-quiescence decisions in pairs of daughters after mitosis in the context of prostate cancer - how it might arise and how this could contribute to tumor heterogeneity.

## Dormancy regulation at the tissue and organismal levels

Beyond the cellular level, higher order mechanisms are required to coordinate, maintain or impose cell dormancy in the organism. Three articles in this Research Topic highlight such high order mechanisms in development and evolution.

Body-wide changes across different cell and tissue types can be mapped to hormonal fluctuations. However, cell-type specificity of dormancy-regulation pathways needs more explanation. [Li et al.](#) report that a Ca<sup>2+</sup>-dependent secreted signal Stc1a (glycoprotein) in zebrafish suppresses local IGF-Akt-mTOR signaling and promotes the quiescence of Ca<sup>2+</sup>-sensitive epithelial cells (ionocytes). Ionocytes functionally resemble mammalian renal epithelia, suggesting a potential role of Ca<sup>2+</sup>-dependent pathways in regulating renal cell quiescence, with implications for kidney disease.

Cells *in vivo* experience interstitial fluid flows whose effects on cell dormancy are little known. By modeling cellular behaviors in microfluidic chambers, [Liu et al.](#) showed a faster extracellular flow drives cells to a more shallow quiescence, by increasing shear stress and extracellular factor replacement. This finding may help us understand how physico-chemical cues affect heterogeneous quiescence-proliferation balance *in situ*, impacting tissue dynamics.

A comprehensive review by [van der Weijden and Bulut-Karslioglu](#) addresses the connection between diapause, a reversible pause of early embryonic development, and the maintenance of potency and dormancy in adult stem cells. They survey diapause in a number of species and discuss body-wide signals at different diapause stages for dormancy induction, maintenance, and exit. Overall, this review identifies gaps in knowledge of dormant embryo and adult stem cells, understanding of which could permit interventions in diseases where quiescence is pathologically altered.

## Dormancy, diseases, and evolution

It is important to understand dormancy in the context of disease. Senescent cells accumulate during aging and in response to chemo- and radio-therapy in cancer treatment. Senescent cells contribute to aging processes and may promote tumorigenesis, and thus efforts are directed towards trying to eliminate senescent cells. [He et al.](#) discuss the challenges and ways forward in generating new senolytic treatments, particularly, how to target the increased apoptotic resistance of senescent cells.

As well as senescence, dormant cells contribute to cancer progression in other ways. For example, dormant cells are more resistant to chemotherapy than proliferating cells, and tumor cells can migrate from the primary tumor and lodge at metastatic sites in dormant states before reawakening years, or even decades, later, driving tumor relapse. [Wiecek et al.](#) tackles the question of which mutational processes give rise to dormant cells in tumors, as a route to start to understand how to tackle tumor dormancy and improve patient outcomes. By taking the vast amount of data from the TCGA database and profiling tumors across cancer types for signatures of tumor dormancy, they

identify an intriguing link between tumor dormancy and APOBEC-mediated mutagenesis.

Finally, [Daignan-Fornier et al.](#) discusses how quiescent states that emerged in unicellular organisms as a survival mechanism may have been adapted as multicellular organisms emerged. In this regard, quiescence may have co-evolved with and acted as a mechanism to promote cell specialization across different cell and tissue types.

Together, the articles in this Research Topic cover features and implications of cellular dormancy states in evolution, development and disease, and highlight the gaps that remain for a more mechanistic understanding.

## Author contributions

GY, JD, and AB wrote and revised the editorial.

## References

- Coller, H. A., Sang, L., and Roberts, J. M. (2006). A new description of cellular quiescence. *PLoS Biol.* 4, e83. doi:10.1371/journal.pbio.0040083
- Kwon, J. S., Everetts, N. J., Wang, X., Wang, W., Della Croce, K., Xing, J., et al. (2017). Controlling depth of cellular quiescence by an Rb-E2F network switch. *Cell Rep.* 20, 3223–3235. doi:10.1016/j.celrep.2017.09.007

## Conflict of interest

The authors declare that the research was conducted in the absence of any commercial or financial relationships that could be construed as a potential conflict of interest.

## Publisher's note

All claims expressed in this article are solely those of the authors and do not necessarily represent those of their affiliated organizations, or those of the publisher, the editors and the reviewers. Any product that may be evaluated in this article, or claim that may be made by its manufacturer, is not guaranteed or endorsed by the publisher.

- Rodgers, J. T., King, K. Y., Brett, J. O., Cromie, M. J., Charville, G. W., Maguire, K. K., et al. (2014). mTORC1 controls the adaptive transition of quiescent stem cells from G0 to G(Alert). *Nature* 510, 393–396. doi:10.1038/nature13255



# Calcium State-Dependent Regulation of Epithelial Cell Quiescence by Stanniocalcin 1a

Shuang Li<sup>1,2,3</sup>, Chengdong Liu<sup>3†</sup>, Allison Goldstein<sup>3</sup>, Yi Xin<sup>3</sup>, Caihuan Ke<sup>1,2</sup> and Cunming Duan<sup>3\*</sup>

<sup>1</sup> State Key Laboratory of Marine Environmental Science, Xiamen University, Xiamen, China, <sup>2</sup> College of Ocean and Earth Sciences, Xiamen University, Xiamen, China, <sup>3</sup> Department of Molecular, Cellular, and Developmental Biology, University of Michigan, Ann Arbor, MI, United States

## OPEN ACCESS

### Edited by:

Guang Yao,  
University of Arizona, United States

### Reviewed by:

Shaojun Du,  
University of Maryland, Baltimore,  
United States  
Zhongzhou Yang,  
Nanjing University, China

### \*Correspondence:

Cunming Duan  
cduan@umich.edu  
orcid.org/0000-0001-6794-2762

### † Present address:

Chengdong Liu,  
Key Laboratory of Mariculture  
(Ministry of Education), Ocean  
University of China, Qingdao, China

### Specialty section:

This article was submitted to  
Cell Growth and Division,  
a section of the journal  
Frontiers in Cell and Developmental  
Biology

**Received:** 01 February 2021

**Accepted:** 08 March 2021

**Published:** 09 April 2021

### Citation:

Li S, Liu C, Goldstein A, Xin Y,  
Ke C and Duan C (2021) Calcium  
State-Dependent Regulation  
of Epithelial Cell Quiescence by  
Stanniocalcin 1a.  
Front. Cell Dev. Biol. 9:662915.  
doi: 10.3389/fcell.2021.662915

The molecular mechanisms regulating cell quiescence-proliferation balance are not well defined. Using a zebrafish model, we report that Stc1a, a secreted glycoprotein, plays a key role in regulating the quiescence-proliferation balance of  $\text{Ca}^{2+}$  transporting epithelial cells (ionocytes). Zebrafish *stc1a*, but not the other *stc* genes, is expressed in a  $\text{Ca}^{2+}$  state-dependent manner. Genetic deletion of *stc1a*, but not *stc2b*, increased ionocyte proliferation, leading to elevated body  $\text{Ca}^{2+}$  levels, cardiac edema, body swelling, and premature death. The increased ionocyte proliferation was accompanied by an increase in the IGF1 receptor-mediated PI3 kinase-Akt-Tor signaling activity in ionocytes. Inhibition of the IGF1 receptor, PI3 kinase, Akt, and Tor signaling reduced ionocyte proliferation and rescued the edema and premature death in *stc1a*<sup>-/-</sup> fish, suggesting that Stc1a promotes ionocyte quiescence by suppressing local IGF signaling activity. Mechanistically, Stc1 acts by inhibiting Papp-aa, a zinc metalloproteinase degrading Igfbp5a. Inhibition of Papp-aa proteinase activity restored ionocyte quiescence-proliferation balance. Genetic deletion of *papp-aa* or its substrate *igfbp5a* in the *stc1a*<sup>-/-</sup> background reduced ionocyte proliferation and rescued the edema and premature death. These findings uncover a novel and  $\text{Ca}^{2+}$  state-dependent pathway regulating cell quiescence. Our findings also provide new insights into the importance of ionocyte quiescent-proliferation balance in organismal  $\text{Ca}^{2+}$  homeostasis and survival.

**Keywords:** PAPP-A, IGFBP-5, IGF1 receptor, Akt, Tor, ionocytes, zebrafish

## INTRODUCTION

Maintaining a pool of quiescent cells that can be rapidly reactivated upon appropriate stimulation is critical for tissue repair, wound healing, and regeneration. This is particularly critical for highly renewable tissues such as epithelia (Valcourt et al., 2012; Cheung and Rando, 2013; Collier, 2019). Dysregulation of the cell quiescence-proliferation balance can lead to human diseases such as cancer, autoimmune diseases, and fibrosis (Kitaori et al., 2009; Fiore et al., 2018). Recent studies

in genetically tractable organisms suggest that the nutrient sensitive insulin/insulin-like growth factor (IGF)-PI3 kinase-AKT-mTOR signaling pathway plays a key role in regulating the cell quiescence-proliferation decision. Studies in *Drosophila* have shown that adult neural stem cells can be reactivated in response to dietary amino acids attributed to increased insulin release from neighboring glia cells (Britton and Edgar, 1998; Chell and Brand, 2010; Sousa-Nunes et al., 2011; Huang and Wang, 2018). Likewise, mouse genetic studies revealed that IGF2 plays a key role in reactivating hematopoietic stem cells (HSCs), neural stem cell, and intestinal stem cells (Venkatraman et al., 2013; Ferron et al., 2015; Ziegler et al., 2015; Ziegler et al., 2019). Activating mTOR signaling by deleting the Tsc gene in mouse HSCs stimulates their cell cycle re-entry and proliferation (Chen et al., 2008). Conversely, inhibition of mTOR signaling in mice preserved the long-term self-renewal and the hematopoietic capacity of HSCs (Chen et al., 2009). This regulation is not limited to adult stem cells. mTORC1 signaling has been shown to promote naïve T cells to exit quiescence and proliferate (Yang et al., 2013).

While the importance of the insulin/IGF-PI3 kinase-AKT-mTOR signaling pathway in quiescence-proliferation regulation has become evident, an outstanding question is how this central hormonal pathway is activated in such a cell type-specific manner. Recently, we have developed a zebrafish model, in which a population of quiescent epithelial cells, known as ionocytes or NaR cells, can be induced to reenter the active cell cycle (Dai et al., 2014; Liu et al., 2017). NaR cells take up  $\text{Ca}^{2+}$  from the surrounding aquatic habitat to maintain body  $\text{Ca}^{2+}$  homeostasis (Hwang, 2009; Yan and Hwang, 2019). While largely quiescent when zebrafish larvae are kept in  $\text{Ca}^{2+}$ -rich embryo rearing media, these cells rapidly re-enter the active cell cycle and proliferate when  $\text{Ca}^{2+}$  is depleted or reduced from the media (i.e., low  $[\text{Ca}^{2+}]$  stress) (Dai et al., 2014; Liu et al., 2017). As the case in *Drosophila* and mouse adult stem cells, NaR cell quiescence to proliferation transition is regulated by the cell type-specific activation of the IGF-PI3 kinase-Akt-Tor signaling (Dai et al., 2014; Liu et al., 2017). Further studies suggested that IGF binding protein 5a (Igfbp5a), a secreted protein capable of binding IGFs with high-affinity and regulating IGF bioavailability to its receptors, and its major proteinase, pregnancy-associated plasma protein-a (Papp-aa), are highly expressed in NaR cells (Liu et al., 2018; Liu et al., 2020). Genetic deletion of *igfbp5a*, *papp-aa*, or inhibition of Papp-aa-mediated Igfbp5a proteolytic cleavage all abolishes NaR cell reactivation and proliferation (Liu et al., 2018, 2020). These findings suggest that Papp-aa-mediated Igfbp5a proteolysis plays a key role in activating IGF signaling locally and in promoting NaR cell quiescence exit and proliferation. Further analyses showed that the Papp-aa-mediated Igfbp5a proteolysis is inhibited by a post-transcriptional mechanism under normal  $[\text{Ca}^{2+}]$  conditions. This in turn promotes NaR cell quiescence (Liu et al., 2020). The molecular nature of this  $[\text{Ca}^{2+}]$ -dependent mechanism, however, is unknown.

Stanniocalcin 1 (Stc1) is a dimeric glycoprotein originally discovered from the corpuscles of Stannius (CS) in teleost fish in the 1960s (Wagner and Dimattia, 2006). Early studies

showed that surgical removal of CS led to elevated calcium uptake, increased blood calcium level, and the appearance of kidney stones in fish (Fontaine, 1964; Pang, 1971; Fenwick, 1974), leading to the notion that CS contains a hypocalcemic hormone. The active CS component was purified and named as Stc1 (Wagner and Dimattia, 2006; Yeung et al., 2012). Mature Stc1 contains 11 conserved cysteine residues and a N-linked glycosylation site. The first 10 cysteines form intramolecular disulfide bridges and the 11th cysteine forms a disulfide bond linking the two monomers, which stabilizes the functional dimer (Yamashita et al., 1995). It is now clear that zebrafish genome contains 4 *stc* genes (Schein et al., 2012) and they are called by different names in the literature and in different databases. Hereafter, they will be referred as *stc1a*, *stc1b*, *stc2a*, and *stc2b* following Schein et al. (2012). In good agreement with the notion that Stc1 is a hypocalcemic hormone, forced expression by mRNA injection and morpholino-based knockdown of Stc1 in zebrafish altered  $\text{Ca}^{2+}$  uptake and changed NaR cell number, although these manipulations also changed the uptake of other ions as well as other ionocyte types (Tseng et al., 2009; Chou et al., 2015).

Although Stc1 was originally discovered in fish and was considered a teleost fish-specific hormone for several decades, it is now clear that multiple *Stc/STC* genes are present in mammals including humans (Gagliardi et al., 2005; Wagner and Dimattia, 2006; Yeung et al., 2012). Humans have two *STC* genes, *STC1* and *STC2*. There is limited and conflicting evidence on whether STCs play any major role in calcium uptake in mammals (Gagliardi et al., 2005; Wagner and Dimattia, 2006; Yeung et al., 2012). Overexpressing human *STC1* or *STC2* in transgenic mice resulted in reduced body size (Johnston et al., 2010). Biochemical studies showed that *STC1* and *STC2* can bind to PAPP-A/A2 *in vitro* and inhibit PAPP-A/A2-mediated IGFBP4 and IGFBP5 proteolytic cleavage (Argente et al., 2017). Clinical studies suggested that human individuals carrying loss-of-function mutations in the *STC2* gene had greater adult height and this was linked to reduced PAPP-A activity and increased local IGF signaling activity (Marouli et al., 2017). These observations led us to hypothesized that one or more Stc proteins regulates NaR cell quiescence by inhibiting Papp-aa-mediated Igfbp5a proteolysis and suppress IGF signaling.

In this study, we report that the expression of *stc1a*, but not the other 3 *stc* genes, is regulated in a  $[\text{Ca}^{2+}]$  state-dependent manner in zebrafish embryos. Genetic deletion of *stc1a* resulted in elevated IGF signaling in NaR cells and increased NaR cell proliferation, leading to increased body  $\text{Ca}^{2+}$  levels, body edema, and premature death. These phenotypes were rescued by double deletion of *stc1a* with *papp-aa* or *igfbp5a*. Moreover, inhibition of IGF signaling reduced NaR cell proliferation and rescued the edema and premature death in *stc1a*<sup>-/-</sup> fish.

## MATERIALS AND METHODS

### Chemicals and Reagents

Chemical and molecular biology reagents were purchased from Fisher Scientific (Pittsburgh, PA) unless otherwise



noted. BMS-754807 was purchased from Active Biochemicals Co. Batimastat and  $\text{ZnCl}_2$  were purchased from Sigma (St. Louis, MO, United States), MK2206 from ChemieTek (Indianapolis, IN), wortmannin and Rapamycin from Calbiochem (Gibbstown, NJ). The Phospho-Akt antibody was purchased from Cell Signaling Technology (Danvers, MA, United States) and restriction enzymes were purchased from New England BioLabs (Ipswich, MA, United States). Primers, TRIzol, M-MLV reverse transcriptase were purchased from Life Technologies (Carlsbad, CA, United States). Anti-Digoxigenin-AP antibodies was purchased from Roche (Basel, Switzerland). The pT3.Cas 9-UTRglobin vector was a gift from Dr. Yonghua Sun, Institute of Hydrobiology, Chinese Academy of Sciences.

## Experimental Animals

Zebrafish were maintained, crossed, and staged in accordance to standard guidelines (Kimmel et al., 1995; Westerfield, 2000). Embryos and larvae were raised at 28.5°C in standard E3 embryo medium. Three additional embryo media containing 0.2, 0.02, and 0.001 mM  $[\text{Ca}^{2+}]$  were prepared as previously reported (Dai et al., 2014). To inhibit pigmentation, 0.003% (w/v) N-phenylthiourea was added to these solutions. The *Tg(igfbp5a:GFP)* and *igfbp5a*<sup>-/-</sup> fish lines were generated in previous studies (Liu et al., 2018, 2020). The *papp-aa*<sup>p170/+</sup> fish were a kind gift from the Marc Wolman lab. The *stc2b*<sup>+/-</sup> fish (*stc2b*<sup>sc24026</sup>, ZIRC# ZL10776) were obtained from ZIRC. All experiments were conducted in accordance with the guidelines approved by the Institutional Committee on the Use and Care of Animals, University of Michigan.

## RT-qPCR

Total RNA was extracted from pooled zebrafish embryos and larvae. RNA was reverse-transcribed to cDNA using oligo(dT)18 primer and M-MLV (Promega). qPCR was performed using SYBR Green (Bio-Rad) on a StepONE PLUS real-time thermocycler (Applied Biosystems). PCR primers were designed based on the 4 zebrafish *stc* gene sequences obtained from the Ensemble database (Ensemble gene numbers are: *stc1a*, ENSDARG00000058476, *stc1b*, ENSDARG0000003303, *stc2a*, ENSDARG00000056680, and *stc2b*, ENSDARG00000102206). The expression level of a target gene transcript was normalized by  $\beta$ -actin mRNA or 18S RNA levels. The primers used are: *stc1a*-qPCR-F: 5'-CCAGCTGCTTCAAAACAAACC-3', *stc1a*-qPCR-R: 5'-ATGGAGCGTTTTCTGGCGA-3', *stc1b*-qPCR-F: 5'-CCAAGCCACTTTCCCAACAG-3', *stc1b*-qPCR-R: 5'-ACCCACCACGAGTCTCCATTC-3', *stc2a*-qPCR-F: 5'-TATGGTCTTCCAGCTTCAGCG-3', *stc2a*-qPCR-R: 5'-CGAGTAATGGCTTCCTTCACCT-3', *stc2b*-qPCR-F: 5'-CACAAGAAAAGACTGTCTCTGCAGA-3', *stc2b*-qPCR-R: 5'-GGTAGTGACATCTGGGACGG-3', *papp-aa*-qPCR-F: 5'-AAAGAGGAGGGCGTTCAAG-3', *papp-aa*-qPCR-R: 5'-TGCAGCGGATCACATTAGAG-3' (Liu et al., 2020), *18s*-qPCR-F: 5'-AATCGCATTTGCCATCACCG-3', *18s*-qPCR-R: 5'-TCACCACCCTCTCAACCTCA-3',  $\beta$ -actin-qPCR-F: 5'-GATCTGGCATCACACCTTCTAC-3',  $\beta$ -actin-qPCR-R: 5'-CCTGGATGGCCACATACAT-3'.

## Generation of *stc1a*<sup>-/-</sup> Fish Lines and Transient Knockdown of *stc1a* by CRISPR/Cas9

Two sgRNAs targeting the *stc1a* gene were designed using CHOPCHOP<sup>1</sup>. Their sequences are: *stc1a*-sgRNA-1, 5'-GCAGAGCGCCATTCAGACAG-3' and *stc1a*-sgRNA-2, 5'-GCAGATCTCGTGCATGCCGT-3'. Mixed sgRNA (30–40 ng/ $\mu$ l) and Cas 9 mRNA (200–400 ng/ $\mu$ l) were injected into *Tg(igfbp5a:GFP)* embryos at the 1-cell stage (Xin and Duan, 2018). A subset of injected F0 embryos was used to identify indels. DNA was isolated from individual embryos and analyzed by PCR followed by hetero-duplex assays (HRMA) as reported (Liu et al., 2018). For transient knockout experiments, the remaining injected F0 embryos were raised in E3 embryo medium to 3 dpf and transferred to the intended embryo medium from 3 to 5 dpf as previously reported (Dai et al., 2014). To generate stable *stc1a*<sup>-/-</sup> fish lines, injected F0 embryos were raised to adulthood and crossed with *Tg(igfbp5a:GFP)* or wild-type fish. F1 fish were raised to adulthood and genotyped. After confirming indels by DNA sequencing, the heterozygous F1 fish were intercrossed to generate F2 fish.

## Genotyping

Genomic DNA was isolated from individual or pooled fish as reported (Liu et al., 2018). HRMA was performed to genotype *igfbp5a*<sup>-/-</sup>, *papp-aa*<sup>-/-</sup> fish and siblings following published methods (Liu et al., 2018, 2020). The *stc1a* mutant fish genotyping was performed by PCR using the following primers: *stc1a*-gt-F, 5'-TGAAAACCACTGCCTTAAATTG-3', *stc1a*-gt-R, 5'-GTAGCTCTACCGATCCCAAATG-3'. The progenies of *stc2b*<sup>+/-</sup> intercrosses were genotyped by direct DNA sequencing.

## Morphology Analysis

Body length, somite number and head trunk angles were measured as described (Kamei et al., 2011; Liu et al., 2018). The bright-field images were acquired using a stereomicroscope (Leica MZ16F, Leica, Wetzlar, Germany) equipped with a QImaging QICAM camera (QImaging, Surrey, BC, Canada).

## Total Body $\text{Ca}^{2+}$ Assay

The sample preparation was carried out as reported (Elizondo et al., 2010). Briefly, fish larvae were anesthetized using MS-222. In each group, 35 zebrafish larvae were pooled and washed twice with deionized water, and dried at 65°C for 60 min. Next, 125  $\mu$ l 1M HCl was added to each tube and incubated overnight at 95°C with shaking. Samples were centrifuged and the supernatant was collected. Total calcium content was measured using a commercial kit (ab102505, Abcam, United States) following the manufacturer's instruction.

## Live Imaging and Microscopy

NaR cells were quantified as previously reported (Liu et al., 2017). Briefly, embryos and larvae were anesthetized with MS-222. Larvae were mounted and subjected to fluorescent imaging using

<sup>1</sup><http://chopchop.cbu.uib.no>

the Leica MZ16F stereo microscope. Image J was used for image analysis and data quantification.

## Immunostaining and Whole Mount *in situ* Hybridization

Whole mount immunostaining and *in situ* hybridization were performed as described previously (Dai et al., 2014). Briefly, zebrafish larvae were fixed in 4% paraformaldehyde and permeabilized in methanol. They were incubated overnight with the phospho-Akt antibody in 4°C, followed by incubation with an anti-rabbit HRP antibody (Jackson ImmunoResearch, West Grove, PA, United States) and nickel-diaminobenzidine staining. For *in situ* hybridization, *igfbp5a* mRNA signal was detected using a digoxigenin (DIG)-labeled antisense riboprobe. Larvae were incubated in an anti-DIG-AP antibody or dinitrophenol following published methods (Dai et al., 2014).

## Drug Treatment

All drugs used in this study, except ZnCl<sub>2</sub>, were dissolved in DMSO and further diluted in double-distilled water. ZnCl<sub>2</sub> was dissolved in distilled water. Zebrafish larvae were treated with ZnCl<sub>2</sub>, batimastat, BMS-754807, and other drugs from 3 to 5 dpf (Dai et al., 2014; Liu et al., 2017). Drug solutions were changed daily. 5 dpf larvae were then collected for immunostaining, *in situ* hybridization or fluorescent imaging.

## Statistical Analysis

Statistical tests were carried out using GraphPad Prism 8 software (GraphPad Software, Inc., San Diego, CA). Values are shown as means ± SEM. Statistical significance between experimental groups was performed using unpaired two-tailed *t*-test, Chi-square test, long-rank test and one-way ANOVA followed by Tukey's multiple comparison test. Statistical significances were accepted at *P* < 0.05 or greater.

## RESULTS

### The Expression of *stc1a* Gene Is Regulated by Ca<sup>2+</sup> Levels

To determine whether changing Ca<sup>2+</sup> levels affect *stc* expression, zebrafish embryos were raised in embryo media containing varying concentrations of [Ca<sup>2+</sup>]. As shown in **Figures 1A–D**, the levels of *stc1a* mRNA, but not those of *stc1b*, *stc2a*, and *stc2b*, were increased with increasing [Ca<sup>2+</sup>] levels. Similar results were obtained in larval fish (**Supplementary Figure 1A**). Next, we used *papp-aa*<sup>−/−</sup> and *trpv6*<sup>−/−</sup> mutants to investigate the effect of body Ca<sup>2+</sup> levels. Both mutant fish suffer from severe calcium deficiency and had greatly reduced body Ca<sup>2+</sup> levels compared to their siblings (Xin et al., 2019; Liu et al., 2020). The levels of *stc1a* mRNA were significantly lower in the *papp-aa*<sup>−/−</sup> mutant fish compared to those of the wildtype siblings (**Figure 1E**). The mRNA levels of *stc1b*, *stc2a*, and

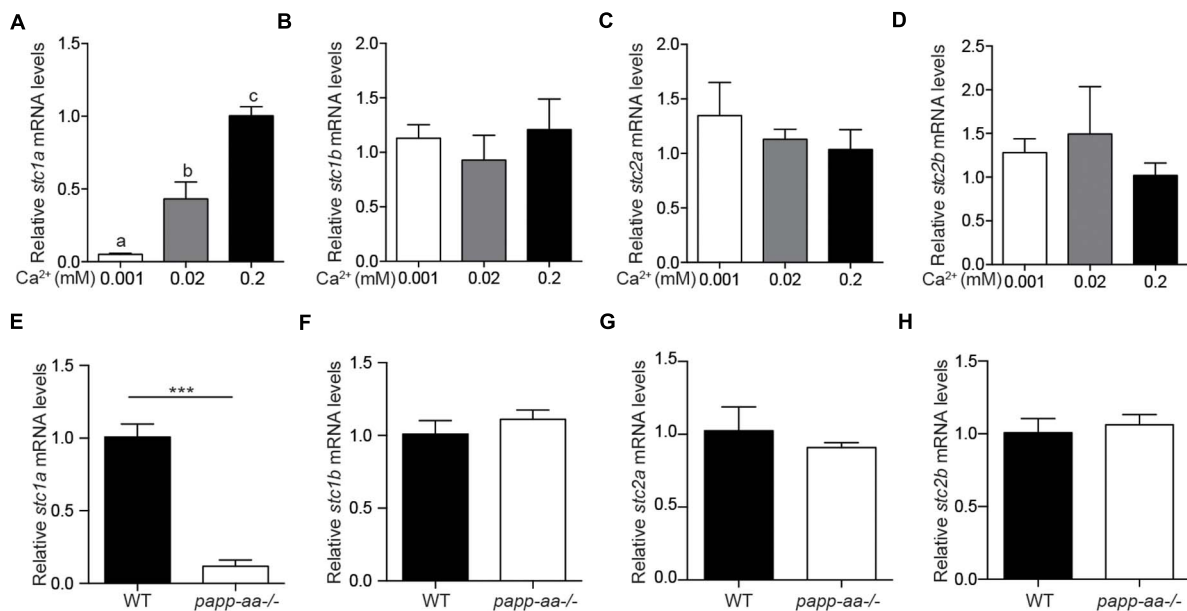


**FIGURE 1 |** The expression of *stc1a*, but not other *stc* genes, is regulated by Ca<sup>2+</sup> levels. **(A–D)** Wild-type zebrafish embryos were raised in embryo media containing the indicated Ca<sup>2+</sup> concentration until 3 days post fertilization (dpf). The mRNA expression levels of *stc1a* **(A)**, *stc1b* **(B)**, *stc2a* **(C)**, and *stc2b* **(D)** were determined by qRT-PCR and normalized by  $\beta$ -actin mRNA levels. Data shown are from 3 independent experiments, each containing 10–15 embryos/group. In this and all subsequent figures, data shown are Mean ± SEM unless stated otherwise. Different letters indicate significant differences between groups by one-way ANOVA followed by Tukey's multiple comparison test (*P* < 0.05) unless stated otherwise. **(E–H)** Zebrafish of the indicated genotypes were raised in E3 embryo medium until 5 dpf. The mRNA levels of *stc1a* **(E)**, *stc1b* **(F)**, *stc2a* **(G)**, and *stc2b* **(H)** were measured, normalized, and shown. Data shown are from 3 independent experiments, each containing 10–15 larvae/group. \*\*\**P* < 0.001 by unpaired two-tailed *t*-test.

*stc2b* were comparable between *papp-aa*<sup>-/-</sup> and wild-type fish (Figures 1F–H). Similarly, the *stc1a* mRNA level in the calcium deficient *trpv6*<sup>-/-</sup> mutant fish was significantly lower compared to those of the siblings (Supplementary Figure 1B). These data suggest that the expression of *stc1a*, but not the other *stc* genes, is regulated in a [Ca<sup>2+</sup>]-dependent manner in zebrafish embryos.

## Genetic Deletion of *stc1a* Leads to Elevated NaR Cell Proliferation, Increased Body Ca<sup>2+</sup> Content, Body Swelling, and Premature Death

To determine the *in vivo* function of Stc1a, three *stc1a* mutant fish lines, i.e., *stc1a* (+17), *stc1a* ( $\Delta 18 + 1$ ), and *stc1a* ( $\Delta 35$ ), were generated using CRISPR/Cas 9 (Supplementary Figure 2A). All 3 mutants are predicted to be null mutations (Figure 2A). Progenies of *stc1a* (+17)<sup>+/-</sup> intercrosses, which were a mixture of homozygous, heterozygous, and wild type embryos, were raised and analyzed in a double-blind fashion.

No difference in the body size, development speed, and gross morphology was detected among the 3 genotypes until 3 dpf (Figures 2B–F). At 4 dpf, many *stc1a* (+17)<sup>-/-</sup> mutant fish displayed cardiac edema (Figure 2B). The cardiac edema phenotype became more pronounced at 5 dpf. In addition, mutant fish had no inflated swim bladder (Figure 2B). By 6 and 7 dpf, mutant fish showed severe body swelling and death rate increased (Figures 2B,G). Similar results were obtained in *stc1a* ( $\Delta 18 + 1$ )<sup>-/-</sup> fish (Supplementary Figures 2B–G). In comparison, *stc2b*<sup>-/-</sup> fish showed no morphological defects or premature death (Supplementary Figure 3). These findings suggest that while Stc1a does not affect embryonic patterning and growth, it is essential for larval survival.

Because the known role of fish Stc1 in epithelial Ca<sup>2+</sup> uptake and body Ca<sup>2+</sup> balance, we measured total body Ca<sup>2+</sup> levels. Measuring blood Ca<sup>2+</sup> levels in zebrafish embryos/larvae is not feasible because of their tiny size. Compared to the siblings, the total body Ca<sup>2+</sup> levels in *stc1a*<sup>-/-</sup> mutants were significantly greater (Figure 3A). Next, the possible

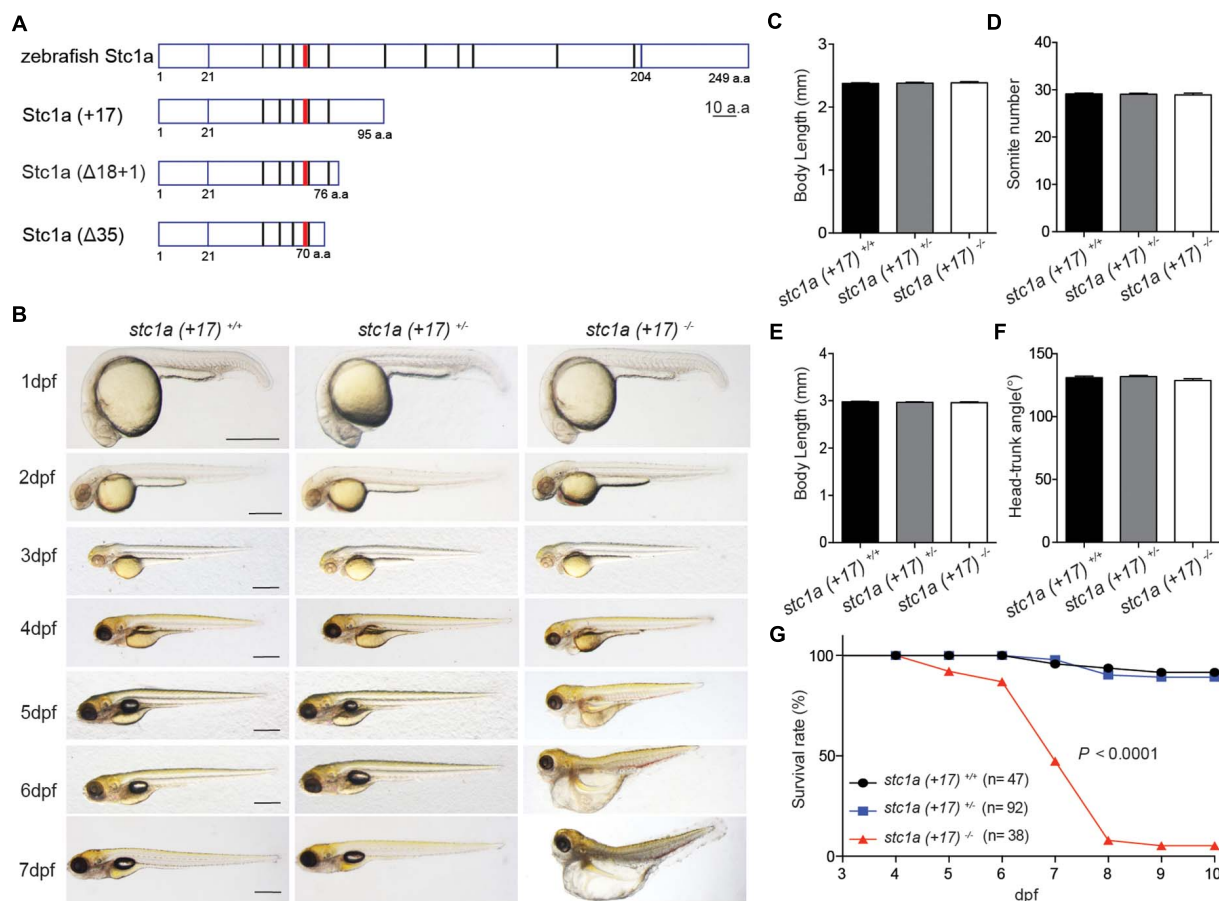


**FIGURE 2 |** Genetic deletion of *stc1a* results in cardiac edema, body swelling, and premature death. **(A)** Schematic diagram of Stc1a protein and the indicated mutants. The N-linked glycosylation site and conserved cysteine residues are shown by red and black bars, respectively. **(B)** Morphology of fish of the indicated genotypes at the indicated stages. Lateral views with anterior to the left and dorsal up. Scale bar = 0.5 mm. **(C–F)** Body length, somite number, and head-trunk angle of the indicated genotypes at 24 hpf **(C,D)** and 48 hpf **(E,F)**.  $n = 15$ –42 fish/group. **(G)** Survival curves. Progenies of *stc1a* (+17)<sup>+/-</sup> intercrosses were raised in E3 embryo medium. Dead embryos were collected daily and genotyped individually. The survival curves of indicated genotypes and the total fish numbers are shown.  $P < 0.0001$  by log-rank test.



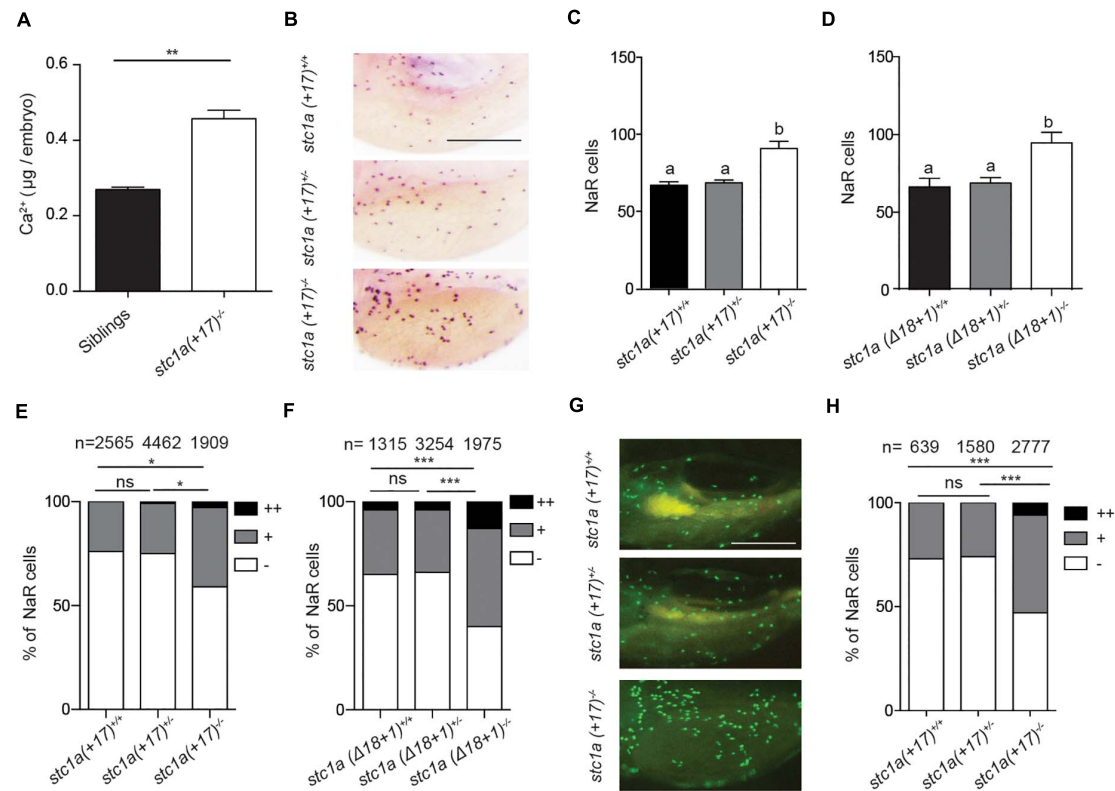


**FIGURE 3 |** Genetic deletion of *stc1a* results in elevated body  $\text{Ca}^{2+}$  content and increased NaR cell proliferation. **(A)** Total body  $\text{Ca}^{2+}$  content in 5 dpf zebrafish larvae of the indicated genotypes. Data shown are from 3 independent experiments, each containing 35 larvae/group. **\*\*** $P < 0.01$  by unpaired two-tailed *t*-test. **(B–D)** Progenies of *stc1a* (+17) $^{+/-}$  intercrosses **(C)** or progenies of *stc1a* ( $\Delta18 + 1$ ) $^{+/-}$  intercrosses **(D)** were raised in the E3 embryo medium to 5 dpf. NaR cells were detected by *in situ* hybridization using an *igfbp5a* cRNA probe. After NaR cells were visualized and quantified in each fish, fish were genotyped individually. Representative images are shown in **(B)** and quantified data in **(C,D)**. Scale bar = 0.2 mm.  $n = 33\text{--}70$  larvae/group **(C)** and  $19\text{--}46$  larvae/group **(D)**. **(E,F)** NaR cells in 5 dpf larvae of the indicated genotypes were scored following a published proliferation scoring index (Liu et al., 2018). Cells that divided 0, 1, or 2 times were scored as -, +, and ++. **\* $P < 0.05$**  and **\*\*\* $P < 0.001$**  by Chi-square test. Total number of cells is shown above the bar. **(G,H)** Progenies of *stc1a* (+17) $^{+/-}$ ; *Tg* (*igfbp5a*: *GFP*) intercrosses were raised in E3 embryo medium until 5 dpf. GFP-expressing NaR cells were scored as described in **(E)**. Representative images are shown in **(G)** and quantified results in **(H)**. Scale bar = 0.2 mm. **\*\*\* $P < 0.001$**  by Chi-square test.

changes in NaR cells were examined. For this, progenies of *stc1a* (+17) $^{+/-}$  intercrosses were subjected to *in situ* hybridization analysis using a specific NaR cell maker (Liu et al., 2017). *stc1a* (+17) $^{-/-}$  fish had significantly more NaR cells than their wild-type and heterozygous siblings (Figures 3B,C). Similar increases in NaR cell number were also observed in *stc1a* ( $\Delta18 + 1$ ) $^{-/-}$  (Figure 3D) and *stc1a* ( $\Delta35$ ) $^{-/-}$  fish (Supplementary Figure 4A). In comparison, *stc2b* $^{-/-}$  deletion did not increase NaR cell number (Supplementary Figure 4B). Notably, NaR cells in the *stc1a* $^{-/-}$  mutant fish were often observed as cell clusters, an indicator of newly divided cells (Figure 3B). Quantification results showed that the NaR proliferation index was greater in *stc1a* (+17) $^{-/-}$ , ( $\Delta18 + 1$ ) $^{-/-}$ , and *stc1a* ( $\Delta35$ ) $^{-/-}$  fish (Figures 3E,F and Supplementary Figure 4C). No change in NaR cell proliferation was detected in *stc2b* $^{-/-}$  fish (Supplementary Figure 4D). To investigate possible changes in NaR proliferation further, we generated a *stc1a* (+17) $^{-/-}$ ; *Tg*(*igfbp5a*:*GFP*) fish line. The *Tg*(*igfbp5a*:*GFP*) fish is a reporter fish line, in which NaR cell proliferation can be

visualized in real time in live fish larvae (Liu et al., 2017). A significantly higher NaR cell proliferation rate was detected in *stc1a* (+17) $^{-/-}$  fish compared with the siblings (Figures 3G,H). These findings suggest that genetic deletion of *stc1a* results in elevated NaR cell proliferation and higher body  $\text{Ca}^{2+}$  content.

### Stc1a Action in NaR Cells Requires Papp-aa and Igfbp5a

Gene expression indicated higher *papp-aa* mRNA levels in *stc1a* (+17) $^{-/-}$  fish compared with their siblings (Figure 4A). Knockdown of *Stc1a* using gRNAs resulted in a significant increase in NaR cell number (Figure 4B). This increase was reduced by treatment with  $\text{ZnCl}_2$  or batimastat, two distinct Papp-aa inhibitors (Tallant et al., 2006; Liu et al., 2020; Figure 4B), suggesting Papp-aa-mediated proteolysis is critical. This action is IGF signaling-dependent since it was abolished by treatment with BMS-754807, an IGF1 receptor inhibitor (Figure 4B).

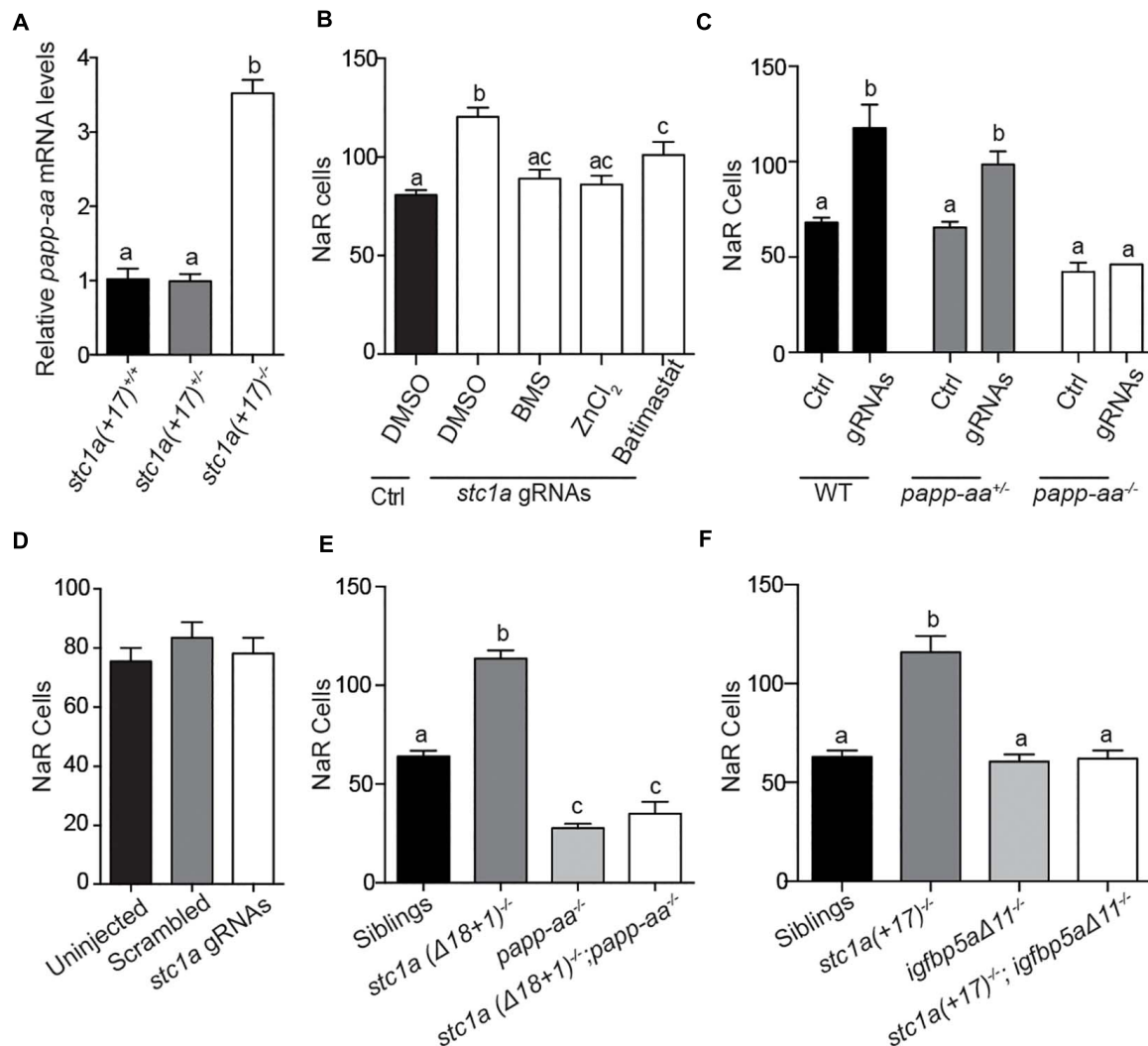


**FIGURE 4 |** Papp-aa and Igfbp5a are indispensable for Stc1a action in NaR cells. **(A)** Embryos of the indicated genotypes were raised in E3 embryo medium until 5 dpf. The mRNA levels of *papp-aa* were measured and normalized.  $n = 15\text{--}17$  larvae/group. **(B)** *Tg(igfbp5a: GFP)* embryos were injected with *stc1a* targeting gRNAs and Cas9 mRNA at the 1-cell stage. Embryos were raised in E3 embryo medium. The injected embryos were treated with BMS-754807 (BMS, 0.3  $\mu\text{M}$ ), ZnCl<sub>2</sub> (8  $\mu\text{M}$ ), or Batimastat (200  $\mu\text{M}$ ) from 3 to 5 dpf. NaR cells were quantified and shown.  $n = 20\text{--}39$  larvae/group. **(C,D)** Progeny of *papp-aa<sup>+/-</sup>*; *Tg(igfbp5a: GFP)* intercrosses **(C)** or *igfbp5a<sup>-/-</sup>*; *Tg(igfbp5a: GFP)* intercrosses **(D)** were injected with *stc1a* targeting gRNAs and Cas9 mRNA. The injected embryos were raised and NaR cells were quantified at 5 dpf. Each larva was genotyped afterward.  $n = 5\text{--}19$  larvae/group **(C)** and  $n = 39\text{--}43$  larvae/group **(D)**. **(E,F)** Larvae of the indicated genotypes were raised in E3 embryo medium and NaR cells were quantified at 5 dpf.  $n = 9\text{--}78$  larvae/group **(E)** and  $n = 4\text{--}34$  larvae/group **(F)**.

If Stc1a acts via suppressing the Papp-aa-mediated Igfbp5a proteolysis, then the loss of Stc1a should not affect NaR cell quiescence-proliferation balance in the absence of Papp-aa or Igfbp5a. Indeed, while knockdown of Stc1a resulted in significant increases in NaR cell proliferation in wild-type and heterozygous siblings, it did not have such an effect in *pappaa<sup>-/-</sup>*; *Tg(igfbp5a:GFP)* embryos (**Figure 4C**). Likewise, knockdown of Stc1a in *igfbp5a<sup>-/-</sup>*; *Tg(igfbp5a:GFP)* fish did not increase NaR cell proliferation (**Figure 4D**). This was tested further by generating stable double mutant fish. While permanent deletion of *stc1a* significantly increased NaR cell reactivation, it had no such effect in the *papp-aa<sup>-/-</sup>* background (**Figure 4E**) or in the *igfbp5a<sup>-/-</sup>* background (**Figure 4F**). These genetic data

suggest that Stc1a promotes NaR cell quiescence in a Papp-aa and Igfbp5a-dependent manner.

### Stc1a Promotes NaR Cell Quiescence by Suppressing IGF Signaling in NaR Cells

To determine whether local IGF signaling plays a role in elevated NaR cell proliferation in *stc1a<sup>-/-</sup>* fish, phospho-Akt immunostaining analysis was performed as previously reported (Dai et al., 2014). Compared with siblings, *stc1a* (+17)<sup>-/-</sup> larvae had significantly more phospho-Akt positive cells in the yolk sac region (**Figure 5A**). This increase was abolished by the addition of the IGF1 receptor inhibitor BMS-754807

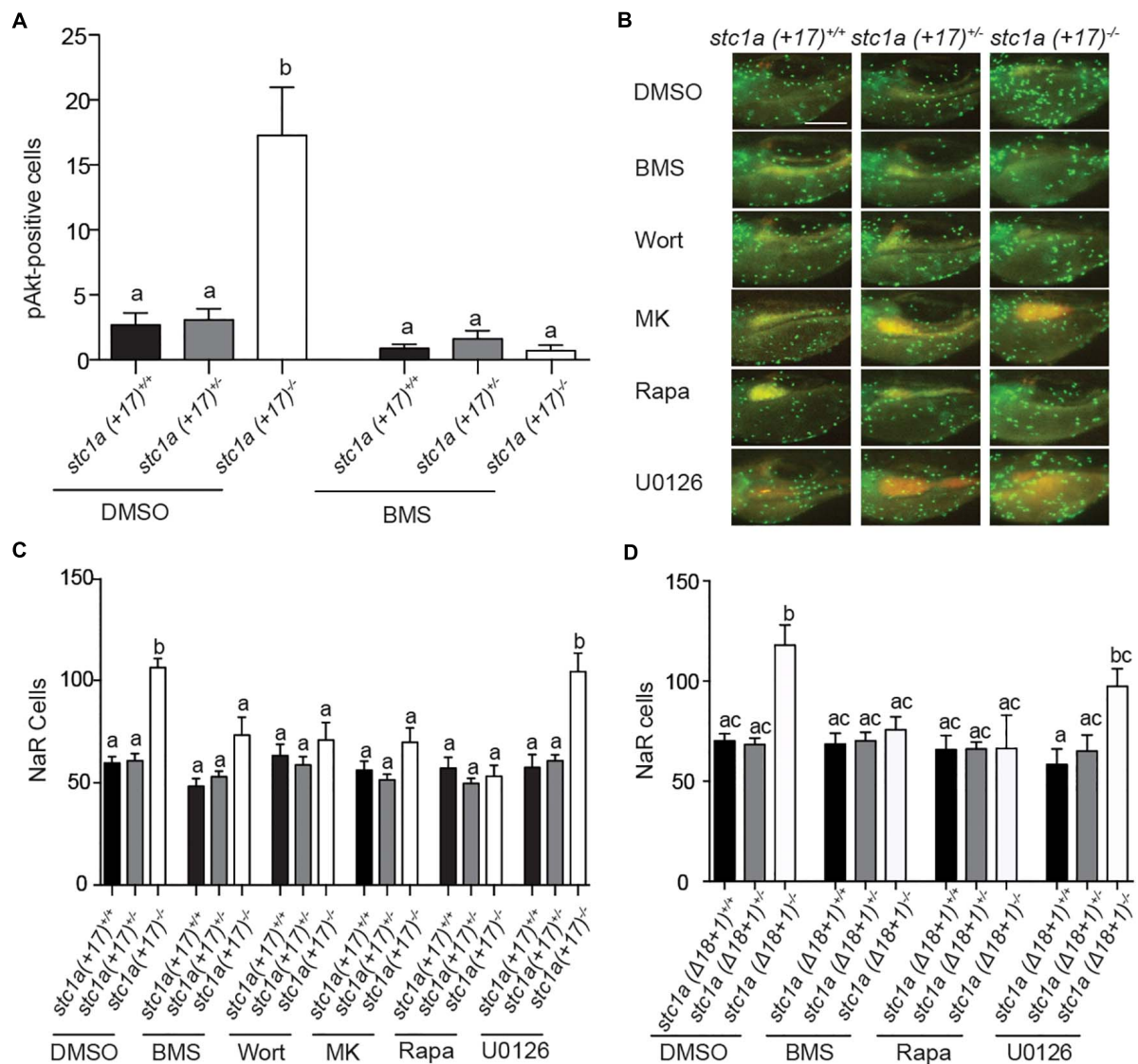


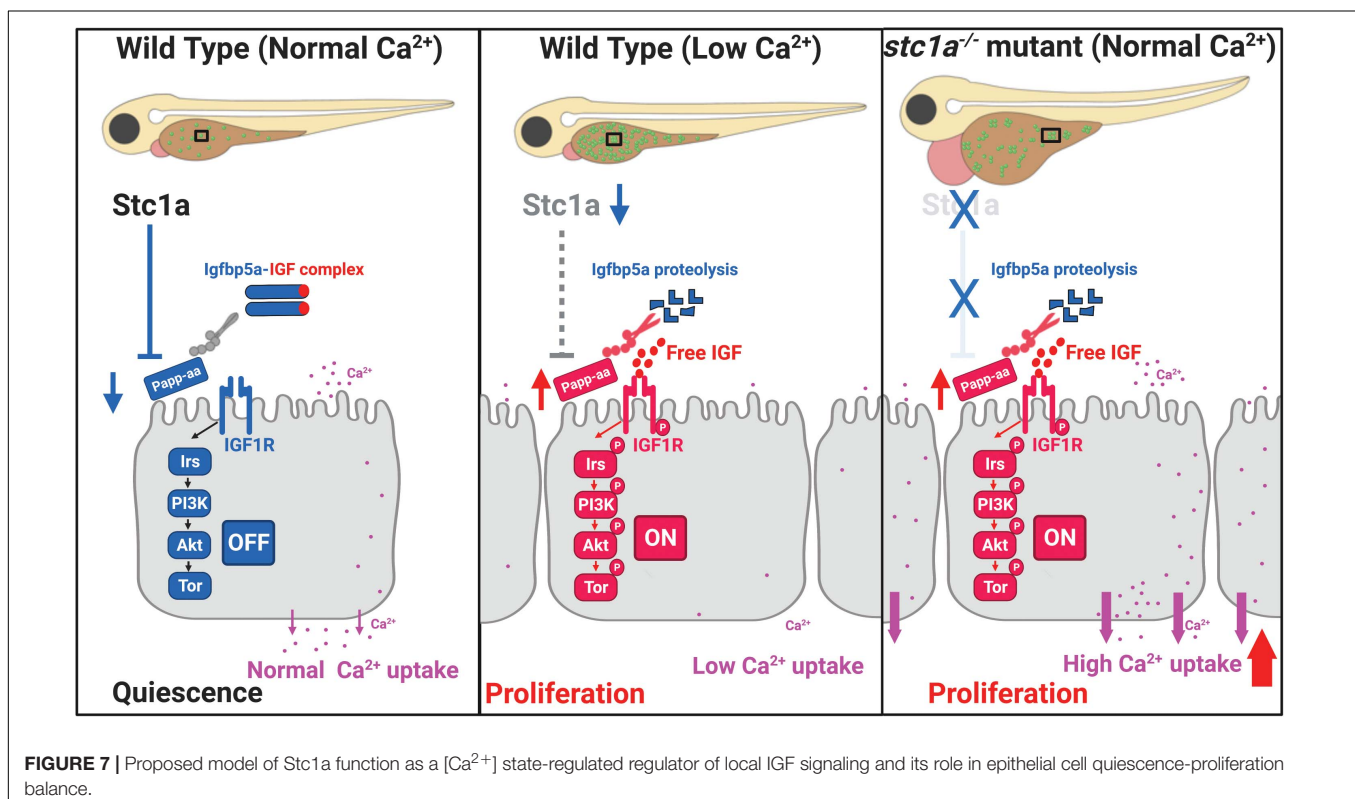
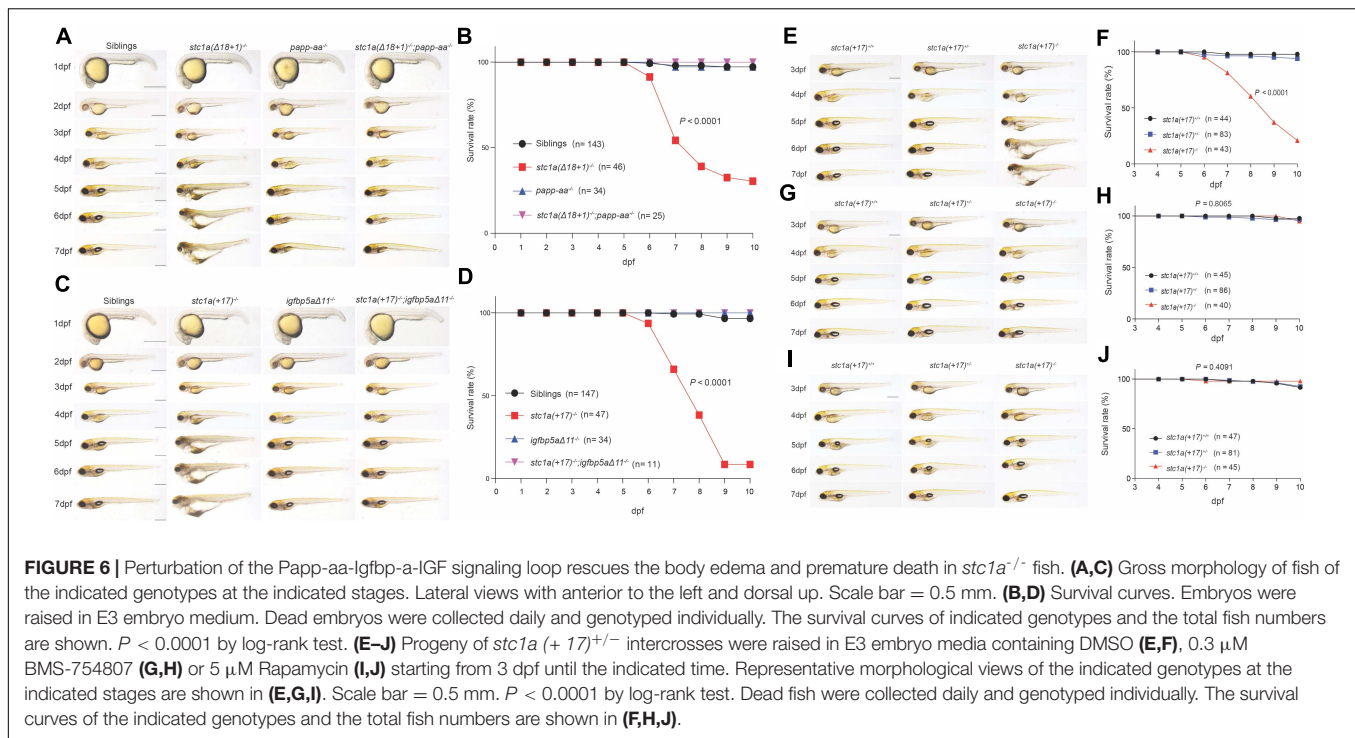
**FIGURE 5 |** Stc1a promotes NaR cell quiescence by suppressing IGF-PI3 kinase-Akt-Tor signaling in NaR cells. **(A)** Progenies of *stc1a (+17)<sup>+/-</sup>; Tg (igfbp5a: GFP)* intercrosses were raised in E3 embryo medium to 3 dpf and treated with DMSO or 0.3  $\mu$ M BMS-754807 (BMS). Two days later, fish were fixed and phospho-Akt positive cells in the yolk sac region were detected by immunostaining. These fish were genotyped individually afterward.  $n = 14$ –47 larvae/group. **(B,C)** Progeny of *stc1a (+17)<sup>+/-</sup>; Tg (igfbp5a: GFP)* intercrosses were raised in E3 embryo medium and treated with DMSO, 0.3  $\mu$ M BMS-754807 (BMS), 0.06  $\mu$ M Wortmannin (Wort), 8  $\mu$ M MK2206 (MK), 5  $\mu$ M Rapamycin (Rapa), or 10  $\mu$ M U0126 from 3 to 5 dpf. After NaR cells were quantified, these fish were genotyped individually. Representative images **(B)** and quantified data are shown **(C)**.  $n = 7$ –35 larvae/group. Scale bar = 0.2 mm. **(D)** Progeny of *stc1a (Δ18+1)<sup>+/-</sup>; Tg (igfbp5a: GFP)* intercrosses were raised in E3 embryo medium to 3 dpf and treated with DMSO, 0.3  $\mu$ M BMS-754807 (BMS), 5  $\mu$ M Rapamycin (Rapa), or 10  $\mu$ M U0126 from 3 to 5 dpf. NaR cells were quantified as described above.  $n = 4$ –28 larvae/group.

(Figure 5A). Moreover, BMS-754807 treatment reduced NaR cell number in *stc1a (+17)<sup>-/-</sup>* larvae to that of the siblings (Figures 5B,C). Likewise, treatments with the PI3 kinase inhibitor wortmannin, Akt inhibitor MK2206, and Tor inhibitor rapamycin all decreased NaR cell proliferation (Figures 5B,C). The addition of the MEK inhibitor U0126 had no such effect level (Figures 5B,C). Similar results were obtained with *stc1a (Δ18+1)<sup>-/-</sup>* fish (Figure 5D). These data suggest that genetic deletion of *stc1a* increases NaR cell proliferation via activating the IGF1 receptor-mediated PI3 kinase-Akt-Tor signaling in NaR

cells. Therefore, Stc1a promotes NaR cell quiescence state by suppressing local IGF signaling.

### The Body Edema and Premature Death in *stc1a<sup>-/-</sup>* Fish Are Rescued by Perturbing the Papp-aa-Igfbp5a-IGF Signaling Axis

The cardiac edema, body swelling, and premature death phenotypes in *stc1a<sup>-/-</sup>* fish were unexpected. We postulated that these phenotypes may be related to the altered NaR cell



quiescence-proliferation balance in the *stc1a*<sup>-/-</sup> mutant fish. We tested this idea using *stc1a*<sup>-/-</sup>;*papp-aa*<sup>-/-</sup> double mutant fish. While *stc1a*<sup>-/-</sup> fish developed cardiac and body edema, and had elevated death rate, *stc1a*<sup>-/-</sup>;*papp-aa*<sup>-/-</sup> double mutants

did not display these phenotypes (Figure 6A). The survival curve of *stc1a*<sup>-/-</sup>;*papp-aa*<sup>-/-</sup> double mutant fish was similar to their wild-type and heterozygous siblings (Figure 6B). Likewise, permanent deletion of *igfbp5a* in the *stc1a*<sup>-/-</sup> background



prevented the development of edema, swelling and premature death (**Figures 6C,D**). Finally, treatment of *stc1a*<sup>-/-</sup> fish with BMS-754807 eliminated the edema, body swelling and prevented the mutant fish from premature death (**Figures 6E–H**). Inhibition of Tor signaling had similar results (**Figures 6I,J**). The cardiac edema, body swelling, and premature death phenotypes in *stc1a*<sup>-/-</sup> fish occur due to elevated IGF signaling and NaR cell quiescence-proliferation imbalance.

## DISCUSSION

Ca<sup>2+</sup> is an essential ion and plays key roles in a wide range of biological processes. In zebrafish embryos, epithelial Ca<sup>2+</sup> uptake is carried out by NaR cells (Liao et al., 2009; Yan and Hwang, 2019). NaR cells are functionally equivalent to human intestinal and renal epithelial cells and express major molecular components of the transcellular Ca<sup>2+</sup> transport machinery, including the epithelial calcium channel Trpv6 (Hoenderop et al., 2005; Hwang, 2009). In the adult stage, NaR cells are distributed in the intestine, kidney, and gills (a major osmoregulation organ in fish). In the embryonic and larval stages, these cells are located on the yolk sac region (Hwang, 2009). Genetic deletion of *trpv6* resulted in severe Ca<sup>2+</sup> deficiency and premature death in zebrafish (Xin et al., 2019). Epithelial Ca<sup>2+</sup> uptake is regulated by a number of hormones, including parathyroid hormones, vitamin D, isotocin, cortisol, stanniocalcin 1, and IGF1 (Chou et al., 2011, 2015; Dai et al., 2014; Yan and Hwang, 2019). Calcium abundance/availability also changes epithelial Ca<sup>2+</sup> uptake by affecting Trpv6 expression and NaR cell numbers (Liu et al., 2017; Yan and Hwang, 2019). We have previously reported that reducing or depleting Ca<sup>2+</sup> from the embryo media (i.e., low Ca<sup>2+</sup> stress) activates IGF signaling in NaR cells locally and stimulates pre-exiting NaR cells to re-enter the cell cycle and proliferate (Dai et al., 2014; Liu et al., 2017). In this cell-type specific regulation of IGF signaling, IGFBP5/Igfbp5a and its proteinase Papp-aa are key players (Liu et al., 2020; Liu et al., 2018). Under low [Ca<sup>2+</sup>] conditions, Papp-aa degrades Igfbp5a and releases IGFs to activate IGF signaling and promotes NaR proliferation. Under normal [Ca<sup>2+</sup>] conditions, however, the Papp-aa-mediated Igfbp5 proteolysis is inhibited and IGF signaling is suppressed in NaR cells. This promotes NaR cell quiescence (Liu et al., 2020). In this study, we provide genetic, cell biology, and pharmacological evidence suggesting that Stc1a functions as a calcium state-dependent regulator of IGF signaling in NaR cell quiescence and promotes NaR cell quiescence state. Mechanistically, Stc1a suppresses local IGF signaling by inhibiting Papp-aa-mediated Igfbp5a proteolytic cleavage.

Early reports showed that Stc1 expression is stimulated by increasing external [Ca<sup>2+</sup>] via the action of calcium-sensing receptor (CaSR), a G-protein coupled receptor which senses extracellular [Ca<sup>2+</sup>] levels. When kept in high [Ca<sup>2+</sup>] media, cultured rainbow trout CS cells increase Stc1 expression and secretion (Ellis and Wagner, 1995). This increase in Stc1 expression is mediated by CaSR (Radman et al., 2002). Similarly, zebrafish embryos raised in embryo media containing higher

levels of [Ca<sup>2+</sup>] had greater levels of *stc1* mRNA compared to those raised in normal [Ca<sup>2+</sup>] media and this increase is mediated by CaSR (Kwong et al., 2014; Lin et al., 2014). We now understand that teleost fish and mammals have multiple STC/Stc genes. Whether all *stc* genes are regulated in a similar way and act redundantly is less clear. Additionally, whether Stc1 expression is regulated in a similar fashion by body calcium levels *in vivo* has not yet reported. The results of the present study addressed these questions. Our results suggested that the 4 *stc* genes are differentially regulated in zebrafish embryos. Increasing external [Ca<sup>2+</sup>] levels increased *stc1a* mRNA levels in a concentration-dependent manner. This effect is specific to *stc1a* and no such changes were found with *stc1b*, *stc2a*, and *stc2b*. The effects of the body Ca<sup>2+</sup> levels were determined by comparing *stc* mRNA levels in calcium deficient *papp-aa*<sup>-/-</sup> fish and their siblings (Xin et al., 2019; Liu et al., 2020). The levels of *stc1a* mRNA were significantly reduced in the *papp-aa*<sup>-/-</sup> mutant fish compared to their siblings. Papp-aa is a zinc metalloproteinase involved in degrading Igfbps (Liu et al., 2020). Therefore, the reduced *stc1a* mRNA levels in *papp-aa*<sup>-/-</sup> fish is probably caused by the reduced body Ca<sup>2+</sup> levels in *papp-aa*<sup>-/-</sup> fish rather than a direct effect of Papp-aa. This notion was further supported by the reduced *stc1a* mRNA level in the *trpv6*<sup>-/-</sup> mutant fish.

The first Stc1 protein was identified from bony fish in 1960s (Pang, 1973; Wagner and Dimattia, 2006; Yeung et al., 2012). While significant progress has been made in our understanding of Stc proteins over the past decades, the long-term *in vivo* function of fish Stc has not been elucidated due to the lack of a null fish model. Using CRISPR/Cas9, we generated several *stc1a*<sup>-/-</sup> zebrafish lines. Our genetic analysis results reveal that Stc1a is an essential protein. Loss of Stc1a leads to cardiac edema, body swelling, and premature death. Importantly, loss of *stc1a* resulted in elevated NaR cell proliferation and increased NaR cell number, suggesting Stc1a regulates NaR cell quiescence-proliferation balance. The action of Stc1a in NaR cells clearly involves local IGF signaling. Loss of Stc1a activated the IGF1 receptor-mediated Akt signaling in NaR cells. Inhibition of the IGF1 receptor, PI3 kinase, Akt, and Tor all reduced NaR cell proliferation in *stc1a*<sup>-/-</sup> mutant fish. The *papp-aa* mRNA levels were higher in the *stc1a*<sup>-/-</sup> mutant fish. In zebrafish embryos, *papp-aa* mRNA is highly expressed in NaR cells (Liu et al., 2020). The elevated *papp-aa* mRNA level in *stc1a*<sup>-/-</sup> mutant fish is likely an indirect result of increased NaR cell number. We investigated the functional relationship between Stc1a and Papp-aa using genetic and pharmacological approaches. While transient knockdown of Stc1a increased NaR cell proliferation in wild-type fish, it did not have such effect in *papp-aa*<sup>-/-</sup> mutant fish. Likewise, double deletion of *papp-aa* and *stc1a* reduced NaR cell proliferation. Finally, pharmacological inhibition of Papp-aa-mediated proteolysis reduced the NaR cell proliferation in *stc1a*<sup>-/-</sup> mutant fish to the sibling levels, suggesting that Papp-aa and its proteolysis are required for Stc1a action in NaR cells. In further support of this conclusion, knockdown or genetic deletion of *igfbp5a*, which encodes the major Papp-aa substrate Igfbp5a, abolished the NaR cell proliferation in *stc1a*<sup>-/-</sup> mutant fish. Based on these findings, we propose that Stc1a regulates

NaR cell quiescence-proliferation balance in a  $[Ca^{2+}]$  state-dependent manner (Figure 7). Under normal  $[Ca^{2+}]$  conditions, Stc1a is expressed and Stc1a inhibits Papp-aa-mediated Igfbp5a proteolysis. The intact Igfbp5a binds to and sequesters IGFs in the Igfbp5a/IGF complex. This suppresses IGF signaling and promotes NaR cell quiescence (Figure 7, left panel). Under low  $[Ca^{2+}]$  conditions, Stc1a expression is reduced and this inhibitory loop is inactivated and Papp-aa-mediated Igfbp5a proteolysis increased. The free IGFs binds to the IGF1 receptor and activates the IGF1 receptor-mediated PI3 kinase-Akt-Tor signaling in NaR cells. This stimulates NaR cell proliferation and increases NaR cell number. Despite the increased NaR cell number, the body calcium levels are low because the external  $Ca^{2+}$  is depleted (Figure 7, middle panel). In the *stc1a*<sup>-/-</sup> mutant fish, Stc1a is absent and Papp-aa is active. Papp-aa proteolytically cleaves Igfbp5a and releases IGFs from the complex to activate IGF-1 receptor-mediated signaling and promotes NaR cell proliferation. Increased NaR cell number results in elevated  $Ca^{2+}$  uptake and this in turn leads to cardiac edema and body swelling (Figure 7, right panel). While our conclusion is based on findings made in zebrafish, available evidence indicates that this regulatory loop is conserved in mammals. Human STC1 has been shown to bind to PAPP-A and inhibit PAPP-A proteolytic cleavage of IGFBP4 and IGFBP5 *in vitro* (Kløverpris et al., 2015). A recent study in mice suggested that mesenchymal stromal cells secrete STC1 to suppress HSC reactivation and proliferation (Waclawiczek et al., 2020).

It is worth to note that the *stc1a*<sup>-/-</sup> mutant fish phenotypes reported in the present study differ considerably from those reported in Stc1-null mice. Stc1-null mice grew and reproduced normally with no notable anatomical abnormalities (Chang et al., 2005). There are several possible explanations for the differences. Published studies suggest that mammalian STC1 does not appear to play a major role in  $Ca^{2+}$  uptake nor does it act as an endocrine factor (Wagner and Dimattia, 2006; Yeung et al., 2012). Mammals do not have CS glands. The *STC1* gene is expressed in many tissues in mammals and acts mainly in a paracrine and autocrine fashion (Yeung et al., 2012). Another key difference is the habitats. Unlike the terrestrial mammals, zebrafish live in hypoosmotic aquatic habitats (Evans, 2008). Zebrafish must constantly uptake ions such as  $Ca^{2+}$  from the surrounding habitat and continuously remove osmotic water by secreting a large volume of diluted urine to maintain the body osmolarity (Evans, 2008). We speculate that the increased NaR cell number and elevated epithelial  $Ca^{2+}$  uptake in *stc1a*<sup>-/-</sup> mutant fish led to increased osmotic water in the fish body, resulting in cardiac edema and body swelling. This speculation is supported by the fact that when the elevated NaR cell proliferation in *stc1a*<sup>-/-</sup> mutant fish was blocked by inhibiting IGF signaling, the body edema and premature death phenotypes were alleviated. Moreover, genetic deletion of *igfbp5a* or *papp-aa* in the *stc1a*<sup>-/-</sup> background reduced NaR cell proliferation and prevented the cardiac edema, body swelling, and premature death phenotypes. It is also possible that the higher levels of body  $Ca^{2+}$  may play a direct role in heart development and/or cardiac muscle

function. However, we did not notice significant changes in heart development in *stc1a*<sup>-/-</sup> embryos. In fact, the *stc1a*<sup>-/-</sup> mutant fish are indistinguishable from the siblings until 3 dpf. The cardiac edema began to appear around 4 dpf and became more prevalent thereafter. Future studies are needed to clarify whether the higher levels of  $Ca^{2+}$  play a direct role in cardiac muscle.

## CONCLUSION

In conclusion, our analyses reveal a previously unrecognized role of Stc1a as a  $[Ca^{2+}]$  state-dependent epithelial cell quiescence regulator. Stc1a regulates epithelial cell quiescence-proliferation balance by suppressing the local Papp-aa-Igfbp5a-IGF signaling loop. Our study also sheds new light on the functional importance of ionocyte quiescence-proliferation balance in organismal  $Ca^{2+}$  homeostasis and survival. Zebrafish NaR cells are functionally and molecularly similar to human renal epithelial cells. In mammals, dysregulation of IGF signaling has been implicated in abnormal kidney growth. Following unilateral nephrectomy, for example, the contralateral kidney shows compensatory growth in an IGF dependent manner (Rosendahl et al., 1992). Renal expression of IGF-1, IGF1 receptor, IGFBP4, IGFBP5, and PAPP-A are all increased in an autosomal dominant polycystic disease (ADPKD) mouse model (Kashyap et al., 2020). A recent study reported that PAPP-A knockout significantly decreased cyst development and improved kidney injury response in the ADPKD mice (Kashyap et al., 2020). STC1 has been identified as one of the chronic kidney disease genes by genome-wide association studies (Böger and Heid, 2011). Future studies will be needed to elucidate whether STC1 plays a similar role in regulating mammalian renal cell quiescence-proliferation balance via locally expressed PAPP-A, IGFBPs, and IGF signaling.

## DATA AVAILABILITY STATEMENT

The raw data supporting the conclusions of this article will be made available by the authors, without undue reservation.

## ETHICS STATEMENT

The animal study was reviewed and approved by the Institutional Committee on the Use and Care of Animals, University of Michigan.

## AUTHOR CONTRIBUTIONS

CD conceived the study. CD and SL designed the study and wrote the manuscript. SL, CL, AG, and YX performed the study.

SL analyzed the data. CD and CK provided supervision. All authors read the manuscript.

## FUNDING

This work was supported by NSF grant IOS-1557850 and University of Michigan M-Cubed 3 Project U064122 to CD. The funders had no role in study design, data collection and analysis, decision to publish, or preparation of the manuscript.

## REFERENCES

- Argente, J., Chowen, J. A., Pérez-Jurado, L. A., Frystyk, J., and Oxvig, C. (2017). One level up: abnormal proteolytic regulation of IGF activity plays a role in human pathophysiology. *EMBO Mol. Med.* 9, 1338–1345. doi: 10.15252/emmm.201707950
- Böger, C. A., and Heid, I. M. (2011). Chronic kidney disease: novel insights from genome-wide association studies. *Kidney Blood Press. Res.* 34, 225–234. doi: 10.1159/000326901
- Britton, J. S., and Edgar, B. A. (1998). Environmental control of the cell cycle in *Drosophila*: nutrition activates mitotic and endoreplicative cells by distinct mechanisms. *Development*. 125, 2149–2158.
- Chang, A. C. M., Cha, J., Koentgen, F., and Reddel, R. R. (2005). The murine stanniocalcin 1 gene is not essential for growth and development. *Mol. Cell Biol.* 25, 10604–10610. doi: 10.1128/mcb.25.23.10604-10610.2005
- Chell, J. M., and Brand, A. H. (2010). Nutrition-responsive glia control exit of neural stem cells from quiescence. *Cell*. 143, 1161–1173. doi: 10.1016/j.cell.2010.12.007
- Chen, C., Liu, Y., Liu, R., Ikenoue, T., Guan, K. L., Liu, Y., et al. (2008). TSC-mTOR maintains quiescence and function of hematopoietic stem cells by repressing mitochondrial biogenesis and reactive oxygen species. *J. Exp. Med.* 205, 2397–2408. doi: 10.1084/jem.20081297
- Chen, C., Liu, Y., Liu, Y., and Zheng, P. (2009). mTOR regulation and therapeutic rejuvenation of aging hematopoietic stem cells. *Sci. Signal.* 2:ra75. doi: 10.1126/scisignal.2000559
- Cheung, T. H., and Rando, T. A. (2013). Molecular regulation of stem cell quiescence. *Nat. Rev. Mol. Cell Biol.* 14, 329–340. doi: 10.1038/nrm3591
- Chou, M. Y., Hung, J. C., Wu, L. C., Hwang, S. P., and Hwang, P. P. (2011). Isotocin controls ion regulation through regulating ionocyte progenitor differentiation and proliferation. *Cell. Mol. Life Sci.* 68, 2797–2809. doi: 10.1007/s00018-010-0593-2
- Chou, M. Y., Lin, C. H., Chao, P. L., Hung, J. C., Cruz, S. A., and Hwang, P. P. (2015). Stanniocalcin-1 controls ion regulation functions of ion-transporting epithelium other than calcium balance. *Int. J. Biol. Sci.* 11, 122–132. doi: 10.7150/ijbs.10773
- Coller, H. A. (2019). The paradox of metabolism in quiescent stem cells. *FEBS Lett.* 593, 2817–2839. doi: 10.1002/1873-3468.13608
- Dai, W., Bai, Y., Hebda, L., Zhong, X., Liu, J., Kao, J., et al. (2014). Calcium deficiency-induced and TRP channel-regulated IGF1R-PI3K-Akt signaling regulates abnormal epithelial cell proliferation. *Cell Death Differ.* 21, 568–581. doi: 10.1038/cdd.2013.177
- Elizondo, M. R., Budi, E. H., and Parichy, D. M. (2010). trpm7 regulation of in vivo cation homeostasis and kidney function involves stanniocalcin 1 and fgf23. *Endocrinology* 151, 5700–5709. doi: 10.1210/en.2010-0853
- Ellis, T. J., and Wagner, G. F. (1995). Post-transcriptional regulation of the stanniocalcin gene by calcium. *J. Biol. Chem.* 270, 1960–1965.
- Evans, D. H. (2008). Teleost fish osmoregulation: what have we learned since August Krogh, Homer Smith, and Ancel Keys. *Am. J. Physiol. Regul. Integr. Comp. Physiol.* 295, R704–R713. doi: 10.1152/ajpregu.90337.2008
- Fenwick, J. C. (1974). The corpuscles of stannius and calcium regulation in the North American eel (*Anguilla rostrata* LeSueur). *Gen. Comp. Endocrinol.* 23, 127–135. doi: 10.1016/0016-6480(74)90121-x

## ACKNOWLEDGMENTS

We thank Ms. Helena Li, University of Michigan, for proofreading this manuscript.

## SUPPLEMENTARY MATERIAL

The Supplementary Material for this article can be found online at: <https://www.frontiersin.org/articles/10.3389/fcell.2021.662915/full#supplementary-material>

- Ferron, S., Radford, E., Domingo-Muelas, A., Kleine, I., Ramme, A., Gray, D., et al. (2015). Differential genomic imprinting regulates paracrine and autocrine roles of IGF2 in mouse adult neurogenesis. *Nat. Commun.* 6:8265. doi: 10.1038/ncomms9265
- Fiore, A., Ribeiro, P. F., and Bruni-Cardoso, A. (2018). Sleeping beauty and the microenvironment enchantment: microenvironmental regulation of the proliferation-quiescence decision in normal tissues and in cancer development. *Front. Cell Dev. Biol.* 6:59. doi: 10.3389/fcell.2018.00059
- Fontaine, M. (1964). [Stannius' corpuscles and ionic (Ca, K, Na) of the interior environment of the eel (*Anguilla anguilla* L.)]. *C. R. Hebd. Seances Acad. Sci.* 259, 875–878.
- Gagliardi, A. D., Kuo, E. Y., Raulic, S., Wagner, G. F., and DiMattia, G. E. (2005). Human stanniocalcin-2 exhibits potent growth-suppressive properties in transgenic mice independently of growth hormone and IGFs. *Am. J. Physiol. Endocrinol. Metab.* 288, E92–E105. doi: 10.1152/ajpendo.00268.2004
- Hoenderop, J. G., Nilius, B., and Bindels, R. J. (2005). Calcium absorption across epithelia. *Physiol. Rev.* 85, 373–422. doi: 10.1152/physrev.00003.2004
- Huang, J., and Wang, H. (2018). Hsp83/Hsp90 physically associates with Insulin receptor to promote neural stem cell reactivation. *Stem Cell Rep.* 11, 883–896. doi: 10.1016/j.stemcr.2018.08.014
- Hwang, P. P. (2009). Ion uptake and acid secretion in zebrafish (*Danio rerio*). *J. Exp. Biol.* 212, 1745–1752. doi: 10.1242/jeb.026054
- Johnston, J., Ramos-Valdes, Y., Stanton, L. A., Ladhani, S., Beier, F., and DiMattia, G. E. (2010). Human stanniocalcin-1 or -2 expressed in mice reduces bone size and severely inhibits cranial intramembranous bone growth. *Transgenic Res.* 19, 1017–1039. doi: 10.1007/s11248-010-9376-7
- Kamei, H., Ding, Y., Kajimura, S., Wells, M., Chiang, P., and Duan, C. (2011). Role of IGF signaling in catch-up growth and accelerated temporal development in zebrafish embryos in response to oxygen availability. *Development*. 138, 777–786. doi: 10.1242/dev.056853
- Kashyap, S., Hein, K. Z., Chini, C. C., Lika, J., Warner, G. M., Bale, L. K., et al. (2020). Metalloproteinase PAPP-A regulation of IGF-1 contributes to polycystic kidney disease pathogenesis. *JCI Insight* 5:135700. doi: 10.1172/jci.insight.135700
- Kimmel, C. B., Ballard, W. W., Kimmel, S. R., Ullmann, B., and Schilling, T. F. (1995). Stages of embryonic development of the zebrafish. *Dev. Dyn.* 203, 253–310. doi: 10.1002/aja.1002030302
- Kitaori, T., Ito, H., Schwarz, E. M., Tsutsumi, R., Yoshitomi, H., Oishi, S., et al. (2009). Stromal cell-derived factor 1/CXCR4 signaling is critical for the recruitment of mesenchymal stem cells to the fracture site during skeletal repair in a mouse model. *Arthritis Rheum.* 60, 813–823. doi: 10.1002/art.24330
- Kløverpris, S., Mikkelsen, J. H., Pedersen, J. H., Jepsen, M. R., Laursen, L. S., Petersen, S. V., et al. (2015). Stanniocalcin-1 potently inhibits the proteolytic activity of the metalloproteinase pregnancy-associated plasma protein-a. *J. Biol. Chem.* 290, 21915–21924. doi: 10.1074/jbc.M115.650143
- Kwong, R. W., Auprix, D., and Perry, S. F. (2014). Involvement of the calcium-sensing receptor in calcium homeostasis in larval zebrafish exposed to low environmental calcium. *Am. J. Physiol. Regul. Integr. Comp. Physiol.* 306, R211–R221. doi: 10.1152/ajpregu.00350.2013
- Liao, B. K., Chen, R. D., and Hwang, P. P. (2009). Expression regulation of Na<sup>+</sup>-K<sup>+</sup>-ATPase alpha1-subunit subtypes in zebrafish gill ionocytes. *Am. J. Physiol.*

- Regul. Integr. Comp. Physiol.* 296, R1897–R1906. doi: 10.1152/ajpregu.00029.2009
- Lin, C. H., Su, C. H., and Hwang, P. P. (2014). Calcium-sensing receptor mediates  $\text{Ca}^{2+}$  homeostasis by modulating expression of PTH and stanniocalcin. *Endocrinology* 155, 56–67. doi: 10.1210/en.2013-1608
- Liu, C., Dai, W., Bai, Y., Chi, C., Xin, Y., He, G., et al. (2017). Development of a whole organism platform for phenotype-based analysis of IGF1R-PI3K-Akt-Tor Action. *Sci. Rep.* 7:1994. doi: 10.1038/s41598-017-01687-3
- Liu, C., Li, S., Noer, P. R., Kjaer-Sorensen, K., Juhl, A. K., Goldstein, A., et al. (2020). The metalloproteinase Papp-aa controls epithelial cell quiescence-proliferation transition. *Elife* 9:e52322. doi: 10.7554/eLife.52322
- Liu, C., Xin, Y., Bai, Y., Lewin, G., He, G., Mai, K., et al. (2018).  $\text{Ca}^{2+}$  concentration-dependent premature death of *igfbp5a*<sup>-/-</sup> fish reveals a critical role of IGF signaling in adaptive epithelial growth. *Sci. Signal.* 11:eaa2231. doi: 10.1126/scisignal.aat2231
- Marouli, E., Graff, M., Medina-Gomez, C., Lo, K. S., Wood, A. R., Kjaer, T. R., et al. (2017). Rare and low-frequency coding variants alter human adult height. *Nature* 542:186. doi: 10.1038/nature21039
- Pang, P. K. (1971). The relationship between corpuscles of stannius and serum electrolyte regulation in killifish, *Fundulus heteroclitus*. *J. Exp. Zool.* 178, 1–8. doi: 10.1002/jez.1401780102
- Pang, P. K. (1973). Endocrine control of calcium metabolism in teleosts. *Am. Zool.* 13, 775–792.
- Radman, D. P., McCudden, C., James, K., Nemeth, E. M., and Wagner, G. F. (2002). Evidence for calcium-sensing receptor mediated stanniocalcin secretion in fish. *Mol. Cell. Endocrinol.* 186, 111–119. doi: 10.1016/s0303-7207(01)00643-8
- Rosendahl, W., Föll, J., Blum, W., and Ranke, M. B. (1992). Increased insulin-like growth factor-II tissue concentrations during compensatory kidney growth in infantile rats. *Pediatr. Nephrol.* 6, 527–531. doi: 10.1007/bf00866493
- Schein, V., Cardoso, J. C., Pinto, P. I., Anjos, L., Silva, N., Power, D. M., et al. (2012). Four stanniocalcin genes in teleost fish: structure, phylogenetic analysis, tissue distribution and expression during hypercalcemic challenge. *Gen. Comp. Endocrinol.* 175, 344–356. doi: 10.1016/j.ygcen.2011.11.033
- Sousa-Nunes, R., Yee, L. L., and Gould, A. P. (2011). Fat cells reactivate quiescent neuroblasts via TOR and glial insulin relays in *Drosophila*. *Nature* 471, 508–512. doi: 10.1038/nature09867
- Tallant, C., García-Castellanos, R., Seco, J., Baumann, U., and Gomis-Rüth, F. X. (2006). Molecular analysis of ulilysin, the structural prototype of a new family of metzincin metalloproteases. *J. Biol. Chem.* 281, 17920–17928. doi: 10.1074/jbc.M600907200
- Tseng, D. Y., Chou, M. Y., Tseng, Y. C., Hsiao, C. D., Huang, C. J., Kaneko, T., et al. (2009). Effects of stanniocalcin 1 on calcium uptake in zebrafish (*Danio rerio*) embryo. *Am. J. Physiol. Regul. Integr. Comp. Physiol.* 296, R549–R557. doi: 10.1152/ajpregu.90742.2008
- Valcourt, J. R., Lemons, J. M., Haley, E. M., Kojima, M., Demuren, O. O., and Collier, H. A. (2012). Staying alive: metabolic adaptations to quiescence. *Cell Cycle* 11, 1680–1696. doi: 10.4161/cc.19879
- Venkatraman, A., He, X. C., Thorvaldsen, J. L., Sugimura, R., Perry, J. M., Tao, F., et al. (2013). Maternal imprinting at the H19-Igf2 locus maintains adult haematopoietic stem cell quiescence. *Nature* 500, 345–349. doi: 10.1038/nature12303
- Waclawiczek, A., Hamilton, A., Rouault-Pierre, K., Abarrategi, A., Albornoz, M. G., Miraki-Moud, F., et al. (2020). Mesenchymal niche remodeling impairs hematopoiesis via stanniocalcin 1 in acute myeloid leukemia. *J. Clin. Invest.* 130, 3038–3050. doi: 10.1172/jci133187
- Wagner, G. F., and Dimattia, G. E. (2006). The stanniocalcin family of proteins. *J. Exp. Zool. A Comp. Exp. Biol.* 305, 769–780. doi: 10.1002/jez.a.313
- Westerfield, M. (2000). *The Zebrafish Book: a Guide for the Laboratory use of Zebrafish*. Eugene, OR: Univ. of Oregon Press.
- Xin, Y., and Duan, C. (2018). Microinjection of antisense morpholinos, CRISPR/Cas9 RNP, and RNA/DNA into zebrafish embryos. *Hypoxia Springer* 1742, 205–211. doi: 10.1007/978-1-4939-7665-2-18
- Xin, Y., Malick, A., Hu, M., Liu, C., Batah, H., Xu, H., et al. (2019). Cell-autonomous regulation of epithelial cell quiescence by calcium channel Trpv6. *Elife* 8:e48003. doi: 10.7554/eLife.48003
- Yamashita, K., Koide, Y., Itoh, H., Kawada, N., and Kawauchi, H. (1995). The complete amino acid sequence of chum salmon stanniocalcin, a calcium-regulating hormone in teleosts. *Mol. Cell. Endocrinol.* 112, 159–167. doi: 10.1016/0303-7207(95)03590-4
- Yan, J. J., and Hwang, P. P. (2019). Novel discoveries in acid-base regulation and osmoregulation: a review of selected hormonal actions in zebrafish and medaka. *Gen. Comp. Endocrinol.* 277, 20–29. doi: 10.1016/j.ygcen.2019.03.007
- Yang, K., Shrestha, S., Zeng, H., Karmaus, P. W., Neale, G., Vogel, P., et al. (2013). T cell exit from quiescence and differentiation into Th2 cells depend on raptor-mTORC1-mediated metabolic reprogramming. *Immunity* 39, 1043–1056. doi: 10.1016/j.immuni.2013.09.015
- Yeung, B. H., Law, A. Y., and Wong, C. K. (2012). Evolution and roles of stanniocalcin. *Mol. Cell. Endocrinol.* 349, 272–280. doi: 10.1016/j.mce.2011.11.007
- Ziegler, A. N., Feng, Q., Chidambaram, S., Testai, J. M., Kumari, E., Rothbard, D. E., et al. (2019). Insulin-like growth factor II: an essential adult stem cell niche constituent in brain and intestine. *Stem Cell Rep.* 12, 816–830. doi: 10.1016/j.stemcr.2019.02.011
- Ziegler, A. N., Levison, S. W., and Wood, T. L. (2015). Insulin and IGF receptor signalling in neural-stem-cell homeostasis. *Nat. Rev. Endocrinol.* 11, 161–170. doi: 10.1038/nrendo.2014.208

**Conflict of Interest:** The authors declare that the research was conducted in the absence of any commercial or financial relationships that could be construed as a potential conflict of interest.

Copyright © 2021 Li, Liu, Goldstein, Xin, Ke and Duan. This is an open-access article distributed under the terms of the Creative Commons Attribution License (CC BY). The use, distribution or reproduction in other forums is permitted, provided the original author(s) and the copyright owner(s) are credited and that the original publication in this journal is cited, in accordance with accepted academic practice. No use, distribution or reproduction is permitted which does not comply with these terms.





# Cell Cycle Re-entry in the Nervous System: From Polyploidy to Neurodegeneration

Shyama Nandakumar, Emily Rozich and Laura Buttitta\*

Department of Molecular, Cellular and Developmental Biology, University of Michigan, Ann Arbor, MI, United States

## OPEN ACCESS

### Edited by:

Guang Yao,  
University of Arizona, United States

### Reviewed by:

Mireille Khacho,  
University of Ottawa, Canada  
Alexandra Chittka,  
Queen Mary University of London,  
United Kingdom

### \*Correspondence:

Laura Buttitta  
buttitta@umich.edu

### Specialty section:

This article was submitted to  
Cell Growth and Division,  
a section of the journal  
Frontiers in Cell and Developmental  
Biology

**Received:** 21 April 2021

**Accepted:** 19 May 2021

**Published:** 24 June 2021

### Citation:

Nandakumar S, Rozich E and  
Buttitta L (2021) Cell Cycle Re-entry  
in the Nervous System: From  
Polyploidy to Neurodegeneration.  
*Front. Cell Dev. Biol.* 9:698661.  
doi: 10.3389/fcell.2021.698661

Terminally differentiated cells of the nervous system have long been considered to be in a stable non-cycling state and are often considered to be permanently in G0. Exit from the cell cycle during development is often coincident with the differentiation of neurons, and is critical for neuronal function. But what happens in long lived postmitotic tissues that accumulate cell damage or suffer cell loss during aging? In other contexts, cells that are normally non-dividing or postmitotic can or re-enter the cell cycle and begin replicating their DNA to facilitate cellular growth in response to cell loss. This leads to a state called polyploidy, where cells contain multiple copies of the genome. A growing body of literature from several vertebrate and invertebrate model organisms has shown that polyploidy in the nervous system may be more common than previously appreciated and occurs under normal physiological conditions. Moreover, it has been found that neuronal polyploidization can play a protective role when cells are challenged with DNA damage or oxidative stress. By contrast, work over the last two and a half decades has discovered a link between cell-cycle reentry in neurons and several neurodegenerative conditions. In this context, neuronal cell cycle re-entry is widely considered to be aberrant and deleterious to neuronal health. In this review, we highlight historical and emerging reports of polyploidy in the nervous systems of various vertebrate and invertebrate organisms. We discuss the potential functions of polyploidization in the nervous system, particularly in the context of long-lived cells and age-associated polyploidization. Finally, we attempt to reconcile the seemingly disparate associations of neuronal polyploidy with both neurodegeneration and neuroprotection.

**Keywords:** neurodegeneration, polyploidy, cell cycle, endomitosis, aging

## INTRODUCTION

The prolonged maintenance of a non-dividing state is critical for the proper functioning of long lived cells in various tissues throughout the lifespan of an organism. The cells of the nervous system; neurons and glia, are some of the longest lived in many animals. It is known that maintaining a non-dividing state in these cells is critical for brain function (Frade, 2000; Aranda-Anzaldo and Dent, 2017).

In a majority of adult metazoan cells including neurons, muscles, and most epithelial cells, the G0 associated with terminal differentiation is thought to be permanent (Zacksenhaus et al., 1996; Cunningham et al., 2002; Huh et al., 2004; Buttitta and Edgar, 2007; O'Farrell, 2011). These cells exit the cell cycle with a diploid (2C) DNA content. Studies over the past

few years have suggested that there are several overlapping and redundant biological pathways that influence the establishment and maintenance of G0 in terminally differentiated tissues, including the upregulation of the activity of negative regulators of the cell cycle, as well as changes in transcription and chromatin (Reviewed in Galderisi et al., 2003; Buttitta and Edgar, 2007; Oyama et al., 2014; Davis and Dyer, 2010; Duronio and Xiong, 2013; Ruijtenberg and van den Heuvel, 2016).

## ARE ALL TERMINALLY DIFFERENTIATED NEURONS PERMANENTLY DIPLOID, AND IN G0?

It has long been speculated that some neurons and glia in the CNS may be polyploid (Mann and Yates, 1973a; Yates and Mann, 1973; Bregnard et al., 1975). Recent work is beginning to confirm this, as well as indicate that polyploid cells in the nervous system may be more prevalent than previously thought, and these findings have important implications in the physiology and pathology of the nervous system. We begin with an introduction to variant cell cycles and examples of variant cell cycles in the nervous system across species (Figure 1).

### Variant Cell Cycles

The canonical cell cycle starts with a diploid cell containing two copies of each chromosome, and at the end of one cycle, results in two daughter cells, each diploid with two copies of each chromosome. Exceptions to this can be seen in several cell types and organisms across the animal and plant kingdoms (Edgar and Orr-Weaver, 2001; Frawley and Orr-Weaver, 2015). Variant cell cycles which give rise to a cell that contains more than two copies of the genome are classified as endoreduplication or endoreplication cycles. The resulting cell is polyploid in DNA content. There are different types of endoreplication cycles, and different contexts in which cells employ them to become polyploid.

Endoreplication cycles utilize parts of the cell cycle machinery to replicate DNA, but these cycles are curtailed and result in one cell with increased DNA content instead of two cells. Endoreplication cycles can involve only cycles of DNA replication and growth (termed endocycles) resulting in one nucleus with increased DNA content, or a cycle of with replication mitosis without an ensuing cytokinesis (termed endomitosis), resulting in two or more nuclei in one cell (Figure 1).

### Endocycles

Endocycles are variant cell cycles characterized by alternating Gap and DNA synthesis phases (Edgar and Orr-Weaver, 2001). In flies, endocycling is thought to be driven predominantly by an oscillation of Cyclin E/CDK2 activity and controlled by the transcriptional activity of E2F (Duronio and O'Farrell, 1995; Edgar and Orr-Weaver, 2001; Zielke et al., 2011; Moon and Kim, 2019). Another important factor that plays a role in endocycle progression is the APC/C<sup>Frz/cdh1</sup> which ensures

not only the degradation of mitotic CDKs, but also the timely degradation of geminin in S phase to prevent re-replication (Edgar et al., 2014). In mammals, variant or non-canonical E2Fs are employed specifically during endocycles implying a specialized role for these regulatory factors (Pandit et al., 2012; Matondo et al., 2018).

Several types of cells in various organisms employ endocycles during development or in contexts of cellular damage. Developmentally regulated endocycles occurs in some cells during development to aid the growth of the organism—cells generated by these endocycles usually possess several to several hundred copies of the genome, and often grow very large in size. It is interesting to note that developmentally regulated endocycles can generate cells of vastly varying ploidies depending on the tissue and context. While the enterocytes of the fly intestinal epithelium show average ploidies of 32–64C, nurse cells of the ovaries and cells of the salivary gland can be up to 1,024C (Frawley and Orr-Weaver, 2015).

Some examples of developmentally regulated endocycles in flies include the larval epidermis, salivary gland, fat body and some Sub-perineurial glia of the blood brain barrier (Hammond and Laird, 1985; Britton and Edgar, 1998; Lee et al., 2009; Unhavaithaya and Orr-Weaver, 2012; Von Stetina et al., 2018). In the adult fly, the enterocytes in the gut, the nurse and follicle cells of the ovary in adult females (Royzman et al., 2002; Fox and Duronio, 2013). These are all very large cells which either serve a biosynthetic demand or crucial barrier function. The cells resulting from these endocycles are usually constitutively polyploid.

While developmental endocycles have been well studied in *Drosophila*, they are also present and widespread in other eukaryotes. Several tissues in plants such as leaves, roots and trichomes have cells that endocycle after terminal differentiation to support growth (De Veylder et al., 2011; Frawley and Orr-Weaver, 2015; Lang and Schnittger, 2020). In mammals, the most studied example of endocycling is hepatocytes in the liver, and the trophoblast giant cells of the placenta. Just like in the fly, the different polyploid cells in mammals can exhibit varied levels of polyploidy. Polyploid hepatocytes contain 4–8C DNA content, however, trophoblast giant cells can have over 1,000 copies of the genome (Roszell et al., 1978; Severin et al., 1984; Zuckermann and Head, 1986; Jensen et al., 1989; Melchiorri et al., 1993; Zybina and Zybina, 1996; Klisch et al., 1999; Celton-Morizur and Desdouets, 2010). It is interesting to note here that highly polyploid cells such as nurse cells and trophoblast giant cells which provide critical trophic support are short lived, suggesting that the degree of polyploidy may influence the longevity of a cell. As cases of polyploidy continue to be uncovered, it is becoming clear this is a widely used cellular mechanism, yet the polyploid state remains poorly understood. Understanding the extent to which polyploidy is used during normal development and in abnormal conditions, will help reveal common features of the polyploid state. To facilitate communication across research areas, we have developed a searchable polyploidy literature atlas that encompasses organisms and model systems across eukarya. We envision this literature atlas could serve as a “living document,”

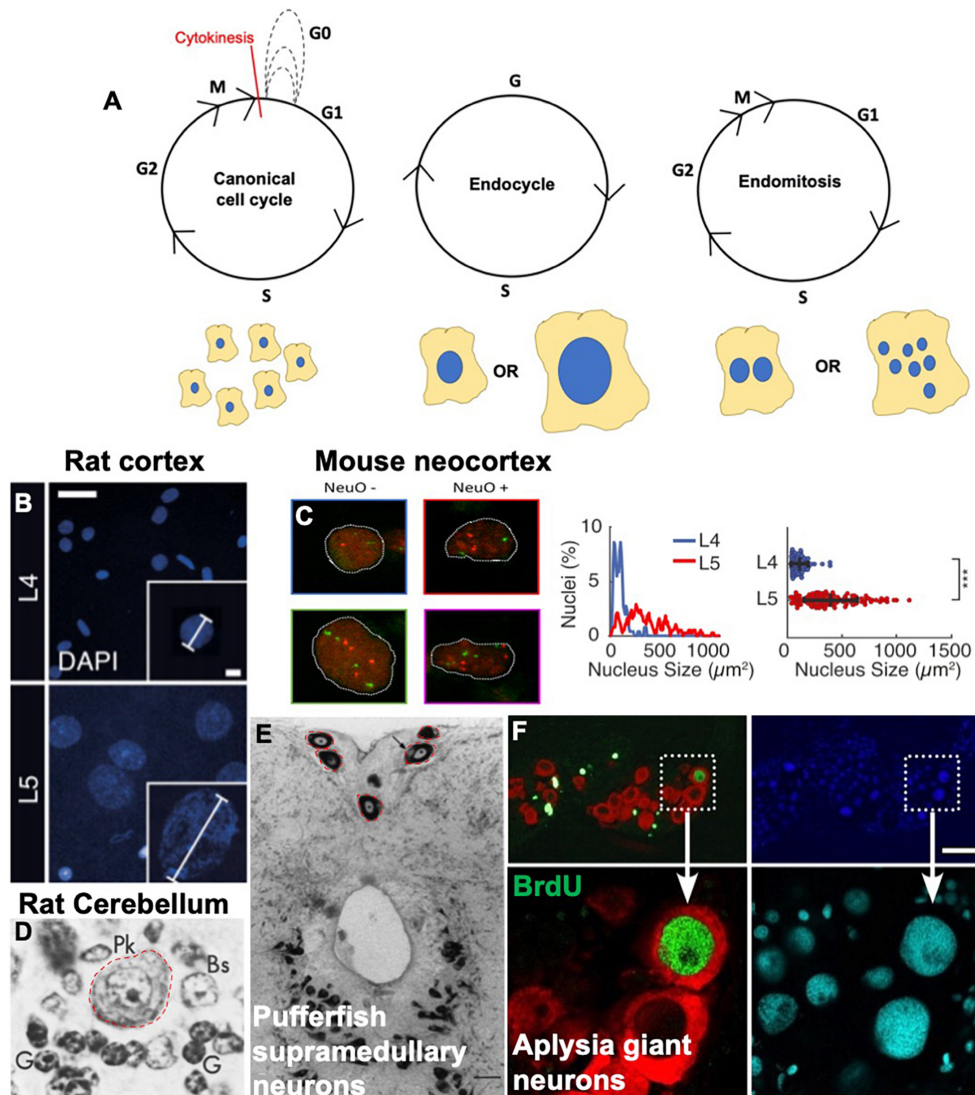


**FIGURE 1 |** Variant cell cycles and polyploidy in neurons. **(A)** Cartoons showing the progression of the canonical cell cycle and two variant cell cycles: the endocycle and the endomitotic cycle. Multiple repeated canonical cell cycles result in numerous daughter cells with diploid DNA content, whereas endocycles result in cells with tetraploid or greater ( $>4C$ ) DNA content and endomitosis can result in either binucleate or multinucleate cells. **(B–F)** Examples of polyploid neurons from the literature. **(B)** Nuclear DAPI staining and quantification showing larger, polyploid pyramidal neurons in the rat cortical layer <https://doi.org/10.1016/j.celrep.2017.08.069>. Scale bars = 25 and 5  $\mu\text{M}$  for inset. **(C)** Polyploid neurons in the developing mouse neocortex from <https://doi.org/10.1093/textcom/tgaa063>. This study used a combination of flow cytometry and FISH combined with immunostaining against various neuronal markers to determine polyploidy. NeuO is a neuronal marker. Mouse neocortex has both polyploid neurons and non-neurons, both show increased number of red and green foci (FISH probes against loci on chromosomes 11 and 2, respectively). **(D)** Large polyploid purkinje neurons from rat cerebellum, outlined in red. Reprinted from Herman and Lapham (1973) with permission from Elsevier. License Number 5079560753665 (to author LB). **(E)** Red outlines and black arrows indicate polyploid supramedullary neurons of pufferfish *Diodon holanctus* stained with toluidine blue. Scale bar = 100  $\mu\text{M}$ . Reprinted from Cuoghi and Marini (2001) with permission from Elsevier. License number 5053261503241 (to author SN). **(F)** Giant neurons in an Aplysia (slug) brain, positive for BrdU in green. Nuclei are stained with DAPI in blue and cyan, and red staining indicates FISH against mRNA of neurotransmitter achatin. Data from <https://www.ncbi.nlm.nih.gov/pmc/articles/PMC6622835>. Scale bar = 125  $\mu\text{M}$ .

an organizational structure and collection that will evolve as work on polyploidy progresses<sup>1</sup>.

In addition to cells that undergo developmentally regulated endocycles to become constitutively polyploid, some cells show a capacity to enter an endocycle in contexts of wounding and

damage (facultative). These will be discussed in the following sections.

## Endomitosis

Endomitosis is another variant cell cycle which differs from endocycles in that it produces a cell with two or more nuclei. Endomitoses comprise a  $G_1$ , S,  $G_2$ , and a mitosis

<sup>1</sup><https://sites.google.com/umich.edu/polyploidyatlas/home>

without cytokinesis (Edgar and Orr-Weaver, 2001; Frawley and Orr-Weaver, 2015). Thus, the regulation of endomitoses is different from that of an endocycle. Endomitotic cell cycles are characterized by a failure to undergo cytokinesis which results in binucleate or multinucleate cells. Endomitotic cells are less common than endocycling cells.

Endomitoses are best studied in the platelet-producing megakaryocyte cells in mammals (Zhang et al., 1996; Zimmet and Ravid, 2000; Ravid et al., 2002; Bluteau et al., 2009). Some SPGs in the fly blood brain barrier are known to become multinucleate by endomitosis (Eliades et al., 2010; Unhavaithaya and Orr-Weaver, 2012; Von Stetina et al., 2018). Examples of endomitosis giving rise to binucleate cells are cardiomyocytes in mouse and human hearts, lactating mammary epithelial cells and the binucleate cells of the *Drosophila* accessory gland (Stephen et al., 2009; Pandit et al., 2013; Paradis et al., 2014; Taniguchi et al., 2014, 2018; Box et al., 2019).

## Polyploidy in the Nervous System: From Mollusk to Man

### Slugs do It Best

Sea slugs of the *Aplysia* species have long been used in studies of olfaction and memory formation (Coggeshall et al., 1970; Nagle et al., 1993; Sattelle and Buckingham, 2006; Moroz, 2011; Yamagishi et al., 2012, 2011; Kukushkin et al., 2019). These slugs possess giant neurons (roughly the size of one fly brain) which are perhaps the most extreme example of somatic polyploidy, possessing up to 600,000 copies of the genome (600,000C)! While we still do not know exactly why these neurons are so large, it is speculated that in “simpler” animals, one large cell can perform the functions of several smaller cells, trading off “complexity” for capacity (Frade and López-Sánchez, 2010; Mandrioli et al., 2010).

### Drosophila

Endocycling has been observed in the *Drosophila* peripheral nervous system in the bristle cell lineage. Bristle cells are mechanoreceptive cells in the fly thorax. While it has been known for over 30 years that these cells become polyploid (up to 8C) during development (Fung et al., 2008), recent work has provided mechanistic insight into how these cells become polyploid. The bristle lineage consists of a neuron, a glial cell, a sheath cell, and one socket and one shaft cell. The shaft and socket cells become polyploid in a Cyclin A/CDK2 dependent manner, unlike most other tissues in fly which employ CyclinE/CDK2 oscillations to become polyploid (Audibert et al., 2005; Furman and Bukharina, 2008; Sallé et al., 2012).

The Sub-perineurial glia that form the protective blood brain barrier for the CNS in the fly become highly polyploid during development (Unhavaithaya and Orr-Weaver, 2012). These large cells adopt either an endocycle or an endomitosis depending on their location (Von Stetina et al., 2018) to become polyploid and support the rapidly growing larval brain during development. Inhibition of polyploidization in these cells results in impaired blood brain barrier function.

Our recent work has shown that neurons and glia become polyploid in the fly brain, specifically in the adult (Nandakumar et al., 2020). Our study found that the optic lobes show higher

levels of polyploidy than the central brain and the ventral nerve cord. We also showed that an increase in polyploidy occurs within the first week after eclosion. In addition, exogenous DNA damage and oxidative stress can induce even higher levels of polyploidy, and the polyploid cells are protected from cell death.

### Teleost Supramedullary Neurons

Several species of teleosts are also known to possess a small number of highly polyploid neurons called supramedullary neurons on the dorsal surface of the spinal cord or the rostral spinal cord (Nakajima et al., 1965; Bennett and Nakajima, 1967; Mola et al., 2001; Dampney et al., 2003). Depending on the species of fish, these neurons can have anywhere between 100 to over 5,000 copies of the genome. These neurons are very small in number, and have been proposed as a good *in vivo* model for electrophysiology studies due to their prominent size and convenient location. These large cells are thought to have a neuro-endocrine function as some species of puffer fish produce noradrenalin (Mola et al., 2002; Mola and Cuoghi, 2004). The need for biosynthesis of large amounts of adrenaline may underlie the polyploidy in these cells, however, this has not been functionally tested.

### Other Vertebrates and Mammals

Initial observations of polyploidy in vertebrate brains involved the study of neurons and glia in the cerebellum by three different groups in the 1960s and 1970s (Lapham, 1963, 1968; Herman and Lapham, 1969, 1973; Lentz and Lapham, 1969, 1970; Lapham et al., 1971; Mann and Yates, 1973a,b, 1979; Mann et al., 1976; Swartz and Bhatnagar, 1981). While these studies reported differing numbers, they concluded that the cerebellum does indeed possess polyploid cells. One study measured the proportion of polyploid cells at different ages in the human cerebellum and found that there was no increase in the proportion of polyploid of neurons or glia between ages 8 and 72, suggesting that unlike the liver and heart, the proportion of polyploidy remains constant in the human brain with age. These early studies speculated that the polyploidization may contribute to cerebellar memory and specialized function due to their increased transcriptional output (Mann and Yates, 1973b).

In addition to cytometric measurements, studies in the 1900s also made histological observations of neuronal nuclear hypertrophy in various mammals such as mice, rats, dogs, rhesus monkeys and even humans (Verhaart and Voogd, 1962; Lapham, 1963; Bregnard et al., 1975, 1979; Ribeiro, 2006; Toscano et al., 2009).

In mammals, most observations of neuronal polyploidy or hypertrophy report larger, mononucleate cells. However, there are a couple of very interesting exceptions: neurons of the dorsal root and pelvic ganglia, neurons of the superior cervical ganglion (SCG), neurons of enteric ganglia, and neurons innervating the heart (Bunge et al., 1967; Smith, 1970; Forsman et al., 1989; Ribeiro, 2006; Hunter et al., 2018). Binucleate SCG neurons have been observed in rats, rabbits, capybaras, guinea pigs, and humans.

The observations of larger, mononucleate polyploid neurons in the brain, and binucleate neurons in the autonomic nervous



system also presents an interesting distinction worth exploring in future studies. What is the function of neuronal binucleation in involuntary actions? Does binucleation support secretory functions in neurons?

Modern genetic approaches investigating potential cell cycle re-entry in vertebrate brains began taking shape in the early 2000's. In recent years, observations of bona fide polyploidy in neurons of the retinal ganglion of the chicken and mouse, cerebral cortex of the rat and neocortex of the mouse have been made using modern flow cytometry and high resolution imaging techniques (Morillo et al., 2010; López-Sánchez and Frade, 2013; Ovejero-Benito and Frade, 2015; Martin et al., 2017; Jungas et al., 2020). Work from the Frade lab has shown that the neurons of the retinal ganglion become tetraploid in an E2F-dependent manner. However, this endoreplication program is differentially regulated in chick and mouse central nervous system, as p27<sup>kip1</sup> is necessary for tetraploidization in the chick, but not the mouse RGCs (López-Sánchez and Frade, 2013; Ovejero-Benito and Frade, 2013, 2015). Further advances in imaging and flow cytometry techniques have identified polyploid pyramidal neurons in the cerebrum of the rat, and the neocortex of the mouse, but the function and underlying cause for their polyploidy remain elusive (Sigl-Glückner and Brecht, 2017; Jungas et al., 2020). These studies show sufficient evidence that polyploidization does indeed occur in higher vertebrates, suggesting that neuronal polyploidization may be a well conserved phenomenon. However, while these studies have made detailed observations of polyploidy in neurons, the precise function of polyploidization under each of these conditions remains unknown.

## Why Become Polyploid?

### Increased Biosynthetic Capacity

Why do some cells become polyploid? What are the benefits of entering a variant cell cycle rather than undergoing cell division? Constitutively polyploid cells, as mentioned before, mainly perform two important functions: they usually have increased biosynthetic capacity, and they maintain barrier function (Reviewed in Edgar and Orr-Weaver, 2001; Lee et al., 2009; Øvrebo and Edgar, 2018). Polyploid cells with more copies of the genome can increase cell size and metabolic functions efficiently. Undergoing cell division involves cell rounding, cytoskeletal rearrangements and potential loss of cell-cell contacts (Sauer, 1935; Erenpreisa and Cragg, 2001; Lancaster et al., 2013; Frawley and Orr-Weaver, 2015). This can be problematic in cells performing important barrier functions. Endocycling can therefore be a way for these cells to grow in size and genome copy number without increasing in cell number.

Speculation about the role that tetraploidy plays in neurons has varied from generation of neuronal diversity to increased capacity for dendritic arborization. One study performed over 30 years ago (Szaro and Tompkins, 1987) compared the dendritic arbors of two *Xenopus* species, one diploid species and another which displays whole organism tetraploidy (where the entire organism has a larger genome). This study showed that while the brains from these two organisms were the same

size, the neurons from the tetraploid species showed longer dendritic segments as well as larger dendritic arbors. This could mean that tetraploid neurons are able to make more synaptic connections and participate in larger neuronal networks, contributing to functional diversity. Polyploid neurons could also, as a virtue of increased biosynthetic capacity, increase production of neurotransmitters, resulting in robust signaling.

In glial cells, increased biosynthetic capacity in wrapping glia as a result of endocycling could ensure better sheathing of axon bundles and enhanced neuronal conductivity. Similarly, increased biosynthetic capacity could improve phagocytic glial function and aid in better clearance of cellular debris in the adult brain. Glial cells provide the bulk of the metabolic support to the neurons in the brain. In flies, glial glycolysis has been shown to be essential for neuronal survival (Volkenhoff et al., 2015) in the adult brain. Glial polyploidization might be a way for some glial cells in the central nervous system to increase their metabolic capacity.

### Wound Healing and Compensatory Growth

Cells in the *Drosophila* adult abdominal epithelium respond to wounding by re-entering the cell cycle as well as undergoing cell fusion to become polyploid, and close the wound. Induction of the endocycle in these cells is dependent on the upregulation of E2F by the Hippo/Yorkie pathway as well as the degradation of mitotic cyclins by APC/C<sup>Fzr</sup>. Polyploidization is also known to play a role in wound healing in the mammalian corneal endothelium, heart and keratinocytes (Werner et al., 2007; Losick et al., 2013, 2016; Trakala and Malumbres, 2014; Trakala et al., 2015; Losick, 2016; Gandarillas et al., 2019; Grendler et al., 2019). Polyploid fat body cells of the *Drosophila* pupa and wax moth larvae respond to wounding by migrating to lesion sites and forming a “plug” to prevent infection by maintaining the epithelial barrier (Rowley and Ratcliffe, 1978; Franz et al., 2018).

Endoreplication has also been implicated in alternate modes of regeneration and response to cell loss. The liver remains best studied in this context as well in mammals, but recent studies have shown that polyploidization occurs in renal tubular epithelial cells in response to ischemic damage (Melchiorri et al., 1993; Lazzeri et al., 2018; Matsumoto et al., 2020). Other examples of endocycling in response to cell loss include the epicardium of the zebrafish heart (Uroz et al., 2019). In *Drosophila*, the enterocytes of the intestinal epithelium, the follicle cells of the ovary and the main cells of the accessory gland can cope with induced cell death by engaging a compensatory cellular hypertrophy or endocycle program to maintain tissue size and homeostasis (Tamori and Deng, 2013; Edgar et al., 2014; Shu et al., 2018; Øvrebo and Edgar, 2018; Box et al., 2019). In the fly optic lobe, where increase in polyploidy is accompanied by a steady loss of diploid cells, polyploidization may serve a compensatory role by enabling neurons to form more synaptic connections to compensate for cell loss to maintain visual acuity (Nandakumar et al., 2020).

### DNA Damage Resistance and Repair

One additional benefit of polyploidy is resistance to DNA damage conferred by the number of copies of the genome—somatic

mutations in one copy of a gene will not greatly impact the capacity of the cell to function since it will have many other copies of the genome. For over 80 years, scientists have observed that polyploid cells are able to endure and survive DNA damage better than diploid cells (Muntzing and Prakken, 1941). The resistance to DNA damage is attributed, in most part, to the number of copies of a gene that a polyploid cell has. If a cell has several “spares”, DNA damage caused by random somatic mutation to one copy of a crucial gene will not impede the cell’s ability to function or survive, as it will have more copies of the gene (D’Alessandro and d’Adda di Fagagna, 2017). The earliest studies on the resistance polyploid cells show to DNA damage were performed in the 1940s (Muntzing and Prakken, 1941). These studies compared the response of whole organism tetraploids to diploid rye plants and linked the resistance to radiation damage to ploidy variations.

Functional studies in genetic model organisms have since furthered our understanding of how some polyploid cells may resist DNA damage. The most prominent model used to understand the relationship between polyploidy and DNA damage resistance has been the various polyploid tissues in *Drosophila*. Studies in the follicle cells, fat body as well as salivary glands in the fly have shown that endocycling cells do not undergo apoptosis as a result of induced genome instability (Mehrotra et al., 2008). These polyploid cells can tolerate high levels of DNA damage, and harbor double strand breaks to their DNA, but do not undergo apoptosis. Further studies have shown that low levels of the tumor suppressor protein p53 in these endocycling cells is responsible for conferring their resistance to cell death (Mehrotra et al., 2008; Zhang et al., 2014). The tumor suppressor p53 is responsible for activating the expression of proapoptotic genes *hid*, *reaper* and *grim* in *Drosophila*, and these proteins are in turn upstream of the caspase cascade. Low levels of p53 in some *Drosophila* polyploid cells, combined with chromatin-level silencing of the pro-apoptotic genes confer high levels of resistance to DNA damage-induced cell death in these cells (Mehrotra et al., 2008; Zhang et al., 2014; Park et al., 2019).

Studies of cancer cells show that polyploidy can be induced by DNA damage. This is frequently observed in cancer cells which lack cell cycle checkpoints. Failure of cytokinesis or premature exit from the cell cycle without undergoing mitosis often results in tetraploid cancer cells. Several types of carcinomas with inactivated p53 or Rb have cells with hyperploid DNA content. Severe telomere attrition has been implicated in these cases as the source of DNA damage (Lazzerini Denchi et al., 2006; Davoli and de Lange, 2011). Polyploid cells are protected from DNA damage, and polyploidy can be induced by DNA damage. This suggests that polyploidy has been employed in several types of tissues and organisms as a robust adaptation to DNA damage.

Our recent work in *Drosophila* brains indicates that the rate of accumulation of polyploidy in adults can be exacerbated by damaging agents such as DNA damage or oxidative stress. Our experiments demonstrated that exogenous DNA damage leads to increased polyploidy, and that polyploid cells are protected from DNA damage induced cell death. Exposure to paraquat and UV both elicit a DNA damage response in the brain, and result in increased polyploidy.

Other work in *Drosophila* has shown that transposon silencing becomes compromised with age in the brain and has been linked with conditions of aging, neurodegeneration and decline in brain function (Abrusán, 2012; De Cecco et al., 2013; Li et al., 2013; Krug et al., 2017; Chang and Dubnau, 2019; Chang et al., 2019). This has been termed the “transposon storm” hypothesis of aging and neurodegeneration. Transposon reactivation has also recently been observed in aging fly guts, albeit at different levels (Riddiford et al., 2020). Could transposon reactivation represent a portion of the endogenous DNA damage that cells in the brain have to endure and overcome as they age?

Another potential source of DNA damage is DNA damage associated with high transcriptional activity (Hill et al., 2016; Langellotti et al., 2016). Highly transcribed loci in the genome are known to be susceptible to damage as a result of RNA:DNA hybrid formation. Recent work has shown that proteins implicated in neurodegenerative diseases such as TDP-43 are involved in preventing and contributing to repair at sites of transcription associated DNA damage. Age associated decline in TDP43 (Herrup and Arendt, 2002; Bonda et al., 2010a,b), coupled with high levels of transcription in neurons could contribute to unresolved DNA damage resulting from transcription-associated DNA lesions.

Transcriptional analysis of the aging fly brain shows age-associated reduction ATP metabolism, oxidative phosphorylation and cellular respiration (Nandakumar et al., 2020). This may indicate compromised mitochondrial function, which is a known hallmark of aging and a well known source of cellular oxidative stress (López-Otín et al., 2013). Compromised mitochondrial function can lead to increased levels of intracellular peroxide and superoxide radicals which can lead to oxidative DNA damage. Oxidized bases in DNA may evoke the need for base or nucleotide excision repair pathways to repair lesions.

## CONCLUSION AND FUTURE PERSPECTIVES

### Age-Dependent Accumulation of Polyploidy—A Common Theme in Long-Lived Tissues?

In the murine liver and the heart which have been extensively studied in the context of polyploidy: most cells are diploid at birth, with polyploidy appearing at the onset of weaning and acquisition of sexual maturity. A similar pattern of onset of polyploidization is also observed in the pancreas of mice and rats, the lacrimal glands of male rats. In addition, an increase in the proportion of polyploid cells with age has been observed and reported in the adrenal and thyroid glands (Teir, 1949; Geschwind et al., 1958; Carriere and Patterson, 1962; Paulini and Mohr, 1975; Gahan, 1977; Gilbert and Pfitzer, 1977; Roszell et al., 1978; Bohman et al., 1985; Nguyen and Ravid, 2010). In all of these cases, the proportion of polyploid cells increases rapidly at first, and then gradually over age.

The liver and lacrimal glands exhibit endocrine dependent onset of polyploidy, with the liver being dependent on thyroid

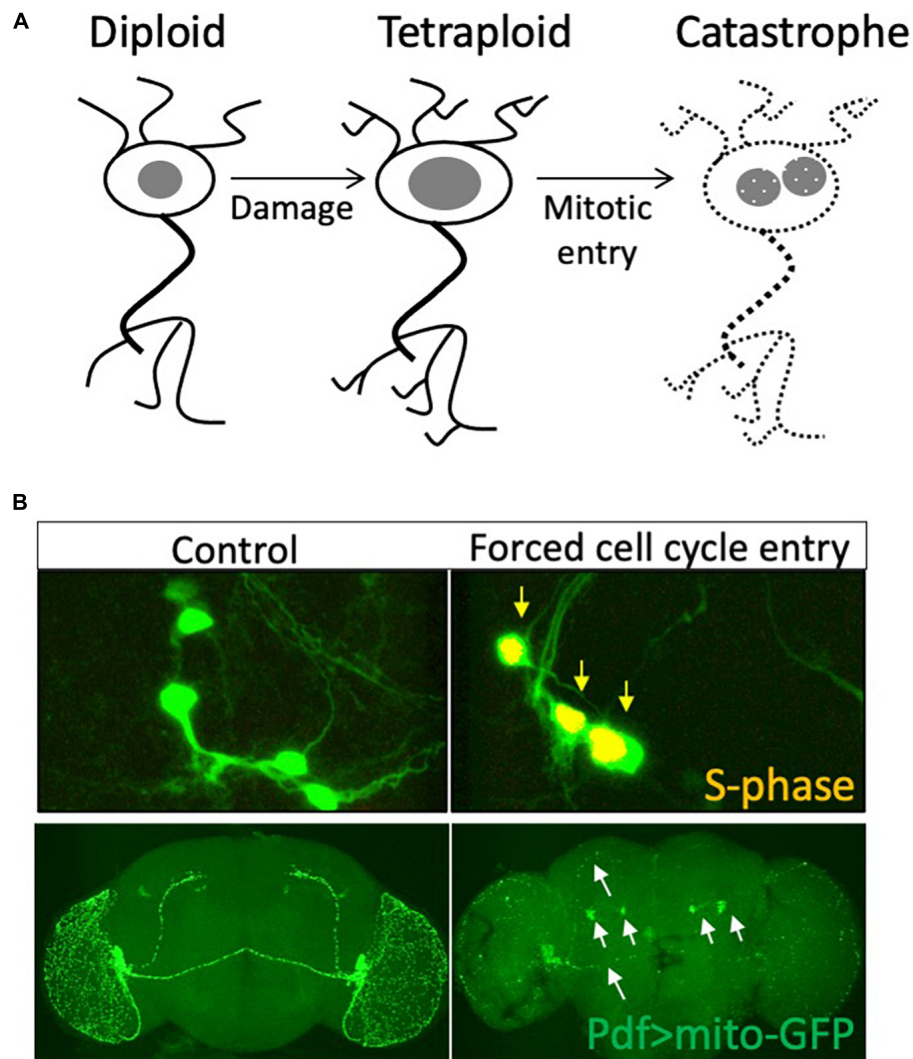


**FIGURE 2** | Is cell cycle re-entry both neuroprotective and neurodegenerative? **(A)** Neurons may enter the cell cycle and increase nuclear DNA content in response to tissue damage. This polyploid state may be neuroprotective, while further progression in the cell cycle into mitosis or sustained cell cycle re-entry may lead to axonal fragmentation and neurodegeneration. **(B)** We forced sustained cell cycle re-entry in postmitotic PDF neurons of the *Drosophila* brain and found this led to axonal fragmentation (white arrows) and degeneration of these neurons in the adult brain, abrogating circadian rhythm regulation. Data from Grushko and Buttitta (2015).

and thymus function, and the lacrimal glands, on male gonads for polyploidization. The liver shows diet-dependent increase in polyploidy levels: rats on a restricted diet showed lower levels of accumulated polyploidy whereas rats feeding *ad libitum* showed higher levels of polyploidy accumulation with age, suggesting that the polyploidization of the liver is dependent on metabolic need and adaptive in nature (Paulini and Mohr, 1975; Enesco et al., 1991).

Similarly, observations of polyploidy and binucleation in cardiomyocytes have been made in several organisms (Brodsky et al., 1991, 1994; Hirose et al., 2019; Derks and Bergmann, 2020; Gan et al., 2020). Recent work has linked the onset of polyploidy to endocrine cues and show that the polyploidy is also marked by a metabolic shift from glycolysis to oxidative

phosphorylation upon polyploidization (Hirose et al., 2019). Induced polyploidy in zebrafish hearts results in reduced regenerative capacity (González-Rosa et al., 2018). Further, binucleate cells and polyploidy increase with age as well as in diseased hearts (Clubb et al., 1987; Dzau and Gibbons, 1988; Lombardi et al., 1989; Brodsky et al., 1994; Derks and Bergmann, 2020). This has led to the prevailing notion that polyploidization in the heart is generally not beneficial. The current opinion in the cardiology field that binucleation directly hampers cardiac regeneration potential linking the lack of binucleation or polyploidization with regenerative capacity may be incomplete. Adult mammals and birds (endotherms) show cardiac polyploidy while amphibians and teleosts (ectotherms) do not (Derks and Bergmann, 2020). While most studies



view polyploidization in the heart simply as a loss of regenerative potential, the idea that perhaps the acquisition of polyploidy, instead, is an adaptation to endothermic conditions and oxidative stress warrants further inquiry. Cardiomyocytes and neurons are among the longest lived cells in a mammalian body, perhaps polyploidization may underlie their longevity?

## Cell Cycle Re-entry and Neurodegeneration

A large body of work over the last two decades has drawn a link between cell cycle re-entry and neurodegeneration. The first studies describing this showed increased immunostaining for cell cycle proteins in conditions of neurodegeneration such as Alzheimer's disease (AD) or AD models (Yang et al., 2006; Herrup and Yang, 2007; Khurana and Feany, 2007; Rimkus et al., 2008; Chen et al., 2010; Moh et al., 2011; Herrup, 2012; Frade and Ovejero-Benito, 2015). Since then, multiple models have been developed and several groups have corroborated this finding: brains exhibiting neurodegeneration also have cells that express cell cycle genes and proteins associated with the cell cycle. An enduring hypothesis emerged: that cell cycle re-entry in neurons is aberrant, and a marker of neurodegeneration including in human. Neurodegeneration is also marked by apoptosis and loss of neurons. The most common conclusion is that aberrant cell cycle re-entry causes cell death in neurons which, in turn, results in neurodegeneration. This hypothesis could also explain the appearance of neurons entering the cell cycle and bi-nucleate neurons even in pre-clinical cases of Alzheimer's disease (Nagy, 1999, 2000; Zhu et al., 2008).

Markers of cell cycle re-entry have been observed in several other neuropathologies, including down's syndrome (McShea et al., 1999), vascular dementia (Pelegrí et al., 2008), Huntington's disease (Ranganathan and Bowser, 2003; Liu et al., 2015) and amyotrophic lateral sclerosis (ALS) (Ranganathan and Bowser, 2003; Liu et al., 2015; Manickam et al., 2018, 2020). In addition, neuronal cell cycle protein expression has been observed upon induction of iron toxicity (McShea et al., 1997; Wen et al., 2004), ischemia (Park et al., 2000; Marathe et al., 2015), and excitotoxicity (Chow et al., 2019; Iqbal et al., 2020). Altered metabolism and endocrine function have also been implicated in aberrant cell cycle re-entry in neurons (Atwood and Bowen, 2015). These studies suggest that cell cycle re-entry in the mammalian brain may be a common response to a plethora of acute as well as chronic neurological stressors.

## REFERENCES

- Abrusán, G. (2012). Somatic transposition in the brain has the potential to influence the biosynthesis of metabolites involved in Parkinson's disease and schizophrenia. *Biol. Direct* 7:41. doi: 10.1186/1745-6150-7-41
- Aranda-Anzaldo, A., and Dent, M. A. R. (2017). Why cortical neurons cannot divide, and why do they usually die in the attempt? *J. Neurosci. Res.* 95, 921–929. doi: 10.1002/jnr.23765
- Atwood, C. S., and Bowen, R. L. (2015). The endocrine dyscrasia that accompanies menopause and andropause induces aberrant cell cycle signaling that triggers re-entry of post-mitotic neurons into the cell cycle, neurodysfunction, neurodegeneration and cognitive disease. *Horm. Behav.* 76, 63–80. doi: 10.1016/j.yhbeh.2015.06.021

Is cell cycle re-entry associated with neurodegeneration always deleterious? Most studies published in the past two decades argue that cell cycle re-entry leads to cell death. However additional S-phase entry in differentiating neurons is not always associated with cell death (Ferguson et al., 2002; MacPherson et al., 2003). An alternate hypothesis is that cell cycle re-entry in neurons is not a cause, but rather a consequence of cell loss. Consistent with this hypothesis, our work in *Drosophila* has shown that neurons that undergo cell cycle re-entry and become polyploid are protected from cell death (Nandakumar et al., 2020), indicating that there are contexts where cell cycle re-entry in neurons is protective (Ippati et al., 2021). Congruent with our findings, a recent study using live imaging and fluorescent cell cycle reporters in the mouse hippocampus has shown that cell cycle entry in mature neurons protects cells from amyloid-beta toxicity and resultant cell death (Ippati et al., 2021). One possibility is that cell cycle re-entry that proceeds into mitosis leads to neurodegeneration (Ruggiero et al., 2012), while partial cell cycle re-entry is neuroprotective (Figure 2).

Currently the relationship between neurodegeneration-associated cell cycle re-entry and neuronal polyploidy remains unclear. Are these distinct phenomena? The inherent cellular diversity of the mammalian brain, the diversity of approaches and conditions used in the different studies cited make this a challenging question to address. Future studies using a combination of quantitative DNA content measurements, modern imaging techniques and genetically tractable model systems will shed light on the relationship between neuronal polyploidization and neurodegeneration.

## AUTHOR CONTRIBUTIONS

SN and ER researched the literature and compiled the Polyploidy Atlas database. SN wrote the manuscript with input from ER and LB. All authors contributed to the article and approved the submitted version.

## FUNDING

This work was supported by the National Institutes of Health (R01 GM127367).

- Audibert, A., Simon, F., and Ghossein, M. (2005). Cell cycle diversity involves differential regulation of Cyclin E activity in the *Drosophila* bristle cell lineage. *Development* 132, 2287–2297. doi: 10.1242/dev.01797
- Bennett, M. V., and Nakajima, Y. (1967). Physiology and ultrastructure of electrotonic junctions. I. Supramedullary neurons. *J. Neurophysiol.* 30, 161–179.
- Bluteau, D., Lordier, L., Di Stefano, A., Chang, Y., Raslova, H., Debili, N., et al. (2009). Regulation of megakaryocyte maturation and platelet formation. *J. Thromb. Haemost.* 7(Suppl. 1), 227–234. doi: 10.1111/j.1538-7836.2009.03398.x
- Bohman, R., Tamura, C. T., Doolittle, M. H., and Cascarano, J. (1985). Growth and aging in the rat: changes in total protein, cellularity, and polyploidy in various organs. *J. Exp. Zool.* 233, 385–396. doi: 10.1002/jez.1402330307



- Bonda, D. J., Bajić, V. P., Spremo-Potparevic, B., Casadesus, G., Zhu, X., Smith, M. A., et al. (2010a). Review: cell cycle aberrations and neurodegeneration. *Neuropathol. Appl. Neurobiol.* 36, 157–163. doi: 10.1111/j.1365-2990.2010.01064.x
- Bonda, D. J., Lee, H., Kudo, W., Zhu, X., Smith, M. A., and Lee, H. (2010b). Pathological implications of cell cycle re-entry in Alzheimer disease. *Expert Rev. Mol. Med.* 12:e19. doi: 10.1017/S146239941000150X
- Box, A. M., Church, S. J., Hayes, D., Nandakumar, S., Taichman, R. S., and Buttitta, L. (2019). Endocycles support tissue growth and regeneration of the adult *Drosophila* accessory gland. *BioRxiv* [preprint]. doi: 10.1101/719013
- Bregnard, A., Knüsel, A., and Kuenzle, C. C. (1975). Are all the neuronal nuclei polyploid? *Histochemistry* 43, 59–61. doi: 10.1007/BF00490154
- Bregnard, A., Ruch, F., Lutz, H., and Kuenzle, C. C. (1979). Histones and DNA increase synchronously in neurons during early postnatal development of the rat forebrain cortex. *Histochemistry* 61, 271–279. doi: 10.1007/BF00508448
- Britton, J. S., and Edgar, B. A. (1998). Environmental control of the cell cycle in *Drosophila*: nutrition activates mitotic and endoreplicative cells by distinct mechanisms. *Development* 125, 2149–2158.
- Brodsky, V., Chernyaev, A. L., and Vasilyeva, I. A. (1991). Variability of the cardiomyocyte ploidy in normal human hearts. *Virchows Arch. B. Cell Pathol. Incl. Mol. Pathol.* 61, 289–294. doi: 10.1007/BF02890430
- Brodsky, V., Sarkisov, D. S., Arefyeva, A. M., Panova, N. W., and Gvasava, I. G. (1994). Polyploidy in cardiac myocytes of normal and hypertrophic human hearts; range of values. *Virchows Arch.* 424, 429–435. doi: 10.1007/BF00190566
- Bunge, M. B., Bunge, R. P., Peterson, E. R., and Murray, M. R. (1967). A light and electron microscope study of long-term organized cultures of rat dorsal root ganglia. *J. Cell Biol.* 32, 439–466. doi: 10.1083/jcb.32.2.439
- Buttitta, L. A., and Edgar, B. A. (2007). Mechanisms controlling cell cycle exit upon terminal differentiation. *Curr. Opin. Cell Biol.* 19, 697–704. doi: 10.1016/j.ceb.2007.10.004
- Carriere, R., and Patterson, D. (1962). The counting of mono- and binucleated cells in tissue sections. *Anat. Rec.* 142, 443–456. doi: 10.1002/ar.1091420402
- Celton-Morizur, S., and Desdouets, C. (2010). Polyploidization of liver cells. *Adv. Exp. Med. Biol.* 676, 123–135. doi: 10.1007/978-1-4419-6199-0\_8
- Chang, Y.-H., and Dubnau, J. (2019). The gypsy endogenous retrovirus drives non-cell-autonomous propagation in a *Drosophila* TDP-43 model of neurodegeneration. *Curr. Biol.* 29, 3135–3152.e4. doi: 10.1016/j.cub.2019.07.071
- Chang, Y.-H., Keegan, R. M., Prazak, L., and Dubnau, J. (2019). Cellular labeling of endogenous retrovirus replication (CLEVR) reveals de novo insertions of the gypsy retrotransposable element in cell culture and in both neurons and glial cells of aging fruit flies. *PLoS Biol.* 17:e3000278. doi: 10.1371/journal.pbio.3000278
- Chen, J., Cohen, M. L., Lerner, A. J., Yang, Y., and Herrup, K. (2010). DNA damage and cell cycle events implicate cerebellar dentate nucleus neurons as targets of Alzheimer's disease. *Mol. Neurodegener.* 5:60. doi: 10.1186/1750-1326-5-60
- Chow, H.-M., Shi, M., Cheng, A., Gao, Y., Chen, G., Song, X., et al. (2019). Age-related hyperinsulinemia leads to insulin resistance in neurons and cell-cycle-induced senescence. *Nat. Neurosci.* 22, 1806–1819. doi: 10.1038/s41593-019-0505-1
- Clubb, F. J., Bell, P. D., Kriseman, J. D., and Bishop, S. P. (1987). Myocardial cell growth and blood pressure development in neonatal spontaneously hypertensive rats. *Lab. Invest.* 56, 189–197.
- Coggeshall, R. E., Yaksta, B. A., and Swartz, F. J. (1970). A cytophotometric analysis of the DNA in the nucleus of the giant cell, R-2, in Aplysia. *Chromosoma* 32, 205–212. doi: 10.1007/bf00286009
- Cunningham, J. J., Levine, E. M., Zindy, F., Goloubeva, O., Roussel, M. F., and Smeyne, R. J. (2002). The cyclin-dependent kinase inhibitors p19(Ink4d) and p27(Kip1) are coexpressed in select retinal cells and act cooperatively to control cell cycle exit. *Mol. Cell. Neurosci.* 19, 359–374. doi: 10.1006/mcne.2001.1090
- Cuoghi, B., and Marini, M. (2001). Ultrastructural and cytochemical features of the supramedullary neurons of the pufferfish *Diodon holacanthus* (L.) (Osteichthyes). *Tissue Cell* 33, 491–499. doi: 10.1054/tice.2001.0203
- D'Alessandro, G., and d'Adda di Fagnana, F. (2017). Transcription and DNA damage: holding hands or crossing swords? *J. Mol. Biol.* 429, 3215–3229. doi: 10.1016/j.jmb.2016.11.002
- Dampney, R. A. L., Horiuchi, J., Tagawa, T., Fontes, M. A. P., Potts, P. D., and Polson, J. W. (2003). Medullary and supramedullary mechanisms regulating sympathetic vasomotor tone. *Acta Physiol. Scand.* 177, 209–218. doi: 10.1046/j.1365-201X.2003.01070.x
- Davis, D. M., and Dyer, M. A. (2010). Retinal progenitor cells, differentiation, and barriers to cell cycle reentry. *Curr. Top. Dev. Biol.* 93, 175–188. doi: 10.1016/B978-0-12-385044-7.00006-0
- Davoli, T., and de Lange, T. (2011). The causes and consequences of polyploidy in normal development and cancer. *Annu. Rev. Cell Dev. Biol.* 27, 585–610. doi: 10.1146/annurev-cellbio-092910-154234
- De Cecco, M., Criscione, S. W., Peterson, A. L., Neretti, N., Sedivy, J. M., and Kreiling, J. A. (2013). Transposable elements become active and mobile in the genomes of aging mammalian somatic tissues. *Aging (Albany NY)* 5, 867–883. doi: 10.18632/aging.100621
- De Veylder, L., Larkin, J. C., and Schnittger, A. (2011). Molecular control and function of endoreplication in development and physiology. *Trends Plant Sci.* 16, 624–634. doi: 10.1016/j.tplants.2011.07.001
- Derks, W., and Bergmann, O. (2020). Polyploidy in cardiomyocytes: roadblock to heart regeneration? *Circ. Res.* 126, 552–565. doi: 10.1161/CIRCRESAHA.119.315408
- Duronio, R. J., and O'Farrell, P. H. (1995). Developmental control of the G1 to S transition in *Drosophila*: cyclin E is a limiting downstream target of E2F. *Genes Dev.* 9, 1456–1468. doi: 10.1101/gad.9.12.1456
- Duronio, R. J., and Xiong, Y. (2013). Signaling pathways that control cell proliferation. *Cold Spring Harb. Perspect. Biol.* 5:a008904. doi: 10.1101/cshperspect.a008904
- Dzau, V. J., and Gibbons, G. H. (1988). Cell biology of vascular hypertrophy in systemic hypertension. *Am. J. Cardiol.* 62, 30G–35G. doi: 10.1016/0002-9149(88)90029-x
- Edgar, B. A., and Orr-Weaver, T. L. (2001). Endoreplication cell cycles: more for less. *Cell* 105, 297–306. doi: 10.1016/S0092-8674(01)00334-8
- Edgar, B. A., Zielke, N., and Gutierrez, C. (2014). Endocycles: a recurrent evolutionary innovation for post-mitotic cell growth. *Nat. Rev. Mol. Cell Biol.* 15, 197–210. doi: 10.1038/nrm3756
- Eliades, A., Papadantonakis, N., and Ravid, K. (2010). New roles for cyclin E in megakaryocytic polyploidization. *J. Biol. Chem.* 285, 18909–18917. doi: 10.1074/jbc.M110.102145
- Enesco, H. E., Shimokawa, I., and Yu, B. P. (1991). Effect of dietary restriction and aging on polyploidy in rat liver. *Mech. Ageing Dev.* 59, 69–78. doi: 10.1016/0047-6374(91)90074-a
- Erenpreisa, J., and Cragg, M. S. (2001). Mitotic death: a mechanism of survival? A review. *Cancer Cell Int.* 1:1. doi: 10.1186/1475-2867-1-1
- Ferguson, K. L., Vanderluit, J. L., Hébert, J. M., McIntosh, W. C., Tibbo, E., MacLaurin, J. G., et al. (2002). Telencephalon-specific Rb knockouts reveal enhanced neurogenesis, survival and abnormal cortical development. *EMBO J.* 21, 3337–3346. doi: 10.1093/emboj/cdf338
- Forsman, C. A., Lindh, B., Elfvin, L. G., and Hallman, H. (1989). Measurements of the DNA amount in mono- and binucleate cells in the celiac superior mesenteric ganglion of the guinea pig. *Anat. Embryol.* 179, 587–590. doi: 10.1007/BF00315700
- Fox, D. T., and Duronio, R. J. (2013). Endoreplication and polyploidy: insights into development and disease. *Development* 140, 3–12. doi: 10.1242/dev.080531
- Frade, J. M. (2000). Unscheduled re-entry into the cell cycle induced by NGF precedes cell death in nascent retinal neurones. *J. Cell Sci.* 113(Pt 7), 1139–1148.
- Frade, J. M., and López-Sánchez, N. (2010). A novel hypothesis for Alzheimer disease based on neuronal tetraploidy induced by p75 (NTR). *Cell Cycle* 9, 1934–1941. doi: 10.4161/cc.9.10.11582
- Frade, J. M., and Ovejero-Benito, M. C. (2015). Neuronal cell cycle: the neuron itself and its circumstances. *Cell Cycle* 14, 712–720. doi: 10.1080/15384101.2015.1004937
- Franz, A., Wood, W., and Martin, P. (2018). Fat body cells are motile and actively migrate to wounds to drive repair and prevent infection. *Dev. Cell* 44, 460–470.e3.
- Frawley, L. E., and Orr-Weaver, T. L. (2015). Polyploidy. *Curr. Biol.* 25, R353–R358. doi: 10.1016/j.cub.2015.03.037

- Fung, S., Wang, F., Chase, M., Godt, D., and Hartenstein, V. (2008). Expression profile of the cadherin family in the developing *Drosophila* brain. *J. Comp. Neurol.* 506, 469–488. doi: 10.1002/cne.21539
- Furman, D. P., and Bukharina, T. A. (2008). How *Drosophila melanogaster* Forms its Mechanoreceptors. *Curr. Genomics* 9, 312–323. doi: 10.2174/138920208785133271
- Gahan, P. B. (1977). Increased levels of euploidy as a strategy against rapid ageing in diploid mammalian systems: an hypothesis. *Exp. Gerontol.* 12, 113–116. doi: 10.1016/0531-5565(77)90021-3
- Galderisi, U., Jori, F. P., and Giordano, A. (2003). Cell cycle regulation and neural differentiation. *Oncogene* 22, 5208–5219. doi: 10.1038/sj.onc.1206558
- Gan, P., Patterson, M., and Sucov, H. M. (2020). Cardiomyocyte polyploidy and implications for heart regeneration. *Annu. Rev. Physiol.* 82, 45–61. doi: 10.1146/annurev-physiol-021119-034618
- Gandarillas, A., Sanz-Gómez, N., and Freije, A. (2019). Polyploidy and the mitosis path to epidermal cell fate. *Cell Cycle* 18, 359–362. doi: 10.1080/15384101.2019.1568766
- Geschwind, I. I., Alfert, M., and Schooley, C. (1958). Liver regeneration and hepatic polyploidy in the hypophysectomized rat. *Exp. Cell Res.* 15, 232–235. doi: 10.1016/0014-4827(58)90080-6
- Gilbert, P., and Pfitzer, P. (1977). Facultative polyploidy in endocrine tissues. *Virchows Arch. B Cell Pathol.* 25, 233–242.
- González-Rosa, J. M., Sharpe, M., Field, D., Soonpaa, M. H., Field, L. J., Burns, C. E., et al. (2018). Myocardial polyploidization creates a barrier to heart regeneration in zebrafish. *Dev. Cell* 44, 433–446.e7.
- Grendler, J., Lowgren, S., Mills, M., and Losick, V. P. (2019). Wound-induced polyploidization is driven by Myc and supports tissue repair in the presence of DNA damage. *Development* 146:dev173005. doi: 10.1242/dev.173005
- Grushko, O., and Buttitta, L. (2015). A sensitive assay for hyperploidy and cell death in *Drosophila* brain using the attune™ acoustic focusing cytometer. *BioProbes* 71, 6–9.
- Hammond, M. P., and Laird, C. D. (1985). Control of DNA replication and spatial distribution of defined DNA sequences in salivary gland cells of *Drosophila melanogaster*. *Chromosoma* 91, 279–286. doi: 10.1007/BF00328223
- Herman, C. J., and Lapham, L. W. (1969). Neuronal polyploidy and nuclear volumes in the cat central nervous system. *Brain Res.* 15, 35–48. doi: 10.1016/0006-8993(69)90308-4
- Herman, C. J., and Lapham, L. W. (1973). Differential effects of tissue processing on tetraploid neurons as compared with diploid neurons and glia. *Brain Res.* 54, 43–50. doi: 10.1016/0006-8993(73)90032-2
- Herrup, K. (2012). The contributions of unscheduled neuronal cell cycle events to the death of neurons in Alzheimer's disease. *Front. Biosci. (Elite Ed)* 4:2101–2109. doi: 10.2741/527
- Herrup, K., and Arendt, T. (2002). Re-expression of cell cycle proteins induces neuronal cell death during Alzheimer's disease. *J. Alzheimers Dis.* 4, 243–247.
- Herrup, K., and Yang, Y. (2007). Cell cycle regulation in the postmitotic neuron: oxymoron or new biology? *Nat. Rev. Neurosci.* 8, 368–378. doi: 10.1038/nrn2124
- Hill, S. J., Mordes, D. A., Cameron, L. A., Neuberg, D. S., Landini, S., Eggan, K., et al. (2016). Two familial ALS proteins function in prevention/repair of transcription-associated DNA damage. *Proc. Natl. Acad. Sci. U.S.A.* 113, E7701–E7709. doi: 10.1073/pnas.1611673113
- Hirose, K., Payumo, A. Y., Cutie, S., Hoang, A., Zhang, H., Guyot, R., et al. (2019). Evidence for hormonal control of heart regenerative capacity during endothermy acquisition. *Science* 364, 184–188. doi: 10.1126/science.aar2038
- Huh, M. S., Parker, M. H., Scimè, A., Parks, R., and Rudnicki, M. A. (2004). Rb is required for progression through myogenic differentiation but not maintenance of terminal differentiation. *J. Cell Biol.* 166, 865–876. doi: 10.1083/jcb.200403004
- Hunter, D. V., Smaila, B. D., Lopes, D. M., Takatoh, J., Denk, F., and Ramer, M. S. (2018). Advillin is expressed in all adult neural crest-derived neurons. *Eneuro* 5, 1–16. doi: 10.1523/ENEURO.0077-18.2018
- Ippati, S., Deng, Y., van der Hoven, J., Heu, C., van Hummel, A., Chua, S. W., et al. (2021). Rapid initiation of cell cycle reentry processes protects neurons from amyloid- $\beta$  toxicity. *Proc. Natl. Acad. Sci. U.S.A.* 118:e2011876118. doi: 10.1073/pnas.2011876118
- Iqbal, N., Zhu, Li, and Chua, S. C. (2020). Neuronal cell cycle events link caloric intake to obesity. *Trends Endocrinol. Metab.* 31, 46–52. doi: 10.1016/j.tem.2019.09.001
- Jensen, R., Pier, A. C., Kaltenbach, C. C., Murdoch, W. J., Becerra, V. M., Mills, K. W., et al. (1989). Evaluation of histopathologic and physiologic changes in cows having premature births after consuming Ponderosa pine needles. *Am. J. Vet. Res.* 50, 285–289.
- Jungas, T., Joseph, M., Fawal, M.-A., and Davy, A. (2020). Population dynamics and neuronal polyploidy in the developing neocortex. *BioRxiv* [preprint]. doi: 10.1101/2020.06.29.177469
- Khurana, V., and Feany, M. B. (2007). Connecting cell-cycle activation to neurodegeneration in *Drosophila*. *Biochim. Biophys. Acta* 1772, 446–456. doi: 10.1016/j.bbdis.2006.10.007
- Klisch, K., Hecht, W., Pfarrer, C., Schuler, G., Hoffmann, B., and Leiser, R. (1999). DNA content and ploidy level of bovine placental trophoblast giant cells. *Placenta* 20, 451–458. doi: 10.1053/plac.1999.0402
- Krug, L., Chatterjee, N., Borges-Monroy, R., Hearn, S., Liao, W.-W., Morrill, K., et al. (2017). Retrotransposon activation contributes to neurodegeneration in a *Drosophila* TDP-43 model of ALS. *PLoS Genet.* 13:e1006635. doi: 10.1371/journal.pgen.1006635
- Kukushkin, N. V., Williams, S. P., and Carew, T. J. (2019). Neurotropic and modulatory effects of insulin-like growth factor II in Aplysia. *Sci. Rep.* 9:14379. doi: 10.1038/s41598-019-50923-5
- Lancaster, O. M., Le Berre, M., Dimitracopoulos, A., Bonazzi, D., Zlotek-Zlotkiewicz, E., Picone, R., et al. (2013). Mitotic rounding alters cell geometry to ensure efficient bipolar spindle formation. *Dev. Cell* 25, 270–283. doi: 10.1016/j.devcel.2013.03.014
- Lang, L., and Schnittger, A. (2020). Endoreplication – a means to an end in cell growth and stress response. *Curr. Opin. Plant Biol.* 54, 85–92. doi: 10.1016/j.pbi.2020.02.006
- Langelotti, S., Romano, V., Romano, G., Klima, R., Feiguin, F., Cragnaz, L., et al. (2016). A novel *Drosophila* model of TDP-43 proteinopathies: N-terminal sequences combined with the Q/N domain induce protein functional loss and locomotion defects. *Dis. Model. Mech.* 9, 659–669. doi: 10.1242/dmm.023382
- Lapham, L. W. (1963). Cytologic and cytochemical studies of neuroglia. *Arch. Neurol.* 9:194. doi: 10.1001/archneur.1963.00460080104013
- Lapham, L. W. (1968). Tetraploid DNA content of Purkinje neurons of human cerebellar cortex. *Science* 159, 310–312. doi: 10.1126/science.159.3812.310
- Lapham, L. W., Lentz, R. D., Woodward, D. J., Hoffer, B. J., and Herman, C. J. (1971). Postnatal development of tetraploid DNA content in the Purkinje neuron of the rat: an aspect of cellular differentiation. *UCLA Forum Med. Sci.* 14, 61–71.
- Lazzeri, E., Angelotti, M. L., Peired, A., Conte, C., Marschner, J. A., Maggi, L., et al. (2018). Endocycle-related tubular cell hypertrophy and progenitor proliferation recover renal function after acute kidney injury. *Nat. Commun.* 9:1344. doi: 10.1038/s41467-018-03753-4
- Lazzerini Denchi, E., Celli, G., and de Lange, T. (2006). Hepatocytes with extensive telomere deprotection and fusion remain viable and regenerate liver mass through endoreduplication. *Genes Dev.* 20, 2648–2653. doi: 10.1101/gad.1453606
- Lee, H. O., Davidson, J. M., and Duronio, R. J. (2009). Endoreplication: polyploidy with purpose. *Genes Dev.* 23, 2461–2477. doi: 10.1101/gad.1829209
- Lentz, R. D., and Lapham, L. W. (1969). A quantitative cytochemical study of the DNA content of neurons of rat cerebellar cortex. *J. Neurochem.* 16, 379–384.
- Lentz, R. D., and Lapham, L. W. (1970). Postnatal development of tetraploid DNA content in rat purkinje cells: a quantitative cytochemical study. *J. Neuropathol. Exp. Neurol.* 29, 43–56. doi: 10.1097/00005072-197001000-00004
- Li, W., Prazak, L., Chatterjee, N., Grüniger, S., Krug, L., Theodorou, D., et al. (2013). Activation of transposable elements during aging and neuronal decline in *Drosophila*. *Nat. Neurosci.* 16, 529–531. doi: 10.1038/nn.3368
- Liu, K.-Y., Shyu, Y.-C., Barbaro, B. A., Lin, Y.-T., Chern, Y., Thompson, L. M., et al. (2015). Disruption of the nuclear membrane by perinuclear inclusions of mutant huntingtin causes cell-cycle re-entry and striatal cell death in mouse and cell models of Huntington's disease. *Hum. Mol. Genet.* 24, 1602–1616. doi: 10.1093/hmg/ddu574

- Lombardi, D. M., Owens, G. K., and Schwartz, S. M. (1989). Ploidy in mesenteric vessels of aged spontaneously hypertensive and Wistar-Kyoto rats. *Hypertension* 13, 475–479. doi: 10.1161/01.hyp.13.5.475
- López-Otín, C., Blasco, M. A., Partridge, L., Serrano, M., and Kroemer, G. (2013). The hallmarks of aging. *Cell* 153, 1194–1217. doi: 10.1016/j.cell.2013.05.039
- López-Sánchez, N., and Frade, J. M. (2013). Genetic evidence for p75NTR-dependent tetraploidy in cortical projection neurons from adult mice. *J. Neurosci.* 33, 7488–7500. doi: 10.1523/JNEUROSCI.3849-12.2013
- Losick, V. P. (2016). Wound-Induced polyploidy is required for tissue repair. *Adv. Wound Care (New Rochelle)* 5, 271–278. doi: 10.1089/wound.2014.0545
- Losick, V. P., Fox, D. T., and Spradling, A. C. (2013). Polyploidization and cell fusion contribute to wound healing in the adult *Drosophila* epithelium. *Curr. Biol.* 23, 2224–2232. doi: 10.1016/j.cub.2013.09.029
- Losick, V. P., Jun, A. S., and Spradling, A. C. (2016). Wound-Induced polyploidization: regulation by hippo and JNK signaling and conservation in mammals. *PLoS One* 11:e0151251. doi: 10.1371/journal.pone.0151251
- MacPherson, D., Sage, J., Crowley, D., Trumpp, A., Bronson, R. T., and Jacks, T. (2003). Conditional mutation of Rb causes cell cycle defects without apoptosis in the central nervous system. *Mol. Cell Biol.* 23, 1044–1053. doi: 10.1128/MCB.23.3.1044-1053.2003
- Mandrioli, M., Mola, L., Cuoghi, B., and Sonetti, D. (2010). Endoreplication: a molecular trick during animal neuron evolution. *Q. Rev. Biol.* 85, 159–169. doi: 10.1086/652341
- Manickam, N., Radhakrishnan, R. K., Vergil Andrews, J. F., Selvaraj, D. B., and Kandasamy, M. (2020). Cell cycle re-entry of neurons and reactive neuroblastosis in Huntington's disease: possibilities for neural-glial transition in the brain. *Life Sci.* 263:118569. doi: 10.1016/j.lfs.2020.118569
- Manickam, V., Dhakshinamoorthy, V., and Perumal, E. (2018). Iron oxide nanoparticles induces cell cycle-dependent neuronal apoptosis in mice. *J. Mol. Neurosci.* 64, 352–362. doi: 10.1007/s12031-018-1030-5
- Mann, D. M. A., Yates, P. O., and Barton, C. M. (1976). Development of polyploid glial classes in the human cerebellum and their relationship to purkinje cells. *Neuropathol. Appl. Neurobiol.* 2, 433–437. doi: 10.1111/j.1365-2990.1976.tb00517.x
- Mann, D. M., and Yates, P. O. (1973a). Polyploidy in the human nervous system. 1. The DNA content of neurones and glia of the cerebellum. *J. Neurol. Sci.* 18, 183–196. doi: 10.1016/0022-510x(73)90005-1
- Mann, D. M., and Yates, P. O. (1973b). Polyploidy in the human nervous system. 2. Studies of the glial cell populations of the Purkinje cell layer of the human cerebellum. *J. Neurol. Sci.* 18, 197–205. doi: 10.1016/0022-510x(73)90006-3
- Mann, D. M., and Yates, P. O. (1979). A quantitative study of the glia of the Purkinje cell layer of the cerebellum in mammals. *Neuropathol. Appl. Neurobiol.* 5, 71–76.
- Marathe, S., Liu, S., Brai, E., Kaczarowski, M., and Alberi, L. (2015). Notch signaling in response to excitotoxicity induces neurodegeneration via erroneous cell cycle reentry. *Cell Death Differ.* 22, 1775–1784. doi: 10.1038/cdd.2015.23
- Martin, D., Xu, J., Porretta, C., and Nichols, C. D. (2017). Neurocytometry: flow cytometric sorting of specific neuronal populations from human and rodent brain. *ACS Chem. Neurosci.* 8, 356–367. doi: 10.1021/acscchemneuro.6b00374
- Matondo, R. B., Moreno, E., Toussaint, M. J. M., Tooten, P. C. J., van Essen, S. C., van Liere, E. A., et al. (2018). Atypical E2f functions are critical for pancreas polyploidization. *PLoS One* 13:e0190899. doi: 10.1371/journal.pone.0190899
- Matsumoto, T., Wakefield, L., Tarlow, B. D., and Grompe, M. (2020). In vivo lineage tracing of polyploid hepatocytes reveals extensive proliferation during liver regeneration. *Cell Stem Cell* 26, 34–47.e3.
- McShea, A., Harris, P. L., Webster, K. R., Wahl, A. F., and Smith, M. A. (1997). Abnormal expression of the cell cycle regulators P16 and CDK4 in Alzheimer's disease. *Am. J. Pathol.* 150, 1933–1939.
- McShea, A., Wahl, A. F., and Smith, M. A. (1999). Re-entry into the cell cycle: a mechanism for neurodegeneration in Alzheimer disease. *Med. Hypotheses* 52, 525–527. doi: 10.1054/mehy.1997.0680
- Mehrotra, S., Maqbool, S. B., Kolpakas, A., Murnen, K., and Calvi, B. R. (2008). Endocycling cells do not apoptose in response to DNA rereplication genotoxic stress. *Genes Dev.* 22, 3158–3171. doi: 10.1101/gad.1710208
- Melchiorri, C., Chieco, P., Zedda, A. I., Coni, P., Ledda-Columbano, G. M., and Columbano, A. (1993). Ploidy and nuclearity of rat hepatocytes after compensatory regeneration or mitogen-induced liver growth. *Carcinogenesis* 14, 1825–1830. doi: 10.1093/carcin/14.9.1825
- Moh, C., Kubiak, J. Z., Bajic, V. P., Zhu, X., Smith, M. A., and Lee, H.-G. (2011). Cell cycle deregulation in the neurons of Alzheimer's disease. *Results Probl. Cell Differ.* 53, 565–576. doi: 10.1007/978-3-642-19065-0\_23
- Mola, L., and Cuoghi, B. (2004). The supramedullary neurons of fish: present status and goals for the future. *Brain Res. Bull.* 64, 195–204. doi: 10.1016/j.brainresbull.2004.07.010
- Mola, L., Cuoghi, B., Mandrioli, M., and Marini, M. (2001). DNA endoreplication in the clustered supramedullary neurons of the pufferfish diodon *Holacanthus* L. (Osteichthyes). *Histochem. J.* 33, 59–63.
- Mola, L., Sassi, D., and Cuoghi, B. (2002). The supramedullary cells of the teleost *Coris julis* (L.): a noradrenergic neuronal system. *Eur. J. Histochem.* 46, 329–332. doi: 10.4081/1744
- Moon, N. S., and Kim, M. (2019). E2F-dependent genetic oscillators control endoreplication. *BioRxiv* [preprint]. doi: 10.1101/858746
- Morillo, S. M., Escoll, P., de la Hera, A., and Frade, J. M. (2010). Somatic tetraploidy in specific chick retinal ganglion cells induced by nerve growth factor. *Proc. Natl. Acad. Sci. U.S.A.* 107, 109–114. doi: 10.1073/pnas.0906121107
- Moroz, L. L. (2011). Aplysia. *Curr. Biol.* 21, R60–R61. doi: 10.1016/j.cub.2010.11.028
- Muntzing, A., and Prakken, R. (1941). Chromosomal aberrations in rye populations. *Hereditas* 27, 273–308. doi: 10.1111/j.1601-5223.1941.tb03261.x
- Nagle, G. T., van Heumen, W. R., Knock, S. L., Garcia, A. T., McCullough, D. A., and Kurosky, A. (1993). Occurrence of a furin-like prohormone processing enzyme in Aplysia neuroendocrine bag cells. *Comp. Biochem. Physiol. B* 105, 345–348.
- Nagy, Z. (1999). Mechanisms of neuronal death in Down's syndrome. *J. Neural Transm. Suppl.* 57, 233–245. doi: 10.1007/978-3-7091-6380-1\_15
- Nagy, Z. (2000). Cell cycle regulatory failure in neurones: causes and consequences. *Neurobiol. Aging* 21, 761–769. doi: 10.1016/s0197-4580(00)00223-2
- Nakajima, Y., Pappas, G. D., and Bennett, M. V. (1965). The fine structure of the supramedullary neurons of the puffer with special reference to endocellular and pericellular capillaries. *Am. J. Anat.* 116, 471–491. doi: 10.1002/aja.1001160303
- Nandakumar, S., Grushko, O., and Buttitta, L. A. (2020). Polyploidy in the adult *Drosophila* brain. *elife* 9, 54385. doi: 10.7554/eLife.54385
- Nguyen, H. G., and Ravid, K. (2010). "Polyploidy: mechanisms and cancer promotion in hematopoietic and other cells," in *Polyploidization and Cancer Advances in Experimental Medicine and Biology*, ed. R. Y. C. Poon (New York, NY: Springer New York), 105–122. doi: 10.1007/978-1-4419-6199-0\_7
- O'Farrell, P. H. (2011). Quiescence: early evolutionary origins and universality do not imply uniformity. *Philos. Trans. R Soc. Lond. B Biol. Sci.* 366, 3498–3507. doi: 10.1098/rstb.2011.0079
- Ovejero-Benito, M. C., and Frade, J. M. (2013). Brain-derived neurotrophic factor-dependent cdk1 inhibition prevents G2/M progression in differentiating tetraploid neurons. *PLoS One* 8:e64890. doi: 10.1371/journal.pone.0064890
- Ovejero-Benito, M. C., and Frade, J. M. (2015). p27(Kip1) participates in the regulation of endoreplication in differentiating chick retinal ganglion cells. *Cell Cycle* 14, 2311–2322. doi: 10.1080/15384101.2015.1044175
- Øvrebo, J. I., and Edgar, B. A. (2018). Polyploidy in tissue homeostasis and regeneration. *Development* 145:dev156034. doi: 10.1242/dev.156034
- Oyama, K., El-Nachef, D., Zhang, Y., Sdek, P., and MacLellan, W. R. (2014). Epigenetic regulation of cardiac myocyte differentiation. *Front. Genet.* 5:375. doi: 10.3389/fgene.2014.00375
- Pandit, S. K., Westendorp, B., and de Bruin, A. (2013). Physiological significance of polyploidization in mammalian cells. *Trends Cell Biol.* 23, 556–566. doi: 10.1016/j.tcb.2013.06.002
- Pandit, S. K., Westendorp, B., Nantasanti, S., van Liere, E., Tooten, P. C. J., Cornelissen, P. W. A., et al. (2012). E2F8 is essential for polyploidization in mammalian cells. *Nat. Cell Biol.* 14, 1181–1191. doi: 10.1038/ncb2585
- Paradis, A. N., Gay, M. S., and Zhang, L. (2014). Binucleation of cardiomyocytes: the transition from a proliferative to a terminally differentiated state. *Drug Discov. Today* 19, 602–609. doi: 10.1016/j.drudis.2013.10.019
- Park, D. S., Obeidat, A., Giovanni, A., and Greene, L. A. (2000). Cell cycle regulators in neuronal death evoked by excitotoxic stress: implications for



- neurodegeneration and its treatment. *Neurobiol. Aging* 21, 771–781. doi: 10.1016/s0197-4580(00)00220-7
- Park, J.-H., Nguyen, T. T. N., Lee, E.-M., Castro-Aceituno, V., Wagle, R., Lee, K.-S., et al. (2019). Role of p53 isoforms in the DNA damage response during *Drosophila* oogenesis. *Sci. Rep.* 9:11473. doi: 10.1038/s41598-019-47913-y
- Paulini, K., and Mohr, W. (1975). Hormone-dependent Polyploidy in the Glandula orbitalis externa and Glandula infraorbitalis of Animals of Different Age. *Beitr. Pathol.* 156, 65–74. doi: 10.1016/S0005-8165(75)80086-2
- Pelegri, C., Duran-Vilaregut, J., del Valle, J., Crespo-Biel, N., Ferrer, I., Pallàs, M., et al. (2008). Cell cycle activation in striatal neurons from Huntington's disease patients and rats treated with 3-nitropropionic acid. *Int. J. Dev. Neurosci.* 26, 665–671. doi: 10.1016/j.ijdevneu.2008.07.016
- Ranganathan, S., and Bowser, R. (2003). Alterations in G(1) to S phase cell-cycle regulators during amyotrophic lateral sclerosis. *Am. J. Pathol.* 162, 823–835. doi: 10.1016/S0002-9440(10)63879-5
- Ravid, K., Lu, J., Zimmet, J. M., and Jones, M. R. (2002). Roads to polyploidy: the megakaryocyte example. *J. Cell. Physiol.* 190, 7–20. doi: 10.1002/jcp.10035
- Ribeiro, A. A. C. M. (2006). Size and number of binucleate and mononucleate superior cervical ganglion neurons in young capybaras. *Anat. Embryol.* 211, 607–617. doi: 10.1007/s00429-006-0113-1
- Riddiford, N., Siudeja, K., van den Beek, M., Boumard, B., and Bardin, A. J. (2020). Evolution and genomic signatures of spontaneous somatic mutation in *Drosophila* intestinal stem cells. *BioRxiv* [preprint]. doi: 10.1101/2020.07.20.188979
- Rimkus, S. A., Katzenberger, R. J., Trinh, A. T., Dodson, G. E., Tibbetts, R. S., and Wassarman, D. A. (2008). Mutations in String/CDC25 inhibit cell cycle re-entry and neurodegeneration in a *Drosophila* model of Ataxia telangiectasia. *Genes Dev.* 22, 1205–1220. doi: 10.1101/gad.1639608
- Roszell, J. A., Fredi, J. L., and Irving, C. C. (1978). The development of polyploidy in two classes of rat liver nuclei. *Biochim. Biophys. Acta BBA Nucleic Acids Protein Synth.* 519, 306–316. doi: 10.1016/0005-2787(78)90084-9
- Rowley, A. F., and Ratcliffe, N. A. (1978). A histological study of wound healing and hemocyte function in the wax-moth *Galleria mellonella*. *J. Morphol.* 157, 181–199. doi: 10.1002/jmor.1051570206
- Royzman, I., Hayashi-Hagihara, A., Dej, K. J., Bosco, G., Lee, J. Y., and Orr-Weaver, T. L. (2002). The E2F cell cycle regulator is required for *Drosophila* nurse cell DNA replication and apoptosis. *Mech. Dev.* 119, 225–237. doi: 10.1016/S0925-4773(02)00388-X
- Ruggiero, R., Kale, A., Thomas, B., and Baker, N. E. (2012). Mitosis in neurons: roughhex and APC/C maintain cell cycle exit to prevent cytokinetic and axonal defects in *Drosophila* photoreceptor neurons. *PLoS Genet.* 8:e1003049. doi: 10.1371/journal.pgen.1003049
- Ruijtenberg, S., and van den Heuvel, S. (2016). Coordinating cell proliferation and differentiation: Antagonism between cell cycle regulators and cell type-specific gene expression. *Cell Cycle* 15, 196–212. doi: 10.1080/15384101.2015.1120925
- Sallé, J., Campbell, S. D., Gho, M., and Audibert, A. (2012). CycA is involved in the control of endoreplication dynamics in the *Drosophila* bristle lineage. *Development* 139, 547–557. doi: 10.1242/dev.069823
- Sattelle, D. B., and Buckingham, S. D. (2006). Invertebrate studies and their ongoing contributions to neuroscience. *Invert. Neurosci.* 6, 1–3. doi: 10.1007/s10158-005-0014-7
- Sauer, F. C. (1935). Mitosis in the neural tube. *J. Comp. Neurol.* 62, 377–405. doi: 10.1002/cne.900620207
- Severin, E., Meier, E. M., and Willers, R. (1984). Flow cytometric analysis of mouse hepatocyte ploidy. I. Preparative and mathematical protocol. *Cell Tissue Res.* 238, 643–647. doi: 10.1007/BF00219883
- Shu, Z., Row, S., and Deng, W.-M. (2018). Endoreplication: the good, the bad, and the ugly. *Trends Cell Biol.* 28, 465–474. doi: 10.1016/j.tcb.2018.02.006
- Sigl-Glöckner, J., and Brecht, M. (2017). Polyploidy and the cellular and areal diversity of rat cortical layer 5 pyramidal neurons. *Cell Rep.* 20, 2575–2583. doi: 10.1016/j.celrep.2017.08.069
- Smith, R. B. (1970). Binucleate neurons in the human foetal heart. *Experientia* 26:772. doi: 10.1007/BF02232542
- Stephen, M. J., Poindexter, B. J., Moolman, J. A., Sheikh-Hamad, D., and Bick, R. J. (2009). Do binucleate cardiomyocytes have a role in myocardial repair? Insights using isolated rodent myocytes and cell culture. *Open Cardiovasc. Med. J.* 3, 1–7. doi: 10.2174/1874192400903010001
- Swartz, F. J., and Bhatnagar, K. P. (1981). Are CNS neurons polyploid? A critical analysis based upon cytophotometric study of the DNA content of cerebellar and olfactory bulbular neurons of the bat. *Brain Res.* 208, 267–281. doi: 10.1016/0006-8993(81)90557-6
- Szaro, B. G., and Tompkins, R. (1987). Effect of tetraploidy on dendritic branching in neurons and glial cells of the frog, *Xenopus laevis*. *J. Comp. Neurol.* 258, 304–316. doi: 10.1002/cne.902580210
- Tamori, Y., and Deng, W.-M. (2013). Tissue repair through cell competition and compensatory cellular hypertrophy in postmitotic epithelia. *Dev. Cell* 25, 350–363. doi: 10.1016/j.devcel.2013.04.013
- Taniguchi, K., Kokuryo, A., Imano, T., Minami, R., Nakagoshi, H., and Adachi-Yamada, T. (2014). Isoform-specific functions of Mud/NuMA mediate binucleation of *Drosophila* male accessory gland cells. *BMC Dev. Biol.* 14:46. doi: 10.1186/s12861-014-0046-5
- Taniguchi, K., Kokuryo, A., Imano, T., Nakagoshi, H., and Adachi-Yamada, T. (2018). Binucleation of accessory gland lobe contributes to effective ejection of seminal fluid in *Drosophila melanogaster*. *Zool. Sci.* 35, 446–458. doi: 10.2108/zsl70188
- Teir, H. (1949). On the sizes of the nuclei in the glandula infraorbitalis of the white rat. *Acta Pathol. Microbiol. Scand.* 26, 620–635. doi: 10.1111/j.1699-0463.1949.tb00761.x
- Toscano, C. P., de Melo, M. P., Matera, J. M., Loesch, A., and Ribeiro, A. A. C. M. (2009). The developing and restructuring superior cervical ganglion of guinea pigs (*Cavia porcellus* var. albina). *Int. J. Dev. Neurosci.* 27, 329–336. doi: 10.1016/j.ijdevneu.2009.03.006
- Trakala, M., and Malumbres, M. (2014). The functional relevance of polyploidization in the skin. *Exp. Dermatol.* 23, 92–93. doi: 10.1111/exd.12305
- Trakala, M., Rodríguez-Acebes, S., Maroto, M., Symonds, C. E., Santamaría, D., Ortega, S., et al. (2015). Functional reprogramming of polyploidization in megakaryocytes. *Dev. Cell* 32, 155–167. doi: 10.1016/j.devcel.2014.12.015
- Unhavaithaya, Y., and Orr-Weaver, T. L. (2012). Polyploidization of glia in neural development links tissue growth to blood-brain barrier integrity. *Genes Dev.* 26, 31–36. doi: 10.1101/gad.177436.111
- Uroz, M., Garcia-Puig, A., Tekeli, I., Elozegui-Artola, A., Abenza, J. F., Marín-Llauradó, A., et al. (2019). Traction forces at the cytokinetic ring regulate cell division and polyploidy in the migrating zebrafish epicardium. *Nat. Mater.* 18, 1015–1023. doi: 10.1038/s41563-019-0381-9
- Verhaart, W. J., and Voogd, J. (1962). Hypertrophy of the inferior olives in the cat. *J. Neuropathol. Exp. Neurol.* 21, 92–104. doi: 10.1097/00005072-196201000-00008
- Volkenhoff, A., Weiler, A., Letzel, M., Stehling, M., Klämbt, C., and Schirmeier, S. (2015). Glial glycolysis is essential for neuronal survival in *Drosophila*. *Cell Metab.* 22, 437–447. doi: 10.1016/j.cmet.2015.07.006
- Von Stetina, J. R., Frawley, L. E., Unhavaithaya, Y., and Orr-Weaver, T. L. (2018). Variant cell cycles regulated by Notch signaling control cell size and ensure a functional blood-brain barrier. *Development* 145:dev157115. doi: 10.1242/dev.157115
- Wen, Y., Yang, S., Liu, R., Brun-Zinkernagel, A. M., Koulen, P., and Simpkins, J. W. (2004). Transient cerebral ischemia induces aberrant neuronal cell cycle re-entry and Alzheimer's disease-like tauopathy in female rats. *J. Biol. Chem.* 279, 22684–22692. doi: 10.1074/jbc.M311768200
- Werner, S., Krieg, T., and Smola, H. (2007). Keratinocyte-fibroblast interactions in wound healing. *J. Invest. Dermatol.* 127, 998–1008. doi: 10.1038/sj.jid.5700786
- Yamagishi, M., Ito, E., and Matsuo, R. (2011). DNA endoreplication in the brain neurons during body growth of an adult slug. *J. Neurosci.* 31, 5596–5604. doi: 10.1523/JNEUROSCI.0179-11.2011
- Yamagishi, M., Ito, E., and Matsuo, R. (2012). Whole genome amplification in large neurons of the terrestrial slug *Limax*. *J. Neurochem.* 122, 727–737. doi: 10.1111/j.1471-4159.2012.07822.x
- Yang, Y., Varvel, N. H., Lamb, B. T., and Herrup, K. (2006). Ectopic cell cycle events link human Alzheimer's disease and amyloid precursor protein transgenic mouse models. *J. Neurosci.* 26, 775–784. doi: 10.1523/JNEUROSCI.3707-05.2006
- Yates, P. O., and Mann, D. M. (1973). Polyploidy in the human nervous system. *J. Pathol.* 110:vii.
- Zacksenhaus, E., Jiang, Z., Chung, D., Marth, J. D., Phillips, R. A., and Gallie, B. L. (1996). pRb controls proliferation, differentiation, and death of skeletal muscle

- cells and other lineages during embryogenesis. *Genes Dev.* 10, 3051–3064. doi: 10.1101/gad.10.23.3051
- Zhang, B., Mehrotra, S., Ng, W. L., and Calvi, B. R. (2014). Low levels of p53 protein and chromatin silencing of p53 target genes repress apoptosis in *Drosophila* endocycling cells. *PLoS Genet.* 10:e1004581. doi: 10.1371/journal.pgen.1004581
- Zhang, Y., Wang, Z., and Ravid, K. (1996). The cell cycle in polyploid megakaryocytes is associated with reduced activity of cyclin B1-dependent cdc2 kinase. *J. Biol. Chem.* 271, 4266–4272. doi: 10.1074/jbc.271.8.4266
- Zhu, X., Siedlak, S. L., Wang, Y., Perry, G., Castellani, R. J., Cohen, M. L., et al. (2008). Neuronal binucleation in Alzheimer disease hippocampus. *Neuropathol. Appl. Neurobiol.* 34, 457–465. doi: 10.1111/j.1365-2990.2007.00908.x
- Zielke, N., Kim, K. J., Tran, V., Shibutani, S. T., Bravo, M.-J., Nagarajan, S., et al. (2011). Control of *Drosophila* endocycles by E2F and CRL4(CDT2). *Nature* 480, 123–127. doi: 10.1038/nature10579
- Zimmet, J., and Ravid, K. (2000). Polyploidy. *Exp. Hematol.* 28, 3–16. doi: 10.1016/S0301-472X(99)00124-1
- Zuckermann, F. A., and Head, J. R. (1986). Isolation and characterization of trophoblast from murine placenta. *Placenta* 7, 349–364.
- Zybina, E. V., and Zybina, T. G. (1996). “Polytene chromosomes in mammalian cells,” in *International Review of Cytology*, ed. K. W. Jeon (Amsterdam: Elsevier), 53–119. doi: 10.1016/S0074-7696(08)62220-2

**Conflict of Interest:** The authors declare that the research was conducted in the absence of any commercial or financial relationships that could be construed as a potential conflict of interest.

Copyright © 2021 Nandakumar, Rozich and Buttitta. This is an open-access article distributed under the terms of the Creative Commons Attribution License (CC BY). The use, distribution or reproduction in other forums is permitted, provided the original author(s) and the copyright owner(s) are credited and that the original publication in this journal is cited, in accordance with accepted academic practice. No use, distribution or reproduction is permitted which does not comply with these terms.



# Pan-Cancer Survey of Tumor Mass Dormancy and Underlying Mutational Processes

Anna Julia Wiecek<sup>1†</sup>, Daniel Hadar Jacobson<sup>1,2†</sup>, Wojciech Lason<sup>1†</sup> and Maria Secrier<sup>1\*</sup>

<sup>1</sup> Department of Genetics, Evolution and Environment, UCL Genetics Institute, University College London, London, United Kingdom, <sup>2</sup> UCL Cancer Institute, Paul O'Gorman Building, University College London, London, United Kingdom

## OPEN ACCESS

### Edited by:

Guang Yao,  
The University of Arizona,  
United States

### Reviewed by:

Joseph William Landry,  
Virginia Commonwealth University,  
United States  
Hai Hu,  
Sun Yat-sen Memorial Hospital, China

### \*Correspondence:

Maria Secrier  
m.secrier@ucl.ac.uk

<sup>†</sup> These authors have contributed  
equally to this work and share first  
authorship

### Specialty section:

This article was submitted to  
Cell Growth and Division,  
a section of the journal  
Frontiers in Cell and Developmental  
Biology

**Received:** 21 April 2021

**Accepted:** 17 June 2021

**Published:** 09 July 2021

### Citation:

Wiecek AJ, Jacobson DH,  
Lason W and Secrier M (2021)  
Pan-Cancer Survey of Tumor Mass  
Dormancy and Underlying Mutational  
Processes.  
Front. Cell Dev. Biol. 9:698659.  
doi: 10.3389/fcell.2021.698659

Tumor mass dormancy is the key intermediate step between immune surveillance and cancer progression, yet due to its transitory nature it has been difficult to capture and characterize. Little is understood of its prevalence across cancer types and of the mutational background that may favor such a state. While this balance is finely tuned internally by the equilibrium between cell proliferation and cell death, the main external factors contributing to tumor mass dormancy are immunological and angiogenic. To understand the genomic and cellular context in which tumor mass dormancy may develop, we comprehensively profiled signals of immune and angiogenic dormancy in 9,631 cancers from the Cancer Genome Atlas and linked them to tumor mutagenesis. We find evidence for immunological and angiogenic dormancy-like signals in 16.5% of bulk sequenced tumors, with a frequency of up to 33% in certain tissues. Mutations in the *CASP8* and *HRAS* oncogenes were positively selected in dormant tumors, suggesting an evolutionary pressure for controlling cell growth/apoptosis signals. By surveying the mutational damage patterns left in the genome by known cancer risk factors, we found that aging-induced mutations were relatively depleted in these tumors, while patterns of smoking and defective base excision repair were linked with increased tumor mass dormancy. Furthermore, we identified a link between APOBEC mutagenesis and dormancy, which comes in conjunction with immune exhaustion and may partly depend on the expression of the angiogenesis regulator *PLG* as well as interferon and chemokine signals. Tumor mass dormancy also appeared to be impaired in hypoxic conditions in the majority of cancers. The microenvironment of dormant cancers was enriched in cytotoxic and regulatory T cells, as expected, but also in macrophages and showed a reduction in inflammatory Th17 signals. Finally, tumor mass dormancy was linked with improved patient survival outcomes. Our analysis sheds light onto the complex interplay between dormancy, exhaustion, APOBEC activity and hypoxia, and sets directions for future mechanistic explorations.

**Keywords:** tumor mass dormancy, mutational signatures, immunity, angiogenesis, APOBEC, hypoxia

## INTRODUCTION

Tumor evolution is shaped by a variety of internal and external forces that act at different stages during cancer development, sometimes in an antagonistic manner, and drive distinct trajectories to advanced disease (Gerlinger et al., 2014; McGranahan and Swanton, 2017; Temko et al., 2018). Within this rapidly changing context, adaptation of cancer cells is paramount for survival and

much of it is achieved through cellular plasticity (Yuan et al., 2019). As a manifestation of this plasticity, cancer dormancy has emerged as an important contributor to the early stages of tumor development, as well as to cancer progression and metastatic dissemination (Jahanban-Esfahlan et al., 2019; Phan and Croucher, 2020; Park and Nam, 2020). Its two facets, cellular dormancy driven by arrest in the G0 state of the cell cycle (Phan and Croucher, 2020), and tumor mass dormancy (TMD), described as an equilibrium between cell proliferation and cell death shaped by the microenvironment that constrains tumor growth (Holmgren et al., 1995; Aguirre-Ghiso, 2007; Wang et al., 2019), are complementary but distinct mechanisms that contribute to the plasticity of cancer expansion (Shen and Clairambault, 2020; Huang, 2021). The former concept had already been coined by Hadfield (1954) and has since led to the generation of more detailed mechanistic insights explaining its regulation by the DREAM complex (Sadasivam and DeCaprio, 2013; MacDonald et al., 2017; Kim et al., 2021), with key dependencies on the p53/p21 activation axis (Itahana et al., 2002; Barr et al., 2017; Heldt et al., 2018). The latter, initially termed “population dormancy” by Gimbrone et al. (1972) and then renamed to tumor mass dormancy, remains poorly understood due to the lack of suitable data and models (Boire et al., 2019).

The theoretical model of TMD is embedded into the “3Es of immunoediting” paradigm (Dunn et al., 2004b), arising as a temporary equilibrium between tumor elimination and immune escape (Koebel et al., 2007; Teng et al., 2008). As the cancer lesion develops, a period of immunoediting follows when the immune system interacts with the malignant cells establishing a dynamic equilibrium: the immunogenic cells are eliminated, and non-immunogenic tumor cells arise (Dunn et al., 2004a). This keeps the tumor in a dormant state (Aguirre-Ghiso, 2007; Wang et al., 2019), hypothesized to account for the “latency” between the initiation of the first mutator phenotype and symptom manifestation in early disease, or for the disease-free period preceding cancer recurrence (Gužvić and Klein, 2013; Damen et al., 2020). During this period of dormancy, the continued cytotoxic response triggered by pro-inflammatory signaling cytokines like interferon  $\gamma$ , as well as prolonged exposure to pro-inflammatory signaling in general, causes the cytotoxic cells to become inactive, a phenomenon known as T cell exhaustion (Dunn et al., 2006; Yi et al., 2010; Wherry and Kurachi, 2015). Finally, the angiogenic switch or immune escape shifts the balance in favor of cancer progression (Jahanban-Esfahlan et al., 2019).

A variety of molecular mechanisms have been proposed to mediate these switches. The urokinase receptor (uPAR) regulates tumor growth by controlling  $\beta 1$  integrin signaling which drives a cascade of Ras/ERK mitogenic activation via the focal adhesion kinase (FAK) and the EGF receptor (EGFR) (Aguirre Ghiso et al., 1999; Aguirre Ghiso, 2002; Liu et al., 2002; White et al., 2004). Downregulation of any of these components has been shown to lead to tumor growth arrest and dormancy (Aguirre-Ghiso, 2007). Additionally, blocking uPAR activates p38, which induces dormancy under p53 upregulation and downregulation of JUN (Ranganathan et al., 2006). Metastatic lesions appear to manifest reduced p38 activity under sustained

ERK activation. As a result, a low ERK:p38 protein expression ratio is often employed to assess tumor dormancy (Aguirre-Ghiso et al., 2003). This state is further corroborated by a limited ability in recruiting new blood vessels and vasculature remodeling, resulting in angiogenic dormancy (Moserle et al., 2009). This condition is often characterized by VEGF inhibition in the presence of anti-angiogenic factors such as angiostatin, endostatin, thrombospondin, etc., or chemokines (CXCL9 and CXCL10) (Aguirre-Ghiso, 2007; Lyu et al., 2013; Senft and Ronai, 2016; Park and Nam, 2020).

Overall, it is clear that TMD results from an interplay between immunological and angiogenic dormancy, where cell growth is counterbalanced by apoptosis due to poor vascularization and immune cytotoxicity, followed by exhaustion. It becomes evident that the states of T cell exhaustion and dormancy are not a simple dysfunction, but a purposeful homeostatic mechanism enabling the prevention of pathological immune responses. Hence, it is of crucial importance to be able to identify and target the dormant tumors early. This temporary equilibrium state provides a unique clinical opportunity, but its prevalence in cancer and the genetic determinants that may sustain it are currently unknown.

In this study, we surveyed the landscape of TMD along the two axes that shape it, immunological and angiogenic dormancy, in a cohort of 9,631 tumors from 31 tissues available from the Cancer Genome Atlas (TCGA). We show that TMD can be captured from bulk sequencing datasets, that it is pervasive across a variety of cancer types and that its emergence is linked with key somatic alterations. We also investigate the environmental context of TMD and its relevance in the clinic.

## RESULTS

### Pan-Cancer Characterization of Immunological, Angiogenic, and Tumor Mass Dormancy

To evaluate the levels of immunological and angiogenic dormancy across multiple cancer tissues, we manually curated lists of genes associated with the two programs from the literature (**Supplementary Table 1**). The lists included receptor molecules, as well as soluble mediators, surface and structural proteins, enzymes and transcription factors, several of which are observed to be frequently mutated during cancer development (**Supplementary Figure 1**). Immunological and angiogenic dormancy program scores were assigned on a per-sample basis using two distinct methodologies that exploited the expression of genes associated with either process, focusing either on differences between up/downregulated gene activity (‘scaled difference of means’) or on the largest variation explained by principal component analysis (‘PCA’) (see section “Materials and Methods,” **Supplementary Figures 2–4**). Both immunological and angiogenic dormancy represent potential mechanisms for restricting the expansion of primary tumor cell populations due to either impaired vascularization or immunosurveillance (Aguirre-Ghiso, 2007), therefore both processes can contribute to the development of TMD. As such, an overall per-patient



TMD program score was also derived using the expression of genes associated with both types of dormancy. We assessed the robustness of the two scoring methods to changes in the gene signature employed or small variations in gene expression, and showed that the ‘scaled difference of means’ approach was comparatively more stable to such fluctuations (**Supplementary Figure 5**). Therefore, we chose this method for the downstream analysis.

Having established a framework for quantifying immunological, angiogenic and tumor mass dormancy programs, we next profiled these cellular programs across 9,631 samples of solid primary tumors from TCGA. We observed a spectrum of TMD across tumors that ranges from highly dormant to highly expanding (**Figures 1A–C** and **Supplementary Figures 6, 7**). TMD is thought to emerge when tumor cell proliferation is balanced by apoptosis due to factors such as limitations in blood supply or an active immune system (Holmgren et al., 1995). Consequently, primary tumor samples with high TMD program scores (upper quartile of the score range) which also showed a proliferation/apoptosis ratio below 1 (see section “Materials and Methods”), indicative of limited primary tumor lesion expansion, were classed as exhibiting TMD (**Figure 1D**). Overall, 16.5% of samples across different tissues exhibited substantial evidence for a TMD-like phenotype (with up to 33% prevalence in certain cancers) and they were further subdivided into those indicating angiogenic dormancy (4.4%), immunological dormancy (5%), or both (7%) (**Figure 1E** and **Supplementary Table 2**). Head and neck (32%), sarcoma (32%) and breast (26%) cancer were among the cancers with highest rates of TMD. Angiogenic dormancy alone was most widespread in breast (14%) and head and neck cancers (13%). Some rarer cancers like thymoma or pheochromocytoma and paraganglioma also showed a remarkably high prevalence of TMD (~33% each) with the latter also exhibiting the highest immune-mediated dormancy (21%). The systematic differences in TMD program scores across different tissues (**Figures 1E,F**) suggest that the tissue environment may impact the ability of the tumor to enter a TMD state. Across the board, immune-mediated dormancy levels appeared higher than those of angiogenic dormancy, suggesting a dominant role for immune surveillance in determining TMD.

Even though TMD is expected to manifest primarily in early forming tumors (Dunn et al., 2004b), we surprisingly found that a sizeable proportion of late-stage tumors also exhibited similarly high TMD-linked activity levels (**Supplementary Figure 8**). When comparing the prevalence of TMD between early- and late-stage cancers, expanding tumors appeared enriched in the later stages (Fisher’s exact test  $p < 0.0001$ , 1.5-fold enrichment), as expected. Remarkably, samples with angiogenic dormancy were also marginally enriched (1.3-fold) in late-stage cancers (Fisher’s exact test  $p < 0.05$ ).

## The Genomic Background of TMD

To gain a better understanding of the genomic context in which TMD can develop, we asked whether samples with high and low TMD differed in their association with known drivers of tumorigenesis. We found 15 genes with either a statistically significant enrichment or a depletion of mutations

within samples classed as showing TMD across the 31 solid cancer tissues, with several depletion signals characterizing both early- and late-stage tumors (Fisher’s exact test adjusted  $p < 0.05$ , **Figure 2A**, **Supplementary Figures 9A, 10A**, and **Supplementary Table 3**). Furthermore, mutations in *MUC4*, a gene involved in angiogenesis and metastasis (Zhi et al., 2014), were specifically enriched in stomach adenocarcinoma, while *EGFR*, *FAT3/4*, *LRP1B*, *KAT6B* mutations, mainly linked with cell proliferation and immune responses (Katoh, 2012; Simó-Riudalbas et al., 2015; Sigismund et al., 2018; Chen et al., 2019), were depleted in colon cancer (Fisher’s exact test adjusted  $p < 0.05$ , **Supplementary Figure 11**). Many of these findings were reaffirmed using a random forest classification approach (**Supplementary Figure 12**).

The results of the pan-cancer analysis largely reflected the balance of proliferation, cell death and pro/anti-angiogenic signals (Semenza, 2003; Naumov et al., 2006; Aguirre-Ghiso, 2007) one would expect in the context of dormancy. Two genes stood out as having a ~5-fold enrichment of mutations in patients displaying TMD: *HRAS* and *CASP8*. Interestingly, while *HRAS* alterations were positively associated with dormancy, other members of the same oncogenic family, *KRAS* and *NRAS* showed a depletion of mutations in the context of this phenotype. Specifically, we found an enrichment of *HRAS* hotspot mutations at the Q61 and G13 positions across all solid primary tumor samples, but a depletion of *KRAS* G13 and G12, as well as *NRAS* Q61 hotspot alterations (**Supplementary Figure 13**). Two of these hotspots presented cancer stage specificity: *HRAS* G13 mutations were enriched in TMD in late-stage cancers, while *KRAS* G12 mutations were depleted in early-stage tumors (**Supplementary Figures 9B, 10B**). The oncogenic activation of the Ras protein has been associated with pro-angiogenic signaling through the repression of thrombospondin-1 (Watnick et al., 2015). It has been suggested that while distinct oncogenic Ras alterations might have similar ability to promote cell cycle progression, they might have different abilities to induce the pro-angiogenic program (Aguirre-Ghiso, 2007), which may explain the discrepancy of mutation signals in the RAS genes in relation to TMD.

*CASP8*, a gene encoding a cysteine-aspartic acid protease involved in the execution of apoptosis by cleaving and thereby activating caspase-3 and caspase-7 (Tummers and Green, 2017), was also preferentially mutated in dormancy. While *CASP8* loss of function would be predicted to impair the ability of cancer cells to initiate apoptosis, silencing of *CASP8* in breast cancer cell lines has also been shown to decrease cancer cell growth by delaying G0/G1- to S-phase transition and increasing the expression of CDK inhibitors p21 and p27 (De Blasio et al., 2016).

The genes presenting a depletion of point mutations within dormant samples identified by our analysis have key functions in regulating tumor growth, including *TP53*, the master regulator that coordinates signals of stress such as DNA damage and aberrant growth signaling and can induce cell cycle arrest or apoptosis (Polyak et al., 1997; Vogelstein et al., 2000), or *APC*, which suppresses tumor growth through repression of the Wnt signaling pathway (Boman and Fields, 2013). Both the *APC* and *DCC* genes promote



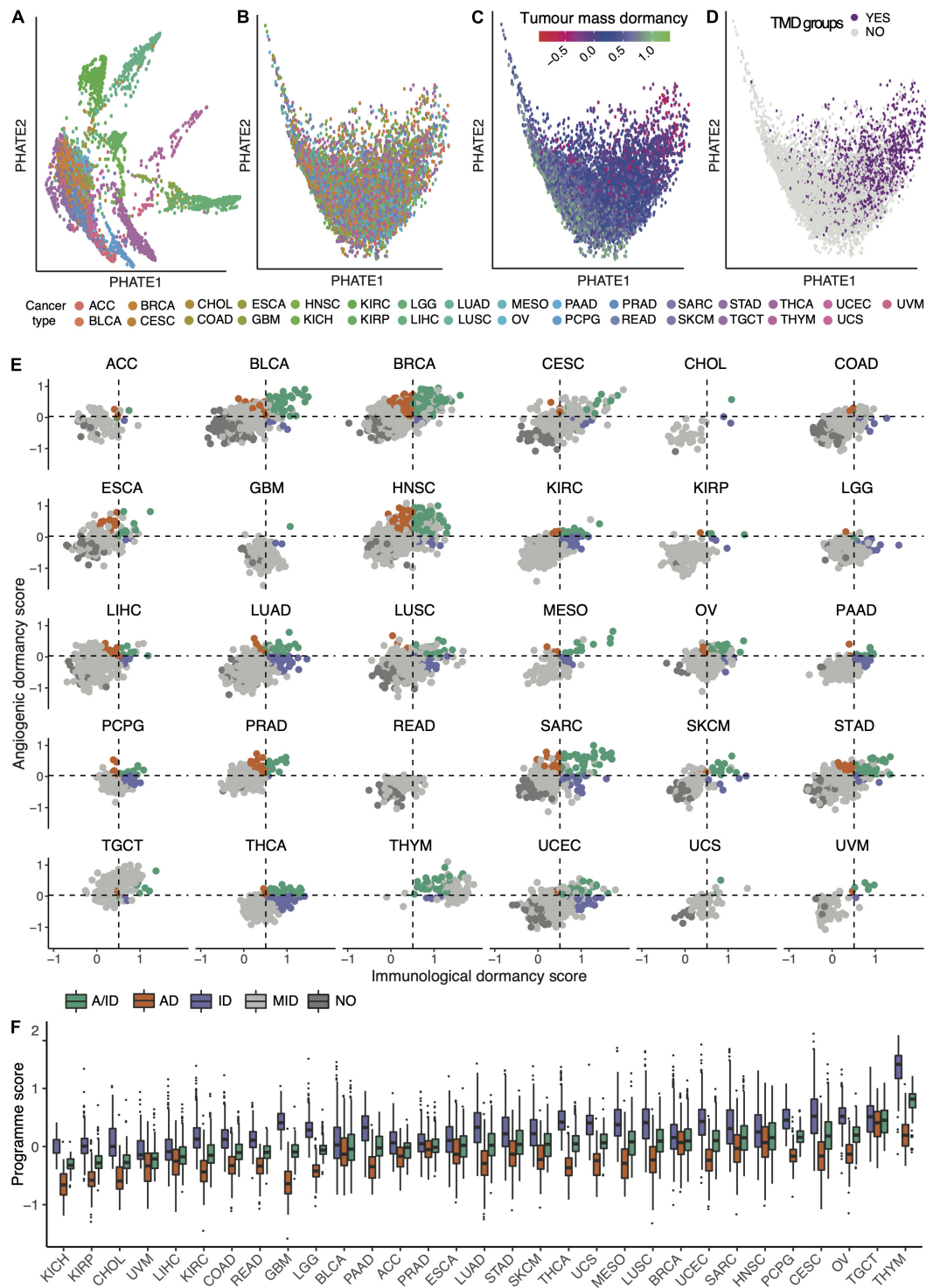


**FIGURE 1 |** The pan-cancer landscape of tumor mass dormancy (TMD). **(A–D)** PHATE dimensionality reduction applied to 9,631 primary tumor samples based on the expression of genes within the TMD and exhaustion programs before **(A)** and after **(B–D)** removal of tissue specific expression patterns. The maps are colored by their corresponding tissue type **(A,B)**, TMD program score **(C)** and TMD status **(D)**. **(E)** Relationship between immunological and angiogenic program scores within individual TCGA cancer tissues. Samples are colored by their angiogenic (orange, AD), immunological (purple, ID) and tumor mass (green, A/ID) dormancy status. Samples showing no evidence of TMD (NO) are colored in dark gray, and slowly expanding tumors in light gray (MID). Horizontal and vertical dashed lines represent the upper quartile of the pan-cancer angiogenic and immunological dormancy program scores, respectively. KICH was not plotted because it lacked TMD samples. **(F)** Variation in TMD, immunological and angiogenic dormancy scores across primary tumor TCGA samples stratified by tissue type. The tissues are sorted by their TMD levels.

apoptosis by downregulation of survivin gene expression (Zhang et al., 2001) and caspase-9 cleavage (Forcet et al., 2001), respectively. Control of tumor vascularization was reflected in depletion of mutations in *PRDM16*, which inhibits angiogenesis by suppressing the expression of a HIF target semaphorin 5B (Kundu et al., 2020), and in *NCO1A*, a transcriptional coactivator that upregulates the expression of the VEGF $\alpha$  pro-angiogenic factor (Qin et al., 2015). Mutations in the *IDH1* gene, shown to be depleted in samples with TMD, result in the production of the 2-hydroxyglutarate metabolite which regulates the activity of  $\alpha$ -ketoglutarate dependent dioxygenases and causes the ubiquitination and proteasomal degradation of *HIF1A*, a key sensor of hypoxia and initiator of angiogenesis (Ye et al., 2013). Moreover, 2-hydroxyglutarate can also result in the downregulation of leukocyte chemotaxis factors (Turcan et al., 2012; Tommasini-Ghelfi et al., 2019), which could contribute to the ability of tumor cells to escape immunological dormancy through immune system evasion.

In addition to the enrichment analysis, using a maximum-likelihood dN/dS method (Martincorena et al., 2017) we detected signals of positive selection for mutations within *CASP8* and *HRAS* in samples with TMD, but not in expanding tumor samples (Figure 2B). In contrast, *IDH1* and *NRAS*, both of which showed a depletion of mutations within TMD samples, showed signals of positive selection only in expanding tumors (Figure 2B). Interestingly, *CASP8* showed similarly increased mutation rate both in early- and late-stage cancers with TMD, while *HRAS* mutations appeared linked with TMD only in late-stage tumors – pointing toward a timing specificity of TMD-linked evolutionary pressures (Supplementary Figure 14). The associations between mutations in these genes and TMD were also validated in an independent dataset from the International Cancer Genome Consortium (ICGC), along with several others including *KRAS* and *TP53* (Supplementary Figure 15). While signals of positive selection are more difficult to validate in the sparser independent cohorts available due to the limited sample size, nevertheless *CASP8* and *TP53* selection signals were robustly recovered both

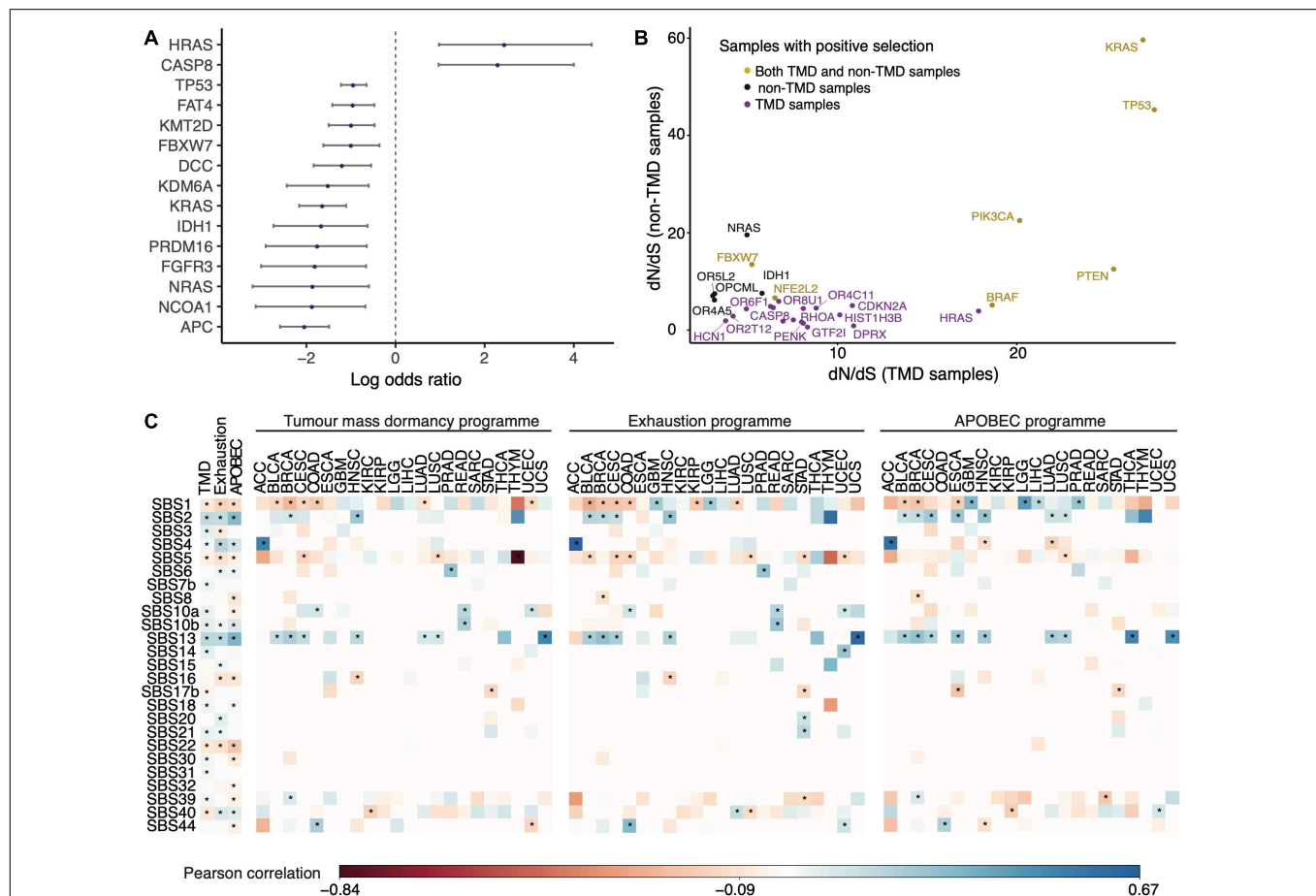


**FIGURE 2 |** Genomic drivers and mutational processes linked with TMD. **(A)** Genes presenting an enrichment or depletion of mutations within high TMD samples. Blue circles represent odds ratios on a log2 scale and the confidence intervals for each of the individual Fisher's exact tests are depicted. **(B)** Genes showing signals of positive selection in samples with high (purple) and low (black) TMD, as well as across both groups (yellow). **(C)** Matrices depicting the Pearson correlation between mutational signatures and the TMD, exhaustion and APOBEC programs, both pan-cancer (first 3 columns) and within individual cancer tissues. Statistically significant correlations ( $p < 0.05$ ) are highlighted with an asterisk. Only signatures with at least one significant correlation are shown.

in oral cancers from ICGC as well as in breast cancers from the METABRIC cohort (**Supplementary Figure 16**). These findings support the importance of *CASP8* and *RAS* mutational status in the context of TMD.

In terms of broader structural variation in the genome, we found no copy number alteration events (amplifications and deletions) specifically enriched in tumors with TMD (data not shown), potentially because such events would be preferentially selected for in fast growing tumors. Moreover, tumors with angiogenic and immunological dormancy showed a modest, but significant decrease in mutational burden when compared to tumors without TMD (**Supplementary Figure 17**).

## Mutational Processes Linked With Dormancy and Exhaustion

In addition to investigating the links with specific driver events, we also set out to characterize broader mutational processes associated with TMD. Different risk factors of cancer induce DNA damage in the cells in a context dependent manner, such that nucleotide substitution patterns associated with such mutational processes can be observed within cancer genomes. These patterns of trinucleotide substitutions are termed “mutational signatures” and have been widely characterized across cancers (Alexandrov et al., 2013a, 2020). We carried out a mutational signature analysis to survey the contribution of known mutagenic processes and risk factors to the genomes of dormant tumors. The mutational signature prevalence was correlated with dormancy and exhaustion program scores (**Figure 2C**, left and center panels).

We observed that exposure to signatures SBS1, originating from aging-induced deamination of 5-methylcytosines (Alexandrov et al., 2015), SBS5, also ageing-like, and SBS22, linked with aristolochic acid exposure (Jelaković et al., 2015), decreased as TMD and exhaustion increased. In contrast, smoking (SBS4) and defective base excision repair linked with polymerase epsilon or *NTHL1* mutations (SBS10a/b, SBS30) (Shivji et al., 1995; Jager et al., 2019) were associated with an increase in TMD. Finally, we noted a consistently strong correlation between TMD/exhaustion and mutational signatures SBS2 and SBS13, associated with mutagenesis induced by a class of cytidine deaminases called APOBEC (apolipoprotein B mRNA editing catalytic polypeptide-like) (Alexandrov et al., 2020). These enzymes induce mutagenesis in viral genetic material and are part of the anti-viral defense, but can also act on and damage host DNA (Green and Weitzman, 2019). The correlation of these mutational footprints of APOBEC with TMD was observed both pan-cancer and across individual cancer types, including bladder, breast, cervical and head and neck cancers (**Figure 2C**). Reassuringly, there was a similarly strong correlation between SBS2 and SBS13 and the mean expression of the AID/APOBEC cytidine deaminases (**Figure 2C**, right panel). All the correlations highlighted were consistent between early- and late-stage cancers (**Supplementary Figure 18**).

## Dormancy and Exhaustion Programs Correlate With APOBEC Enzymatic Activity

To further explore the association between TMD and exhaustion with APOBEC mutagenesis, we calculated the correlation of our program scores and the mean expression of genes belonging to the APOBEC family (**Figures 3A–F**). Across all cancers and regardless of clinical stage, we observed significant correlations between the activity of the APOBEC program as a whole, TMD and exhaustion programs (**Figures 3A–G** and **Supplementary Figures 19–23**). These associations were stronger than would be expected by chance (**Supplementary Figure 24**) and consistently validated in independent datasets from ICGC and cBioPortal (**Supplementary Figures 25–28**). In particular, we observed a marked association between APOBEC mutagenesis and immunological dormancy, which we stipulate may precede or come in conjunction with immune exhaustion, the latter showing the strongest correlation.

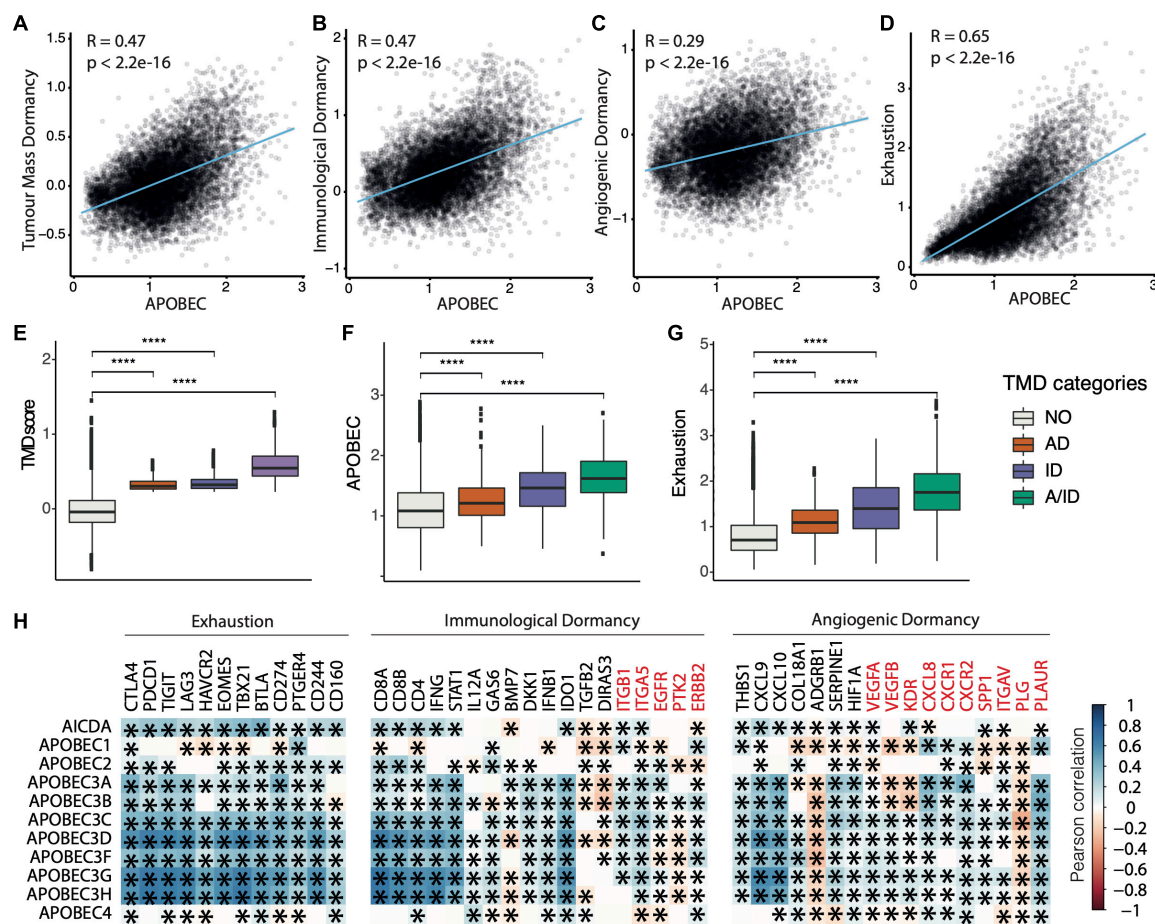
We also observed positive correlations between most but not all genes included in the immunological, angiogenic and exhaustion programs, on the one side, and the expression of the AID/APOBEC enzyme family members, on the other (**Figure 3H**). This may be because of downstream regulation of expression, e.g., through mRNA degradation, compartmentalization, or inhibition of transcription. Notably, among all genes, the correlation was highest for the mRNAs of enzymatically active APOBEC3 and AID members of the APOBEC family. The correlation scores were similar for *APOBEC3A-H*, which is to be expected as these genes form a cluster on chromosome 22. Within the TMD program, type II interferon  $\gamma$  and the interferon-upregulated genes such as *STAT1* showed a positive correlation with APOBEC. This is interesting as interferon  $\gamma$  signaling is associated with anti-tumor response by favoring rejection of highly immunogenic tumors (Mittal et al., 2014; Benci et al., 2016). However, prolonged interferon  $\gamma$  signaling promotes epigenetic changes to *STAT1* and the expression of ligands for multiple T cell inhibitory receptors (Benci et al., 2016). Thus, we would expect a spectrum of exhaustion signaling to be present within the tumor, ranging from cells signaling danger to cells with anti-cytotoxic response. Anti-angiogenic markers, such as the urokinase receptor *PLAUR*, which downregulate angiogenic processes and thus restrict the supply of T cells (Oh et al., 2003), were also positively correlated with APOBEC expression. Similar associations were observed for several immune checkpoints (*CD244*, *CD166*, *TIGIT*, *CTLA4*, and *PDCD1*) and exhaustion markers (*EOMES* and *TBX21*).

Overall, the multiple correlations between APOBEC expression and the dormancy/exhaustion levels in tumors suggest a complex interplay between the activity of APOBEC deaminases and the immune microenvironment, which we set out to explore in greater depth.

## TMD Activity Differences in the Context of APOBEC Mutagenesis

To further elucidate the association between TMD and APOBEC activity, we sought to investigate the specific TMD signals





that might have the strongest links with APOBEC-attributable mutagenesis, as quantified by the single-base substitution mutational signatures SBS2 and SBS13. In order to identify APOBEC-enriched tumors, we employed t-distributed stochastic neighbor embedding (tSNE) to cluster samples based on their overall mutational signature profiles (Figures 4A,B). Unsurprisingly, the clustering was impacted by the tumor tissue of origin, as mutational signatures are often tissue-specific (Degasperi et al., 2020) (Figure 4A). However, samples enriched for APOBEC-associated mutations, defined as the total enrichment of signatures SBS2 and SBS13, covered a fairly heterogeneous set of tissues (Figure 4B). Groups with distinct mutagenesis patterns were defined using expectation-maximization clustering (Supplementary Figure 29), and the procedure was repeated 100 times to obtain robust clusters. Samples were defined as APOBEC-enriched if they fell into the APOBEC-associated cluster more than 50 times (see section “Materials and Methods”), which broadly overlaps with the

APOBEC enrichment score approach developed by Roberts et al. (2013) (Supplementary Figure 30).

To determine whether APOBEC mutagenesis was specifically associated with particular aspects of the TMD program, we used random forest classifiers to rank TMD genes based on how much their expression helps to distinguish between the APOBEC-enriched and depleted groups (see section “Materials and Methods”). The accuracies for predicting APOBEC enrichment across 100 built models were remarkably high and broadly replicable (mean AUC = 0.8354, range: 0.8203–0.8534) (Figures 4C,D). Additionally, the gene ranking in the models was also highly reproducible (Figure 4E). *PLG*, which encodes for the plasminogen protein and triggers angiostatin release to inhibit angiogenesis (Oh et al., 2003), displayed the highest importance by far, defined as the mean associated decrease in Gini index following its removal from a model (mean = 119.2). Upon further investigation of *PLG* expression, we found that its high predictive importance could



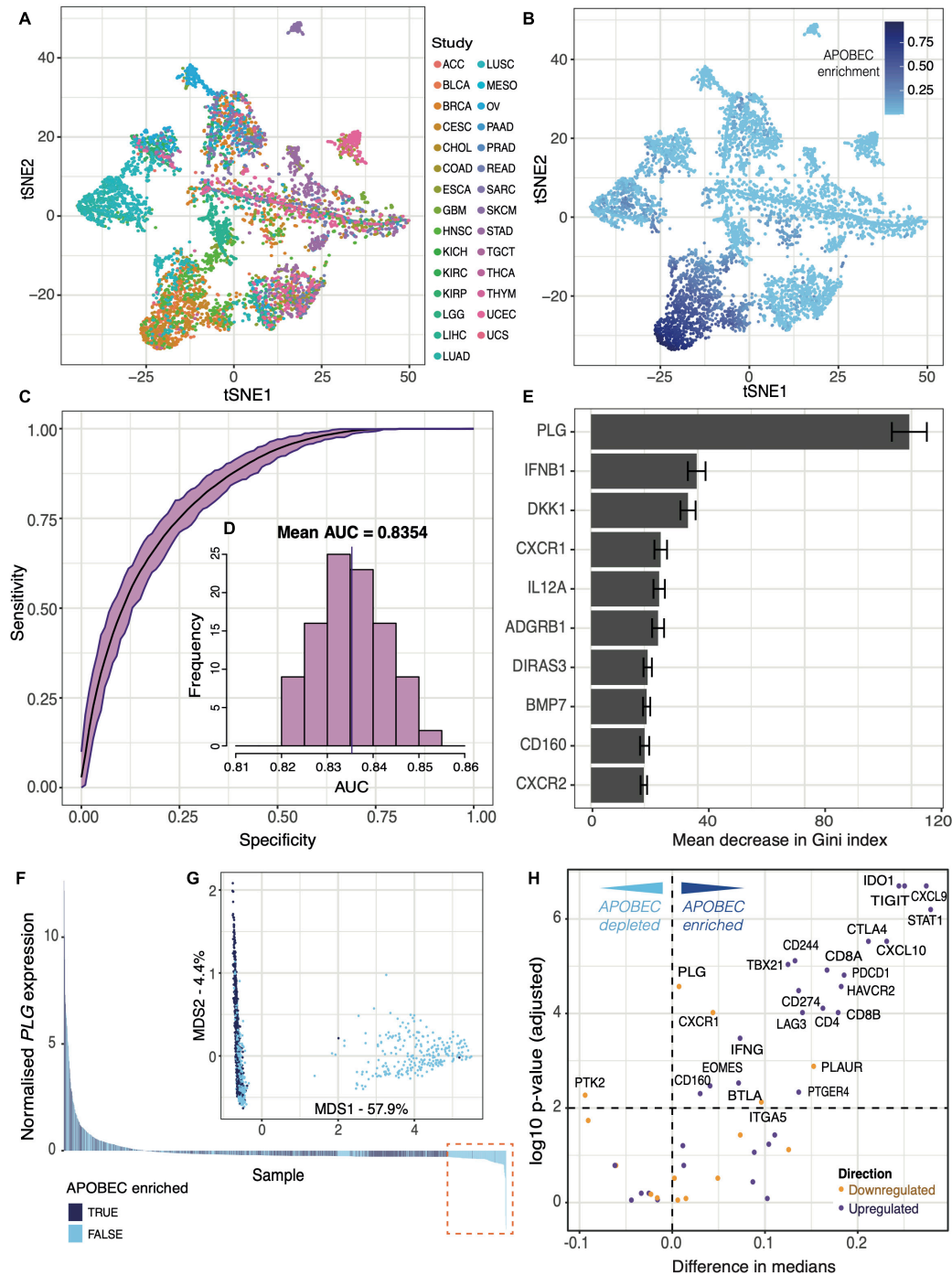


**FIGURE 4 |** Tumor mass dormancy and exhaustion programs distinguish an APOBEC mutagenesis cluster. tSNE dimensionality reduction of 6,410 primary tumor samples based on single-base substitution signature profiles labeled by (A) TCGA study and (B) the total contribution of mutations from APOBEC signatures SBS2 and SBS13. (C) Receiver operating characteristic (ROC) curves of 100 random forest classifiers of APOBEC signature enrichment based on expression of genes involved in the TMD and exhaustion programs. (D) Distribution of Area Under Curve (AUC) values across all 100 random forest classifiers. (E) The top 10 ranked genes with highest importance for APOBEC signature enrichment classification, ranked by mean associated decrease in Gini index across all 100 classifiers. (F) Waterfall plot displaying samples included in an exemplary classifier ranked by normalized *PLG* expression, colored by APOBEC enrichment labels. The dashed orange box highlights the subset of samples with low *PLG* expression and marked depletion of APOBEC signatures. (G) Multidimensional scaling plot displaying samples included in the exemplary classifier. (H) Volcano plot displaying the difference in median normalized expression for each gene involved in the TMD and exhaustion programs between APOBEC-enriched and non-enriched groups, colored by anticipated direction of regulation. Differences in medians above 0 correspond to an increase in expression in the APOBEC-enriched group. Genes with a difference in median < 0 would instead be higher expressed in the non-enriched cluster (APOBEC depleted). A significance cut-off of  $p < 0.01$  was applied after Benjamini–Hochberg multiple testing correction.

largely be attributed to a substantial group of low-*PLG*-expressing samples which were not labeled as APOBEC-enriched (**Figure 4F**). This becomes more apparent when considering the multidimensional scaling plot attributable to one of the random forest classifiers, which clearly displays a segregated cluster of non-APOBEC-enriched samples defined by a specific *PLG* expression threshold derived from the classifier (**Figure 4G**). Therefore, APOBEC mutagenesis appears to be completely lacking in the cases when *PLG* is not expressed, suggesting a link between APOBEC enzymatic activity and the uPA/uPAR system of angiogenic modulation.

Finally, we compared the expression of genes associated with TMD between APOBEC mutagenesis enriched and depleted groups. The large majority of genes whose upregulation drives TMD displayed a higher median expression in APOBEC-enriched samples compared with non-enriched samples (**Figure 4H**). It is worth noting that some genes were found to be significantly changed whilst displaying negligible difference in medians, likely reflecting the effects of a large sample size rather than a real biological difference. Overall, these results reaffirm the positive correlation between TMD and APOBEC enzyme activity, apparent both from an expression and mutagenesis perspective.

## Heterogeneity of TMD Maintenance in Hypoxic Conditions

Owing to the reported association between hypoxic environments and angiogenesis (Chen et al., 2009), we next sought to investigate whether hypoxia might differentially impact TMD. Hypoxia was quantified on a per-sample basis using established transcriptional signatures (see section “Materials and Methods”), and the calculation procedure was validated using three separate hypoxia signatures (**Supplementary Figure 31**).

From a pan-cancer perspective, we observed that hypoxia scores were significantly lower in samples displaying any type of dormancy, compared to samples with no evidence of TMD (**Figure 5A**). This was further corroborated by grouping tumors into distinct subsets (bins) based on their hypoxia levels: the proportion of samples with no evidence of TMD increased significantly as hypoxia scores increased (**Figure 5B**). In particular, we noted the lowest hypoxia levels appearing in tumors with angiogenic dormancy. These results align with the established consensus that the hypoxia-inducible factor (HIF) pathway is a key regulator of angiogenesis (Pugh and Ratcliffe, 2003; Krock et al., 2011), with angiogenic dormancy expected to develop in normoxic conditions. Similar patterns were also observed on a tissue-specific basis, particularly in the cases of sarcoma, stomach, lung squamous and esophageal carcinomas (**Figure 5C**). Cancer studies which tended to present low hypoxia, such as pheochromocytoma and paraganglioma (PCPG), thymoma (THYM) and thyroid carcinoma (THCA) often presented some evidence of TMD, whereas studies presenting high hypoxia, such as colon and rectum adenocarcinomas (COAD/READ) and glioblastoma (GBM), were abundant in expanding tumors (**Supplementary Figure 32**). Notable exceptions included bladder cancer and uveal melanoma, both of which presented samples with evidence

of TMD at the higher end of their respective hypoxia spectra (**Figures 5C–F**). While prior research has highlighted HIF-1 $\alpha$  expression as a promoter of angiogenesis and tumor invasion in bladder carcinoma (Theodoropoulos et al., 2004) and metastasis in uveal melanoma (Asnaghi et al., 2014), our analysis suggests that a period of TMD-induced latency may also be compatible with hypoxia in these cancers.

While a considerable heterogeneity across cancer tissues was observed, patterns of decreased hypoxia in the context of TMD were noted in the majority of cancers (**Figures 5D–F**). This would imply that hypoxia may be an impediment to TMD maintenance across the majority of tumors, consistent with its increased prevalence in the later stages of tumor development (Petrova et al., 2018).

## The Microenvironmental Context of TMD

Since TMD is by definition dependent on immune surveillance, we also set out to confirm this and potentially identify new components of the cancer microenvironment which are permissive to this type of dormancy. Specifically, because the balance in the populations of immune and stromal cells is central to forming anti-tumor responses, we investigated how immune composition might be shaped in the context of TMD, exhaustion and APOBEC programs. Using cell type-specific transcriptional markers (see section “Materials and Methods”), we observed strong positive correlations between TMD and various types of T cells (**Figure 6A**). Antitumoral cytotoxic cells such as CD8+ and CD4+ T cells, Th1/2 cells, as well as tumor promoting regulatory cells and macrophages were correlated with the APOBEC, exhaustion and dormancy programs. This observation is in line with the mechanism proposed in the literature whereby an initial immune response caused by neoantigens presented by the dormant tumors is followed by exhaustion of such signals (Ghorani et al., 2020). In addition to their cytotoxic activity, CD8+ and CD4+ T cells have been previously shown to limit tumor growth through the secretion of anti-proliferative cytokines, such as interferon  $\gamma$  which can stimulate the expression of p21 and p27 cell cycle inhibitors (Chin et al., 1996; Wall et al., 2003), and antiangiogenic chemokines, such as CXCL9 and CXCL10 (Ikeda et al., 2002).

Compared to Th1 and Th2 cells, natural killer (NK) cells showed a weaker correlation with dormancy programs, consistent with reports of tumor growth control by the immune system being mostly associated with adaptive T cell responses (Finn, 2006). The microenvironment of samples with high TMD was also depleted in inflammatory Th17 cells, which secrete the angiogenesis inducer IL-17A (Bailey et al., 2014). Interestingly, samples displaying signals of angiogenic dormancy had higher enrichment of Th2 instead of Th1 cells. While the Th1 activity is linked with interferon  $\gamma$  production and tumor suppression, Th2 activity has been implicated in cancer progression (Zhao et al., 2019). Despite the broader heterogeneity of T helper cell signals, they showed a similar overall trend as that of cytotoxic and dendritic cells when projected across the TMD landscape (**Figures 6B–D**). All these classes except for the Th2 cells appeared most enriched in tumors with evidence of both immunological and angiogenic dormancy (**Figure 6E**). Similar

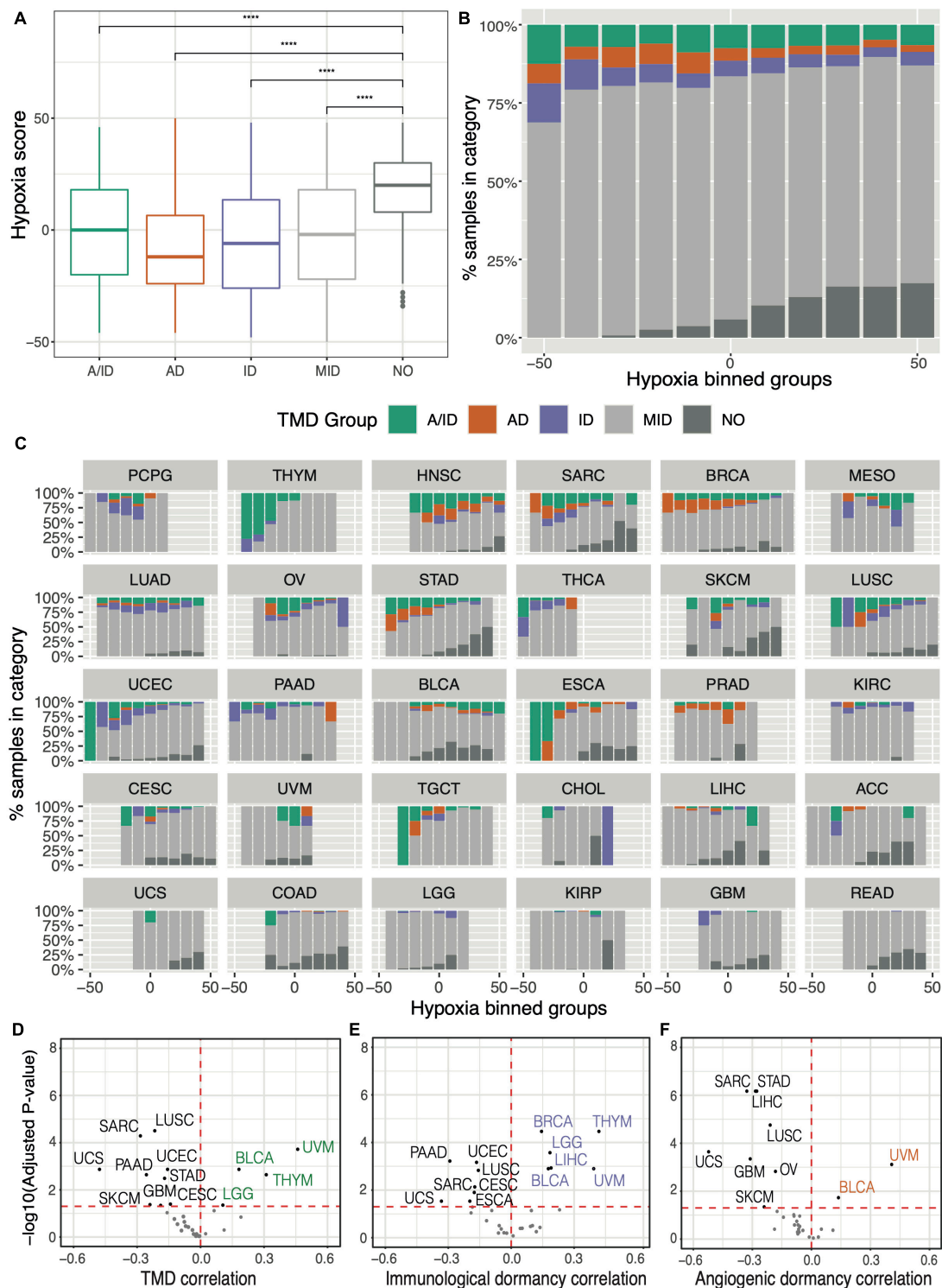


**FIGURE 5 |** Tumor mass dormancy is reduced in the context of hypoxia. **(A)** Comparison of hypoxia scores across samples falling within distinct TMD categories: both angiogenic and immunological dormancy (A/ID), angiogenic dormancy (AD), immunological dormancy (ID), slowly expanding tumors (MID), expanding tumors without evidence of TMD (NO). **(B,C)** Distributions of dormancy status within hypoxia groups, defined by binning the hypoxia scores into intervals of 10: **(B)** pan-cancer, and **(C)** by TCGA cancer tissue, arranged in descending proportion of dormant samples. KICH was not plotted because it lacked TMD samples. **(D–F)** Volcano plots displaying the cancer-study-specific Pearson correlations of **(D)** TMD, **(E)** immunogenic dormancy and **(F)** angiogenic dormancy program scores against hypoxia scores. Cancers showing an increased dormancy in the context of hypoxia are highlighted in corresponding colors, while cancers with high dormancy in normoxic conditions are depicted in black. \*\*\*\* $p < 0.0001$ .

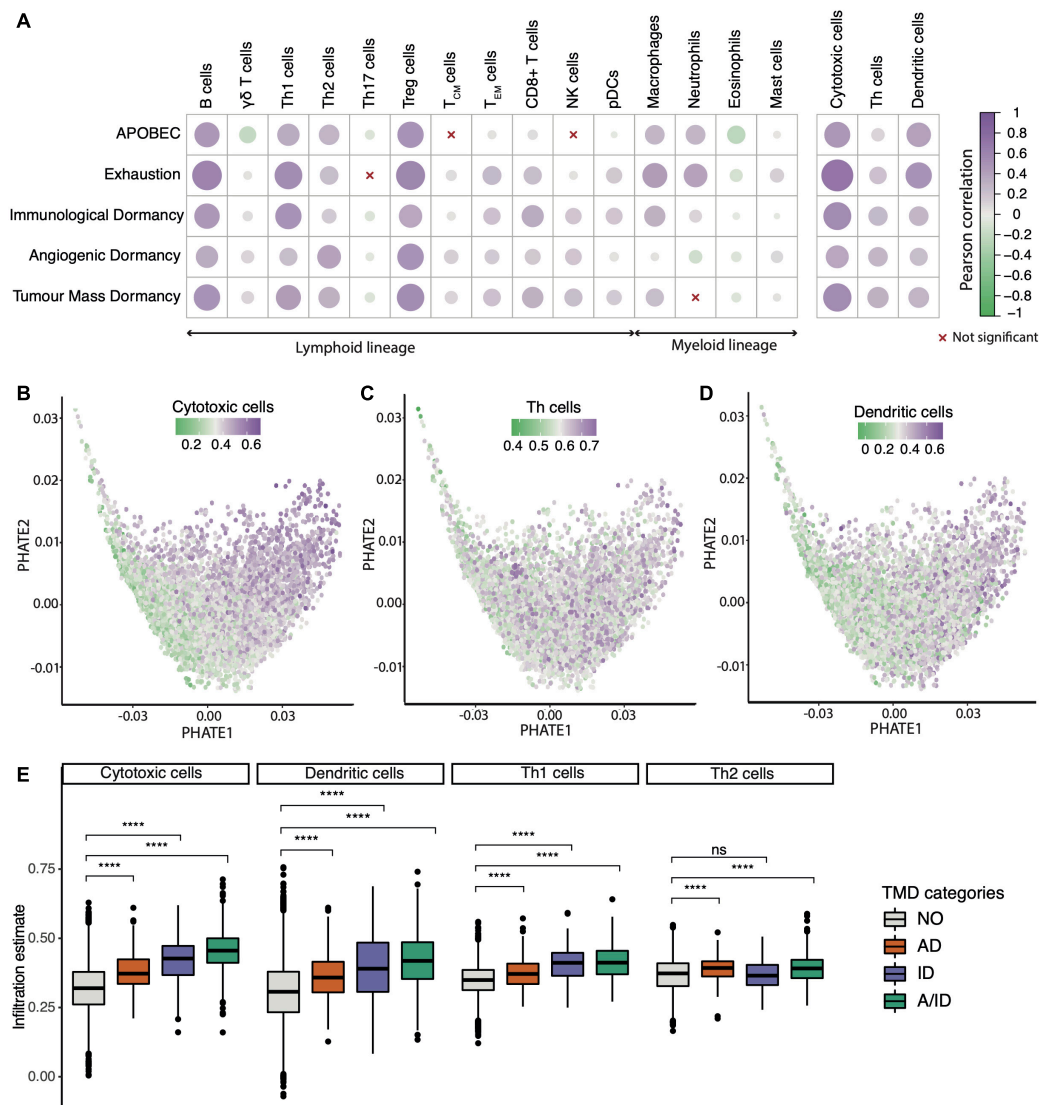


**FIGURE 6 |** Tumor microenvironment activity correlates with the TMD program. **(A)** Correlation between cell infiltration estimates and the APOBEC, exhaustion and dormancy program scores across the TCGA primary tumor samples. The three broader categories on the right hand side summarize the combined marker expression for all cytotoxic, T helper and dendritic cells. **(B–D)** PHATE dimensionality reduction of 9,631 primary tumor samples, based on the expression of genes driving the TMD and exhaustion programs, with removal of tissue specific expression patterns and colored by **(B)** cytotoxic cell enrichment score, **(C)** Th cell enrichment score and **(D)** dendritic cell enrichment score. **(E)** Cytotoxic T cell, Th1/Th2 and dendritic cell abundance compared between samples with angiogenic dormancy (AD), immunological dormancy (ID), both angiogenic and immunological dormancy (A/ID) and samples without TMD (NO); \*\*\*\* $p < 0.00001$ .

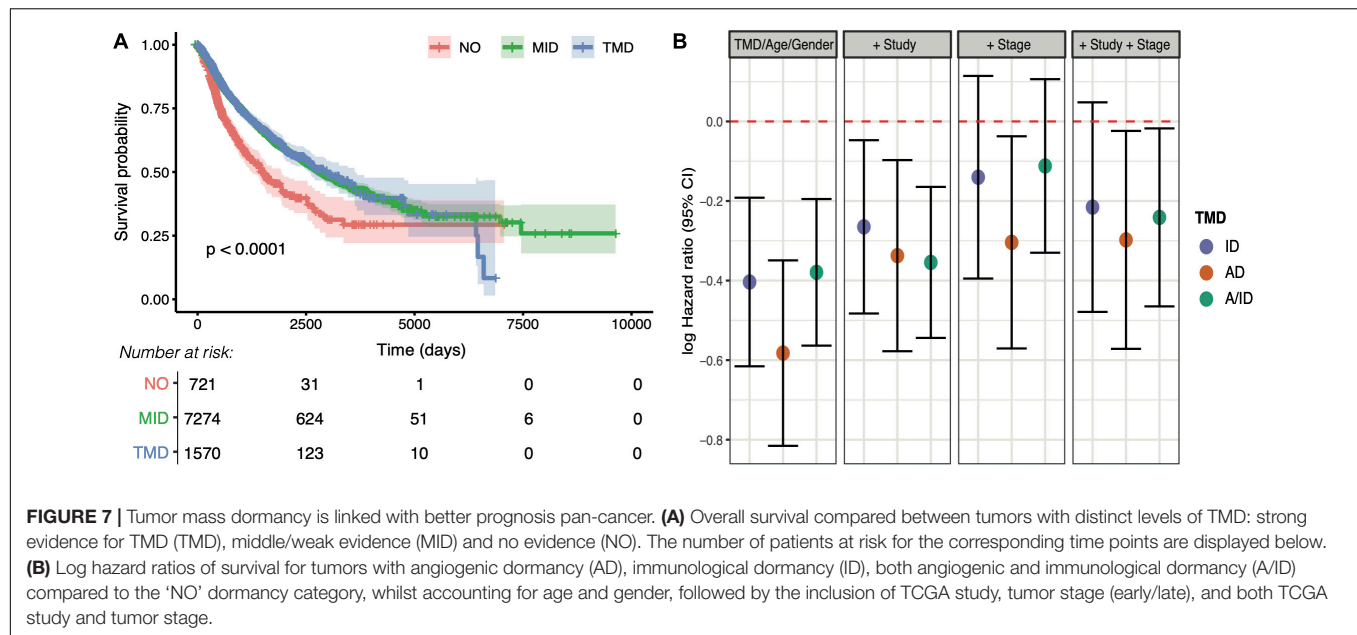
associations were observed for early- and late-stage cancers (**Supplementary Figures 33–36**).

## TMD Is Prognostic in Cancer

To understand the clinical relevance of TMD, we carried out survival analysis and found that patients with expanding tumors that presented no evidence of TMD had a significantly reduced prognosis (**Figure 7A**), consistent with the expectation that fast-proliferating tumors should be more aggressive than their dormant counterparts. To further dissect the potential sources of this variation along the immunity/angiogenesis axis, we employed Cox proportional hazards models to determine

the effects of different types of dormancy on survival whilst accounting for potential confounders such as patient age, gender, cancer type, and tumor stage. While all three categories were associated with decreased risk when compared to patients with no evidence of TMD, much of this variation was accounted for by tumor stage, with only angiogenic and tumor mass dormancy still marginally significant after correction (**Figure 7B** and **Supplementary Figures 37–41**). While the tumor stage effect may not be fully uncoupled from the TMD effect, TMD did present a marginal protective role within the early-stage tumors (stages I/II), as well as a larger protective role in late-stage tumors (stages III/IV) (**Supplementary Figure 42**).





## DISCUSSION

The TMD is a key state in tumor development and progression, but its evolutionary constraints are largely unknown. In this study, we have presented an overview of TMD across 31 cancer tissues and highlighted potential novel genomic hallmarks of this state. While TMD remains a poorly characterized program whose current known markers are undoubtedly incomplete, our approach to evaluating TMD in bulk tumors through an equilibrium of proliferation, apoptosis, cytotoxicity, exhaustion, and angiogenesis signals has enabled us to systematically capture this temporary state across a variety of cancers. We show that TMD-like signals are present across a multitude of cancer tissues, and that immunological and angiogenic dormancy are not always concomitant. We confirm many of the expected associations reported in the literature, including lower mutational burden, correlations with CD8+, regulatory and helper T cells (Teng et al., 2008), improved prognosis (Park and Nam, 2020) and a strong link with immune exhaustion (Mittal et al., 2014). Exhaustion is a phenotype that likely immediately follows TMD, but in our analysis the two states are largely overlapping. This is most likely due to the bulk nature of the samples analyzed, where we may be capturing parts of the tumor that starting to expand in addition to areas still displaying TMD. Interestingly, we find TMD tends to occur in normoxic rather than hypoxic environments in the majority of cases, which is different than what is observed for cellular quiescence (Qiu et al., 2017; Butturini et al., 2019).

In addition to expected associations, our methodology has also enabled us to capture previously unreported links between TMD and clinical or genomic characteristics. Firstly, while TMD would be expected to dominate in early-stage tumors, we also notice TMD-like signals in a comparable fraction of late-stage tumors (18%) (Supplementary Figure 8). In the absence of longitudinal data that could shed further light onto the causes, we

can only hypothesize this could be due to a mechanism of slowly advancing cancers that are maintained in a semi-TMD state, potentially enabled by a strong, consistent immune response.

Secondly, we find that oncogenic mutations in *CASP8* (inactivating) and *HRAS* (activating) are positively selected for during the development of TMD. This is either because they might confer an advantage in terms of maintaining TMD, or because they might enable cells to escape TMD and expand further. Interestingly, the selection pressure on *CASP8* in the context of TMD was seen across the entire tumor progression spectrum, while *HRAS* mutations appeared positively selected specifically in late-stage tumors. Counterbalancing these selective forces are *KRAS* hotspots that are preferentially depleted in the context of TMD. These findings could suggest distinct adaptive mechanisms in the context of early forming versus disseminated cancer in a temporary dormant state, as well as a complex “tug-of-war”-like regulation of tumor growth/arrest via Ras oncogenesis. Beyond these mutational associations, most of the classical cancer drivers were amplified or deleted preferentially in non-dormant tumors, while TMD appeared largely devoid of specific copy number marks. These observations may be partly explained by an association with early stage cancers, where these changes have not yet occurred as a means of expansion and escape from immune surveillance.

In concordance with the reduced rate of cell proliferation in TMD, we found that aging-induced mutations, which are believed to accumulate at a relatively constant rate in cancer, were lesser represented in dormant tumors. Correlations between TMD and several other mutational processes (smoking, defective DNA repair) were noted, which might suggest that multiple neoplastic mechanisms that are tissue-specific could favor this state.

A remarkably consistent signal came from the mutagenesis trace left by the APOBEC enzyme family. APOBEC activity

appeared strongly linked with the exhaustion signals that presumably follow TMD, and with immunological dormancy. Several studies (Burns et al., 2013; Swanton et al., 2015; Yamazaki et al., 2019) have proposed that APOBEC expression may be one of the drivers of tumorigenesis, suggesting a role for APOBECs in evading the immune response. APOBEC3 signatures are prevalent in leukaemias (Rebhandl et al., 2014), while AID was demonstrated to induce hypermutation and chromosomal translocation in B cell lymphomas (Robbiani and Nussenzweig, 2013). On the other hand, APOBEC may promote the formation of neoantigens and activate cytotoxic T cell responses. It was shown that the APOBEC3 class of enzymes is upregulated in immune cells (monocytes, macrophages and pDCs) upon treatment with interferon  $\gamma$  (Wang et al., 2008; Stenglein et al., 2010). In ovarian carcinoma, the expression of APOBEC3G was positively correlated with T cell infiltration, expression of cytotoxic granzyme and perforin (GZMB and PRF1), and improved clinical outcome (Leonard et al., 2016). Moreover, APOBEC mutagenesis has previously been linked with responses to immunotherapy in lung, melanoma and head and neck cancers (Wang et al., 2018; Faden et al., 2019; Driscoll et al., 2020) through the induction of heteroclitic neoepitopes. We have demonstrated increased APOBEC mutagenesis in a TMD setting across multiple tumor types, and have shown that this process appears linked with the regulation of angiogenesis by the uPAR system. It is possible that the mutational footprint left in the genome by such activity enables immune recognition and maintenance of TMD in the time span until exhaustion and immune escape occurs. This could suggest a window of opportunity for the employment of checkpoint inhibitors, possibly in combination with APOBEC inhibitors, in early-stage tumors with TMD.

Our pan-cancer analysis unveils a complex interplay between TMD, exhaustion and APOBEC activity, and a mutational context that may enable these phenotypes to develop. However, it is possible that some of the associations uncovered may be due to the direct association between APOBEC activity and immune responses/exhaustion or hypoxia, which have been previously reported in the literature as highlighted above, rather than with tumor mass dormancy itself. Future experimental studies will be needed to verify and further understand the implications of increased APOBEC mutagenesis in a TMD-specific context. Moreover, changes in gene expression may not accurately reflect changes in the abundance of protein products in our defined dormancy and exhaustion programs. Biochemical assays and studies in model organisms will give a more definite answer to the nature of these relationships.

An important limitation of this analysis consists in the fact that there are no currently available datasets describing transcriptional changes specifically in the context of tumor mass dormancy. This phenotype is difficult to study due to its temporary nature and few model systems for this state exist. We have therefore not been able to unequivocally determine whether the chosen scoring method and even the cut-offs employed for assessing TMD capture this phenomenon in the most accurate manner. However, we are taking a conservative approach focusing only on the most extreme values, which are most likely

to reflect this state. This approach appears methodologically robust to small fluctuations in expression/gene signatures, and the associations identified have been validated in independent datasets. Moreover, the key findings of CASP8 positive selection in TMD, associations with APOBEC mutagenesis and cytotoxic microenvironment were also reproducible using the PCA-based scoring methodology (**Supplementary Figures 43–48**). Further experimental evidence is needed to verify the biological nature of these associations and the most appropriate way of evaluating TMD, once experimental model systems for this state will have become more widely available and easier to study.

Another limitation refers to the fact that the samples analyzed have been profiled using bulk sequencing methods, which means that we are only capturing an average cellular signal across the entire tumor which may not reflect its true heterogeneity. Furthermore, since TMD is a temporary phenotype, a single static snapshot of tumors, even in this large dataset, may not be sufficient to capture the entire array of TMD phenotypes that might develop in different tissues. Therefore, multi-regional sequencing and longitudinal studies should be conducted in the future to shed further light on the diversity and dynamics of TMD phenotypes.

Furthermore, our study focused mainly on pan-cancer markers of TMD, due to the scarcity of this phenotype. From our analyses, we observe TMD is frequent in certain tissues such as head and neck, breast, bone, and has weak evidence or complete absence of signals in others, e.g., chromophobe renal cell carcinoma. Some of the smaller studies from TCGA may be insufficiently powered to capture such signals. Therefore, future studies should focus on an in-depth characterization of TMD in distinct tissues and should be able to pinpoint tissue-specific genomic markers linked to TMD. Finally, the potential genomic biomarkers of dormancy that we identified need to be confirmed through experimental validation in suitable *in vitro/in vivo* models of TMD.

Overall, our study provides evidence for TMD, immunological and angiogenic dormancy signals across a variety of cancer types, and highlights key associated intrinsic and extrinsic hallmarks, including CASP8/RAS dependencies, APOBEC mutagenesis and hypoxia. These findings pave the way for further exploration of the mechanisms underlying TMD emergence, maintenance and exit.

## MATERIALS AND METHODS

### Datasets

FPKM normalized RNA-sequencing expression data as well as mutation annotation files aligned against the hg38 genome from the Muse pipeline, were downloaded using the TCGA *Abiolinks* R package (Colaprico et al., 2016) for 9,712 treatment-naïve primary tumor TCGA samples across 31 solid cancer types. For patients with multiple samples available, one RNA-seq barcode entry was randomly selected for each individual patient resulting in 9,631 total entries. All expression data were log-transformed for downstream analysis.

For validation, RNA-seq and matched whole-genome sequencing data were downloaded for 12 cancer studies from the ICGC Data Portal (Zhang et al., 2019), accompanied by RNA-seq and matched targeted sequencing from cBioPortal (Cerami et al., 2012) for the following datasets: *blca\_mskcc\_solit\_2012* = Bladder Cancer (MSKCC, J Clin Onco 2013); *brca\_metabric* = Breast Cancer (METABRIC, Nature 2012 and Nat Commun 2016); *prad\_mskcc* = Prostate Adenocarcinoma (MSKCC, Cancer Cell 2010); *sarc\_mskcc* = Sarcoma (MSKCC/Broad, Nat Genet 2010); whole-genome sequencing from *rt\_target\_2018\_pub* = Pediatric Rhabdoid Tumor (TARGET, 2018) and *prostate\_dkfz\_2018* = Prostate Cancer (DKFZ, Cancer Cell 2018); and whole-exome sequencing from: *brca\_smc\_2018* = Breast Cancer (SMC 2018); *GIS031* = Lung adenocarcinoma (GIS, Nat Genet 2019); *paad\_qcmg\_uq\_2016* = Pancreatic Adenocarcinoma (QCMG, Nature 2016); *prad\_broad* = Prostate Adenocarcinoma (Broad/Cornell, Nat Genet 2012); *utuc\_cornell\_baylor\_mdacc\_2019* = Upper Tract Urothelial Carcinoma (Cornell/Naylor/MDACC, Nat Commun 2019); *wt\_target\_2018\_pub* = Pediatric Wilm's Tumor (TARGET, 2018). The data were processed and analyzed in the same manner as the TCGA data.

## Quantifying the Dormancy, Exhaustion and APOBEC Programs

Mean log-transformed expression values of genes deemed to be associated with a given program by manual curation of the literature (**Supplementary Table 1**) were used to produce per-sample program scores for TMD, immunological/angiogenic dormancy, exhaustion and APOBEC activity. We have specifically selected genes that have been associated with immunological and angiogenic dormancy, rather than generic immunity or angiogenesis processes, in order to ensure that any associations identified downstream are likely to be TMD-related.

The APOBEC and exhaustion program scores were calculated by taking the mean expression of genes within the respective programs, as all genes in the programs were expected to be upregulated in the respective states.

The angiogenic and immunological dormancy (AD/ID) program scores, as well as the TMD scores, were calculated using two different approaches:

### Scaled Difference of Means

For every sample in the cohort, a score  $S$  was derived by subtracting the sum of expression values of downregulated genes ( $E_d$ ) in the respective program from the sum of expression values of upregulated genes ( $E_u$ ) and dividing by the total number of genes within the program ( $N_u + N_d$ , where  $N_u$  is the total number of upregulated genes and  $N_d$  is the total number of downregulated genes):

$$S = \frac{\sum_i^{N_u} E_{u,i} - \sum_j^{N_d} E_{d,j}}{N_u + N_d}$$

## Principal Component Analysis (PCA)

Principal component analysis was performed across the pan-cancer dataset using the up- and downregulated gene signature of the respective program. The dormancy score was extracted as the coordinate of the first principal component (PC1).

The proliferation/apoptosis ratio was calculated by dividing the average expression of E2F target genes [including MKI67, a classical proliferation marker (Miller et al., 2018)], obtained from the “HALLMARK\_E2F\_TARGETS” gene list, by the average expression of genes involved in apoptosis from the “HALLMARK\_APOPTOSIS” gene list. Both gene lists are part of the “H: hallmark gene sets” collection deposited at MSigDB.

Samples with high TMD were identified as being within the upper quartile of the TMD program score range and presenting a ratio of proliferation/apoptosis < 1. Dormant samples were further classified as having immunological and/or angiogenic dormancy based on whether they were in the upper quartile of the angiogenic (AD) and/or immunological dormancy (ID) program score range, respectively. Samples with no evidence for TMD (expanding tumors, marked as ‘NO’) were identified as being in the lower quartile of the TMD program score range and showing a ratio of proliferation/apoptosis > 1. The remaining samples (‘MID’ category) were classed as having middle levels of expansion with some weak potential evidence of dormancy, but biologically unlikely to be dormant.

## Assessing the Robustness of the AD/ID Program Scores

To assess the relative robustness of the three methodologies employed to calculate the TMD and AD/ID scores, we took two approaches:

- (1) We systematically removed one gene from the respective program at a time and recalculated the scores.
- (2) A small amount of random noise was added to the expression of each gene in the signature, measured in each sample and scores were recalculated. The *jitter* R function was used to introduce variable amounts of noise in the data, by changing the factor variable level between 1 and 200. For each level of noise, the approach was repeated 100 times and the scores were recalculated.

The overall variability of the fold changes in the new score compared to the original scores was compared between the ‘scaled difference of means’ and PCA-based methods.

## Assessing the Robustness of APOBEC Associations

Correlations between the mean expression of APOBEC-related genes and random gene expression programs were calculated by randomly selecting an equal number of genes to that found in the TMD signatures (35) from the genome and assessing the mean expression correlation with APOBEC activity. 1,000 iterations were performed. Associations varied as shown in **Supplementary Figure 24**, and were consistently



lower than the one calculated for TMD. *P*-values were frequently significant, but this is likely due to the large number of samples.

## PHATE Dimensionality Reduction

The *phateR* R package (Moon et al., 2019) was used to perform the dimensionality reduction based on the expression of genes associated with the TMD and exhaustion programs. A constant seed was used for reproducibility. The *ComBat* function from the *sva* R package (Leek et al., 2012) was used to remove tissue-specific expression patterns from the TCGA RNA-seq data.

## Association Between Cancer Driver Mutations and TMD

The COSMIC database (Tate et al., 2019) was used to source a list of 723 known drivers of tumorigenesis (Tiers 1 + 2). COSMIC genes mutated in at least 1% of samples across all solid primary tumor samples were tested for enrichment or depletion of mutations between samples with high and low TMD using a Fisher's exact test. Only missense, nonsense, non-stop, frameshift deletion/insertion and inframe insertion/deletion mutations were considered in the analysis. For *HRAS*, *KRAS*, and *NRAS*, a Fisher's exact test was also performed to test for enrichment or depletion of specific recurrent hotspot mutations, reported by the cBioPortal data hub and based in part on methodology from Chang et al. (2016) and Gao et al. (2017). The analysis was also repeated on a cancer-by-cancer basis, where COSMIC genes mutated in at least 5% of samples within the cancer-specific study sample were tested for enrichment or depletion of mutations with TMD samples. The *p*-values were corrected using Benjamini–Hochberg (BH) procedure to accommodate for multiple testing.

Enrichment analysis was reaffirmed using a random forest classification approach. This was conducted using the *randomForest* R package. A balanced dataset of samples with high and low TMD was generated by utilizing all samples with low TMD (*n* = 657), and randomly sampling an equal number of samples with high TMD (*n* = 1,154). The resulting random forest consisted of 500 trees, and mutation enrichment was determined by calculating the mean decrease in Gini index between the two groups following the removal of a gene.

To identify genes that are positively selected in the context of TMD, we carried out dN/dS analysis separately for high and low TMD samples using the *dNdScv* R package (Martincorena et al., 2017), run with default parameters.

## Mutational Signature Analysis

Mutational signature contributions were inferred using *deconstructSigs* (Rosenthal et al., 2016) and the choice of signatures was further informed using results from *SigProfiler* (Alexandrov et al., 2013b). Only samples with at least 50 mutations were employed in the analysis, for a total of 6,410 samples.

*SigProfiler* was used to infer mutational signatures from TCGA whole-exome sequencing data. For each TCGA study

of interest, input mutational matrices were generated using the *SigProfilerMatrixGeneratorR* function using all samples containing at least 50 mutations and aligning the MAF files to the hg38 genome build. *SigProfilerExtractorR* was used to extract *de novo* mutational signatures for each cancer type. For each study, the solution with the greatest number of mutational signatures was chosen, for which also the sum of the solution stability (calculated average silhouette coefficient) and minimum stability exceeded 1, and the minimum stability value did not fall below 0.4. For the selected solutions, the identity of the mutational signatures was determined by calculating cosine similarities with COSMIC v3.1 mutational signatures.

Mutational signatures from whole-exome sequencing data were also inferred using the *deconstructSigs* R package. MAF files were aligned against the hg38 genome build and the COSMIC v3.1 mutational signatures were employed in the analysis. For each cancer type, the contribution of all signatures within the *deconstructSigs* solution was set to 0, apart from SBS1, SBS5, signatures identified in the corresponding *SigProfiler* solution, as well as signatures which contribute on average at least 5% of mutations across all samples within the *deconstructSigs* solution. For cancer types where *SigProfiler* did not result in a stable solution, the *deconstructSigs* solution was used with the contribution of all signatures set to 0, apart from SBS1, SBS5 as well as signatures which contribute at least 5% of mutations across samples within the *deconstructSigs* solution.

## Tumor Microenvironment Deconvolution From Bulk RNA-Seq Data

The tumor microenvironment cell infiltration scores were calculated using the *ConsensusTME* R package (Jiménez-Sánchez et al., 2019) based on gene sets from Bindea et al. (2013). Cell abundance was estimated from the TCGA bulk RNA-seq data using single sample Gene Set Enrichment Analysis (ssGSEA). Broader categories (cytotoxic cells, Th cells, dendritic cells) were scored by combining the expression across subtype-specific markers.

## Identification of APOBEC Mutagenesis Clusters

First, APOBEC enrichment scores were calculated using the *sigminer* R package (Wang et al., 2020). Next, the mutational signature profiles of 6,410 samples underwent dimensionality reduction with tSNE using the *Rtsne* R package, followed by expectation-maximization clustering using the *EMCluster* R package. The optimal number of clusters was determined by considering the associated increase in log-likelihood pertaining to additional clusters and was assumed to be equivalent for all applications of tSNE (Supplementary Figure 9A). Whilst substantial increases were associated with both 10 and 17 clusters, we selected 10 clusters in order to prevent the cluster of APOBEC-enriched samples from being segmented. The APOBEC-enriched cluster was identified as the cluster with the highest median collective enrichment of APOBEC signatures SBS2 and SBS13. The procedure was conducted 100



times and samples which appeared in the APOBEC-enriched cluster on more than 50 occasions were labeled as 'APOBEC enriched.'

## Random Forest Modeling of APOBEC Mutagenesis-Gene Expression Associations

Z-score normalization of RNA-sequencing expression data was applied across each cancer type individually. The FPKM-normalized values were log-transformed, and the results for each gene were transformed into a  $Z \sim N(0,1)$  distribution using the scale function in R. Only genes involved in the dormancy and exhaustion programs were considered as input in the classifier.

Genes whose expression contributed to APOBEC enrichment classification were identified using machine learning via a random forest approach, conducted using the *randomForest* R package. In total, 5,850 samples were included for which Z-scores and mutational signature profiles were available. Each random forest model required all samples labeled as APOBEC-enriched ( $n = 952$ ), and an equal number of samples taken randomly without replacement from the non-APOBEC-enriched samples to generate balanced groups. Each random forest consisted of 1,000 trees. The importance of each gene in the model, measured as the associated mean decrease in Gini index following its removal, was also calculated. This procedure was run 100 times.

Changes in median gene expression between the APOBEC enriched and non-enriched groups (Figure 4H) were determined using a two-sample Wilcoxon rank-sum test. P-values were corrected for multiple testing using the Benjamini–Hochberg procedure.

## Calculation of Hypoxia Scores

Hypoxia scores were calculated using three transcription-based hypoxia signatures referred to as Buffa (Buffa et al., 2010), West (Eustace et al., 2013), and Winter (Winter et al., 2007), following the calculation procedure detailed by Bhandari et al. (2019). Genes which were included in the curated dormancy or exhaustion signatures were subsequently removed from the respective hypoxia signature. Scores were calculated based on the pan-cancer cohort to enable variation in hypoxia between cancer types to be identified. Since we observed a high degree of agreement between the three signatures (Supplementary Figure 11), the Buffa signature was employed in the downstream analysis on account of its use as a reference by Bhandari et al. (2019). A binning approach with a window size of 10 was employed to further subdivide tumors into discrete subgroups with increasing levels of hypoxia.

## Survival Analysis

Survival analysis was conducted via the *survival* R package. Hazard ratios were calculated using Cox proportional hazards models and were displayed using the *finalfit* R package. Survival curves were calculated

using the Kaplan–Meier formula, and plotted using the *survminer* R package.

## Statistics

Pairwise correlations were calculated using the Pearson correlation statistics. The *corrplot* R package was used to carry out statistical analysis and visualize the correlation matrices. Groups were compared using the Student's *t*-test, Wilcoxon rank-sum test or Kruskal–Wallis test as appropriate. Multiple testing correction was applied using the Benjamini–Hochberg method. The significance threshold was taken as  $p < 0.05$ .

## Code

All code developed for the purpose of this analysis can be found at the following repository: <https://github.com/secrierlab/tumourMassDormancy/tree/v1.0>.

## DATA AVAILABILITY STATEMENT

Publicly available datasets were analyzed in this study. This data can be found here: <https://portal.gdc.cancer.gov/> (TCGA Genomics Data Commons Data Portal).

## ETHICS STATEMENT

Ethical review and approval was not required for the study on human participants in accordance with the local legislation and institutional requirements. Written informed consent for participation was not required for this study in accordance with the national legislation and the institutional requirements.

## AUTHOR CONTRIBUTIONS

MS designed and supervised the study. AW, DJ, and WL performed the analyses. All authors wrote and approved the manuscript.

## FUNDING

AW and DJ were supported by MRCDTP grants (MR/N013867/1). MS was supported by a UKRI Future Leaders Fellowship (MR/T042184/1), an Academy of Medical Sciences Springboard Award (SBF004\1042), and a Wellcome Trust Seed Award in Science (215296/Z/19/Z).

## SUPPLEMENTARY MATERIAL

The Supplementary Material for this article can be found online at: <https://www.frontiersin.org/articles/10.3389/fcell.2021.698659/full#supplementary-material>

## REFERENCES

- Aguirre Ghiso, J. A. (2002). Inhibition of FAK signaling activated by urokinase receptor induces dormancy in human carcinoma cells in vivo. *Oncogene* 21, 2513–2524. doi: 10.1038/sj.onc.1205342
- Aguirre Ghiso, J. A., Kovalski, K., and Ossowski, L. (1999). Tumor dormancy induced by downregulation of urokinase receptor in human carcinoma involves integrin and MAPK signaling. *J. Cell Biol.* 147, 89–104. doi: 10.1083/jcb.147.1.89
- Aguirre-Ghiso, J. A. (2007). Models, mechanisms and clinical evidence for cancer dormancy. *Nat. Rev. Cancer* 7, 834–846. doi: 10.1038/nrc2256
- Aguirre-Ghiso, J. A., Estrada, Y., Liu, D., and Ossowski, L. (2003). ERK(MAPK) activity as a determinant of tumor growth and dormancy; regulation by p38(SAPK). *Cancer Res.* 63, 1684–1695.
- Alexandrov, L. B., Jones, P. H., Wedge, D. C., Sale, J. E., Campbell, P. J., Nik-Zainal, S., et al. (2015). Clock-like mutational processes in human somatic cells. *Nat. Genet.* 47, 1402–1407. doi: 10.1038/ng.3441
- Alexandrov, L. B., Kim, J., Haradhvala, N. J., Huang, M. N., Tian Ng, A. W., Wu, Y., et al. (2020). The repertoire of mutational signatures in human cancer. *Nature* 578, 94–101. doi: 10.1038/s41586-020-1943-3
- Alexandrov, L. B., Nik-Zainal, S., Wedge, D. C., Aparicio, S. A., Behjati, S., Biankin, A. V., et al. (2013a). Signatures of mutational processes in human cancer. *Nature* 500, 415–421. doi: 10.1038/nature12477
- Alexandrov, L. B., Nik-Zainal, S., Wedge, D. C., Campbell, P. J., and Stratton, M. R. (2013b). Deciphering signatures of mutational processes operative in human cancer. *Cell Rep.* 3, 246–259. doi: 10.1016/j.celrep.2012.12.008
- Asnaghi, L., Lin, M. H., Lim, K. S., Lim, K. J., Tripathy, A., Wendeborn, M., et al. (2014). Hypoxia promotes uveal melanoma invasion through enhanced Notch and MAPK activation. *PLoS One* 9:e105372. doi: 10.1371/journal.pone.0105372
- Bailey, S. R., Nelson, M. H., Himes, R. A., Li, Z., Mehrotra, S., and Paulos, C. M. (2014). Th17 cells in cancer: the ultimate identity crisis. *Front. Immunol.* 5:276. doi: 10.3389/fimmu.2014.00276
- Barr, A. R., Cooper, S., Heldt, F. S., Butera, F., Stoy, H., Mansfeld, J., et al. (2017). DNA damage during S-phase mediates the proliferation-quiescence decision in the subsequent G1 via p21 expression. *Nat. Commun.* 8:14728. doi: 10.1038/ncomms14728
- Benci, J. L., Xu, B., Qiu, Y., Wu, T. J., Dada, H., Twyman-Saint Victor, C., et al. (2016). Tumor interferon signaling regulates a multigenic resistance program to immune checkpoint blockade. *Cell* 167, 1540–1554.e12. doi: 10.1016/j.cell.2016.11.022
- Bhandari, V., Hoey, C., Liu, L. Y., Lalonde, E., Ray, J., Livingstone, J., et al. (2019). Molecular landmarks of tumor hypoxia across cancer types. *Nat. Genet.* 51, 308–318. doi: 10.1038/s41588-018-0318-2
- Bindea, G., Mlecnik, B., Tosolini, M., Kirilovsky, A., Waldner, M., Obenaus, A. C., et al. (2013). Spatiotemporal dynamics of intratumoral immune cells reveal the immune landscape in human cancer. *Immunity* 39, 782–795. doi: 10.1016/j.immuni.2013.10.003
- Boire, A., Coffelt, S. B., Quezada, S. A., Vander Heiden, M. G., and Weeraratna, A. T. (2019). Tumour dormancy and reawakening: opportunities and challenges. *Trends Cancer* 5, 762–765. doi: 10.1016/j.trecan.2019.10.010
- Boman, B. M., and Fields, J. Z. (2013). An APC:WNT counter-current-like mechanism regulates cell division along the human colonic crypt axis: a mechanism that explains how APC mutations induce proliferative abnormalities that drive colon cancer development. *Front. Oncol.* 3:244. doi: 10.3389/fonc.2013.00244
- Buffa, F. M., Harris, A. L., West, C. M., and Miller, C. J. (2010). Large meta-analysis of multiple cancers reveals a common, compact and highly prognostic hypoxia metagene. *Br. J. Cancer* 102, 428–435. doi: 10.1038/sj.bjc.6605450
- Burns, M. B., Temiz, N. A., and Harris, R. S. (2013). Evidence for APOBEC3B mutagenesis in multiple human cancers. *Nat. Genet.* 45, 977–983. doi: 10.1038/ng.2701
- Butturini, E., Carcereri de Prati, A., Boriero, D., and Mariotto, S. (2019). Tumor dormancy and interplay with hypoxic tumor microenvironment. *Int. J. Mol. Sci.* 20:4305. doi: 10.3390/ijms20174305
- Cerami, E., Gao, J., Dogrusoz, U., Gross, B. E., Sumer, S. O., Aksoy, B. A., et al. (2012). The cBio cancer genomics portal: an open platform for exploring multidimensional cancer genomics data. *Cancer Discov.* 2, 401–404. doi: 10.1158/2159-8290.CD-12-0095
- Chang, M. T., Asthana, S., Gao, S. P., Lee, B. H., Chapman, J. S., Kandoth, C., et al. (2016). Identifying recurrent mutations in cancer reveals widespread lineage diversity and mutational specificity. *Nat. Biotechnol.* 34, 155–163. doi: 10.1038/nbt.3391
- Chen, H., Chong, W., Wu, Q., Yao, Y., Mao, M., and Wang, X. (2019). Association of *LRPIB* mutation with tumor mutation burden and outcomes in melanoma and non-small cell lung cancer patients treated with immune check-point blockades. *Front. Immunol.* 10:1113. doi: 10.3389/fimmu.2019.01113
- Chen, L., Endler, A., and Shibasaki, F. (2009). Hypoxia and angiogenesis: regulation of hypoxia-inducible factors via novel binding factors. *Exp. Mol. Med.* 41, 849–857. doi: 10.3858/emmm.2009.41.12.103
- Chin, Y. E., Kitagawa, M., Su, W. C., You, Z. H., Iwamoto, Y., and Fu, X. Y. (1996). Cell growth arrest and induction of cyclin-dependent kinase inhibitor p21 WAF1/CIP1 mediated by STAT1. *Science* 272, 719–722. doi: 10.1126/science.272.5262.719
- Colaprico, A., Silva, T. C., Olsen, C., Garofano, L., Cava, C., Garolini, D., et al. (2016). TCGAAbiolinks: an R/Bioconductor package for integrative analysis of TCGA data. *Nucleic Acids Res.* 44:e71. doi: 10.1093/nar/gkv1507
- Damen, M. P. F., van Rheenen, J., and Scheele, C. L. G. J. (2020). Targeting dormant tumor cells to prevent cancer recurrence. *FEBS J.* doi: 10.1111/febs.15626
- De Blasio, A., Di Fiore, R., Morreale, M., Carlisi, D., Drago-Ferrante, R., Montalbano, M., et al. (2016). Unusual roles of caspase-8 in triple-negative breast cancer cell line MDA-MB-231. *Int. J. Oncol.* 48, 2339–2348. doi: 10.3892/ijo.2016.3474
- Degasperi, A., Amarante, T. D., Czarnecki, J., Shooter, S., Zou, X., Glodzik, D., et al. (2020). A practical framework and online tool for mutational signature analyses show inter-tissue variation and driver dependencies. *Nat. Cancer* 1, 249–263. doi: 10.1038/s43018-020-0027-5
- Driscoll, C. B., Schuelke, M. R., Kottke, T., Thompson, J. M., Wongthida, P., Tonne, J. M., et al. (2020). APOBEC3B-mediated corruption of the tumor cell immunopeptidome induces heteroclitic neoepitopes for cancer immunotherapy. *Nat. Commun.* 11:790. doi: 10.1038/s41467-020-14568-7
- Dunn, G. P., Koebel, C. M., and Schreiber, R. D. (2006). Interferons, immunity and cancer immunoediting. *Nat. Rev. Immunol.* 6, 836–848. doi: 10.1038/nri1961
- Dunn, G. P., Old, L. J., and Schreiber, R. D. (2004a). The immunobiology of cancer immunosurveillance and immunoediting. *Immunity* 21, 137–148. doi: 10.1016/j.immuni.2004.07.017
- Dunn, G. P., Old, L. J., and Schreiber, R. D. (2004b). The three Es of cancer immunoediting. *Annu. Rev. Immunol.* 22, 329–360. doi: 10.1146/annurev.immunol.22.012703.104803
- Eustace, A., Mani, N., Span, P. N., Irlam, J. J., Taylor, J., Betts, G. N., et al. (2013). A 26-gene hypoxia signature predicts benefit from hypoxia-modifying therapy in laryngeal cancer but not bladder cancer. *Clin. Cancer Res.* 19, 4879–4888. doi: 10.1158/1078-0432.CCR-13-0542
- Faden, D. L., Ding, F., Lin, Y., Zhai, S., Kuo, F., Chan, T. A., et al. (2019). APOBEC mutagenesis is tightly linked to the immune landscape and immunotherapy biomarkers in head and neck squamous cell carcinoma. *Oral. Oncol.* 96, 140–147. doi: 10.1016/j.oraloncology.2019.07.020
- Finn, O. J. (2006). Human tumor antigens, immunosurveillance, and cancer vaccines. *Immunol. Res.* 36, 73–82. doi: 10.1385/IR.36:1:73
- Forcet, C., Ye, X., Granger, L., Corset, V., Shin, H., Bredesen, D. E., et al. (2001). The dependence receptor DCC (deleted in colorectal cancer) defines an alternative mechanism for caspase activation. *Proc. Natl. Acad. Sci. U.S.A.* 98, 3416–3421. doi: 10.1073/pnas.051378298
- Gao, J., Chang, M. T., Johnsen, H. C., Gao, S. P., Sylvester, B. E., Sumer, S. O., et al. (2017). 3D clusters of somatic mutations in cancer reveal numerous rare mutations as functional targets. *Genome Med.* 9:4. doi: 10.1186/s13073-016-0393-x
- Gerlinger, M., McGranahan, N., Dewhurst, S. M., Burrell, R. A., Tomlinson, I., and Swanton, C. (2014). Cancer: evolution within a lifetime. *Annu. Rev. Genet.* 48, 215–236. doi: 10.1146/annurev-genet-120213-092314
- Ghorani, E., Reading, J. L., Henry, J. Y., de Massy, M. R., Rosenthal, R., Turati, V., et al. (2020). The T cell differentiation landscape is shaped by tumour mutations in lung cancer. *Nat. Cancer* 1, 546–561. doi: 10.1038/s43018-020-0066-y
- Gimbrone, M. A., Leapman, S. B., Cotran, R. S., and Folkman, J. (1972). Tumor dormancy in vivo by prevention of neovascularization. *J. Exp. Med.* 136, 261–276. doi: 10.1084/jem.136.2.261

- Green, A. M., and Weitzman, M. D. (2019). The spectrum of APOBEC3 activity: from anti-viral agents to anti-cancer opportunities. *DNA Repair. (Amst)* 83:102700. doi: 10.1016/j.dnarep.2019.102700
- Gužvić, M., and Klein, C. A. (2013). Cancer dormancy: time to explore its clinical relevance. *Breast Cancer Res.* 15:321. doi: 10.1186/bcr3590
- Hadfield, G. (1954). The dormant cancer cell. *Br. Med. J.* 2, 607–610. doi: 10.1136/bmj.2.4888.607
- Heldt, F. S., Barr, A. R., Cooper, S., Bakal, C., and Novák, B. (2018). A comprehensive model for the proliferation-quiescence decision in response to endogenous DNA damage in human cells. *Proc. Natl. Acad. Sci. U.S.A.* 115, 2532–2537. doi: 10.1073/pnas.1715345115
- Holmgren, L., O'Reilly, M. S., and Folkman, J. (1995). Dormancy of micrometastases: balanced proliferation and apoptosis in the presence of angiogenesis suppression. *Nat. Med.* 1, 149–153. doi: 10.1038/nm0295-149
- Huang, S. (2021). Reconciling non-genetic plasticity with somatic evolution in cancer. *Trends Cancer* 7, 309–322. doi: 10.1016/j.trecan.2020.12.007
- Ikedo, H., Old, L. J., and Schreiber, R. D. (2002). The roles of IFN gamma in protection against tumor development and cancer immunoediting. *Cytokine Growth Factor Rev.* 13, 95–109. doi: 10.1016/s1359-6101(01)00038-7
- Itahana, K., Dimri, G. P., Hara, E., Itahana, Y., Zou, Y., Desprez, P. Y., et al. (2002). A role for p53 in maintaining and establishing the quiescence growth arrest in human cells. *J. Biol. Chem.* 277, 18206–18214. doi: 10.1074/jbc.M201028200
- Jager, M., Blokzijl, F., Kuijk, E., Bertl, J., Vougioukalaki, M., Janssen, R., et al. (2019). Deficiency of nucleotide excision repair is associated with mutational signature observed in cancer. *Genome Res.* 29, 1067–1077. doi: 10.1101/gr.246223.118
- Jahanban-Esfahlan, R., Seidi, K., Manjili, M. H., Jahanban-Esfahlan, A., Javaheri, T., and Zare, P. (2019). Tumor cell dormancy: threat or opportunity in the fight against cancer. *Cancers (Basel)* 11:1207. doi: 10.3390/cancers11081207
- Jelaković, B., Castells, X., Tomić, K., Ardin, M., Karanović, S., and Zavadil, J. (2015). Renal cell carcinomas of chronic kidney disease patients harbor the mutational signature of carcinogenic aristolochic acid. *Int. J. Cancer* 136, 2967–2972. doi: 10.1002/ijc.29338
- Jiménez-Sánchez, A., Cast, O., and Miller, M. L. (2019). Comprehensive benchmarking and integration of tumor microenvironment cell estimation methods. *Cancer Res.* 79, 6238–6246. doi: 10.1158/0008-5472.CAN-18-3560
- Kato, M. (2012). Function and cancer genomics of FAT family genes (review). *Int. J. Oncol.* 41, 1913–1918. doi: 10.3892/ijo.2012.1669
- Kim, M. J., Cervantes, C., Jung, Y. S., Zhang, X., Zhang, J., Lee, S. H., et al. (2021). PAF remodels the DREAM complex to bypass cell quiescence and promote lung tumorigenesis. *Mol. Cell* 81, 1698–1714.e6. doi: 10.1016/j.molcel.2021.02.001
- Koebel, C. M., Vermi, W., Swann, J. B., Zerafa, N., Rodig, S. J., Old, L. J., et al. (2007). Adaptive immunity maintains occult cancer in an equilibrium state. *Nature* 450, 903–907. doi: 10.1038/nature06309
- Krock, B. L., Skuli, N., and Simon, M. C. (2011). Hypoxia-induced angiogenesis: good and evil. *Genes Cancer* 2, 1117–1133. doi: 10.1177/1947601911423654
- Kundu, A., Nam, H., Shelar, S., Chandrashekar, D. S., Brinkley, G., Karki, S., et al. (2020). PRDM16 suppresses HIF-targeted gene expression in kidney cancer. *J. Exp. Med.* 217:e20191005. doi: 10.1084/jem.20191005
- Leek, J. T., Johnson, W. E., Parker, H. S., Jaffe, A. E., and Storey, J. D. (2012). The sva package for removing batch effects and other unwanted variation in high-throughput experiments. *Bioinformatics* 28, 882–883. doi: 10.1093/bioinformatics/bts034
- Leonard, B., Starrett, G. J., Maurer, M. J., Oberg, A. L., Van Bockstal, M., Van Dorpe, J., et al. (2016). APOBEC3G Expression Correlates with T-Cell infiltration and improved clinical outcomes in high-grade serous ovarian carcinoma. *Clin. Cancer Res.* 22, 4746–4755. doi: 10.1158/1078-0432.CCR-15-2910
- Liu, D., Aguirre Ghiso, J., Estrada, Y., and Ossowski, L. (2002). EGFR is a transducer of the urokinase receptor initiated signal that is required for in vivo growth of a human carcinoma. *Cancer Cell* 1, 445–457. doi: 10.1016/s1535-6108(02)00072-7
- Lyu, T., Jia, N., Wang, J., Yan, X., Yu, Y., Lu, Z., et al. (2013). Expression and epigenetic regulation of angiogenesis-related factors during dormancy and recurrent growth of ovarian carcinoma. *Epigenetics* 8, 1330–1346. doi: 10.4161/epi.26675
- MacDonald, J., Ramos-Valdes, Y., Perampalam, P., Litovchick, L., DiMattia, G. E., and Dick, F. A. (2017). A systematic analysis of negative growth control implicates the DREAM complex in cancer cell dormancy. *Mol. Cancer Res.* 15, 371–381. doi: 10.1158/1541-7786.MCR-16-0323-T
- Martincorena, I., Raine, K. M., Gerstung, M., Dawson, K. J., Haase, K., Van Loo, P., et al. (2017). Universal patterns of selection in cancer and somatic tissues. *Cell* 171, 1029–1041.e21. doi: 10.1016/j.cell.2017.09.042
- McGranahan, N., and Swanton, C. (2017). Clonal heterogeneity and tumor evolution: past, present, and the future. *Cell* 168, 613–628. doi: 10.1016/j.cell.2017.01.018
- Miller, I., Min, M., Yang, C., Tian, C., Gookin, S., Carter, D., et al. (2018). Ki67 is a graded rather than a binary marker of proliferation versus quiescence. *Cell Rep.* 24, 1105–1112.e5. doi: 10.1016/j.celrep.2018.06.110
- Mittal, D., Gubin, M. M., Schreiber, R. D., and Smyth, M. J. (2014). New insights into cancer immunoediting and its three component phases—elimination, equilibrium and escape. *Curr. Opin. Immunol.* 27, 16–25. doi: 10.1016/j.coi.2014.01.004
- Moon, K. R., van Dijk, D., Wang, Z., Gigante, S., Burkhardt, D. B., Chen, W. S., et al. (2019). Visualizing structure and transitions in high-dimensional biological data. *Nat. Biotechnol.* 37, 1482–1492. doi: 10.1038/s41587-019-0336-3
- Moserle, L., Amadori, A., and Indraco, S. (2009). The angiogenic switch: implications in the regulation of tumor dormancy. *Curr. Mol. Med.* 9, 935–941. doi: 10.2174/156652409789712800
- Naumov, G. N., Bender, E., Zurakowski, D., Kang, S. Y., Sampson, D., Flynn, E., et al. (2006). A model of human tumor dormancy: an angiogenic switch from the nonangiogenic phenotype. *J. Natl. Cancer Inst.* 98, 316–325. doi: 10.1093/jnci/dij068
- Oh, C. W., Hoover-Plow, J., and Plow, E. F. (2003). The role of plasminogen in angiogenesis *in vivo*. *J. Thromb. Haemost.* 1, 1683–1687. doi: 10.1046/j.1538-7836.2003.00182.x
- Park, S. Y., and Nam, J. S. (2020). The force awakens: metastatic dormant cancer cells. *Exp. Mol. Med.* 52, 569–581. doi: 10.1038/s12276-020-0423-z
- Petrova, V., Annicchiarico-Petruzzelli, M., Melino, G., and Amelio, I. (2018). The hypoxic tumour microenvironment. *Oncogenesis* 7:10. doi: 10.1038/s41389-017-0011-9
- Phan, T. G., and Croucher, P. I. (2020). The dormant cancer cell life cycle. *Nat. Rev. Cancer* 20, 398–411. doi: 10.1038/s41568-020-0263-0
- Polyak, K., Xia, Y., Zweier, J. L., Kinzler, K. W., and Vogelstein, B. (1997). A model for p53-induced apoptosis. *Nature* 389, 300–305. doi: 10.1038/38525
- Pugh, C. W., and Ratcliffe, P. J. (2003). Regulation of angiogenesis by hypoxia: role of the HIF system. *Nat. Med.* 9, 677–684. doi: 10.1038/nm0603-677
- Qin, L., Xu, Y., Ma, G., Liao, L., Wu, Y., Li, Y., et al. (2015). NCOA1 promotes angiogenesis in breast tumors by simultaneously enhancing both HIF1 $\alpha$ - and AP-1-mediated VEGF $\alpha$  transcription. *Oncotarget* 6, 23890–23904. doi: 10.18632/oncotarget.4341
- Qiu, G. Z., Jin, M. Z., Dai, J. X., Sun, W., Feng, J. H., and Jin, W. L. (2017). Reprogramming of the tumor in the hypoxic niche: the emerging concept and associated therapeutic strategies. *Trends Pharmacol. Sci.* 38, 669–686. doi: 10.1016/j.tips.2017.05.002
- Ranganathan, A. C., Zhang, L., Adam, A. P., and Aguirre-Ghiso, J. A. (2006). Functional coupling of p38-induced up-regulation of BiP and activation of RNA-dependent protein kinase-like endoplasmic reticulum kinase to drug resistance of dormant carcinoma cells. *Cancer Res.* 66, 1702–1711. doi: 10.1158/0008-5472.CAN-05-3092
- Rebhandl, S., Huemer, M., Gassner, F. J., Zaborsky, N., Hebenstreit, D., Catakovic, K., et al. (2014). APOBEC3 signature mutations in chronic lymphocytic leukemia. *Leukemia* 28, 1929–1932. doi: 10.1038/leu.2014.160
- Robbiani, D. F., and Nussenzweig, M. C. (2013). Chromosome translocation, B cell lymphoma, and activation-induced cytidine deaminase. *Annu. Rev. Pathol.* 8, 79–103. doi: 10.1146/annurev-pathol-020712-164004
- Roberts, S. A., Lawrence, M. S., Klimczak, L. J., Grimm, S. A., Fargo, D., Stojanov, P., et al. (2013). An APOBEC cytidine deaminase mutagenesis pattern is widespread in human cancers. *Nat. Genet.* 45, 970–976. doi: 10.1038/ng.2702
- Rosenthal, R., McGranahan, N., Herrero, J., Taylor, B. S., and Swanton, C. (2016). DeconstructSigs: delineating mutational processes in single tumors distinguishes DNA repair deficiencies and patterns of carcinoma evolution. *Genome Biol.* 17:31. doi: 10.1186/s13059-016-0893-4
- Sadasivam, S., and DeCaprio, J. A. (2013). The DREAM complex: master coordinator of cell cycle-dependent gene expression. *Nat. Rev. Cancer* 13, 585–595. doi: 10.1038/nrc3556
- Semenza, G. L. (2003). Targeting HIF-1 for cancer therapy. *Nat. Rev. Cancer* 3, 721–732. doi: 10.1038/nrc1187



- Senft, D., and Ronai, Z. A. (2016). Immunogenic, cellular, and angiogenic drivers of tumor dormancy—a melanoma view. *Pigment Cell Melanoma Res.* 29, 27–42. doi: 10.1111/pcmr.12432
- Shen, S., and Clairambault, J. (2020). Cell plasticity in cancer cell populations. *F1000Res* 9:F1000FacultyRev–635. doi: 10.12688/f1000research.24803.1
- Shivji, M. K., Podust, V. N., Hübscher, U., and Wood, R. D. (1995). Nucleotide excision repair DNA synthesis by DNA polymerase epsilon in the presence of PCNA, RFC, and RPA. *Biochemistry* 34, 5011–5017. doi: 10.1021/bi00015a012
- Sigismund, S., Avanzato, D., and Lanzetti, L. (2018). Emerging functions of the EGFR in cancer. *Mol. Oncol.* 12, 3–20. doi: 10.1002/1878-0261.12155
- Simó-Riudalbas, L., érez-Salvia, M. P., Setien, F., Villanueva, A., Moutinho, C., Martínez-Cardús, A., et al. (2015). KAT6B is a tumor suppressor histone H3 Lysine 23 acetyltransferase undergoing genomic loss in small cell lung cancer. *Cancer Res.* 75, 3936–3945. doi: 10.1158/0008-5472.CAN-14-3702
- Stenglein, M. D., Burns, M. B., Li, M., Lengyel, J., and Harris, R. S. (2010). APOBEC3 proteins mediate the clearance of foreign DNA from human cells. *Nat. Struct. Mol. Biol.* 17, 222–229. doi: 10.1038/nsmb.1744
- Swanton, C., McGranahan, N., Starrett, G. J., and Harris, R. S. (2015). APOBEC enzymes: mutagenic fuel for cancer evolution and heterogeneity. *Cancer Discov.* 5, 704–712. doi: 10.1158/2159-8290.CD-15-0344
- Tate, J. G., Bamford, S., Jubb, H. C., Sondka, Z., Beare, D. M., Bindal, N., et al. (2019). COSMIC: the catalogue of somatic mutations in cancer. *Nucleic Acids Res.* 47 (D1), D941–D947. doi: 10.1093/nar/gky1015
- Temko, D. I., Tomlinson, P. M., Severini, S., Schuster-Böckler, B., and Graham, T. A. (2018). The effects of mutational processes and selection on driver mutations across cancer types. *Nat. Commun.* 9:1857. doi: 10.1038/s41467-018-04208-6
- Teng, M. W., Swann, J. B., Koebel, C. M., Schreiber, R. D., and Smyth, M. J. (2008). Immune-mediated dormancy: an equilibrium with cancer. *J. Leukoc. Biol.* 84, 988–993. doi: 10.1189/jlb.1107774
- Theodoropoulos, V. E., Lazaris, A. C., Sofras, F., Gerzelis, I., Tsoukala, V., Ghikonti, I., et al. (2004). Hypoxia-inducible factor 1 alpha expression correlates with angiogenesis and unfavorable prognosis in bladder cancer. *Eur. Urol.* 46, 200–208. doi: 10.1016/j.eururo.2004.04.008
- Tommasini-Ghelfi, S., Murnan, K., Kouri, F. M., Mahajan, A. S., May, J. L., and Stegh, A. H. (2019). Cancer-associated mutation and beyond: the emerging biology of isocitrate dehydrogenases in human disease. *Sci. Adv.* 5:eaaw4543. doi: 10.1126/sciadv.aaw4543
- Tummers, B., and Green, D. R. (2017). Caspase-8: regulating life and death. *Immunol. Rev.* 277, 76–89. doi: 10.1111/imr.12541
- Turcan, S., Rohle, D., Goenka, A., Walsh, L. A., Fang, F., Yilmaz, E., et al. (2012). IDH1 mutation is sufficient to establish the glioma hypermethylator phenotype. *Nature* 483, 479–483. doi: 10.1038/nature10866
- Vogelstein, B., Lane, D., and Levine, A. J. (2000). Surfing the p53 network. *Nature* 408, 307–310. doi: 10.1038/35042675
- Wall, L., Burke, F., Smyth, J. F., and Balkwill, F. (2003). The anti-proliferative activity of interferon-gamma on ovarian cancer: in vitro and in vivo. *Gynecol. Oncol.* 88 (1 Pt 2), S149–S151. doi: 10.1006/gyno.2002.6707
- Wang, F. X., Huang, J., Zhang, H., and Ma, X. (2008). APOBEC3G upregulation by alpha interferon restricts human immunodeficiency virus type 1 infection in human peripheral plasmacytoid dendritic cells. *J. Gen. Virol.* 89 (Pt 3), 722–730. doi: 10.1099/vir.0.83530-0
- Wang, H. F., Wang, S. S., Huang, M. C., Liang, X. H., Tang, Y. J., and Tang, Y. L. (2019). Targeting immune-mediated dormancy: a promising treatment of cancer. *Front. Oncol.* 9:498. doi: 10.3389/fonc.2019.00498
- Wang, S., Huimin, L., Minfang, S., Zaoke, H., Tao, W., Xuan, W., et al. (2020). Copy number signature analyses in prostate cancer reveal distinct etiologies and clinical outcomes. *medRxiv [Preprint]* doi: 10.1101/2020.04.27.20082404
- Wang, S., Jia, M., He, Z., and Liu, X. S. (2018). APOBEC3B and APOBEC mutational signature as potential predictive markers for immunotherapy response in non-small cell lung cancer. *Oncogene* 37, 3924–3936. doi: 10.1038/s41388-018-0245-9
- Watnick, R. S., Rodriguez, R. K., Wang, S., Blois, A. L., Rangarajan, A., Ince, T., et al. (2015). Thrombospondin-1 repression is mediated via distinct mechanisms in fibroblasts and epithelial cells. *Oncogene* 34, 2823–2835. doi: 10.1038/ncr.2014.228
- Wherry, E. J., and Kurachi, M. (2015). Molecular and cellular insights into T cell exhaustion. *Nat. Rev. Immunol.* 15, 486–499. doi: 10.1038/nri3862
- White, D. E., Kurpios, N. A., Zuo, D., Hassell, J. A., Blaess, S., Mueller, U., et al. (2004). Targeted disruption of beta1-integrin in a transgenic mouse model of human breast cancer reveals an essential role in mammary tumor induction. *Cancer Cell* 6, 159–170. doi: 10.1016/j.ccr.2004.06.025
- Winter, S. C., Buffa, F. M., Silva, P., Miller, C., Valentine, H. R., Turley, H., et al. (2007). Relation of a hypoxia metagene derived from head and neck cancer to prognosis of multiple cancers. *Cancer Res.* 67, 3441–3449. doi: 10.1158/0008-5472.CAN-06-3322
- Yamazaki, H., Shirakawa, K., Matsumoto, T., Hirabayashi, S., Murakawa, Y., Kobayashi, M., et al. (2019). Endogenous APOBEC3B overexpression constitutively generates DNA substitutions and deletions in myeloma cells. *Sci. Rep.* 9:7122. doi: 10.1038/s41598-019-43575-y
- Ye, D., Ma, S., Xiong, Y., and Guan, K. L. (2013). R-2-hydroxyglutarate as the key effector of IDH mutations promoting oncogenesis. *Cancer Cell.* 23, 274–276. doi: 10.1016/j.ccr.2013.03.005
- Yi, J. S., Cox, M. A., and Zajac, A. J. (2010). T-cell exhaustion: characteristics, causes and conversion. *Immunology* 129, 474–481. doi: 10.1111/j.1365-2567.2010.03255.x
- Yuan, S., Norgard, R. J., and Stanger, B. Z. (2019). Cellular plasticity in cancer. *Cancer Discov.* 9, 837–851. doi: 10.1158/2159-8290.CD-19-0015
- Zhang, J., Bajari, R., Andric, D., Gerthoffert, F., Lepsa, A., Nahal-Bose, H., et al. (2019). The international cancer genome consortium data portal. *Nat. Biotechnol.* 37, 367–369. doi: 10.1038/s41587-019-0055-9
- Zhang, T., Otevrel, T., Gao, Z., Ehrlich, S. M., Fields, J. Z., and Boman, B. M. (2001). Evidence that APC regulates survivin expression: a possible mechanism contributing to the stem cell origin of colon cancer. *Cancer Res.* 61, 8664–8667.
- Zhao, X., Liu, J., Ge, S., Chen, C., Li, S., Wu, X., et al. (2019). Saikosaponin a inhibits breast cancer by regulating Th1/Th2 Balance. *Front. Pharmacol.* 10:624. doi: 10.3389/fphar.2019.00624
- Zhi, X., Tao, J., Xie, K., Zhu, Y., Li, Z., Tang, J., et al. (2014). MUC4-induced nuclear translocation of  $\beta$ -catenin: a novel mechanism for growth, metastasis and angiogenesis in pancreatic cancer. *Cancer Lett.* 346, 104–113. doi: 10.1016/j.canlet.2013.12.021

**Conflict of Interest:** The authors declare that the research was conducted in the absence of any commercial or financial relationships that could be construed as a potential conflict of interest.

Copyright © 2021 Wiecek, Jacobson, Lason and Secrier. This is an open-access article distributed under the terms of the Creative Commons Attribution License (CC BY). The use, distribution or reproduction in other forums is permitted, provided the original author(s) and the copyright owner(s) are credited and that the original publication in this journal is cited, in accordance with accepted academic practice. No use, distribution or reproduction is permitted which does not comply with these terms.





# Cell Cycle Commitment and the Origins of Cell Cycle Variability

Robert F. Brooks<sup>1,2\*</sup>

<sup>1</sup> Molecular and Clinical Sciences Research Institute, St George's, University of London, London, United Kingdom,

<sup>2</sup> Department of Anatomy, King's College London, London, United Kingdom

## OPEN ACCESS

### Edited by:

Alexis Ruth Barr,  
London Institute of Medical Sciences,  
Medical Research Council,  
United Kingdom

### Reviewed by:

P. K. Vinod,  
International Institute of Information  
Technology, Hyderabad, India  
Steve Cappell,  
National Cancer Institute (NCI),  
United States  
Hee Won Yang,  
Columbia University, United States

### \*Correspondence:

Robert F. Brooks  
rbrooks@sgul.ac.uk

### Specialty section:

This article was submitted to  
Cell Growth and Division,  
a section of the journal  
Frontiers in Cell and Developmental  
Biology

**Received:** 20 April 2021

**Accepted:** 22 June 2021

**Published:** 23 July 2021

### Citation:

Brooks RF (2021) Cell Cycle  
Commitment and the Origins of Cell  
Cycle Variability.  
Front. Cell Dev. Biol. 9:698066.  
doi: 10.3389/fcell.2021.698066

Exit of cells from quiescence following mitogenic stimulation is highly asynchronous, and there is a great deal of heterogeneity in the response. Even in a single, clonal population, some cells re-enter the cell cycle after a sub-optimal mitogenic signal while other, seemingly identical cells, do not, though they remain capable of responding to a higher level of stimulus. This review will consider the origins of this variability and heterogeneity, both in cells re-entering the cycle from quiescence and in the context of commitment decisions in continuously cycling populations. Particular attention will be paid to the role of two interacting molecular networks, namely the RB-E2F and APC/C<sup>CDH1</sup> “switches.” These networks have the property of bistability and it seems likely that they are responsible for dynamic behavior previously described kinetically by Transition Probability models of the cell cycle. The relationship between these switches and the so-called Restriction Point of the cell cycle will also be considered.

**Keywords:** cell cycle variability, restriction point, bistable switches, RB-E2F switch, APC/C<sup>CDH1</sup> switch, transition probability, quiescence, heterogeneity

## INTRODUCTION

When starved of growth factors, normal mammalian cells cease proliferating and arrest in a quiescent state outside the cell cycle, now commonly referred to as G0 (Holley and Kiernan, 1968; Burk, 1970). On re-addition of growth factors (typically in the form of serum), the cells resume cycling but only after a long lag comparable to the duration of the entire cell cycle of rapidly proliferating cells (Burk, 1970; Temin, 1971). This lag is independent of the concentration of growth factors or serum, even though these have widespread effects on cellular growth (mass increase) and metabolism (Temin, 1971; Brooks, 1975, 1976). Following the lag, the cells start entering S phase asynchronously, at a rate determined by the level of growth factors (Brooks, 1975, 1976). If the growth factors are removed again at any point, even before the end of the lag, many cells continue on into S phase and mitosis in the absence of further stimulation (Todaro et al., 1965; Burk, 1970; Temin, 1971; Brooks, 1976). Cells therefore appear to become committed to re-enter the cell cycle sometime before they reach S phase. This point of commitment, after which subsequent progress through the cell cycle becomes independent of growth factors, is known as the Restriction Point (Pardee, 1974). For normal, growth factor-dependent cells, the Restriction Point is widely regarded as a critical decision point that must be passed in each and every cell cycle (Planas-Silva and Weinberg, 1997). Underscoring its importance, regulation of this transition appears to be defective in most if not all cancers (Malumbres and Barbacid, 2009).

In recent years there has been a great deal of progress in understanding the molecular details of the Restriction Point – see Pennycook and Barr (2020) for an excellent recent review. However, what determines the timing of the Restriction Point remains far from clear. When stimulated from quiescence, some cells (even in clonal populations) require much higher levels of growth factors than others to be triggered into S phase (Brooks et al., 1984). Even with maximal stimulation, the cells enter S phase at different times over many hours, indicating asynchronous passage of the Restriction point (Brooks, 1975, 1976). This asynchrony and heterogeneity is often regarded merely as a nuisance, limiting the utility of serum starvation/refeeding as a means to synchronize the cell cycle. However, an alternative view is that the variability may actually be saying something about the way in which cell cycle commitment is regulated. At the very least, understanding the origin of the variability is essential to any complete understanding of cell cycle regulation. In this article, some of the causes of this variability will be explored, with a particular focus on the RB-E2F and APC/C<sup>CDH1</sup> bistable switches (Stallaert et al., 2019; Pennycook and Barr, 2020). These have the property of excitability and increasingly seem likely to lie behind key all-or-none commitment steps in the cell cycle.

## THE RB-E2F BISTABLE SWITCH

It is now widely accepted (Planas-Silva and Weinberg, 1997; Johnson and Skotheim, 2013; Stallaert et al., 2019; Pennycook and Barr, 2020) that passage of the Restriction Point is regulated by the RB-E2F pathway (**Figure 1**). RB in this context refers to a family of so-called pocket proteins that includes RB itself, the product of the retinoblastoma susceptibility gene, together with p130 and p107 (Cobrinik, 2005). RB family proteins bind to members of the E2F family of transcription factors, repressing the expression of E2F-target genes either directly or through recruitment of chromatin modifiers such as histone deacetylase (Cobrinik, 2005; Choi and Anders, 2014). Of particular importance are E2F1-3a, needed for the expression of many genes required for DNA synthesis and cell cycle progression (Bertoli et al., 2013). Indeed, knock-out of these E2Fs prevents cell cycle re-entry from quiescence (Wu et al., 2001) while ectopic overexpression alone is sufficient to drive quiescent cells into S phase (Johnson et al., 1993). Likewise, elimination of E2F repression by knock-out of all three RB family members prevents cell cycle exit into quiescence (Sage et al., 2000). For more detail of the distinctive roles of the different Rb family proteins, see **Box 1**.

Mitogenic stimulation leads to the expression of cyclin D (**Figure 1**), a family of three closely related proteins, D1–D3 (in mammals) whose pattern of expression is partly cell type specific and partly dependent on the signaling pathway (Sherr, 1995; Choi and Anders, 2014). Cyclin D1 is induced by the RAS-MAPK pathway in particular, but also by Wnt/ $\beta$ -catenin, Notch, JAK-STAT or Hedgehog signaling (Klein and Assoian, 2008; Choi and Anders, 2014). Cyclin D2 is induced by Myc (Bouchard et al., 1999), which in turn is elevated by growth

factor stimulation. Cyclin D3 is less-well studied but is widely expressed and may be important in lymphoid cells (Sicinska et al., 2003). All three bind to and activate cyclin dependent kinases 4 and 6 (CDK4,6) and, seemingly being of equivalent activity, will be referred to collectively hereafter as Cyclin D, for simplicity. The active CDK4,6/Cyclin D then phosphorylates RB family proteins – its major substrates (Sherr, 1995; Choi and Anders, 2014). The precise details of phosphorylation are complex, and will be revisited later. For now, phosphorylation on multiple sites (“hyperphosphorylation”) leads to dissociation of RB proteins from E2F, allowing the latter to activate expression of target genes (Mittnacht, 1998; Bracken et al., 2004; Choi and Anders, 2014). Among these, cyclin E is of particular importance (**Figure 1**). Following induction, cyclin E binds to CDK2. The active CDK2-cyclin E complex then, in turn, contributes to the hyperphosphorylation of RB, further promoting the release of E2F, and further expression of cyclin E in a positive feedback loop (Yao et al., 2008; Johnson and Skotheim, 2013; Weinberg, 2013; Pennycook and Barr, 2020). The targets of E2F also include E2F1-3, contributing another positive feedback loop promoting E2F activity (Bracken et al., 2004). In addition, elevation of Myc activity in response to growth factor stimulation, besides promoting expression of Cyclin D (Bouchard et al., 1999), also directly induces expression of E2F1-3 (Leone et al., 2001) as well as promoting E2F-mediated transcription (Leung et al., 2008), further contributing to Cyclin E expression and RB suppression (**Figure 1**).

The positive feedback loops within the RB-E2F pathway confer the property of bistability, such that E2F activity can only be sustained at steady-state at one of two levels: either low (E2F-Off) or high (E2F-On) (Yao et al., 2008). Once above a critical threshold, E2F levels will drive inexorably upwards to the high steady state due to the positive feedback. From then on, the level of Cyclin E-CDK2 becomes sufficient to maintain the hyperphosphorylation of RB without the need for further input from Cyclin D-CDK4,6. This switch is postulated to represent passage of the Restriction Point since, after it, growth factor stimulation, and Cyclin D expression, are no longer needed to maintain E2F activity (Yao et al., 2008).

Experimental evidence that the RB-E2F pathway does indeed behave as a bistable switch came from using a green fluorescent protein (GFP)-construct under the control of the E2F1 promoter as an E2F reporter (Yao et al., 2008). After stimulating quiescent cells with a high level of serum growth factors, E2F activity rose to a high level in all cells in the population, with most going on to enter S phase. However, when stimulated with suboptimal levels of serum, the level of E2F activity became bimodal within the population, with some cells maintaining the low level of the quiescent controls, while other cells in the same population switched to a high level of E2F. This bifurcation of E2F activity within the population showed that the RB-E2F switch was able to convert continuous, graded levels of growth stimulation into all-or-none responses at the cellular level. Importantly, the cells that subsequently went on into S phase were from those that switched to high-E2F.

That some cells switch to high E2F under suboptimal conditions while others do not was attributed to cellular noise

**BOX 1 |** Distinct roles of Rb family members in cell cycle-regulated gene expression.

Rb family members are often treated as though they were largely equivalent in function (as in **Figure 1**), insofar as they all bind to E2F transcription factors, and this interaction is disrupted by CDK-mediated phosphorylation. This, however, is an oversimplification. Rb binds preferentially to the activator E2Fs (E2F1, E2F2, and E2F3a), whereas p107 (RBL-1) and p130 (RBL-2) associate primarily with E2F4 and E2F5, which function mainly as repressors of transcription (Cobrinik, 2005). In quiescent cells, the level of activator E2Fs is low and the expression of genes needed for entry into the cell cycle is actively and specifically repressed by E2F4, in association with p130 (Takahashi et al., 2000; Sadasivam and DeCaprio, 2013; Schade et al., 2019). However, E2F4 and p130 do not act alone but function along with MuvB as part of the so-called DREAM complex, made up of DP, RB-like, E2F4 (or E2F5) and MuvB (Sadasivam and DeCaprio, 2013; Schade et al., 2019). The multi-subunit MuvB component binds to the CHR (cell cycle genes homology region) elements found in "late" cell cycle genes. This enables the DREAM complex to suppress both late cell cycle genes as well as E2F-dependent "early" genes, in quiescence.

After mitogenic stimulation, phosphorylation of p130 by CDK4,6/cyclin D, midway through the pre-replicative lag, leads to disruption of the DREAM complex, the dissociation of E2F4 (Schade et al., 2019) and its replacement by E2F1, E2F2, and E2F3 (Takahashi et al., 2000). This in turn allows expression of "early" cell cycle genes. Sometime after this, MuvB (presumably still bound to the CHR elements of late cell cycle genes, maintaining suppression) is joined by BMYB (itself a product of early gene expression) (Sadasivam and DeCaprio, 2013). The BMYB-MuvB complex in turn recruits FOXM1 which, after phosphorylation (probably by CDK4,6/cyclin D – Anders et al., 2011) induces expression of late cell cycle genes in G2 (Sadasivam and DeCaprio, 2013).

Although p130 and the DREAM complex contribute to the suppression of cell cycle gene expression in quiescence, RB itself (which is not able to form complexes with MuvB) appears to play a greater role (Schade et al., 2019). Quiescent cells lacking RB show a significant de-repression of cell cycle gene expression whereas cells lacking p130 do not (Schade et al., 2019). However, cells lacking both p130 and RB show a greater de-repression of cell cycle genes than cells lacking RB only, confirming that DREAM does play a part in suppression (Schade et al., 2019). The greater role of RB was attributed to the inhibition of the activator E2Fs (1-3) still needed for gene expression after repression by E2F4 is relieved. Nevertheless, Takahashi et al. (2000) were unable to detect an association of RB with the cell cycle gene promoters examined at any time after mitogenic stimulation, even after the point half-way through the pre-replicative lag when E2F4 is replaced by E2F1, E2F2 and E2F3. This is consistent more with RB sequestering the activator E2Fs away from the promoters until after its hyperphosphorylation, rather than direct promoter repression (Cobrinik, 2005). Importantly, DREAM and RB appear to regulate the same set of genes, with little evidence for differential expression (Schade et al., 2019).

The exact role of p107 continues to be unclear. Its level is highest in proliferating cells and it is the product of an early E2F-regulated gene switched on during entry into the cycle from quiescence (Schade et al., 2019). It is also upregulated in cells deficient in p130 (Schade et al., 2019). Nevertheless, although p107 is able to complex with MuvB, there was little evidence for it doing so in p130-deficient cells (Schade et al., 2019). The limited de-repression of cell cycle-regulated cells in p130-deficient cells does not therefore seem to be due to compensatory replacement of p130 by p107 in forming the DREAM complex. It is also noteworthy that siRNA knock-down of p107 in cells lacking both RB and p130 did not lead to any consistent, additional changes in gene expression (Schade et al., 2019). There is no evidence therefore for a set of genes repressed specifically by p107. Evidently, the precise contribution of p107 to cell cycle regulation remains to be determined.

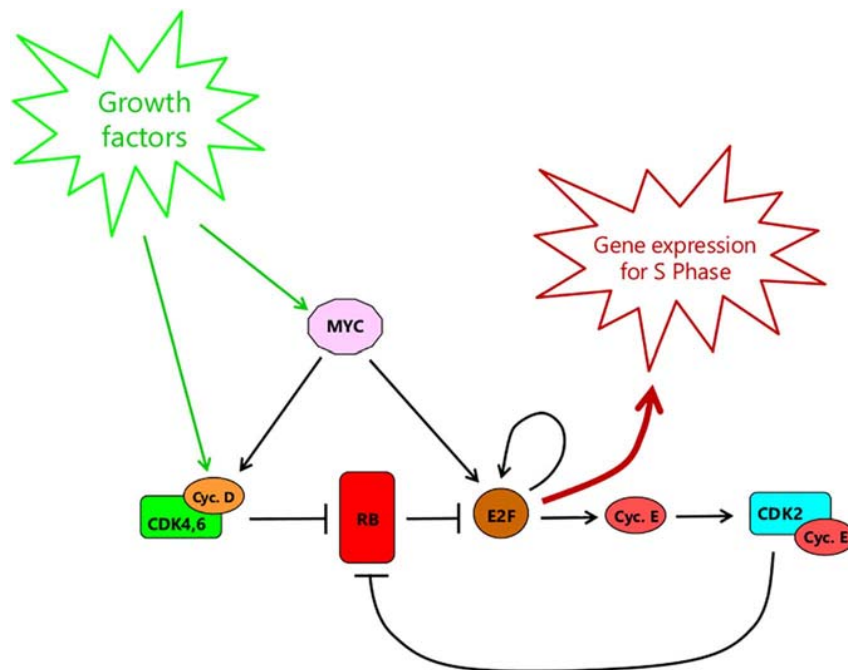


**FIGURE 1 |** The RB-E2F bistable switch, as outlined by Yao et al. (2008). RB represents the pocket protein family consisting of RB itself, p130 and p107. E2F refers to all activator forms, namely E2F1, E2F2, and E2F3a complexed with a dimerization partner DP1 or DP2. This simplified view of the RB-E2F pathway continues to be useful and conceptually valid. However, see Box 1 for discussion of the distinctive roles of the different RB family members that underlie the pathway.

in pathway dynamics around the threshold, due either to small numbers of interacting molecules or to small differences in parameter values resulting from the previous history of the cell

(size variation, for example, or local differences in cell density) (Yao et al., 2008). Later, a stochastic version of the model was indeed able to generate asynchronous switching within a

population (Lee et al., 2010). Moreover, it was able to reproduce the apparently first order kinetics of entry into S phase observed experimentally, in which a constant fraction of the cells enters S phase per unit time (Brooks, 1975, 1976). These kinetics had previously been taken as evidence for the Transition Probability model of Smith and Martin (Smith and Martin, 1973) which proposed the existence of a rate-limiting commitment step in the cell cycle occurring stochastically with constant probability over time under steady-state conditions.

## THE RB-E2F SWITCH AND HETEROGENEITY IN EXIT FROM QUIESCENCE

Although the stochastic version of the RB-E2F switch is able to reproduce some of the observed asynchrony in entry into S phase after stimulation from quiescence, it fails to account for other aspects of the kinetics. In particular, the model predicts that the lag between stimulation and cell cycle entry should depend on the level of stimulation (Lee et al., 2010). As already indicated, this is not the case. Rather, the lag before the first cells reach S phase is independent of growth factor (serum) concentration, even though the subsequent rate of entry into S phase varies (Brooks, 1975, 1976). Moreover, when the cells are first stimulated with a low (suboptimal) level of serum and the level raised again at the end of the first lag, there is another lag, identical to the first, before the rate of entry into S increases for a second time (Brooks, 1976). It is as though only a fraction of the population responded to the first stimulus, the rest remaining in the quiescent state until a second (higher) stimulus was able to move them out of arrest and on toward S phase. This would imply heterogeneity, even in a clonal population, such that some cells can respond to a low level of growth factors whereas others cannot.

That such heterogeneity does indeed exist was shown by later experiments in which the response to low levels of serum was followed over a much longer period. In the original experiments with observations limited to around 24 h, the rate of entry into S phase after stimulation did indeed appear first-order, following the lag, with a rate constant dependent on the level of serum. The expectation was that all cells would eventually reach S phase, if followed for long enough, even with very low levels of stimulation. This, however, is not what happens. When cells stimulated with low serum were followed over days, the rate of entry into S phase slowed, with the fraction of cells entering S phase reaching a plateau (Brooks et al., 1984). This was not because the low level of serum added was “used up” since the medium was renewed daily. Instead, it is clear that only some cells were able to respond to the low level of serum, with those responding doing so asynchronously, over many hours. However if, after reaching the plateau, the serum concentration was raised further, the previously unresponsive cells then entered S phase (Brooks et al., 1984). Thus, the non-responsive cells had not become incapable of responding, they merely needed a higher level of stimulation.

Similar results were obtained when cells were followed by timelapse microscopy rather than  $^3\text{H}$ -thymidine

autoradiography. However, in this case it was possible to see that some of the cells triggered to divide in response to low serum went on to divide again, in some cases several times, while many cells in the same field failed to respond at all (Brooks et al., 1984; Brooks and Riddle, 1988a). This might suggest an inherited element determining sensitivity to growth factors. However, attempts to enrich for responding cells by prolonged culture in low serum (3 weeks) were not successful (Brooks et al., 1984). Following such selection, the cells were no more responsive than the controls.

Such heterogeneity *within* a population is not predicted by the simple, stochastic version of the RB-E2F bistable switch (Lee et al., 2010). Although the inclusion of stochastic noise enables it to reproduce asynchrony in exit from quiescence, the model predicts that all cells should eventually do so, even with low levels of stimulation, given long enough, which (as already discussed) is not what happens. However, a later, extended version of the model, explicitly including a role for CDK-inhibitors such as p21 and p27, may provide an explanation (Kwon et al., 2017). Systematic varying of the model parameters showed that certain ones, in particular those affecting Cyclin-CDK activity or RB-phosphorylation status, had a marked effect on the threshold for switching (Kwon et al., 2017). Raising the threshold makes it more difficult to exit quiescence, increasing both the time required and the level of stimulation needed. Such an increase in threshold was shown to provide a compelling explanation for the well-established observation that cells do indeed go deeper and deeper into quiescence the longer they are starved of mitogenic stimulation, requiring both longer to re-enter the cycle on re-stimulation and a higher level of stimulation (Kwon et al., 2017). Later, it was shown that raising the threshold even further was able to account for a shift from deep quiescence to senescence and irreversible cell cycle arrest (Fujimaki et al., 2019; Fujimaki and Yao, 2020).

Although variation in the activation threshold of the RB-E2F switch is able to account for different levels of quiescence, in the published simulations the parameters are assumed (for simplicity) to have the same values in all cells of the population at the same time (other than stochastic noise). In practice this is unlikely to be the case. It is more probable that some parameters may vary within the population, even between adjacent cells, giving them different activation thresholds for responding to mitogenic stimulation. Of the possible parameters that might be implicated, the levels of CDK-inhibitors such as p27 and p21 are particularly attractive candidates. Simulations showed that these were among the strongest coarse tuners of the threshold in the model. In keeping with this, experimentally increased levels of p21 did indeed raise the activation threshold (Kwon et al., 2017; Heldt et al., 2018). Moreover, levels of p27 are known to increase in quiescence (Coats et al., 1996), and are heterogeneous within a population, with those cells reaching S phase after a short serum pulse being the ones with the lowest levels (Hitomi et al., 2006). It therefore seems probable that differences between individual cells in the levels of p27 or p21 contribute significantly to the heterogeneity in growth factor dependence within a quiescent population. This, of course, does not preclude the possibility that other components of the RB-E2F



switch also contribute to the heterogeneity, such as levels of RB family proteins.

## EXIT INTO QUIESCENCE IN CYCLING POPULATIONS

Heterogeneity is seen not only in populations of quiescent cells responding to mitogenic stimulation. It is also a feature of continuously cycling cells. Recent developments in live cell imaging have enabled cell cycle transitions to be followed with unprecedented precision in real time. Of particular value has been the use of a fluorescent sensor based on a fragment of human DNA helicase B (DHB) that moves from the nucleus to the cytoplasm on phosphorylation (Spencer et al., 2013). This was originally thought to be selective for Cyclin-dependent kinase 2 (CDK2) but later shown to be responsive to both CDK1 and CDK2, complexed with either cyclins E or A (Schwarz et al., 2018), and is henceforth referred to here as CDK/E,A activity. Using this sensor, CDK/E,A activity is seen to drop rapidly at mitosis (Spencer et al., 2013), with the onset of cyclin A destruction, as illustrated in **Figure 2A**. Following mitosis, in most proliferating cells (of many different lines), CDK/E,A activity immediately begins rising again (CDK/E,A<sup>increasing</sup> cells), increasing monotonically to a peak at the next mitosis (**Figure 2A**). The pattern of this increase for the majority of cells is broadly similar but it is noteworthy that individual traces differ, indicating a significant degree of asynchrony (Spencer et al., 2013). The increase is driven first by cyclin E accumulation, in conjunction with CDK2, and then by cyclin A accumulation as it replaces cyclin E, with CDK2 later supplemented by CDK1 (Spencer et al., 2013; Barr et al., 2016; Schwarz et al., 2018). However, as indicated in **Figure 2A**, in a significant minority of cells (typically of the order of 15–30% of the population, depending on cell type), the CDK/E,A activity fails to rise again immediately after mitosis (CDK/E,A<sup>low</sup> cells), either remaining low for the remainder of the experiment or increasing again after a variable delay, indicating the start of another cycle (Spencer et al., 2013; Arora et al., 2017; Yang et al., 2017; Moser et al., 2018; Min et al., 2020). These CDK/E,A<sup>low</sup> cells have hypophosphorylated RB and remain mitogen sensitive for re-entry into the cycle, indicating that they are pre-Restriction Point cells in G0 (Spencer et al., 2013; Cappell et al., 2016; Arora et al., 2017; Moser et al., 2018). The CDK/E,A<sup>increasing</sup> cells, however, appear to be committed to the next cell cycle from birth. They already have hyperphosphorylated RB from the very start of the cycle and are insensitive to mitogen withdrawal or MAPK pathway inhibition (Spencer et al., 2013; Yang et al., 2017; Min et al., 2020). Indeed, mitogen withdrawal or MAPK pathway inhibition must be applied during the mother cell cycle to prevent or delay cell cycle re-entry in the CDK/E,A<sup>increasing</sup> daughters (Spencer et al., 2013; Yang et al., 2017; Min et al., 2020).

This bifurcation in CDK/E,A activity occurs within what is otherwise a homogeneous population. For rapidly growing cells, it is attributable in large part to induction and variable expression of p21 (Spencer et al., 2013; Overton et al., 2014; Arora et al., 2017; Barr et al., 2017; Yang et al., 2017; Moser et al., 2018;

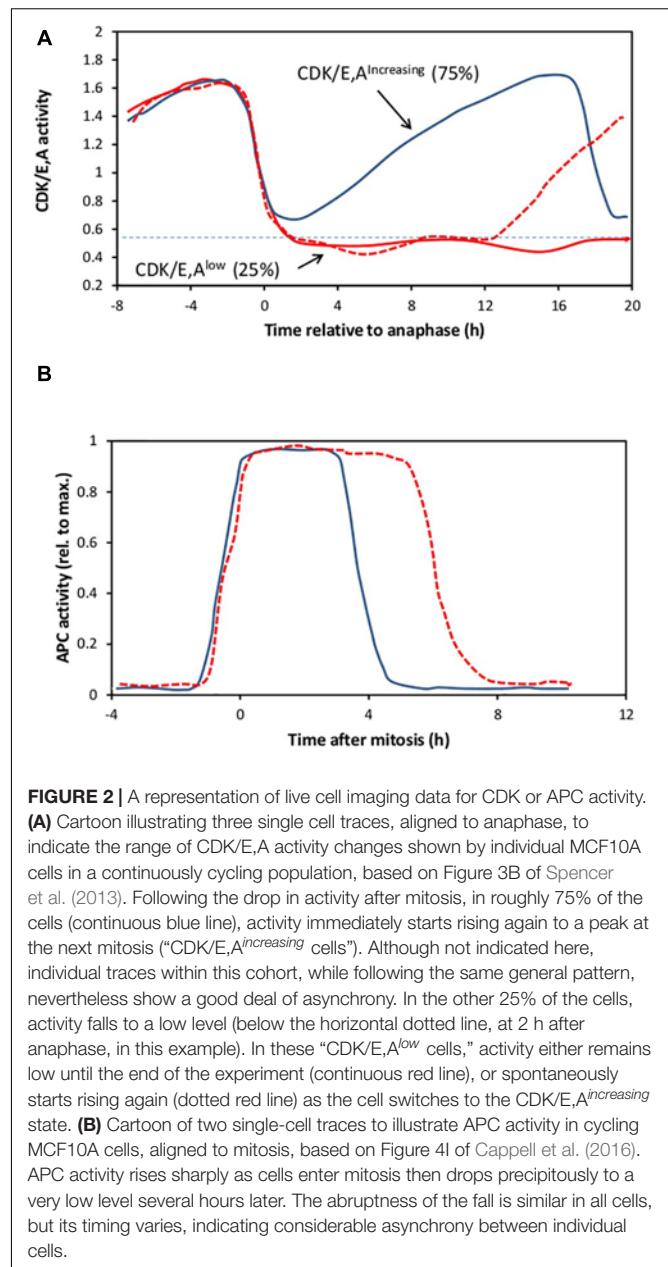


**FIGURE 2 |** A representation of live cell imaging data for CDK or APC activity. **(A)** Cartoon illustrating three single cell traces, aligned to anaphase, to indicate the range of CDK/E,A activity changes shown by individual MCF10A cells in a continuously cycling population, based on Figure 3B of Spencer et al. (2013). Following the drop in activity after mitosis, in roughly 75% of the cells (continuous blue line), activity immediately starts rising again to a peak at the next mitosis ("CDK/E,A<sup>increasing</sup> cells"). Although not indicated here, individual traces within this cohort, while following the same general pattern, nevertheless show a good deal of asynchrony. In the other 25% of the cells, activity falls to a low level (below the horizontal dotted line, at 2 h after anaphase, in this example). In these "CDK/E,A<sup>low</sup> cells," activity either remains low until the end of the experiment (continuous red line), or spontaneously starts rising again (dotted red line) as the cell switches to the CDK/E,A<sup>increasing</sup> state. **(B)** Cartoon of two single-cell traces to illustrate APC activity in cycling MCF10A cells, aligned to mitosis, based on Figure 4I of Cappell et al. (2016). APC activity rises sharply as cells enter mitosis then drops precipitously to a very low level several hours later. The abruptness of the fall is similar in all cells, but its timing varies, indicating considerable asynchrony between individual cells.

Heldt et al., 2018). Thus, p21 levels are higher in the out-of-cycle CDK/E,A<sup>low</sup> cells and decline as cells re-enter the cycle and switch to the CDK/E,A<sup>increasing</sup> state. Importantly, in populations of rapidly proliferating cells, the dropping out of cycle marked by the bifurcation in CDK/E,A activity is much reduced after knockdown of p21 with siRNA or gene inactivation, supporting a causal role for p21 in cell cycle exit (Spencer et al., 2013; Overton et al., 2014; Barr et al., 2017; Heldt et al., 2018).

The induction of p21 in some cells but not others is, in turn, due to a p53-mediated DNA-damage response in the mother cell, passed on through mitosis to the daughter cells (Arora et al., 2017; Barr et al., 2017; Yang et al., 2017; Heldt et al., 2018). This DNA-damage response is most likely a result of replication

stress (e.g., stalled replication forks) during S phase in the mother cell (Harrigan et al., 2011; Lukas et al., 2011; Koundrioukoff et al., 2013; Moreno et al., 2016). Such replication stress is a fairly frequent (and expected) occurrence in mammalian DNA replication, though other causes of endogenous DNA damage are also possible. Experimentally induced replication stress or DNA-damage in the mother cell cycle from treatment with low doses of aphidicolin or neocarzinostatin (insufficient to cause arrest in G2), also led to elevated levels of p21 in daughter cells and increased exit from the cycle into the CDK/E,A<sup>low</sup> state (Arora et al., 2017; Barr et al., 2017; Yang et al., 2017).

Consistent with the involvement of a DNA damage response, cells with high levels of p21 exhibit a higher frequency of DNA-damage foci (positive for 53BP1 or  $\gamma$ H2AX) than cells with low p21 (Arora et al., 2017; Barr et al., 2017). In turn, the greater the number of DNA-damage foci, the longer it takes for the cells to re-enter the cycle and start increasing CDK/E,A activity once more (Arora et al., 2017). Nevertheless, not all CDK/E,A<sup>low</sup> cells have high p21 (Spencer et al., 2013) or show DNA damage foci (Arora et al., 2017) and it was suggested that the presence of foci may account for only around 50% of the cells that undergo transient arrest after mitosis (Arora et al., 2017). This raises the possibility that the transient arrest of some cells may be due to something other than a DNA-damage response and elevated p21. In this connection, it is worth noting that Hs68 human fibroblasts immortalized with hTERT, growing optimally in high serum, have cycle times ranging from around 10–12 h to more than 95 h (Nassrally et al., 2019). With S + G2 being no more than 10–12 h (the minimum cycle time), the more than 70% of cells dividing with ages greater than 22 h would have spent longer than 10 h in G1, a length taken (in some studies) as indicative of cell cycle exit (Barr et al., 2017). Nevertheless, only 10–15% of proliferating Hs68-hTERT typically show 53BP1-positive foci (Nassrally et al., 2019), indicating that the majority of slow transits through G1 in this cell type must have been due to something other than a DNA-damage response. This additional factor may be related to proliferation rate *per se*.

In the original experiments of Spencer et al. (2013) using MCF10A cells in full growth medium, roughly 25% of the cells left the cycle after each mitosis into the CDK/E,A<sup>low</sup> state (Figure 2A). However, in later work by Overton et al. (2014) using the same cell type, there was no such cell cycle heterogeneity under high growth factor conditions (20 ng/ml EGF; 5% serum). Only when growth factor stimulation was reduced fourfold (to 5 ng/ml EGF; 1.25% serum) did cells exit the cycle after mitosis with the frequency reported by Spencer et al. (2013). Thus, in the original experiments, the cells may not have been growing at quite their maximum rate, for reasons unknown, despite being in similar high growth factor medium. This slightly reduced growth rate may have contributed to some of the cell cycle drop-out after mitosis, in addition to a DNA-damage response. The lack of any bifurcation in CDK/E,A activity in a line of MCF10A cells deleted for both alleles of p21 was taken as evidence that the drop-out was entirely dependent on p21 (Spencer et al., 2013), as noted previously. However, the p21<sup>-/-</sup> MCF10A cells used had acquired a reduced dependence on EGF during their isolation (Bachman et al., 2004), compared to the

parental line, and may therefore have been less sensitive to any slight deficiency in the growth conditions. A role for reduced mitogenic stimulation in the bifurcation in CDK/E,A activity, in addition to a DNA-damage response mediated by p21, cannot therefore be ruled out.

Further support for the possible importance of growth rate and the level of mitogenic stimulation, in contributing to the heterogeneity in cell exit after mitosis, comes from the results obtained with Swiss 3T3 cells. It was reported that these cells, nominally growing optimally but with an average cycle time of ~30 h, showed a very high rate of cell cycle drop-out after mitosis, with 77% of the cells passing into the CDK/E,A<sup>low</sup> state (Spencer et al., 2013). However, in my own laboratory, Swiss 3T3 cells in high serum grew at twice the rate, with a median cycle time of around 15 h, and showed no such cell cycle heterogeneity. Rather, cell cycle drop-out was seen only when the cells were grown in sub-optimal serum concentrations (Brooks and Riddle, 1988a,b). It seems probable therefore that some of the bifurcation in CDK/E,A activity seen with Swiss 3T3 cells (Spencer et al., 2013) may have been a consequence of a suboptimal growth rate (due, perhaps to medium composition, which was not specified), and not due solely to a stress response to DNA damage mediated by p53-p21.

Given that mitogen reduction is known to lead to the induction of p27 and that its expression is heterogeneous in quiescent populations (Coats et al., 1996; Hitomi et al., 2006), such suboptimal growth could lead to the upregulation of p27 in some cells. This would be expected to add to the contribution of p21 in driving the bifurcation in CDK/E,A activity. Clearly, live cell imaging experiments looking at both p21 and p27 simultaneously are needed to help unpick their relative importance under different conditions, in different cell types. Until this is done, a role for p27 in causing some of the transient cell cycle exit into the CDK/E,A<sup>low</sup> state, in proliferating populations, cannot be ruled out.

## BYPASS OF THE RESTRICTION POINT IN CONTINUOUSLY CYCLING CELLS

As already discussed, in continuously cycling cells, some 15–30% of the population typically enter the CDK/E,A<sup>low</sup> state after mitosis in which CDK/E,A activity fails to increase immediately (Figure 2A). These cells are born with hypophosphorylated RB and require mitogenic stimulation to re-enter the cycle. For these cells, the standard Restriction Point model seems appropriate. However, CDK/E,A<sup>increasing</sup> cells, the majority, have hyperphosphorylated RB from birth and are independent of mitogenic stimulation for continued progress through the cell cycle. These cells are, it seems, already committed to the next cell cycle from birth, which calls into question the idea that the Restriction Point is a critical decision point in G1 which *all* cells must pass through before continuing to the next cycle.

The key determinant of whether cells enter the CDK/E,A<sup>increasing</sup> or CDK/E,A<sup>low</sup> paths appears to be the level of CDK4,6/D activity immediately after mitosis (Yang et al., 2017; Min et al., 2020). This in turn depends on the levels of

cyclin D inherited from the mother cell, along with any p21/p27. Importantly, interruption of mitogenic signaling with a MEK inhibitor at any point in the mother cell cycle, even for as little as 1 h, affects the level of cyclin D attained at the end of G2 (Min et al., 2020). This is not due to a direct effect on cyclin D expression but rather to a decrease in overall translation rate which persists to the end of G2, whenever the pulse of MEK inhibitor is given earlier in the cycle. Conversely, treatment of mother cells with the CDK4,6 inhibitor palbociclib (which blocks the cell cycle but not cell growth in mass) produces enlarged cells with elevated translation capacity. These enlarged cells no longer respond to transient MEK inhibition with a reduction in the proportion of CDK/E,A<sup>increasing</sup> cells after mitosis (Min et al., 2020). That Cyclin D is the critical aspect of translation capacity was shown by knockdown of all three cyclin D genes in mother cells with siRNA, leading to a reduced proportion of CDK/E,A<sup>increasing</sup> daughter cells. Conversely, overexpression of cyclin D1 in mother cells, increased the proportion of CDK/E,A<sup>increasing</sup> daughter cells (Min et al., 2020).

These findings provide good evidence for the importance of cyclin D levels and CDK4/D activity in driving the bifurcation in CDK/E,A activity after mitosis. They also offer insight into two other fundamental features of the vertebrate cell cycle. Firstly, since sister cells would inherit identical concentrations of cyclin D from the mother cell, along with any p21 or p27, this would lead to similar cell cycle trajectories immediately afterward, potentially explaining much of the well-known correlation in sibling cycle times (Minor and Smith, 1974; Brooks et al., 1980). Secondly, since the level of cyclin D at the end of G2 is related to overall translation rate, large cells, with a high translational capacity, would generate large daughter cells with high cyclin D. These in turn would be expected to have shorter than average G1 times, providing a possible explanation for at least some of the observed inverse correlation between cell size and G1 duration (Shields et al., 1978; Ginzberg et al., 2018; Min et al., 2020; Zatulovskiy and Skotheim, 2020).

## THE RELATIVE CONTRIBUTIONS OF CDK4,6/CYCLIN D AND CDK2/CYCLIN E IN RB HYPERPHOSPHORYLATION

According to the standard model of the Restriction Point (Planas-Silva and Weinberg, 1997; Pennycook and Barr, 2020), CDK4,6/Cyclin D initiates phosphorylation of RB sufficient to partially derepress E2F, leading to the expression of cyclin E. This in turn activates CDK2 to fully phosphorylate (hyperphosphorylate) RB, promoting further expression of cyclin E and setting up the positive feedback loop essential to the bistability of the RB-E2F switch (Figure 1). An ingrained notion in this scheme is that CDK4,6/D is insufficient on its own for full phosphorylation of RB but instead requires help from CDK2/E, which eventually replaces it altogether. These ideas are challenged by the observation that CDK/E,A<sup>increasing</sup> cells are already mitogen independent and have fully phosphorylated RB from birth, when CDK/E activity is at its lowest (Spencer et al., 2013; Moser et al., 2018; Chung et al., 2019). Moreover,

treatment with the CDK4,6 inhibitor palbociclib at any point in G1, right up to shortly before entry into S phase, reverses RB-hyperphosphorylation rapidly and completely (Chung et al., 2019). This is true not only of the CDK/E,A<sup>increasing</sup> cells in cycling populations, but also of cells stimulated from quiescence that had become mitogen independent (i.e., post-Restriction Point) several hours earlier (Chung et al., 2019). Only after entry into S phase is RB hyperphosphorylation independent of CDK4,6/D (insensitive to palbociclib) and instead dependent solely on CDK/E,A activity (and sensitive to a CDK2 inhibitor) (Chung et al., 2019).

On the face of it, these observations suggest that there is no role at all for CDK2/E activity in RB hyperphosphorylation throughout G1, calling into question the validity of the RB-E2F bistable switch as the basis for the Restriction Point (Yao et al., 2008). However, the findings of Chung et al. (2019) are in apparent conflict with compelling evidence from Narasimha et al. (2014) that CDK4,6/cyclin D is only able to monophosphorylate RB and that hyperphosphorylation does not occur until after the appearance of CDK2/Cyclin E activity in “late” G1. These studies made use of isoelectric focusing to separate unphosphorylated RB from isoforms phosphorylated on 1, 2, 3, ..., up to 14 sites. Mitogen-stimulated human fibroblasts and other cell types had only monophosphorylated RB until an abrupt shift to fully phosphorylated RB (on 14 sites) coincident with the appearance of CDK2/Cyclin E activity in what was described as “late” G1 (though the timing of DNA synthesis was not shown). The kinase responsible for the RB monophosphorylation was confirmed as CDK4,6/cyclin D by its absence in Cyclin D triple-knockout mouse embryo fibroblasts (lacking all three cyclin D genes) and by its sensitivity to palbociclib and p16 (which disrupts CDK4,6-cyclin D complexes), whereas the hyperphosphorylation was sensitive to a CDK2-inhibitor. Remarkably, the monophosphorylated RB was phosphorylated on any one, but *only* one, of 14 different sites. The different monophosphorylated RB isoforms differed slightly in their affinity for different E2F family members, but all appeared active in suppressing E2F function. This raises the question as to how cyclin E is ever switched on, in order to trigger CDK2/Cyclin E-mediated RB-hyperphosphorylation, leading Narasimha et al. (2014) to invoke the existence of some other mechanism for inducing cyclin E expression not involving E2F.

The contrary conclusions of Chung et al. (2019) that CDK4,6/D alone is sufficient for RB hyperphosphorylation depend heavily on the use of palbociclib to inhibit CDK4,6/D activity. However, recent studies of the crystal structure of trimeric complexes between CDK4, cyclin D1 and either p21 or p27 indicate that the action of palbociclib is much more nuanced than previously appreciated (Guiley et al., 2019; Sherr, 2019). Although p21 and p27 are strong inhibitors of CDK1,2/E,A activity, their action on CDK4,6/D has been less clear-cut. In contrast to other CDK-cyclin complexes, CDK4,6 associates poorly with cyclin D, requiring the assistance of assembly factors, which include Hsp90, Cdc37 and p21 or p27. Indeed, mouse embryo fibroblasts lacking both p21 and p27 are unable to form active CDK4-Cyclin D complexes (Cheng et al., 1999). The structural studies of Guiley et al. showed how p21 and p27 are



able to bring CDK4 and Cyclin D together, facilitating complex formation and promoting conformational changes conducive to enzymatic activity (Guiley et al., 2019). Nevertheless, the p21-CDK4-Cyclin D1 trimer lacked kinase activity, making p21 an inhibitor, consistent with single-cell imaging data from Yang et al. (2017). (This, of course, implies that p21 would need to dissociate from the CDK4-cyclin D dimer after facilitating assembly if it is to function as a promoter of activity.) As with p21, the binding of p27 was also inhibitory until, that is, it is phosphorylated on Tyr74 (a site lacking in p21). Assayed *in vitro*, the resulting tyrosine-phosphorylated p27-CDK4-Cyclin D1 trimer was an active kinase for RB and other CDK4/D targets such as CDC6. Moreover, the tyrosine-phosphorylated trimer had a lower  $K_m$  for ATP than the CDK4-Cyclin D1 dimer (0.4 mM vs. 1.5 mM), leading to the suggestion that tyrosine-phosphorylated p27 is an allosteric *activator* of CDK4-Cyclin D1 (Guiley et al., 2019). However, since ATP levels inside cells are

typically in the mM range, the change in  $K_m$  is unlikely to have any major impact on physiological activity. More significant was the finding that the kinase activity of the tyrosine-phosphorylated trimer was not inhibited by palbociclib at all (Guiley et al., 2019), in contrast to the strong inhibition of the CDK4-Cyclin D1 dimer. Indeed, the binding of p27 and palbociclib to Cdk4 were found to be mutually exclusive. Furthermore, in cells arrested in G1 after prolonged treatment with palbociclib (for 48 h), levels of RB kinase activity in Cdk4 or cyclin D1 immunoprecipitates remained unchanged. Instead, there was a reduction in the RB kinase activity associated with CDK2 due, at least in part, to increased levels of p21 in the immunoprecipitates. Guiley et al. concluded that the cell cycle arrest induced by palbociclib was due to an indirect inhibition of CDK2, possibly through disrupting the p21-CDK4-Cyclin D1 trimer, leading to an accumulation of CDK4 monomer bound to palbociclib, and freeing the otherwise sequestered p21 to inhibit CDK2 (Guiley et al., 2019).

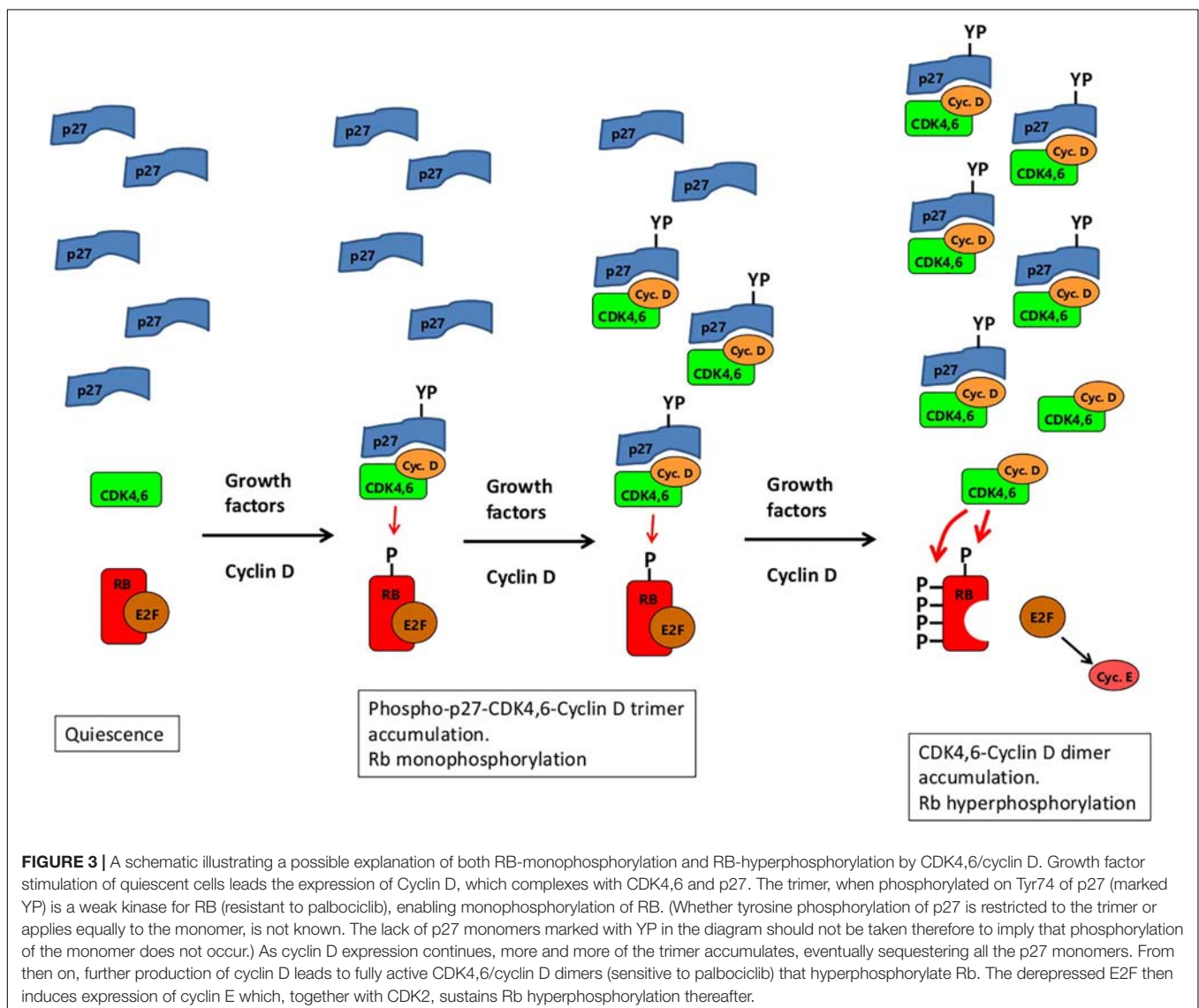


**FIGURE 3 |** A schematic illustrating a possible explanation of both RB-monophosphorylation and RB-hyperphosphorylation by CDK4,6/cyclin D. Growth factor stimulation of quiescent cells leads the expression of Cyclin D, which complexes with CDK4,6 and p27. The trimer, when phosphorylated on Tyr74 of p27 (marked YP) is a weak kinase for RB (resistant to palbociclib), enabling monophosphorylation of RB. (Whether tyrosine phosphorylation of p27 is restricted to the trimer or applies equally to the monomer, is not known. The lack of p27 monomers marked with YP in the diagram should not be taken therefore to imply that phosphorylation of the monomer does not occur.) As cyclin D expression continues, more and more of the trimer accumulates, eventually sequestering all the p27 monomers. From then on, further production of cyclin D leads to fully active CDK4,6/cyclin D dimers (sensitive to palbociclib) that hyperphosphorylate Rb. The derepressed E2F then induces expression of cyclin E which, together with CDK2, sustains Rb hyperphosphorylation thereafter.



Although the tyrosine-phosphorylated p27-CDK4-Cyclin D1 trimer was said to be an active RB kinase, this depends on how kinase activity is measured. Using a recombinant fragment of RB consisting of amino acids 771–874, the trimer was just as active as the CDK4-Cyclin D1 dimer. However, this RB fragment lacks a C-terminal alpha helix (amino acids 892–912) that provides an essential docking site required for efficient binding to CDK4,6-Cyclin D (Topacio et al., 2019). Using a larger RB fragment (amino acids 771–928) containing this docking site, the tyrosine-phosphorylated p27-CDK4-Cyclin D1 trimer is a *far less* active kinase than the CDK4-Cyclin D1 dimer, with a 13-fold lower  $V_{max}$  (Guiley et al., 2019). Thus, far from being an activator, p27 is an inhibitor of kinase activity for RB-substrates with an intact C-terminal tail. This could potentially explain the monophosphorylation of RB (Figure 3). On mitogenic stimulation of quiescent cells, the first cyclin D to be produced will be complexed with both CDK4,6 and p27 (Figure 3). After phosphorylation of p27 on Tyr74 (most likely by Src-like kinases, themselves responsive to mitogenic stimulation – Chu et al., 2007), the trimeric complex would gain sufficient kinase activity to be able to start the phosphorylation of RB (Figure 3). However, after adding the first phosphate, the association between RB and the trimer could conceivably be weakened (perhaps due to altered electrostatic charge), encouraging dissociation. Even without such weakening, by not being able to hold on tightly to the C-terminal docking helix due to blocking by p27 (Guiley et al., 2019), the p27-CDK4,6-cyclin D1 trimer might dissociate from RB before the addition of any further phosphates to it. If so, then only after sufficient cyclin D has been produced to sequester all the p27 in the cell, will CDK4,6/cyclin D dimer start to appear with full activity toward RB to ensure its hyperphosphorylation (Figure 3). (This built-in delay could be of value in enabling the cell to grow in mass before reaching a point of commitment to the next cell cycle.) Note that a possible argument against this scenario – that RB monophosphorylation was reported to be blocked by palbociclib (Narasimha et al., 2014) – can be dismissed because the palbociclib appears to have been added at the time of serum step-up, before the induction of cyclin D. As a result, the palbociclib would have bound first to CDK4,6 monomer (Guiley et al., 2019), preventing its subsequent association with cyclin D and p27.

If these speculations are correct, then the RB hyperphosphorylation seen in CDK2/E<sup>increasing</sup> cells immediately after mitosis could conceivably be due entirely to palbociclib-sensitive CDK4,6/cyclin D dimers, even though these may be a minor fraction of the total CDK4,6/cyclin D in the cell (Guiley et al., 2019). Nevertheless, when nearing the end of G1, cells have elevated levels of CDK2/E activity, just below those needed for entry into S phase. On inhibiting fully active CDK4,6/cyclin D dimers with palbociclib, there should be sufficient CDK2/E activity remaining to sustain RB hyperphosphorylation in the absence of CDK4,6/cyclin D activity. Instead, Chung et al. (2019) found complete reversal of RB hyperphosphorylation after just 15 min treatment with palbociclib. This implies that the CDK2/E present has no activity toward RB, which is difficult to understand. The most likely explanation would seem to be that palbociclib causes rapid

dissociation of CDK4-Cyclin D1 trimer complexes with p27 or p21, freeing the sequestered p21/p27 to inhibit the CDK2/E, i.e., an indirect inhibition of CDK2 activity by palbociclib, as suggested by Guiley et al. (2019). Consistent with this, the activity of CDK2/E is seen to start falling immediately after the addition of palbociclib (Chung et al., 2019). Thus, the provocative suggestion of Chung et al. (2019) that Cyclin E plays no role in RB hyperphosphorylation until after the G1/S transition remains to be established, by ruling out any indirect inhibition of CDK2/E by palbociclib. This could perhaps be done by repeating the experiments with cells deficient for both p21 and p27. In this case, palbociclib should be unable to reverse RB hyperphosphorylation and block entry into S phase after the point of mitogen independence (passage of the Restriction Point), as there would be no sequestered p21 or p27 to relocate to and inhibit CDK2/E. However, cells lacking both p21 and p27 may be compromised in their assembly of active CDK4,6/cyclin D complexes (Cheng et al., 1999), which would complicate the experiments.

## APC/C<sup>CDH1</sup> INACTIVATION

In continuous cycling cells or in cells stimulated from quiescence, there comes a point in G1 when CDK2/E,A activity starts to rise inexorably and monotonically, indicating the start of the next cycle (Figure 2A). Activity reaches a peak at mitosis, after which it declines rapidly toward a baseline. As the level rises from baseline to peak, a threshold is reached when the cell becomes irreversibly committed to entry into S phase (Spencer et al., 2013; Barr et al., 2016; Schwarz et al., 2018; Chung et al., 2019). A similar requirement to achieve a threshold level of CDK activity for entry into S phase is also seen in Fission yeast (Coudreuse and Nurse, 2010), suggesting that this is a universal requirement. An important question that follows on from this is how a gradually increasing level of CDK activity is translated into an abrupt, all-or-none commitment to enter S phase. Recent live-cell imaging studies suggest that inactivation of the Anaphase Promoting Complex or Cyclosome (APC/C), a multimeric ubiquitin E3-ligase, may be key to this.

The activity of APC/C depends on two substrate-recognition adaptor proteins, CDC20 and CDH1 (reviewed, Peters, 2006). Anaphase is brought about by APC/C complexed with CDC20. On exit from mitosis, CDC20 dissociates from APC/C and is replaced by CDH1, maintaining APC/C activity throughout G1. This prevents the accumulation of many proteins needed for S phase (see later). Switching off APC/C<sup>CDH1</sup> is therefore essential for entry into S phase and in keeping with this, CDH1 knockdown accelerates the G1/S transition (Sigl et al., 2009; Yuan et al., 2014).

By using a fluorescent reporter construct consisting of a fragment of geminin (a well-established APC/C target) conjugated to mCherry (Sakaue-Sawano et al., 2008), it has been possible to follow the activity of APC/C<sup>CDH1</sup> in living cells, in real time (Cappell et al., 2016). Remarkably, APC/C<sup>CDH1</sup> activity was found to disappear extremely abruptly in a switch-like manner (as illustrated in Figure 2B), over a span of about an hour (Cappell et al., 2016). The inactivation of APC/C<sup>CDH1</sup> occurred at different

times in different cells (**Figure 2B**), but was always just before the onset of S phase. For cells stimulated from quiescence, this was several hours after RB hyperphosphorylation and passage of the Restriction Point (apparent mitogen independence). The inactivation of APC/C<sup>CDH1</sup> required CDK2/E activity and was blocked by a low dose of a CDK1,2 inhibitor or by knockdown of cyclin E with siRNA (though not cyclin A). However, once inactivated (“off”), APC/C<sup>CDH1</sup> could not be switched on again with the same low dose of CDK1,2 inhibitor (Cappell et al., 2016, 2018), consistent with inactivation being an irreversible transition. For the cells in which CDK/E,A activity does not rise immediately after M (the CDK/E,A<sup>low</sup> population), APC/C<sup>CDH1</sup> activity remains “on” for as long as CDK/E,A activity continues to be low. However, once CDK/E,A activity starts to rise, APC/C<sup>CDH1</sup> inactivation typically follows 3–5 h later, suggesting a requirement to reach a threshold level of activity.

A schematic illustrating the major interacting networks surrounding APC/C<sup>CDH1</sup> and its connections to the RB-E2F switch and the onset of DNA synthesis, is shown in **Figure 4**. The abruptness of the fall in APC/C<sup>CDH1</sup> activity, once it starts (**Figure 2B**), is unaffected by a pan-cullin inhibitor (Cappell et al., 2016). This indicates that the sudden, sharp fall in APC/C<sup>CDH1</sup> activity is not dependent on the SCF (Skp1/CUL1/F-box protein) family of cullin E3 ubiquitin ligases that become active from late G1 to the end of G2, following APC/C<sup>CDH1</sup> inactivation (**Figure 4**). In keeping with this, knockdown of the SCF-substrate adaptor Cyclin F, with siRNA, also failed to alter the kinetics of APC/C<sup>CDH1</sup> inactivation (Cappell et al., 2018), even though SCF<sup>CyclinF</sup> is able to target CDH1 for destruction, and vice versa (Choudhury et al., 2016). Thus, the potential double-negative feedback loop between APC/C<sup>CDH1</sup> and SCF<sup>CyclinF</sup> (Choudhury et al., 2016) – see **Figure 4** – does not appear to be involved in controlling the abruptness of APC/C<sup>CDH1</sup> inactivation (Cappell et al., 2018), though it could contribute to its timing or the maintenance of inactivation once it has occurred. Likewise, knockdown of another SCF-substrate adaptor, SKP2, with siRNA, also fails to alter the kinetics of APC/C<sup>CDH1</sup> inactivation (Cappell et al., 2018). This shows that the abruptness of inactivation is not the result of increased CDK2/E activity following SCF<sup>SKP2</sup>-mediated elimination of p21 or p27 from inhibitory complexes with CDK2/E (Barr et al., 2016, 2017), though again some contribution to timing or maintenance of the APC/C<sup>CDH1</sup> switch cannot be ruled out (**Figure 4**). In contrast, siRNA-mediated knockdown of the APC/C<sup>CDH1</sup> inhibitor EMI1 *does* slow the rate of APC/C<sup>CDH1</sup> inactivation (Cappell et al., 2016, 2018). Moreover, although inactivation of APC/C<sup>CDH1</sup> still occurs after elimination of EMI1, after a delay during which CDK/E activity continues to rise, it is no longer irreversible to treatment with a low dose of CDK1,2 inhibitor. In addition, overexpression of EMI1 brought forward the abrupt inactivation of APC/C<sup>CDH1</sup> (Cappell et al., 2016). Thus EMI1 controls the timing, abruptness and irreversibility of APC/C<sup>CDH1</sup> suggesting that it plays a key part in the bistability of the switch (**Figure 4**). This bistability arises because EMI1 is both a substrate of APC/C<sup>CDH1</sup> at low concentrations, and an inhibitor of it at high concentrations, creating a double-negative feedback loop (Cappell et al., 2018).

Expression of EMI1 is induced by E2F (Hsu et al., 2002) after RB hyperphosphorylation and the RB-E2F switch (**Figure 4**). Initially, the newly made EMI1 is targeted for destruction by APC/C<sup>CDH1</sup>, keeping its concentration low. However, as CDK2/E activity rises, it phosphorylates and gradually inhibits APC/C<sup>CDH1</sup> allowing EMI1 to evade destruction and start accumulating. On reaching a threshold, EMI1 switches from being a substrate to being an inhibitor, further suppressing APC/C<sup>CDH1</sup>. This favors yet further accumulation of EMI1 culminating in complete inactivation of APC/C<sup>CDH1</sup>. Thus, the threshold for this switch is governed by both the level of CDK2/E activity and the concentration of EMI1. Without EMI1, inactivation of APC/C<sup>CDH1</sup> can still occur but requires a much higher CDK2/E activity, thereby delaying the switch. Conversely, upregulation of EMI1 brings forward the switch (Cappell et al., 2016, 2018).

## APC/C<sup>CDH1</sup> INACTIVATION MARKS THE POINT OF NO RETURN IN THE CELL CYCLE

Passage of the Restriction Point – usually equated with flipping of the RB/E2F switch and the acquisition of mitogen independence – is widely considered to be the critical point of no return in the cell cycle, when cells become irreversibly committed to the next cycle. However, the fact that entry into S phase can be blocked by palbociclib almost right up to the G1/S transition, with reversal of RB hyperphosphorylation, calls this into question (Chung et al., 2019). Regardless of the precise mechanism of action of palbociclib (as discussed earlier), this indicates a continuing role for CDK4,6/D (either direct, through RB phosphorylation, or indirect, through sequestering p27 or p21 away from CDK2/E) almost right up to the start of DNA synthesis. In contrast, once APC/C<sup>CDH1</sup> is inactivated, palbociclib is no longer able to arrest the cycle, consistent with inactivation being an irreversible transition.

In addition to treatment with palbociclib, cellular stress has also been reported to reverse passage of the Restriction Point, returning cells to quiescence (Cappell et al., 2016). When “early” G1 cells were exposed to a low dose of neocarzinostatin (NCS) to induce DNA damage, at a time when RB was already hyperphosphorylated and CDK/E,A activity had started to rise, some of the cells transiently reverted to having unphosphorylated/monophosphorylated RB, and the rise in CDK/E,A activity was delayed (for around 8 h). In addition, APC/C<sup>CDH1</sup> activity remained “on.” Similar results were seen after hypertonic treatment or exposure to hydrogen peroxide. If, after treatment with NCS, the cells were deprived of mitogens, most of those that reverted to unphosphorylated/monophosphorylated RB remained in this state, maintaining low CDK/E,A activity, suggesting a return to quiescence and the regaining of mitogen dependence. Consistent with this, when mitogens were restored, the cells resumed cycling, with CDK/E,A activity rising once more, followed by APC/C<sup>CDH1</sup> inactivation. However, the lag between mitogen restoration and the rise in CDK/E,A activity or APC/C<sup>CDH1</sup>

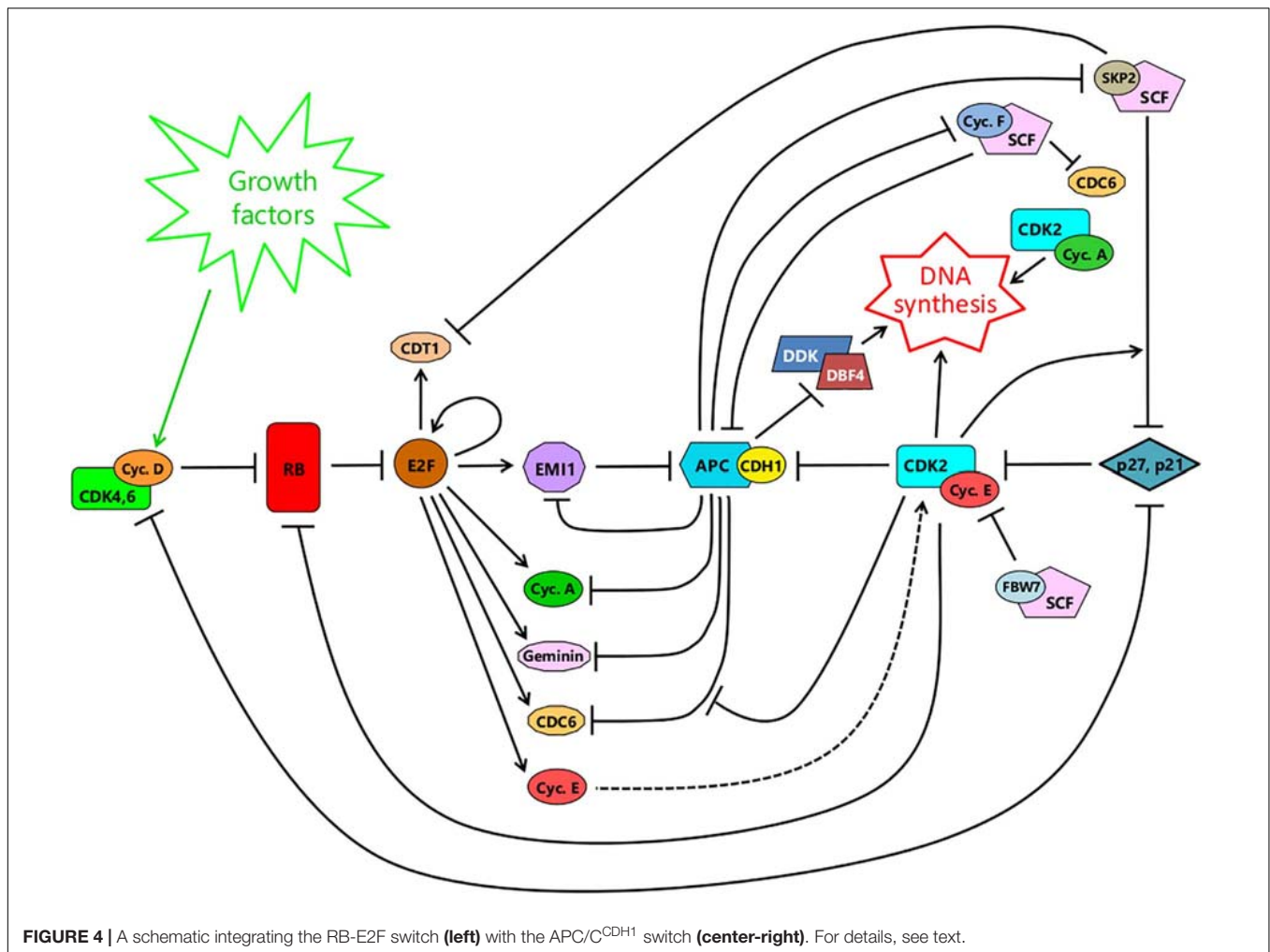


**FIGURE 4** | A schematic integrating the RB-E2F switch (left) with the APC/C<sup>CDH1</sup> switch (center-right). For details, see text.

loss was very short (less than 4 h, though rather imprecise) – much less than the normal pre-replicative lag (of around 12 h). Evidently, stress exposure had not returned the cells to a normal quiescent (G0) state. Nevertheless, the same stress exposures given after APC/C<sup>CDH1</sup> had switched off were without effect, and did not lead to APC/C<sup>CDH1</sup> reactivation. This reinforces the conclusion that once APC/C<sup>CDH1</sup> has been inactivated, the cell passes into a state from which it cannot easily return.

One of the few interventions known to allow reactivation of APC/C<sup>CDH1</sup> once it is switched off involves the knockdown of EMI1 (Barr et al., 2016; Cappell et al., 2016, 2018). However, such reactivation, after entry into S phase, leads to re-replication of DNA (Barr et al., 2016), so is not without deleterious consequences for the cell.

The only other intervention known to induce APC/C<sup>CDH1</sup> reactivation, after it has been switched off, is DNA damage (Wiebusch and Hagemeyer, 2010; Segeren et al., 2020). On the face of it, this might seem to contradict the findings of Cappell et al. (2016), who found no such reactivation, as indicated above. However, the time span of these studies is quite different. Starting with cells that had just undergone APC/C<sup>CDH1</sup> inactivation, Cappell et al. (2016) found no reactivation, following a short

pulse with a low dose of NCS, over the next 8 h. In the studies by Wiebusch and Hagemeyer (2010) and Segeren et al. (2020), somewhat higher levels of DNA damaging agents also produced little change in APC/C<sup>CDH1</sup> activity over the first 6 h. Only *after* this did APC/C<sup>CDH1</sup> levels start to rise, reaching a maximum roughly 12 h later. This reactivation of APC/C<sup>CDH1</sup> was accompanied by the loss of EMI1, through degradation and the suppression of transcription (Wiebusch and Hagemeyer, 2010). Importantly, experimental upregulation of EMI1 in S phase through knock-out of the E2F repressors E2F7/8, or overexpression of an activator E2F (E2F3), prevented the reactivation of APC/C<sup>CDH1</sup> (Segeren et al., 2020) after DNA damage, again underscoring the importance of EMI1 in maintaining the APC/C<sup>CDH1</sup> off-state (c.f. Figure 4). The pathway through which DNA damage brings about APC/C<sup>CDH1</sup> reactivation involves the induction of p53, which in turn acts partly through transactivation of E2F7 (and suppression of EMI1), but in particular through upregulation of p21 (Wiebusch and Hagemeyer, 2010; Segeren et al., 2020). Exactly how p21 contributes to the reactivation of APC/C<sup>CDH1</sup> was not established, but it is likely to be through inhibition of CDK2/cyclin E (c.f. Figure 4). Previously, Cappell et al. (2018)



had reported no reactivation of APC/C<sup>CDH1</sup> once it had switched off, using the maximum tolerated dose of a small molecule CDK1,2 inhibitor. However, the very high levels of p21 seen after DNA damage (Wiebusch and Hagemeyer, 2010; Segeren et al., 2020) may have achieved a more-complete inhibition of CDK2/cyclin E, sufficient to reverse the switch (Cappell et al., 2018). As with EMI1 knock-down above (Barr et al., 2016), the consequences of this premature reactivation of APC/C<sup>CDH1</sup>, after DNA damage, are not benign, and include cell senescence (Wiebusch and Hagemeyer, 2010) or re-replication (Segeren et al., 2020). Clearly, inappropriate reversal of the APC/C<sup>CDH1</sup> switch is not something easily tolerated.

## APC/C<sup>CDH1</sup> INACTIVATION REPRESENTS A CHANGE OF STATE IN THE CELL CYCLE

Following the sudden inactivation of APC/C<sup>CDH1</sup>, ubiquitin-mediated proteolysis in the cell cycle shifts abruptly from being APC/C<sup>CDH1</sup>-dependent to primarily SCF-dependent, marking a fundamental change of state (Figure 5). Prior to this transition, CDH1 is stable, targeting APC/C to the destruction of its own inhibitor, EMI1 (as already discussed). Also targeted are Cyclin F (Choudhury et al., 2016) and SKP2 (Bashir et al., 2004; Wei et al., 2004), substrate adaptors for SCF, keeping them “switched off.” After the transition switching off APC/C<sup>CDH1</sup>, EMI1 is stabilized and maintains the suppression of APC/C<sup>CDH1</sup>. Since cyclin F is no longer eliminated, SCF<sup>cyclinF</sup> also now accumulates, targeting CDH1 for proteolysis and further reinforcing the irreversibility of APC/C<sup>CDH1</sup> inactivation (Choudhury et al., 2016). Similarly, stabilization of SKP2 after APC/C<sup>CDH1</sup> inactivation leads to the formation of SCF<sup>SKP2</sup>, which targets any p21 or p27 present for proteolysis, after they have been phosphorylated by CDK2/E (Lu and Hunter, 2010). The active CDK2/E released would in turn further assist in maintaining the suppression of APC/C<sup>CDH1</sup> (Figure 4). Indeed, since phosphorylation of SKP2 on Ser64 by CDK2/E can prevent its interaction with APC/C<sup>CDH1</sup> (Rodier et al., 2008), stabilizing it, it is possible that some SCF<sup>SKP2</sup> may appear even before full APC/C<sup>CDH1</sup> inactivation, contributing to the timing of the switch, through p21 or p27 elimination and CDK2/E activation (Barr et al., 2016, 2017; Heldt et al., 2018).

Prior to the APC/C<sup>CDH1</sup> “off” transition, factors required for DNA synthesis are actively destroyed. These include Cyclin A, which maintains CDK2 activity after the decline of Cyclin E following the start of S phase, and DBF4, an activator of CDC7 kinase, also known as DDK (DBF4-dependent kinase) (Figure 4). Conversely, the licensing of replication origins is favored. Licensing involves recruiting the MCM helicase to origins of replication, mediated by the licensing factors CDT1 and CDC6. These in turn bind to the hexameric Origin Recognition Complex (ORC1-6) assembled at potential initiation sites along the DNA (Blow and Dutta, 2005; Fragkos et al., 2015). Expression of both CDT1 and CDC6 is induced by E2F (Figure 4). However, CDC6 is initially targeted for destruction by APC/C<sup>CDH1</sup> until it gets phosphorylated by CDK2/cyclin E, which blocks recognition by

CDH1, stabilizing it (Mailand and Diffley, 2005; Figure 4). This opens up a window for origin licensing between the appearance of CDK2/cyclin E and the inactivation of APC/C<sup>CDH1</sup>.

After the inactivation of APC/C<sup>CDH1</sup>, DBF4 and cyclin A are no longer targeted for proteolysis and are able to accumulate, facilitating, along with CDK2 and cyclin E, the initiation of DNA synthesis (Fragkos et al., 2015). At the same time, CDC6 and CDT1 become targeted for destruction by SCF<sup>cyclinF</sup> and SCF<sup>SKP2</sup> respectively (Figures 4, 5), terminating the capacity for further origin licensing (or re-licensing). In addition, geminin (an inhibitor of CDT1 through direct binding), is now able to accumulate (Figures 4, 5), reinforcing the suppression of origin licensing. Thus, after APC/C<sup>CDH1</sup> inactivation, cells pass from a state where origin licensing is possible but DNA replication is not, to one where the initiation of DNA synthesis can occur but relicensing cannot.

## THE G1/S TRANSITION AND THE INITIATION OF DNA SYNTHESIS

Entry into S phase, marked by the initiation of DNA synthesis, occurs with inevitability and very quickly (in an hour or so), after APC/C<sup>CDH1</sup> is switched off (Cappell et al., 2016). When DNA synthesis begins in a given cell, it does so simultaneously at dozens of separate replication foci scattered throughout the nucleus (Newport, 1996). This would seem to suggest a sudden, global change of state acting throughout the nucleus to trigger the onset of DNA synthesis at multiple origins, but what this might be remains unclear. The firing of replication origins requires both CDK activity (driven by either cyclin E or cyclin A) and DDK activity (driven by DBF4) (Fragkos et al., 2015). As discussed earlier, CDK/E,A activity increases rather gradually during G1 and it is difficult to see how just attaining a threshold could have the switch-like precision to trigger the synchronous firing of numerous, dispersed replication foci, each consisting of multiple replication origins. The requirement for DDK activity explains why the initiation of DNA synthesis cannot take place before APC/C<sup>CDH1</sup> is switched off since it is only after this that DBF4 is able to accumulate (Figure 5). However, the gradual accumulation of DBF4, after the switch, again makes it difficult to explain simultaneous initiation at multiple foci, at the start of S phase. The fact that it requires *both* CDK and DDK activity adds an element of cooperativity, but synchronous origin firing remains difficult to understand in the absence of a switch-like mechanism acting throughout the nucleus.

Although the number of licensed origins declines with time during quiescence, in recently quiescent cells enough origins remain licensed for the isolated (intact) nuclei to enter DNA synthesis when transferred into cytoplasmic S phase extracts from *Xenopus* eggs (Sun et al., 2000). Nevertheless, individual nuclei apparently begin DNA synthesis at different times, despite being present in the same S phase cytoplasm (Holla et al., 1994, 1996). The asynchrony is not correlated with differences in nuclear transport (Sun et al., 2001) and is therefore unlikely to be caused by differences between nuclei in the time taken to accumulate replication factors to a critical threshold. Instead, individual



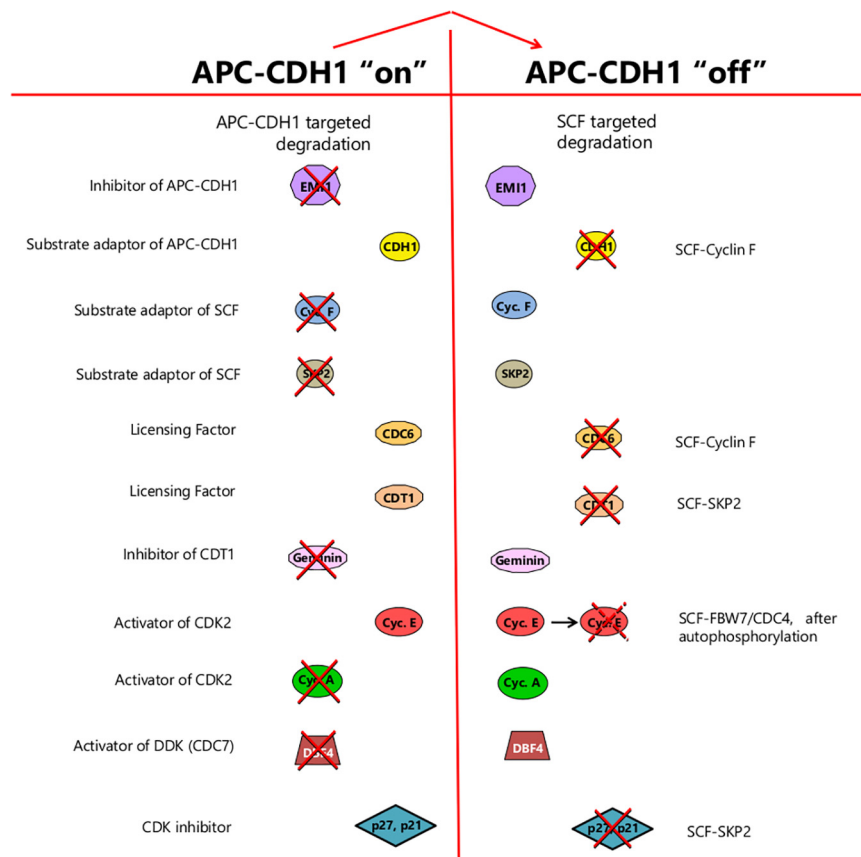


**FIGURE 5 |** The change of state resulting from APC/C<sup>CDH1</sup> inactivation. Prior to this transition, the cell is in a state where proteolysis targeted by APC/C<sup>CDH1</sup> predominates, leading to the elimination of EMI1, its own inhibitor, together with substrate adaptors for the SCF-ubiquitin ligase, and components needed for DNA synthesis such as DBF4 and cyclin A. Factors required for replication origin licensing (CDC6 and CDT1) are stable whereas geminin – an inhibitor of CDT1 and hence licensing – is destroyed. Following the switch, SCF-mediated-proteolysis is promoted by the stabilization of its substrate adaptors (such as SKP2 and cyclin F). Origin firing becomes possible on accumulation of DBF4, acting together with CDK2 activity promoted first by cyclin E, then cyclin A, with activity further enhanced by p27 and/or p21 elimination. Origin relicensing is prevented in part by SCF-targeted degradation of the CDC6 and CDT1 licensing factors together with CDT1 suppression through geminin accumulation. Thus, at the point of APC/C<sup>CDH1</sup> inactivation, the cell passes from a state where origin licensing is possible but origin-firing is prevented, to one where origin-firing becomes possible but relicensing is suppressed. The change of state, once it occurs, is irreversible due to EMI1 stabilization and SCF-mediated elimination of CDH1.

quiescent nuclei must vary in their sensitivity to the replication-inducing factors in *Xenopus* egg extracts. Remarkably, when permeabilized binucleate cells are added to such extracts, *both* nuclei of a pair show identical levels of DNA synthesis suggesting synchrony in the timing of initiation, even though different pairs of nuclei start DNA synthesis at different times (Holo et al., 1996). Clearly, whatever determines the sensitivity of nuclei to the inducers of DNA synthesis, it is a property shared by nuclei formed in a common cytoplasm. (The binucleate cells were generated by blocking cytokinesis with cytochalasin B, prior to serum withdrawal to render them quiescent.) One possibility that might explain this is the degree of chromatin condensation. It is well known that different sets of replication origins fire at different (and reproducible) times throughout S phase, with heterochromatin (the most-condensed) replicating late (Fragkos et al., 2015). Thus the differences between pairs of binucleates in the time taken to start replicating may simply reflect the degree of chromatin compaction at the time of permeabilization and

exposure to egg cytoplasm. That such chromatin differences exist may be inferred from the studies of Yen and Pardee (1979), who noted for quiescent 3T3 cells that nuclear volume varied over a twofold range, despite DNA content being the same. Moreover, the cells with the largest nuclei (and, presumably, the most dispersed chromatin) were the first to start DNA synthesis after serum stimulation. Thus, the first nuclei to start DNA synthesis in egg extracts may simply be the ones with the most-open chromatin. This in turn offers a plausible explanation for the apparently simultaneous firing at multiple replication foci scattered throughout the nucleus on entry into S phase. These clusters of early firing origins are simply those in the most open chromatin, able to respond to the lowest level of replication-inducers as the cell first enters S phase, with origins in more-compacted chromatin firing later as the concentration of inducers in the nucleus rises, or the chromatin becomes decondensed. The apparently synchronous firing of multiple foci at the start of S phase may therefore be a reflection merely of

similar origin-sensitivity (accessibility), rather than the response to some global change of state extending throughout the nucleus at the time of the G1/S transition, downstream of APC/C<sup>CDH1</sup> inactivation. If so, then the interval between the APC/C<sup>CDH1</sup> “off” transition and the start of DNA synthesis, though short, would be expected to show some variation, inversely with nuclear volume (a surrogate for chromatin compaction). However, any such variance would be expected to be shared by sister cells, as with the nuclei of binucleates.

## BISTABLE SWITCHES AND RANDOM TRANSITIONS IN THE CELL CYCLE

For cells stimulated to re-enter the cell cycle from quiescence, the APC/C<sup>CDH1</sup> inactivation switch is triggered by the rise in CDK2/E activity that follows on from passage of the Restriction Point, which in turn is triggered by RB-hyperphosphorylation and the RB-E2F switch. It seems reasonable to ask whether these two bistable switches might correspond to the two random transitions postulated in the revised Transition Probability model (Brooks et al., 1980).

The original version of the Transition Probability model (Smith and Martin, 1973) proposed that cell cycle commitment involved a single random transition in G1, the probability of which varied with conditions. The transition, if it existed, divided the cycle into two parts, an A state in G1 in which cells “waited” for commitment to occur, and a deterministic B phase (the rest of the cell cycle, including S, G2, M and part of G1) which cells were obliged to complete, once started. The model accounted for the connection between cell cycle variability and the regulation of proliferation, for the exponential tail of the distribution of cycle times and for various other aspects of cell cycle kinetics including the invariable difficulty of synchronizing cells from one cycle to the next. Nevertheless, at first sight the model seemed unlikely since it was known that the cycle times of sister cells were highly correlated, with correlation coefficients typically of the order of 0.5. If each cycle were initiated purely at random then there is no reason why sister cell cycle times should be any more alike than random pairs. Nevertheless, sister cells rarely divide at exactly the same time and it transpired that the distribution of *differences* between sister cell cycle times (the so-called  $\beta$ -curve) was a near perfect exponential, indicating that all of the differences could be accounted for solely in terms of a single random transition (Minor and Smith, 1974; Shields, 1977, 1978; Shields and Smith, 1977). Cycle times as a whole, however, are more variable than predicted by a single random transition. It follows that B phase must vary in general, while being identical in sister cells.

The Two Transition extension of the Smith and Martin model (Brooks et al., 1980; Brooks, 1981) arose from attempts to account for the lag preceding entry into S phase following the restoration of serum to serum-starved, quiescent cells. After the lag, cells entered S phase with what appeared to be first order kinetics, as discussed earlier, consistent with the Smith and Martin model (Brooks, 1975, 1976). The random transition – if there was one – had to be placed toward the end of the lag, since this was always much longer than the minimum G1 of continuously cycling cells.

Consistent with this, the rate of entry into S phase declines quite quickly after removing the serum once more (Brooks, 1976). To explain the lag, and its independence on the level of stimulation, it was proposed that some lengthy process or processes, taking up most of the lag (and therefore called L) had to be completed before entry into S phase became possible. Process L was considered to start stochastically (the so-called Q transition), with a probability dependent on the level of stimulation. On completion of L, the cell was competent to undergo commitment to enter S phase, this corresponding to the Smith and Martin transition. At the same time, the “clock” was reset so that L could begin again (stochastically) in readiness for the next cell cycle. However, since L was longer than S + G2, it would be completed after mitosis in G1 of the daughter cells. Accordingly, sister cells would reach the point of commitment to S phase (the Smith and Martin transition) at the same time, thereby explaining both the sibling correlation and the exponential distribution of differences between sisters.

The two transition version of the Transition Probability model turned out to provide a remarkably good *quantitative* description of cell cycle variability in continuously cycling cells using just two parameters (the two transition probabilities), both of which were fixed in advance by the observed cell cycle statistics (standard deviation of cycle times, the mean or standard deviation of differences between sibling cycle times, and the sibling correlation), rather than curve-fitting (Brooks et al., 1980, 1983; Brooks, 1981, 1985). But, the nature of process L was never identified; early hopes that it might correspond to the biogenesis of mitotic centers (centrosomes) were not fulfilled (Brooks and Richmond, 1983; Alvey, 1985). In addition, many alternative models of cell cycle variability have been proposed and kinetics alone are insufficient to distinguish between them (Castor, 1980; Cooper, 1982; Yao, 2014; Arata and Takagi, 2019). Also lacking at the time was any plausible biological basis for the random transitions. Accordingly, transition probability models (and other kinetic models of the cell cycle) largely fell from view in favor of efforts to understand the molecular basis of cell cycle control. However, developments in systems biology have shown how interacting networks of continuous processes containing positive or double-negative feedback loops can generate bistability and ultrasensitivity, switching abruptly and irreversibly from one steady state to another with minimal perturbation (Thron, 1997; Aguda and Tang, 1999; Qu et al., 2003; Novák and Tyson, 2004; Yao et al., 2008; Stallaert et al., 2019). Such behavior could well provide an explanation for probabilistic transitions in terms of the now established molecular players in cell cycle control. A reconsideration of the two-transition model therefore seems timely.

Early studies indicated that the A state transition of the original Smith and Martin transition probability model – if it existed – must be located very close (within an hour or so) to the start of S phase (Brooks, 1977). A good case can be made that this transition corresponds to the abrupt and irreversible inactivation of APC/C<sup>CDH1</sup>. This event occurs at very different times in different cells (Cappell et al., 2016, 2018; Chung et al., 2019). It is triggered by the rise in CDK/E, A activity, the onset of which also shows a great deal of variability in timing between

individual cells (Spencer et al., 2013; Overton et al., 2014; Arora et al., 2017; Barr et al., 2017; Moser et al., 2018). In cycling cells, the timing of the rise in CDK/E,A activity depends on the level of CDK4,6/D activity immediately after mitosis, which in turn depends on mitogenic signaling or replication stress in the mother cell (Spencer et al., 2013; Arora et al., 2017; Barr et al., 2017; Yang et al., 2017; Chung et al., 2019; Min et al., 2020). This means that sister cells are in a similar state at birth and likely to reach the point when CDK/E,A activity starts to rise at the same time, accounting for much (possibly all) of the correlation between sister cell cycle times. However, subsequent activation of the APC/C<sup>CDH1</sup> switch is likely to occur at different times in sister cells due to stochastic variation. It seems possible that such differences in APC/C<sup>CDH1</sup> inactivation account for the majority of variation between siblings in the timing of S phase entry, and subsequently mitosis. For continuously cycling cells, the differences between sister cell cycle times are an almost perfect exponential distribution (the so-called  $\beta$ -curve), providing the most compelling evidence for the Smith & Martin A state transition, as already discussed). It would therefore be of considerable interest to know whether differences in the timing of APC/C<sup>CDH1</sup> inactivation in siblings are also exponentially distributed and identical to the differences in sister cell cycle times (the  $\beta$ -curve).

Although evidence for one random transition in the cell cycle remains good ( $\beta$ -curves), that for a second transition was always much less secure (Brooks, 1985). When the differences in sibling cycle times are subtracted, the left-over variation in cycle times within the population is well described by an exponential distribution (Brooks et al., 1980). However, it is likely that almost any other skewed distribution could fit just as well (Brooks, 1985). For cells re-entering the cycle from quiescence, it is clear that there is a great deal of population heterogeneity in the level of mitogenic stimulus required, with some cells much more sensitive than others. Transition probability models provide no insight into this heterogeneity. However, stochastic activation of a bistable RB-E2F switch, coupled with a variable switching threshold within the population (Kwon et al., 2017) due to known heterogeneity in the level of CDK-inhibitors such as p27 (Hitomi et al., 2006), is an attractive possibility.

Although the RB-E2F switch is widely accepted as the basis of the Restriction Point, as already discussed, in many types of continuously cycling cells, the majority are post-Restriction Point from birth, in so far as they continue on to S phase without further need of mitogenic stimulation (Spencer et al., 2013; Schwarz et al., 2018). The apparent lack of requirement for an RB-E2F switch can be explained if the level of CDK4,6/D activity is sufficiently high to stimulate enough active E2F (i.e., above the threshold required) to generate self-sustaining levels of cyclin E, from the start of G1. The level of CDK4,6/D activity after mitosis will depend on the extent of p21 and/or p27 expression, together with the amount of cyclin D protein inherited from the mother cell (Min et al., 2020). The levels of p21, p27 and cyclin D at the start of G1 clearly vary from cell to cell, but will be inherited more or less equally by sister cells, accounting for the sibling correlation. However, there is no obvious role for the RB-E2F bistable switch, or any other probabilistic transition in the mother cell cycle,

in explaining the post-Restriction Point state of daughter cells from birth. Evidently, the RB-E2F switch is not an obligatory feature of each and every cell cycle but a special case applicable to cells re-entering the cycle from quiescence, or to cells born with a level of CDK4,6/D activity below the threshold required to achieve self-sustaining levels of cyclin E without mitogens (the CDK/E,A<sup>low</sup> cohort).

In conclusion, evidence for one random transition in the cell cycle (the Smith and Martin “A” transition, located very close to the start of S phase, continues to be compelling, and it seems very plausible that it could correspond to the APC/C<sup>CDH1</sup> inactivation switch. For continuously cycling cells, the existence of a second random transition (the “Q” transition of the modified model; Brooks et al., 1980), no longer seems likely, despite the excellent quantitative predictions of the model. For quiescent cells responding to mitogens, a good case can be made that the RB/E2F switch is the basis of the Restriction Point. Nevertheless, as discussed in an earlier section, stochastic noise in switching seems to be a less important contributor to variability than factors leading to differences in the threshold for switching between cells (Kwon et al., 2017), in accounting for the variation in growth factor sensitivity within a population.

## OTHER SOURCES OF VARIATION IN THE CELL CYCLE

If there is no probabilistic transition in the mother cell determining levels of p21, p27, and cyclin D at the start of G1 in daughter cells, then understanding the reasons why these vary between cells becomes important. It is already established that p21 levels reflect replication stress or unrepaired DNA damage in the mother cell, indicating a purely deterministic contribution to cell cycle variability (Arora et al., 2017; Barr et al., 2017; Yang et al., 2017). Factors regulating p27 expression are less well understood, other than that levels are generally low in rapidly cycling cells and rise when cells become quiescent (Coats et al., 1996; Hitomi et al., 2006). However, in contrast to non-transformed cells, rapidly cycling HeLa cells, which lack functioning RB-family proteins, have high levels of p27 in G1 (Barr et al., 2016), perhaps substituting for the lack of an intact RB-E2F network. Further studies of the factors generating variability in p27 expression at the level of single cells, and the contribution of such variability to cell cycle timing, would seem to be a priority.

As for variability in the amount of cyclin D inherited by daughter cells, this is determined by differences in translational capacity at the end of G2 in mother cells (Min et al., 2020). Translational capacity is a reflection of the number of ribosomes per cell, at least in part, and is therefore an indicator of cell size. The bigger the cell, the greater will be the total amount of cyclin D made in any moment in time, even though the translation rate per ribosome is likely to be similar between cells of different size. Since cyclin D is a nuclear protein, it will be concentrated in the nucleus. Bigger mother cells would therefore be expected to achieve a higher *nuclear* concentration of cyclin D than small cells, a difference that would be passed on to daughter cells.

In turn, the higher nuclear levels of cyclin D in large daughters would accelerate their transit through G1, compared to small daughters. Cyclin D levels may therefore provide a link between translational capacity – and hence cell size – and cell cycle timing, potentially explaining (for mammalian cells) the widely observed inverse relationship between cell size and cell cycle time (Prescott, 1956; Fantes, 1977; Johnston et al., 1977; Miyata et al., 1978; Shields et al., 1978). A similar role in linking translation rate to the speed of transit through G1 has also been proposed for Cln3 (a functional homolog of cyclin D) in budding yeast (Polymenis and Schmidt, 1997; Litsios et al., 2019).

If the variation in cyclin D abundance at mitosis is due primarily to variation in cell size, then the faster transit of large daughters through G1 (due to high cyclin D), compared to small daughters, would narrow the dispersion of size by the time of the next mitosis. However, stochastic variation in the timing of the APC/C<sup>CDH1</sup> inactivation switch, would generate renewed variation in cell size at division by affecting cycle length. These two conflicting processes – one decreasing size variance and the other increasing it – may help to explain how distributions of cell size remain stable over time under steady state conditions. Of course, many other factors are involved in the regulation of cell size but further consideration of this important topic is beyond the scope of this article. Instead, the reader is referred to Zatulovskiy and Skotheim (2020) for an excellent recent review.

## CONCLUDING REMARKS

As reviewed here, the recent technical innovations in live-cell imaging have revolutionized the study of cell cycle regulation and have brought renewed attention to the existence of cell cycle variability. Ostensibly identical cells clearly undergo critical transitions at different ages and with the focus on individual cells, this variability becomes difficult to ignore. The parallel developments in systems biology in understanding the role of positive-feedback loops in generating molecular switches have also provided invaluable insight into how cell cycle transitions might be controlled (Thron, 1997; Aguda and Tang, 1999; Qu et al., 2003; Novák and Tyson, 2004; Yao et al., 2008; Stallaert et al., 2019). One such bistable switch – APC/C<sup>CDH1</sup> inactivation – has emerged as the most likely candidate for the point of no return in the mammalian cell cycle (Cappell et al., 2018), and noisy activation of the switch may well prove to be the basis of the elusive Smith and Martin random transition. Should this not turn out to be the case, then the origin of the exponential distribution of differences between sister cell cycle times would return as an important unanswered question.

For cell cycles as a whole, the variability is well-described by two random transitions (Brooks et al., 1980). However, no obvious candidate for the second transition has yet emerged. Instead, this additional variability, shared by sister cells, is likely to be a composite of several sources, of which cell size may be one of the most important. Cell size, as a determinant of translational capacity, influences the amount of cyclin D and CDK4,6 activity inherited by daughter cells, and the timing of the next cell cycle. In addition, nuclear size, again usually shared by

sister cells, seems likely to determine the time taken to respond to the inducers of DNA synthesis present once the cell is committed to enter S phase.

As for the Restriction Point – the moment when cell cycle progress becomes independent of mitogenic stimulation – this can no longer be regarded as an obligatory and irreversible decision point in each and every cell cycle that all cells must pass through. Rather, for many cell types, the majority of rapidly cycling cells are already mitogen-independent from birth. Such cells inherit a level of CDK4,6/D activity above the threshold needed to generate sufficient cyclin E to maintain RB hyperphosphorylation in the absence of further mitogenic stimulation. However, cells born with a level of CDK4,6/D activity below the threshold lose RB hyperphosphorylation and return to a state of mitogen dependence for further progress though the cell cycle. For these, and for long-term quiescent cells, the Restriction Point concept remains valid. Indeed, stochastic activation of the RB-E2F switch may contribute to some of the variability in their subsequent re-entry into the cell cycle, though a bigger contribution seems to come from heterogeneity in the switching threshold, most likely due to differences between cells in the levels of CDK inhibitors (p27, p21). As for the notion that passage of the Restriction Point is strictly irreversible, this now requires qualification. Although it is not reversible with normal, physiological interventions (such as growth factor removal), pharmacological blocking of CDK4,6/D and (probably) CDK2/E activity (indirectly) leads to a loss of RB hyperphosphorylation and a return to mitogen dependence (Cappell et al., 2016). This is not possible after the APC/C<sup>CDH1</sup> inactivation transition.

It is to be expected that further refinements of live-cell imaging techniques will lead to ever fuller understanding of why cell cycles are so variable. Nevertheless, it is worth emphasizing that this will require great precision in determining the timing of intracellular events. Classical cell biology approaches have led to the conclusion that most cell cycle variability is in G1 and that the duration of S + G2 is relatively constant (Sisken and Morasca, 1965; Tobey, 1973; Shields et al., 1978; Brooks et al., 1983; Zetterberg and Larsson, 1985). In contrast, recent live-cell imaging studies using a fluorescent PCNA reporter have concluded that G1, S, and G2 are all independently variable (Chao et al., 2019). However, this rests on noise-free determination of entry into and exit from S phase. These transitions are assessed by changes in the granularity of PCNA fluorescence (nuclear foci). In most cases, this is unambiguous, but with a few cells it is difficult to say precisely when S phase begins and ends (especially the former). Indeed, this is apparent in Figure 2E of Chao et al. (2017) where a few cells in S phase have very few PCNA foci. Such measurement uncertainty would increase the apparent variance in phase length estimates, possibly explaining the disparity with the older work. Measurement noise may also be an issue in determining CDK/E,A activity. This involves determining the ratio of nuclear to cytoplasmic levels of the DHB reporter. As such, the estimate is affected by the variance in both the nuclear and cytoplasmic measurements, which widens the confidence intervals. Added to this, the measurements may be affected by cell motility. As cells move, they round up and flatten out periodically, to varying degrees. This is likely to affect



the thickness of cytoplasm in the region of the ring around the nucleus used for quantitating reporter fluorescence. This could lead to variation in the fluorescence signal independent of any change in CDK/E,A activity. Such noise could well account for some of the differences in activity traces shown by different cells. Quantitating, or better, eliminating any such measurement noise is likely to become important in the discrimination between models.

It has often been said that cell division is too important to be left to chance yet variability seems to be embedded in the very fabric of cell cycle control. There are very good reasons why it should be. In free-living, single-cell organisms, cell cycle entry is controlled by nutrient availability. When nutrients are restored to starved cells, it would be undesirable for all of them to commit immediately to cell cycle re-entry, in case the restoration of nutrients is short-lived. If starvation conditions rapidly return, this could compromise survival of cells already committed to cell division. It is clearly advantageous for the timing of commitment to vary between cells, particularly in response to suboptimal conditions, where a graded response is needed in the population such that some cells respond and others do not. In the case of multicellular organisms, cell division is controlled less by nutrient supply than by growth factor signaling in the context of tissue

homeostasis. After wounding, new cells are required to repair the deficit, but it is important that not all cells in the tissue respond to the stimulus, to avoid an overshoot. This is not just a matter of having a localized stimulus in the proximity of the wound. In partial hepatectomy, cell division resumes throughout the liver remnant, not just at the cut edge, yet the response is proportional to need (the extent of hepatectomy). Ensuring a graded response to the level of mitogens is clearly of fundamental importance. *A priori*, this requires either an inherently probabilistic response to mitogenic stimuli, with probability proportional to the stimulus, or the generation of actual differences between cells in the threshold for response – or most likely both, as has been discussed here. Uncovering all the mechanisms involved clearly remains an important goal. In recent years, progress in understanding the molecular details of critical cell cycle transitions within individual cells has been impressive. There is now every reason to hope that in the very near future, a full, molecular understanding of the origins of the variability will be forthcoming.

## AUTHOR CONTRIBUTIONS

RB wrote and completed the review.

## REFERENCES

- Aguda, B. D., and Tang, Y. (1999). The kinetic origins of the restriction point in the mammalian cell cycle. *Cell Prolif.* 32, 321–335. doi: 10.1046/j.1365-2184.1999.3250321.x
- Alvey, P. L. (1985). An investigation of the centriole cycle using 3T3 and CHO cells. *J. Cell Sci.* 78, 147–162. doi: 10.1242/jcs.78.1.147
- Anders, L., Ke, N., Hydbring, P., Choi, Y., Widlund, H., Chick, J., et al. (2011). A Systematic Screen for CDK4/6 Substrates Links FOXM1 Phosphorylation to Senescence Suppression in Cancer Cells. *Cancer Cell* 20, 620–634. doi: 10.1016/j.ccr.2011.10.001
- Arata, Y., and Takagi, H. (2019). Quantitative Studies for Cell-Division Cycle Control. *Frontiers in Physiology* 10:1022.
- Arora, M., Moser, J., Phadke, H., Basha, A. A., and Spencer, S. L. (2017). Endogenous Replication Stress in Mother Cells Leads to Quiescence of Daughter Cells. *Cell Reports* 19, 1351–1364. doi: 10.1016/j.celrep.2017.04.055
- Bachman, K. E., Blair, B. G., Brenner, K., Bardelli, A., Arena, S., Zhou, S., et al. (2004). 21 (WAF1/CIP1) Mediates the Growth Response to TGF- $\beta$  in Human Epithelial Cells. *null* 3, 221–225. doi: 10.4161/cbt.3.2.666
- Barr, A. R., Cooper, S., Heldt, F. S., Butera, F., Stoy, H., Mansfeld, J., et al. (2017). DNA damage during S-phase mediates the proliferation-quiescence decision in the subsequent G1 via 21 expression. *Nature Communications* 8, 14728.
- Barr, A. R., Heldt, F. S., Zhang, T., Bakal, C., and Novák, B. (2016). A Dynamical Framework for the All-or-None G1/S Transition. *Cell Systems* 2, 27–37. doi: 10.1016/j.cels.2016.01.001
- Bashir, T., Dorrello, N. V., Amador, V., Amador, V. F., Guardavaccaro, D. F., and Pagano, M. (2004). Control of the SCF(Skp2-Cks1) ubiquitin ligase by the APC/C(Cdh1) ubiquitin ligase. *Nature* 428, 190–193. doi: 10.1038/nature02330
- Bertoli, C., Skotheim, J. M., and de Bruin, R. A. M. (2013). Control of cell cycle transcription during G1 and S phases. *Nature Reviews Molecular Cell Biology* 14, 518–528. doi: 10.1038/nrm3629
- Blow, J. J., and Dutta, A. (2005). Preventing re-replication of chromosomal DNA. *Nature Reviews Molecular Cell Biology* 6, 476–486. doi: 10.1038/nrm1663
- Bouchard, C., Thieke, K., Maier, A., Saffrich, R., Hanley-Hyde, J., Ansorge, W., et al. (1999). Direct induction of cyclin D2 by Myc contributes to cell cycle progression and sequestration of 27. *EMBO J.* 18, 5321–5333. doi: 10.1093/emboj/18.19.5321
- Bracken, A. P., Ciro, M., Cocito, A., and Helin, K. (2004). E2F target genes: unraveling the biology. *Trends in Biochemical Sciences* 29, 409–417. doi: 10.1016/j.tibs.2004.06.006
- Brooks, R. F. (1975). The kinetics of serum-induced initiation of DNA synthesis in BHK21/c13 cells, and the influence of exogenous adenosine. *J. Cell. Physiol.* 86, 369–377. doi: 10.1002/jcp.1040860409
- Brooks, R. F. (1976). Regulation of the fibroblast cell cycle by serum. *Nature* 260, 248–250. doi: 10.1038/260248a0
- Brooks, R. F. (1977). Continuous protein synthesis is required to maintain the probability of entry into S phase. *Cell* 12, 311–317. doi: 10.1016/0092-8674(77)90209-4
- Brooks, R. F. (1981). “Variability in the cell cycle and the control of proliferation,” in *The cell cycle*, ed. P. C. L. John (Cambridge: Cambridge University Press), 35–61.
- Brooks, R. F. (1985). “The transition probability model: successes, limitations and deficiencies,” in *Temporal Order*, eds L. Rensing and N. I. Jaeger (Berlin: Springer-Verlag), 304–314. doi: 10.1007/978-3-642-70332-4\_49
- Brooks, R. F., and Richmond, F. N. (1983). Microtubule-organizing centres during the cell cycle of 3T3 cells. *J. Cell Sci.* 61, 231–245. doi: 10.1242/jcs.61.1.231
- Brooks, R. F., and Riddle, P. N. (1988a). Differences in growth factor sensitivity between individual 3T3 cells arise at high frequency: possible relevance to cell senescence. *Expl. Cell Res.* 174, 378–387. doi: 10.1016/0014-4827(88)90308-4
- Brooks, R. F., and Riddle, P. N. (1988b). The 3T3 cell cycle at low proliferation rates. *J. Cell Sci.* 90, 601–612. doi: 10.1242/jcs.90.4.601
- Brooks, R. F., Bennett, D. C., and Smith, J. A. (1980). Mammalian cell cycles need two random transitions. *Cell* 19, 493–504. doi: 10.1016/0092-8674(80)90524-3
- Brooks, R. F., Richmond, F. N., Riddle, P. N., and Richmond, K. M. V. (1984). Apparent heterogeneity in the response of quiescent Swiss 3T3 cells to serum growth factors: implications for the transition probability model and parallels with “cellular senescence” and “competence”. *J. Cell. Physiol.* 121, 341–350. doi: 10.1002/jcp.1041210211
- Brooks, R. F., Riddle, P. N., Richmond, F. N., and Marsden, J. (1983). The G1 distribution of “G1-less” V79 Chinese hamster cells. *Expl. Cell Res.* 148, 127–142. doi: 10.1016/0014-4827(83)90193-3
- Burk, R. R. (1970). One-step growth cycle for BHK21-13 hamster fibroblasts. *Exp. Cell Res* 63, 309–316. doi: 10.1016/0014-4827(70)90218-1

- Cappell, S. D., Chung, M., Jaimovich, A., Spencer, S. L., and Meyer, T. (2016). Irreversible APC<sup>Cdh1</sup> Inactivation Underlies the Point of No Return for Cell-Cycle Entry. *Cell* 166, 167–180. doi: 10.1016/j.cell.2016.05.077
- Cappell, S. D., Mark, K. G., Garbett, D., Pack, L. R., Rape, M., and Meyer, T. (2018). EM1 switches from being a substrate to an inhibitor of APC/CCDH1 to start the cell cycle. *Nature* 558, 313–317. doi: 10.1038/s41586-018-0199-7
- Castor, L. N. (1980). A G1 rate model accounts for the cell-cycle kinetics attributed to “transition probability”. *Nature* 287, 857–859. doi: 10.1038/287857a0
- Chao, H. X., Fakhreddin, R. I., Shimerov, H. K., Kedziora, K. M., Kumar, R. J., Perez, J., et al. (2019). Evidence that the human cell cycle is a series of uncoupled, memoryless phases. *Mol. Syst. Biol.* 15, e8604.
- Chao, H. X., Poovey, C. E., Privette, A. A., Grant, G. D., Chao, H. Y., Cook, J. G., et al. (2017). Orchestration of DNA Damage Checkpoint Dynamics across the Human Cell Cycle. *Cell Systems* 5, 445–459. doi: 10.1016/j.cels.2017.09.015
- Cheng, M., Olivier, P., Diehl, J. A., Fero, M., Roussel, M. F., Roberts, J. M., et al. (1999). The p21Cip1 and p27Kip1 CDK “inhibitors” are essential activators of cyclin D-dependent kinases in murine fibroblasts. *EMBO J.* 18, 1571–1583. doi: 10.1093/emboj/18.6.1571
- Choi, Y. J., and Anders, L. (2014). Signaling through cyclin D-dependent kinases. *Oncogene* 33, 1890–1903. doi: 10.1038/onc.2013.137
- Choudhury, R., Bonacci, T., Arceci, A., Lahiri, D., Mills, C. A., Kernan, J. L., et al. (2016). APC/C and SCF<sup>Cyclin F</sup> Constitute a Reciprocal Feedback Circuit Controlling S-Phase Entry. *Cell Reports* 16, 3359–3372. doi: 10.1016/j.celrep.2016.08.058
- Chu, I., Sun, J., Arnaout, A., Kahn, H., Hanna, W., Narod, S., et al. (2007). 27 Phosphorylation by Src Regulates Inhibition of Cyclin E-Cdk2. *Cell* 128, 281–294. doi: 10.1016/j.cell.2006.11.049
- Chung, M., Liu, C., Yang, H. W., Köberlin, M. S., Cappell, S. D., and Meyer, T. (2019). Transient Hysteresis in CDK4/6 Activity Underlies Passage of the Restriction Point in G1. *Molecular Cell* 76, 1–12.
- Coats, S., Flanagan, M., Nourse, J., and Roberts, J. (1996). Requirement of p27Kip1 for restriction point control of the fibroblast cell cycle. *Science* 272, 877–880. doi: 10.1126/science.272.5263.877
- Cobrinik, D. (2005). Pocket proteins and cell cycle control. *Oncogene* 24, 2796–2809. doi: 10.1038/sj.onc.1208619
- Cooper, S. (1982). The continuum model: statistical implications. *J Theor. Biol* 94, 783–800. doi: 10.1016/0022-5193(82)90078-9
- Coudreuse, D., and Nurse, P. (2010). Driving the cell cycle with a minimal CDK control network. *Nature* 468, 1074–1079. doi: 10.1038/nature09543
- Fantes, P. A. (1977). Control of cell size and cycle time in *Schizosaccharomyces pombe*. *J Cell Sci* 24, 51–67. doi: 10.1242/jcs.24.1.51
- Fragkos, M., Ganier, O., Coulombe, P., and Mechali, M. (2015). DNA replication origin activation in space and time. *Nat Rev. Mol. Cell Biol* 16, 360–374. doi: 10.1038/nrm4002
- Fujimaki, K., and Yao, G. (2020). Cell dormancy plasticity: quiescence deepens into senescence through a dimmer switch. *Physiological Genomics* 52, 558–562. doi: 10.1152/physiolgenomics.00068.2020
- Fujimaki, K., Li, R., Chen, H., Della Croce, K., Zhang, H. H., Xing, J., et al. (2019). Graded regulation of cellular quiescence depth between proliferation and senescence by a lysosomal dimmer switch. *PNAS* 116, 22624. doi: 10.1073/pnas.1915905116
- Ginzberg, M. B., Chang, N., D’Souza, H., Patel, N., Kafri, R., and Kirschner, M. W. (2018). Cell size sensing in animal cells coordinates anabolic growth rates and cell cycle progression to maintain cell size uniformity. *Elife* 7, e26957.
- Guiley, K. Z., Stevenson, J. W., Lou, K., Barkovich, K. J., Kumarasamy, V., Wijeratne, T. U., et al. (2019). 27 allosterically activates cyclin-dependent kinase 4 and antagonizes palbociclib inhibition. *Science* 366, eaaw2106. doi: 10.1126/science.aaw2106
- Harrigan, J. A., Belotserkovskaya, R., Coates, J., Dimitrova, D. S., Polo, S. E., Bradshaw, C. R., et al. (2011). Replication stress induces 53BP1-containing OPT domains in G1 cells. *J Cell Biol* 193, 97–108. doi: 10.1083/jcb.201011083
- Heldt, F. S., Barr, A. R., Cooper, S., Bakal, C., and Novák, B. (2018). A comprehensive model for the proliferation-quiescence decision in response to endogenous DNA damage in human cells. *PNAS* 115, 2532. doi: 10.1073/pnas.1715345115
- Hitomi, M., Yang, K., Guo, Y., Fretthold, J., Harwalkar, J., and Stacey, D. (2006). p27Kip1 and Cyclin Dependent Kinase 2 Regulate Passage Through the Restriction Point. *Cell Cycle* 5, 2281–2289. doi: 10.4161/cc.5.19.3318
- Hola, M., Castleden, S., Howard, M., and Brooks, R. F. (1994). Initiation of DNA synthesis by nuclei from scrape-ruptured quiescent mammalian cells in high speed supernatants of *Xenopus* egg extracts. *J. Cell Sci.* 107, 3045–3053. doi: 10.1242/jcs.107.11.3045
- Hola, M., Howard, M., Nawaz, F. N., Castleden, S., and Brooks, R. F. (1996). Individual nuclei differ in their sensitivity to the cytoplasmic inducers of DNA synthesis: implications for the origin of cell cycle variability. *Expl. Cell Res.* 229, 350–359. doi: 10.1006/excr.1996.0380
- Holley, R. W., and Kiernan, J. A. (1968). “Contact inhibition” of cell division in 3T3 cells. *Proc. Natl. Acad. Sci. U. S. A.* 60, 300–304. doi: 10.1073/pnas.60.1.300
- Hsu, J. Y., Reimann, J. D. R., Sørensen, C. S., Lukas, J., and Jackson, P. K. (2002). E2F-dependent accumulation of hEmi1 regulates S phase entry by inhibiting APC<sup>Cdh1</sup>. *Nature Cell Biology* 4, 358–366. doi: 10.1038/ncb785
- Johnson, A., and Skotheim, J. M. (2013). Start and the restriction point. *Current. Opinion. in Cell Biology* 25, 717–723. doi: 10.1016/j.celb.2013.07.010
- Johnson, D. G., Schwarz, J. K., Cress, W. D., and Nevins, J. R. (1993). Expression of transcription factor E2F1 induces quiescent cells to enter S phase. *Nature* 365, 349–352. doi: 10.1038/365349a0
- Johnston, G. C., Pringle, J. R., and Hartwell, L. H. (1977). Coordination of growth with cell division in the yeast *Sacharomyces cerevisiae*. *Expl. Cell Res.* 105, 79–98. doi: 10.1016/0014-4827(77)90154-9
- Klein, E. A., and Assoian, R. K. (2008). Transcriptional regulation of the cyclin D1 gene at a glance. *J. Cell Sci.* 121, 3853. doi: 10.1242/jcs.039131
- Koundrioukoff, S., Carignon, S., Técher, H., Letessier, A., Brison, O., and Debatisse, M. (2013). Stepwise Activation of the ATR Signaling Pathway upon Increasing Replication Stress Impacts Fragile Site Integrity. *PLoS Genetics* 9:e1003643. doi: 10.1371/journal.pgen.1003643
- Kwon, J. S., Everetts, N. J., Wang, X., Wang, W., Croce, K. D., Xing, J., et al. (2017). Controlling Depth of Cellular Quiescence by an Rb-E2F Network Switch. *Cell Reports* 20, 3223–3235. doi: 10.1016/j.celrep.2017.09.007
- Lee, T. J., Yao, G., Bennett, D. C., Nevins, J. R., and You, L. (2010). Stochastic E2F Activation and Reconciliation of Phenomenological Cell-Cycle Models. *PLoS Biol* 8:e1000488. doi: 10.1371/journal.pbio.1000488
- Leone, G., Sears, R., Huang, E., Rempel, R., Nuckolls, F., Park, C. H., et al. (2001). Myc Requires Distinct E2F Activities to Induce S Phase and Apoptosis. *Molecular Cell* 8, 105–113. doi: 10.1016/s1097-2765(01)00275-1
- Leung, J. Y., Ehmann, G. L., Giangrande, P. H., and Nevins, J. R. (2008). A role for Myc in facilitating transcription activation by E2F1. *Oncogene* 27, 4172–4179. doi: 10.1038/onc.2008.55
- Litsios, A., Huberts, D. H. E. W., Terpstra, H. M., Guerra, P., Schmidt, A., Buczak, K., et al. (2019). Differential scaling between G1 protein production and cell size dynamics promotes commitment to the cell division cycle in budding yeast. *Nature Cell Biology* 21, 1382–1392. doi: 10.1038/s41556-019-0413-3
- Lu, Z., and Hunter, T. (2010). Ubiquitylation and proteasomal degradation of the 21(Cip1), p27(Kip1) and p57(Kip2) CDK inhibitors. *Cell Cycle* 9, 2342–2352. doi: 10.4161/cc.9.12.11988
- Lukas, C., Savic, V., Bekker-Jensen, S., Doil, C., Neumann, B., Sølvhøj Pedersen, R., et al. (2011). 53BP1 nuclear bodies form around DNA lesions generated by mitotic transmission of chromosomes under replication stress. *Nature Cell Biology* 13, 243–253. doi: 10.1038/ncb2201
- Mailand, N., and Diffley, J. F. X. (2005). CDKs Promote DNA Replication Origin Licensing in Human Cells by Protecting Cdc6 from APC/C-Dependent Proteolysis. *Cell* 122, 915–926. doi: 10.1016/j.cell.2005.08.013
- Malumbres, M., and Barbacid, M. (2009). Cell cycle, CDKs and cancer: a changing paradigm. *Nat Rev Cancer* 9, 153–166. doi: 10.1038/nrc2602
- Min, M., Rong, Y., Tian, C., and Spencer, S. (2020). Temporal integration of mitogen history in mother cells controls proliferation of daughter cells. *Science* 368, 1261–1265. doi: 10.1126/science.aay824
- Minor, P. D., and Smith, J. A. (1974). Explanation of degree of correlation of sibling generation times in animal cells. *Nature*. 248, 241–243. doi: 10.1038/248241a0
- Mittnacht, S. (1998). Control of pRB phosphorylation. *Current Opinion. in Genetics & Development* 8, 21–27. doi: 10.1016/s0959-437x(98)80057-9
- Miyata, H., Miyata, M., and Ito, M. (1978). The cell cycle in the fission yeast, *Schizosaccharomyces pombe*. I. Relationship between cell size and cycle time. *Cell Struct. & Funct.* 3, 39–46. doi: 10.1247/csf.3.39
- Moreno, A., Carrington, J. T., Albergante, L., Al Mamun, M., Haagensen, E. J., Komseli, E. S., et al. (2016). Unreplicated DNA remaining from unperturbed

- S phases passes through mitosis for resolution in daughter cells. *PNAS* 113, E5757–E5764.
- Moser, J., Miller, I., Carter, D., and Spencer, S. L. (2018). Control of the Restriction Point by Rb and 21. *PNAS* 115, E8219.
- Narasimha, A. M., Kaulich, M., Shapiro, G. S., Choi, Y. J., Sicinski, P., and Dowdy, S. F. (2014). Cyclin D activates the Rb tumor suppressor by mono-phosphorylation. *Elife* 3, e02872.
- Nassrally, M. S., Lau, A., Wise, K., John, N., Kotecha, S., Lee, K. L., et al. (2019). Cell cycle arrest in replicative senescence is not an immediate consequence of telomere dysfunction. *Mechanisms of Ageing and Development* 179, 11–22. doi: 10.1016/j.mad.2019.01.009
- Newport, J. Y. (1996). Organization of DNA into foci during replication. *Curr. Opin. Cell Biol.* 8, 365–368. doi: 10.1016/s0955-0674(96)80011-1
- Novák, B., and Tyson, J. J. (2004). A model for restriction point control of the mammalian cell cycle. *Journal of Theoretical Biology* 230, 563–579. doi: 10.1016/j.jtbi.2004.04.039
- Overton, K. W., Spencer, S. L., Noderer, W. L., Meyer, T., and Wang, C. L. (2014). Basal 21 controls population heterogeneity in cycling and quiescent cell cycle states. *Proc. Natl. Acad. Sci. USA* 111, E4386–E4393.
- Pardee, A. B. (1974). A restriction point for control of normal animal cell proliferation. *Proc. Natl. Acad. Sci. U. S. A.* 71, 1286–1290. doi: 10.1073/pnas.71.4.1286
- Pennycook, B. R., and Barr, A. R. (2020). Restriction point regulation at the crossroads between quiescence and cell proliferation. *FEBS Lett.* 594, 2046–2060. doi: 10.1002/1873-3468.13867
- Peters, J. M. (2006). The anaphase promoting complex/cyclosome: a machine designed to destroy. *Nature Reviews Molecular Cell Biology* 7, 644–656. doi: 10.1038/nrm1988
- Planas-Silva, M. D., and Weinberg, R. A. (1997). The restriction point and control of cell proliferation. *Current Opinion in Cell Biology* 9, 768–772. doi: 10.1016/s0955-0674(97)80076-2
- Polymenis, M., and Schmidt, E. V. (1997). Coupling of cell division to cell growth by translational control of the G1 cyclin CLN3 in *Yeast*. *Genes & Development* 11, 2522–2531. doi: 10.1101/gad.11.19.2522
- Prescott, D. M. (1956). Relation between cell growth and cell division. II. The effect of cell size on cell growth rate and generation time in *Amoeba proteus*. *Exp. Cell Res.* 11, 86–98. doi: 10.1016/0014-8287(56)90192-6
- Qu, Z., MacLellan, W. R., and Weiss, J. N. (2003). Dynamics of the Cell Cycle: Checkpoints, Sizers, and Timers. *Biophysical Journal* 85, 3600–3611. doi: 10.1016/s0006-3495(03)74778-x
- Rodier, G., Coulombe, P., Tanguay, P. L., Boutonnet, C., and Meloche, S. (2008). Phosphorylation of Skp2 regulated by CDK2 and Cdc14B protects it from degradation by APC(Cdh1) in G1 phase. *EMBO J.* 27, 679–691. doi: 10.1038/emboj.2008.6
- Sadasivam, S., and DeCaprio, J. A. (2013). The DREAM complex: master coordinator of cell cycle-dependent gene expression. *Nat. Rev. Cancer* 13, 585–595. doi: 10.1038/nrc3556
- Sage, J., Mulligan, G. J., Attardi, L. D., Miller, A., Chen, S., Williams, B., et al. (2000). Targeted disruption of the three Rb-related genes leads to loss of G(1) control and immortalization. *Genes Dev.* 14, 3037–3050. doi: 10.1101/gad.843200
- Sakaue-Sawano, A., Kurokawa, H., Morimura, T., Hanyu, A., Hama, H., Osawa, H., et al. (2008). Visualizing Spatiotemporal Dynamics of Multicellular Cell-Cycle Progression. *Cell* 132, 487–498. doi: 10.1016/j.cell.2007.12.033
- Schade, A. E., Oser, M. G., Nicholson, H. E., and DeCaprio, J. A. (2019). Cyclin D–CDK4 relieves cooperative repression of proliferation and cell cycle gene expression by DREAM and RB. *Oncogene* 38, 4962–4976. doi: 10.1038/s41388-019-0767-9
- Schwarz, C., Johnson, A., Kõivomägi, M., Zatulovskiy, E., Kravitz, C. J., Donic, A., et al. (2018). A Precise Cdk Activity Threshold Determines Passage through the Restriction Point. *Molecular Cell* 69, 253–264. doi: 10.1016/j.molcel.2017.12.017
- Segeren, H. A., van Rijnberk, L. M., Moreno, E., Riemers, F. M., van Lie, E. A., Yuan, R., et al. (2020). Excessive E2F Transcription in Single Cancer Cells Precludes Transient Cell-Cycle Exit after DNA Damage. *Cell Reports* 33, 108449. doi: 10.1016/j.celrep.2020.108449
- Sherr, C. J. (1995). D-type cyclins. *Trends in biochemical sciences* 20, 187–190.
- Sherr, C. J. (2019). Surprising regulation of cell cycle entry. *Science* 366, 1315. doi: 10.1126/science.aaz4043
- Shields, R. (1977). Transition probability and the origin of variation in the cell cycle. *Nature* 267, 704–707. doi: 10.1038/267704a0
- Shields, R. (1978). Further evidence for a random transition in the cell cycle. *Nature* 273, 755–758. doi: 10.1038/273755a0
- Shields, R., and Smith, J. A. (1977). Cells regulate their proliferation through alterations in transition probability. *J. Cell. Physiol.* 91, 345–356. doi: 10.1002/jcp.1040910304
- Shields, R., Brooks, R. F., Riddle, P. N., Capellaro, D. F., and Delia, D. (1978). Cell size, cell cycle and transition probability in mouse fibroblasts. *Cell* 15, 469–474. doi: 10.1016/0092-8674(78)90016-8
- Sicinska, E., Aifantis, I., Le Cam, L., Swat, W., Borowski, C., Yu, Q., et al. (2003). Requirement for cyclin D3 in lymphocyte development and T cell leukemias. *Cancer Cell* 4, 451–461. doi: 10.1016/s1535-6108(03)00301-5
- Sigl, R., Wandke, C., Rauch, V., Kirk, J., Hunt, T., and Geley, S. (2009). Loss of the mammalian APC/C activator FZR1 shortens G1 and lengthens S phase but has little effect on exit from mitosis. *J. Cell Sci.* 122, 4208. doi: 10.1242/jcs.054197
- Sisken, J. E., and Morasca, J. (1965). Intrapopulation kinetics of the mitotic cycle. *J. Cell Biol.* 25, 179–189. doi: 10.1083/jcb.25.2.179
- Smith, J. A., and Martin, L. (1973). Do cells cycle? *Proc. Natl. Acad. Sci. U. S. A.* 70, 1263–1267.
- Spencer, S. L., Cappell, S. D., Tsai, F. C., Overton, K. W., Wang, C. L., and Meyer, T. (2013). The Proliferation-Quiescence Decision Is Controlled by a Bifurcation in CDK2 Activity at Mitotic Exit. *Cell* 155, 369–383. doi: 10.1016/j.cell.2013.08.062
- Stallaert, W., Kedziora, K. M., Chao, H. X., and Purvis, J. E. (2019). Bistable switches as integrators and actuators during cell cycle progression. *FEBS Lett* 593, 2805–2816. doi: 10.1002/1873-3468.13628
- Sun, W. H., Hola, M., Baldwin, N., Pedley, K., and Brooks, R. F. (2001). Heterogeneity in nuclear transport does not affect the timing of DNA synthesis in quiescent mammalian cells induced to replicate in *Xenopus* egg extracts. *Cell Prolif.* 34, 55–67. doi: 10.1046/j.1365-2184.2001.00196.x
- Sun, W. H., Hola, M., Pedley, K., Tada, S., Blow, J. J., Todorov, I. T., et al. (2000). The replication capacity of intact mammalian nuclei in *Xenopus* egg extracts declines with quiescence, but the residual DNA synthesis is independent of *Xenopus* MCM proteins. *J. Cell Sci.* 113, 683–695. doi: 10.1242/jcs.113.4.683
- Takahashi, Y., Rayman, J. B., and Dynlacht, B. D. (2000). Analysis of promoter binding by the E2F and pRB families in vivo: distinct E2F proteins mediate activation and repression. *Genes & Development* 14, 804–816.
- Temin, H. M. (1971). Stimulation by serum of multiplication of stationary chicken cells. *J. Cell Physiol* 78, 161–170. doi: 10.1002/jcp.1040780202
- Thron, C. D. (1997). Bistable biochemical switching and the control of the events of the cell cycle. *Oncogene* 15, 317–325. doi: 10.1038/sj.onc.1201190
- Tobey, R. A. (1973). “Production and Characterization of Mammalian Cells Reversibly Arrested in G1 by Growth in Isoleucine-Deficient Medium,” in *Methods in Cell Biology*, ed. D. M. Prescott (Cambridge, MA: Academic Press), 67–112. doi: 10.1016/s0091-679x(08)60048-5
- Todaro, G. J., Lazar, G. K., and Green, H. (1965). The initiation of cell division in a contact-inhibited mammalian cell line. *J. Cell Physiol* 66, 325–333. doi: 10.1002/jcp.1030660310
- Topacio, B. R., Zatulovskiy, E., Cristea, S., Xie, S., Tambo, C. S., Rubin, S. M., et al. (2019). Cyclin D–Cdk4,6 Drives Cell-Cycle Progression via the Retinoblastoma Protein’s C-Terminal Helix. *Molecular Cell* 74, 758–770. doi: 10.1016/j.molcel.2019.03.020
- Wei, W., Ayad, N. G., Wan, Y., Zhang, G. J., Kirschner, M. W., and Kaelin, W. G. (2004). Degradation of the SCF component Skp2 in cell-cycle phase G1 by the anaphase-promoting complex. *Nature* 428, 194–198. doi: 10.1038/nature02381
- Weinberg, R. A. (2013). *The Biology of Cancer*. Garland.
- Wiebusch, L., and Hagemeier, C. (2010). 53- and p21-dependent premature APC/C–Cdh1 activation in G2 is part of the long-term response to genotoxic stress. *Oncogene* 29, 3477–3489. doi: 10.1038/onc.2010.99
- Wu, L., Timmers, C., Maiti, B., Saavedra, H. I., Sang, L., Chong, G. T., et al. (2001). The E2F1–3 transcription factors are essential for cellular proliferation. *Nature* 414, 457–462. doi: 10.1038/35106593
- Yang, H. W., Chung, M., Kudo, T., and Meyer, T. (2017). Competing memories of mitogen and 53 signalling control cell-cycle entry. *Nature* 549, 404–408. doi: 10.1038/nature23880
- Yao, G. (2014). Modelling mammalian cellular quiescence. *Interface Focus* 4, 20130074. doi: 10.1098/rsfs.2013.0074

- Yao, G., Lee, T. J., Mori, S., Nevins, J. R., and You, L. (2008). A bistable Rb-E2F switch underlies the restriction point. *Nature Cell Biology* 10, 476–482. doi: 10.1038/ncb1711
- Yen, A., and Pardee, A. B. (1979). Role of nuclear size in cell growth initiation. *Science* 204, 1315. doi: 10.1126/science.451539
- Yuan, X., Srividhya, J., De Luca, T., Lee, J. H., and Pomerening, J. R. (2014). Uncovering the role of APC-Cdh1 in generating the dynamics of S-phase onset. *MBoC* 25, 441–456. doi: 10.1091/mbc.e13-08-0480
- Zatulovskiy, E., and Skotheim, J. M. (2020). On the Molecular Mechanisms Regulating Animal Cell Size Homeostasis. *Trends in Genetics* 36, 360–372. doi: 10.1016/j.tig.2020.01.011
- Zetterberg, A., and Larsson, O. (1985). Kinetic analysis of regulatory events in G1 leading to proliferation or quiescence of Swiss 3T3 cells. *Proc. Natl. Acad. Sci. U. S. A.* 82, 5365–5369. doi: 10.1073/pnas.82.16.5365

**Conflict of Interest:** The author declares that the research was conducted in the absence of any commercial or financial relationships that could be construed as a potential conflict of interest.

**Publisher's Note:** All claims expressed in this article are solely those of the authors and do not necessarily represent those of their affiliated organizations, or those of the publisher, the editors and the reviewers. Any product that may be evaluated in this article, or claim that may be made by its manufacturer, is not guaranteed or endorsed by the publisher.

Copyright © 2021 Brooks. This is an open-access article distributed under the terms of the Creative Commons Attribution License (CC BY). The use, distribution or reproduction in other forums is permitted, provided the original author(s) and the copyright owner(s) are credited and that the original publication in this journal is cited, in accordance with accepted academic practice. No use, distribution or reproduction is permitted which does not comply with these terms.





# Molecular Regulation of Paused Pluripotency in Early Mammalian Embryos and Stem Cells

Vera A. van der Weijden and Aydan Bulut-Karslioglu\*

Max Planck Institute for Molecular Genetics, Berlin, Germany

## OPEN ACCESS

### Edited by:

Alexis Ruth Barr,  
Medical Research Council,  
United Kingdom

### Reviewed by:

Carla Mulas,  
University of Cambridge,  
United Kingdom  
Harry Leitch,  
Medical Research Council,  
United Kingdom

### \*Correspondence:

Aydan Bulut-Karslioglu  
aydan.karslioglu@molgen.mpg.de

### Specialty section:

This article was submitted to  
Cell Growth and Division,  
a section of the journal  
Frontiers in Cell and Developmental  
Biology

**Received:** 11 May 2021

**Accepted:** 06 July 2021

**Published:** 27 July 2021

### Citation:

van der Weijden VA and  
Bulut-Karslioglu A (2021) Molecular  
Regulation of Paused Pluripotency  
in Early Mammalian Embryos  
and Stem Cells.  
Front. Cell Dev. Biol. 9:708318.  
doi: 10.3389/fcell.2021.708318

The energetically costly mammalian investment in gestation and lactation requires plentiful nutritional sources and thus links the environmental conditions to reproductive success. Flexibility in adjusting developmental timing enhances chances of survival in adverse conditions. Over 130 mammalian species can reversibly pause early embryonic development by switching to a near dormant state that can be sustained for months, a phenomenon called *embryonic diapause*. Lineage-specific cells are retained during diapause, and they proliferate and differentiate upon activation. Studying diapause thus reveals principles of pluripotency and dormancy and is not only relevant for development, but also for regeneration and cancer. In this review, we focus on the molecular regulation of diapause in early mammalian embryos and relate it to maintenance of potency in stem cells *in vitro*. Diapause is established and maintained by active rewiring of the embryonic metabolome, epigenome, and gene expression in communication with maternal tissues. Herein, we particularly discuss factors required at distinct stages of diapause to induce, maintain, and terminate dormancy.

**Keywords:** embryonic diapause, pluripotency, dormancy, metabolism, transcription, miRNA, signaling pathways, stem cells

## INTRODUCTION

Five momentous periods characterize the storyline of most animal life: fertilization, embryonic development, juvenility, sexual maturation, and reproduction. The reproductive drive motivates all of these steps, with the ultimate goal of contributing an individual's genes to the next generations. Numerous reproductive tactics are employed to maximize the fitness of the young. For example, red-sided garter snakes store sperm for up to 1 year after mating to adjust the timing of fertilization, and to allow post-copulatory sexual selection. Wallabies mate within 1 h after giving birth and always rear an offspring, ensuring that any lost pouch young can be replaced as quickly as possible. In developing embryos of many species, the precursors of oocyte and sperm, primordial germ cells, are put aside even before the early embryo has established major tissues for itself, which may reduce the likelihood of *de novo* mutations in the germline (Milholland et al., 2017).

Most fish and amphibians produce numerous offspring, of which only a small percentage survives juvenility. In contrast, mammals produce 1–15 offspring at once and look after them a considerably long time thereby increasing the chances of juvenile survival. For this reason, the mammalian investment in each offspring during gestation, lactation and further nurturing of the young is energetically and temporally expensive, for which the necessary resources may not exist at all times. From a species' survival point of view, flexible adjustment of reproductive timing in

response to metabolic and environmental restrictions could make the difference between survival and extinction. In more moderate circumstances, such flexibility enhances reproductive efficiency.

Fertilization initiates the progressive development of the embryo. Within the first few days of development, most mammalian embryos activate their genome for transcription, go through a few cell divisions, and organize into the first embryonic structure called the blastocyst. Embryonic and extraembryonic cells are already allocated, yet undifferentiated, in the blastocyst. Although it takes place *in vivo*, this pre-implantation period of embryonic development is self-sufficient, as the fertilized oocyte can proceed through the same developmental steps in a minimally enriched culture medium *ex vivo*. Once at the blastocyst stage, and if the uterus is receptive, the embryo implants and proceeds with further developmental steps including gastrulation and organogenesis. *Ex vivo* cultured blastocysts cannot sustain pluripotency under standard culture conditions and collapse within 2–3 days (Bulut-Karslioglu et al., 2016). Thus, blastocysts can only be cultured transiently in regular embryo culture medium. Taken together, mammalian early development proceeds through sequential steps coordinated by maternal and embryonic programs, and is largely unyielding to temporal adjustments of individual steps. However, many mammalian species can delay embryonic development at the blastocyst stage to adjust the timing of birth such that the offspring and the mother will have a better chance of survival during the energetically demanding lactational period and beyond. Here we focus on delayed development by inhibition of embryo implantation, also called delayed implantation or *embryonic diapause*. A few other species, such as some bats, can delay development after implantation, which is beyond the scope of this review. Importantly, many other vertebrates and non-vertebrates such as several species of nematodes, crustaceans, fish, and birds can also suspend development in accordance with environmental conditions. Although also referred to as diapause, non-mammalian embryos are commonly *paused* at more complex embryonic stages (e.g., with fully specified tissues in the annual killifish) compared to the blastocyst, and are thus largely out of the focus of this review. However, where appropriate, we discuss potentially common regulatory mechanisms between mammalian and non-mammalian embryonic diapause.

## Mammalian Diapause Is a Feature of the Blastocyst





Although the embryos of some species such as cow begin gastrulation before implantation (van Leeuwen et al., 2015; Pfeffer et al., 2017), the blastocyst is usually the stage at which mammalian embryos implant. Therefore, it is also the stage that diapause occurs in the absence of implantation. The embryo is only conducive to diapause at the blastocyst stage, and not earlier, even when diapause is induced experimentally *in vivo* and *ex vivo* (Bulut-Karslioglu et al., 2016; Renfree and Fenelon, 2017). Many mammalian embryos fail to develop beyond the cleavage stages due to genetic aberrations or other causes (van der Weijden and Ulbrich, 2020). Pausing of embryos at the blastocyst stage, and therefore after cleavage stages, would readily integrate

this initial quality control, such that only successfully developing embryos would be kept dormant for further development (van der Weijden and Ulbrich, 2020).

Most mammalian (eutherian) blastocysts contain three different cell types: cells on the outside of the embryo, the trophoblast (TE), are the precursors of the placenta; and cells on the inside of the blastocyst, the inner cell mass, are a mix of precursors of embryonic tissues (the epiblast, Epi) and the yolk sac (the primitive endoderm, PrE). Stem cells representing the three early embryo cell types can be derived from the blastocyst and cultured *in vitro*. Trophoblast stem (TS) cells represent the trophoblast layer and can be differentiated into distinct trophoblast cells (Tanaka et al., 1998). Embryonic stem (ES) cells represent the epiblast and can generate all embryonic cell types across the three germ layers, as well as germ cells, therefore are pluripotent (Evans and Kaufman, 1981; Martin, 1981). Extraembryonic endoderm (XEN) stem cells represent the PrE and can be differentiated into more committed endodermal cells representing the yolk sac (Kunath et al., 2005). For clarity, we will refer to the early embryonic cells (Epi, PrE, TE) as cell types, and their *in vitro* counterparts as stem cells. The three early embryo stem cell types have distinct transcriptional and epigenetic profiles *in vitro* (ES, TS, and XEN) and *in vivo* (TE, Epi, and PrE) (Blakeley et al., 2015). Thus, common and distinct molecular regulators may be required to induce and maintain diapause in the different embryonic cell types. Furthermore, signaling and crosstalk between the different cell types likely instruct the paused stem cell states. Technical and material limitations usually prevent separate investigation of TE, Epi, and PrE cells *in vivo*. Stem cell models are thus valuable tools to dissect mechanisms regulating the three lineages. Although stem cell lines have so far been established in several mammalian species, most notably from rodents and humans, it remains a challenge to establish stem cell models of most wildlife species (Stanton et al., 2019). Except for mink, many diapause species lack stem cell models to date (Sukoyan et al., 1992; Menzorov et al., 2015), challenging identification and validation of molecular and genetic regulators of embryonic diapause. Derivation and induction of stem cells benefit from mapping and understanding of the transcriptional networks controlling embryonic cell types. Current low-input and single-cell transcriptomics and chromatin accessibility mapping technology allows blueprinting of gene networks in single embryos and cells (Blakeley et al., 2015; Wu et al., 2016; Guo et al., 2017). Application of these techniques to diapause embryos will expand the understanding of diapause pathways. It could further allow stem cell derivation from blastocysts or reprogramming of somatic cells to pluripotency via introduction of transcription factors governing each lineage.

## Triggers of Diapause and Reactivation

Diapause was first observed in the European roe deer (*Capreolus capreolus*) in 1854 (Bischoff, 1854). It is now known that over 130 mammalian species across eutherians and marsupials undergo diapause (Renfree and Fenelon, 2017; **Figure 1**). The duration of diapause is independent of gestational length and is rather a function of the prolongation required to optimally adjust the timing of birth (Renfree and Fenelon, 2017). Diapause is

Mammalian diapause				
	 Mouse	 Roe deer	 Mink	 Wallaby
# of embryos	6-12	1-4	2-12	1
occurrence	facultative	obligate	obligate	facultative or obligate
duration	up to ~40 days	4-5 months	2 weeks	11 months
post-implantation gestation length	16 days	4-5 months	31 days	9 days
growth during diapause	first 5 days	continuously	no proliferation	no proliferation
embryo cell number (diapause start-end)	140-200 cells	100-20k cells	250-500 cells	80 cells
embryo morphology	hatched blastocyst elongated	hatched blastocyst lemon shaped	blastocyst in zona pellucida	blastocyst in zona pellucida, mucin layer and shell coat

**FIGURE 1 |** Mammalian diapause characteristics in the mouse, roe deer, mink, and wallaby. Embryo morphology, diapause duration, and embryo number differ between species. Diapause duration is independent of the length of post-implantation gestation. Diapause is triggered either seasonally (obligate) or due to lactational stress (facultative). Embryo reactivation is triggered by alterations in photoperiod (mink, wallaby, roe deer) or end of lactation (mouse, wallaby).

either obligate or facultative, the latter case being triggered by lactational stress. The American mink (*Neovison vison*) employs obligate diapause every mating season and adjusts the length of diapause according to the timing of mating (diapause length is 1–2 weeks) (Murphy, 2012). Exit from diapause is triggered by increasing daylight (photoperiod) following the March equinox in the northern hemisphere (Pilbeam et al., 1979; Murphy et al., 1981; Douglas et al., 1998). Blastocysts of the house mouse (*Mus musculus*) undergo diapause if lactation and pregnancy occur at the same time. Diapause regulation is most intensely studied in mice, due to the availability of *in vivo*, *ex vivo* and *in vitro* models and the feasibility of functional gene perturbations. Diapause can be experimentally induced in the mouse by surgical removal of ovaries (ovariectomy) at embryonic day E3.5 or by injection of estrogen antagonists (Weitlauf and Greenwald, 1968; Hunter and Evans, 1999), both of which counteract the estrogen surge prior to implantation. In addition to eliminating estrogen, progesterone supplementation is required to sustain the pregnancy. Mouse diapause can be sustained for up to 36 days and possibly longer *in vivo* (twice as long as gestation), however, embryo loss occurs over time (Arena et al., 2021). Exit from diapause is triggered by an increase in uterine receptivity that either occurs when lactation ends or can be experimentally induced by injection of estradiol. Mouse blastocysts can also be induced to enter a diapause-like paused state *ex vivo* via a few alternate methods for variable durations, including chemical inhibition of the cytoplasmic kinase mTOR (up to 30 days after blastocyst formation) (Bulut-Karslioglu et al., 2016), inhibition of the transcriptional regulator Myc (18 h) (Scognamiglio et al., 2016), and overexpression of the microRNA let-7 (up to 14 days) (Liu et al., 2020). These molecular regulators are further

discussed below. Importantly, any *ex vivo* pausing method should be reversible and should not compromise the developmental potential of the blastocyst. Retransfer experiments in which paused, then released embryos are transferred to pseudopregnant surrogate female mice are necessary to test the developmental competence of experimentally paused embryos.

Marsupials also use diapause to adjust reproductive timing. Tammar wallabies (*Macropus eugenii*) generate one embryo per fertilization cycle, which undergoes both seasonal and lactational diapause for a remarkable 11 months (Renfree and Fenelon, 2017). After activation, marsupial embryos do not *per se* implant but loosely attach to the uterine wall, where they develop for about 26 days (Fenelon et al., 2017). The duration of diapause thus exceeds the duration of gestation by 10-fold in tammar wallabies. Wallaby diapause also differs from mouse and roe deer in that the blastocyst does not hatch out of its three embryonic coats (zona pellucida, mucin layer, and the shell coat) during diapause (Renfree and Fenelon, 2017). In contrast, mice, rats, and roe deer blastocysts have one embryonic coat (zona pellucida), out of which they hatch before diapause and eventual implantation. Additionally, marsupial blastocysts neither have an inner cell mass nor show differential staining of Epi, TE, or PrE markers in the blastocyst, suggesting that cell fate specification has not happened at this stage (Frankenberg et al., 2013). Exit from diapause in wallabies is triggered either by removal of the pouch young and its sucking stimulus, or by the onset of the summer solstice in the southern hemisphere (Renfree and Fenelon, 2017). Despite the occurrence of embryonic diapause in over 130 mammals, we do not have even a basic understanding of diapause duration and regulation in most species, including vulnerable species such as the panda bear.

## Are Embryos in Diapause Truly Dormant?

Dormancy represents a cellular state with reduced metabolic activity and little or no proliferation. For clarity, here we define dormancy as a complete loss of proliferation. We use the term “quiescence” only when evidence supports exit of cells from cell cycle. Embryonic diapause is characterized by a significant reduction in proliferation. But not all diapause embryos are truly dormant. About 10% of cells in the roe deer blastocyst proliferate throughout diapause, with the embryo expanding from 300 to 20,000 cells within 4 months (Rüegg et al., 2020). The inner cell mass proliferates less than the TE. The inner cell mass also undergoes morphological changes, from round to flattened to cyst to disc, indicating active restructuring and communication between the cells, even at the low rate of proliferation (Rüegg et al., 2020).

The mouse embryo cells reach near complete dormancy after 5 days in diapause. Kamemizu and Fujimori (2019) used the FUCCI model combined with staining of the proliferation marker Ki67 to investigate the cell cycle status of diapause mouse embryos over time and showed significant differences in the TE and ICM responses to diapause. While mural trophoblast (opposite side to ICM) largely stops proliferating 1 day after induction of diapause, polar trophoblast and the ICM gradually decrease proliferation over the next 4 days, reaching near-complete dormancy by diapause day 8.5 (D8.5, also called equivalent day of gestation 8.5, EDG8.5) (McLaren, 1968; Kamemizu and Fujimori, 2019). The sequence is reversed during exit from diapause, where the embryonic side (ICM and polar TE) activates before the mural TE. Prolonged diapause leads to a deeper dormant state which takes longer to activate. Upon activation and retransfer of EDG4.5 and EDG10.5 embryos, the authors found a 0.5–1 day delay in development of EDG10.5 embryos (Kamemizu and Fujimori, 2019).

The mouse embryo grows by about 140 cells and an estimated 4 times the volume during diapause compared to E4.0 blastocysts (Kamemizu and Fujimori, 2019). The epiblast and PrE do not grow, and, in contrast, can shrink by 40–50% (Battle-Morera et al., 2008). As a result, the TE grows significantly during the course of diapause. As mural TE ceases proliferation by E4.5–E5.5, the polar TE should then be responsible for most TE proliferation. TE proliferation, together with potential stretching as evidenced by increased distance between TE nuclei, are likely responsible for the characteristic elongated shape of the mouse embryo in diapause. We note that there is great variability between mouse embryos of the same strain as well as between strains in terms of cell proliferation and epiblast size. This phenotypic variation may affect the consequent developmental competence of the embryos and needs to be taken into account when determining sample sizes in mouse diapause experiments to robustly identify novel diapause markers and regulators.

## Conservation of Diapause Potential in Non-diapausing Species

Whether diapause is conserved across mammals is an intriguing question. Eutherian blastocysts generally follow the same blueprint of pre-implantation development, although exact cell

type-defining factors might vary between species (Blakeley et al., 2015; Nakamura et al., 2016; Petropoulos et al., 2016; Bernardo et al., 2018; Boroviak et al., 2018; Gerri et al., 2020). In this respect, more species might be capable of diapause than those actually employing it. To test whether non-diapausing species are responsive to dormancy triggers in the diapause uterus, interspecies transfer experiments have been performed. Embryos from two closely related species, the mink and the ferret (*Mustela putorius furo*) were transferred reciprocally (Chang, 1968). Ferret embryos showed delayed development and did not implant in the mink uterus under diapause, while normally diapausing mink embryos activated and implanted into the ferret uterus. An independent study showed sheep embryos undergoing diapause in the mouse uterus under diapause conditions, which upon activation and retransfer were able to give rise to live-born lambs (Ptak et al., 2012). These studies point to uterine control of diapause induction and maintenance and the conservation of diapause pathways, at least in mammals that have been studied. Although diapause is initially triggered by the non-receptivity of the uterus to an otherwise implantation-ready blastocyst, soluble uterine factors likely sustain the diapause state, as mouse and mink embryos in diapause do not remain dormant in basic culture medium lacking growth factors or relevant metabolites beyond a few days (Naeslund, 1979; Fenelon and Murphy, 2017). Therefore, the diapause uterine fluid is instructive in rewiring genetic pathways for maintenance of early embryonic dormancy.

## The Possibility of Diapause in Humans

A proven case of human diapause has never been documented. In naturally conceived pregnancies, precise determination of the exact time of fertilization or implantation is unlikely. Thus, if natural diapause exists in humans, it could only be detected by studying pregnancies following transfer of *in vitro* fertilized (IVF) embryos. Although sparse evidence shows that a large delay between transfer and implantation is possible (e.g., one case study shows a 5-week delay Grinstead and Avery, 1996), large-scale studies have not found such outliers. Naturally conceived human embryos implant 7–11 days after ovulation, although a range of 6–18 days was observed (Wilcox et al., 1999). Importantly, late implantation is associated with a higher rate of pregnancy loss. Late implantation, without a reduced cell proliferation of the embryo, may be caused by natural factors such as delayed uterine receptivity. However, xenobiotic factors such as those resulting from smoking also cause a higher rate of late implantation and pregnancy loss (Jukic et al., 2011). Taken together, there is currently no evidence that humans might use natural diapause as a reproductive strategy. It is important to note that, if diapause occurs in humans, it will most likely be triggered by lactational or nutritional stress. In this context, clinical studies present a challenge, since participants are very unlikely to experience such stresses. On occasions where mothers experience such stresses, e.g., during famines and droughts, reproduction timelines have not been analyzed. Moreover, the natural variation of gestation length in humans makes the detection of a potentially short diapause period challenging.

Similar to the ability of ferret and sheep embryos to undergo diapause as mentioned above, it is possible that human embryos



might have retained or acquired a capacity for diapause. This possibility can only be tested *ex vivo* using surplus embryos donated by IVF patients. Many IVF surplus embryos develop suboptimally, there is genetic variation in the human population and there is naturally more variable developmental rates of human embryos compared to captive-bred species, making it challenging to achieve statistical power. Nonetheless, qualitative evidence can be obtained. Indeed, Liu et al. (2020) recently showed a slight delay in the development of human blastocysts upon treatment with extracellular vesicles carrying the microRNA let-7g (52% vs. 30% day 7 survival in treated vs. control embryos). Human blastocysts were also reported to undergo diapause when coated with a mucin-mimicking synthetic gel, however, these did not retain the characteristic blastocyst morphology (Canton et al., 2016). Taken together, this evidence suggests that human diapause, if it occurs, likely lasts just a few days.

## Why Is It Important to Understand the Regulation of Diapause?

In progressive embryonic development, pluripotency co-occurs with proliferation and proliferation regulates gene activity. Mouse ES cells clearly illustrate this relationship, where high proliferative capacity is linked to hyper-transcription and -translation, which in turn promote open chromatin through gene turnover of transcriptional and euchromatin modifiers (Bulut-Karslioglu et al., 2018). In contrast, maintenance of pluripotency in diapause does not depend on proliferation. The diapause epiblast maintains naïve pluripotency networks and at the same time presents a distinct and largely suppressed transcriptional profile in response to altered cell proliferation (Boroviak et al., 2015). As such, diapause offers a unique model to dissect pluripotency and proliferation networks.

In addition to preserving the first three cell types in the embryo over longer periods, diapause might also enhance pluripotency. Indeed, the first ES cells (mouse) were derived from diapause embryos (Evans and Kaufman, 1981) and comparative analyses has shown that diapause embryos more efficiently gave rise to ES cells for the initial strain employed (129) as well as hitherto refractory strains (Brook and Gardner, 1997). The increased efficiency cannot be explained by increased embryo size, since epiblasts were extracted for ES derivation and later studies showed that the epiblast cell number does not increase, and contrarily may decrease during diapause (Batlle-Morera et al., 2008). Thus, embryonic dormancy likely enhances the ability to give rise to ES cells. Whether this effect is due to rewiring of transcriptional and epigenetic landscapes or by other means is unclear to date. An intriguing possibility is that potentially enhanced DNA repair during diapause might in several species enable the emergence of a healthier embryo upon diapause exit. Indeed, DNA repair proteins are expressed at higher levels during killifish diapause (Wagner and Podrabsky, 2015; Hu et al., 2020), but whether repair activity is enhanced in killifish and mammals during diapause needs to be further investigated. Enhanced autophagy and lower oxidative damage may be two alternative mechanisms that increase the fitness of the diapause embryo (see

below). The above outlined potential benefits might result in a higher developmental potential of individual diapause epiblasts, however, further studies directly addressing its developmental capacity e.g., via chimera formation are required.

Prolonged diapause, on the other hand, may compromise the fitness of the embryo. In mice, fewer diapause embryos (Arena et al., 2021) and resulting fetuses (Weitlauf and Greenwald, 1968) are recovered with longer duration of diapause. Also, *ex vivo* survival of embryos in a diapause-like state diminishes over time (Bulut-Karslioglu et al., 2016; Liu et al., 2020). Metabolic restrictions, maternal or embryonic pathways may underlie diminishing embryo survival. Understanding metabolic and genetic regulation of diapause is thus critical to overcome the embryo lethality or compromised developmental competence. Under culture conditions tailored to species-specific requirements, diapause could be induced and maintained for longer periods *ex vivo*. Artificial reproductive technology would greatly benefit from such progress, especially in wildlife and captive-bred species for which cryopreservation is either not adaptable or compromises embryo fitness (Wauters et al., 2020). Prolonged blastocyst maintenance would also extend the time window for genetic selection or manipulation of embryos.

Embryo studies allow identification of transcriptional networks critical for survival of each cell type. The required transcription factors (TF) or cytokines can then be engineered and utilized to derive ES or extraembryonic stem cells or to reprogram somatic cells (Williams et al., 1988; Takahashi and Yamanaka, 2006). Some key factors enabling generation of pluripotent stem cells are only required in diapause and not in proliferative blastocysts, suggesting that pluripotency maintenance and establishment may be regulated by non-overlapping mechanisms. For example, leukemia inhibitory factor (LIF), a cytokine that allows maintenance of ES cell pluripotency (Smith et al., 1988; Williams et al., 1988), is dispensable in proliferative blastocysts (Stewart et al., 1992). Although the LIF pathway is not strictly necessary for ES derivation or maintenance *in vitro* (Ying et al., 2008), knockout of the LIF receptor component gp130 results in loss of the pluripotent epiblast during prolonged diapause (Nichols et al., 2001), providing a clear example of an *in vitro* pluripotency maintenance factor with physiological roots in diapause. Unraveling diapause networks may thus enable generation of ES cells from species with no established ES cell models.

## Other Phenomena With a Regulatory Basis Potentially Similar to Diapause

Dormancy-activation cycles underlie stem cell function in many somatic tissues, such as in the hematopoietic and mesenchymal systems (Marescal and Cheeseman, 2020). Although tissue-specific stem cells are not pluripotent and have transcriptional networks tailored to the tissue type and activation cues, dormancy and its reversibility in embryonic and adult tissues may share a regulatory basis. Furthermore, dormant cancer cells, which usually arise as a result of therapy resistance, also show similarities to diapause embryo cells (Dhimolea et al., 2021; Duy et al., 2021; Rehman et al., 2021). For example, metabolic profiles

of dormant stem cells are remarkably similar across tissues and species, with globally decreased oxidative phosphorylation and an increased dependency on lipolysis (Kinder et al., 2010; Singh et al., 2016; Marescal and Cheeseman, 2020). Similarly, autophagy is enhanced in diapause cells, as well as in tissue stem cells and in dormant cancer cells (Lee et al., 2011; Bulut-Karslioglu et al., 2016; Hen and Barkan, 2019). The cytoplasmic kinase, mTOR is a major growth regulator that promotes proliferation in virtually every tissue (Laplanche and Sabatini, 2012). Inhibition of its activity induces diapause in mouse embryos (Bulut-Karslioglu et al., 2016) and is necessary for tissue stem cell dormancy, as evidenced by loss of tissue stem cell pools in hyperactive mTOR mutants (Kharas et al., 2010; Zhang et al., 2015; Hu et al., 2017). Diapause studies may thus not only unravel developmental pathways, but also increase our understanding of tissue stem cell biology and cancer dormancy. The ability of stem cells to tolerate and adjust to various stressors in diapause could signify their capacity to resist to other stressors such as bacterial infections in *C. elegans* that the embryo might encounter during development (Ren and Ambros, 2015).

## MOLECULAR REGULATION OF DIAPAUSE

### Uterine Receptivity and Hormonal Regulation of Diapause

Seasonal and lactational diapause are hormonally regulated by a number of hormones including prolactin, estrogen, and progesterone, acting in different manners in different taxa (Renfree and Fenelon, 2017). Here we summarize the main hormonal changes leading to diapause and reactivation of the early mammalian embryo.

Once at the blastocyst stage, the mammalian embryo is ready to implant into the uterine wall. Normally, a glycoprotein layer called mucins covers the uterine surface and acts as a barrier to implantation due to its anti-adhesive property (Carson et al., 1998). In mice, the estrogen surge on day 4 and, more importantly, the continuously high progesterone levels lead to temporary stripping of the mucin layer and provides a window of implantation (Surveyor, 1995). Lactation-induced decrease of gonadotrophin release by the pituitary gland and consequently lower estrogen levels cause a delay in embryo implantation (Whitten, 1955). Experimentally, surgical removal of ovaries or injection of estrogen antagonists reduce estrogen levels and induce diapause in mice (McCormack and Greenwald, 1974; Hunter and Evans, 1999). High progesterone levels are required throughout diapause to sustain the pregnancy. The embryo remains in close proximity to the uterine wall throughout diapause, in fact it localizes to pockets of uterine tissue called crypts in the implantation position (**Figure 2**), with the mural TE more proximally located to the uterus in the mouse (in contrast, the human embryo implants from the polar side) (Kamemizu and Fujimori, 2019). This positioning may enable close communication between the maternal tissue and the embryo via diffusible factors in the uterine fluid or via extracellular vesicles. Diapause is terminated *in vivo*

upon decrease of lactation-induced prolactin followed by an increase in estrogen. Experimentally, injection of estradiol terminates diapause. The diapause mouse embryo activates within 12 h of the estrogen surge, although precise time of activation may vary depending on the length of diapause (Kamemizu and Fujimori, 2019).

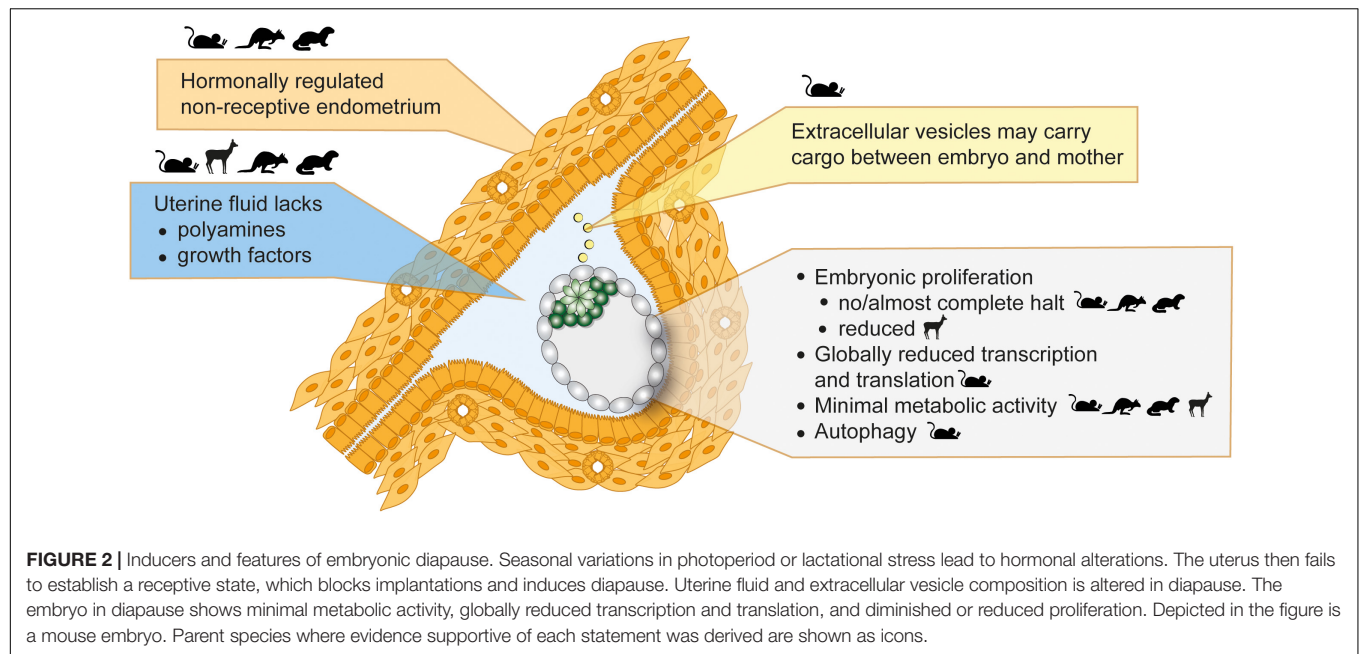
In tammar wallaby, diapause is induced and maintained by inhibition of the corpus luteum-secreted progesterone via high plasma prolactin levels (Hinds, 1989; Hinds and Tyndale-Biscoe, 2012). Suckling of the pouch young or photoperiod-induced melatonin alterations control plasma prolactin levels (Shaw and Renfree, 1984). Between 48 and 72 h post decrease of prolactin levels either after the summer solstice or upon loss of the pouch young, the corpus luteum increases the secretion of progesterone, which leads to embryo reactivation and eventual implantation on day 17. The delayed reactivation of the embryo might be due to slow diffusion of activating factors through the embryonic shell coat.

The mink differs from mouse and wallaby in that neither prolactin nor progesterone is highly secreted during diapause (Møller, 1973; Douglas et al., 1994). Mink diapause is largely controlled by photoperiod-mediated changes in nocturnal melatonin levels. Following the March equinox, decreased melatonin levels lead to an increase in prolactin, progesterone secretion from the corpus luteum, endometrium receptivity, and embryo reactivation 3 days later (Pilbeam et al., 1979; Murphy et al., 1981; Stoufflet et al., 1989).

The failure of the uterus to establish a receptive state under the influence of upstream hormonal regulation is likely the principal cause for the initiation of diapause (**Figure 2**). This notion is further supported by genetic studies. LIF is secreted by the uterine glandular epithelium cells in response to estradiol and is necessary for implantation (Stewart et al., 1992). Maternal LIF knock-out (KO) results in non-implanted blastocysts with morphological features of diapause (Stewart et al., 1992). LIF expression correlates with the implantation window also in mink, Western spotted skunk, and humans (Song et al., 1998; Hirzel et al., 1999; Aghajanova, 2004). Although low LIF levels correlate with failed implantations in humans, a requirement for LIF in human implantation has not been proven (Aghajanova, 2004). Other important regulators of implantation and diapause are the muscle segment homeobox genes *Msx1* and *Msx2* (Daikoku et al., 2011). *Msx* genes are repressed directly by LIF, thus are highly expressed in the uterine luminal and glandular epithelial cells during diapause (mouse, mink, wallaby) and downregulated for implantation (Cha et al., 2013). Mouse diapause can be induced but not maintained in *Msx* KO mothers (Cha et al., 2013). However, whether *Msx* upregulation is sufficient to induce diapause is unclear and inducible overexpression in the uterus is necessary to prove causality. Taken together, uterus non-receptivity suffices to trigger diapause, however, additional factors are likely necessary to maintain prolonged pausing.

### The Uterine Microenvironment

The uterine fluid comprises of growth factors, soluble metabolites and extracellular vesicles, and serves as a communication medium between the embryo and the mother. Uterine fluid composition, i.e., free amino acids, glucose, lactate, and pyruvate



concentrations, is tailored to the developing embryo (Harris et al., 2005), indicating stage-specific metabolic requirements across species, e.g., cattle (Forde et al., 2014), sheep (Gao et al., 2009), mice (Kelleher et al., 2016), and pig (Kim et al., 2013). Metabolite uptake is also regulated in a stage-specific manner by altered expression of metabolite transporters (Winkle, 2001). During diapause, the embryo stays in close proximity to the uterus and responds to diffusible factors such as LIF (Nichols et al., 2001). The uterine tissue, uterine fluid, and the embryo have been separately studied to identify molecular regulators of diapause. Reactivation from diapause is clearly associated with increased soluble growth factors in the uterine fluid, e.g., epidermal growth factor (EGF) and heparin-binding EGF (HBEGF) in the tammar wallaby (Fenelon et al., 2017), together with increased expression of growth factor receptors in the blastocyst, e.g., EGFR increase in mouse 12–24 h after estradiol injection (Hamatani et al., 2004). The absence of growth factors does not induce diapause in *ex vivo* cultured embryos, indicating that growth factor pathways are more relevant for reactivation.

Absence of certain metabolites do induce or maintain diapause, as shown by delayed activation of diapause mouse blastocysts *ex vivo* in the absence of glucose, and by delayed implantation of mink and mouse blastocysts *in vivo* in the absence of polyamines (Naeslund, 1979; Fenelon and Murphy, 2017). Polyamines are synthesized from ornithine, arginine, proline, and methionine by ODC1 downstream of mTOR in response to prolactin and play important roles in reproductive physiology by regulating endothelial cell growth and proliferation, cell migration, and via antioxidant functions (Lenis et al., 2017). Chemical inhibition of uterine ODC1 induces diapause in both mink and mouse blastocysts and uterine ODC1 is upregulated upon reactivation (Lefèvre et al., 2011b; Fenelon and Murphy, 2017). Likewise, polyamine abundance, i.e., less spermine, more spermidine and putrescine, likely increase upon

reactivation in the uterine fluid of roe deer (van der Weijden et al., 2019). Other diapause-associated microenvironmental changes include adhesion- and cell cycle-related proteins, further corroborating maternal control over embryo attachment and proliferation (Lefèvre et al., 2011a; Martin et al., 2016; van der Weijden et al., 2019).

## Metabolic Profile of the Diapause Embryo

Similar to other dormant cells, the diapause embryo presents a significantly lowered metabolic rate with altered usage of metabolic pathways (Naeslund et al., 1980; Lee et al., 2011; Hussein et al., 2020; Sousa et al., 2020). The diapause mouse ICM is metabolically more quiescent compared to TE, suggesting cell type-specific regulation of metabolic activity (Houghton, 2006). In general, reduced oxidative phosphorylation, structurally altered mitochondria and increased autophagy characterize the diapause metabolism (Naeslund et al., 1980; Lee et al., 2011; Hussein et al., 2020; Sousa et al., 2020). Reactivation from diapause results in activation of mitochondria in the mural TE, as evidenced by increased mitochondrial membrane potential (Fu et al., 2014). However, the role of glycolysis is less clear, with studies reporting either increased or decreased glycolysis downstream of mTOR inhibition in ES cells and in diapause embryos (Fu et al., 2014; Boroviak et al., 2015; Hussein et al., 2020; Sousa et al., 2020). Reactivated mouse embryos display a rapid increase in expression of glycolytic pathway genes (Fu et al., 2014) as well as pyruvate and glucose uptake (Spindler et al., 1996). Reactivation is delayed in the absence of glucose (Naeslund, 1979) pointing to the critical role of glycolysis in exit from diapause (Spindler et al., 1996). The glutamine transporter Slc38a1 is also upregulated in the ICM during diapause and inhibition



of it is detrimental to the embryos capacity to pause (Hussein et al., 2020).

Although RNA, protein, and metabolome profiling provide insights into metabolic pathway usage, real-time measurement of metabolic activity via colorimetric assays or the Seahorse system has the potential to provide more direct evidence of metabolic activity. However, these assays often require a large number of cells and therefore direct metabolic characterization of embryos remains challenging.

Dormant stem cells across tissues and species utilize lipid reserves for maintenance (Kinder et al., 2010; Singh et al., 2016). Recently, lipids have been shown to be a major energy source during diapause as well. Free fatty acids and phospholipid phosphatidylcholine are in greater abundance in diapause blastocysts compared to proliferating embryos, suggesting active lipolysis (Hussein et al., 2020). The lipid content of the mouse oocyte is relatively low compared to other species (4 ng compared to 161 ng in the pig, 63 in cows, and 89 in sheep) (Loewenstein and Cohen, 1964; McEvoy et al., 2000; Sturmey and Leese, 2003). Nonetheless, removal of lipid droplets from mouse zygotes impairs the survival of the diapause blastocysts, indicating active utilization during diapause (Arena et al., 2021). This functional evidence is supported by molecular analysis of different lipid species during diapause, which found depletion of neutral lipids usually enriched in lipid droplets (e.g., triacylglycerol) and increase in processed intermediates such as phosphatidylcholines and fatty acids (Hussein et al., 2020). Intriguingly, and contrary to this finding, fatty acid oxidation was shown to counteract a naturally arising quiescent subpopulation in mouse ES cells, with inhibition of it increasing the  $G_0$  population from 4 to ~17% (Khoo et al., 2020).

The metabolic profile of a cell not only determines energy availability and levels of cellular building blocks, it also affects the epigenome, genome integrity, and cellular fitness. Preimplantation development takes place in a hypoxic environment, with intrauterine oxygen levels ranging from 1.5% in the rhesus monkey to 5.3% in rabbits and hamsters (Fischer and Bavister, 1993). The low-capacity oxidative phosphorylation mandated by hypoxia is further lowered during diapause, which may result in less oxidative DNA damage in the diapause embryo (Houghton, 2021). In addition, existing DNA damage may be more efficiently repaired during diapause. Cells turn to autophagy when other energy sources do not suffice to sustain the energy needs or reduced uptake or metabolism do not allow the use of existing resources. In addition to providing energy, autophagy also clears out defective organelles, mostly mitochondria, which is more prone to oxidative DNA damage compared to genomic DNA. Increased autophagy is a common feature of diapause (Lee et al., 2011; Hu et al., 2020) and dormancy and may in this way enhance cellular fitness. Fu et al. (2014), however, showed that mitochondria numbers remain constant during diapause. Thus, how autophagy contributes to overall diapause metabolism remains unclear. In contrast to its short-term benefits, ongoing autophagy could, in the long-term, compromise embryo health if organelles are depleted below a threshold required to sustain the embryo. Indeed, mouse embryos that have been diapause longer than 10 days resulted in fewer fetuses, potentially due to poorer

development of fetal placenta vessels (Weitlauf and Greenwald, 1968). In this sense autophagy may not be an important factor in cell nutrition in species with long periods of diapause such as the tammar wallaby (Renfree and Fenelon, 2017).

## Cell Cycle

Dormancy mandates alterations in cell cycle progression and, indeed, cell cycle related genes are among the most altered between dormant and activated blastocysts. Evidence supports p21-mediated cell cycle control at the G1/S checkpoint, thereby retaining cells in the G0/G1 phase and reducing DNA replication (Hamatani et al., 2004; Kamemizu and Fujimori, 2019). Diapausing killifish cells similarly arrest at G0/G1, and upon activation immediately enter the S phase (Dolfi et al., 2019). In mice, it has been suggested that cell cycle arrest is estrogen-mediated and thus controlled maternally via downregulation of the tumor repressor Brcal and upregulation of the anti-proliferation gene Btg1 (Hamatani et al., 2004).

In mouse ES cells, induction of a paused-like state by inhibition of mTOR reduces the proliferation rate while distribution of cells among the stages of the cell cycle is only modestly altered, suggesting that paused-like cells proceed through the cell cycle, albeit at a very slow pace (Bulut-Karslioglu et al., 2016). In contrast, Myc inhibition, which also leads to a diapause-like state, enriches  $G_0/G_1$  cells and depletes the S phase (Scognamiglio et al., 2016). Although the latter cell cycle profile is closer to true dormancy, the Myc-inhibited cells cannot be sustained longer than a day. These findings suggest that *in vivo* and *in vitro* regulation of diapause might be distinct and warrants further studies on cell cycle control in paused pluripotency or embryonic stem cell dormancy.

## GENOMIC REGULATION

Cell cycle and metabolism rewiring appear to be hallmarks of diapause, as expected from a largely dormant state. Yet, distinguishing causal and consequential alterations in diapause remains a challenge. Several RNA and protein profiling studies have mapped gene expression changes during diapause to identify altered pathways and to isolate inducers of diapause and reactivation. Here we outline in detail the recent advances in genomic regulation of diapause. We note that functional perturbations are necessary to show causality. In addition, we caution the reader to take the following critical confounding factors into account when applicable: (1) significant inter-embryo heterogeneity in diapause response, as evidenced by variable durations of pausing *in vivo* and *ex vivo*, may conceal changes if pooled embryo profiling is performed, (2) whole-blastocyst analysis may prevent identification of Epi-, TE-, and PrE-specific regulators, (3) static analysis (i.e., comparing a single time point vs. control) likely misses dynamically altered pathways, and (4) gene expression levels cannot be precisely mapped, due to global reductions in RNA and protein levels, unless exogenous spike-in controls are used. Despite these complications, exciting new insights into genomic regulation have illuminated diapause biology in the recent years.



## Chromatin Rewiring in Diapause: Cause or Consequence?

Epigenetic marks, such as post-translational modifications of histones, DNA and RNA, together with TFs and chromatin remodelers, regulate gene activity. Epigenetic modifications either control or result from transcriptional activity. Irrespective of causality, highly transcribed or repressed genes show characteristic histone modifications, e.g., histone acetylation is associated with high transcriptional output (Bannister and Kouzarides, 2011). Additionally, the chromatin state is linked to metabolism, as for example the citric acid intermediate  $\alpha$ -ketoglutarate affects DNA and histone methylation levels (Donohoe and Bultman, 2012). As such, chromatin rewiring is an expected outcome of diapause, although a detailed characterization is missing. Chromatin of ICM cells is particularly sensitive to diapause and shows depletion of histone acetylation such as H4K16ac (Bulut-Karslioglu et al., 2016). Interestingly, knock-out of MOF, the enzyme that acetylates H4K16, increases the naturally-occurring dormant subpopulation of ES cells observed in the study, suggesting that depletion of histone acetylation could induce pausing by reducing global transcriptional output (Khoa et al., 2020). On the contrary, inhibition of histone acetyltransferase activity via chemical inhibitors does not suffice to pause mouse blastocysts *ex vivo* (Bulut-Karslioglu et al., 2016).

Transcriptional activity reduces the abundance of heterochromatin (Ahmad and Henikoff, 2001), therefore global reductions in transcription and associated histone acetylation in diapause may result in abundant heterochromatin. In agreement, electron microscopy analysis of diapause vs. active blastocysts revealed more condensed nucleoli and abundant heterochromatin in Epi and TE cells, which decondensed within 12 h of reactivation (Fu et al., 2014). Polycomb-mediated H3K27me<sub>3</sub>, which represses transcription, represses key metabolic and developmental genes during killifish diapause (Hu et al., 2020) and may also play a role in maintaining diapause in mammals. Although most of the genome is silent and potentially heterochromatinized during diapause, the diapause epiblast retains naïve pluripotency features (Boroviak et al., 2015). Additionally, a subset of genes is upregulated and possibly induces or maintains dormancy (Hamatani et al., 2004; Bulut-Karslioglu et al., 2016). The regulatory pathways by which such genes escape silencing is a question that invites attention in the coming years.

## Transcription and Translation Are Globally Reduced During Diapause

Inhibition of cellular growth and proliferation during diapause leads to global reductions in transcription and translation, resulting in smaller cell size. Paused-like ES cells have 2–4-fold less RNA per cell and are smaller than proliferative ES cells (Bulut-Karslioglu et al., 2016). Dormant cells across different systems, e.g., tissue stem cells, are smaller than their activated counterparts and have reduced transcriptional and translational output (Rodgers et al., 2014). The impact of reduced transcriptional and translational capacity is particularly

relevant for the imminent expansion of the epiblast after implantation. Pluripotent cells of the late epiblast are among the most rapidly proliferating cells, with one cell division taking ~5–6 h (Snow, 1977). This rapid proliferative rate mandates prolific transcription and translation. In proliferative ES cells, levels of transcription and associated chromatin modifications such as histone acetylation are acutely responsive to translational output, which is in turn correlated with transcriptional output (Schwanhäusser et al., 2011; Percharde et al., 2017; Bulut-Karslioglu et al., 2018). Reactivation of the diapause embryo, combined with the fast proliferative rate of the early post-implantation embryo, requires a major ramp-up in transcriptional and translational output. How the transcription-translation cycle builds back to prior levels and the associated chromatin regulation is an area of interest for future studies. In other situations requiring an accelerated transcriptional response, e.g., signal-induced transcription at heat shock or hormone-responsive genes (Sawarkar et al., 2012), pre-loaded RNA polymerase and chromatin modifiers enable rapid activation. Similar regulation may be utilized in diapause, as mouse embryos reactivate within 12 h after release from diapause (Kamemizu and Fujimori, 2019). In addition, post-transcriptional and post-translational mechanisms such as miRNA activity complement nascent regulation to achieve repression and on-demand activation of proliferative pathways.

## Transcriptional Networks and Cellular Signaling in Diapause

Stem cell identity is governed by transcriptional networks downstream of cellular signaling pathways (Young, 2011). Altered signaling pathway activity defines transcriptional outputs and can result in cell state or fate switches. In the mouse, pluripotency is maintained through combinatorial activity of master TFs such as Oct4, Klf4, Esrrb, Sox2, and Nanog under the control of signaling pathways such as Fgf/Mek/Erk, Wnt, or LIF/Jak-Stat. Long-term pluripotency maintenance during diapause entails distinct signaling pathway activity as compared to only transient regulation in proliferative blastocysts. For instance, although the cytokine leukemia inhibitory factor (LIF) is expressed in the blastocyst (Nichols et al., 1996), it is dispensable for early embryo development (Stewart et al., 1992). It is, however, required to maintain pluripotency during diapause, as gp130 (LIF receptor component) knock-out embryos lose the epiblast during diapause (Nichols et al., 2001). ES cell pluripotency is alternatively maintained through inhibition of the differentiation-promoting Mek/Erk pathway and enhancement of Wnt pathway activity (Ying et al., 2008). Wnt activity is minimal in the early embryo but is increased during diapause (Boroviak et al., 2015), illustrating another case where prolonged pluripotency maintenance in ES cultures has physiological roots in diapause. In general, naïve pluripotency networks are intact in the diapause epiblast, indicating active maintenance of pluripotency despite global transcriptional silencing (Boroviak et al., 2015). However, the effect of diapause on PrE- and TE-specific transcriptional networks is unclear. Technical challenges in dissecting Epi, PrE, and TE cells in the blastocyst so

far prevented comparative studies of stem cell networks and crosstalk between the three cell types in the diapause blastocyst. Of note, although PrE is clearly defined in the diapause blastocyst, observations suggest altered transcriptional networks, e.g., all Gata4<sup>+</sup> PrE cells were shown to retain Oct4 expression, in contrast to only a subset of Gata4<sup>+</sup>/Oct4<sup>+</sup> cells in normal mouse blastocysts (Batlle-Morera et al., 2008; **Figure 3**). ICM cell numbers decrease by half (Epi) and 40% (PrE) during diapause (Batlle-Morera et al., 2008). Thus, the remaining ICM cells during diapause may be selectively retained based on their transcriptional state, allowing them to express both Gata4 and Oct4, or transcriptional rewiring may override previous separation of Gata4<sup>+</sup> and Oct4<sup>+</sup> in a subset of cells. Mouse trophoblast shows signs of apoptosis during diapause, and its deterioration may underlie embryo loss in prolonged diapause (Bulut-Karslioglu et al., 2016). Thus, whether TE identity and transcriptional networks remain uncompromised is unclear. Species in which a single embryo experiences an extremely long diapause, such as the tammar wallaby, likely safeguard cellular potency via multiple redundant mechanisms, as the loss of the single embryo would have significant consequences on the species' survival. Interestingly, wallaby blastocysts are composed of a monolayer of cells without an ICM, which may underlie their increased resistance to prolonged pausing.

A prominent pathway in controlling embryonic diapause in mice is the PI3K/mTOR pathway. mTOR promotes cell growth, and thus proliferation, via direct control over translation, metabolism, and transcription (Laplanche and Sabatini, 2012). It acts as a cellular rheostat to adjust cellular growth to the availability of nutrients and energy. Modulation of mTOR activity is necessary for dormancy-activation cycles in adult stem cells, as hyperactive mTOR results in loss of stem cell pools (Kharas et al., 2010; Zhang et al., 2015; Hu et al., 2017). Similar to dormant tissue stem cells, the mTOR pathway is downregulated in the diapause epiblast, suggesting that the PI3K/insulin/mTOR axis governs dormancy decisions in mammals (Boroviak et al., 2015). Importantly, inhibition of mTOR activity induces diapause in mouse blastocysts *ex vivo* for up to 30 days (Bulut-Karslioglu et al., 2016). This diapause-like state can also be applied to ES cells in culture via treatment with catalytic mTOR inhibitors. The paused-like ES cells show characteristics of diapause such as a reduced metabolic rate, globally downregulated transcription and translation, and a transcriptional signature reminiscent of the diapause epiblast. Establishment of such *in vitro* diapause-mimicking stem cell culture conditions is critical to overcome technical and material limitations in embryo studies and for detailed mapping and functional investigation of regulatory networks.

Although translational inhibition is one of the most prominent consequences of mTOR inhibition, inhibition of translation does not suffice to induce diapause *ex vivo* (Bulut-Karslioglu et al., 2016), suggesting that combinatorial control downstream of mTOR inhibition drives cellular adaptation to diapause. A major regulator that controls global transcription as well as specific gene networks is TF Myc (Kress et al., 2015). Myc is a component of the pluripotency network and is also functional across somatic tissues (Kress et al., 2015). Myc activity

is reduced in diapause (Boroviak et al., 2015) and its inhibition can induce a diapause-like state for short periods (18–24 h in mouse blastocysts) (Scognamiglio et al., 2016).

## Wnt Pathway Activity and the Interplay With Cellular Polarization

In contrast to reduced mTOR and Myc signaling, Wnt activity is transiently increased during diapause in the epiblast (Fan et al., 2020). The Wnt pathway is stimulated via multiple ligands (Wnt1-16 in mice and humans with variants, in total 19 genes) and can assume conflicting roles in promoting pluripotency or differentiation in a cell type specific and context-dependent manner (ten Berge et al., 2008, 2011). Wnt is also an upstream regulator of cellular polarization, thus spearheading epithelial-mesenchymal transition in gastrulation and body patterning. The ICM of the pre-implantation embryo comprises of unpolarized cells (Rivera-Pérez and Hadjantonakis, 2014). Immediately after implantation the ICM polarizes, assumes a rosette-shaped pattern, creates a lumen and undergoes morphological transformation to generate the classical “egg cylinder” of the mouse post-implantation epiblast (the post-implantation morphology is species-dependent, e.g., in human the post-implantation epiblast forms a disc shape) (Rivera-Pérez and Hadjantonakis, 2014). Morphological changes in the epiblast correspond to progression of the embryo along the pluripotency spectrum, i.e., from rosette (Neagu et al., 2020) to formative (Kinoshita et al., 2021) to primed pluripotency (Brons et al., 2007; Tesar et al., 2007). Interestingly, the late-stage diapause epiblast (EDG9.5 onward) assumes a polarized pattern despite retaining naïve pluripotency networks (Fu et al., 2014; Fan et al., 2020). Fan et al. (2020) recently showed that transient Wnt activity during early stages of mouse diapause (peaking at EDG7.5 and downregulated by EDG9.5) is required to delay polarization and retain naïve pluripotency of the Epi cells. Polarization is prevented via the naïve pluripotency TF *Esrrb*. The epiblast of *Esrrb* null blastocysts is not maintained during prolonged diapause (Fan et al., 2020). Wnt pathway activity thus promotes naïve pluripotency and prevents polarization in ES cells, as well as in the diapause epiblast, despite its dispensability in normal blastocysts. These observations indicate that establishment of diapause is thus an active process that entails both transcriptional rewiring and morphological alterations. Open questions that remain unanswered are how naïve pluripotency is retained once the epiblast polarizes at EDG9.5 and whether other naïve pluripotency factors are indispensable for epiblast maintenance during diapause.

Wnt pathway activity controls cell polarity by modulating the activities of ROCK and JNK kinases, which control cellular cytoskeleton structure including e.g., actin polymerization. In addition,  $\beta$ -catenin is required for cell adhesion by connecting E-cadherin and  $\alpha$ -catenin (Drees et al., 2005). Following the trend for general Wnt activity,  $\beta$ -catenin is also dispensable for normal blastocyst formation (Haegel et al., 1995; Huelsken et al., 2000). Yet,  $\beta$ -catenin null blastocysts collapse upon induction of diapause (before EDG5.5) (Fan et al., 2020). This more severe

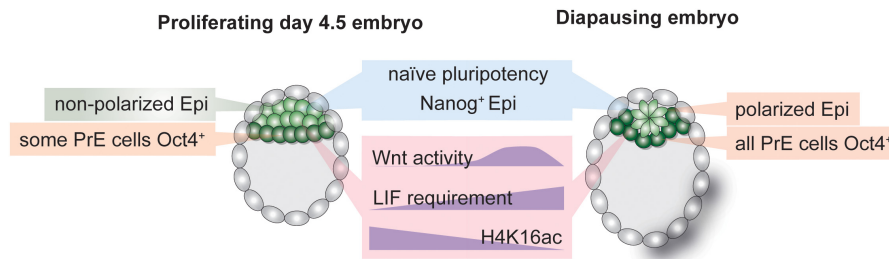


**FIGURE 3 |** Hallmarks of the inner cell mass (ICM) of normal and diapause blastocysts. Establishment and maintenance of diapause entails alterations in cellular signaling pathways, transcriptional networks and the chromatin state. The epiblast retains naïve pluripotency during diapause but is polarized due to transient Wnt pathway activity. LIF is required to sustain the epiblast throughout diapause. The transcription-associated histone H4K16 acetylation is depleted in diapause ICM.

phenotype compared to *Esrrb* KO suggests the involvement of cellular adhesion pathways in establishing the diapause state (Fan et al., 2020). Indeed, several genomic profiling studies comparing diapause and active blastocysts documented altered expression of cellular adhesion genes (Hamatani et al., 2004; Fu et al., 2014; van der Weijden et al., 2019). Adhesion pathways and the cytoskeleton are not merely structural components of the cell, but also affect transcriptional networks, as they are additionally involved in signaling pathways and chromatin regulation (Klages-Mundt et al., 2018; Griffith et al., 2021). Thus, altered adhesion properties may have an impact on the diapause blastocyst at multiple levels, e.g., by altering implantation capacity of the TE and polarity of the epiblast, by maintaining the blastocoel and adjusting the blastocyst in its new elongated form, and by altering transcriptional networks to adapt cellular states. Detailed analysis on how adhesion, mechanotransduction, and cytoskeleton pathways impact stem cell states in diapause are missing to date.

## Post-transcriptional and Post-translational Gene Regulation in Diapause

Post-transcriptional mechanisms, such as miRNA-based gene control, are critical regulators of gene activity. Indeed, only about 40% of gene activity is explainable by nascent transcription, although the exact fraction is cell-type dependent (Buccitelli and Selbach, 2020). MicroRNAs (miRNA) are small non-coding RNAs that largely repress gene activity via transcriptional silencing, transcript degradation or translation inhibition (Treiber et al., 2019). MiRNA-mediated gene repression combines sequence specificity with promiscuity (due to short seed sequence and by allowing mismatches), thereby allowing control of multiple target genes at once (O'Brien et al., 2018). Combinatorial miRNA activity, i.e., multiple miRNAs controlling a given gene and one miRNA controlling multiple genes, provides pathway-level control (Bartel and Chen, 2004) and thus is suited to mediate cell state shifts that entail alterations of many pathways. Furthermore, miRNAs usually control metabolic, proliferation, apoptosis, and developmental pathways, all of which are essential components of diapause. As such, miRNAs are potential prominent regulators of diapause and therefore

have attracted attention. As miRNA activity fine-tunes gene expression and increases the robustness of genetic programs, miRNA-mediated control of diapause likely acts in combination with other regulatory units to achieve the final outcome (Bartel and Chen, 2004).

The evidence for miRNA function in diapause largely originates from genomic profiling studies. Diapause results in altered miRNA profiles in many mammalian and non-mammalian species (silk worms (Fan et al., 2017), mosquito (Meuti et al., 2018), *C. elegans* (Meuti et al., 2018), mouse (Liu et al., 2012)). It is therefore possible that distinct miRNAs mediate diapause induction, maintenance, and reactivation. Cell-type specific miRNAs may mediate tissue specificity. For example, in *C. elegans* diapause, the miRNA miR-71 suppresses the growth-promoting PI3K/insulin pathway and miR-235 acts downstream of the insulin pathway to arrest development, pointing at the central role of the insulin pathway in diapause control across species. Knock-outs of these miRNAs are not lethal in diapause, suggesting auxiliary roles in dormancy transition. In the mouse, overexpression of let-7, among the first miRNAs to be discovered in *C. elegans* and a major regulator of developmental timing, induces *ex vivo* diapause by suppressing mTOR and Myc activities and by inhibiting polyamine synthesis (Liu et al., 2020). In mouse diapause, let-7 is of maternal origin and is transferred to the embryo via extracellular vesicles (Figure 2), exemplifying direct maternal control of the embryonic state (Liu et al., 2020). The authors state that let-7 can also induce diapause in human embryos, however, the duration and rate of pausing is marginal (day 7 survival 52% vs. 30%, day 8 survival 5% vs. 0% in let-7 vs. control embryos).

Given the promise of miRNA control over diapause, it is desirable to dissect spatial and temporal regulation by combinatorial action of miRNAs. Mechanistically, miRNA targets are easy to predict but hard to precisely define, since sequence complementarity may not suffice. Studies focusing on individual miRNAs would benefit from identification of miRNA targets. Dissection of downstream pathways can enhance our understanding of *how* miRNAs regulate diapause. MiRNAs are often in feedback control with cellular pathways and active miRNA levels are regulated either transcriptionally, post-transcriptionally (with selective processing), or via sequestration of mature miRNAs, thus acute functional



perturbations are necessary to dissect the regulatory complexity of miRNA activity (Treiber et al., 2019).

Many miRNAs have oncogenic activity (Dhawan et al., 2018). Given the importance of understanding dormancy pathways in cancer, investigating miRNA-mediated dormancy in diapause may enlighten oncogenic miRNA activity. miRNAs are assembled into extracellular vesicles and circulating oncogenic miRNAs are used as cancer biomarkers (Hou et al., 2015). It is an intriguing possibility to use circulating miRNAs as potential diapause biomarkers, especially in wildlife species where diapause detection has otherwise not been successful.

Among other post-transcriptional or -translational regulators of pluripotency maintenance in diapause are mRNA stability, alternative splicing, and protein localization. Cnot3, a deadenylator that controls RNA stability, is required to maintain the pluripotent epiblast during mouse diapause by targeting mRNAs of differentiation genes for degradation (Zheng et al., 2016). Cnot3 is not required in normal blastocysts and its deletion is only embryonic lethal at ~E6.5, thereby illustrating the occurrence of another regulator required for prolonged pluripotency maintenance in ES cells and in diapause (Zheng et al., 2016). Lkb1, an upstream regulator of the starvation-induced AMPK kinase, is controlled by alternative splicing during diapause (Hussein et al., 2020). Other genes such as the developmental TF Pitx1, which also regulates prolactin expression, are also subject to alternative splicing in diapause (Hussein et al., 2020). Finally, the Forkhead family TFs Foxo1/3/4 are associated with dormant states in *C. elegans* (Sun et al., 2017), tammar wallaby, and mink and may control diapause via altered cellular localization in response to altered PI3K/insulin signaling (Fenelon et al., 2017). Although Foxo/Daf-16 has been established as a master regulator of dauer diapause in *C. elegans*, evidence of mammalian Foxo activity in diapause is largely based on stainings and requires functional perturbations (Sun et al., 2017). Foxo function is dispensable for normal development (Kuscu et al., 2019), but is essential to maintain pluripotency in mouse and human ES cells (Zhang et al., 2011), as well as tissue stem cells. This suggests that it may be another factor specifically required to maintain prolonged pluripotency and may be a common inducer of dormancy. Foxo involvement in metabolism, cell cycle, DNA repair control, and protection against oxidative stress (Kops et al., 2002; Fenelon et al., 2017) are highly relevant for diapause, and suggest it may be a master regulator of dormancy.

## OUTLOOK

In this review we highlight the complex biology of diapause that we are only beginning to understand. Current evidence

supports a model in which diapause is initially triggered due to the embryo's inability to implant into the non-receptive uterus. Entry into diapause is followed by morphological, metabolic, and genomic restructuring of the embryo as well as maternal tissues. Soluble and vesicle-delivered factors in the uterine microenvironment mediate maternal-embryo crosstalk and control diapause. Absence of key metabolites, e.g., polyamines, induce diapause and presence of others, e.g., lipids, sustain embryos in diapause. Key pluripotency-maintenance factors, e.g., LIF, are required to maintain the epiblast throughout diapause. Diapause-like states can be induced *ex vivo*, e.g., via mTOR and Myc inhibitors or miRNA supplementations. Taken together, diapause is induced through multiple routes and entails complex restructuring of embryonic and extraembryonic networks.

Current challenges in further investigation of diapause include technical limitations in embryo accessibility, recovery, and manipulation. These challenges illustrate the need for *ex vivo* and *in vitro* diapause model systems. Spatial and temporal regulation can only be understood by designing dynamic experiments and by addressing inter-embryo heterogeneity and cell-type specificity. Implementing single-cell transcriptome and accessibility profiling methods will greatly enhance our understanding of spatiotemporal regulation. Recovering normal or diapause embryos in many wild animals is not feasible and identification of diapause biomarkers would facilitate reproductive technology in these species. ES pluripotency pathways are rooted in prolonged pluripotency maintenance in diapause, thus studying diapause could enable establishment of ES or iPS cells from so-far refractive species.

## AUTHOR CONTRIBUTIONS

VvdW and AB-K conceptualized and co-wrote the manuscript. Both authors contributed to the article and approved the submitted version.

## FUNDING

This work was sponsored by the Swiss National Science Foundation Early Postdoc.Mobility fellowship (P2EZP3\_195682) to VvdW, the Sofja Kovalevskaja Award (Humboldt Foundation) to AB-K and the Max Planck Society.

## ACKNOWLEDGMENTS

We thank members of the Bulut-Karslioglu lab and Bruce Murphy for critical feedback.

## REFERENCES

- Aghajanova, L. (2004). Leukemia inhibitory factor and human embryo implantation. *Ann. N. Y. Acad. Sci.* 1034, 176–183.
- Ahmad, K., and Henikoff, S. (2001). Modulation of a transcription factor counteracts heterochromatic gene silencing in *Drosophila*. *Cell* 104, 839–847.
- Arena, R., Bisogno, S., Gąsior, Ł., Rudnicka, J., Bernhardt, L., Haaf, T., et al. (2021). Lipid droplets in mammalian eggs are utilized during embryonic diapause. *Proc. Natl. Acad. Sci. U.S.A.* 118:e2018362118. doi: 10.1073/pnas.2018362118
- Bannister, A. J., and Kouzarides, T. (2011). Regulation of chromatin by histone modifications. *Cell Res.* 21, 381–395. doi: 10.1038/cr.2011.22



- Bartel, D. P., and Chen, C.-Z. (2004). Micromanagers of gene expression: the potentially widespread influence of metazoan microRNAs. *Nat. Rev. Genet.* 5, 396–400. doi: 10.1038/nrg1328
- Battle-Morera, L., Smith, A., and Nichols, J. (2008). Parameters influencing derivation of embryonic stem cells from murine embryos. *Genesis* 46, 758–767. doi: 10.1002/dvg.20442
- Bernardo, A. S., Jouneau, A., Marks, H., Kensche, P., Kobolak, J., Freude, K., et al. (2018). Mammalian embryo comparison identifies novel pluripotency genes associated with the naïve or primed state. *Biol. Open* 7:bio033282. doi: 10.1242/bio.033282
- Bischoff, T. L. W. (1854). *Entwicklungsgeschichte des Rehes*. Giessen: J. Bicker'sche Buchhandlung.
- Blakeley, P., Fogarty, N. M. E., del Valle, I., Wamaitha, S. E., Hu, T. X., Elder, K., et al. (2015). Defining the three cell lineages of the human blastocyst by single-cell RNA-seq. *Development* 142, 3151–3165. doi: 10.1242/dev.123547
- Boroviak, T., Loos, R., Lombard, P., Okahara, J., Behr, R., Sasaki, E., et al. (2015). Lineage-specific profiling delineates the emergence and progression of naive pluripotency in mammalian embryogenesis. *Dev. Cell* 35, 366–382. doi: 10.1016/j.devcel.2015.10.011
- Boroviak, T., Stirparo, G. G., Dietmann, S., Hernando-Herraez, I., Mohammed, H., Reik, W., et al. (2018). Single cell transcriptome analysis of human, marmoset and mouse embryos reveals common and divergent features of preimplantation development. *Development* 145:dev167833. doi: 10.1242/dev.167833
- Brons, I. G. M., Smithers, L. E., Trotter, M. W. B., Rugg-Gunn, P., Sun, B., Lopes, S. M. C., et al. (2007). Derivation of pluripotent epiblast stem cells from mammalian embryos. *Nature* 448, 191–195. doi: 10.1038/nature05950
- Brook, F. A., and Gardner, R. L. (1997). The origin and efficient derivation of embryonic stem cells in the mouse. *Proc. Natl. Acad. Sci. U.S.A.* 94, 5709–5712. doi: 10.1073/pnas.94.11.5709
- Buccitelli, C., and Selbach, M. (2020). mRNAs, proteins and the emerging principles of gene expression control. *Nat. Rev. Genet.* 21, 630–644. doi: 10.1038/s41576-020-0258-4
- Bulut-Karslioglu, A., Bichele, S., Jin, H., Macrae, T. A., Hejna, M., Gertsenstein, M., et al. (2016). Inhibition of mTOR induces a paused pluripotent state. *Nature* 540, 119–123. doi: 10.1038/nature20578
- Bulut-Karslioglu, A., Macrae, T. A., Osés-Prieto, J. A., Covarrubias, S., Percharde, M., Ku, G., et al. (2018). The transcriptionally permissive chromatin state of embryonic stem cells is acutely tuned to translational output. *Cell Stem Cell* 22, 369–383.e8. doi: 10.1016/j.stem.2018.02.004
- Canton, I., Warren, N. J., Chahal, A., Amps, K., Wood, A., Weightman, R., et al. (2016). Mucin-inspired thermoresponsive synthetic hydrogels induce stasis in human pluripotent stem cells and human embryos. *ACS Central Sci.* 2, 65–74. doi: 10.1021/acscentsci.5b00370
- Carson, D. D., Desouza, M. M., and Regisford, E. G. C. (1998). Mucin and proteoglycan functions in embryo implantation. *Bioessays* 20, 577–583.
- Cha, J., Sun, X., Bartos, A., Fenelon, J., Lefèvre, P., Daikoku, T., et al. (2013). A new role for muscle segment homeobox genes in mammalian embryonic diapause. *Open Biol.* 3:130035. doi: 10.1098/rsob.130035
- Chang, M. C. (1968). Reciprocal insemination and egg transfer between ferrets and mink. *J. Exp. Zool.* 168, 49–59. doi: 10.1002/jez.1401680105
- Daikoku, T., Cha, J., Sun, X., Tranguch, S., Xie, H., Fujita, T., et al. (2011). Conditional deletion of MSX homeobox genes in the uterus inhibits blastocyst implantation by altering uterine receptivity. *Dev. Cell* 21, 1014–1025. doi: 10.1016/j.devcel.2011.09.010
- Dhawan, A., Scott, J. G., Harris, A. L., and Buffa, F. M. (2018). Pan-cancer characterisation of microRNA across cancer hallmarks reveals microRNA-mediated downregulation of tumour suppressors. *Nat. Commun.* 9:5228. doi: 10.1038/s41467-018-07657-1
- Dhimolea, E., Simoes, R., de, M., Kansara, D., Al'Khafaji, A., Bouysson, J., et al. (2021). An embryonic diapause-like adaptation with suppressed Myc activity enables tumor treatment persistence. *Cancer Cell* 39, 240–256.e11. doi: 10.1016/j.ccell.2020.12.002
- Dolfi, L., Ripa, R., Antebi, A., Valenzano, D. R., and Cellerino, A. (2019). Cell cycle dynamics during diapause entry and exit in an annual killifish revealed by FUCCI technology. *EvoDevo* 10:29. doi: 10.1186/s13227-019-0142-5
- Donohoe, D. R., and Bultman, S. J. (2012). Metaboloepigenetics: interrelationships between energy metabolism and epigenetic control of gene expression. *J. Cell. Physiol.* 227, 3169–3177. doi: 10.1002/jcp.24054
- Douglas, D. A., Houde, A., Song, J. H., Farookhi, R., Concannon, P. W., and Murphy, B. D. (1998). Luteotropic hormone receptors in the ovary of the mink (*Mustela vison*) during delayed implantation and early-postimplantation gestation. *Biol. Reprod.* 59, 571–578. doi: 10.1095/biolreprod59.3.571
- Douglas, D. A., Pierson, R. A., and Murphy, B. D. (1994). Ovarian follicular development in mink (*Mustela vison*). *Reproduction* 100, 583–590. doi: 10.1530/jrf.0.1000583
- Drees, F., Pokutta, S., Yamada, S., Nelson, W. J., and Weis, W. I. (2005).  $\alpha$ -catenin is a molecular switch that binds E-Cadherin- $\beta$ -catenin and regulates actin-filament assembly. *Cell* 123, 903–915. doi: 10.1016/j.cell.2005.09.021
- Duy, C., Li, M., Teater, M., Meydan, C., Garrett-Bakelman, F. E., Lee, T. C., et al. (2021). Chemotherapy induces senescence-like resilient cells capable of initiating AML recurrence. *Cancer Discov.* 11, 1542–1561. doi: 10.1158/2159-8290.cd-20-1375
- Evans, M. J., and Kaufman, M. H. (1981). Establishment in culture of pluripotent cells from mouse embryos. *Nature* 292, 154–156. doi: 10.1038/292154a0
- Fan, R., Kim, Y. S., Wu, J., Chen, R., Zeuschner, D., Mildner, K., et al. (2020). Wnt/Beta-catenin/Esrrb signalling controls the tissue-scale reorganization and maintenance of the pluripotent lineage during murine embryonic diapause. *Nat. Commun.* 11:5499. doi: 10.1038/s41467-020-19353-0
- Fan, W., Zhong, Y., Qin, M., Lin, B., Chen, F., Yan, H., et al. (2017). Differentially expressed microRNAs in diapausing versus HCl-treated Bombyx embryos. *PLoS One* 12:e0180085. doi: 10.1371/journal.pone.0180085
- Fenelon, J. C., and Murphy, B. D. (2017). Inhibition of polyamine synthesis causes entry of the mouse blastocyst into embryonic diapause. *Biol. Reprod.* 97, 119–132. doi: 10.1093/biolre/iox060
- Fenelon, J. C., Shaw, G., Frankenberg, S. R., Murphy, B. D., and Renfree, M. B. (2017). Embryo arrest and reactivation: potential candidates controlling embryonic diapause in the tammar wallaby and mink. *Biol. Reprod.* 96, 877–894. doi: 10.1093/biolre/iox019
- Fischer, B., and Bavister, B. D. (1993). Oxygen tension in the oviduct and uterus of rhesus monkeys, hamsters and rabbits. *Reproduction* 99, 673–679. doi: 10.1530/jrf.0.0990673
- Forde, N., Simintiras, C. A., Sturmey, R., Mamo, S., Kelly, A. K., Spencer, T. E., et al. (2014). Amino acids in the uterine luminal fluid reflects the temporal changes in transporter expression in the endometrium and conceptus during early pregnancy in cattle. *PLoS One* 9:e100010. doi: 10.1371/journal.pone.0100010
- Frankenberg, S., Shaw, G., Freyer, C., Pask, A. J., and Renfree, M. B. (2013). Early cell lineage specification in a marsupial: a case for diverse mechanisms among mammals. *Development* 140, 965–975. doi: 10.1242/dev.091629
- Fu, Z., Wang, B., Wang, S., Wu, W., Wang, Q., Chen, Y., et al. (2014). Integral proteomic analysis of blastocysts reveals key molecular machinery governing embryonic diapause and reactivation for implantation in mice. *Biol. Reprod.* 90, 52–52. doi: 10.1095/biolreprod.113.115337
- Gao, H., Wu, G., Spencer, T. E., Johnson, G. A., Li, X., and Bazer, F. W. (2009). Select nutrients in the ovine uterine lumen. I. amino acids, glucose, and ions in uterine luminal flushings of cyclic and pregnant ewes. *Biol. Reprod.* 80, 86–93. doi: 10.1095/biolreprod.108.071597
- Gerri, C., McCarthy, A., Alanis-Lobato, G., Demtschenko, A., Bruneau, A., Loubesac, S., et al. (2020). Initiation of a conserved trophectoderm program in human, cow and mouse embryos. *Nature* 587, 443–447. doi: 10.1038/s41586-020-2759-x
- Griffith, B. G. C., Upstill-Goddard, R., Brunton, H., Grimes, G. R., Biankin, A. V., Serrels, B., et al. (2021). FAK regulates IL-33 expression by controlling chromatin accessibility at c-Jun motifs. *Sci. Rep.* 11:229. doi: 10.1038/s41598-020-80111-9
- Grinstead, J., and Avery, B. (1996). A sporadic case of delayed implantation after *in-vitro* fertilization in the human? *Hum. Reprod.* 11, 651–654.
- Guo, F., Li, L., Li, J., Wu, X., Hu, B., Zhu, P., et al. (2017). Single-cell multi-omics sequencing of mouse early embryos and embryonic stem cells. *Cell Res.* 27, 967–988. doi: 10.1038/cr.2017.82
- Haegel, H., Larue, L., Ohsugi, M., Fedorov, L., Herrenknecht, K., and Kemler, R. (1995). Lack of beta-catenin affects mouse development at gastrulation. *Development* 121, 3529–3537. doi: 10.1242/dev.121.11.3529
- Hamatani, T., Daikoku, T., Wang, H., Matsumoto, H., Carter, M. G., Ko, M. S. H., et al. (2004). Global gene expression analysis identifies molecular pathways distinguishing blastocyst dormancy and activation. *Proc. Natl. Acad. Sci. U.S.A.* 101, 10326–10331. doi: 10.1073/pnas.0402597101

- Harris, S. E., Gopichandran, N., Picton, H. M., Leese, H. J., and Orsi, N. M. (2005). Nutrient concentrations in murine follicular fluid and the female reproductive tract. *Theriogenology* 64, 992–1006. doi: 10.1016/j.theriogenology.2005.01.004
- Hen, O., and Barkan, D. (2019). Dormant disseminated tumor cells and cancer stem/progenitor-like cells: similarities and opportunities. *Semin. Cancer Biol.* 60, 157–165. doi: 10.1016/j.semcancer.2019.09.002
- Hinds, L. A. (1989). Morning pulse of prolactin maintains seasonal quiescence in the tammar, *Macropus eugenii*. *Reproduction* 87, 735–744. doi: 10.1530/jrf.0.0870735
- Hinds, L. A., and Tyndale-Biscoe, C. H. (2012). Daily prolactin pulse inhibits the corpus luteum during lactational quiescence in the marsupial, *Macropus eugenii*. *Reprod. Fertil. Dev.* 25, 456–461. doi: 10.1071/rd11228
- Hirzel, D. J., Wang, J., Das, S. K., Dey, S. K., and Mead, R. A. (1999). Changes in uterine expression of leukemia inhibitory factor during pregnancy in the western spotted skunk. *Biol. Reprod.* 60, 484–492. doi: 10.1095/biolreprod60.2.484
- Hou, B., Ishinaga, H., Midorikawa, K., Shah, S. A., Nakamura, S., Hiraku, Y., et al. (2015). Circulating microRNAs as novel prognosis biomarkers for head and neck squamous cell carcinoma. *Cancer Biol. Ther.* 16, 1042–1046. doi: 10.1080/15384047.2015.1045692
- Houghton, F. D. (2006). Energy metabolism of the inner cell mass and trophoblast of the mouse blastocyst. *Differentiation* 74, 11–18. doi: 10.1111/j.1432-0436.2006.00052.x
- Houghton, F. D. (2021). HYPOXIA AND REPRODUCTIVE HEALTH: hypoxic regulation of preimplantation embryos: lessons from human embryonic stem cells. *Reproduction* 161, F41–F51. doi: 10.1530/rep-20-0322
- Hu, C.-K., Wang, W., Brind'Amour, J., Singh, P. P., Reeves, G. A., Lorincz, M. C., et al. (2020). Vertebrate diapause preserves organisms long term through Polycomb complex members. *Science* 367, 870–874. doi: 10.1126/science.aaw2601
- Hu, J. K.-H., Du, W., Shelton, S. J., Oldham, M. C., DiPersio, C. M., and Klein, O. D. (2017). An FAK-YAP-mTOR signaling axis regulates stem cell-based tissue renewal in mice. *Cell Stem Cell* 21, 91–106.e6. doi: 10.1016/j.stem.2017.03.023
- Huelsken, J., Vogel, R., Brinkmann, V., Erdmann, B., Birchmeier, C., and Birchmeier, W. (2000). Requirement for  $\beta$ -catenin in anterior-posterior axis formation in mice. *J. Cell Biol.* 148, 567–578. doi: 10.1083/jcb.148.3.567
- Hunter, S. M., and Evans, M. (1999). Non-surgical method for the induction of delayed implantation and recovery of viable blastocysts in rats and mice by the use of tamoxifen and Depo-Provera. *Mol. Reprod. Dev.* 52, 29–32.
- Hussein, A. M., Wang, Y., Mathieu, J., Margaretha, L., Song, C., Jones, D. C., et al. (2020). Metabolic control over mTOR-dependent diapause-like state. *Dev. Cell* 52, 236–250.e7. doi: 10.1016/j.devcel.2019.12.018
- Jukic, A. M. Z., Weinberg, C. R., Baird, D. D., and Wilcox, A. J. (2011). The association of maternal factors with delayed implantation and the initial rise of urinary human chorionic gonadotrophin. *Hum. Reprod.* 26, 920–926. doi: 10.1093/humrep/der009
- Kamemiz, C., and Fujimori, T. (2019). Distinct dormancy progression depending on embryonic regions during mouse embryonic diapause. *Biol. Reprod.* 100, 1204–1214. doi: 10.1093/biolre/iox017
- Kelleher, A. M., Burns, G. W., Behura, S., Wu, G., and Spencer, T. E. (2016). Uterine glands impact uterine receptivity, luminal fluid homeostasis and blastocyst implantation. *Sci. Rep.* 6:38078. doi: 10.1038/srep38078
- Kharas, M. G., Okabe, R., Ganis, J. J., Gozo, M., Khandan, T., Pakinat, M., et al. (2010). Constitutively active AKT depletes hematopoietic stem cells and induces leukemia in mice. *Blood* 115, 1406–1415.
- Khoa, L. T. P., Tsan, Y.-C., Mao, F., Kremer, D. M., Sajjakulnukit, P., Zhang, L., et al. (2020). Histone Acetyltransferase MOF blocks acquisition of quiescence in ground-state ESCs through activating fatty acid oxidation. *Cell Stem Cell* 27, 441–458.e10. doi: 10.1016/j.stem.2020.06.005
- Kim, J., Song, G., Wu, G., Gao, H., Johnson, G. A., and Bazer, F. W. (2013). Arginine, leucine, and glutamine stimulate proliferation of porcine trophoblast cells through the MTOR-RPS6K-RPS6-EIF4EBP1 signal transduction pathway. *Biol. Reprod.* 88:113. doi: 10.1095/biolreprod.112.105080
- Kinder, M., Wei, C., Shelat, S. G., Kundu, M., Zhao, L., Blair, I. A., et al. (2010). Hematopoietic stem cell function requires 12/15-lipoxygenase-dependent fatty acid metabolism. *Blood* 115, 5012–5022. doi: 10.1182/blood-2009-09-243139
- Kinoshita, M., Barber, M., Mansfield, W., Cui, Y., Spindlow, D., Stirparo, G. G., et al. (2021). Capture of mouse and human stem cells with features of formative pluripotency. *Cell Stem Cell* 28, 453–471.e8. doi: 10.1016/j.stem.2020.11.005
- Klages-Mundt, N. L., Kumar, A., Zhang, Y., Kapoor, P., and Shen, X. (2018). The nature of actin-family proteins in chromatin-modifying complexes. *Front. Genet.* 9:398. doi: 10.3389/fgene.2018.00398
- Kops, G. J. P. L., Dansen, T. B., Polderman, P. E., Saarloos, I., Wirtz, K. W. A., Coffey, P. J., et al. (2002). Forkhead transcription factor FOXO3a protects quiescent cells from oxidative stress. *Nature* 419, 316–321. doi: 10.1038/nature01036
- Kress, T. R., Sabò, A., and Amati, B. (2015). MYC: connecting selective transcriptional control to global RNA production. *Nat. Rev. Cancer* 15, 593–607. doi: 10.1038/nrc3984
- Kunath, T., Arnaud, D., Uy, G. D., Okamoto, I., Chureau, C., Yamanaka, Y., et al. (2005). Imprinted X-inactivation in extra-embryonic endoderm cell lines from mouse blastocysts. *Development* 132, 1649–1661. doi: 10.1242/dev.01715
- Kuscu, N., Gungor-Ordueri, N. E., Sozen, B., Adiguzel, D., and Celik-Ozenci, C. (2019). FoxO transcription factors 1 regulate mouse preimplantation embryo development. *J. Assist. Reprod. Gen.* 36, 2121–2133. doi: 10.1007/s10815-019-01555-1
- Laplanche, M., and Sabatini, D. M. (2012). mTOR signaling in growth control and disease. *Cell* 149, 274–293. doi: 10.1016/j.cell.2012.03.017
- Lee, J.-E., Oh, H.-A., Song, H., Jun, J. H., Roh, C.-R., Xie, H., et al. (2011). Autophagy regulates embryonic survival during delayed implantation. *Endocrinology* 152, 2067–2075.
- Lefèvre, P. L. C., Palin, M.-F., Beaudry, D., Dobias-Goff, M., Desmarais, J. A., Llerena, E. M. V. et al. (2011a). Uterine signaling at the emergence of the embryo from obligate diapause. *Am. J. Physiol. Endocrinol. Metab.* 300, E800–E808. doi: 10.1152/ajpendo.00702.2010
- Lefèvre, P. L. C., Palin, M.-F., Chen, G., Turecki, G., and Murphy, B. D. (2011b). Polyamines are implicated in the emergence of the embryo from obligate Diapause. *Endocrinology* 152, 1627–1639. doi: 10.1210/en.2010-0955
- Lenis, Y. Y., Elmetwally, M. A., Maldonado-Estrada, J. G., and Bazer, F. W. (2017). Physiological importance of polyamines. *Zygote* 25, 244–255. doi: 10.1017/s0967199417000120
- Liu, W. M., Cheng, R. R., Niu, Z. R., Chen, A. C., Ma, M. Y., Li, T., et al. (2020). Let-7 derived from endometrial extracellular vesicles is an important inducer of embryonic diapause in mice. *Sci. Adv.* 6:eaa7070. doi: 10.1126/sciadv.aaz7070
- Liu, W.-M., Pang, R. T. K., Cheong, A. W. Y., Ng, E. H. Y., Lao, K., Lee, K.-F., et al. (2012). Involvement of microRNA Lethal-7a in the regulation of embryo implantation in mice. *PLoS One* 7:e37039. doi: 10.1371/journal.pone.0037039
- Loewenstein, J. E., and Cohen, A. I. (1964). Dry mass, lipid content and protein content of the intact and zona-free mouse ovum. *J. Embryol. Exp. Morphol.* 12, 113–121. doi: 10.1242/dev.12.1.113
- Marescal, O., and Cheeseman, I. M. (2020). Cellular mechanisms and regulation of quiescence. *Dev. Cell* 55, 259–271. doi: 10.1016/j.devcel.2020.09.029
- Martin, F. C., Ang, C.-S., Gardner, D. K., Renfree, M. B., and Shaw, G. (2016). Uterine flushing proteome of the tammar wallaby after reactivation from diapause. *Reproduction* 152, 491–505.
- Martin, G. R. (1981). Isolation of a pluripotent cell line from early mouse embryos cultured in medium conditioned by teratocarcinoma stem cells. *Proc. Natl. Acad. Sci. U.S.A.* 78, 7634–7638. doi: 10.1073/pnas.78.12.7634
- McCormack, J. T., and Greenwald, G. S. (1974). Evidence for a preimplantation rise in oestradiol-17 $\beta$  levels on day 4 of pregnancy in the mouse. *Reproduction* 41, 297–301. doi: 10.1530/jrf.0.0410297
- McEvoy, T. G., Coull, G. D., Broadbent, P. J., Hutchinson, J. S., and Speake, B. K. (2000). Fatty acid composition of lipids in immature cattle, pig and sheep oocytes with intact zona pellucida. *J. Reprod. Fertil.* 118, 163–170. doi: 10.1530/jrf.0.1180163
- McLaren, A. (1968). A study of blastocysts during delay and subsequent implantation in lactating mice. *J. Endocrinol.* 42, 453–463. doi: 10.1677/joe.0.0420453
- Menzorov, A. G., Matveeva, N. M., Markakis, M. N., Fishman, V. S., Christensen, K., Khabarova, A. A., et al. (2015). Comparison of American mink embryonic stem and induced pluripotent stem cell transcriptomes. *BMC Genomics* 16:S6. doi: 10.1186/1471-2164-16-s13-s6

- Meuti, M. E., Bautista-Jimenez, R., and Reynolds, J. A. (2018). Evidence that microRNAs are part of the molecular toolkit regulating adult reproductive diapause in the mosquito, *Culex pipiens*. *PLoS One* 13:e0203015. doi: 10.1371/journal.pone.0203015
- Milholland, B., Dong, X., Zhang, L., Hao, X., Suh, Y., and Vijg, J. (2017). Differences between germline and somatic mutation rates in humans and mice. *Nat. Commun.* 8:15183. doi: 10.1038/ncomms15183
- Møller, O. M. (1973). The progesterone concentrations in the peripheral plasma of the mink (*Mustela vison*) during pregnancy. *J. Endocrinol.* 56, 121–132. doi: 10.1677/joe.0.0560121
- Murphy, B. (2012). Embryonic diapause: advances in understanding the enigma of seasonal delayed implantation. *Reprod. Domest. Anim.* 47, 121–124. doi: 10.1111/rda.12046
- Murphy, B. D., Concannon, P. W., Travis, H. F., and Hansel, W. (1981). Prolactin: the hypophyseal factor that terminates embryonic diapause in mink. *Biol. Reprod.* 25, 487–491. doi: 10.1095/biolreprod25.3.487
- Naeslund, G. (1979). The effect of glucose-, arginine- and leucine-deprivation on mouse blastocyst outgrowth *in vitro*. *Ups. J. Med. Sci.* 84, 9–20.
- Naeslund, G., Lundkvist, Ö., and Nilsson, B. O. (1980). Transmission electron microscopy of mouse blastocysts activated and growth-arrested *in vivo* and *in vitro*. *Anat. Embryol.* 159, 33–48. doi: 10.1007/bf00299253
- Nakamura, T., Okamoto, I., Sasaki, K., Yabuta, Y., Iwatani, C., Tsuchiya, H., et al. (2016). A developmental coordinate of pluripotency among mice, monkeys and humans. *Nature* 537, 57–62. doi: 10.1038/nature19096
- Neagu, A., van Genderen, E., Escudero, I., Verwegen, L., Kurek, D., Lehmann, J., et al. (2020). *In vitro* capture and characterization of embryonic rosette-stage pluripotency between naive and primed states. *Nat. Cell Biol.* 22, 534–545. doi: 10.1038/s41556-020-0508-x
- Nichols, J., Chambers, I., Taga, T., and Smith, A. (2001). Physiological rationale for responsiveness of mouse embryonic stem cells to gp130 cytokines. *Development* 128, 2333–2339. doi: 10.1242/dev.128.12.2333
- Nichols, J., Davidson, D., Taga, T., Yoshida, K., Chambers, I., and Smith, A. (1996). Complementary tissue-specific expression of LIF and LIF-receptor mRNAs in early mouse embryogenesis. *Mech. Dev.* 57, 123–131. doi: 10.1016/0925-4773(96)00531-x
- O'Brien, J., Hayder, H., Zayed, Y., and Peng, C. (2018). Overview of MicroRNA biogenesis, mechanisms of actions, and circulation. *Front. Endocrinol.* 9:402. doi: 10.3389/fendo.2018.00402
- Percharde, M., Bulut-Karslioglu, A., and Ramalho-Santos, M. (2017). Hypertranscription in development, stem cells, and regeneration. *Dev. Cell* 40, 9–21. doi: 10.1016/j.devcel.2016.11.010
- Petropoulos, S., Edsgård, D., Reinius, B., Deng, Q., Panula, S. P., Codeluppi, S., et al. (2016). Single-Cell RNA-Seq reveals lineage and X chromosome dynamics in human preimplantation embryos. *Cell* 165, 1012–1026. doi: 10.1016/j.cell.2016.03.023
- Pfeffer, P. L., Smith, C. S., Maclean, P., and Berg, D. K. (2017). Gene expression analysis of bovine embryonic disc, trophoblast and parietal hypoblast at the start of gastrulation. *Zygote* 25, 265–278. doi: 10.1017/s0967199417000090
- Pilbeam, T. E., Concannon, P. W., and Travis, H. F. (1979). The annual reproductive cycle of mink (*Mustela Vison*). *J. Anim. Sci.* 48, 578–584. doi: 10.2527/jas1979.483578x
- Ptak, G. E., Tacconi, E., Czernik, M., Toschi, P., Modlinski, J. A., and Loi, P. (2012). Embryonic diapause is conserved across mammals. *PLoS One* 7:e33027. doi: 10.1371/journal.pone.0033027
- Rehman, S. K., Haynes, J., Collignon, E., Brown, K. R., Wang, Y., Nixon, A. M. L., et al. (2021). Colorectal cancer cells enter a diapause-like DTP state to survive chemotherapy. *Cell* 184, 226–242.e21. doi: 10.1016/j.cell.2020.11.018
- Ren, Z., and Ambros, V. R. (2015). Caenorhabditis elegans microRNAs of the let-7 family act in innate immune response circuits and confer robust developmental timing against pathogen stress. *Proc. Natl. Acad. Sci. U.S.A.* 112, E2366–E2375. doi: 10.1073/pnas.1422858112
- Renfree, M. B., and Fenelon, J. C. (2017). The enigma of embryonic diapause. *Development* 144, 3199–3210. doi: 10.1242/dev.148213
- Rivera-Pérez, J. A., and Hadjantonakis, A.-K. (2014). The Dynamics of morphogenesis in the early mouse embryo. *Cold. Spring Harb. Perspect. Biol.* 7:a015867. doi: 10.1101/cshperspect.a015867
- Rodgers, J. T., King, K. Y., Brett, J. O., Cromie, M. J., Charville, G. W., Maguire, K. K., et al. (2014). mTORC1 controls the adaptive transition of quiescent stem cells from G0 to GAlert. *Nature* 510, 393–396. doi: 10.1038/nature13255
- Rüegg, A., Bernal, S., Moser, F., Rutzen, I., and Ulbrich, S. (2020). Trophoblast and embryoblast proliferate at slow pace in the course of embryonic diapause in the roe deer (*Capreolus capreolus*). *Biosci. Proc.* 10, 181–196. doi: 10.1530/biosci.10.013
- Sawarkar, R., Sievers, C., and Paro, R. (2012). Hsp90 globally targets paused RNA polymerase to regulate gene expression in response to environmental stimuli. *Cell* 149, 807–818. doi: 10.1016/j.cell.2012.02.061
- Schwanhäusser, B., Busse, D., Li, N., Dittmar, G., Schuchhardt, J., Wolf, J., et al. (2011). Global quantification of mammalian gene expression control. *Nature* 473, 337–342. doi: 10.1038/nature10098
- Scognamiglio, R., Cabezas-Wallscheid, N., Thier, M. C., Altamura, S., Reyes, A., Prendergast, Á. M., et al. (2016). Myc depletion induces a pluripotent dormant state mimicking diapause. *Cell* 164, 668–680. doi: 10.1016/j.cell.2015.12.033
- Shaw, G., and Renfree, M. B. (1984). Concentrations of oestradiol-17 $\beta$  in plasma and corpora lutea throughout pregnancy in the tammar, *Macropus eugenii*. *Reproduction* 72, 29–37. doi: 10.1530/jrf.0.0720029
- Singh, S. R., Zeng, X., Zhao, J., Liu, Y., Hou, G., Liu, H., et al. (2016). The lipolysis pathway sustains normal and transformed stem cells in adult *Drosophila*. *Nature* 538, 109–113. doi: 10.1038/nature19788
- Smith, A. G., Heath, J. K., Donaldson, D. D., Wong, G. G., Moreau, J., Stahl, M., et al. (1988). Inhibition of pluripotential embryonic stem cell differentiation by purified polypeptides. *Nature* 336, 688–690. doi: 10.1038/336688a0
- Snow, M. H. L. (1977). Gastrulation in the mouse: growth and regionalization of the epiblast. *Development* 42, 293–303.
- Song, J. H., Houde, A., and Murphy, B. D. (1998). Cloning of leukemia inhibitory factor (LIF) and its expression in the uterus during embryonic diapause and implantation in the mink (*Mustela vison*). *Mol. Reprod. Dev.* 51, 13–21.
- Sousa, M. I., Correia, B., Rodrigues, A. S., and Ramalho-Santos, J. (2020). Metabolic characterization of a paused-like pluripotent state. *Biochim. Biophys. Acta* 1864:129612. doi: 10.1016/j.bbagen.2020.129612
- Spindler, R. E., Renfree, M. B., and Gardner, D. K. (1996). Carbohydrate uptake by quiescent and reactivated mouse blastocysts. *J. Exp. Zool.* 276, 132–137.
- Stanton, M. M., Tzatzalos, E., Donne, M., Kolundzic, N., Helgason, I., and Ilic, D. (2019). Prospects for the use of induced pluripotent stem cells in animal conservation and environmental protection. *Stem Cells Transl. Med.* 8, 7–13. doi: 10.1002/sctm.18-0047
- Stewart, C. L., Kaspar, P., Brunet, L. J., Bhatt, H., Gadi, I., Köntgen, F., et al. (1992). Blastocyst implantation depends on maternal expression of leukaemia inhibitory factor. *Nature* 359, 76–79. doi: 10.1038/359076a0
- Stoufflet, I., Mondain-Monval, M., Simon, P., and Martinet, L. (1989). Patterns of plasma progesterone, androgen and oestrogen concentrations and *in-vitro* ovarian steroidogenesis during embryonic diapause and implantation in the mink (*Mustela vison*). *Reproduction* 87, 209–221. doi: 10.1530/jrf.0.0870209
- Sturmey, R. G., and Leese, H. J. (2003). Energy metabolism in pig oocytes and early embryos. *Reproduction* 126, 197–204. doi: 10.1530/rep.0.1260197
- Sukoyan, M. A., Golubitsa, A. N., Zhelezova, A. I., Shilov, A. G., Vatolin, S. Y., Maximovsky, L. P., et al. (1992). Isolation and cultivation of blastocyst-derived stem cell lines from American mink (*Mustela vison*). *Mol. Reprod. Dev.* 33, 418–431. doi: 10.1002/mrd.1080330408
- Sun, X., Chen, W.-D., and Wang, Y.-D. (2017). DAF-16/FOXO transcription factor in aging and longevity. *Front. Pharmacol.* 8:548. doi: 10.3389/fphar.2017.00548
- Surveyor, G. A. (1995). Expression and steroid hormonal control of Muc-1 in the mouse uterus. *Endocrinology* 136, 3639–3647. doi: 10.1210/en.136.8.3639
- Takahashi, K., and Yamanaka, S. (2006). Induction of pluripotent stem cells from mouse embryonic and adult fibroblast cultures by defined factors. *Cell* 126, 663–676. doi: 10.1016/j.cell.2006.07.024
- Tanaka, S., Kunath, T., Hadjantonakis, A.-K., Nagy, A., and Rossant, J. (1998). Promotion of trophoblast stem cell proliferation by FGF4. *Science* 282, 2072–2075. doi: 10.1126/science.282.5396.2072
- ten Berge, D., Koole, W., Fuerer, C., Fish, M., Eroglu, E., and Nusse, R. (2008). Wnt signaling mediates self-organization and axis formation in embryoid bodies. *Cell Stem Cell* 3, 508–518. doi: 10.1016/j.stem.2008.09.013
- ten Berge, D., Kurek, D., Blauwkamp, T., Koole, W., Maas, A., Eroglu, E., et al. (2011). Embryonic stem cells require Wnt proteins to prevent differentiation to epiblast stem cells. *Nat. Cell Biol.* 13, 1070–1075. doi: 10.1038/ncb2314
- Tesar, P. J., Chenoweth, J. G., Brook, F. A., Davies, T. J., Evans, E. P., Mack, D. L., et al. (2007). New cell lines from mouse epiblast share defining features with human embryonic stem cells. *Nature* 448, 196–199. doi: 10.1038/nature05972

- Treiber, T., Treiber, N., and Meister, G. (2019). Regulation of microRNA biogenesis and its crosstalk with other cellular pathways. *Nat. Rev. Mol. Cell Biol.* 20, 5–20. doi: 10.1038/s41580-018-0059-1
- van der Weijden, V. A., Bick, J., Bauersachs, S., Arnold, G. J., Fröhlich, T., Drews, B., et al. (2019). Uterine fluid proteome changes during diapause and resumption of embryo development in roe deer. *Reproduction* 1, 13–24. doi: 10.1530/rep-19-0022
- van der Weijden, V. A., and Ulbrich, S. E. (2020). Embryonic diapause in roe deer: a model to unravel embryo-maternal communication during pre-implantation development in wildlife and livestock species. *Theriogenology* 158, 105–111. doi: 10.1016/j.theriogenology.2020.06.042
- van Leeuwen, J., Berg, D. K., and Pfeffer, P. L. (2015). Morphological and gene expression changes in cattle embryos from hatched blastocyst to early gastrulation stages after transfer of *in vitro* produced embryos. *PLoS One* 10:e0129787. doi: 10.1371/journal.pone.0129787
- Wagner, J. T., and Podrabsky, J. E. (2015). Extreme tolerance and developmental buffering of UV-C induced DNA damage in embryos of the annual killifish *Austrofundulus limnaeus*. *J. Exp. Zool. Part Ecol. Genet. Physiol.* 323, 10–30. doi: 10.1002/jez.1890
- Wauters, J., Jewgenow, K., Goritz, F., and Hildebrandt, T. (2020). Could embryonic diapause facilitate conservation of endangered species? *Biosci. Proc.* 10, 76–84. doi: 10.1530/biosciproc.10.005
- Weitlauf, H. M., and Greenwald, G. S. (1968). Survival of blastocysts in the uteri of ovariectomized mice. *Reproduction* 17, 515–520. doi: 10.1530/jrf.0.0170515
- Whitten, W. K. (1955). Endocrine studies on delayed implantation in lactating mice. *J. Endocrinol.* 13, 1–6. doi: 10.1677/joe.0.0130001
- Wilcox, A. J., Baird, D. D., and Weinberg, C. R. (1999). Time of implantation of the conceptus and loss of pregnancy. *N. Engl. J. Med.* 340, 1796–1799. doi: 10.1056/nejm199906103402304
- Williams, R. L., Hilton, D. J., Pease, S., Willson, T. A., Stewart, C. L., Gearing, D. P., et al. (1988). Myeloid leukaemia inhibitory factor maintains the developmental potential of embryonic stem cells. *Nature* 336, 684–687. doi: 10.1038/336684a0
- Winkle, L. J. (2001). Amino acid transport regulation and early embryo development. *Biol. Reprod.* 64, 1–12. doi: 10.1095/biolreprod64.1.1
- Wu, J., Huang, B., Chen, H., Yin, Q., Liu, Y., Xiang, Y., et al. (2016). The landscape of accessible chromatin in mammalian preimplantation embryos. *Nature* 534, 652–657. doi: 10.1038/nature18606
- Ying, Q.-L., Wray, J., Nichols, J., Batlle-Morera, L., Doble, B., Woodgett, J., et al. (2008). The ground state of embryonic stem cell self-renewal. *Nature* 453, 519–523. doi: 10.1038/nature06968
- Young, R. A. (2011). Control of the embryonic stem cell state. *Cell* 144, 940–954. doi: 10.1016/j.cell.2011.01.032
- Zhang, P., Liang, X., Shan, T., Jiang, Q., Deng, C., Zheng, R., et al. (2015). mTOR is necessary for proper satellite cell activity and skeletal muscle regeneration. *Biochem. Biophys. Res. Commun.* 463, 102–108. doi: 10.1016/j.bbrc.2015.05.032
- Zhang, X., Yalcin, S., Lee, D.-F., Yeh, T.-Y. J., Lee, S.-M., Su, J., et al. (2011). FOXO1 is an essential regulator of pluripotency in human embryonic stem cells. *Nat. Cell Biol.* 13, 1092–1099. doi: 10.1038/ncb2293
- Zheng, X., Yang, P., Lackford, B., Bennett, B. D., Wang, L., Li, H., et al. (2016). CNOT3-Dependent mRNA deadenylation safeguards the pluripotent state. *Stem Cell Rep.* 7, 897–910. doi: 10.1016/j.stemcr.2016.09.007

**Conflict of Interest:** The authors declare that the research was conducted in the absence of any commercial or financial relationships that could be construed as a potential conflict of interest.

**Publisher's Note:** All claims expressed in this article are solely those of the authors and do not necessarily represent those of their affiliated organizations, or those of the publisher, the editors and the reviewers. Any product that may be evaluated in this article, or claim that may be made by its manufacturer, is not guaranteed or endorsed by the publisher.

Copyright © 2021 van der Weijden and Bulut-Karslioglu. This is an open-access article distributed under the terms of the Creative Commons Attribution License (CC BY). The use, distribution or reproduction in other forums is permitted, provided the original author(s) and the copyright owner(s) are credited and that the original publication in this journal is cited, in accordance with accepted academic practice. No use, distribution or reproduction is permitted which does not comply with these terms.





# Cell Cycle Entry Control in Naïve and Memory CD8<sup>+</sup> T Cells

David A. Lewis<sup>1\*</sup> and Tony Ly<sup>2,3\*</sup>

<sup>1</sup> Ashworth Laboratories, Institute of Immunology and Infectious Research, University of Edinburgh, Edinburgh, United Kingdom, <sup>2</sup> Wellcome Centre for Cell Biology, University of Edinburgh, Edinburgh, United Kingdom, <sup>3</sup> Centre for Gene Regulation and Expression, University of Dundee, Dundee, United Kingdom

CD8<sup>+</sup> T cells play important roles in immunity and immuno-oncology. Upon antigen recognition and co-stimulation, naïve CD8<sup>+</sup> T cells escape from dormancy to engage in a complex programme of cellular growth, cell cycle entry and differentiation, resulting in rapid proliferation cycles that has the net effect of producing clonally expanded, antigen-specific cytotoxic T lymphocytes (CTLs). A fraction of activated T cells will re-enter dormancy by differentiating into memory T cells, which have essential roles in adaptive immunity. In this review, we discuss the current understanding of cell cycle entry control in CD8<sup>+</sup> T cells and crosstalk between these mechanisms and pathways regulating immunological phenotypes.

**Keywords:** quiescence, T cell, proliferation, cell cycle, T cell activation

## OPEN ACCESS

### Edited by:

Guang Yao,  
University of Arizona, United States

### Reviewed by:

Sander Van Den Heuvel,  
Utrecht University, Netherlands  
Jing Qu,  
Institute of Zoology, (CAS), China

### \*Correspondence:

David A. Lewis  
D.A.Lewis-1@sms.ed.ac.uk  
Tony Ly  
tly@dundee.ac.uk

### Specialty section:

This article was submitted to  
Cell Growth and Division,  
a section of the journal  
Frontiers in Cell and Developmental  
Biology

**Received:** 18 June 2021

**Accepted:** 07 September 2021

**Published:** 06 October 2021

### Citation:

Lewis DA and Ly T (2021) Cell  
Cycle Entry Control in Naïve  
and Memory CD8<sup>+</sup> T Cells.  
Front. Cell Dev. Biol. 9:727441.  
doi: 10.3389/fcell.2021.727441

## INTRODUCTION

CD8<sup>+</sup> T cells are an important component of the acquired immune response. They have a role in limiting viral infection and cancer progression through recognising key viral/tumour antigens on the infected cell surface and targeting them for destruction (Kim and Ahmed, 2010). T cells are the product of central selection, a process in which newly developed progenitor T cells go through differentiation and numerous divisions, becoming lineage restricted toward the naïve CD8<sup>+</sup> T cell phenotype. These naïve T cells then lie dormant predominately within the lymph nodes (Carpenter and Bosselut, 2010). Naïve CD8<sup>+</sup> T cells are activated by antigen presenting cells. The activation phase is characterised by major rewiring of their cellular proteomes and metabolism. Activated T cells then rapidly proliferate in what is known as the expansion phase (**Figure 1A**). During this phase, the doubling rate averages at 6–8 h with some studies demonstrating a peak doubling time of 4.5 h, or even 2 h (Kurts et al., 1997; Yoon et al., 2010). Also during this phase, T cells will begin to differentiate toward one of two T effector ( $T_{eff}$ ) phenotypes, the short lived effector cell (SLEC) which die during the subsequent contraction phase, and the memory progenitor cells (MPEC) which survive beyond the contraction phase. MPECs then differentiate toward one of the memory T cell phenotypes, e.g., the central memory T cell ( $T_{cm}$ ), and effector memory T cell ( $T_{em}$ ). The role of SLECs is to clear the infection, which is done by targeted release of cytolytic granzymes and perforins to infected cells. Following the clearance of infection, memory T cells remain in a state of dormancy, with  $T_{cm}$  localising to the lymph nodes, and  $T_{em}$  remaining in the periphery. Like naïve T cells, they await antigen stimulation in order to activate and proliferate, but have a higher antigenic threshold and more quickly initiate proliferation (Mehlhof-Williams and Bevan, 2014). This enables memory T cells to act as early responders to repeat infections.

What factors determine whether daughter cells from an activated naïve T cell move toward the MPEC or SLEC phenotype are a topic of active debate. It is generally agreed, however, that SLECs represent a fully differentiated form of T cell, which develop full effector function in exchange of proliferative potential and survival that typify MPECS. Complementing this model are studies that

demonstrate differences in cell cycle progression between the phenotypes, with SLECs progressing at a much faster rate than MPEC (Kinjyo et al., 2015; Kretschmer et al., 2020) demonstrating a link between control of proliferation and differentiation.

In this review, we will first present an overview on cell cycle regulation based on various mammalian model systems. We then examine the pathways controlling CD8<sup>+</sup> T cell differentiation and proliferation with reference to the cell cycle regulation pathways outlined prior and explore potential crosstalk between these two key processes.

## CELL CYCLE REGULATION

The cell cycle is divided into four phases (Figure 1B). In the first gap phase (G1), the cell prepares for DNA replication (S). This is followed by a second gap phase (G2) when the cell prepares for mitosis (M). Quiescent, or G0 cells enter the cell cycle by first transiting through G1. During G1, cells pass through a commitment step called the restriction point (R). Before R, cells are susceptible to cell cycle arrest by mitogen starvation. However, beyond R, progression through the cell cycle is mitogen-independent in human fibroblasts. The time cells spend in pre-R G1 is heterogeneous compared with the time spent in the remaining phases of the cell cycle (Zetterberg and Larsson, 1985; Zetterberg et al., 1995). Additionally mitogen starved cells which exit to G0 and are reintroduced to mitogen have been observed to take up to an additional 8 h to reach and complete mitosis compared to cells cultured in mitogen-replete conditions (Zetterberg and Larsson, 1991). Thus, G0, pre-R and post-R G1 can be considered distinct phases that are distinguished in their mitogen responsiveness and in the length of time needed to progress to S-phase. It should be noted, however, that it is as yet unclear if the restriction point as described in fibroblasts exists within T cells. This is due to the differences in mitogenic signalling within T cells which make the model established in fibroblasts more challenging to test in T cells.

Key proteins that control cell cycle progression include (1) the cyclin proteins, which rise and fall in abundance at key stages of cell cycle, (2) the cyclin-dependent kinases (CDKs) which become active when bound to their cognate cyclins, and (3) the CDK inhibitor proteins (CDKi) which control cell cycle progression at key check points in response to mitogen starvation or cellular stress (e.g., DNA damage).

### CDK-Rb-E2F

Cyclins, CDKs, and CDKis have key roles in regulating the activity of E2 factor F (E2F), a transcription factor that promotes the expression of cell cycle genes, including the cyclins and CDKs themselves.

In G0 and pre-R G1, E2F mediated transcription will be inhibited by pocket proteins Retinoblastoma protein (Rb), p107, and p130, preventing the cell from progressing to S phase (Stengel et al., 2009). An active kinase complex is formed by interaction of cyclin D with either CDK4 or CDK6, and this

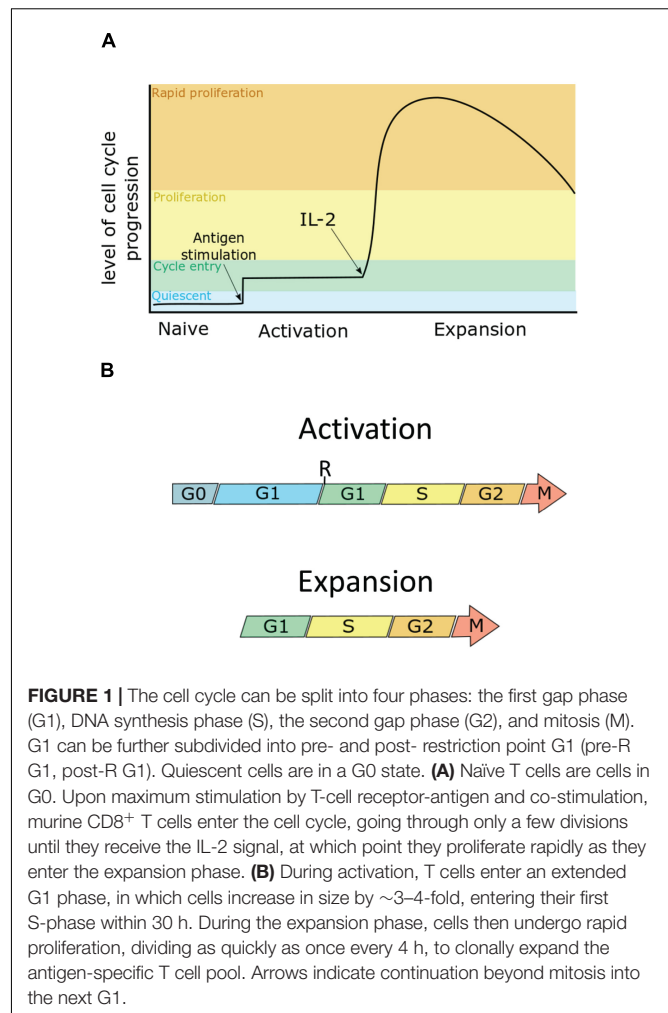


**FIGURE 1** | The cell cycle can be split into four phases: the first gap phase (G1), DNA synthesis phase (S), the second gap phase (G2), and mitosis (M). G1 can be further subdivided into pre- and post- restriction point G1 (pre-R G1, post-R G1). Quiescent cells are in a G0 state. **(A)** Naïve T cells are cells in G0. Upon maximum stimulation by T-cell receptor-antigen and co-stimulation, murine CD8<sup>+</sup> T cells enter the cell cycle, going through only a few divisions until they receive the IL-2 signal, at which point they proliferate rapidly as they enter the expansion phase. **(B)** During activation, T cells enter an extended G1 phase, in which cells increase in size by ~3–4-fold, entering their first S-phase within 30 h. During the expansion phase, cells then undergo rapid proliferation, dividing as quickly as once every 4 h, to clonally expand the antigen-specific T cell pool. Arrows indicate continuation beyond mitosis into the next G1.

kinase activity mediates hyperphosphorylation of Rb, causing Rb to decouple from E2F, and thereby enable E2F to promote upregulation of its targets. Such targets include a large number of S phase-promoting proteins, including cyclin E and cyclin A. Cyclin E will form a complex with CDK2 which amongst other processes will contribute to Rb hyperphosphorylation, resulting in a positive feedback loop that activates E2F (Dyson, 1998). Recent work suggests that CDK4/6 regulates cellular processes other than those downstream of E2F. Cyclin D3-CDK6 phosphorylates key enzymes in the glycolysis pathway, diverting metabolites from glycolysis into the pentose phosphate pathway to promote redox balance (via production of NADPH) and cellular anabolism (e.g., by generating nucleotide precursors) (Wang et al., 2017).

Cyclin-dependent kinases activities can be inhibited by stoichiometric binding to CDKis, of which there are two main families: the INK4 family consisting of p16, p15, p18, and p19 which inhibit Cyclin D-CDK4/6 complex; and the Cip/Kip family which consists of p27, p21, and p57 that inhibit cyclin-CDK complexes, and are able to induce cell cycle arrest at G1 phase (Sherr and Roberts, 1999). The regulation of CDK4/6

complexes by the Cip/Kip family members are more complex. Cip/Kip proteins can promote the formation of cyclin-CDK complexes and in the absence of p21 or p27, cyclin D-CDK complexes do not form (Labaer et al., 1997; Cheng et al., 1999). Trimeric species containing p27 phosphorylated on tyrosine 74, cyclin D, and CDK4 retain kinase activity (Guiley et al., 2019). On the other hand, high levels of p21 inhibit CDK4 (Labaer et al., 1997). Cip/Kip proteins are inactivated by post-translational modification and degradation. For example, tyrosine phosphorylation on p27 by mitogen-activated tyrosine kinases disrupts the inhibitory interaction of p27 with CDK2 and promotes p27 degradation (Grimmler et al., 2007),

## Anaphase Promoting Complex/Cyclosome

Stability of cyclin, CDK and CDKi proteins are controlled post-translationally in a cell cycle regulated manner by E3 ubiquitin ligases. The anaphase promoting complex/cyclosome (APC/C) is a large, multi-subunit E3 ligase that targets many proteins, including cyclins and other E2F targets, for destruction in mitosis and G1. The APC/C has two co-activators, Cell Division Cycle (Cdc) 20 and Fizzy-related protein homolog-1 (Fzr1) (also known as Cdh1). The substrate adaptor functions of Cdc20 are primarily in mitosis, whereas Cdh1 is important in mitotic exit and G1. Indeed, inactivation of the APC/C-Cdh1 has been shown to be a second crucial step in promoting the transition from G1 to S (Cappell et al., 2016). Thus, proteins required for G1/S are upregulated by increased synthesis via transcription by E2F and increased stability via APC/C inactivation. APC/C inactivation in G1 is mediated by multiple mechanisms, including phosphorylation of Cdh1 (Kramer et al., 2000) by CDK2 (Lukas et al., 1999) and by the accumulation the pseudosubstrate inhibitor protein, F-box only protein 5 (Fbxo5) [also known as the early mitotic inhibitor 1 (Emi1)] (Cappell et al., 2018). Additionally, there are deubiquitinases (DUBs), including ubiquitin specific peptidase 37 (Usp37), which stabilise APC/C substrates by removing ubiquitin chains that would otherwise target these proteins for proteasomal destruction (Huang et al., 2011).

## ACTIVATION PHASE (TCR INDUCED PROLIFERATION)

T cell activation and proliferation requires three stimulation signals, antigenic stimulation via the T cell receptor (TCR), co-receptor signalling from professional antigen presenting cells via CD28, and cytokine stimulation primarily driven by interleukin (IL)-2. Stimulation of the TCR alone results in anergy. Anergic cells do not produce IL-2, fail to proliferate, and become unresponsive to further stimulation attempts. A dual signal of TCR and CD28 induces production of IL-2 and proliferation within the first 24 h. IL-2 stimulation through the IL-2 receptor (IL-2R) enables rapid proliferation as the cells enter the expansion phase (Mondino et al., 2006).

As depicted in **Figure 2A**, TCR stimulation leads to phosphorylation of lymphocyte-specific protein tyrosine kinase

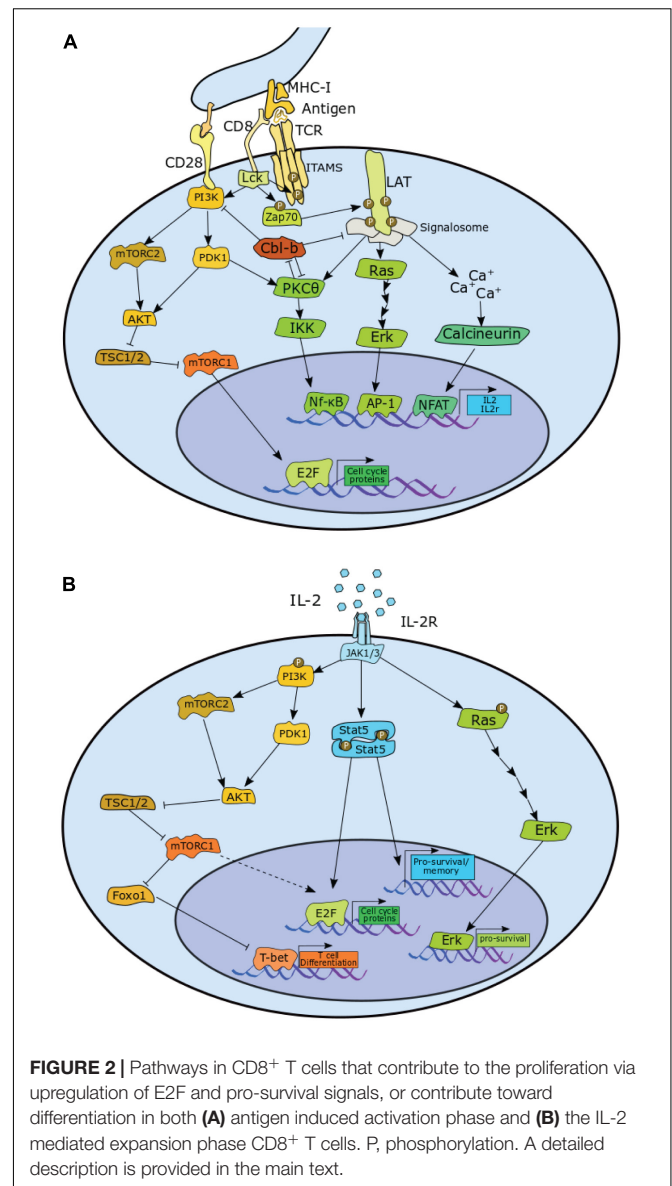


**FIGURE 2 |** Pathways in CD8<sup>+</sup> T cells that contribute to the proliferation via upregulation of E2F and pro-survival signals, or contribute toward differentiation in both (A) antigen induced activation phase and (B) the IL-2 mediated expansion phase CD8<sup>+</sup> T cells. P, phosphorylation. A detailed description is provided in the main text.

(Lck), which in return phosphorylates the  $\zeta$  chains of the TCR along the immunoreceptor tyrosine-based activation motifs (ITAMS). This enables recruitment of TCR-associated protein 70 (Zap70), which is subsequently phosphorylated by Lck. Zap70 then phosphorylates four key sites on the linker for activation of T cells (LAT) which allows for recruitment of proteins into the LAT signalosome. The downstream effect is activation of the Rat sarcoma (Ras)/extracellular signal-related kinase (Erk)/Activator protein 1 (AP-1) pathway, Protein kinase C- $\theta$  (PKC $\theta$ )/ $\kappa$ B kinase (IKK)/nuclear factor- $\kappa$ B (NF- $\kappa$ B) pathway, and the calcium-dependent Calcineurin/nuclear factor of activated T cells (NFAT) pathway (Brownlie and Zamoyska, 2013; Hwang et al., 2020). The transcription factors downstream of these pathways, NFAT, NF- $\kappa$ B, and AP-1 all contribute to the transcription of *IL2* and also contribute to the transcription of *IL2RA*, which encodes the  $\alpha$ -chain of the IL-2 receptor (CD25) (Liao et al., 2013).

Protein tyrosine kinase positively regulates phosphoinositide-dependent kinase 1 (PDK1) activity, which stimulates two major pathways: PKC $\theta$ /IKK/NF- $\kappa$ B pathway and the Akt strain transforming (AKT)/mammalian target of rapamycin complex 1 (mTORC1) pathway. Lck mediates this via activation of phosphoinositide 3-Kinase (PI3K), which is enhanced by co-receptor CD28 stimulation. PI3K is also responsible for enabling the assembly of mTOR complex 2 (mTORC2), which activates AKT, enabling it to target its substrates, such as the mTORC1 inhibitor, Hamartin (TSC1)/Tuberin (TSC2), thereby upregulating mTORC1 activity (Brownlie and Zamoyska, 2013; Jutz et al., 2016; Spolski et al., 2018; Hwang et al., 2020).

With TCR stimulation alone, however, the components of the LAT signalosome, as well as PKC $\theta$  are targeted for degradation by the E3-Ubiquitin ligase casitas B-lineage lymphoma proto-oncogene (Cbl)-b. Cbl-b also has the effect of reducing PI3K activity by preventing formation of phosphatidylinositol-3-phosphate (PIP3). The net effect of this is a sharp reduction in NFAT, NF $\kappa$ B, AP-1, and mTOR activity, resulting in the cell becoming anergic (Liu et al., 2014).

CD28 stimulation counteracts this effect by enhancing PKC $\theta$  activity, which promotes degradation of Cbl-b. Indeed, loss of PKC $\theta$  activity further decreases transcription factor activity downstream of LAT (Gruber et al., 2009), while knockout of CD28 leads to a reduction in proliferation (Li et al., 2004). Conversely, both Cbl-b deletion and Cbl-b inactive mutation enables T cell proliferation and production of IL-2 in the absence of CD28 signal. Loss of Cbl-b activity greatly enhances CD28-mediated proliferation and IL-2 production (Paolino et al., 2011). Consistent with a role in negatively regulating activation, Cbl-b also emerged as a top hit in a CRISPR genetic screen for regulators of secondary activation in human CD8 $^{+}$  T cells (Shifrut et al., 2018).

Interestingly, there is no requirement for Lck in the activation of memory T cells upon secondary infection by LCMV *in vivo*. The frequency of antigen-specific T cells after secondary challenge to antigen was unaffected in memory cells depleted of Lck compared to Lck-replete cells, suggesting that proliferation is unaffected by Lck depletion. Re-challenged Lck-depleted cells also produced comparable levels of interferon (IFN)- $\gamma$  to that of Lck-replete cells. This is in direct contrast to naïve cells depleted of Lck, which do not proliferate in response to antigen (Tewari et al., 2006). In addition, *ex vivo* memory T cells seem more reliant on cytokine signalling to induce proliferation, with antigen and CD28 stimulation alone proving insufficient to trigger proliferation in memory T cells (Cho et al., 1999).

## Mammalian Target of Rapamycin Complex, Cell Growth, and E2 Factor F

T cell receptor/CD28 stimulation of naïve cells is sufficient to initiate proliferation. TCR/CD28 stimulation leads to phosphorylation of Rb, expression of cyclin E, cyclin A, and CDK2, and the degradation of p27 (Appleman et al., 2000). Rapamycin, an inhibitor of mTOR, induces a severe delay in proliferation (D'Souza and Lefrançois, 2003), resulting in decreased levels of cyclin D3 and cyclin E. And while cyclin

D3 levels recover 3–5 days following rapamycin treatment, cyclin E remains low, suggesting a dependence on mTOR for antigen-induced E2F activation. Although the exact mechanism is unknown, expression of a rapamycin resistant mutant of p70<sup>S6k</sup> (also known as S6K) rescues E2F activity in rapamycin-treated cells; thereby demonstrating that mTOR activity promotes cell cycle progression by activating E2F through S6K (Brennan et al., 1999). In contrast to wild-type cells, proliferation of IL-2 $^{-/-}$  cells is arrested completely by rapamycin. In addition, stimulator of interferon genes (STING) activity reduces levels of cyclins A and E, and Cdk1, leading to a reduction in activation induced proliferation. STING inhibits mTOR, reduces S6K activity, reduces phosphorylation of eukaryotic translation initiation factor 4E (eIF4E)-binding protein (4E-BP1), and reduces STAT5 phosphorylation, leading to decreased levels of S-phase promoting proteins (Imanishi et al., 2019). Together these results suggest that IL-2 signalling contributes to proliferation in an mTOR-independent manner as outlined in **Figure 2B**. Interestingly, mTOR inhibition does not delay cells in the expansion phase (Colombetti et al., 2006).

Canonically there are three E2F isoforms which promote proliferation, E2F1-3, and that activation of these transcription factors are essential to cell cycle progression (Wu et al., 2001). However, it has been shown that in CD8 $^{+}$  T cells, E2F1-3 can have both positive and negative effects on cell cycle progression. Single knockout of either E2F1 or E2F2 results in reduction in proliferation, while a double knockout yields a hyperproliferative phenotype and reduced antigenic threshold (Murga et al., 2001; Zhu et al., 2001). In addition to this, CD8 $^{+}$  T cells deficient in E2F1 show much reduced activation induced cell death (Gao et al., 2004). CD8 $^{+}$  T cells are not the only cell line in which E2F behaves in a non-canonical fashion. In retinal cells Myc mediated proliferation has been shown to persist even in the absence of E2F1-3 proving these E2Fs to be largely non-essential for these cells (Chen et al., 2009), while in progenitor cell lines approaching terminal differentiation, E2F1-3 seem to have a cell cycle repressive role upon forming a complex with Rb (Chong et al., 2009). It is, however, difficult to say whether similar processes are occurring within CD8 $^{+}$  T cells post activation as the precise molecular regulators of E2F transcription targets have yet to be fully explored.

mTOR also upregulates the c-Myc transcription factor, which has a crucial role in T cell metabolism (Vartanian et al., 2011; Wang et al., 2011; Waickman and Powell, 2012) and expression of several cell cycle regulators, including p27, cyclins, and CDKs (Dang et al., 2006). T cells lacking c-Myc have defects in glycolysis, glutaminolysis, cell growth, and proliferation. Indeed, compared to wild type, c-Myc knockout cells show decreased levels of CDK4, CDK2, and Cdc25A (Wang et al., 2011). Furthermore, Raptor deficient cells that have impaired mTORC1 activity show reduced levels of key transcription factors including Myc, but also GA-binding protein alpha chain (Gabpa), yin yang (YY)1, and Sterol Regulatory Element Binding Transcription Factor (Srebf)1, all of which are associated with mitochondrial function (Tan et al., 2017).



## Cyclin-Dependent Kinase Regulation of T Cell Activation

CDKi proteins interfere with the pathways downstream of TCR stimulation. p27 is a key negative regulator of IL-2 production in anergic CD4<sup>+</sup> T cells (Boussiotis et al., 2000). Ectopic expression of p27, but not p21, suppresses IL-2 production in CD4<sup>+</sup> T cells. Depletion of p27 in stimulated Jurkat T cells enhances transcription of an IL-2 luciferase reporter construct and enhanced cellular AP-1 activity. The proposed mechanism is that p27 directly binds JAB1/COPS5, a subunit of the COP9 signalosome and positive regulates AP-1, inducing translocation of AP-1 from the nucleus to the cytoplasm (Tomoda et al., 1999), thereby suppressing IL-2 transcription (Boussiotis et al., 2000). Whether this effect extends to CD8<sup>+</sup> T cells is yet to be determined.

There is significant interest in the roles of CDK4/6 in immunomodulation, and how small molecule inhibitors of CDK4/6 affect immune cell phenotypes. Recent data using CDK4/6 inhibitors (CDK4/6i) suggest a direct role of Cyclin-CDKs in controlling T cell differentiation. Three CDK4/6i are FDA-approved for HR+ breast cancer: palbociclib (PD-0332991), abemaciclib (LY2835219), and ribociclib (LEE011). Numerous clinical trials are ongoing for the treatment of other solid tumours (Álvarez-Fernández and Malumbres, 2020). Extensive reviews on this topic already exist and lie outside the scope of this review (Chaikovsky and Sage, 2018; Ameratunga et al., 2019). Interestingly, recent evidence suggests these inhibitors function similarly to the INK4 family of proteins by binding to monomeric CDK4/6 (Guiley et al., 2019). Proliferation of CD4<sup>+</sup> Treg cells is inhibited by CDK4/6 inhibition whereas proliferation of CD8<sup>+</sup> cells is relatively unaffected (Goel et al., 2017). Indeed, CD8<sup>+</sup> T cell function can be augmented by CDK4/6 inhibition. Treatment of CD8<sup>+</sup> T cells with CDK4/6 inhibitors enhances NFAT activity, increasing expression of CD25 and production of IL-2 and granzyme B, indicating that CDK6 may have a role in limiting T cell effector differentiation (Deng et al., 2018). Indeed, loss of CDK6 in T cells led to an increase in IL-2 production, and was also seen to impair type I interferon signalling events and increased metabolic processes resulting in enhanced ATP production and maximal respiration in addition to affecting proliferation (Klein et al., 2021).

In summary, T cell activation produces a signalling cascade that triggers a change in gene expression that promotes cell growth, increased anabolic metabolism, and stimulation of nascent CDK/E2F activities. The significant rewiring of the proteome and metabolism is important for supporting the next phase of CD8<sup>+</sup> T cell differentiation, in which activated cells rapidly proliferate to clonally expand antigen-specific CTLs.

## EXPANSION PHASE (IL-2 DRIVEN PROLIFERATION)

A key regulator of CD8<sup>+</sup> T cell proliferation in the expansion phase is IL-2, a cytokine and potent T cell mitogen (Smith and Ruscetti, 1981) that is produced primarily by

activated CD4<sup>+</sup> and CD8<sup>+</sup> T cells (Nelson, 2004). Upon activation, CD8<sup>+</sup> T cells secrete IL-2 and express a high affinity IL-2 receptor subunit, CD25. Blockade of IL-2 leads to reduced proliferation (Mishima et al., 2017). While TCR stimulation alone has been shown to be sufficient to induce proliferation of CD8<sup>+</sup> T cells, the absence of IL-2 signal results in suboptimal expansion and cell cycle slower progression (D'Souza and Lefrançois, 2003). In addition, the presence of IL-2 in culture reduces the minimum threshold of TCR signalling required to enter cell cycle (Au-Yeung et al., 2017).

Continuous exposure to IL-2 is essential for prolonged expansion. IL-2 starvation leads to reduced cell viability, loss of CD25 expression, and decreased cellular protein content, including many major cell cycle regulators: cyclin D2, cyclin D3, cyclin A, cyclin B1, cyclin B2, CDK4, CDK6, CDK1, p15, and p21. Notably, p27 is one of the few proteins to increase as a result of IL-2 starvation (Rollings et al., 2018). p27 is implicated in controlling cell cycle exit in the contraction phase. *In vivo* experiments utilising p27 KO CD8<sup>+</sup> T cells continued to expand up to day 11 post immunisation, while WT began contraction by day 8. The effect of p27 is more pronounced for MPECs than SLECs. MPEC cells maintained their higher populations as late as 30 days post immunisation, while SLEC p27 knockouts generally returned to similar cell numbers as WT cells by day 15. This difference in response is likely due to MPECs expressing higher pro-survival factors and having a greater capacity for IL-2 production than SLECs (Singh et al., 2010).

Whereas studies consistently show that p27<sup>-/-</sup> mice exhibit splenic and thymic hyperplasia (Fero et al., 1996; Kiyokawa et al., 1996; Nakayama et al., 1996), the data for p21<sup>-/-</sup> mice are conflicting (Balomenos et al., 2000). Activated p21<sup>-/-</sup>, p27<sup>-/-</sup> double knockout (DKO) splenocytes are hyperproliferative *in vitro*. Freshly isolated splenocytes from p21<sup>-/-</sup> but not p27<sup>-/-</sup> mice, had a higher frequency of CD25 expressing naïve CD4<sup>+</sup> and CD8<sup>+</sup> T cells. The percentage of CD25<sup>+</sup> cells in activated DKO or p27<sup>-/-</sup> splenocyte cultures were elevated by ~10% relative to wild type, or to p21<sup>-/-</sup> (Wolfrum et al., 2004), which may enhance T cell sensitivity to IL-2, and therefore mitogen-induced proliferation.

Downstream of IL-2 receptor activation is the STAT5 pathway (Moriggl et al., 1999a), which is known to positively regulate proliferation. STAT5 activation induces homeostatic proliferation in naïve CD8<sup>+</sup> T cells, even in the absence of cytokine stimulation (Burchill et al., 2003), and in activated T cells, like mTOR, STAT5 enhances E2F activity by activating S6K (Lockyer et al., 2007). STAT5 KO T cells have reduced cell cycle regulators, including cyclin D2, cyclin D3, cyclin E, cyclin A, and CDK6 (Moriggl et al., 1999b) while inhibition of STAT5 results in a dose dependent loss of Cyclin E (Lai et al., 2009). All of these proteins play important roles in G1-S phase progression. STAT5 signalling upregulates levels of pro-survival proteins Bcl-2 and Bcl-X<sub>L</sub>. Additionally, STAT5 upregulates c-Myc, further implicating it as an important mediator of CD8<sup>+</sup> T cell proliferation (Lord et al., 2000). Constitutively active STAT5 promotes homeostatic proliferation and survival of CD8<sup>+</sup> T cells. Interestingly, STAT5 also enhances presence of T memory cell phenotype, increasing the frequency of cells expressing key

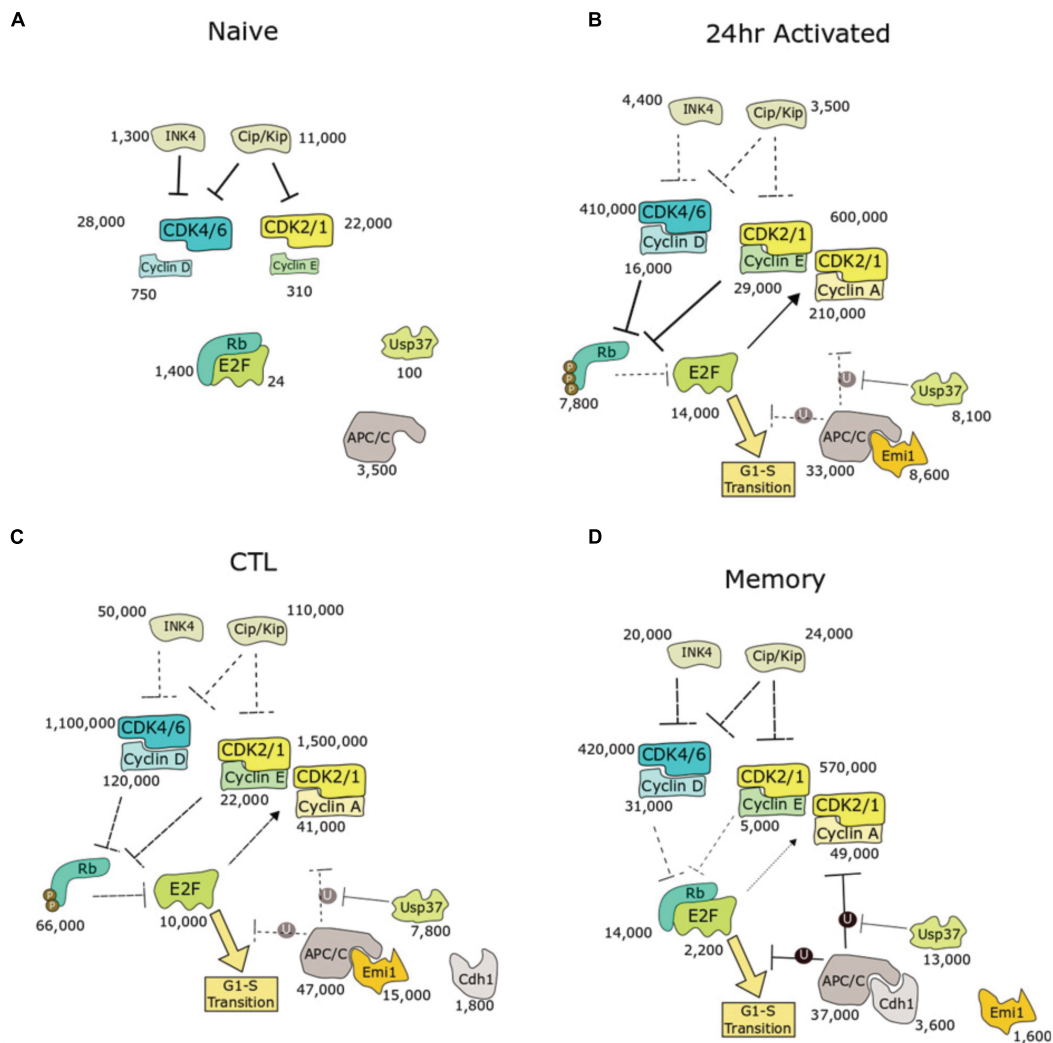


**FIGURE 3 |** Biochemical pathway analysis of cell cycle entry in murine CD8<sup>+</sup> T cells with protein copies measured by quantitative proteomics. Four populations were presented: **(A)** quiescent naïve, **(B)** activation phase, **(C)** expansion phase toward SLEC phenotype, or **(D)** expansion phase toward MPEC phenotype. Numbers indicate copy number of each protein as determined by quantitative proteomics, acquired from ImmPress ("ImmPress.co.uk," University of Dundee). For protein families (e.g., INK4, CIP/KIP, cyclins, and CDKs), summed copies are shown. E2F copies represent the sum of E2Fs 1–3. Median subunit copy number is shown for the APC/C. Mechanisms predicted to be dominant are highlighted in bold lines, whereas suppressed pathways are indicated by dotted lines. P, phosphorylation; U, ubiquitination.

memory markers including CD127, CD122, CD62L, and Bcl-2 (Hand et al., 2010).

As previously noted, CDK4/6 inhibitors are shown to enhance CD25 expression during activation. However, post expansion phase, cells that have been previously exposed to the inhibitors produce a greater pool of memory T cells by upregulating Max Dimerization Protein (Mxd)4, a negative regulator of Myc/Max formation (Heckler et al., 2021). Interestingly, this event seems to be independent of cell cycle arrest, suggesting a role for CDK4/6 in affecting T cell development (Heckler et al., 2021; Lelliott et al., 2021).

mTOR is also upregulated by IL-2 via the PI3K/AKT pathway. However, other pathways contribute more strongly to T cell proliferation in the expansion phase, as inhibiting

mTOR in this phase does not arrest proliferation (Howden et al., 2019). Similarly, naïve CD8<sup>+</sup> treated with AKT inhibitors responded less to stimulation, with proliferation severely reduced by day 2 of the culture in a dose dependent manner (Cho et al., 2013). If treated 3 days post activation, however, AKT inhibition resulted in little impact on proliferation (Macintyre et al., 2011).

Conversely, T cells expressing constitutively activated AKT were defective in memory T cell development *in vivo*. These cells have reduced CD127, CD122, CD62L, and Bcl-2 (Hand et al., 2010). CD127 reduction is predominately controlled by PI3K/AKT activity in a STAT5 independent way, as STAT5 knockout cells had little impact on CD127 (Xue et al., 2002). Constitutively active AKT cells also showed poor STAT5

phosphorylation in response to any cytokine stimulation, and as a result had a defect in homeostatic proliferation.

Taken together, these data suggest that a principal role of the IL2R/PI3K/AKT/mTOR pathway is the differentiation of T cells toward the SLEC phenotype, which occurs in parallel to IL2R/STAT5. The latter is the dominant pathway that promotes upregulation of cell cycle regulatory proteins and therefore proliferation of CD8<sup>+</sup> T cells.

Cyclin E/A-CDK2 complexes phosphorylate numerous substrates, including targets outside of canonical cell cycle pathways that directly regulate DNA replication and mitosis. For example, cyclin E/A-CDK2 phosphorylates and inhibits Foxo1 within a number of cancer cell lines (Huang et al., 2006). In T cells, mTOR drives differentiation toward SLEC phenotype by phosphorylation of Foxo1, an inhibitor of SLEC phenotype transcription factor T-box expressed in T cells (T-bet) (Rao et al., 2010; Michelini et al., 2013; Pollizzi et al., 2015). Thus, CDK2-mediated inhibition of Foxo1 raises the intriguing possibility that CDK2 may also have a role in enhancing T-bet activity, and thus provide a mechanism by which high CDK2 expression can enhance differentiation. However, this has yet to be demonstrated in T cells.

## THE CELL CYCLE CONTROL PROTEIN NETWORK IN T CELLS

T cell activation and their differentiation into effector and memory cells provides exemplar systems to study the G0 to G1 transition in non-immortalised cells in the physiological context of the adaptive immune response. The proteomes of these cells have been characterised to high depth using mass spectrometry-based proteomics, enabling detailed measurements of protein copies per cell in naïve and activated murine CD8<sup>+</sup> T cells (Howden et al., 2019; Marchingo et al., 2020). The Immunological Proteomic Resource (ImmPres) is an open access public resource consolidating proteomics experiments carried out on murine immune cell populations, including effector and memory CD8<sup>+</sup> T cell states.<sup>1</sup> We therefore used these publicly available data to evaluate the copies of key cell cycle proteins in naïve, activated (24 h), CTL (IL-2), and memory (IL-15) cell populations (Figure 3).

These data show that naïve cells have proportionally higher numbers of CDKs for each CDK (CIP/KIP and INK4) and very low abundance of cyclins. For example, naïve cells express 3,800 copies of p27 and less than 1,000 copies each of cyclin D2 and cyclin D3. In addition, levels of activating E2F transcription factors (20 copies) are two orders of magnitude lower than their stoichiometric inhibitor, Rb (1,400 copies). E2F activity is therefore strongly inhibited, which maintains naïve cells in quiescence. Interestingly, of the CIP/KIP family of proteins, p27 is higher expressed than p21 except during IL-2 mediated expansion, supporting a role of p27 over p21 as a regulator of quiescence and homeostatic proliferation in T cells.

Upon activation, E2F levels increase 500-fold to 14,000 copies, contributing to a gene expression programme that promotes G1/S progression. For example, levels of CDK1/2/4/6, cyclin D, cyclin E, and cyclin A are all upregulated. Intriguingly, while Rb levels increase in activated T cells to 7,800 copies. There is a 3-fold increase in cyclin D2, and 8-fold increase in cyclin D3, and around a 30-fold increase in CDK4/6 copies, while p27 decreases 19-fold. Interestingly, CD8<sup>+</sup> T cells can bypass CDK4/6 inhibition (Goel et al., 2017), leading to slowed proliferation (Heckler et al., 2021; Lelliott et al., 2021), but not arrest. The major changes observed copies in the Rb-E2F pathway may contribute to this resistance to G1 arrest by CDK4/6 inhibitors.

Inactivation of the APC/C is another mechanism to promote G1/S transition (Cappell et al., 2018). Median copies of the core APC/C subunits increase from 3,500 copies in naïve to 33,000 copies in activated T cells. Interestingly, Cdh1, the co-activator and substrate adaptor subunit of APC/C during G1, is undetectable in naïve and activated T cells. Likewise, Emi1 is undetectable in naïve. However, Emi1, an E2F target, increases to 8,600 copies in activated T cells.

Interleukin-2-mediated differentiation into CTLs is accompanied by a nearly 10-fold increase in Rb levels relative to 24 h activated T cells. Unlike newly activated T cells, which have nearly 2-fold excess E2F to Rb, CTLs contain far higher copies of Rb (66,000) to E2F (10,000). Thus, in CTLs there are sufficient levels of Rb, when not phosphorylated by CDK, to suppress all copies of E2F. However, copies of cyclins and CDKs are much higher in CTLs, leading to high activity of CDKs, which phosphorylate and inactivate Rb. These two mechanisms of E2F activation, Rb phosphorylation and excess E2F, suggest that newly activated T cells and CTLs may have differential sensitivity to pharmacological inhibition of CDK2/4/6.

Memory T cells produced by culture with IL-15 proliferate slower. In contrast to CTLs, memory T cells have reduced levels of cyclins and CDK2/4/6. However, like CTLs, copies of Rb (14,000) exceed copies of E2F (2,200). This may make memory T cells more sensitive toward Rb-mediated inhibition of E2F activity compared to naïve and 24-activated T cells. Memory T cells have increased copies of APC-C/Cdh1 (3,600) compared to CTLs, which also may contribute to extending G1 phase by keeping cyclin levels low.

## CONCLUDING REMARKS

Immune cells play critical roles in normal physiology, pathology, and the development of new therapies to treat disease. Understanding fundamental mechanisms for how proliferation is controlled in T cells will be important in making advances in these areas of immunological research. This is highlighted by recent studies showing that CDK4/6 inhibitors affect proliferation of CD4<sup>+</sup> T<sub>reg</sub> cells, but not CTLs (Goel et al., 2017), and enhance functions of checkpoint-activated CD8<sup>+</sup> T cells (Deng et al., 2018). These results suggest that there are major differences between CD4<sup>+</sup> and CD8<sup>+</sup> T cells in G1 control, which will be interesting to explore in future studies. Deeper insights into how the cell cycle control network is structured

<sup>1</sup><http://www.immpres.co.uk/>



in different immune subsets may provide important clues into the mode of action of these inhibitors on immune cells and an opportunity to identify new targets for modulating immune cell proliferation and function.

## AUTHOR CONTRIBUTIONS

DL prepared the figures. DL and TL wrote the manuscript. Both authors contributed to the article and approved the submitted version.

## REFERENCES

- Álvarez-Fernández, M., and Malumbres, M. (2020). Mechanisms of sensitivity and resistance to CDK4/6 inhibition. *Cancer Cell* 37, 514–529.
- Ameratunga, M., Kipps, E., Okines, A. F. C., and Lopez, J. S. (2019). To cycle or fight—CDK4/6 inhibitors at the crossroads of anticancer immunity. *Clin. Cancer Res.* 25, 21–28.
- Appleman, L. J., Berezovskaya, A., Grass, I., and Boussiotis, V. A. (2000). CD28 costimulation mediates T cell expansion via IL-2-independent and IL-2-dependent regulation of cell cycle progression. *J. Immunol.* 164, 144–151. doi: 10.4049/jimmunol.164.1.144
- Au-Yeung, B. B., Smith, G. A., Mueller, J. L., Heyn, C. S., Jaszczak, R. G., Weiss, A., et al. (2017). IL-2 modulates the TCR signaling threshold for CD8 but Not CD4 T cell proliferation on a single-cell level. *J. Immunol.* 198, 2445–2456. doi: 10.4049/jimmunol.1601453
- Balomenos, D., Martín-Caballero, J., García, M. I., Prieto, I., Flores, J. M., Serrano, M., et al. (2000). The cell cycle inhibitor P21 controls T-cell proliferation and sex-linked lupus development. *Nat. Med.* 6, 171–176. doi: 10.1038/72272
- Boussiotis, V. A., Freeman, G. J., Taylor, P. A., Berezovskaya, A., Grass, I., Blazar, B. R., et al. (2000). P27(Kip1) functions as an anergy factor inhibiting interleukin 2 transcription and clonal expansion of alloreactive human and mouse helper T lymphocytes. *Nat. Med.* 6, 290–297. doi: 10.1038/73144
- Brennan, P., Babbage, J. W., Thomas, G., and Cantrell, D. (1999). P70s6k integrates phosphatidylinositol 3-kinase and rapamycin-regulated signals for E2F regulation in T lymphocytes. *Mol. Cell. Biol.* 19, 4729–4738. doi: 10.1128/mcb.19.7.4729
- Brownlie, R. J., and Zamoyska, R. (2013). T cell receptor signalling networks: branched, diversified and bounded. *Nat. Rev. Immunol.* 13, 257–269.
- Burchill, M. A., Goetz, C. A., Prlic, M., O'Neil, J. J., Harmon, I. R., Bensinger, S. J., et al. (2003). Distinct effects of STAT5 activation on CD4 + and CD8 + T Cell homeostasis: development of CD4 + CD25 + regulatory T cells versus CD8 + memory T cells. *J. Immunol.* 171, 5853–5864. doi: 10.4049/jimmunol.171.11.5853
- Cappell, S. D., Chung, M., Jaimovich, A., Spencer, S. L., and Meyer, T. (2016). Irreversible APCDh1 inactivation underlies the point of no return for cell-cycle entry. *Cell* 166, 167–180. doi: 10.1016/j.cell.2016.05.077
- Cappell, S. D., Mark, K. G., Garbett, D., Pack, L. R., Rape, M., and Meyer, T. (2018). EMI1 switches from being a substrate to an inhibitor of APC/CCDH1 to start the cell cycle. *Nature* 558, 313–317. doi: 10.1038/s41586-018-0199-7
- Carpenter, A. C., and Bosselut, R. (2010). Decision checkpoints in the thymus. *Nat. Immunol.* 11, 666–673.
- Chaikovskiy, A. C., and Sage, J. (2018). Beyond the cell cycle: enhancing the immune surveillance of tumors via CDK4/6 inhibition. *Mol. Cancer Res.* 16, 1454–1457.
- Chen, D., Pacal, M., Wenzel, P., Knoepfler, P. S., Leone, G., and Bremner, R. (2009). Division and apoptosis in the E2f-Deficient retina. *Nature* 462:925. doi: 10.1038/NATURE08544
- Cheng, M., Olivier, P., Diehl, J. A., Fero, M., Roussel, M. F., Roberts, J. M., et al. (1999). “The P21(Cip1) and P27(Kip1) CDK ‘inhibitors’ are essential activators of cyclin D-dependent kinases in murine fibroblasts. *EMBO J.* 18, 1571–1583. doi: 10.1093/emboj/18.6.1571
- Cho, B. K., Wang, C., Sugawa, S., Eisen, H. N., and Chen, J. (1999). Functional differences between memory and naive CD8 T Cells. *Proc. Natl. Acad. Sci. U.S.A.* 96, 2976–2981. doi: 10.1073/pnas.96.6.2976

## FUNDING

TL was supported by a Sir Henry Dale Fellowship funded by the Wellcome Trust and the Royal Society (206211/A/17/Z). DL was supported by a BBSRC EASTBIO Ph.D. Studentship.

## ACKNOWLEDGMENTS

We thank the Ly, Cantrell, and Zamoyska groups for helpful discussions.

- Cho, J.-H., Kim, H.-O., Kim, K.-S., Yang, D.-H., Surh, C. D., and Sprent, J. (2013). Unique features of naive CD8 + T Cell activation by IL-2. *J. Immunol.* 191, 5559–5573. doi: 10.4049/jimmunol.1302293
- Chong, J.-L., Wenzel, P. L., Sáenz-Robles, M. T., Nair, V., Ferrey, A., Hagan, J. P., et al. (2009). E2F1-3 switch from activators in progenitor cells to repressors in differentiating cells. *Nature* 462:930. doi: 10.1038/NATURE08677
- Colombetti, S., Basso, V., Mueller, D. L., and Mondino, A. (2006). Prolonged TCR/CD28 engagement drives IL-2-independent t cell clonal expansion through signaling mediated by the mammalian target of rapamycin. *J. Immunol.* 176, 2730–2738. doi: 10.4049/jimmunol.176.5.2730
- Dang, C. V., O'Donnell, K. A., Zeller, K. I., Nguyen, T., Osthus, R. C., and Li, F. (2006). The C-Myc target gene network. *Semin. Cancer Biol.* 16, 253–264.
- Deng, J., Wang, E. S., Jenkins, R. W., Li, S., Dries, R., Yates, K., et al. (2018). CDK4/6 inhibition augments antitumor immunity by enhancing T-cell activation. *Cancer Discov.* 8, 216–233. doi: 10.1158/2159-8290.CD-17-0915
- D'Souza, W. N., and Lefrançois, L. (2003). IL-2 Is not required for the initiation of CD8 T cell cycling but sustains expansion. *J. Immunol.* 171, 5727–5735. doi: 10.4049/jimmunol.171.11.5727
- Dyson, N. (1998). The regulation of E2F by PRB-family proteins. *Genes Dev.* 12, 2245–2262.
- Fero, M. L., Rivkin, M., Tasch, M., Porter, P., Carow, C. E., Firpo, E., et al. (1996). A syndrome of multiorgan hyperplasia with features of gigantism, tumorigenesis, and female sterility in P27Kip1-deficient mice. *Cell* 85, 733–744. doi: 10.1016/S0092-8674(00)81239-8
- Gao, X., Tewari, K., Svaren, J., and Suresh, M. (2004). Role of cell cycle regulator E2F1 in regulating CD8 T Cell responses during acute and chronic viral infection. *Virology* 324, 567–576. doi: 10.1016/J.VIROL.2004.04.012
- Goel, S., DeCristo, M. J., Watt, A. C., BrinJones, H., Sceneay, J., Li, B. B., et al. (2017). CDK4/6 inhibition triggers anti-tumor immunity. *Nature* 548:471. doi: 10.1038/NATURE23465
- Grimmler, M., Wang, Y., Mund, T., Cilenšek, Z., Keidel, E. M., Waddell, M. B., et al. (2007). Cdk-inhibitory activity and stability of P27Kip1 are directly regulated by oncogenic tyrosine kinases. *Cell* 128, 269–280. doi: 10.1016/j.cell.2006.11.047
- Gruber, T., Hermann-Kleiter, N., Hinterleitner, R., Fresser, F., Schneider, R., Gastl, G., et al. (2009). PKC-θ modulates the strength of t cell responses by targeting Cbl-b for ubiquitination and degradation. *Sci. Signal.* 2, ra30–ra30. doi: 10.1126/scisignal.2000046
- Guiley, K. Z., Stevenson, J. W., Lou, K., Barkovich, K. J., Kumarasamy, V., Wijeratne, T. U., et al. (2019). P27 allosterically activates cyclin-dependent kinase 4 and antagonizes palbociclib inhibition. *Science* 366:6471. doi: 10.1126/science.aaw2106
- Hand, T. W., Cui, W., Woo Jung, Y., Sefik, E., Joshi, N. S., Chande, A., et al. (2010). Differential effects of STAT5 and PI3K/AKT signaling on effector and memory CD8 T-cell survival. *Proc. Natl. Acad. Sci. U. S. A.* 107, 16601–16606. doi: 10.1073/pnas
- Heckler, M., Ali, L. R., Clancy-Thompson, E., Qiang, L., Ventre, K. S., Lenehan, P., et al. (2021). Inhibition of CDK4/6 promotes CD8 T cell memory formation 1 2. *Cancer Discov.* [Epub ahead of print]. doi: 10.1158/2159-8290.CD-20-1540
- Howden, A. J. M., Hukelmann, J. L., Brenes, A., Spinelli, L., Sinclair, L. V., Lamond, A. I., et al. (2019). Quantitative analysis of T cell proteomes and environmental sensors during T cell differentiation. *Nat. Immunol.* 20, 1542–1554. doi: 10.1038/s41590-019-0495-x



- Huang, H., Regan, K. M., Lou, Z., Chen, J., and Tindall, D. J. (2006). CDK2-dependent phosphorylation of FOXO1 as an apoptotic response to DNA damage. *Science* (80-). 314, 294–297. doi: 10.1126/science.1130512
- Huang, X. D., Summers, M. K., Pham, V., Lill, J. R., Liu, J., Lee, G., et al. (2011). Deubiquitinase USP37 is activated by CDK2 to antagonize APCCDH1 and promote S phase entry. *Mol. Cell* 42, 511–523. doi: 10.1016/j.molcel.2011.03.027
- Hwang, J. R., Byeon, Y., Kim, D., and Park, S. G. (2020). Recent insights of T cell receptor-mediated signaling pathways for T cell activation and development. *Exp. Mol. Med.* 52, 750–761.
- Imanishi, T., Unno, M., Kobayashi, W., Yoneda, N., Matsuda, S., Ikeda, K., et al. (2019). Reciprocal regulation of STING and TCR signaling by MTORC1 for T-cell activation and function. *Life Sci Alliance* 2:e201800282. doi: 10.26508/lsa.201800282
- Jutz, S., Leitner, J., Schmetterer, K., Doel-Perez, I., Majdic, O., Grabmeier-Pfistershammer, K., et al. (2016). Assessment of costimulation and coinhibition in a triple parameter T cell reporter line: simultaneous measurement of NF-KB, NFAT and AP-1. *J. Immunol. Methods* 430, 10–20. doi: 10.1016/j.jim.2016.01.007
- Kim, P. S., and Ahmed, R. (2010). Features of responding T cells in cancer and chronic infection. *Curr. Opin. Immunol.* 22, 223–230. doi: 10.1016/j.coi.2010.02.005
- Kinjyo, I., Qin, J., Tan, S.-Y., Wellard, C. J., Mrass, P., Ritchie, W., et al. (2015). Real-time tracking of cell cycle progression during CD8+ effector and memory T-cell differentiation. *Nat. Commun.* 6:6301. doi: 10.1038/ncomms7301
- Kiyokawa, H., Kineman, R. D., Manova-Todorova, K. O., Soares, V. C., Huffman, E. S., Ono, M., et al. (1996). Enhanced growth of mice lacking the cyclin-dependent kinase inhibitor function of P27Kip1. *Cell* 85, 721–732. doi: 10.1016/S0092-8674(00)81238-6
- Klein, K., Witalisz-Siepracka, A., Gotthardt, D., Agerer, B., Locker, F., Grausenburger, R., et al. (2021). T cell-intrinsic CDK6 is dispensable for antiviral and anti-tumor responses in vivo. *Front. Immunol.* 12:650977. doi: 10.3389/FIMMU.2021.650977
- Kramer, E. R., Scheuringer, N., Podtelebnikov, A. V., Mann, M., and Peters, J. M. (2000). Mitotic regulation of the APC activator proteins CDC20 and CDH1. *Mol. Biol. Cell* 11, 1555–1569. doi: 10.1091/mbc.11.5.1555
- Kretschmer, L., Flossdorf, M., Mir, J., Cho, Y. L., Plambeck, M., Treise, I., et al. (2020). Differential expansion of t central memory precursor and effector subsets is regulated by division speed. *Nat. Commun.* 11, 1–12. doi: 10.1038/s41467-019-13788-w
- Kurts, C., Kosaka, H., Carbone, F. R., Miller, J. F. A. P., and Heath, W. R. (1997). Class I-restricted cross-presentation of exogenous self-antigens leads to deletion of autoreactive CD8+ T cells. *J. Exp. Med.* 186, 239–245. doi: 10.1084/jem.186.2.239
- Labae, J., Garrett, M. D., Stevenson, L. F., Slingerland, J. M., Sandhu, C., Chou, H. S., et al. (1997). New functional activities for the P21 family of CDK inhibitors. *Genes Dev.* 11, 847–862. doi: 10.1101/gad.11.7.847
- Lai, Y.-P., Lin, C.-C., Liao, W.-J., Tang, C.-Y., and Chen, S.-C. (2009). CD4 + T Cell-derived IL-2 signals during early priming advances primary CD8 + T cell responses. *PLoS One* 4:7766. doi: 10.1371/journal.pone.0007766
- Lelliott, E. J., Kong, I. Y., Zethoven, M., Ramsbottom, K. M., Martelotto, L. G., Meyran, D., et al. (2021). CDK4/6 inhibition promotes anti-tumor immunity through the induction of T Cell memory. *Cancer Discov.* [Epub ahead of print]. doi: 10.1158/2159-8290.CD-20-1554
- Li, D., Gál, I., Vermes, C., Alegre, M.-L., Chong, A. S. F., Chen, L., et al. (2004). Cutting edge: Cbl-b: one of the key molecules tuning CD28- and CTLA-4-mediated T cell costimulation. *J. Immunol.* 173, 7135–7139. doi: 10.4049/jimmunol.173.12.7135
- Liao, W., Lin, J. X., and Leonard, W. J. (2013). Interleukin-2 at the crossroads of effector responses, tolerance, and immunotherapy. *Immunity* 38, 13–25.
- Liu, Q., Langdon, W. Y., and Zhang, J. (2014). E3 ubiquitin ligase Cbl-b in innate and adaptive immunity. *Cell Cycle* 13, 1875–1884.
- Lockyer, H. M., Tran, E., and Nelson, B. H. (2007). STAT5 is essential for Akt/P70S6 kinase activity during IL-2-induced lymphocyte proliferation. *J. Immunol.* 179, 5301–5308. doi: 10.4049/jimmunol.179.8.5301
- Lord, J. D., McIntosh, B. C., Greenberg, P. D., and Nelson, B. H. (2000). The IL-2 receptor promotes lymphocyte proliferation and induction of the c- Myc, Bcl-2, and Bcl-x genes through the trans- activation domain of stat5. *J. Immunol.* 164, 2533–2541. doi: 10.4049/jimmunol.164.5.2533
- Lukas, C., Sørensen, C. S., Kramer, E., Santoni-Ruglu, E., Lindene, C., Peters, J. M., et al. (1999). Accumulation of cyclin B1 requires E2F and cyclin-A-dependent rearrangement of the anaphase-promoting complex. *Nature* 401, 815–818. doi: 10.1038/44611
- Macintyre, A. N., Finlay, D., Preston, G., Sinclair, L. V., Waugh, C. M., Tamas, P., et al. (2011). Protein kinase B controls transcriptional programs that direct cytotoxic T cell fate but is dispensable for T cell metabolism. *Immunity* 34, 224–236. doi: 10.1016/j.immuni.2011.01.012
- Marchingo, J. M., Sinclair, L. V., Howden, A. J., and Cantrell, D. A. (2020). Quantitative analysis of how Myc controls T cell proteomes and metabolic pathways during T cell activation. *Elife* 9:e53725. doi: 10.7554/ELIFE.53725
- Mehlhop-Williams, E. R., and Bevan, M. J. (2014). Memory CD8+ T cells exhibit increased antigen threshold requirements for recall proliferation. *J. Exp. Med.* 211, 345–356. doi: 10.1084/jem.20131271
- Michelin, R. H., Doedens, A. L., Goldrath, A. W., and Hedrick, S. M. (2013). Differentiation of CD8 memory T cells depends on foxo1. *J. Exp. Med.* 210, 1189–1200. doi: 10.1084/jem.20130392
- Mishima, T., Fukaya, S., Toda, S., Ando, Y., Matsunaga, T., and Inobe, M. (2017). Rapid G0/1 transition and cell cycle progression in CD8+ T cells compared to CD4+ T cells following in vitro stimulation. *Microbiol. Immunol.* 61, 168–175. doi: 10.1111/1348-0421.12479
- Mondino, A., Colombetti, S., Basso, V., and Mueller, D. L. (2006). Mammalian target of rapamycin through signaling mediated by the IL-2-independent T cell clonal expansion prolonged TCR/CD28 engagement drives. *J. Immunol.* 176, 2730–2738.
- Moriggl, R., Sexl, V., Piekorz, R., Topham, D., and Ihle, J. N. (1999a). Stat5 activation is uniquely associated with cytokine signaling in peripheral T cells. *Immunity* 11, 225–230. doi: 10.1016/S1074-7613(00)80097-7
- Moriggl, R., Topham, D. J., Teglund, S., Sexl, V., McKay, C., Wang, D., et al. (1999b). Stat5 is required for IL-2-induced cell cycle progression of peripheral T cells. *Immunity* 10, 249–259. doi: 10.1016/S1074-7613(00)80025-4
- Murga, M., Fernández-Capetillo, O., Field, S., Moreno, B., Borlado, L., Fujiwara, Y., et al. (2001). Mutation of E2F2 in mice causes enhanced T lymphocyte proliferation, leading to the development of autoimmunity. *Immunity* 15, 959–970. doi: 10.1016/S1074-7613(01)00254-0
- Nakayama, K., Ishida, N., Shirane, M., Inomata, A., Inoue, T., Shishido, N., et al. (1996). Mice lacking P27Kip1 display increased body size, multiple organ hyperplasia, retinal dysplasia, and pituitary tumors. *Cell* 85, 707–720. doi: 10.1016/S0092-8674(00)81237-4
- Nelson, B. H. (2004). IL-2, regulatory T cells, and tolerance. *J. Immunol.* 172, 3983–3988. doi: 10.4049/jimmunol.172.7.3983
- Paolino, M., Thien, C. B. F., Gruber, T., Hinterleitner, R., Baier, G., Langdon, W. Y., et al. (2011). Essential role of E3 ubiquitin ligase activity in Cbl-b- regulated T cell functions. *J. Immunol.* 186, 2138–2147. doi: 10.4049/jimmunol.1003390
- Pollizzi, K. N., Patel, C. H., Sun, I. H., Oh, M. H., Waickman, A. T., Wen, J., et al. (2015). MTORC1 and MTORC2 selectively regulate CD8+ T cell differentiation. *J. Clin. Invest.* 125, 2090–2108. doi: 10.1172/JCI77746
- Rao, R. R., Li, Q., Odunsi, K., and Shrikant, P. A. (2010). The mtor kinase determines effector versus memory CD8+ T cell fate by regulating the expression of transcription factors T-bet and eomesodermin. *Immunity* 32, 67–78. doi: 10.1016/j.immuni.2009.10.010
- Rollings, C. M., Sinclair, L. V., Brady, H. J. M., Cantrell, D. A., and Ross, S. H. (2018). Interleukin-2 shapes the cytotoxic T cell proteome and immune environment-sensing programs. *Sci. Signal* 11:ea8112.
- Sherr, C. J., and Roberts, J. M. (1999). CDK inhibitors: positive and negative regulators of G1-phase progression. *Genes Dev.* 13, 1501–1512. doi: 10.1101/gad.13.12.1501
- Shifrut, E., Carnevale, J., Tobin, V., Roth, T. L., Woo, J. M., Bui, C. T., et al. (2018). Genome-wide CRISPR screens in primary human T cells reveal key regulators of immune function. *Cell* 175, 1958–1971.e15. doi: 10.1016/j.cell.2018.10.024
- Singh, A., Jatzek, A., Plisch, E. H., Srinivasan, R., Svaren, J., and Suresh, M. (2010). Regulation of memory CD8 T-cell differentiation by cyclin-dependent kinase inhibitor P27Kip1. *Mol. Cell. Biol.* 30, 5145–5159. doi: 10.1128/mcb.01045-09
- Smith, K. A., and Ruscetti, F. W. (1981). T-cell growth factor and the culture of cloned functional T cells. *Adv. Immunol.* 31, 137–175. doi: 10.1016/S0065-2776(08)60920-7

- Spolski, R., Li, P., and Leonard, W. J. (2018). Biology and regulation of IL-2: from molecular mechanisms to human therapy. *Nat. Rev. Immunol.* 18, 648–659.
- Stengel, K. R., Thangavel, C., Solomon, D. A., Angus, S. P., Zheng, Y., and Knudsen, E. S. (2009). Retinoblastoma/P107/P130 pocket proteins. proteins dynamics and interactions with target gene promoters. *J. Biol. Chem.* 284, 19265–19271. doi: 10.1074/jbc.M808740200
- Tan, H., Yang, K., Li, Y., Shaw, T. I., Wang, Y., Blanco, D. B., et al. (2017). Integrative proteomics and phosphoproteomics profiling reveals dynamic signaling networks and bioenergetics pathways underlying T cell activation. *Immunity* 46, 488–503. doi: 10.1016/j.immuni.2017.02.010
- Tewari, K., Walent, J., Svaren, J., Zamoyska, R., and Suresh, M. (2006). Differential requirement for Lck during primary and memory CD8+ T cell responses. *Proc. Natl. Acad. Sci. U.S.A.* 103, 16388–16393. doi: 10.1073/pnas.0602565103
- Tomoda, K., Kubota, Y., and Kato, J. Y. (1999). Degradation of the cyclin-dependent-kinase inhibitor P27(Kip1) is instigated by Jab1. *Nature* 398, 160–165. doi: 10.1038/18230
- Vartanian, R., Masri, J., Martin, J., Cloninger, C., Holmes, B., Artinian, N., et al. (2011). AP-1 regulates cyclin D1 and c-MYC transcription in an AKT-dependent manner in response to MTOR inhibition: role of AIP4/Itch-mediated JUNB degradation. *Mol. Cancer Res.* 9, 115–130. doi: 10.1158/1541-7786.MCR-10-0105
- Waickman, A. T., and Powell, J. D. (2012). MTOR, metabolism, and the regulation of T-cell differentiation and function. *Immunol. Rev.* 249, 43–58. doi: 10.1111/j.1600-065X.2012.01152.x
- Wang, H., Nicolay, B. N., Chick, J. M., Gao, X., Geng, Y., Ren, H., et al. (2017). The metabolic function of cyclin D3-CDK6 kinase in cancer cell survival. *Nature* 546, 426–430. doi: 10.1038/nature22797
- Wang, R., Dillon, C. P., Shi, L. Z., Milasta, S., Carter, R., Finkelstein, D., et al. (2011). The transcription factor Myc controls metabolic reprogramming upon T lymphocyte activation. *Immunity* 35, 871–882. doi: 10.1016/j.immuni.2011.09.021
- Wolfrum, L. A., Walz, T. M., James, Z., Fernandez, T., and Letterio, J. J. (2004). P21 Cip1 and P27 Kip1 act in synergy to alter the sensitivity of naive T cells to TGF- $\beta$ -mediated G1 arrest through modulation of IL-2 responsiveness. *J. Immunol.* 173, 3093–3102. doi: 10.4049/jimmunol.173.5.3093
- Wu, L., Timmers, C., Maiti, B., Saavedra, H. I., Sang, L., Chong, G. T., et al. (2001). The E2F1–3 transcription factors are essential for cellular proliferation. *Nature* 414, 457–462. doi: 10.1038/35106593
- Xue, H. H., Kovanen, P. E., Pise-Masison, C. A., Berg, M., Radovich, M. F., Brady, J. N., et al. (2002). IL-2 negatively regulates IL-7 receptor  $\alpha$  chain expression in activated T lymphocytes. *Proc. Natl. Acad. Sci. U.S.A.* 99, 13759–13764. doi: 10.1073/pnas.212214999
- Yoon, H., Kim, T. S., and Braciale, T. J. (2010). The cell cycle time of CD8+ T cells responding in vivo is controlled by the type of antigenic stimulus. *PLoS One* 5:e15423. doi: 10.1371/journal.pone.0015423
- Zetterberg, A., and Larsson, O. (1985). Kinetic analysis of regulatory events in G1 leading to proliferation or quiescence of swiss 3T3 cells. *Proc. Natl. Acad. Sci. U.S.A.* 82, 5365–5369. doi: 10.1073/pnas.82.16.5365
- Zetterberg, A., and Larsson, O. (1991). Coordination between cell growth and cell cycle transit in animal cells. *Cold Spring Harb. Symp. Quant. Biol.* 56, 137–147. doi: 10.1101/SQB.1991.056.01.018
- Zetterberg, A., Larsson, O., and Wiman, K. G. (1995). What is the restriction point? *Curr. Opin. Cell Biol.* 7, 835–842. doi: 10.1016/0955-0674(95)80067-0
- Zhu, J. W., Field, S. J., Gore, L., Thompson, M., Yang, H., Fujiwara, Y., et al. (2001). E2F1 and E2F2 determine thresholds for antigen-induced T-cell proliferation and suppress tumorigenesis. *Mol. Cell. Biol.* 21:8547. doi: 10.1128/MCB.21.24.8547-8564.2001

**Conflict of Interest:** The authors declare that the research was conducted in the absence of any commercial or financial relationships that could be construed as a potential conflict of interest.

**Publisher's Note:** All claims expressed in this article are solely those of the authors and do not necessarily represent those of their affiliated organizations, or those of the publisher, the editors and the reviewers. Any product that may be evaluated in this article, or claim that may be made by its manufacturer, is not guaranteed or endorsed by the publisher.

Copyright © 2021 Lewis and Ly. This is an open-access article distributed under the terms of the Creative Commons Attribution License (CC BY). The use, distribution or reproduction in other forums is permitted, provided the original author(s) and the copyright owner(s) are credited and that the original publication in this journal is cited, in accordance with accepted academic practice. No use, distribution or reproduction is permitted which does not comply with these terms.



# Quiescence Through the Prism of Evolution

Bertrand Daignan-Fornier<sup>†</sup>, Damien Laporte<sup>†</sup> and Isabelle Sagot<sup>\*\*</sup>

Univ. Bordeaux, CNRS, IBGC, UMR 5095, Bordeaux, France

## OPEN ACCESS

### Edited by:

Jyotsna Dhawan,  
Centre for Cellular & Molecular  
Biology (CCMB), India

### Reviewed by:

Alexandre Bruni-Cardoso,  
University of São Paulo, Brazil  
David Goode,  
Peter MacCallum Cancer Centre,  
Australia

### \*Correspondence:

Isabelle Sagot  
isabelle.sagot@ibgc.cnrs.fr

<sup>†</sup>These authors have contributed  
equally to this work and share senior  
authorship

### Specialty section:

This article was submitted to  
Cell Growth and Division,  
a section of the journal  
Frontiers in Cell and Developmental  
Biology

**Received:** 21 July 2021

**Accepted:** 11 October 2021

**Published:** 29 October 2021

### Citation:

Daignan-Fornier B, Laporte D and  
Sagot I (2021) Quiescence Through  
the Prism of Evolution.  
Front. Cell Dev. Biol. 9:745069.  
doi: 10.3389/fcell.2021.745069

Being able to reproduce and survive is fundamental to all forms of life. In primitive unicellular organisms, the emergence of quiescence as a reversible proliferation arrest has most likely improved cell survival under unfavorable environmental conditions. During evolution, with the repeated appearances of multicellularity, several aspects of unicellular quiescence were conserved while new quiescent cell intrinsic abilities arose. We propose that the formation of a microenvironment by neighboring cells has allowed disconnecting quiescence from nutritional cues. In this new context, non-proliferative cells can stay metabolically active, potentially authorizing the emergence of new quiescent cell properties, and thereby favoring cell specialization. Through its co-evolution with cell specialization, quiescence may have been a key motor of the fascinating diversity of multicellular complexity.

**Keywords:** quiescence, multicellularity, evolution, unicellular organism, microenvironment

## QUIESCENCE IN UNICELLULAR ORGANISMS

Life is characterized by the ability of self-reproduction. However, natural selection, which is key to Darwinian evolution, operates on inherited variations that increase individual's ability not only to reproduce but also to survive. This duality started with the very first unicellular organisms for which there was a need for trade-off between proliferation and long-term survival in changing environments. In this early scenario, quiescence could have emerged as an adaptive reversible proliferation arrest. Quiescence, which is not strictly required for life to multiply, might have resulted from the need to control proliferation in response to unfavorable environmental conditions that otherwise would compromise viability by disconnecting cell division from cell growth. At this time, quiescence might have represented an extreme form of slow growth and been a passive consequence of a massive anabolism slow-down due to resource limitation. Similarly, in contemporary unicellular prokaryotes or eukaryotes, the cessation of cell cycle progression *per se* may still be just a rather passive outcome of a drastic anabolic diminution. This was proposed for *Saccharomyces cerevisiae* cells that were observed to cease to proliferate in various cell cycle phases (Brauer et al., 2008; Daignan-Fornier and Sagot, 2011a,b; Klosinska et al., 2011; Laporte et al., 2011; Broach, 2012) as well as for *Cryptococcus neoformans* (Takeo et al., 1995) and *Schizosaccharomyces pombe* (Costello et al., 1986; Wei et al., 1993).

Yet, in modern unicellular organisms, additional quiescent cell properties improving survival capacities have appeared. These new intrinsic abilities involve dedicated molecular processes that protect cells from adversities (Rittershaus et al., 2013; Zhang and Cao, 2017). For example, the cellular response for survival can engage the storage of various energetic macromolecules, the nature of which depends on both the limiting resource and the species (Montrose et al., 2020).

This was demonstrated in *S. cerevisiae* and *Chlamydomonas reinhardtii*, in which the metabolic rewiring upon quiescence establishment is highly dependent on the nature of the exhausted nutrient (Klosinska et al., 2011; Broach, 2012; Takeuchi and Benning, 2019). In addition, quiescence establishment is often accompanied by the remodeling of organelles and the reorganization of cellular machineries. This has been particularly documented in quiescent *S. cerevisiae* in which multiple reorganizations were observed, including the hyper-condensation of the genome, the rearrangement of the mitochondrial network, or the aggregation of enzymes (O'Connell et al., 2012; Prouteau et al., 2017; Sagot and Laporte, 2019b; Miles et al., 2021). Some of these reorganizations are the consequences of variations in the cytoplasm physico-chemical properties occurring upon proliferation to quiescence transition (Joyner et al., 2016; Munder et al., 2016; Heimlicher et al., 2019). Others may be the outcome of a dedicated signaling pathway. The possible, yet not mandatory, physiological “raisons d’être” of many of these cellular reorganizations are still puzzling, but it has been speculated that the accumulation of reserves of macromolecules, such as osmoprotective polymers, or cellular machineries, such as ribosomes, may be a key for adaptation in a changing environment (Argüelles, 2000; Yu et al., 2020). Altogether, the diverse properties of quiescent cells, which probably have evolved in different ways in function of both the cell types and the environmental conditions, exemplify the plasticity of this cellular state (Sagot and Laporte, 2019a,b).

In parallel, it seems that unicellular organisms have evolved a fast and efficient quiescence exit. For example, *S. cerevisiae* responds immediately to an extracellular food supply (Zhang et al., 2019) and many of the cellular machineries reorganized upon quiescence establishment, such as the actin cytoskeleton or the proteasome, are mobilized within seconds upon carbon replenishment (Sagot et al., 2006; Laporte et al., 2008, 2011). Furthermore, during the first step of resuscitation from chlorosis of nitrogen starved cyanobacteria, an almost instantaneous increase in the adenosine triphosphate (ATP) level is observed upon addition of sodium nitrate (Neumann et al., 2021), just as in quiescent *S. cerevisiae* upon glucose re-feeding (Laporte et al., 2011). Besides, in *S. cerevisiae*, the polymerase II is poised onto promoter of genes that are critical for proliferation resumption (Radonjic et al., 2005). In parallel, the chromatin remodeling complex (RSC) is bound to genes induced upon quiescence exit and facilitates rapid gene expression firing, despite a globally repressive chromatin state maintained compacted by histone specific modifications (McKnight et al., 2015; Swygert et al., 2019; Cucinotta et al., 2021). Hence, unicellular quiescent cells seem to be prepared to respond rapidly to favorable conditions and mechanisms accompanying quiescence establishment may be an asset for the competition within a given environment. Of note, this propensity to swiftly exit quiescence has been proposed to be the Achilles’ heel of persisters pathogenic bacteria that can be deceived by specific metabolites that trigger quiescence exit and as such expose them to killing drugs (Amato et al., 2014; Prax and Bertram, 2014). Thus, in contemporary unicellular organisms, quiescence establishment involves reorganizations to improve both sustained protection and fitness upon quiescence exit.

Finally, in both prokaryotes and some unicellular eukaryotes, it has been observed that the longer the time spent in quiescence, the slower the resumption of proliferation, suggesting that quiescence might deepen with time by unknown mechanisms that remains to be deciphered (Su et al., 1996; Laporte et al., 2017; Pu et al., 2019).

Overall, the rationale governing quiescence reflects an opportunistic behavior that seems very well-adapted to inter-individual competition in a fluctuating environment. Yet, while in unicellular species, cell and organism are synonymous, in multicellular entities, the two scales are distinct. How did cellular quiescence evolve in this context?

## QUIESCENCE IN RUDIMENTARY MULTICELLULAR ORGANISMS

In *C. reinhardtii*, as in other unicellular algae (*Chlorella*, *Scenedesmus*), non-favorable environmental conditions induce not only a cell cycle arrest but also cell clumping into large aggregates made of few tens to thousand quiescent cells held together by an extracellular matrix. This multicellular form favors resistance to starvation, desiccation, and freezing. When conditions become favorable again, aggregates disassemble in few minutes and cells re-proliferate (Sathe and Durand, 2016; de Carpentier et al., 2019). In this case, quiescence is still a survival form, but it is associated with the formation of a dedicated multicellular assembly. *Dictyostelium discoideum* also propagates as a single cell in a nutrient rich environment, and upon nutrient exhaustion, just as other dictyostelids, it may opt for several strategies. Unicellular forms can just stop proliferating, forming a so-called solitary quiescent cells that survive short periods of starvation. Alternatively, a cell can encyst to form a unicellular quiescent microcyst that is able to survive long period of scarcity. Nutritional depletion, when combined with dark and humid environment can also lead to the initiation of a sexual cycle that will end up by the formation of a dormant macrocyst from a diploid giant cell. Finally, upon starvation, *D. discoideum* cells can also start to secrete both chemoattractant and extracellular matrix and aggregate into a multicellular sorogen, that can eventually form a stalk, named fruiting body, in which some cells differentiate into dormant spores that will disseminate and germinate when external conditions will become favorable again (Dubravcic et al., 2014; Kin and Schaap, 2021). Thus, in dictyostelids, cellular quiescence is still associated to survival in non-optimal environmental conditions, but combined with multicellularity, it contributes to improve propagation.

In the above examples, planktonic organisms can switch to a temporary multicellular lifestyle to improve survival. Symmetrically, volvocine green algae species, which live as spherical assembly of thousands of cells in rich freshwater habitats, can produce dormant unicellular zygotes capable of surviving adverse conditions. The return to a favorable environment triggers meiosis and haploid offspring reproduces asexually to ultimately rebuild a multicellular form (Hallmann, 2011). Similarly, many multicellular organisms use quiescent unicellular spore as a mean to both face unfavorable conditions



and disseminate. These quiescent spores can be generated asexually, such as conidiospores produced by several kind of filamentous fungi like *Neurospora crassa* (Turian and Matikian, 1966; Ruger-Herreros and Corrochano, 2020), or *via* sexual reproduction like ascospores formed by ascomycetes (Bennett and Turgeon, 2016) or micro- and macro-spores generated by algae (Maggs and Callow, 2003). In these rudimentary multicellular species, quiescence is a combination between a survival mode and a mean to disseminate robust single-celled propagules.

## QUIESCENCE IN MORE COMPLEX MULTICELLULAR ORGANISMS

### Suspended Animation at the Whole Organism Scale

Where multicellularity has become obligatory, some selected survival strategies were no longer based on cellular quiescence but rather take place at the whole organism scale. In that situation, extended period of inactivity, either adaptive or programmed, were developed. Cryptobiosis is an extreme form of inactivity that can lead to an almost complete cessation of the body metabolism. It includes freezing, desiccation, hypoxia and osmobiogenesis. This state of “suspended animation” is observed in lichen or mosses, but also in invertebrate such as nematodes or tardigrades. It is also widely used by a variety of phytoplankton species that can persist for multiple decades in a quiescent resting state (Ellegaard and Ribeiro, 2018). This adaptive reaction allows surviving unpredictable unfavorable conditions. By contrast, organism dormancy is programmed and widely found in plants and animals. Dormancy can either be an obligated part of the life cycle, such as a given developmental stage like diapause, or a seasonal arrest that anticipates predictable environmental non-favorable conditions, such as hibernation (for an excellent review see Withers and Cooper, 2010). Yet, many multicellular species do not have recourse to suspended animation to survive.

### Key Aspects of Unicellular Quiescence Have Been Conserved in Multicellular Species

In multicellular organisms, cell death is no longer synonymous to organism death and within a multicellular body, dead cells are generally replaced to preserve tissue homeostasis. In adults, this replacement relies on stem cells that are capable of surviving and self-renewing all along the organism's lifetime (Rumman et al., 2015). Quiescence favors stem cells preservation by preventing the accumulation of replication-induced mutations (Fuchs, 2009; Cheung and Rando, 2013; Tümpel and Rudolph, 2019). Quiescence also permits stem cells to have an inherent low metabolic activity. In particular, the low rate of oxygen consumption reduces the impact of deleterious oxidation accrual thereby limiting the damaging effect of age on cellular macromolecules. Furthermore, as in *S. pombe*, in stem cells, quiescence specific protective and repair mechanisms limit DNA damages, hence avoiding their propagation to daughter cells.

Thus mechanisms implemented in quiescence are critical for both stem cell survival and fitness of the progeny (Mandal et al., 2011; Burkhalter et al., 2015; Gangloff and Arcangioli, 2017; Vitale et al., 2017). In this perspective, stem cell quiescence in multicellular organisms has a survival role quite similar to quiescence in unicellular species.

As observed in unicellular eukaryotes, quiescence establishment in cells of multicellular species is accompanied by the reorganization of cellular machineries. For example, quiescent primary human fibroblasts exhibit a tighter chromatin compaction (Everitts et al., 2013). The proteasome is reorganized into cytoplasmic granules in the root cells of *Arabidopsis thaliana* seedlings (Marshall and Vierstra, 2018) and the actin cytoskeleton form aggregates in non-dividing *Papaver rhoeas* pollen tubes, and rat endothelial cell (Jensen and Larsson, 2004; Poulter et al., 2010). However, to date, the cell biology of plant and animal quiescent cells remains largely underexplored.

Interestingly, quiescent cells from multicellular species can be paused in various cell cycle stages, just as some quiescent unicellular eukaryotes. This is the case of precursor cells of the *Drosophila melanogaster* wing discs that are arrested in G2 waiting for proliferation signals to form bristles (Nègre et al., 2003). Furthermore, an arrest in G2 has been associated with efficient adult stem cell regeneration in a variety of organisms, including hydra, axolotl, and zebrafish (Sutcu and Ricchetti, 2018). In addition, just as in yeast, it was observed that several quiescent stem cells are poised to possibly resume proliferation as fast as possible, an essential step for repair in various tissues (Cao et al., 2017; Relaix et al., 2021). Indeed, in muscle, systemic signals released upon muscle injury, prime some quiescent muscle stem cells into a pre-activated state by transitioning from a G0 state to a G alert state (Rodgers et al., 2014). Similarly, some neural stem cells become pre-activated for reentering the cell cycle more readily upon the next round of injury (Llorens-Bobadilla et al., 2015) and dormant hematopoietic stem cells differ in self-renewal potential and division frequency depending on their individual endogenous CDK6 level (Laurenti et al., 2015). Therefore, just as in unicellular organisms, quiescence exit swiftness is key, but in multicellular species, the trigger has shifted from nutrient cues to repair or renewing signals. Yet the logic stays the same, ensuring the flexibility for quiescent cell to respond to an ever-changing environment.

The co-existence of “deep” next to “alerted” quiescent stem cells indicated that for a given cell type, different kind of quiescent cells coexist within the same tissue, and pointed to an heterogeneity along the quiescence-to-reproliferation trajectory (Ancel et al., 2021). In fact, as in *S. cerevisiae*, differences in quiescence deepness were observed in mammals, in which quiescence exit become slower with age. For example, long-term quiescent hepatocytes (Roth and Adelman, 1974) or fibroblasts (Soprano, 1994; Kwon et al., 2017; Fujimaki et al., 2019) take a longer time to reenter the cell cycle than their younger counterparts and become less and less sensitive to proliferation stimulation. Finally, aged quiescent cells may ultimately transition to senescence, a non-proliferative cellular state that is irreversible (Sousa-Victor et al., 2014; Fujimaki and Yao, 2020). Thus, quiescence deepening reveals the

limitation of cell replacement relying on stemness and is among the strongest candidates for multicellular organism aging.

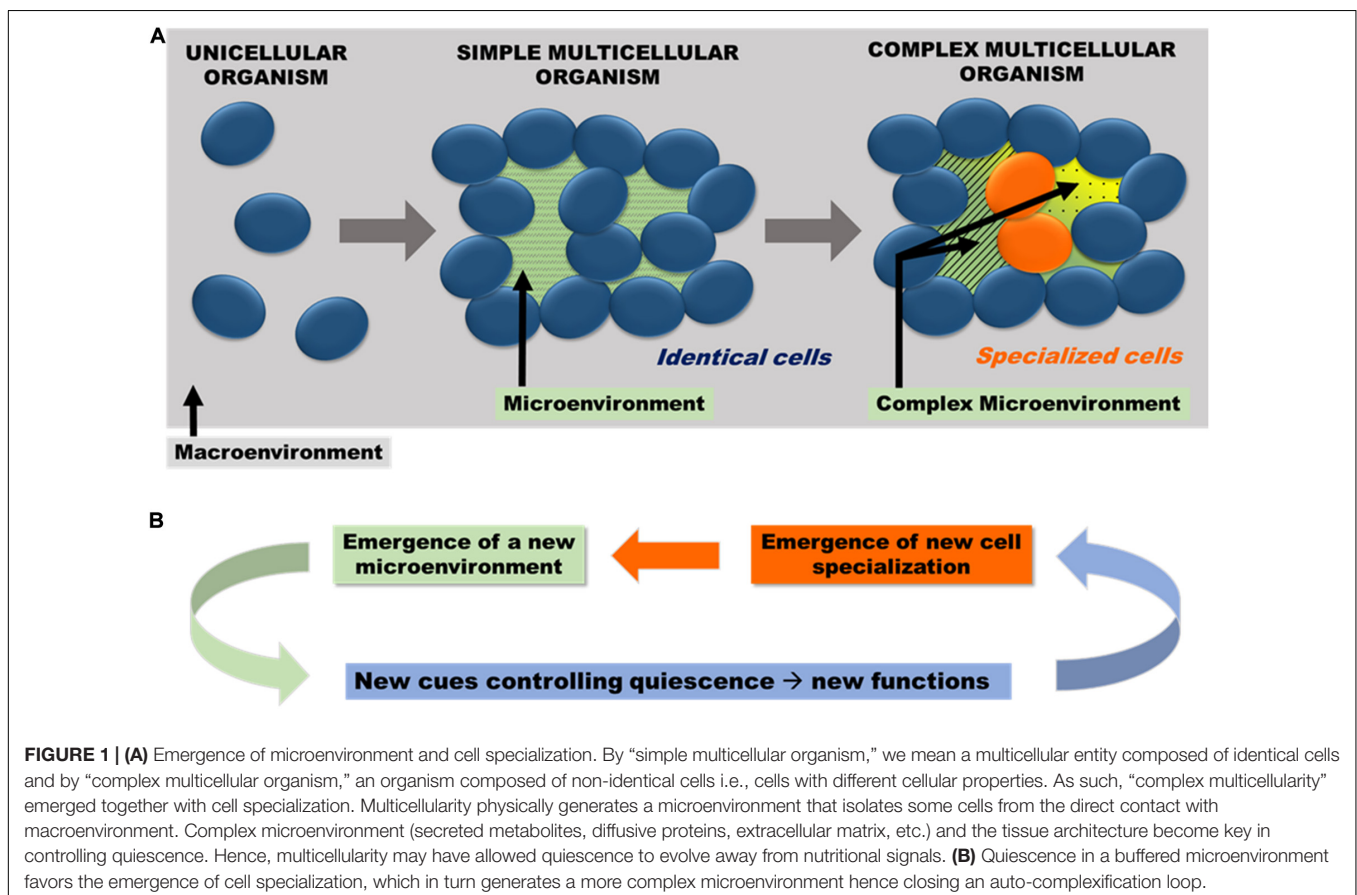
## QUIESCENCE, A MOTOR FOR EVOLUTION?

One of the first route to multicellularity may have been to aggregate in order to improve resistance to unfavorable environment (see for example Smukalla et al., 2008; Lyons and Kolter, 2015). This kind of cell consortium may have dampened niche fluctuation and created a rudimentary microenvironment that might have launched quiescence independency toward the macroenvironment. This primitive microenvironment may have provided a nutrient buffering effect in which cells, although having not enough resources to divide, could do more than just survive. In this context, we propose that quiescent cells could have launched new functions. At the beginning, these new features were probably not too much demanding in terms of metabolic resources, but some of them might have provided a selective advantage, like the ability to move and thus to explore new environments or escape predation. In fact, in many cases, proliferation and specialization became exclusive. As an example, volvox somatic cells can swim thanks to a flagellum but they have lost the capacity to proliferate. Reciprocally, volvox gonidia cells do not have flagella, but they can divide. This swim or

divide specialization echoes the segregation of somatic functions and reproduction into distinct cell types and it thought to be one of the first key steps in the evolution of multicellularity (King, 2004). Furthermore, there are growing evidences that the reverse is true and that rapid cell division favors dedifferentiation (Guo et al., 2014; Matson et al., 2017) and cell transformation (Chen et al., 2019). Thus, we propose that with the emergence of multicellularity, quiescence became no longer confined to a survival form but may have favored cell specialization thereby launching division of labor.

With the complexification of multicellular organisms, proliferation-quiescence transitions detached from the availability in nutrients and became largely independent of the macroenvironment to rely mostly on signals from neighboring cells. Secreted compounds such as metabolites, vesicles or proliferating factors, and importantly, the extracellular matrix, play a crucial role in the control of quiescence, just like physical cues such as the tension induced by the tissue architecture. This has been comprehensively reviewed in Fiore et al. (2018).

The possibility of being quiescent in a plentiful environment could have fostered some specific metabolic activities, as shown for contact-inhibited fibroblasts (Lemons et al., 2010). In fact, in heterotrophs such as humans, a part of quiescent cell metabolism is dedicated to energy production through catabolism, breakdown and re-synthesis of proteins. Part of it can also be devoted to specific processes, such as the synthesis



of extra-cellular matrix (ECM) compounds. Therefore, some dedicated metabolic pathways can be active in the total absence of proliferation (Valcourt et al., 2012). This probably opened new avenues for the emergence of cellular functions specific of quiescent cells. One typical example is the primary cilium, a structure with several key sensing functions that is assembled upon quiescence establishment by many types of mammalian cells (Satir et al., 2010). Thus, quiescence and cell specialization could have progressed hand in hand, progressively moving away quiescence from its ancestral dependency toward the macroenvironment. In this scheme, multicellularity might have arisen first, then, microenvironment and quiescence could have co-evolved, reciprocally acting on each other.

If cell specialization and quiescence co-evolved after the multiple independent emergences of multicellularity, it may be impossible to identify common properties of quiescent cells that would be posterior to multicellularity. However, as discussed above, some ancient quiescence properties inherited from unicellular organisms were conserved. Quiescence, initially selected for its ability to increase survival by slowing down proliferation, would have allowed diversifying cellular functions once reprocessed in a multicellular context. This was made possible because multicellularity eventually isolate some cells from the direct contact with macroenvironment. Hence, through the generation of a microenvironment, multicellularity could have allowed quiescence to evolve away from nutritional signals. This new form of quiescence would have favored the emergence of cell specialization, which in turn would have made the microenvironment more complex, resulting in a sort of relay race between quiescence and multicellularity (**Figure 1**).

## REFERENCES

- Amato, S. M., Fazen, C. H., Henry, T. C., Mok, W. W. K., Orman, M. A., Sandvik, E. L., et al. (2014). The role of metabolism in bacterial persistence. *Front. Microbiol.* 5:70. doi: 10.3389/fmicb.2014.00070
- Ancel, S., Stuelsatz, P., and Feige, J. N. (2021). Muscle stem cell quiescence: controlling stemness by staying asleep. *Trends Cell Biol.* 31, 556–568. doi: 10.1016/j.tcb.2021.02.006
- Argüelles, J. C. (2000). Physiological roles of Trehalose in bacteria and yeasts: a comparative analysis. *Arch. Microbiol.* 174, 217–224. doi: 10.1007/s002030000192
- Bennett, R. J., and Turgeon, B. G. (2016). Fungal sex: the Ascomycota. *Microbiol. Spectr.* 4:5. doi: 10.1128/microbiolspec.FUNK-0005-2016 [Epub ahead of print].
- Brauer, M. J., Huttenhower, C., Airoidi, E. M., Rosenstein, R., Matese, J. C., Gresham, D., et al. (2008). Coordination of growth rate, cell cycle, stress response, and metabolic activity in yeast. *Mol. Biol. Cell* 19, 352–367. doi: 10.1091/mbc.e07-08-0779
- Broach, J. R. (2012). Nutritional control of growth and development in yeast. *Genetics* 192, 73–105. doi: 10.1534/genetics.111.135731
- Burkhalter, M. D., Rudolph, K. L., and Sperka, T. (2015). Genome instability of ageing stem cells—Induction and defence mechanisms. *Age. Res. Rev.* 23, 29–36. doi: 10.1016/j.arr.2015.01.004
- Cao, W., Chen, K., Bolkestein, M., Yin, Y., Verstegen, M. M. A., Bijvelds, M. J. C., et al. (2017). Dynamics of proliferative and quiescent stem cells in liver homeostasis and injury. *Gastroenterology* 153, 1133–1147. doi: 10.1053/j.gastro.2017.07.006
- Chen, X., Burkhardt, D. B., Hartman, A. A., Hu, X., Eastman, A. E., Sun, C., et al. (2019). MLL-AF9 initiates transformation from fast-proliferating myeloid progenitors. *Nat. Commun.* 10:5767. doi: 10.1038/s41467-019-13666-5
- Cheung, T. H., and Rando, T. A. (2013). Molecular regulation of stem cell quiescence. *Nat. Rev. Mol. Cell Biol.* 14, 329–340. doi: 10.1038/nrm3591
- Costello, G., Rodgers, L., and Beach, D. (1986). Fission yeast enters the stationary G0 state from either mitotic G1 or G2. *Curr. Genet.* 11, 119–125.
- Cucinotta, C. E., Dell, R. H., Bracer, K. C., and Tsukiyama, T. (2021). RSC primes the quiescent genome for hypertranscription upon cell-cycle re-entry. *eLife* 10:e09376. doi: 10.7554/eLife.67033
- Daignan-Fornier, B., and Sagot, I. (2011a). Proliferation/quiescence: the controversial “aller-retour”. *Cell Div.* 6:10. doi: 10.1186/1747-1028-6-10
- Daignan-Fornier, B., and Sagot, I. (2011b). Proliferation/quiescence: when to start? where to stop? what to stock? *Cell Div.* 6:20. doi: 10.1186/1747-1028-6-20
- de Carpentier, F., Lemaire, S. D., and Danon, A. (2019). When unity is strength: the strategies used by *Chlamydomonas* to survive environmental stresses. *Cells* 8:1307. doi: 10.3390/cells8111307
- Dubravac, D., van Baalen, M., and Nizak, C. (2014). An evolutionarily significant unicellular strategy in response to starvation in *Dictyostelium* social amoebae. *F1000Research* 3:133. doi: 10.12688/f1000research.4218.2
- Ellegaard, M., and Ribeiro, S. (2018). The long-term persistence of phytoplankton resting stages in aquatic “seed banks”. *Biol. Rev. Camb. Philos. Soc.* 93, 166–183. doi: 10.1111/brv.12338
- Everitt, A. G., Manning, A. L., Wang, X., Dyson, N. J., Garcia, B. A., and Coller, H. A. (2013). H4K20 methylation regulates quiescence and chromatin compaction. *Mol. Biol. Cell* 24, 3025–3037. doi: 10.1091/mbc.E12-07-0529
- Fiore, A. P. Z. P., Ribeiro, P., de, F., and Bruni-Cardoso, A. (2018). Sleeping beauty and the microenvironment enchantment: microenvironmental regulation of the proliferation-quiescence decision in normal tissues and in cancer development. *Front. Cell Dev. Biol.* 6:59. doi: 10.3389/fcell.2018.00059
- Fuchs, E. (2009). The tortoise and the hare: slow-cycling cells in the stem cell race. *Cell* 137, 811–819. doi: 10.1016/j.cell.2009.05.002

This co-evolution between quiescence and cell specialization, by offering major functional and structural opportunities to innovate might have been chief to foster life diversification. Thus, quiescence may have played an important role in multicellular evolution.

## DATA AVAILABILITY STATEMENT

The original contributions presented in the study are included in the article/supplementary material, further inquiries can be directed to the corresponding author.

## AUTHOR CONTRIBUTIONS

All authors listed have made a substantial, direct and intellectual contribution to the work, and approved it for publication.

## FUNDING

This research was funded by the CNRS and the Bordeaux University.

## ACKNOWLEDGMENTS

We would like to thank Pei-Yun Jenny Wu for her comments and advices on this manuscript.

- Fujimaki, K., Li, R., Chen, H., Della Croce, K., Zhang, H. H., Xing, J., et al. (2019). Graded regulation of cellular quiescence depth between proliferation and senescence by a lysosomal dimmer switch. *Proc. Natl. Acad. Sci. U.S.A.* 116, 22624–22634. doi: 10.1073/pnas.1915905116
- Fujimaki, K., and Yao, G. (2020). Cell dormancy plasticity: quiescence deepens into senescence through a dimmer switch. *Physiol. Genom.* 52, 558–562. doi: 10.1152/physiolgenomics.00068.2020
- Gangloff, S., and Arcangioli, B. (2017). DNA repair and mutations during quiescence in yeast. *FEMS Yeast Res.* 17:fox002. doi: 10.1093/femsyr/fox002
- Guo, S., Zi, X., Schulz, V. P., Cheng, J., Zhong, M., Koochaki, S. H. J., et al. (2014). Nonstochastic reprogramming from a privileged somatic cell state. *Cell* 156, 649–662. doi: 10.1016/j.cell.2014.01.020
- Hallmann, A. (2011). Evolution of reproductive development in the volvocine algae. *Sex Plant Reprod.* 24, 97–112. doi: 10.1007/s00497-010-0158-4
- Heimlicher, M. B., Bächler, M., Liu, M., Ibeneche-Nnewiwe, C., Florin, E.-L., Hoenger, A., et al. (2019). Reversible solidification of fission yeast cytoplasm after prolonged nutrient starvation. *J. Cell Sci.* 132:jcs231688. doi: 10.1242/jcs.231688
- Jensen, P. V., and Larsson, L.-I. (2004). Actin microdomains on endothelial cells: association with CD44, ERM proteins, and signaling molecules during quiescence and wound healing. *Histochem. Cell Biol.* 121, 361–369. doi: 10.1007/s00418-004-0648-2
- Joyner, R. P., Tang, J. H., Helenius, J., Dultz, E., Brune, C., Holt, L. J., et al. (2016). A glucose-starvation response regulates the diffusion of macromolecules. *eLife* 5:e09376. doi: 10.7554/eLife.09376
- Kin, K., and Schaap, P. (2021). Evolution of multicellular complexity in the dictyostelid social amoebas. *Genes* 12:487. doi: 10.3390/genes12040487
- King, N. (2004). The unicellular ancestry of animal development. *Dev. Cell* 7, 313–325. doi: 10.1016/j.devcel.2004.08.010
- Klosinska, M. M., Crutchfield, C. A., Bradley, P. H., Rabinowitz, J. D., and Broach, J. R. (2011). Yeast cells can access distinct quiescent states. *Genes Dev.* 25, 336–349. doi: 10.1101/gad.2011311
- Kwon, J. S., Everetts, N. J., Wang, X., Wang, W., Della Croce, K., Xing, J., et al. (2017). Controlling depth of cellular quiescence by an Rb-E2F network switch. *Cell Rep.* 20, 3223–3235. doi: 10.1016/j.celrep.2017.09.007
- Laporte, D., Jimenez, L., Gouleme, L., and Sagot, I. (2017). Yeast quiescence exit swiftness is influenced by cell volume and chronological age. *Microb. Cell* 5, 104–111. doi: 10.15698/mic2018.02.615
- Laporte, D., Lebaudy, A., Sahin, A., Pinson, B., Ceschin, J., Daignan-Fornier, B., et al. (2011). Metabolic status rather than cell cycle signals control quiescence entry and exit. *J. Cell Biol.* 192, 949–957. doi: 10.1083/jcb.201009028
- Laporte, D., Salin, B., Daignan-Fornier, B., and Sagot, I. (2008). Reversible cytoplasmic localization of the proteasome in quiescent yeast cells. *J. Cell Biol.* 181, 737–745. doi: 10.1083/jcb.200711154
- Laurenti, E., Frelin, C., Xie, S., Ferrari, R., Dunant, C. F., Zandi, S., et al. (2015). CDK6 levels regulate quiescence exit in human hematopoietic stem cells. *Cell Stem Cell* 16, 302–313. doi: 10.1016/j.stem.2015.01.017
- Lemons, J. M. S., Feng, X.-J., Bennett, B. D., Legesse-Miller, A., Johnson, E. L., Raitman, I., et al. (2010). Quiescent fibroblasts exhibit high metabolic activity. *PLoS Biol.* 8:e1000514. doi: 10.1371/journal.pbio.1000514
- Llorens-Bobadilla, E., Zhao, S., Baser, A., Saiz-Castro, G., Zwadlo, K., and Martin-Villalba, A. (2015). Single-cell transcriptomics reveals a population of dormant neural stem cells that become activated upon brain injury. *Cell Stem Cell* 17, 329–340. doi: 10.1016/j.stem.2015.07.002
- Lyons, N. A., and Kolter, R. (2015). On the evolution of bacterial multicellularity. *Curr. Opin. Microbiol.* 24, 21–28. doi: 10.1016/j.mib.2014.12.007
- Maggs, C. A., and Callow, M. E. (2003). “Algal spores,” in *ELS* eds Wiley Online Library, John Wiley & Sons (Atlanta, GE: American Cancer Society). doi: 10.1038/npg.els.0000311
- Mandal, P. K., Blanpain, C., and Rossi, D. J. (2011). DNA damage response in adult stem cells: pathways and consequences. *Nat. Rev. Mol. Cell Biol.* 12, 198–202. doi: 10.1038/nrm3060
- Marshall, R. S., and Vierstra, R. D. (2018). Proteasome storage granules protect proteasomes from autophagic degradation upon carbon starvation. *eLife* 7:e34532. doi: 10.7554/eLife.34532
- Matson, J. P., Dumitru, R., Coryell, P., Baxley, R. M., Chen, W., Twaroski, K., et al. (2017). Rapid DNA replication origin licensing protects stem cell pluripotency. *eLife* 6:e30473. doi: 10.7554/eLife.30473
- McKnight, J. N., Boerma, J. W., Breeden, L. L., and Tsukiyama, T. (2015). Global promoter targeting of a conserved lysine deacetylase for transcriptional shutoff during quiescence entry. *Mol. Cell* 59, 732–743. doi: 10.1016/j.molcel.2015.07.014
- Miles, S., Bradley, G. T., and Breeden, L. L. (2021). The budding yeast transition to quiescence. *Yeast* 38, 30–38. doi: 10.1002/yea.3546
- Montrose, K., López Cabezas, R. M., Paukštytė, J., and Saarikangas, J. (2020). Winter is coming: regulation of cellular metabolism by enzyme polymerization in dormancy and disease. *Exp. Cell Res.* 397:112383. doi: 10.1016/j.yexcr.2020.112383
- Munder, M. C., Midtvedt, D., Franzmann, T., Nüske, E., Otto, O., Herbig, M., et al. (2016). A pH-driven transition of the cytoplasm from a fluid- to a solid-like state promotes entry into dormancy. *eLife* 5:e09347. doi: 10.7554/eLife.09347
- Nègre, N., Ghysen, A., and Martinez, A. M. (2003). Mitotic G2-arrest is required for neural cell fate determination in *Drosophila*. *Mech. Dev.* 120, 253–265. doi: 10.1016/s0925-4773(02)00419-7
- Neumann, N., Doello, S., and Forchhammer, K. (2021). Recovery of unicellular cyanobacteria from nitrogen chlorosis: a model for resuscitation of dormant bacteria. *Microb. Physiol.* 31, 78–87. doi: 10.1159/000515742
- O’Connell, J. D., Zhao, A., Ellington, A. D., and Marcotte, E. M. (2012). Dynamic reorganization of metabolic enzymes into intracellular bodies. *Annu. Rev. Cell Dev. Biol.* 28, 89–111. doi: 10.1146/annurev-cellbio-101011-155841
- Poulter, N. S., Staiger, C. J., Rappoport, J. Z., and Franklin-Tong, V. E. (2010). Actin-binding proteins implicated in the formation of the punctate actin foci stimulated by the self-incompatibility response in *Papaver*. *Plant Physiol.* 152, 1274–1283. doi: 10.1104/pp.109.152066
- Prax, M., and Bertram, R. (2014). Metabolic aspects of bacterial persisters. *Front. Cell Infect. Microbiol.* 4:148. doi: 10.3389/fcimb.2014.00148
- Prouteau, M., Desfosses, A., Sieben, C., Bourgoing, C., Lydia Mozaffari, N., Demurtas, D., et al. (2017). TORC1 organized in inhibited domains (TOROIDs) regulate TORC1 activity. *Nature* 550, 265–269. doi: 10.1038/nature24021
- Pu, Y., Li, Y., Jin, X., Tian, T., Ma, Q., Zhao, Z., et al. (2019). ATP-dependent dynamic protein aggregation regulates bacterial dormancy depth critical for antibiotic tolerance. *Mol. Cell* 73, 143–156.e4. doi: 10.1016/j.molcel.2018.10.022
- Radonjic, M., Andrau, J.-C., Lijnzaad, P., Kemmeren, P., Kockelkorn, T. T. J. P., van Leenen, D., et al. (2005). Genome-wide analyses reveal RNA polymerase II located upstream of genes poised for rapid response upon *S. cerevisiae* stationary phase exit. *Mol. Cell* 18, 171–183. doi: 10.1016/j.molcel.2005.03.010
- Relaix, F., Bencze, M., Borok, M. J., Der Vartanian, A., Gattazzo, F., Mademtoglou, D., et al. (2021). Perspectives on skeletal muscle stem cells. *Nat. Commun.* 12:692. doi: 10.1038/s41467-020-20760-6
- Rittershaus, E. S. C., Baek, S.-H., and Sasseti, C. M. (2013). The normalcy of dormancy: common themes in microbial quiescence. *Cell Host Microb.* 13, 643–651. doi: 10.1016/j.chom.2013.05.012
- Rodgers, J. T., King, K. Y., Brett, J. O., Cromie, M. J., Charville, G. W., Maguire, K. K., et al. (2014). mTORC1 controls the adaptive transition of quiescent stem cells from G0 to G(Alert). *Nature* 510, 393–396. doi: 10.1038/nature13255
- Roth, G. S., and Adelman, R. C. (1974). Age-dependent regulation of mammalian DNA synthesis and cell division *in vivo* by Glucocorticoids. *Exp. Gerontol.* 9, 27–31. doi: 10.1016/0531-5565(74)90004-7
- Ruger-Herreros, C., and Corrochano, L. M. (2020). Conidiation in *Neurospora crassa*: vegetative reproduction by a model fungus. *Int. Microbiol.* 23, 97–105. doi: 10.1007/s10123-019-00085-1
- Rumman, M., Dhawan, J., and Kassem, M. (2015). Concise review: quiescence in adult stem cells: biological significance and relevance to tissue regeneration. *Stem Cells* 33, 2903–2912. doi: 10.1002/stem.2056
- Sagot, I., and Laporte, D. (2019b). The cell biology of quiescent yeast - a diversity of individual scenarios. *J. Cell. Sci.* 132:jcs213025. doi: 10.1242/jcs.213025
- Sagot, I., and Laporte, D. (2019a). Quiescence, an individual journey. *Curr. Genet.* 65, 695–699. doi: 10.1007/s00294-018-00928-w
- Sagot, I., Pinson, B., Salin, B., and Daignan-Fornier, B. (2006). Actin bodies in yeast quiescent cells: an immediately available actin reserve? *Mol. Biol. Cell* 17, 4645–4655. doi: 10.1091/mbc.E06-04-0282
- Sathe, S., and Durand, P. M. (2016). Cellular aggregation in *Chlamydomonas* (Chlorophyceae) is chimaeric and depends on traits like cell size and motility. *Eur. J. Phycol.* 51, 129–138. doi: 10.1080/09670262.2015.1107759



- Satir, P., Pedersen, L. B., and Christensen, S. T. (2010). The primary cilium at a glance. *J. Cell Sci.* 123, 499–503. doi: 10.1242/jcs.050377
- Smukalla, S., Caldara, M., Pochet, N., Beauvais, A., Guadagnini, S., Yan, C., et al. (2008). FLO1 is a variable green beard gene that drives biofilm-like cooperation in budding yeast. *Cell* 135, 726–737. doi: 10.1016/j.cell.2008.09.037
- Soprano, K. J. (1994). WI-38 cell long-term quiescence model system: a valuable tool to study molecular events that regulate growth. *J. Cell. Biochem.* 54, 405–414. doi: 10.1002/jcb.240540407
- Sousa-Victor, P., Gutarra, S., García-Prat, L., Rodríguez-Ubreva, J., Ortet, L., Ruiz-Bonilla, V., et al. (2014). Geriatric muscle stem cells switch reversible quiescence into senescence. *Nature* 506, 316–321. doi: 10.1038/nature13013
- Su, S. S., Tanaka, Y., Samejima, I., Tanaka, K., and Yanagida, M. (1996). A nitrogen starvation-induced dormant G0 state in fission yeast: the establishment from uncommitted G1 state and its delay for return to proliferation. *J. Cell. Sci.* 109(Pt 6), 1347–1357.
- Sutcu, H. H., and Ricchetti, M. (2018). Loss of heterogeneity, quiescence, and differentiation in muscle stem cells. *Stem Cell Investig.* 5:9. doi: 10.21037/sci.2018.03.02
- Swygert, S. G., Kim, S., Wu, X., Fu, T., Hsieh, T.-H., Rando, O. J., et al. (2019). Condensin-dependent chromatin compaction represses transcription globally during quiescence. *Mol. Cell* 73, 533–546.e4. doi: 10.1016/j.molcel.2018.11.020
- Takeo, K., Tanaka, R., Miyaji, M., and Nishimura, K. (1995). Unbudded G2 as well as G1 arrest in the stationary phase of the basidiomycetous yeast *Cryptococcus neoformans*. *FEMS Microbiol. Lett.* 129, 231–235.
- Takeuchi, T., and Benning, C. (2019). Nitrogen-dependent coordination of cell cycle, quiescence and TAG accumulation in *Chlamydomonas*. *Biotechnol. Biofuels* 12:292. doi: 10.1186/s13068-019-1635-0
- Tümpel, S., and Rudolph, K. L. (2019). Quiescence: good and bad of stem cell aging. *Trends Cell Biol.* 29, 672–685. doi: 10.1016/j.tcb.2019.05.002
- Turian, G., and Matikian, N. (1966). Conidiation of *Neurospora crassa*. *Nature* 212, 1067–1068. doi: 10.1038/2121067a0
- Valcourt, J. R., Lemons, J. M. S., Haley, E. M., Kojima, M., Demuren, O. O., and Collier, H. A. (2012). Staying alive: metabolic adaptations to quiescence. *Cell Cycle* 11, 1680–1696. doi: 10.4161/cc.19879
- Vitale, I., Manic, G., De Maria, R., Kroemer, G., and Galluzzi, L. (2017). DNA damage in stem cells. *Mol. Cell* 66, 306–319. doi: 10.1016/j.molcel.2017.04.006
- Wei, W., Nurse, P., and Broek, D. (1993). Yeast cells can enter a quiescent state through G1, S, G2, or M phase of the cell cycle. *Cancer Res.* 53, 1867–1870.
- Withers, P. C., and Cooper, C. E. (2010). Metabolic depression: a historical perspective. *Prog. Mol. Subcell. Biol.* 49, 1–23. doi: 10.1007/978-3-642-02421-4\_1
- Yu, R., Campbell, K., Pereira, R., Björkeröth, J., Qi, Q., Vorontsov, E., et al. (2020). Nitrogen limitation reveals large reserves in metabolic and translational capacities of yeast. *Nat. Commun.* 11:1881. doi: 10.1038/s41467-020-15749-0
- Zhang, J., Martinez-Gomez, K., Heinzle, E., and Wahl, S. A. (2019). Metabolic switches from quiescence to growth in synchronized *Saccharomyces cerevisiae*. *Metabolomics* 15:121. doi: 10.1007/s11306-019-1584-4
- Zhang, N., and Cao, L. (2017). Starvation signals in yeast are integrated to coordinate metabolic reprogramming and stress response to ensure longevity. *Curr. Genet.* 63, 839–843. doi: 10.1007/s00294-017-0697-4

**Conflict of Interest:** The authors declare that the research was conducted in the absence of any commercial or financial relationships that could be construed as a potential conflict of interest.

**Publisher's Note:** All claims expressed in this article are solely those of the authors and do not necessarily represent those of their affiliated organizations, or those of the publisher, the editors and the reviewers. Any product that may be evaluated in this article, or claim that may be made by its manufacturer, is not guaranteed or endorsed by the publisher.

Copyright © 2021 Daignan-Fornier, Laporte and Sagot. This is an open-access article distributed under the terms of the Creative Commons Attribution License (CC BY). The use, distribution or reproduction in other forums is permitted, provided the original author(s) and the copyright owner(s) are credited and that the original publication in this journal is cited, in accordance with accepted academic practice. No use, distribution or reproduction is permitted which does not comply with these terms.



# Is There a Histone Code for Cellular Quiescence?

**Kenya Bonitto<sup>1†</sup>, Kirthana Sarathy<sup>1†</sup>, Kaiser Atai<sup>1,2,3</sup>, Mithun Mitra<sup>1,3‡</sup> and Hilary A. Collier<sup>1,3,4\*‡</sup>**

<sup>1</sup> Department of Molecular, Cell, and Developmental Biology, University of California, Los Angeles, Los Angeles, CA, United States, <sup>2</sup> Molecular Biology Interdepartmental Doctoral Program, University of California, Los Angeles, Los Angeles, CA, United States, <sup>3</sup> Department of Biological Chemistry, David Geffen School of Medicine, University of California, Los Angeles, Los Angeles, CA, United States, <sup>4</sup> Molecular Biology Institute, University of California, Los Angeles, Los Angeles, CA, United States

## OPEN ACCESS

### Edited by:

Guang Yao,  
University of Arizona, United States

### Reviewed by:

Venkata Chalamcharla,  
Centre for Cellular & Molecular  
Biology (CCMB), India  
Mary Ann Osley,  
University of New Mexico Health  
Sciences Center, United States

### \*Correspondence:

Hilary A. Collier  
hcollier@ucla.edu

<sup>†</sup> These authors have contributed  
equally to this work and share first  
authorship

<sup>‡</sup> These authors have contributed  
equally to this work and share last  
authorship

### Specialty section:

This article was submitted to  
Cell Growth and Division,  
a section of the journal  
Frontiers in Cell and Developmental  
Biology

**Received:** 12 July 2021

**Accepted:** 17 September 2021

**Published:** 29 October 2021

### Citation:

Bonitto K, Sarathy K, Atai K,  
Mitra M and Collier HA (2021) Is There  
a Histone Code for Cellular  
Quiescence?  
*Front. Cell Dev. Biol.* 9:739780.  
doi: 10.3389/fcell.2021.739780

Many of the cells in our bodies are quiescent, that is, temporarily not dividing. Under certain physiological conditions such as during tissue repair and maintenance, quiescent cells receive the appropriate stimulus and are induced to enter the cell cycle. The ability of cells to successfully transition into and out of a quiescent state is crucial for many biological processes including wound healing, stem cell maintenance, and immunological responses. Across species and tissues, transcriptional, epigenetic, and chromosomal changes associated with the transition between proliferation and quiescence have been analyzed, and some consistent changes associated with quiescence have been identified. Histone modifications have been shown to play a role in chromatin packing and accessibility, nucleosome mobility, gene expression, and chromosome arrangement. In this review, we critically evaluate the role of different histone marks in these processes during quiescence entry and exit. We consider different model systems for quiescence, each of the most frequently monitored candidate histone marks, and the role of their writers, erasers and readers. We highlight data that support these marks contributing to the changes observed with quiescence. We specifically ask whether there is a quiescence histone “code,” a mechanism whereby the language encoded by specific combinations of histone marks is read and relayed downstream to modulate cell state and function. We conclude by highlighting emerging technologies that can be applied to gain greater insight into the role of a histone code for quiescence.

**Keywords:** histone post translational modification, quiescence, histone methylation, histone acetylation, metabolism, histone code

## CELLULAR QUIESCENCE: A STATE OF REVERSIBLE CELL CYCLE EXIT

To maintain physiological homeostasis, many tissues contain a population of cells that can exit the proliferative cell cycle and enter a quiescent state of temporary cell division arrest in response to anti-proliferative cues (Li and Clevers, 2010; Cheung and Rando, 2013; Nakamura-Ishizu et al., 2014; Dhawan and Laxman, 2015; Sun and Buttitta, 2017; Sagot and Laporte, 2019a; Marescal and Cheeseman, 2020). This non-dividing state of cellular quiescence is defined by its reversibility, that is, quiescent cells can reenter the cell cycle upon receiving proliferative signals. Quiescent

cells can be distinguished from other types of non-dividing cells such as senescent or terminally differentiated cells by their temporary exit from the cell cycle and high likelihood of proliferating in response to a triggering stimulus (Sang and Collier, 2009; Cheung and Rando, 2013; Terzi et al., 2016). Quiescent cells must therefore preserve the ability to proliferate at a later time, and protect themselves from entering irreversible states (Collier et al., 2006; Sang and Collier, 2009; Sang et al., 2010; Bjornson et al., 2012).

Cellular quiescence has been studied experimentally in multiple systems including yeast, cultured primary cells, and stem cells (Mitra et al., 2018a; Spain et al., 2018; Yang and Chi, 2018) (Table 1). Some of the gene expression, signaling, and functional changes observed with quiescence are likely specific for a cell type, while others are shared. Transcriptional changes with quiescence have been analyzed using cDNA libraries (Schneider et al., 1988; Coppock et al., 1993), microarrays (Venezia et al., 2004; Collier et al., 2006; Suh et al., 2012; Johnson et al., 2017), next generation sequencing (van Velthoven et al., 2017; Mitra et al., 2018b; Srivastava et al., 2018), and single-cell RNA sequencing methods (Kalakonda et al., 2008; Collier, 2019a). These studies demonstrated widespread gene expression changes with quiescence, some of which are functionally important for the quiescent state (Suh et al., 2012; Johnson et al., 2017; Lee H.N. et al., 2018; Mitra et al., 2018b). These gene expression changes include downregulation of genes involved in cell cycle progression and upregulation of stress response genes (Lemons et al., 2010; Legesse-Miller et al., 2012; Valcourt et al., 2012; Collier, 2019b). Other gene expression changes allow the cell to re-organize metabolic pathways in quiescent cells to better match the availability of nutrients and the metabolic needs of the cell (Lemons et al., 2010; Valcourt et al., 2012; Collier, 2019b). Disruption of these cellular mechanisms can contribute to the occurrence and progression of pathologies related to aging, developmental defects, and cancer (Tumpel and Rudolph, 2019).

In addition to gene expression changes, quiescence is also associated with changes in the packaging of DNA into chromatin. Eukaryotic chromatin can take on two forms—a more condensed and transcriptionally silent form called heterochromatin and a less condensed and more transcriptionally active form called euchromatin (Desjarlais and Tummino, 2016). Within these states, the extent of compaction can vary, for instance, mitotic chromosomes are extremely condensed. Studies using imaging, flow cytometry, Hi-C, and other methods have shown that entry to a quiescent state involves changes in nuclear size, chromatin compaction and 3D genome architecture (Bridger et al., 2000; Everitts et al., 2013a; Guidi et al., 2015; Criscione et al., 2016; Swygert et al., 2019, 2021). In yeast, the transition from exponential phase growth to stationary phase, a quiescent state achieved when yeast deplete their nutrients, is associated with downregulation of gene expression, a more condensed chromatin state (Martinez et al., 2004; Schafer et al., 2008), and more long-range chromosomal interactions (Swygert et al., 2019). In mammals, activation of quiescent lymphocytes is associated with an unpacking of condensed chromatin in a process that can be visualized with electron microscopy (Tokuyasu et al., 1968; Dardick et al., 1983; Setterfield et al., 1983; Grigoryev et al., 2004).

Using circular dichroism, Chiu and Baserga reported a likely change to a more open chromatin structure as quiescent fibroblasts re-enter the cell cycle (Chiu and Baserga, 1975). In contrast, in one study, bovine fibroblasts were reported to have a more relaxed chromatin state in G<sub>0</sub> (quiescent) compared with G<sub>1</sub> cells (Kallingappa et al., 2016).

In addition to changes in gene expression and chromatin compaction, quiescence is also associated with a change in the positioning of chromosomes within the nucleus. In yeast, hyperclustering of telomeres has been reported with quiescence (Guidi et al., 2015; Laporte et al., 2016). When serum was removed from the culture medium of human fibroblasts, chromosomes were repositioned within 15 min in a process that required ATP, actin polymerization, and myosin (Mehta et al., 2010). In another study in human dermal fibroblasts, gene-poor chromosome 18 was found near the edge of the nucleus and gene-rich chromosome 19 was found in the center of the nucleus in proliferating cells. In serum-starved, quiescent fibroblasts, chromosome 18 shifted to a more central location in the nucleus, and there was no longer a difference in the positioning of chromosomes 18 and 19 (Bridger et al., 2000). Taken together, these findings demonstrate changes in gene expression, chromatin compaction and chromosome positioning within the nucleus in quiescent cells.

## HISTONE POST-TRANSLATIONAL MODIFICATIONS AS A POSSIBLE BIOLOGICAL CODE

### Nucleosome Structure and Histone Marks

Eukaryotic genomic DNA is tightly packed inside the nucleus. For mammalian chromosomes, this tight packing results in a 10,000-fold reduction in length (Kornberg and Lorch, 2020). The DNA in chromatin forms complexes with histone proteins that assemble the DNA strands into nucleosomes in a structure that resembles “beads on a string” with the nucleosomes (beads) representing the basic repeating unit of chromatin (Cutter and Hayes, 2015; Zhou et al., 2019; Ghoneim et al., 2021). Each core nucleosome consists of ~147 base pairs (bp) of DNA in a left-handed super-helical conformation wrapped around an octamer of histone proteins (Zhou et al., 2019). The octamer consists of two copies each of histone proteins H2A, H2B, H3, and H4 with each of the two dimers of H2A-H2B interacting with either end of a (H3-H4)<sub>2</sub> tetramer (H4-H3:H3-H4). The core nucleosome is flanked by 10-70 bp of linker DNA and usually a linker histone (H1) (Cutter and Hayes, 2015). The disordered N-terminal tails of all four histone proteins as well as the C-terminal tail of H2A protrude out from the nucleosome core and are sites of diverse post translational modifications (PTMs) or marks such as lysine and arginine methylation, lysine acetylation, and serine and threonine phosphorylation (Bannister and Kouzarides, 2011; Greer and Shi, 2012; Cutter and Hayes, 2015). These histone tails modulate charge, hydrophobicity, and steric access to chromatin (Ghoneim et al., 2021). Histone PTMs

**TABLE 1** | List of *in vitro* and *in vivo* quiescence models.

Quiescence model	Type	Model conditions	References
Yeast	Cell culture	Stationary phase isolation	Allen et al., 2006
Fission yeast	Cell culture	Nitrogen-induced starvation; Glucose deprivation	Hayashi et al., 2018; Zahedi et al., 2020
Human dermal fibroblasts	Cell culture	Serum-starvation; Contact-inhibition	Everitts et al., 2013a; Mitra et al., 2018a
Human lung fibroblasts	Cell culture	Mitogen withdrawal; Contact inhibition; Loss of adhesion	Coller et al., 2006; Dai et al., 2015
Bovine fibroblasts	Cell culture	Serum starvation	Meng et al., 2020; Kallingappa et al., 2016
Human/mouse embryonic stem cells	Cell culture	Isolation from inner cell mass of blastocyst	Khoa et al., 2020
Mouse hematopoietic stem cells	Tissue	Isolation from fetal liver, bone marrow, cord blood	Vizán et al., 2020; Tie et al., 2020
Mouse neural stem cells	Tissue	Isolation from ventricular-subventricular zone of brain	Kalamakis et al., 2019; Obernier et al., 2018
Mouse muscle skeletal cells	Tissue	Isolation from muscle of 2 month-old mice	Boonsanay et al., 2016; Ryall et al., 2015
Human primary myoblasts	Cell culture	Methylcellulose culture medium	Cheedipudi et al., 2015
Mouse hair follicle stem cells	Tissue	Isolation from back, belly, or scalpskin	Kang et al., 2020; Lee et al., 2016; Lien et al., 2011
Human Breast cancer MCF-7 cells	Cell culture	Hormone starvation; Serum starvation	Liu et al., 2017; Bierhoff et al., 2014
Mouse T cells	Tissue	Isolation from spleen	Rawlings et al., 2011
Mouse Fibroblasts	Cell culture	Serum deprivation	Grigoryev et al., 2004

are added and removed by enzymatic proteins referred to as “writers” and “erasers,” respectively (Soshnev et al., 2016; Hyun et al., 2017; Husmann and Gozani, 2019). Histone PTMs serve as recognition sites for proteins (“readers”) that site-specifically bind to chromatin. In some cases, a single protein contains multiple domains and can act as both a reader for one type of PTM and a writer for another PTM (Smeenk and Mailand, 2016). The amino acid residues in the histone globular core can also be post-translationally modified and these core PTMs likely modulate interactions between histones and between histones and DNA (Tessaraz and Kouzarides, 2014).

## What Are the Properties or Functions of Histone Marks?

Histone H3K4me3, H3K36me3, and H3K79me3 and ubiquitylation of H2B marks are often associated with active transcription (Black et al., 2012; Hyun et al., 2017), whereas H3K9me3, H3K27me3, H2A ubiquitylation on lysine 119, and H4K20 methylation are indicators of a silenced chromatin state with reduced gene expression (Black et al., 2012; Hyun et al., 2017). These properties of histone marks are related to the way they interact with chromatin and chromatin binding proteins. Histone PTMs can be envisioned to function by at least two broad categories of mechanisms (Bannister and Kouzarides, 2011). The first involves direct structural effects on the biomechanical properties of DNA (Bannister and Kouzarides, 2011). In this role, histone PTMs can affect the accessibility of DNA, and thus the binding of transcription factors or other proteins that bind enhancers and affect transcription (Bannister and Kouzarides, 2011). Such effects can occur, for instance, when histone PTMs disrupt electrostatic interactions between histones and DNA. Nucleosome core particle has an overall charge of  $-150$  electrons that is contributed by DNA ( $-294$  electrons) and histones ( $+144$  electrons) (Norton et al., 1989; Cortini, 2016; Prakash and Fournier, 2018). Some histone PTMs that are associated

with a more open chromatin state and increased gene expression reduce the positive charges on histones thereby leading to less effective screening of the negative charges on DNA (Prakash and Fournier, 2018). Acetylation, in particular, impairs the affinity of histones for DNA by neutralizing the positive charges and disrupting the ionic interactions between histones and DNA. This results in increased histone mobility and a more open chromatin conformation (Allfrey et al., 1964; Cosgrove et al., 2004). An open chromatin conformation facilitates access to transcription factors and other chromatin binding proteins (Bannister and Kouzarides, 2011). While some modifications such as acetylation may be expected to alter the ionic charge and thus chromatin compaction, others, including methylation, may have more modest impacts on charge and chromatin structure (Bannister and Kouzarides, 2011).

The second way in which histone PTMs can exert a functional effect is by regulating the binding of different chromatin factors. As one example, proteins with PHD fingers and Tudor family of domains can bind lysine methylations (Maurer-Stroh et al., 2003; Champagne and Kutateladze, 2009; Bannister and Kouzarides, 2011). In some cases, multiple different domains can recognize the same lysine methylation (Bannister and Kouzarides, 2011). Another example of histone PTM recognition is the binding of dimeric Heterochromatin Protein 1 (HP1) to the H3K9me3 mark via the chromodomain. This is associated with repressive architecture and chromatin compaction (Bannister et al., 2001; Lachner et al., 2001; Bannister and Kouzarides, 2011).

Genome-wide studies of histone marks have revealed that combinations of histone marks can be used to classify chromatin into different states (Black et al., 2012). In *Arabidopsis*, four chromatin states were identified (Roudier et al., 2011); in *Drosophila*, 5–9 states have been reported (Kharchenko et al., 2011; Riddle et al., 2011); while in human cells, up to 51 chromatin states have been defined (Ernst and Kellis, 2010). In human cells, chromatin states include promoter-associated,



transcription-associated, active intergenic, large-scale repressed, and repeat-associated states, each of which have distinct histone marks and biological roles (Ernst and Kellis, 2010). Different promoter states were defined by patterns of H3K4 methylation, H3K79 methylation, H4K20 methylation, and acetylation (Black et al., 2012). One particular chromatin state that involves a specific combination of histone marks is the bivalent mark (Bernhart et al., 2016). Bivalent marks are often found in the promoters of developmentally regulated genes (Bernstein et al., 2006; Lesch et al., 2013), and are defined by the simultaneous presence of activating marks such as H3K4me1 or H3K4me3, and the repressive chromatin mark H3K27me3 (Voigt et al., 2013). Genes with bivalent marks are repressed, but pre-loaded with RNA polymerase that is “poised” for rapid expression in response to a relevant trigger (Mikkelsen et al., 2007; Margaritis and Holstege, 2008; Gaertner et al., 2012). More recent studies have identified combinatorial marks that establish zones within the nucleus that can be identified by combinations of proteins and histone marks (Takei et al., 2021). These nuclear zones include nuclear speckles, active chromatin, heterochromatin zones and zones within the nucleolus (Takei et al., 2021). The active chromatin zone, for example, was characterized by histone H3K9ac, H3K27ac, H4K16ac, RNA polymerase II serine 5 phosphorylation, and SF3A66 (Takei et al., 2021).

Consistent with the concept of nuclear zones, histone marks may allow for the patterning of chromatin into regions of approximately 0.5-1 megabases with similar properties, termed topological domains as identified by the Hi-C technique (Prakash and Fournier, 2018). Histone modifications have been found to cluster at the genome scale as DNA tends to fold into domains in which the all of the DNA in that domain is labeled with similar histone marks (Dixon et al., 2012; Rao et al., 2014; Barbieri et al., 2017). For instance, H3K4me3-rich, H3K27me3-rich and H3K9me3 rich regions have been found to segregate from each other, and to mark active genes, repressed genes and inactive chromatin, respectively (Prakash and Fournier, 2018). Thus, histone PTMs may be associated with multiple aspects of chromatin including the extent of local compaction, the extent of gene expression and the formation of chromatin domains.

## Do Histone Marks Create a Histone Code?

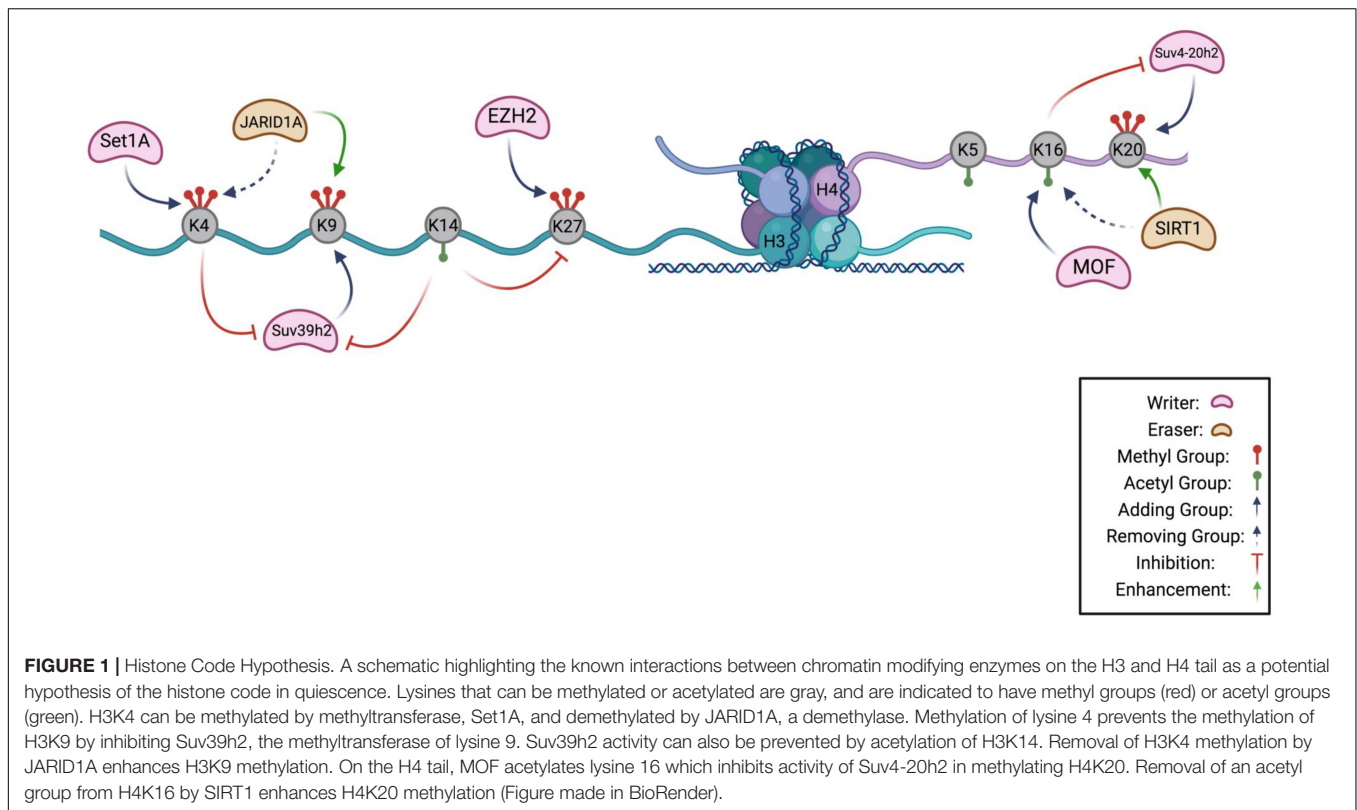
Biological codes that have been previously described include an input system that is translated into an output via adaptors (Prakash and Fournier, 2018). As one example, the genetic code translates sequences of nucleotide codons (input) into a sequence of amino acids (output) using the protein translation apparatus (adapter) (Prakash and Fournier, 2018). Histone PTMs have also been suggested to establish a biological code (Strahl and Allis, 2000; Allis and Jenuwein, 2016). According to the histone code hypothesis, the presence of specific histone marks, and in some cases, possible combinations of histone marks (inputs), provides information to reader proteins (adapters) that interpret the marks or combinations of marks to produce outputs such as gene activation or silencing, chromatin compaction, repair of DNA damage, cell division or differentiation (Strahl and

Allis, 2000; Jenuwein and Allis, 2001; Turner, 2002; Smeenk and Mailand, 2016). Given that histone marks tend to be rapidly re-established after cell division (Everitts et al., 2013a,b), information about a cell's state can be transmitted to descendant cells. Misreading of histone marks has been associated with cancer and developmental defects (Wang and Allis, 2009; Chi et al., 2010; Hyun et al., 2017).

One potential advantage of a histone code would be that combinations of histone marks could provide increased robustness to a system in which different inputs result in specific outcomes (Prakash and Fournier, 2018). Robustness can be achieved with cooperation and redundancy (Prakash and Fournier, 2018). A histone code has been hypothesized to provide a level of proofreading needed so that genes are not turned on or off inappropriately (Prakash and Fournier, 2018). If there are multiple independent histone marks that work in concert to achieve an outcome, then loss of one mark would have only a modest effect on the associated phenotypes (Prakash and Fournier, 2018). Further, comparing the use of histone marks in different species shows that histone modifications have evolutionarily conserved functions and play a similar functional role across eukaryotes (Ho et al., 2014; Prakash and Fournier, 2018).

Generating chromatin states with combinations of histone marks may reflect instances in which the presence of one histone PTM affects the recruitment of enzymes that create another PTM in the same or different histone tails resulting in reproducible output patterns (**Figure 1**). This can be achieved by multi-domain proteins that recognize the histone PTM through the reader domain and utilize a different domain for recruiting a histone writer. As one example, double-stranded DNA breaks serve as a signal to the ATM kinase, which leads to phosphorylation of the H2A variant H2A.X on its C terminal tail (Rogakou et al., 1998; Smeenk and Mailand, 2016). The presence of this mark, called  $\gamma$ -H2AX, creates binding sites for a reader for this mark, Mediator of DNA Damage Checkpoint Protein 1 (MDC1), a protein that recruits factors to the DNA damage site (Stucki et al., 2005), including E3 ligases that ubiquitinate histones (Huen et al., 2007; Kolas et al., 2007; Mailand et al., 2007; Doil et al., 2009). Histone ubiquitin modifications create recruitment platforms for DNA repair factors (Huen et al., 2007; Kolas et al., 2007; Mailand et al., 2007; Doil et al., 2009). Thus, histone modifications can transmit information about the site-specific presence of double strand breaks to affect an outcome, in this case, DNA repair.

Another example in which the presence of a histone mark affects the likelihood of other marks being added occurs during the mitosis phase of the cell cycle. Phosphorylation of Ser10 of histone H3 regulates transcription during interphase (Shimada et al., 2008) and chromosome condensation during mitosis (Wei et al., 1999). Histone H3S10 phosphorylation prevents phosphorylation of Thr6 and Thr11 on the same histone (Cosgrove, 2012; Liokatis et al., 2012). This hierarchy may ensure that phosphorylation of Ser10 during mitosis, which is required for chromosome condensation and separation, does not lead to subsequent formation of dually labeled histones with H3S10 phosphorylation and Thr6 or Thr11 phosphorylation during mitosis (Cosgrove, 2012; Liokatis et al., 2012). This example



provides an instance in which histone marks antagonize each other, and combinations of histone marks are required to ensure a robust functional response.

Histone codes that lead to biologically significant outcomes have been suggested to play a role in neural plasticity (Farrelly and Maze, 2019), genome structure (Prakash and Fournier, 2018), and cancer (Godley and Le Beau, 2012). In neurons, serotonylation of histone H3 glutamine 5 works in conjunction with nearby H3K4me3 marks to regulate transcription (Farrelly et al., 2019; Farrelly and Maze, 2019). The dual H3K4(me3)(Q5serotonin) mark was found to enhance binding of interacting proteins, including the transcription factor complex TFIID (Lauberth et al., 2013; Farrelly et al., 2019; Farrelly and Maze, 2019). In this way, the combination of histone marks results in increased transcription of specific nearby genes.

On the other hand, it is important to note that the model that specific combinations of histone tail PTMs lead to defined biological outcomes has been challenged (Henikoff and Shilatifard, 2011; Morgan and Shilatifard, 2020). One central argument is whether histone modifications are the cause of different transcriptional states or, instead, are formed as a consequence of transcription and other dynamic processes. It has been difficult to resolve this controversy because studying the direct role of a histone PTM is challenging. Traditional genetic tools such as knockdown or overexpression are not sufficient to differentiate the direct versus indirect effects of targeting a histone modifying enzyme that adds or removes a PTM because the enzyme may also act on non-histone substrates (Henikoff and Shilatifard, 2011; Cornett et al., 2019; Corvalan and Collier, 2021).

An alternative strategy to directly assess the role of a histone PTM is to mutate the amino acid residue that bears the PTM. While this strategy can be effective in some organisms such as yeast, it is not practical for higher eukaryotes due to the presence of multiple copies of the genes encoding the most frequently modified histones (Tripputi et al., 1986; Henikoff and Shilatifard, 2011; Soshnev et al., 2016; Corvalan and Collier, 2021).

Debate about the existence of a histone code has also centered on the nature of the histone code. The original paper describing a histone code suggested a code that has been described as hardwired and deterministic (Jenuwein and Allis, 2001), like the genetic code (Morgan and Shilatifard, 2020). With time, an alternative and more complex relationship between histone marks and functional outcomes has been described (Morgan and Shilatifard, 2020). In this potential representation, histone PTMs convey information in a context-dependent manner (Morgan and Shilatifard, 2020). A histone mark can have multiple potential outcomes, and the specific path would depend on multiple factors including the three-dimensional folding of the genome, the local chromatin environment, and the concentrations of the possible downstream effector molecules (Morgan and Shilatifard, 2020).

## Is There a Histone Post-translational Modification Code for Quiescence?

Does a histone code exist for quiescence? Are there specific patterns of histone tail PTMs that dictate or are associated with entry, exit, maintenance, or depth of a quiescent state? If so, do these histone PTMs modulate the physical properties

of the DNA? Do these histone marks directly alter the chromatin accessibility of gene promoters and enhancers to induce molecular and phenotypic changes with quiescence? Alternatively, do these histone PTMs serve as binding sites for readers that recognize the PTMs and effect cellular changes during quiescence? If the histone marks serve as recognition sites, what are the most important effectors and what aspects of quiescence do they control? In this review, we address these questions and compare the findings from multiple

experimental models of quiescence (**Table 1**). Advances in ChIP-seq technology (O'Geen et al., 2011) such as CUT&RUN (Hainer and Fazzio, 2019), CUT&Tag (Kaya-Okur et al., 2019), and HiChIP (Yan et al., 2014) have enabled fine resolution mapping of the genomic position of different histone tail marks (**Table 2**). Mass spectrometry can be used to measure histone epigenetic mark abundance and dynamics in a multiplexed, parallel manner (Volker-Albert et al., 2018) (**Table 2**). Further, advances in imaging such as combining immunofluorescence

**TABLE 2 |** Methods to study histone marks.

Approach	Method(s)	Description	Amount of material	Bulk or single-cell	Global pattern?	References
PCR	ChIP-qPCR	Chromatin is cross-linked, fragmented, and immunoprecipitated (ChIP). DNA is isolated and purified and undergoes PCR	$5 \times 10^5 - 5 \times 10^6$ cells	Bulk	No	Milne et al., 2009
High-throughput sequencing	ChIP-seq	Following ChIP, Next-generation sequencing (NGS) is used to identify DNA fragments and map them against entire genome	$10^5 - 5 \times 10^5$ cells per antibody	Bulk	Yes	O'Geen et al., 2011
	CUT&RUN	Recombinant protein A-micrococcal nuclease fusion recruited to the antibody targeting chromatin protein of interest; DNA fragments near antibody sites are cleaved, released, and sequenced	$5 \times 10^5$ cells	Bulk	Yes	Hainer and Fazzio, 2019
	CUT&Tag	A-Tn5 transposase fusion protein bound to antibody; transposase generates fragment libraries for sequencing	100,000 – 500,000 cells	Bulk	Yes	Kaya-Okur et al., 2019
	Joint RNA-seq and CUT&Tag (Paired-Tag)	CUT&Tag followed by RNA-seq: profiling of histone modifications and transcripts in single cells; generates maps of chromatin state and transcript in various tissues by cell type	~10,000 cells per antibody	Single-cell	Yes	Zhu et al., 2021
	HiChIP	Comprehensive analysis of single-end and paired-end ChIP-seq reads for protein-DNA interactions	$10^6 - 15 \times 10^6$ cells	Bulk	Yes	Yan et al., 2014
Imaging	RNA-seq	RNA is isolated from sample and converted into cDNA libraries which undergo NGS.	$5 \times 10^4 - 5 \times 10^6$ cells	Bulk and single-cell	Yes	Wang et al., 2009; Svensson et al., 2018
	Multicolor IF-based single cell analysis	Using directly labeled histone modification-specific antibodies to monitor histone levels in single cells			No	Hayashi-Takanaka et al., 2020
	Stochastic Optical Reconstruction Microscopy (STORM)	Single fluorophores blink individually and randomly, enabling precise location of photons, eventually forming full images			No	Xu et al., 2018
Mass spectrometry	LC-MS/MS	Allows for quantification of histone modifications and combinations of modifications	$10^6 - 10^7$ cells	single-cell	Yes	Volker-Albert et al., 2018
Flow cytometry	FACS	Cells are prepared accordingly for high-throughput flow cytometry, and gated based on phenotype of interest; allows for investigation of multiple phenotypes in complex samples	$10^5 - 10^6$ cells	single-cell	Yes	Zahedi et al., 2020
Western blot		Protein is isolated from sample, separated by weight and probed for on gel with specific antibodies			No	Egelhofer et al., 2011

with directly labeled histone modification-specific antibodies to monitor histone levels in single cells (Hayashi-Takanaka et al., 2020), sequential fluorescence *in situ* hybridization analysis (Takei et al., 2021), and improved imaging with Stochastic Optical Reconstruction Microscopy (STORM) (Xu et al., 2018), have permitted detailed analysis of the global and site-specific organization of histone marks (Takei et al., 2021). It is important to note that in this review we focus on the most intensively studied histone PTMs, but these are not the only possible candidates by which histones or a histone code could contribute to the changes observed with quiescence. For instance, there may be new histone marks that are specific for quiescence and have not yet been observed, despite mass spectrometry-based histone tail analysis (Everitts et al., 2013a). There are also linker histones and variants of core histones that affect nucleosome structure and function, and consequently chromatin architecture (Kurumizaka et al., 2021). Changes in the compositions of histones and histone linkers could potentially contribute to the functional attributes of quiescent cells, and these are not reviewed here. We conclude by identifying areas for future studies and methodologies that can be used to address existing gaps in our knowledge.

## DIFFERENT QUIESCENCE MODEL SYSTEMS FOR STUDYING HISTONE MARKS

### Yeast Models of Quiescence

Multiple model systems have been used to study the molecular mechanisms of quiescence including yeast, mouse and human cells (Table 1), all of which have different genomes, limiting our ability to make direct comparisons about histone modifications in specific genomic regions. Further, the signals that induce quiescence, and the quiescent state achieved in these model systems differs, which may contribute to differences in the levels of specific histone modifications (Valcourt et al., 2012; Collier, 2019a). Among these model systems, each has advantages and disadvantages, for instance, budding yeast in a haploid state contain only one copy each of the major core histone genes (Eriksson et al., 2012). In haploid yeast, it is possible to alter a single amino acid to test the importance of a specific histone PTM, thus making yeast a particularly attractive model system for such studies.

Budding yeast, such as the well-studied strain *Saccharomyces cerevisiae* (*S. cerevisiae*), participate in both symmetric mitotic cell divisions during the budding process, and meiotic cell divisions during yeast sporulation (Neiman, 2011). All microorganisms, including yeast, spend a majority of their life-cycle in a quiescent state due to a lack of resources in their natural environment (De Virgilio, 2012; Sagot and Laporte, 2019b). Diploid yeast cells can enter a quiescent state in response to nutrient depletion, stress, and even cell wall damage (Miles et al., 2019). *Saccharomyces cerevisiae* initiate quiescence following the exhaustion of nutrients, especially glucose, and have been widely used to study quiescence. Quiescent yeast share some similarities to the quiescent state

of mammals (Gray et al., 2004; Dhawan and Laxman, 2015; Miles et al., 2021). When grown in the laboratory, yeast consume glucose present in their growth medium and when available nutrients have been depleted, the yeast undergo a change termed diauxic shift (Chu and Barnes, 2016) as their metabolic profiles transition from fermentation to respiration, resulting in a decreased growth rate. When no other carbon sources are readily available, the yeast enter stationary phase or quiescence (Galdieri et al., 2010). By fractionating the cells based on differing densities, the non-proliferating stationary phase yeast have been separated into a denser population that is long-lived, and a less dense subpopulation that has been termed “non-quiescent” (Allen et al., 2006). Differences in the accumulation of trehalose and lipids may contribute to the different densities of these populations (Sagot and Laporte, 2019b). Fractionation protocols that purify quiescent yeast have allowed for comparisons of histone modifications in quiescent and proliferative yeast samples (Mews et al., 2014). In budding yeast that initiate quiescence following nutrient exhaustion, there is a genomewide shift in gene expression, with transcriptional repression of genes involved in growth and proliferation including ribosomal genes (Werner-Washburne et al., 1996; Gray et al., 2004; Radonjic et al., 2005; McKnight et al., 2015).

Yeast can also form spores, which can serve as another model for quiescence. When diploid yeast cells undergo meiosis, the meiotic products can differentiate into dormant spores during the process of sporogenesis (Greig, 2009; Duina et al., 2014). The state achieved in dormant microbial spores shares some similarities to the quiescent state achieved by nutrient depletion in *S. cerevisiae* (Greig, 2009; Duina et al., 2014). For instance, spore formation, like quiescence, is reversible as spores germinate to form haploid cells when exposed to nutrients. Spores are distinguished from a quiescent state because quiescent cells maintain some metabolic capacity, maintain membrane potential and do not undergo a morphological differentiation (Rittershaus et al., 2013). Spore formation is characterized by a dramatic decrease in global transcription levels (Xu et al., 2012). As described below, both nutrient limitation and spore formation have been used as models to probe the role of histone PTMs in quiescence in *S. cerevisiae*.

Fission yeast like *Schizosaccharomyces pombe* (*S. pombe*) are also an excellent model for quiescence (Su et al., 1996). During meiosis in fission yeast, asymmetric division takes place in which inheritance of the mother cell's components give rise to four different, unique daughter cells (Higuchi-Sanabria et al., 2014). Removing nitrogen from *S. pombe* causes the yeast to mate with yeast of the opposite mating type followed by replication through meiosis (Freese et al., 1982). However, if there is only one mating type of yeast in the population, the fission yeast arrest in G1-phase and enter quiescence (Nurse and Bissett, 1981; Gangloff et al., 2017). These nitrogen-deprived fission yeast can remain viable for months. Quiescent fission yeast cells are metabolically active, engage stress-responsive signaling and are efficient in DNA damage repair (Su et al., 1996; Mochida and Yanagida, 2006; Ben Hassine and Arcangioli, 2009; Marguerat et al., 2012; Gangloff and Arcangioli, 2017). When fission yeast enter a state of quiescence as non-dividing spores, a gene regulatory program



is activated that includes upregulation of genes needed to adapt to the quiescent state (Su et al., 1996; Sajiki et al., 2009; Takeda and Yanagida, 2010), the nucleus undergoes changes in chromatin compaction, and histone modifications are altered (Neiman, 2011). For all of these reasons, fission yeast represents a valuable model system for studying epigenetic changes with quiescence.

## Fibroblast Models of Quiescence

In multicellular organisms, there are multiple different types of quiescent cells, such as quiescent fibroblasts, immune cells, and stem cells, that serve as model systems for the study of quiescence at the molecular level (Mitra et al., 2018a). Fibroblasts, which are normally quiescent *in vivo*, contribute to the physical form and biomechanics of tissue by secreting growth factors and extracellular matrix proteins. Fibroblasts are organizers of the wound healing process as they can proliferate and replenish dead cells at the wound site and secrete extracellular matrix proteins that contribute to the formation of granulation tissue and scars (Lynch and Watt, 2018). Fibroblasts isolated from different tissues such as skin or lung are relatively easy to culture, and quiescence can easily be achieved by serum starvation, contact inhibition, or loss of adhesion (Coller et al., 2006; Mitra et al., 2018a). When fibroblasts enter a quiescent state, there is a dramatic change in gene expression in which a large fraction of the genome is differentially regulated (Coller et al., 2006; Suh et al., 2012; Mitra et al., 2018b). This change in gene expression is accompanied by significant changes in the abundance and activity of microRNAs (Suh et al., 2012; Johnson et al., 2017), transcript decay rates (Johnson et al., 2017; Mitra et al., 2018b), splicing (Mitra et al., 2018b), and the use of proximal versus distal polyadenylation sites (Mitra et al., 2018b). Fibroblasts are a heterogeneous population of cells. They can be isolated from different locations within the skin including hair follicles, and locations within the dermal layer, such as the papillary and reticular dermis (Sorrell and Caplan, 2004), and they differ based on their location within tissue (Sorrell and Caplan, 2004; Lynch and Watt, 2018). Further, fibroblasts isolated from skin from different anatomical sites have distinct and characteristic transcriptional programs that include extracellular matrix synthesis, lipid metabolism and signaling pathways (Chang et al., 2002). Single-cell sequencing data has shed light on the heterogeneity of fibroblasts (Muhl et al., 2020). While the tissue of origin represents an important contributing factor to the differences among fibroblasts, single cell sequencing has also shown intra-organ heterogeneity (Muhl et al., 2020). Different fibroblast subpopulations have distinct characteristics and the contributions of each fibroblast population to physiology is being actively elucidated (Muhl et al., 2020).

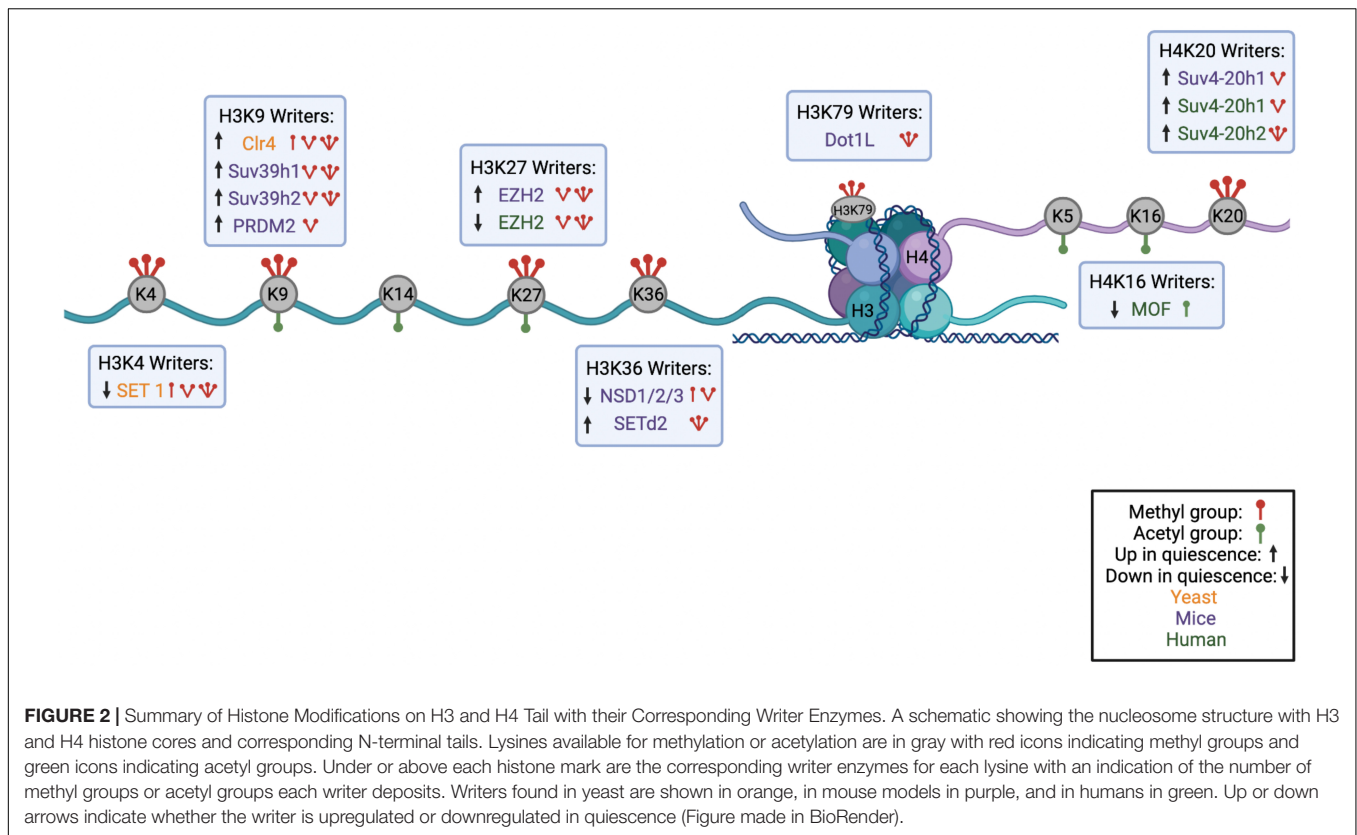
## Stem Cell Models of Quiescence

Adult stem cells are another widely used quiescence model. Stem cells have been used to study quiescence in the context of the tissue-specific niche in which they are located. Many types of stem cells are largely quiescent unless activated to proliferate and differentiate in order to maintain tissue homeostasis and tissue regeneration (Li and Bhatia, 2011; Cheung and Rando, 2013; Coller, 2019b; Urbán and Cheung, 2021). Dysregulation or loss

of stem cell quiescence can result in depletion of a stem cell pool, which can impede tissue regeneration (Cheung and Rando, 2013). Cellular quiescence has been studied in different types of adult stem cells such as hair follicle stem cells (HFSCs) within the skin (Lien et al., 2011; Lee et al., 2016; Rodriguez and Nguyen, 2018), hematopoietic stem cells (HSCs) from bone marrow (Nakamura-Ishizu et al., 2014), neural stem cells (NSCs) in the brain (Basak et al., 2018), and skeletal muscle stem cells (MuSCs) (Fukada et al., 2007). In the skin, the hair follicles that anchor hair to the skin progress through a cycle. During the anagen phase, there is rapid cell proliferation and growth of a new hair follicle. In the catagen phase that follows, the hair stops growing and detaches from the blood supply. Finally, in the telogen phase or resting phase, a new hair grows beneath the existing hair. Quiescent, non-proliferative hair follicle stem cells, which can be identified with cell surface markers including CD34 and CD49 (Garza et al., 2011), reside within a portion of the hair follicle called the bulge during the hair follicle's resting stage, the telogen phase. During the transition from telogen to anagen, HFSCs are activated, exit the bulge and proliferate downward, creating a trail of rapidly proliferating cells (Nowak et al., 2008). These proliferating cells terminally differentiate to give rise to cells that form the new hair shaft and its channel. Hair follicle stem cells have been an important model system for understanding quiescence, including the epigenetics of quiescence.

Another important model system for understanding quiescence is the hematopoietic stem cell (HSC) compartment. HSCs are the stem cells that give rise to other blood cells including both myeloid and lymphoid lineages. In adult animals, hematopoiesis occurs in the bone marrow and the stem cells are only a small fraction of all of the cells present. The HSCs with the greatest capacity for self-renewal in the mouse bone marrow are quiescent HSCs (Wilson et al., 2008; Tesio et al., 2015) which are long-term label retaining and are in a deeply quiescent state (Foudi et al., 2009; Tesio et al., 2015). They are reported to divide only 5 times per lifetime (Foudi et al., 2009; Tesio et al., 2015). In response to infection or chemotherapy, these cells enter the cell cycle and start to proliferate to replenish damaged or lost cells (Wilson et al., 2008; Tesio et al., 2015). HSCs can be identified and isolated from surrounding cells by combinations of cell surface markers, including the presence of CD34 and an absence of markers for specific cell lineages (Sieburg et al., 2006; Dykstra et al., 2007; Kent et al., 2007).

Neural stem cells (NSCs) are present in the developing brain where they generate neurons (Ma et al., 2009). In adult animals, specific regions in the brain contain NSCs that have the capacity to proliferate and generate new neurons, thereby allowing adults to learn and acquire new skills, for instance, the ability to smell new odors (Ma et al., 2009; Obernier et al., 2018; Kalamakis et al., 2019). Like quiescent HFSCs, NSCs *in vivo* are thought to be slowly dividing and can be identified based on their label retention (Ma et al., 2009). These NSCs are depleted as organisms age (Obernier et al., 2018), and recent studies in single cells have shown an increase in quiescent NSCs in older mice compared with younger mice (Kalamakis et al., 2019). Markers for NSCs include expression of glial fibrillary acidic protein and



glycoprotein CD133, along with an absence of differentiated cell markers (Ma et al., 2009).

Finally, muscle stem cells (MuSCs), or muscle satellite cells, represent another valuable quiescence model as MuSCs are mostly quiescent in uninjured tissue (Cheung et al., 2012). Muscle stem cells are crucial for the process of regenerating skeletal muscle (Boonsanay et al., 2016). Upon muscle injury, quiescent satellite cells are activated to re-enter the cell cycle and proliferate (Yin et al., 2013). The proliferating progeny of the muscle satellite cells can differentiate into myotubes that form muscle fibers (Dumont et al., 2015; Boonsanay et al., 2016). Other MuSCs return to quiescence and are available to assist in the repair of subsequent muscle injury events (Yin et al., 2013). *In vivo* analysis of MuSCs has revealed that MuSCs are primed for activation (van Velthoven et al., 2017). The quiescent state of MuSCs has been reported to be an “idling” state for stem cells because widespread, low-level transcription was observed and hypothesized to serve as a means to ensure that the transcription machinery is ready to respond when required (van Velthoven et al., 2017).

Stem cells in these different models are normally found in a quiescent state that is maintained by specific niches that are tightly regulated by intrinsic and extrinsic factors (So and Cheung, 2018). Within these complex niches and diverse tissue compartments, quiescent stem cells are identified by their low RNA content and lack of proliferative markers (Fukada et al., 2007). In many cases, quiescent stem cells can be isolated from the tissue of interest by monitoring the presence and levels of cell-surface markers with fluorescence-activated cell

sorting (FACS), and label-incorporation assays that identify cells that haven’t divided for an extended time (Cheung and Rando, 2013; Nakamura-Ishizu et al., 2014). While this general pattern of quiescent stem cells is reported in multiple tissues, it is important to note that not all stem cells are quiescent, and in some tissues, stem cells are proliferative (Barker et al., 2007).

## H3 METHYLATION WITH QUIESCENCE

Histone H3 has more potential methylation sites than any other histone in the histone octamer. Lysine residues 4, 9, 27, and 36 within the tail region of H3 are the most frequently methylated amino acids (Hyun et al., 2017; Jambhekar et al., 2019). In addition, H3K79, a lysine located within the globular domain of the histone, rather than on the tail, can also be methylated (Farooq et al., 2016). Each of the H3 lysines can be mono- (me), di- (me<sub>2</sub>), or tri-methylated (me<sub>3</sub>) by histone methyltransferases (writers) (Husmann and Gozani, 2019), and the methylation marks can be removed by histone demethylases (erasers). Histone methyltransferases, with the exception of DOT1L, contain a Suppressor of variegation, Enhancer of zeste, and Trithorax (SET) domain that catalyzes methylation of the lysine ε-amino group (Desjarlais and Tummino, 2016). Methylations of different histone lysines have characteristic deposition patterns that support a possible role for them in establishing different types of chromatin either by modulating the accessibility of the DNA to proteins, or by serving as a binding site for readers that act as

effectors. Below we discuss the evidence that each of these marks plays a role individually and in combination in quiescence. Many of these marks have been investigated individually, but not in combination, and thus in many instances, our understanding of how they contribute to a histone code is limited.

## H3K4 Methylation

H3K4me1/me2/me3 are usually associated with gene activation (Jambhekar et al., 2019). H3K4me1, me2, and me3 methylation marks are enriched in enhancers, the 5' ends of genes, and promoters, respectively (Hyun et al., 2017; Jambhekar et al., 2019). Methylation of H3K4 is associated with gene activation and the presence and absence of H3K4 methylation marks provides insight into the genome-wide patterns of active and inactive genes, respectively. Changes in genome-wide H3K4 methylation patterns with quiescence provide insights into gene activation and repression with quiescence. Whether these changes are functionally important for the changes in gene expression with quiescence, or are only correlated with quiescence, and whether H3K4 marks act alone or in combination with other marks or effector proteins, is the subject of active investigation in multiple model systems.

Young and colleagues investigated these questions in budding yeast *S. cerevisiae* by inducing the yeast into quiescence by glucose depletion (diauxic shift) and analyzing the yeast at 7 and 14 days. Overall levels of H3K4me2 were similar between log (proliferating cells) and stationary phase cells containing a mixture of quiescent and non-quiescent cells (Table 3) (Young et al., 2017). Levels of H3K4me3 decreased about 50% in quiescent and non-quiescent stationary phase cells compared with proliferating cells in these studies (Young et al., 2017). In another study focused on cell cycle entry from quiescence, *S. cerevisiae* were maintained in a nutrient depleted environment and then restimulated with complete medium (Mews et al., 2014). In this study, Mews and colleagues found that overall levels of H3K4me1, H3K4me2 and H3K4me3 were similar in log and a mixture of quiescent and non-quiescent stationary phase cells (Mews et al., 2014).

While H3K4me3 levels were similar or changed by 50% in the two studies comparing proliferating and stationary phase budding yeast, there was an observed difference in transcription rate between these two populations of cells. Levels of RNA Pol II CTD residues phospho-Ser5 and phospho-Ser2, which are indicators of transcriptional initiation and elongation, respectively, were high in day 3 post-diauxic cells, and subsequently decreased in day 5 post-diauxic cells (Young et al., 2017). In both proliferating and quiescent cells, H3K4me3 and RNA polymerase II were found at gene promoters, but the distribution of the H3K4me3 mark among promoters shifted with quiescence (Young et al., 2017). H3K4me3 was more abundant at the promoters of growth-associated genes in log phase yeast (Mews et al., 2014). Genes that retained the H3K4me3 mark and RNA Pol II at their promoters in quiescent yeast included genes responsible for stress response, protein catabolism, and energy production (Mews et al., 2014; Young et al., 2017). Thus, an association was observed between the presence of the H4K3me3 histone mark and activation of

genes with quiescence, but further studies would be needed to determine whether this constitutes a “code” and if so, what the functional consequences of this mark are for quiescence.

Further studies have evaluated the functional importance of H3K4 methylation for quiescence in strains of *S. cerevisiae*. *S. cerevisiae* were genetically engineered so that lysine 4 of histone H3 was mutated to alanine. These mutant strains lost reproductive capacity over time, after being introduced into stationary phase, to a greater extent than wild-type yeast (Walter et al., 2014; Young et al., 2017). Further, in this mutant strain, the proportion of non-quiescent cells in the stationary phase increased (Walter et al., 2014; Young et al., 2017). These results indicate that methylation of H3K4 is required for the establishment or maintenance of a quiescent state initiated in response to nutrient depletion.

The effects of removal of H3K4 methylation marks (demethylation) have also been characterized in *S. cerevisiae* during spore production. In *S. cerevisiae* spores, which have very low transcription rates, there is an accumulation of the highly conserved H3K4 demethylase JARID1-family histone 2 (JHD2) during sporulation (Xu et al., 2012) (Figure 1). The spores of JHD2 mutant yeast strain, *jhd2Δ*, show a ~2-fold increase in H3K4me3 and reduced levels of H3K4me1/me2 compared to wild-type spores, suggesting that absence of JHD2 leads to the conversion of H3K4me1/me2 to H3K4me3 (Xu et al., 2012). Studies with wild-type and *jhd2Δ* mutant strains indicated that JHD2 demethylases reduce intergenic transcription induced by H3K4me3 during spore differentiation, promoted protein coding gene transcription, and repressed nucleosome accumulation at transcription start sites (TSSs) of a large subset of ribosomal protein-coding genes. Mutants of *jhd2* exhibited precocious differentiation and the spores formed were sensitive to stress. Since JHD2 needs alpha-ketoglutarate from the TCA cycle for enzymatic function, it is possible that this family of proteins can sense carbon metabolism activity, which in turn regulates transcription in response to nutrient availability (Xu et al., 2012). These findings, taken together, suggest that H3K4me3 may be a mark that can transform information about nutrient availability into a complex pattern of gene expression that has distinct effects on protein coding genes, ribosomal genes and non-coding RNAs.

The role of H3K4 methylation has been studied in the context of quiescent mammalian cells as well. Kallingappa and colleagues compared chromatin states of proliferating bovine adult ear skin fibroblasts in the G1 phase of the cell cycle with chromatin composition of serum-starved, quiescent (G<sub>0</sub>) fibroblasts (Kallingappa et al., 2016). With fluorescence microscopy, quiescent nuclei were found to have a more relaxed or less compact chromatin state, and half the levels of H3K4me3 compared to G1 nuclei (Kallingappa et al., 2016). In mouse B cells, there was a dramatic shift in histone H3K4 methylation with quiescence, with much lower H3K4me2 levels in quiescent mouse B cells compared to cycling mouse B cells (Baxter et al., 2004). Reduction of H3K4me3 levels was also observed in quiescent mouse HSCs in late catagen stage in comparison to proliferating HSCs in early anagen stage (Lee et al., 2016; Kang et al., 2020). Based on ChIP-seq, the H3K4me3 signal generally decreased

**TABLE 3 |** Levels of histone marks in different quiescence systems.

Histone mark	General location	Generally associated with gene activation or repression?	Present within yeast	Up with quiescence	Down with quiescence
H3K4me2	Euchromatin	Gene activation	<i>Saccharomyces cerevisiae</i> ( <i>S. cerevisiae</i> ) <i>Schizosaccharomyces pombe</i> ( <i>S. pombe</i> )		Decreased in sporulating yeast (Xu et al., 2012), mouse skin and HFSCs (Lee et al., 2016), and mouse B lymphocytes (Baxter et al., 2004)
H3K4me3	Euchromatin	Gene activation	<i>S. cerevisiae</i> <i>S. pombe</i>	Increase in adult mouse muscle stem cells (Liu et al., 2013)	Decrease in quiescent yeast (Xu et al., 2012; Young et al., 2017), sporulating yeast (Xu et al., 2012), bovine fibroblasts (Kallingappa et al., 2016), and in HFSCs (Kang et al., 2020)
H3K9me2	Heterochromatin	Gene repression	<i>S. pombe</i>	increased in muscle quiescent stem cells (Cheedipudi et al., 2015)	reduced in yeast (Oya et al., 2019) and bovine fibroblasts (Kallingappa et al., 2016)
H3K9me3	Heterochromatin	Gene repression	<i>S. pombe</i>	increased in MuSCs (Boonsanay et al., 2016)	reduced in mouse skin and HFSCs (Lee et al., 2016), yeast (Oya et al., 2019), and bovine fibroblasts (Kallingappa et al., 2016)
H3K9ac	Euchromatin	Gene activation	<i>S. cerevisiae</i> <i>S. pombe</i>		Global decrease in yeast (Mews et al., 2014)
H3K14ac		Gene activation	<i>S. cerevisiae</i> <i>S. pombe</i>		Decreased in muscle quiescent stem cells and yeast (Cheedipudi et al., 2015; Young et al., 2017)
H3K27me3	Heterochromatin	Gene repression			Decrease in skin and hair stem cells for growth (Kang et al., 2020), in mouse skin and HFSCs (Lee et al., 2016), and in bovine fibroblasts (Kallingappa et al., 2016)
H3K27ac	Euchromatin	Gene activation	<i>S. cerevisiae</i> <i>S. pombe</i>	Increase in neural stem cells (Martynoga et al., 2013)	
H3K36me1/me2/me3	Euchromatin	Gene activation	<i>S. cerevisiae</i> <i>S. pombe</i>	me3 increase in mouse bone marrow cells (Zhou et al., 2018)	reduced in bovine fibroblasts (Meng et al., 2020)
H3K79me1/me2	Heterochromatin		<i>S. cerevisiae</i> <i>S. pombe</i>		loss in yeast (Young et al., 2017)
H4K5ac	Euchromatin	Gene activation	<i>S. cerevisiae</i> <i>S. pombe</i>		Global decrease in yeast (Mews et al., 2014)
H4K16ac	Euchromatin	Gene activation	<i>S. cerevisiae</i> <i>S. pombe</i>		decreased in skeletal muscle stem cells and ESCs (Ryall et al., 2015; Kang et al., 2020)
H4K20me3	Heterochromatin	Gene repression	<i>S. pombe</i>	increased in primary human dermal fibroblasts (Everitts et al., 2013a), in MuSCs (Boonsanay et al., 2016)	

at transcription start sites and overall in quiescent compared with proliferating HSCs, although there was no clear correlation between H3K4me3 marks and gene expression changes with proliferation or quiescence (Lee et al., 2016). These findings suggest that H3K4 methylation may have other roles in addition to transcriptional regulation. Indeed, a recent article re-evaluating the role of histone-modifying enzymes argues that histone H3K4 methylation only has a minor role in transcriptional regulation (Rickels et al., 2017; Morgan and Shilatifard, 2020), but that H3K4 methylation has been associated with DNA recombination, repair, and replication (Daniel and

Nussenzweig, 2012; Acquaviva et al., 2013; Kantidakis et al., 2016).

Similar results were observed in MuSCs where neither the number nor the identify of genes marked by H3K4me3 at their transcription start site changed in activated compared with quiescent stem cells, and quiescence-specific genes retained their H3K4me3 mark at their transcription start site even upon activation (Liu et al., 2013). The authors conclude that H3K4me3 marks genes for transcriptional activation but its presence is not sufficient to determine whether a gene will be expressed (Liu et al., 2013).



Evidence for the importance of H3K4 demethylation as a regulator of quiescence is derived from studies of Retinoblastoma binding protein 2 (RBP2), which can demethylate all the methylation states of H3K4 *in vivo* (Klose et al., 2007). *In vitro*, RBP2 can processively remove the me3 and me2 marks on H3K4 to return the histone to a singly methylated state, but it cannot demethylate the me1 mark (Klose et al., 2007). Hematopoietic stem cells (HSCs) and myeloid progenitors isolated from *Rbp2* knockout mice (*Rbp2*<sup>-/-</sup>) contain a higher proportion of cells exiting quiescence compared to WT. Further, in *Rbp2*<sup>-/-</sup> cells, genes encoding cytokines were marked with higher levels of H3K4me3 and were expressed at higher levels, which could promote proliferation of the HSCs (Klose et al., 2007). In addition to the JmjC domain that is responsible for the demethylase activity, KDM5A/RBP2 also contains 2-3 plant homeodomain (PHD) domains (Klose et al., 2007). Binding of the PHD domain to unmodified H3 peptide activates the KDM5A/RBP2 catalytic activity and results in removal of methyl marks from histone H3K4me3 from a nearby nucleosome (Torres et al., 2015). By coupling the KDM5A/RBP2's ability to read unmodified H3K4 with demethylation of nearby H3K4me3, results in a positive feedback loop that allows the spreading of a chromatin state of demethylated histones (Torres et al., 2015).

The data that are currently available suggest that methylation of H3K4 may play a role in aspects of quiescence, including potentially transcription, but whether this mark is a determinant of gene expression or simply associated with an activated promoter is not yet clear. H3K4 methylation could also contribute to quiescence through its roles in replication, repair or recombination. Establishing whether H3K4 methylation affects quiescence entry or maintenance through direct effects on the biomechanical properties of the DNA or through readers, whether it is part of a histone code, and how this affects functional aspects of quiescence will require additional studies.

## H3K9 Methylation

H3K9 methylation marks are primarily associated with gene repression in heterochromatin regions (Saksouk et al., 2015). H3K9me3 associates with regions of constitutive heterochromatin such as repeat regions of telomeres and centromeres (Saksouk et al., 2015). H3K9me3 is also deposited

at some genomic regions in a tissue-specific manner and plays a role in cell identity (Ninova et al., 2019). Given the observation that in some systems, chromatin is more compact in quiescent than proliferating cells (Bridger et al., 2000; Everts et al., 2013a; Guidi et al., 2015; Criscione et al., 2016; Swygert et al., 2019, 2021), H3K9 methylation is of particular interest as a potential regulator of chromatin compaction with quiescence.

In fission yeast, there is only one H3K9 methyltransferase, Clr4/Suv39H, which adds H3K9me1, me2, and me3 marks (Figure 1, Table 4). Inactivation of Clr4 resulted in viability similar to wild-type cells when nutrients were present, but reduced viability when quiescence was initiated following nitrogen starvation or glucose deprivation (Joh et al., 2016). This trend was also observed in yeast cells with a mutation that converted histone H3 lysine 9 to an alanine, suggesting that H3K9 methylation is important for survival during quiescence (Joh et al., 2016). Global ChIP-seq analysis showed that as fission yeast enter quiescence, the cells accumulate Clr4-dependent H3K9me2 and H3K9me3 marks at euchromatic genes whose transcriptional regulation has been shown to be important for establishing quiescence including genes involved in metabolism, ribosomal genes, cell cycle genes and stress response genes (Joh et al., 2016). In this study, a strong correlation was observed between genes with H3K9me2 marks and the set of genes repressed in G<sub>0</sub> (Joh et al., 2016). The enrichment of H3K9 methylation marks in euchromatic gene regions upon quiescence entry required the small RNAs (sRNAs) associated with RNA interference (RNAi) factor Argonaute (Ago1). Quiescent yeast had a distinct profile of these sRNAs (Joh et al., 2016). Before H3K9 is deposited in these euchromatic regions in quiescent yeast, Ago1-associated sRNAs are expressed from these regions (Joh et al., 2016), and these sRNAs may serve as guides for the deposition of H3K9 methylation marks (Joh et al., 2016). This may reflect a mechanism for regulating the expression of specific genes as yeast enter quiescence. In contrast to euchromatic regions, the levels of H3K9me2 in constitutive heterochromatic regions decline early during quiescence (8h and 24h after starvation) (Oya et al., 2019). These findings support the possibility of a combined histone-RNA code that controls gene expression and viability during quiescence. Surprisingly, the authors observed relatively little overlap between the H3K9me3-enriched genes

**TABLE 4 |** The relationship of histone writers with quiescence.

Histone writers (HGNC ids)	Histone mark	Model	Relationship with cell quiescence	References
SET1	H3K4me1/2/3	Fission Yeast	Downregulated in quiescence	Young et al., 2017
Clr4	H3K9me1/2/3	Fission Yeast	Upregulated in quiescence	Joh et al., 2016
Suv39h1	H3K9me2/3	Mouse Primary Keratinocytes	Upregulated in quiescence	Lee et al., 2016
Suv39h2	H3K9me2/3	Mouse Primary Keratinocytes	Upregulated in quiescence	Lee et al., 2016
PRDM2	H3K9me2	Mouse Myoblasts	Upregulated in quiescence	Cheedipudi et al., 2015
EZH2	H3K27me2/3	Mouse Primary Keratinocytes	Upregulated in quiescence	Lee et al., 2016
NSD1/2/3	H3K36me1/2	Murine Adult Hematopoietic Stem Cells	Downregulated in quiescence	Zhou et al., 2018
SETD2	H3K36me3	Murine Adult Hematopoietic Stem Cells	Upregulated in quiescence	Zhou et al., 2018
MOF	H4K16ac	Human Embryonic Stem Cells	Downregulated in quiescence	Khoa et al., 2020
Suv4-20h1	H4K20me2	Mouse Skeletal Muscle Stem Cells	Upregulated in quiescence	Boonsanay et al., 2016
		Primary Human Dermal Fibroblasts	Upregulated in quiescence	Everts et al., 2013a
Suv4-20h2	H4K20me3	Primary Human Dermal Fibroblasts	Upregulated in quiescence	Everts et al., 2013a

in quiescent cells and the genes that are repressed by Clr4 in quiescence based on RNA-seq analysis of wild-type and *clr4*-deleted yeast strains (Joh et al., 2016). This disconnect between the two genesets shows that additional studies will be needed to clearly determine whether H3K9 methylation plays a role in regulating transcription with quiescence, whether transcriptional regulation by H3K9 is crucial for viability in the quiescent state, and whether the effects of H3K9 in conjunction with short RNAs constitute part of a quiescence histone code.

Similar to the findings in fission yeast, in hair follicles, quiescent HFSCs that were isolated from the late catagen stage of the hair follicle cycle contained considerably lower levels of the H3K9me3 mark compared to proliferating HFSCs isolated from the early anagen stage of the hair follicle cycle (Lee et al., 2016; Kang et al., 2020) (Table 3). In contrast to other studies, Boonsanay et al. found no change in the levels of H3K9me3 between proliferating and quiescent mouse MuSCs (Boonsanay et al., 2016). This study did not measure the global distribution of H3K9 methyl marks, and thus the genomic regions where H3K9 methyl marks are found or how they are redistributed in proliferating and quiescent MuSCs is not known (Boonsanay et al., 2016).

Studies of fibroblasts have also revealed differences in the levels of H3K9 methyl marks with quiescence although the changes observed varies in fibroblasts from different sources. In adult ear skin fibroblasts, overall levels of H3K9me2 and me3 were roughly halved in quiescent cells compared to the same fibroblasts in the G1 phase of the cell cycle, while the levels of H3K9me1 were slightly elevated in quiescent relative to G1 cells (Kallingappa et al., 2016). In contrast, levels of H3K9me3 were modestly elevated in quiescent human dermal fibroblasts compared to proliferating fibroblasts (Everitts et al., 2013a), while levels of H3K9me2 and H3K9me1 were similar (Everitts et al., 2013a). In mouse B lymphocytes, the levels of H3K9me2 and me3 were lower in quiescent cells compared to activated cells (Baxter et al., 2004). Thus, in different quiescence model systems, changes in the levels of H3K9 methylation states are altered, but the specific changes reported have been different depending on the model system, and thus a consistent quiescence program of H3K9 methylation changes has not been observed.

In mammals, there are multiple methyltransferases that add methyl groups to histone H3 lysine 9 including the 17 members of the PRDM family of proteins (Steele-Perkins et al., 2001; Hyun et al., 2017). One of these members, PR domain-containing-2/Rb interacting zinc finger protein (PRDM2/RIZ) is expressed at high levels in quiescent mouse MuSCs *in vivo* (Cheedipudi et al., 2015) (Table 4). Knockdown and overexpression studies of PRDM2/RIZ indicated that in quiescent MuSCs, PRDM2/RIZ prevents lineage commitment and irreversible cell cycle arrest (Cheedipudi et al., 2015). Global analysis using ChIP coupled with DNA microarray (ChIP-Chip) showed that PRDM2 was associated with >4400 gene promoters in quiescent muscle cells that initiate quiescence in suspension culture, that is, loss of adhesion. Approximately 50% of these promoters were also marked with H3K9me2 (Cheedipudi et al., 2015). The PRDM2-associated genes were enriched for differentiation, cell cycle, and

developmental regulators (Cheedipudi et al., 2015). The levels of H3K9 methylation marks (me1, me2, and me3) did not change overall upon knockdown of PRDM2 (Cheedipudi et al., 2015). However, H3K9me2 levels were reduced at the MyoG promoter in G<sub>0</sub> cells, while PRDM2 knockdown cells showed reduced H3K9me2 at the same locus, suggesting that PRDM2 may add methyl groups to generate H3K9me2 at MyoG (Cheedipudi et al., 2015). Further, increased H3K14Ac was observed at the MyoG promoter upon PRDM2 knockdown, supporting a role for PRDM2 in regulating the expression of MyoG, a critical molecule for muscle differentiation (Cheedipudi et al., 2015). These findings support a model in which PRDM2 activation in G<sub>0</sub> ensures that two distinct possible outcomes—myogenesis and cell cycle progression—are poised for reactivation. The findings implicate H3K9 methylation, possibly in combination with other histone marks, in muscle stem cell quiescence and renewal (Cheedipudi et al., 2015).

Thus, while quiescence is generally associated with a reduction in transcription and number of active genes based on H3K4 methylation status as well as other markers, surprisingly in most, but not all, studies, there was not an increase in the H3K9me2 and H3K9me3 marks that might be expected. H3K9me3 is associated with constitutive heterochromatin (Saksouk et al., 2015) and it is possible that the increase in heterochromatin with quiescence reflects an increase in facultative heterochromatin. Nevertheless, even though H3K9me2/3 are not consistently observed to increase with quiescence, in yeast, there is evidence that these marks may be functionally important for the viability of quiescent cells as perturbations that reduce their levels reduce viability of quiescent cells with little effect on cells in full nutrient conditions. The data taken together support a possible role for H3K9 marks as contributors to changes that ensure the viability of quiescent cells, but these effects may be mediated through mechanisms other than transcriptional changes.

## H3K27 Methylation

The H3K27me3 mark is found in multiple model organisms including *Arabidopsis*, *Drosophila*, worms, and the filamentous fungus *Neurospora crassa*, but not yeast (Jamieson et al., 2013). H3K27me3 is a reversible mark of facultative heterochromatin, chromatin that can become compact or open depending upon the circumstance and is not repetitive (Trojer and Reinberg, 2007). H3K27me3 decorates genes that are developmentally regulated and are switched on and off depending upon the stage of development (Jambhekar et al., 2019). The Enhancer of Zeste 1 (EZH1) and EZH2 histone lysine methyltransferases trimethylate H3K27, and are constituents of Polycomb Repressive Complex 2 (PRC2) (Margueron and Reinberg, 2011) (Figures 1, 2, Table 4), while PRC1 stabilizes PRC2 binding to H3K27 and catalyzes monoubiquitination of histone H2A lysine 119 (Margueron and Reinberg, 2011). This ubiquitination mark represses transcription (Lavarone et al., 2019) and promotes chromatin compaction (Wiles and Selker, 2017; Lavarone et al., 2019). The Embryonic Ectoderm Development (EED) protein subunit of the PRC2 complex binds to H3K27me3 and this interaction increases the methyltransferase activity of the complex, resulting in a positive feedback loop that establishes

zones of repressed chromatin (Margueron et al., 2009; DesJarlais and Tummino, 2016).

In some studies, H3K27me3 levels were reduced with quiescence. In bovine fibroblasts, which exhibit more open chromatin with quiescence, H3K27me3 levels were reduced by approximately a half when the fibroblasts entered quiescence in response to serum starvation (Kallingappa et al., 2016). Similarly, protein levels of the members of PRC2—EZH2, EED, and Suppressor of Zeste 12 (SUZ12)—were reduced by about half in G<sub>0</sub> nuclei (Kallingappa et al., 2016). Proteins in the PRC1 polycomb complex were also reduced in quiescent bovine fibroblasts, specifically Polyhomeotic Homolog (PHC1) and Ring Finger Protein 2 (RING2) (Kallingappa et al., 2016). H3K27me3 levels are also reduced in quiescent mouse B lymphocytes compared to activated and cycling B lymphocytes (Baxter et al., 2004).

In contrast, murine chondrocytes (cartilage cells) that entered into a quiescent state by the application of physiological hydrostatic pressure had lower levels of H3K9me3 and higher levels of H3K27me3 compared to control cells that were not subjected to hydraulic pressure (Maki et al., 2021). In primary human dermal fibroblasts, a mass spectrometry-based analysis of histone post-translational modifications revealed higher levels of H3K27me3 in contact-inhibited, quiescent fibroblasts than proliferating fibroblasts (Everitts et al., 2013a). Further dissection of the H3K27me3 signal revealed that levels were particularly high when H3K27me2 was found in combination with H3K36me2 or if H3K27me3 was found on the same histone tail as H3K36me1 and H3K36me2 (Everitts et al., 2013a). This pattern of histone modifications may reflect the fact that H3K36me3 can inhibit the ability of PRC2 to methylate H3K27 (Schmitges et al., 2011; Yuan et al., 2011).

H3K27me3 levels have been observed to be reduced in multiple quiescence model systems involving stem cells. Quiescent mouse HFSCs isolated in the late catagen (quiescent) stage experienced a global decrease in the levels of H3K27me3 along with a decrease in H3K4me3 and H3K9me3, as mentioned in the sections above, compared to cycling HFSCs in early-anagen stage. This hypomethylation of quiescent HFSCs was confirmed using immunofluorescence, western blotting, and ChIP-seq methods (Lee et al., 2016). The levels of H3K27me3 were reduced in 64% of promoters with quiescence in HFSCs (Lee et al., 2016). Surprisingly, the changes in the levels of histone methylation marks, overall, did not correlate with changes in the levels of transcripts for the associated genes in quiescent versus proliferating hair follicle cells (Lee et al., 2016). There were exceptions: a larger than expected fraction of genes highly expressed at all hair cycle stages in the bulge had an increase in the levels of H3K27me3 and a set of genes defined as cell cycle regulators and tumor suppressors had almost no H3K27me3 in quiescent and proliferating HFSCs (Lee et al., 2016). To explore a possible role for decreased histone methylation levels during catagen, the bone morphogenetic protein (BMP) signal which normally maintains quiescence *in vivo* was inhibited, resulting in elevated levels of H3 K4/K9/K27 me3 in quiescent bulge HFSCs (Lee et al., 2016). These findings demonstrate that quiescent HFSCs in the bulge require active BMP signaling in

order to maintain a hypomethylated H3 state (Lee et al., 2016). When keratinocytes, skin epithelial cells, were serum-starved in culture, transcript levels of several histone methyltransferases including EZH2 (forms H3K27me3), SUV39H1 and SUV39H2 (H3K9me3), decreased (Lee et al., 2016), while transcript levels of multiple histone demethylases increased (Lee et al., 2016). The latter include JMJD2a which catalyzes demethylation of histone H3 lysines 9 and 36 (Kim T.D. et al., 2012), UTX which demethylates H3K27me3 (Tang et al., 2017), and JARID1, which acts as a demethylase for H3K4me3 and H3K4me2 (Lee et al., 2016). After chemically inhibiting demethylases specific to the K4, K9, and K27 me3 marks with a cocktail applied to the mouse's skin, cells at the catagen stage failed to generate new hair follicles in the following hair cycle. Thus, the reduction in the H3K4/K9/K27 me3 levels observed in quiescent HFSCs was necessary for the ability of quiescent cells to re-enter the cell cycle (Lee et al., 2016). While these data support the importance of histone demethylation for the quiescent state of HFSCs, it remains unclear whether one, two or all of these marks was required for a functional state, whether these marks maintain chromatin structure or serve as binding sites for effectors, and whether the absence of the methylation marks affected the activity of other marks such as acetylation marks.

Three different studies have investigated the role of H3K27 methylation in quiescent mouse MuSCs (Liu et al., 2013; Cheedipudi et al., 2015; Boonsanay et al., 2016). Liu et al. found that H3K27me3 levels were low in quiescent MuSCs and dramatically increased in activated stem cells (Liu et al., 2013) (Table 3). The transcription start sites of genes expressed at high levels in quiescent stem cells were marked with H3K4me3, but not H3K27me3 (Liu et al., 2013). The 2,019 genes that were marked by H3K27me3 at their transcription start site in quiescent stem cells displayed very low expression levels (Liu et al., 2013). Upon activation, there was a dramatic increase in H3K27me3 in the gene body and intergenic regions (Liu et al., 2013). Boonsanay and colleagues, in contrast, reported that the levels of H3K27me3 were not different between quiescent and proliferating MuSCs (Boonsanay et al., 2016).

Both Boonsanay et al. and Liu et al. discovered changes in the levels of writers and erasers of H3K27me3 as quiescent mouse MuSCs were activated. Liu and colleagues reported that the increase in H3K27me3 marks with activation was associated with higher transcript levels of *Ezh2* and lower levels of the demethylase *Jmjd3* (Liu et al., 2013). Boonsanay and colleagues also found higher levels of PRC2-*Ezh2* in proliferating MuSCs and higher levels of PRC2-*Ezh1* in the quiescent MuSCs (Boonsanay et al., 2016). These findings would be consistent with a study by Margueron and colleagues that showed that *Ezh2* is more closely associated with proliferation, while *Ezh1* is more abundant in non-proliferative adult tissues (Margueron et al., 2008). Margueron and colleagues discovered that PRC2-*Ezh2* effectively catalyzes the formation of H3K27me2/3, while PRC2-*Ezh1* directly represses transcription and compacts chromatin. Additional studies would be needed to determine whether the differences in expression of these methyltransferases results in changes in the genome-wide



distribution of H3K27me2/3, whether there is a direct effect on transcription or chromosome compaction, or whether the shift in the relative abundance of these methyltransferases is functionally important for establishing, maintaining or reversing quiescence in MuSCs.

Cheedipudi and colleagues focused on H3K27me3 levels in MuSCs in the context of their co-existence with H3K4me3 and H3K9me2 and their co-regulation by the H3K9 methyltransferase PRDM2/RIZ. As described in the H3K9 methylation section above, PRDM2/RIZ, an H3K9 methyltransferase, is enriched in quiescent muscle cells *in vitro*, where it participates in stalling differentiation and cell cycle programs, while also maintaining genes involved in differentiation and proliferation poised for future activation (Cheedipudi et al., 2015). Cheedipudi and colleagues found that knocking down PRDM2 resulted in a reduction of H3K4me3 and H3K9me2, and higher levels of H3K27me3 at the cyclin A2 promoter in G<sub>0</sub> MuSCs (Cheedipudi et al., 2015). They conclude that PRDM2 may block the deposition of H3K27me3 silencing marks at the cyclin A2 promoter in G<sub>0</sub>, thereby preserving the gene's potential for reactivation (Cheedipudi et al., 2015). These studies highlight the combinatorial nature of the histone marks during the transition between proliferation and quiescence.

Thus, taken together, substantial changes in H3K27me3 have been observed in different models of quiescence. H3K27me3 may contribute to transcriptional repression in quiescent cells and may contribute to a poised quiescent state, characterized by an ability to re-enter the cell cycle. However, additional studies that probe the genomic location of H3K27me3 in proliferating and quiescent cells in different model system and their functional importance for quiescence will be needed to fully understand the specific role of H3K27 methylation individually or in combination with other marks in quiescence.

## H3K36 Methylation

H3K36 methylation marks are usually deposited across the entire gene body (Hyun et al., 2017; Jambhekar et al., 2019), and are associated with transcriptional activation, dosage compensation, transcriptional repression, and DNA repair (Wagner and Carpenter, 2012). In the study by Young and colleagues described above, quiescent budding yeast *S. cerevisiae* had similar levels of H3K36me2 and H3K36me3 marks compared to proliferating cells (Young et al., 2017). However, the levels of SET Domain containing 2 (Set2) which deposits all three (mono, di, and tri) methylation marks in budding and fission yeast (Morris et al., 2005; Wagner and Carpenter, 2012), were reduced as the cells entered a quiescent state. These findings indicated that H3K36me3 marks were deposited prior to quiescence entry, concomitant with the activity of RNA Pol II.

While yeast has only one H3K36 methyltransferase, humans have eight, including SETD2, the human ortholog of yeast Set2, that generates the H3K36me3 mark *in vivo*, and enzymes of the Nuclear Receptor-binding Set Domain (NSD) family (NSD1/2/3) that deposit H3K36me1 and H3K36me2 marks (Wagner and

Carpenter, 2012) (**Figure 2** and **Table 4**). The trimethylation of H3K36 by SETD2 is highly efficient on an unmethylated H3K36 compared to a H3K36me2 substrate (Husmann and Gozani, 2019). In *Setd2* conditional knockout mice with HSC-specific *Setd2* inactivation, there is a reduction of the number of HSCs in a quiescent state (Zhou et al., 2018). *Setd2* knockout HSCs had a reduced G<sub>0</sub> fraction and increased G1 and S/G2/M phases of the cell cycle (Zhou et al., 2018). In addition, knockout HSCs also exhibited higher levels of apoptosis, reduced stem cell identity, increased differentiation toward progenitors and reduced multiple-lineage terminal differentiation potential (Zhou et al., 2018). *Setd2* knockout mice had mild bone marrow fibrosis, increased erythroid progenitors, but a decreased population of other bone marrow progenitors. As a result, the HSCs from *Setd2* conditional knockout mice were less able to repopulate the hematopoietic system upon transplantation (Zhou et al., 2018). *Setd2* knockout HSCs showed significant reduction of H3K36me3, increased levels of H3K36me1/me2, and increased Nsd1/2/3 at both transcript and protein levels (Zhou et al., 2018). The levels of H3K4me3, H3K79me2, and phosphorylation of Ser2 residue of RNA pol II, all of which are associated with transcriptional elongation, increased in *Setd2* knockout cells. Based on these studies, the authors proposed a model in which, in the absence of SETD2, NSD proteins promote the phosphorylation and elongation of RNA pol II on specific genes, leading to a loss of quiescence (Zhou et al., 2018). The findings support an important role for SETD2 in maintaining the quiescent state of HSCs (Zhou et al., 2018). It is unclear whether SETD2 plays this role through H3K36me3 or non-enzymatic functions such as by affecting cryptic transcription (Carvalho et al., 2013) or alternative splicing (Bhattacharya et al., 2021).

## H3K79 Methylation

In contrast to the previously discussed histone marks that are located on the histone H3 tail, the H3K79 methylation mark is located in the globular domain of H3 (Farooq et al., 2016). H3K79me2 and H3K79me3 are mainly found in the bodies of active genes and are associated with transcription elongation (Mueller et al., 2007). H3K79me2/3 can also maintain enhancer-promoter interactions at a subset of enhancers (Godfrey et al., 2019). H3K79 methylation has also been implicated in telomere silencing (Singer et al., 1998), recombination, DNA repair and cell cycle progression (Nguyen and Zhang, 2011). Monomethylation and trimethylation of H3K79 has been associated with gene activation and gene repression, respectively, in some studies (Barski et al., 2007). Disruptor of Telomere Silencing—Dot1 in yeast and DOT1L in humans—is the only enzyme responsible for methylation of H3K79 in *S. cerevisiae*, *Drosophila*, and humans as knockout of DOT1 in these organisms results in a loss of H3K79 methylation (van Leeuwen et al., 2002; Lee S. et al., 2018) (**Figure 2** and **Table 4**). Both Dot1 and DOT1L can catalyze mono-, di- and trimethylation (Frederiks et al., 2008). Dot1 is the only known non-SET domain-containing methyltransferase (Farooq et al., 2016). *S. cerevisiae* Dot1 does not methylate free histones, only histones in chromatin, in contrast to other histone methyltransferases (Lacoste et al., 2002; Lee S. et al., 2018).



Yeast Dot1 also has histone chaperone activity and is particularly important for nucleosome dynamics and chromatin accessibility on transcribed regions of long genes (Lee S. et al., 2018).

After diauxic shift in *S. cerevisiae*, despite the general shut down of transcription, both the quiescent and non-quiescent yeast populations contained higher levels of the H3K79me3 mark than proliferating yeast cells (Young et al., 2017). However, the quiescent population had reduced H3K79me1 and H3K79me2 levels compared with the non-quiescent population (Young et al., 2017). Levels of Dot1 decreased by day 3 post-starvation and remained low throughout the time course that ended at day 7 (Young et al., 2017). The elevated levels of H3K79me3 and reduced levels of H3K79me1/2, while Dot1 was reduced could reflect that H3K79me3-containing nucleosomes were not turned over, or that demethylases were activated (Young et al., 2017). H3K79me3 was enriched in gene bodies in transcripts expressed specifically in growing cells or specifically in quiescent cells, with no redistribution to non-canonical locations in genes or intergenic regions (Young et al., 2017). Log and quiescent cells contained similar numbers of gene binding sites for H3K79me3 (Young et al., 2017). These marks were established soon after the shift to diauxic growth and then retained in quiescent cells even as transcription was reduced (Young et al., 2017). There was not a strong correlation between RNA polymerase II occupancy and H3K79me3 marks on specific genes in proliferating or quiescent cells (Young et al., 2017).

Mutant *S. cerevisiae* strains that are no longer able to methylate histone H3K4 or ubiquitinate histone H2B showed a shorter chronological lifespan, indicative of reduced ability to re-enter the cell cycle (Young et al., 2017). In contrast, a higher proportion of yeast entered quiescence upon glucose deprivation in H3K79 mutant, and the yeast with H3K79 mutations showed enhanced ability to re-enter the cell cycle (Young et al., 2017). The findings suggest that the presence of a lysine that can be methylated at H3K79 makes cells less able to re-enter the cell cycle after glucose deprivation, and surprisingly, makes the quiescent yeast less fit (Young et al., 2017).

The H3K79 mark has also been implicated in the quiescence of mouse HSCs. In a study described above, knockout of *Setd2*, a histone methyltransferase involved in the addition of the H3K36me3 mark, led to the loss of bone marrow reconstitution after transplantation, with the mouse HSCs exhibiting loss of quiescence, increased apoptosis, and inability to differentiate into multiple lineages (Zhou et al., 2018). When studying the changes at the histone level, it was found that knockout of *Setd2* led to increased expression of NSD1/2/3, which are also H3K36 methyltransferases that generate H3K36me1 and H3K36me2 marks (Zhou et al., 2018). Loss-of-function in *Setd2*, combined with gain-of-function NSD1/2/3, led to an increase in the H3K79me2 mark through recruitment of DOT1L, the H3K79 methyltransferase (Zhou et al., 2018). Together with increased recruitment of histone acetylase Brd4, which recruits the Super Elongation Complex (SEC), DOT1L enhanced RNA Polymerase II elongation and expression of target genes that promote apoptosis and differentiation of quiescent cells (Zhou et al., 2018). This resulted in increased expression of genes including *Myc*, as inhibiting Brd4 or Dot1l reduced markers of

transcription elongation and *Myc* expression (Zhou et al., 2018). The findings support a model where multiple histone-modifying enzymes are co-regulated to affect the choice between quiescence and differentiation (Zhou et al., 2018).

These studies, taken together, suggest H3K79 methylation may play a role in quiescence through mechanisms that involve transcription initiation or elongation, or alternative processes. In yeast, this mark reduces the ability of nutrient-starved cells to proliferate when provided nutrients. In mammalian HSCs, data support H3K79 methylation as part of a complex regulatory code that affects transcription elongation and the fate of quiescent HSCs.

## H4 METHYLATION WITH QUIESCENCE

While the N-terminus of H3 tails exit the nucleosome near DNA entry and exit sites, the tails of histone H4 (residues 1–20) stick out from the nucleosome's face on either side (Ghoneim et al., 2021). DNA breathing dynamics are altered upon removal of either the H3 or H4 tail, suggesting that there is cross-talk between the H3 and H4 tails (Ghoneim et al., 2021). The region encompassing residues 16–23 of H4 contains a high density of arginine and lysine residues that constitutes a basic patch (Ghoneim et al., 2021). In crystal structures, this H4 basic patch interacts with DNA or the cluster of acidic residues called the H2A/H2B acidic patch on the same or nearby nucleosomes (Ghoneim et al., 2021). Histone H4 is mainly methylated at residue K20 in mammalian cells. The methylation of K20 requires the acidic patch, as H4K20 monomethylation is not detected in nucleosomes with a defective acidic patch (Ho et al., 2021). H4K20 methylation is conserved from fission yeast *S. pombe* to humans (Jorgensen et al., 2013). Histone H4K20me1 has been observed in budding yeast *S. cerevisiae* (Edwards et al., 2011).

H4K20me1 can act both as a repressive and an activating mark (Huang et al., 2021). On one hand, H4K20me1 causes chromatin condensation (Lu et al., 2008; Oda et al., 2009), and in mammalian cells, can recruit L3MBTL1, a H4K20me1 reader that can induce nucleosome compaction (Trojer et al., 2007). On the other hand, in the genomes of some mammalian cells, H4K20me1 correlates with gene activation (Barski et al., 2007; Wang et al., 2008; Cui et al., 2009). H4K20me3 has been implicated in heterochromatin maintenance (Kourmouli et al., 2004), and localizes to telomeres (Kourmouli et al., 2004; Schotta et al., 2004; Benetti et al., 2007; Mikkelsen et al., 2007; Marion et al., 2011) and repeated elements, including transposable elements (Martens et al., 2005; Mikkelsen et al., 2007; Montoya-Durango et al., 2009; Rhodes et al., 2016). In addition, H4K20me3 has also been discovered in zinc fingers (Nelson et al., 2016), and promoters of E2F responsive genes (Abbas et al., 2010), histones (Abbas et al., 2010), inflammatory genes (Stender et al., 2012), and ribosomal genes (Bierhoff et al., 2014).

A ChIP-seq study in murine ESCs found that H4K20me3 colocalizes with transcriptionally active marks like H3K4me3 and H3K36me3 (Xu and Kidder, 2018). This bivalent placement of H4K20me3 with activating histone marks suggest a potential combinatorial histone code for a “poised” state. These “poised”

states have been suggested to allow for rapid activation of RNA pol II (Bernstein et al., 2006) during cell state transitions. Sims and colleagues report on another combinatorial code involving H4K20, but in conjunction with H3K9 (Sims et al., 2006). They found that H4K20me3 and H3K9me3 were both enriched in pericentric heterochromatin. H4K20me1 and H4K20me2 were found together with H3K9me1 and H3K9me2, respectively, but in different regions on chromosome arms (Sims et al., 2006). The authors further found that H4K20me1 and H3K9me1 were enriched in the same nucleosome (Sims et al., 2006). What role these bivalent marks play in quiescence is not known and requires additional exploration.

H4K20 methylation status is cell cycle dependent (Pesavento et al., 2008; Oda et al., 2009; Abbas et al., 2010; Centore et al., 2010; Adikes et al., 2020), at least in part because PR-Set-7, the enzyme that generates H4K20me1 (Fang et al., 2002; Nishioka et al., 2002b; Beck et al., 2012), is actively targeted for proteasome-mediated degradation in S phase (Rice et al., 2002; Julien and Herr, 2004; Jorgensen et al., 2007; Abbas et al., 2010; Tardat et al., 2010; Wu et al., 2010). Consistent with these previous reports, in primary human fibroblasts, unmodified H4K20 was most abundant in S phase, less abundant in G2/M cells, and present at low levels in G1 and cells that entered quiescence by contact inhibition for 14 days (Evertts et al., 2013a). H4K20me1 was present at low levels in S phase, increased in G2/M, and increased further in G1 (Evertts et al., 2013a). H4K20me3 represented a small fraction of all of the histones, and was strongly induced with quiescence compared with all other cell cycle phases (Evertts et al., 2013a) (Table 3).

Boonsanay and colleagues investigated the levels of different histone marks in quiescent mouse MuSCs, proliferating MuSCs and differentiated myotubes (Boonsanay et al., 2016). Quiescent MuSCs contained a lower level of H4K20me1, but comparable levels of H4K20me2 to that present in proliferating MuSCs. The levels of H4K20me3 were in the order: differentiated myotubes > quiescent MuSCs > proliferating MuSCs (Boonsanay et al., 2016) (Table 3). In contrast, H3K9me3 and H3K27me3 and euchromatin marker H3K9ac did not change between proliferating and quiescent MuSCs (Boonsanay et al., 2016). Without ChIP-seq data, the distribution of histone H4K20 methylation marks, and the extent of overlap with other histone marks in these different cells is not known.

In mammals, H4K20me1 is catalyzed by PR-SET-7 (Nishioka et al., 2002a) and the methyltransferases KMT5B/Suv4-20h1 and KMT5C/Suv4-20h2, and possibly KMT3E/SMYD3, generate H4K20me2 and H4K20me3 (Rice et al., 2002; Schotta et al., 2004, 2008) (Figures 1, 2, Table 4). Loss of both SUV4-20H enzymes leads to strongly elevated levels of H4K20me1 (Schotta et al., 2008). Electron micrographs of MuSC nuclei with inactivation of Suv4-20h1 revealed a reduction in condensed heterochromatin (Boonsanay et al., 2016). Loss of Suv4-20h1 lead to a reduced population of quiescent cells and increased population of differentiated cells expressing *MyoD* (Boonsanay et al., 2016). In Suv4-20h1-abrogated quiescent MuSCs, there was a reduction in H4K20me2 and nucleosome density, and an increase in H3K4me3, at the distal regulatory region (DRR)

that controls *MyoD* expression (Boonsanay et al., 2016). This indicates that DRR is more accessible in Suv4-20h1 knockout quiescent cells and this may allow expression of differentiation-related gene, *MyoD*. Thus, Suv4-20h1 reduces expression from the *MyoD* locus, resulting in the maintenance and preservation of stem cells in a quiescent state (Boonsanay et al., 2016). Further research will be required to determine whether this is a role for H4K20 methylation exclusively in MuSCs, or whether similar changes occur in other stem cells as well.

The H4K20 monomethyltransferase Pr-set-7 was discovered to regulate NSC quiescence in *Drosophila* (Huang et al., 2021). Targeted DNA adenine methyltransferase identification (TaDa) was used to determine genomic loci where Pr-set7 binds. This analysis revealed Pr-set-7 binds to the promoter and transcriptional start sites of Wnt pathway coactivator earthbound1 (*Ebd1*) and cyclin-dependent kinase 1 (*Cdk1*) (Huang et al., 2021). The mRNA levels of *Ebd1* and *Cdk1* were depleted in *pr-set7* mutant brains (Huang et al., 2021). Thus, by increasing expression of *Cdk1* and *Ebd1* in NSCs, Pr-set7 modulates the cell cycle and Wnt signaling, and thereby promotes NSC reactivation from quiescence (Huang et al., 2021). In these studies, The presence or absence of H4K20me1 in *Ebd1* and *Cdk1* promoters was not determined in this study (Huang et al., 2021).

In primary human dermal fibroblasts, mass spectrometry-based analysis of histone tails revealed that the histone lysine that showed the strongest change in methylation levels with quiescence was H4K20 (Evertts et al., 2013a). H4K20me2, and especially H4K20me3, were highly induced in quiescent cells when compared with proliferating fibroblasts as well as the fibroblasts that were specifically in the G1 phase of the cell cycle and contained the same DNA content as quiescent fibroblasts (Evertts et al., 2013a). In contrast, H4K20me1 levels were reduced in quiescent compared with proliferating fibroblasts. Further knockdown of Suv4-20h1 and Suv4-20h2 methyltransferases that catalyze formation of di and tri-methylated H4K20 with both small hairpin RNAs and small interfering RNAs (siRNAs) resulted in less chromatin compaction, consistent with a potential role for H4K20 trimethylation in chromatin conformation (Evertts et al., 2013a). Knockdown of Suv4-20h2 specifically, with siRNAs, resulted in increased proliferation and more cells in S phase (Evertts et al., 2013a). These findings support a role for Suv4-20h2 in both the regulation of the quiescence-proliferation transition and chromatin compaction with quiescence. Whether there is a direct link between these two activities, and whether they are mediated through H4K20 methylation will require additional studies.

Altogether, these studies highlight the critical role of H4K20 methylation, and in particular, H4K20me3, in regulating the transition between quiescence and proliferation. The consistent upregulation of H3K20me3 in multiple different quiescent models indicates it might play a larger role in establishing the functional state of chromatin in quiescence and may regulate specific gene expression changes necessary for quiescence entry, exit, and maintenance. Given the available data, it is possible that the H4K20 methylation marks act in cooperation with other marks, for instance it has been detected as part of bivalent promoters in combination with H3K4me3

and H3K36me3 (Xu and Kidder, 2018), and as part of heterochromatin in combination with H3K9me3 (Schotta et al., 2004). Taken together, the data support the possibility that H4K20me3 represents one part of a combinatorial code that regulates quiescence.

## HISTONE ACETYLATION WITH QUIESCENCE

### General Properties of Histone Acetylation

An array of conserved lysine residues is present in the N-terminal tails of the four histones forming the nucleosome and these positively charged lysines interact with the DNA and the negatively charged patch formed by H2A/H2B residues of the nearby nucleosome. The tail of histone H4 has the strongest effect on chromatin compaction, followed by the tail of histone H3, which is followed by the tails of histones H2A and H2B (Ghoneim et al., 2021). Histone acetylation weakens the interactions of tails with the DNA and the negative patch, thus making the chromatin more accessible to RNA Pol II (Park and Kim, 2020). In addition to affecting the structural state of the chromatin, acetylation can also affect the proteins bound to chromatin. Lysine acetylation marks on histone tails can be recognized by bromodomain-containing reader proteins (such as chromatin remodelers) that are generally associated with transcriptional activation (Agalioti et al., 2002; Barnes et al., 2019). The removal of acetyl groups by histone deacetylases can modulate the chromatin state to make the chromatin more compact. Further, in some cases, an individual lysine residue can be acetylated, methylated or ubiquitinated, and this establishes a potential for competition among these different lysine modifications.

The N-terminal tail of histone H3 is mainly acetylated at residues K9, K14, K18, and K23, while the corresponding region of H4 is acetylated at residues K5, K8, K12, and K16. Acetylation on H4K16 is particularly linked to unpacking of the chromatin and transcriptional activation—mainly due to diminished interactions between the H4 tail and the H2A/H2B acidic patch (Shogren-Knaak et al., 2006). The periodic nature of the amino acid spacing between the acetylatable lysines in the H3 and H4 tails suggests a potential for cooperative behavior among these amino acids (Strahl and Allis, 2000). In particular, this spacing has been noted to be reminiscent of the 3.6 residues per turn of an  $\alpha$ -helix, raising the possibility that these acetyl marks may act as part of a combinatorial code that provides information about which proteins should bind to chromatin at a specific genomic region (Strahl and Allis, 2000).

The combined presence of histone acetyl marks and other histone modifications have been shown to result in defined outcomes (Winter et al., 2008; Zippo et al., 2009). As one example of this combinatorial effect, Bromodomain PHD Finger Transcription Factor (BPTF), an ATP-dependent chromatin remodeling protein, has increased affinity for histones with two different marks. The presence of H3K4me3 and H4K16ac together results in a 2-fold stronger BPTF binding affinity

than either H3K4me3 or H4K16ac alone (Ruthenburg et al., 2011; Rando, 2012). This effect was not limited to H4K16ac as peptide microarray studies showed an increase in binding of PHD-Bromodomain constructs to histones when H3K4me3 was combined with any of multiple different H3 acetyl states (Fuchs et al., 2011; Rando, 2012). As another example, some proteins bind preferentially when a single epigenetic mark is found by itself, in the absence of another mark (Rando, 2012). This is exemplified by a PHD-Bromo domain chromatin regulator TRIPartite-Motif containing 24 (TRIM24) as this protein binds to H3K23ac to activate estrogen-responsive genes, but this binding is inhibited if H3K4 is also methylated (Tsai et al., 2010; Rando, 2012). Taken together, these reports suggest that a histone acetylation-dependent combinatorial histone code may encode information through the presence of individual histone marks, combinations of marks, their spacing, and the specific readers that recognize the marks. In the sections below, we focus on acetylation of histones H3 and H4 as these have been studied the most in relation to cellular quiescence.

### H3 Acetylation With Quiescence

In budding yeast *S. cerevisiae*, a global decrease in acetylation levels was observed after quiescence entry that parallels the repression of transcriptional activity in quiescence (McKnight et al., 2015). Upon entry into quiescence, the budding yeast cells have lower levels of histone H3 acetylation compared with log phase cells. Immunoblotting for histone H3K9ac, H3K23ac, and pan-acetyl histone H3 revealed a significant reduction in the levels of these marks in quiescent compared with proliferating yeast (McKnight et al., 2015). In a complementary set of studies, using mass spectrometry, Mews et al. showed that when quiescent yeast cells reentered the cell cycle upon nutrient replenishment, there was a burst of histone acetylation, specifically at H3K9 and H3K14, immediately upon cell cycle entry (Mews et al., 2014). In contrast, *de novo* histone methylation occurred at a later cell cycle stage after the acetylation burst. As compared to histone methylation, histone acetylation was more closely correlated with the transcriptional changes that took place soon after the cell cycle entry. Western blot analysis revealed that levels of acetylated histones H4K5ac, H4K8ac, and H3K9ac drop during quiescence and then robustly increase over a 240-min time course after nutrient refeeding. Using ChIP-seq, Mews and colleagues found that when yeast enter stationary phase, H3K9ac levels decreased at genes identified by microarrays as growth genes and increased at genes expressed when yeast initiated quiescence following nutrient exhaustion (Mews et al., 2014). After the nutrients were replenished, acetylation of H3K9 increased at growth genes and decreased at stress response genes (Mews et al., 2014). Histone acetylation rapidly responded to changes in metabolic state, while histone methylation levels were largely constant (Mews et al., 2014). Thus, *S. cerevisiae* undergo a dramatic increase in acetylation, and not methylation, when they re-enter the cell cycle from quiescence as nutrients are re-introduced (Mews et al., 2014; McKnight et al., 2015; Young et al., 2017).

The histone lysine deacetylase Rpd3 has been identified as an important regulator of quiescence entry and maintenance in



*S. cerevisiae* in a study by McKnight and colleagues (McKnight et al., 2015). When the yeast entered quiescence, motifs associated with transcription factors inactivated by nutrient exhaustion were associated with more repressive chromatin structure including more nucleosomes positioned over the motif and lower levels of histone acetylation (McKnight et al., 2015). Motifs for transcriptional activators that function in stress conditions had more open chromatin structure in the quiescent cells (McKnight et al., 2015). A large fraction of transcription factors with binding motifs that exhibit changes in chromatin structure with quiescence function by recruiting Rdp3 lysine deacetylase (McKnight et al., 2015). Deleting Rpd3 did not affect growth in the log phase and Rdp3-deleted cells maintained high viability in log phase (McKnight et al., 2015). Rpd3-deficient cells arrest after glucose exhaustion similarly to wild-type cells. However, fewer quiescent cells are formed in an *rdp3Δ* mutant and the quiescent cells that are formed show reduced long-term survival (McKnight et al., 2015). Analysis of chromatin structure at gene promoters revealed that Rpd3 has a significant role in establishing the transcriptional profile of quiescent cells by affecting the density of histone H3 and the acetylation of histone H4 at the promoters of genes regulated with quiescence (McKnight et al., 2015). The findings, taken together, support histone lysine acetylation as an important regulator of gene expression and viability during quiescence in *S. cerevisiae* (McKnight et al., 2015).

Studies in mouse NIH 3T3 embryonic fibroblasts that were serum starved to induce quiescence and then restimulated with serum addition revealed changes in histone acetylation (Knosp et al., 1991). Using electrophoretic and fluorographic techniques, in 1991, Knosp et al. reported that addition of serum resulted in an increase in the acetylation rate of all core histones within 15 min (Knosp et al., 1991). The sharp increase in acetylation rate was followed by a gradual decline in acetylation rate that continued until 8 h post serum stimulation (Knosp et al., 1991). At 10–12 h after serum stimulation, there was a strong increase in the acetylation rate of all core histones, detected based on increased incorporation of tritium into histone H3 from labeled acetate, a methodology that doesn't distinguish between acetylation of different lysine residues. This increase in acetylation was followed by an increase in histone synthesis (Knosp et al., 1991). The pattern differed among histones: H3 > H2A ~ H2BB > H4 (Knosp et al., 1991). In response to 24 h of serum withdrawal, there was a decrease in DNA synthesis, histone synthesis and histone acetylation (Knosp et al., 1991).

In a more recent study, proliferating and quiescent primary human fibroblasts, were incubated in <sup>13</sup>C-labeled acetate and the rate of histone lysine acetylation was monitored using mass spectrometry (Everitts et al., 2013b). The quiescent fibroblasts accumulated labeled acetylated histones more slowly than proliferating fibroblasts (Everitts et al., 2013b) and differential labeling rates were observed for the acetylation of H3K9, H3K14 and histone H4 (Everitts et al., 2013b). For histone H4, mass spectrometry was used to monitor the extent of acetylation of a peptide that contained lysines K5, K8, K12 and K16 was monitored. Levels of unmodified peptide, peptide with one acetyl group and peptides with two acetyl groups were determined (Everitts et al., 2013b). Incorporation of <sup>13</sup>C in

acetyl groups in quiescent cells was approximately half of that for proliferating cells. Even though the rate of acetylation was faster in proliferating fibroblasts, steady state levels of histone acetylation were similar in proliferating and quiescent fibroblasts (Everitts et al., 2013a,b).

## H4 Acetylation With Quiescence

In yeast, H4 acetylation correlates with transcriptional activation and plays an important role in chromatin decompaction (discussed in more detail in the later section). Using immunoblotting, the overall levels of H4K5ac and H4K8ac were found to decrease sharply during quiescence in budding yeast *S. cerevisiae*. This was followed by a rapid increase of these histone marks during cell cycle reentry when nutrients were reintroduced (Mews et al., 2014). Also using immunoblotting, a reduction in histone H4K12ac was observed in quiescent *S. cerevisiae* (McKnight et al., 2015). Similarly, by mass spectrometry and western blot analysis, two separate studies found that during stationary phase in *S. cerevisiae*, histone acetylation dropped dramatically at H4K5, H4K8, H4K12, and H4K16 compared to their levels in exponential growth phase (Sandmeier et al., 2002; Ngubo et al., 2011).

In mammals, reduced histone acetylation has been associated with a transition to quiescence in pluripotent cells (Khoa et al., 2020). Embryonic stem cells with pluripotent potential are characterized by high levels of histone acetylation, high chromatin accessibility and an active pluripotency transcriptional network. Mouse embryonic stem cells (ESCs) can exist in a proliferative, naïve ground state achieved by maintenance with a MAPK/ERK Kinase (MEK) inhibitor and a Glycogen Synthase Kinase 3 (GSK3) inhibitor (Boroviak et al., 2014). Deletion of histone acetyltransferase Males absent on the first (MOF), which acetylates histone H4 lysine 16 (Finley et al., 2018; Atlasi et al., 2019), resulted in quiescence in mouse ESCs (Figures 1, 2, Table 4). Among the > 200 histone post-translational modifications that were monitored in these MOF-deleted cells, only H4K16ac was significantly decreased (Khoa et al., 2020). Comparing RNA-seq gene expression data with global H4K16ac distribution obtained by ChIP-seq revealed that many genes associated with metabolic processes were regulated in a MOF-dependent manner, especially  $\beta$ -oxidation of fatty acids (Khoa et al., 2020). The degradation of fatty acids provided metabolites for oxidative phosphorylation and energy production in the proliferative state (Khoa et al., 2020). Inhibiting fatty acid oxidation was also sufficient to induce the proliferative ESCs into a quiescent state (Khoa et al., 2020). Taken together, these studies highlight an important role for histone H4 acetylation in regulating the proliferation-quiescence transition.

While addition of H4 acetyl groups is associated with the transition from quiescence to proliferation, the removal of H4 acetyl groups by Sirtuins, a class of histone deacetylases (HDACs), has also been associated with the proliferation-quiescence transition (Ryall et al., 2015) (Figure 1). When mouse MuSCs exit quiescence to begin proliferating, there is a decrease in NAD<sup>+</sup> levels and activity of NAD<sup>+</sup>-dependent sirtuin 1 (SIRT1), an HDAC (Michan and Sinclair, 2007). This reduction in SIRT1 activity results in increased H4K16 acetylation, activation of



muscle gene transcription, premature myogenic differentiation, reduced myofiber size, impaired muscle regeneration, and derepression of muscle developmental genes (Ryall et al., 2015).

These studies taken together support a role for acetylation in modulating transcriptional activation at important genes in different quiescence models. Loss of acetylation marks at genes critical to cell cycle and cell growth define the functional state of the chromatin during quiescence. In yeast and MuSCs, the alterations in acetylation have been functionally linked to quiescence (McKnight et al., 2015; Ryall et al., 2015).

## RNA-MEDIATED ADDITION OF HISTONE MARKS

The mechanisms that dictate where histone marks are deposited are not well-understood. There is an emerging literature that suggests that in some instances, long non-coding RNAs (lncRNAs) can help to direct the deposition of histone epigenetic marks (Batista and Chang, 2013; Hanly et al., 2018). lncRNAs can act as “address-codes” by directing the writers of histone marks to specific chromosomal locations (Batista and Chang, 2013; Hanly et al., 2018). The deposited marks can then affect chromatin conformation, nucleosome positioning and transcription at nearby genes (Faghihi and Wahlestedt, 2009; Guttman et al., 2011). The lncRNA Xist, for example, interacts with polycomb repressive complexes PRC1 and PRC2, which are responsible for the addition of the H3K27me3 mark, and recruiting these complexes is one part of the process by which Xist induces transcriptional silencing of the X chromosomes in female mammals (Kohlmaier et al., 2004; Bousard et al., 2019). Another lncRNA termed HOTAIR represses the HoxD gene locus by recruiting PRC2 for H3K27me3 addition (Rinn et al., 2007). lncRNAs have been confirmed to play critical roles in the establishment and maintenance of heterochromatic regions (Deng et al., 2009).

lncRNAs including *H19* are emerging as critical regulators of quiescence and proliferation in HSCs (Venkatraman et al., 2013; Yildirim et al., 2013; Luo et al., 2015). The *H19-Igf2* locus is an imprinted region that affects organism growth (DeChiara et al., 1991). The differentially methylated region (DMR) upstream of *H19* is the imprinting control region that enforces the expression of *H19* from the maternal allele only while *Igf2* is expressed from the paternal allele (Bartolomei, 2009). Deletion of the maternal, but not the paternal, *H19* DMR in adult mouse HSCs resulted in a activation of quiescent HSCs and reduced function of the HSCs (Venkatraman et al., 2013). When maternal *H19* DMR was deleted, the *Igf2-Igf1r* pathway was activated, the FoxO3 transcription factor translocated from the nucleus to the cytoplasm, and quiescent HSCs were activated to proliferate, resulting in their exhaustion (Venkatraman et al., 2013).

PAPAS lncRNAs have been studied in the context of cell quiescence (Figure 3A). PAPAS, or “promoter and pre-rRNA antisense,” is a heterogeneous group of lncRNAs that are generated when ribosomal DNA (rDNA) is transcribed in the antisense direction and localize to the pre-rRNA coding region and the rDNA promoter (Bierhoff et al., 2010). PAPAS interacts

with Suv-20h2, the methyltransferase that generates H4K20me3, and mediates deposition of this mark at rDNA during quiescence (Bierhoff et al., 2010). PAPAS and H4K20me3 were found to be upregulated in quiescent breast cancer cell line MCF7 generated with an estrogen receptor antagonist (Bierhoff et al., 2014). PAPAS and H4K20me3 are also induced upon terminal differentiation of human colon cancer cells (Caco-2), and upon quiescence in C2C12 mouse myoblasts, and mouse fibroblast-like 3T3-L1 cells (Bierhoff et al., 2014). Knockdown of endogenous PAPAS with siRNAs in MEFs decreased H4K20me3 levels (Bierhoff et al., 2014). Gain- and loss-of-function experiments, RNA-protein binding assays, and chromatin accessibility analysis revealed that PAPAS guides Suv4-20h2 to nucleolar chromatin, reinforcing quiescence-dependent transcriptional repression of ribosomal RNAs through H4K20me3-dependent chromatin compaction (Bierhoff et al., 2014).

Intracisternal A particle (IAP)-specific lncRNAs were found to be involved in H4K20me3-mediated chromatin compaction at IAP retrotransposons (Bierhoff et al., 2014). At IAP elements, both H4K20me3 and Suv4-20h2 levels increased in serum-starved MEFs, and the IAP chromatin was more compact (Bierhoff et al., 2014). Knockdown of IAP lncRNA with locked nucleic acid technology resulted in upregulation of the IAP major 7 kb transcript, supporting a role for the lncRNA in causing repression of the IAP gene, while transfection of IAP lncRNA sequences that interact with Suv4-20h2 resulted in increased Suv4-20h2 and H4K20me3 at IAPs, with no change in H3K9me3 levels (Bierhoff et al., 2010). These studies suggest that lncRNAs may provide another dimensionality to the histone code by potentially providing an address code that directs histone marks to specific genomic positions.

## HISTONE MARKS AND CHROMATIN CONFORMATION DURING QUIESCENCE

Multiple studies have reported changes in chromatin compaction with quiescence with most, but not all studies (Kallingappa et al., 2016), reporting that when cells enter quiescence, their chromatin becomes more compact (Chiu and Baserga, 1975; Setterfield et al., 1983; Evertts et al., 2013a; Swygert et al., 2019). In *S. cerevisiae* budding yeast, quiescence induction was found to induce global changes in chromosomal organization (Rutledge et al., 2015) using a global chromosome conformation capture high-throughput sequencing technology called Hi-C. By monitoring the frequency of interloxi interactions, the study revealed an increase in long range *cis* interactions and a decrease in short range interactions in quiescent yeast cells (Rutledge et al., 2015). The study further found that inter-centromeric interactions decrease during quiescence, while inter-telomeric interactions increase in quiescence, indicating that quiescence maintenance is associated with substantial topological reorganization (Rutledge et al., 2015). Another study has also shown that when yeast enter the stationary phase, the telomeres hypercluster, that is, they colocalize in a single location (Laporte et al., 2016). Mutant yeast strains that lack linker histone Hho1, or condensin, or contain mutations in histone H4 lysine 16 are unable to form these

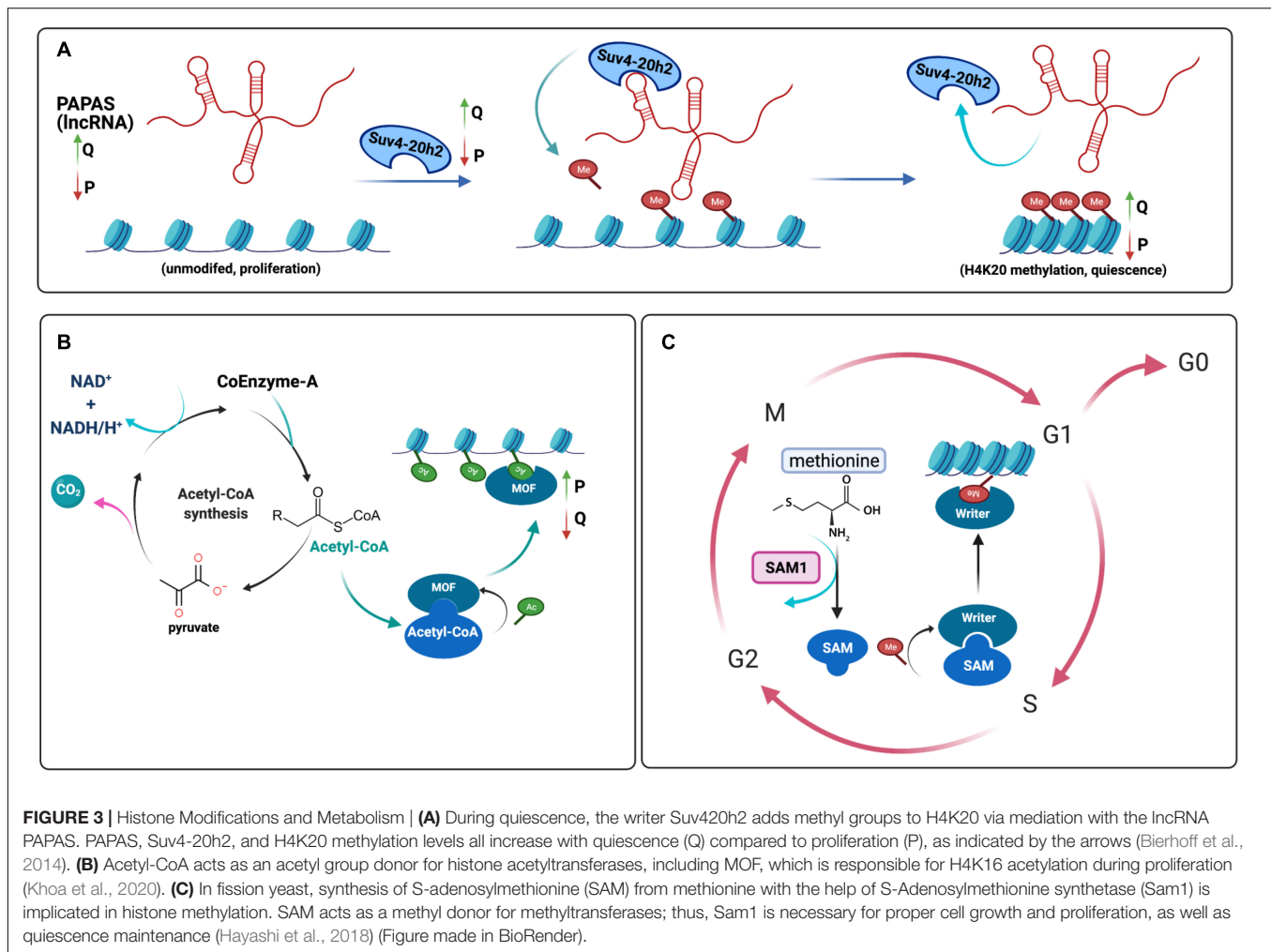


**FIGURE 3 | Histone Modifications and Metabolism | (A)** During quiescence, the writer Suv420h2 adds methyl groups to H4K20 via mediation with the lncRNA PAPAS. PAPAS, Suv4-20h2, and H4K20 methylation levels all increase with quiescence (Q) compared to proliferation (P), as indicated by the arrows (Bierhoff et al., 2014). **(B)** Acetyl-CoA acts as an acetyl group donor for histone acetyltransferases, including MOF, which is responsible for H4K16 acetylation during proliferation (Khoo et al., 2020). **(C)** In fission yeast, synthesis of S-adenosylmethionine (SAM) from methionine with the help of S-Adenosylmethionine synthetase (Sam1) is implicated in histone methylation. SAM acts as a methyl donor for methyltransferases; thus, Sam1 is necessary for proper cell growth and proliferation, as well as quiescence maintenance (Hayashi et al., 2018) (Figure made in BioRender).

telomere hyperclusters (Laporte et al., 2016). A contraction of the nucleolus (Wang et al., 2016) has also been observed in quiescent yeast cells as well.

A study in human diploid fibroblasts investigated changes in chromatin compaction with quiescence (Criscione et al., 2016). Using Formaldehyde Assisted Isolation of Regulatory Elements (FAIRE) to investigate global DNase I sensitivity and chromatin accessibility, quiescent cells were found to be more resistant to DNase I treatment, indicating more compact chromatin (Criscione et al., 2016). This study used Hi-C to show genes switching between A and B compartments with quiescence (Criscione et al., 2016). The A-type compartment has a more open chromatin structure and is enriched for activating marks such as H3K36me3, H3K79me2, H3K27ac, and H3K4me1 (Lieberman-Aiden et al., 2009; Rao et al., 2014). The B-type compartment, on the other hand, is characterized by more densely packed chromatin and correlates with repressive marks such as H3K27me3, H3K9me3, and H4K20me3 (Lieberman-Aiden et al., 2009; Rao et al., 2014). Genes associated with cell proliferation were enriched in the group of genes switching

from A to B compartments as cells entered quiescence (Criscione et al., 2016).

HP1 $\beta$  is a dimeric protein that binds to the H3K9me3 mark in constitutive heterochromatin and can bridge two H3K9me3-containing nucleosomes (Machida et al., 2018). Both HP1 $\beta$  and H3K9me3 localized to constitutive heterochromatin regions in proliferating B lymphocytes, while in quiescent B lymphocytes they did not (Baxter et al., 2004). These findings suggest that the overall structure of DNA may be altered in quiescent B lymphocytes in a way that affects the accessibility of histone writers and readers, especially in constitutive heterochromatin.

One possible mechanism through which the histone code could affect chromatin state during quiescence involves the histone methyltransferase Suv4-20h2 that generates H4K20me3. As mentioned before, H4K20me3 is involved in heterochromatin formation and induces chromatin compaction (Everts et al., 2013a; Hahn et al., 2013). Suv4-20h2 activity and the H4K20me3 mark are upregulated with quiescence (Everts et al., 2013a; Bierhoff et al., 2014). A fluorescence *in situ* hybridization (FISH) analysis performed in primary human dermal fibroblasts

found that contact-inhibited quiescent fibroblasts had more compact chromatin than their proliferating counterparts (Everitts et al., 2013a). Furthermore, knockdown of Suv20h2 resulted in decreased compaction (Everitts et al., 2013a). As described above, crystal structures of nucleosomes reconstituted with histones containing the H4K20me3 mark had alterations in higher order structure (Lu et al., 2008). Fluorescence Recovery After Photobleaching (FRAP) analysis revealed that Suv4-20h2 binds tightly to heterochromatin (Hahn et al., 2013). Other studies have shown that Suv4-20h2 associates with pericentric heterochromatin through multiple, independent interaction sites on its C-terminal domain that directly bind to multiple heterochromatin protein 1 (HP1) molecules (Schotta et al., 2004, 2008; Watanabe et al., 2018). The HP1 protein family consists of three members: HP1 $\alpha$ , HP1 $\beta$ , and HP1 $\gamma$ . HP1 $\alpha$  localizes to heterochromatin, HP1 $\beta$  is found in both heterochromatic and euchromatic regions and HP1 $\gamma$  is associated with actively transcribed genes (Vakoc et al., 2005; Lomberg et al., 2006). Dimeric HP1 $\alpha$  binds two H3K9me3 marks in adjacent nucleosomes and forms a bridge between them, thereby compacting the chromatin (Watanabe et al., 2018). Consequently, the combinatorial effects of the H3K9me3 and H4K20me3 marks together represent an opportunity for a quiescence combinatorial histone code that affects chromatin conformation and induces chromosomal compaction.

Chromatin-bound Suv4-20h2 also recruits the cohesin complex (Hahn et al., 2013), which is composed of rings of Smc1-Smc3 dimers connected by Scc1/Rad21 (Nasmyth, 2011). The cohesin complex can contribute to establishment of the chromatin loop domains at specific DNA regions, thereby inducing chromatin compaction (Maya-Miles et al., 2019). In *Suv4-20h1/Suv4-20h2* double-knockout cells, cohesin was absent from heterochromatic regions in G<sub>0</sub> phase, which showed that Suv4-20h enzymes are required for loading or maintaining cohesin at heterochromatin (Hahn et al., 2013). Reintroducing Suv4-20h2 or only the non-enzymatic clamp domain of Suv4-20h2 rescued the loss of heterochromatin-associated cohesin suggesting the effects of Suv4-20h2 may be mediated independent of its effects on H4K20me3 (Hahn et al., 2013). This ability of Suv4-20h2 to recruit cohesin and compact chromatin may be critical for chromatin compaction with quiescence, as Suv4-20h2-deficient MEFs synchronized in G<sub>0</sub>, contained virtually no cohesin in regions of heterochromatin (Hahn et al., 2013). Additional experiments will be required to understand the functional consequences of a lack of cohesin in heterochromatin in Suv4-20h2-deficient quiescent cells.

## CROSS-TALK BETWEEN HISTONE MARKS AND METABOLISM

An important emerging theme in epigenetic regulation is the close association between histone marks and metabolism. In yeast, metabolic signals such as the presence or absence of glucose can determine whether cells proliferate or arrest (Laporte et al., 2011), and therefore, histone marks that signal the relative abundance of glucose can potentially transmit information about

nutrient abundance in a locus-specific manner to affect gene regulation. The metabolite acetyl-CoA serves as the substrate for histone acetyltransferase enzymes that generate acetylated histones (Kaelin and McKnight, 2013) (**Figure 3B**). Acetyl CoA is formed in mitochondria when pyruvate generated by glycolysis is committed to the TCA cycle (Martinez-Reyes and Chandel, 2020). Citrate formed in the mitochondria can be exported and converted in the cytoplasm to acetyl CoA (Martinez-Reyes and Chandel, 2020). In proliferating yeast and mammalian cells, higher levels of glycolysis and increased export of acetyl CoA from the mitochondria have been observed in proliferating compared with quiescent cells (Frauwrith and Thompson, 2004; Vander Heiden et al., 2009; Lemons et al., 2010). Thus, the metabolic profiles of proliferating cells may facilitate the generation of histone acetylation, and the formation of more open chromatin (Frauwrith and Thompson, 2004; Lemons et al., 2010). The role of histone acetylation in *S. pombe* was investigated with a strain that exhibited a temperature-sensitive mutation in the catalytic region of phosphopantothienoylcysteine synthetase (designated Ppc1) (Nakamura et al., 2012), an enzyme in the biosynthetic pathway for acetyl-CoA. *S. pombe* with mutations that inactivate the ability to synthesize acetyl-CoA fail to acetylate histones and are unable to re-enter the cell cycle after initiating G<sub>0</sub> following nitrogen withdrawal (Nakamura et al., 2012).

In fibroblasts, the oncogene c-MYC has been identified as a transcription factor that can affect global chromatin remodeling (Morrish et al., 2010). In rat fibroblasts, MYC activity increased glucose metabolism and acetyl-CoA production (Morrish et al., 2010). The presence of MYC caused a forty percent increase in <sup>13</sup>C-labeled acetyl-CoA on H4-K16 during cell cycle entry with serum stimulation during the G<sub>0</sub> to S transition (Morrish et al., 2010). Metabolic tracing revealed that in MYC-stimulated cells, MYC increases acetylCoA levels (Morrish et al., 2010). Further, the GCN5 histone acetylase enzyme, an enzyme that is important for histone acetylation in response to nutrients in yeast (McMahon et al., 2000; Cai et al., 2011), is a target of MYC (Morrish et al., 2010).

In addition to a connection between metabolism and histone acetylation, there is also a connection between metabolism and histone methylation. S-adenosylmethionine (SAM) is a metabolite that acts as a donor of methyl groups, which are transferred by methyltransferase enzymes to histones (Kaelin and McKnight, 2013) (**Figure 3C**). In fission yeast, the enzyme responsible for synthesizing SAM, S-adenosylmethionine synthase 1 (Sam1), is required for proper cell growth, proliferation, and quiescence entry and exit (Hayashi et al., 2018). Loss of Sam1 results in reduced levels of H3K4me2 and H3K4me3, and a significant decrease in cell growth and defects in G<sub>2</sub> cell cycle arrest (Hayashi et al., 2018). Yeast with mutations in Sam1 cannot survive in quiescence initiated following nitrogen starvation, and once released from G<sub>0</sub>, they are unable to increase in cell size and restart DNA replication in proliferative conditions (Hayashi et al., 2018).

Taken together, these studies exploring the crosstalk between metabolism and histone marks highlight the close association

between nutrient uptake, proliferation and histone post-translational modifications. How this crosstalk is established and maintained in quiescence is an important area for further exploration.

## GAPS IN THE FIELD AND FUTURE STUDIES

The decision whether to proliferate or exit the proliferative cell cycle requires cells to integrate multiple types of information and execute a complex series of molecular changes that impact many of the cell's activities. Transitioning between a proliferative and quiescent state is associated with many alterations including changes in the expression and activity of specific genes, changes in the conformation of chromatin, and changes in the subnuclear localization of chromosomes. The molecular mechanisms that cells use to make these decisions are actively being investigated and there are likely levels of regulation that have yet to be uncovered. Here we explored the literature to find evidence that histone post-translational modifications serve as a code that interprets information about the activity of signaling pathways and transmits that information to enable the commitment to a proliferative or quiescent state and the functional changes required for this transition.

So, is there a histone code for cellular quiescence? As highlighted in this review, there are multiple lines of evidence that suggest that specific histone modifications alone and in combination are added or removed as cells transition between proliferation and quiescent in multiple model systems. Histone H3K4me<sub>3</sub>, for instance, is found at the promoters of genes that are activated when cells become quiescent. H3K36 methylation is important for establishment and maintenance of the quiescent state in HSCs as inactivation of the SETD2 methyltransferase results in depletion of quiescent HSCs (Wagner and Carpenter, 2012). In quiescent mouse MuSCs, a combination of H3K9 and H3K27 marks was found to regulate cyclin A2 expression and proliferation (Cheedipudi et al., 2015). As another example, H4K20me<sub>3</sub> levels increase in quiescent cells and knockdown of Suv4-20h2 results in a more rapid cell cycle (Everitts et al., 2013a). Finally, changes in the levels of histone acetylation have been observed with the transition between proliferation and quiescence (Ryall et al., 2015), and the close association between nutrient availability and acetyl CoA levels suggests histone acetylation as a possible link between nutrient availability and proliferation (Cai et al., 2011). For each of the marks described, there is evidence that the mark plays a functional role in some aspect of quiescence: quiescence entry, quiescence exit, quiescence maintenance, or quiescence depth. In some cases, functional studies have shown a causative role for a specific reader, writer or eraser. However, in many studies, and for many of the histone PTMs described, it is not clear whether the role of the histone marks is correlative or causative. Also, the contribution of histone marks seems to be context- and cell type-dependent as indicated by our survey of different quiescence models and conditions. For many

of the marks, the direction of change was not consistent in different model systems. For instance, H3K27me<sub>3</sub> was induced in some quiescence models and repressed in others (Baxter et al., 2004; Everitts et al., 2013a; Kallingappa et al., 2016; Maki et al., 2021). Other histone marks appear to be regulated with quiescence in some species, but are absent in others, such as H3K27me<sub>3</sub> which is absent from yeast (Jamieson et al., 2013). Furthermore, quiescence studies have usually focused on one or a few histone marks at a time. Additional studies will be needed to determine whether a well-defined system-dependent or system-independent combinatorial histone code exists for cellular quiescence and how this histone code varies among species and tissues.

The findings in this review show that certain histone marks, and even combinations of histone marks, are altered with quiescence and some of these changes are consistent among model systems. Future studies will be needed that systematically determine the genomewide deposition of histone marks and combinations of histone marks in proliferating and quiescent cells in multiple model systems. These investigations would cover both traditional and non-traditional histone marks in multiple quiescent states. Beyond just comparing proliferating and quiescent cells, these inquiries would look into histone marks in cells that initiate quiescence in response to different signals in the same cell type and cells that have been quiescent for different durations of time to achieve different depths of quiescence (Rodgers et al., 2014; Kwon et al., 2017). While many of the studies we review have not discovered a clear relationship between changes in individual histone marks and altered gene expression (Liu et al., 2013; Lee et al., 2016), a careful analysis of combinations of marks might determine if the changes in the combinatorial pattern of histone marks is a better indicator of gene expression changes with quiescence.

Many questions remain when studying histone marks in quiescence. What triggers the deposition of these marks? In particular, how do different histone writers and readers coordinate to establish marks at the appropriate time? In some cases, establishment and maintenance of histone marks associated with an open chromatin structure and active gene transcription may be achieved through positive feedback loops (Zhang et al., 2015). These positive feedback loops can be formed when proteins that write histone marks also read the same mark (Zhang et al., 2015). For instance, SETD1 complexes not only catalyze the formation of H3K4me<sub>3</sub> marks, but may also recognize the same H3K4me<sub>3</sub> mark, bind to it, and continue to generate additional H3K4me<sub>3</sub> modifications (Shi et al., 2007; Murton et al., 2010; Zhang et al., 2015). Dot1, the H3K79 methyltransferase in yeast (Guan et al., 2013), recognizes modifications on the histone H2B tail and, in human, also binds phosphorylated forms of RNA polymerase II at the transcription start sites of actively transcribed genes (Kim S.K. et al., 2012). H3K4me<sub>3</sub> can recruit histone acetyltransferases that add acetyl groups as well as deacetylases that remove acetyl groups (Zhang et al., 2015), resulting in dynamic turnover of histone acetylation marks when H3K4me<sub>3</sub>, but not other marks such as H3K79me<sub>3</sub> or H3K36me<sub>3</sub>, are present (Crump et al., 2011). For repressive



chromatin, PRC2 not only generates H3K27me3 but also binds to it, resulting in a positive feedback loop in which local chromatin structure allows H3K27me3 to be deposited over chromatin regions to form domains (Hansen et al., 2008; Zhang et al., 2015). Crosstalk between H3K27me3 and monoubiquitinated H2A on lysine 119, H2AK119ub, has also been proposed as enzyme complexes that deposit each mark may recognize the other mark (Blackledge et al., 2014; Cooper et al., 2014; Kalb et al., 2014), allowing for the reinforcement of heterochromatic regions (Zhang et al., 2015). Negative feedback between histone marks also occurs as activating marks can inhibit the activity of enzymes that place repressive marks, and vice versa (Zhang et al., 2015). For instance, activating marks H3K4me2/3 and H3K36me2/3 can inhibit the activity of PRC2 and prevent the deposition of H3K27me3 repressive marks (Schmitges et al., 2011). Experiments in which the impact of modulating a specific reader and writer on the levels of multiple marks in the context of quiescence models may shed light on this question. In particular, such experiments may shed light on how positive and negative feedback loops are interrupted at proliferation-associated genes and reestablished at quiescence-associated genes.

The development and application of new technologies will facilitate future studies investigating how combinations of histone marks coordinate. One valuable approach will be the ability to visualize proliferation and quiescence decisions in organisms in real time. Toward this end, a recent paper describes the adaptation of a biosensor for CDK activity (Spencer et al., 2013) to monitor cell division in two model organisms, *Caenorhabditis elegans* and zebrafish (Adikes et al., 2020). CDK activity was higher at the end of a cell division in cases in which the cell went on to divide (Adikes et al., 2020). Such biosensors could be used in conjunction with visualization of histone marks to assess whether histone marks individually or in combination can predict whether a cell will proliferate.

We anticipate that CRISPR-Cas9 will prove to be a powerful methodology for understanding the impact of histone modifications. One important challenge in understanding the impact of different histone marks and combinations of histone marks has been developing specific systems to test their functional importance. Many studies to date have focused on investigating the role of specific readers and writers with knockdown and knockout approaches. Using CRISPR-Cas9, further studies will likely allow the inactivation of specific histone modifiers using protein degradation systems that allow the proteins to be degraded in proliferating or quiescent cells with defined timing thus permitting a more detailed dissection of their role (Wu et al., 2020).

Functional dissection of histone readers and writers is sometimes complicated as they have non-histone targets as well (Cornett et al., 2019). In fact, nearly 3,000 human non-histone proteins have been reported to have a lysine that can be methylated (Hornbeck et al., 2015; Cornett et al., 2019). An alternative approach is to test for the functional consequences of modifying the histones themselves. To achieve this, CRISPR-Cas9 has been used in *S. cerevisiae*

to generate yeast strains with different combinations of mutations at histone tail lysines for histone H3 and H4, allowing the investigators to assess the effects of loss of different combinations of histone marks (Fu et al., 2021). In *Trypanosoma brucei*, precise editing of genes in multicopy arrays was performed with CRISPR-Cas9, allowing for the replacement of histone H4K4 with H4R4 to mimic the constitutively non-acetylated state. The authors achieved 90% replacement of the 43 histone H4 copies to H4R4 (Vasquez et al., 2018).

CRISPR/Cas9 will also be valuable for its capacity to specifically target chromatin writers and readers to specific genomic regions. As an early example of this technology, “programmable chromatin kinase” dCas9-dMSK1 was generated by fusing nuclease-deficient CRISPR/Cas9 (or dCas9) to a histone H3 kinase (Li et al., 2021). When this protein was targeted to specific promoters with guide RNAs, there was an increase in histone H3 serine 28 phosphorylation at the target genes’ promoters and an increase in expression of the targeted gene. Such studies are likely to be valuable for defining causal connections between histone PTMs, their activity at specific genomic loci, and outcomes such as gene expression and proliferation.

We anticipate that the availability of new technologies that allow us to better visualize the relationships among histone marks and chromosomal organization on a cell-by-cell basis will also benefit studies of the histone code in quiescence. A recent report built upon sequential FISH (seqFISH) and multiplexed FISH methods to target 3,660 loci in individual mouse ES cells (Takei et al., 2021). These studies revealed that nuclear zones were created by combinatorial chromatin patterns (Takei et al., 2021). Repressive histone marks H4K20me3, H3K9me3, and histone variant H2A1 were found together and colocalized with DAPI-rich regions (Takei et al., 2021). A second heterochromatic pattern of H4K20me2, H3K27me3 and H3K27me2 was also observed (Takei et al., 2021). Active histone marks, H3K9ac and H3K27ac, and RNA Polymerase II serine 5 phosphorylation localized to nuclear speckles and were excluded from heterochromatin and nuclear lamina (Takei et al., 2021). Similar studies comparing proliferating and quiescent cells could shed light on the role for a potential histone code in establishing a cell’s proliferative fate. In particular, single cell analyses of proliferating and quiescent cells could reveal patterns that are consistent among cells versus those that are more variable from cell to cell.

We anticipate that with time the role of additional histone PTMs and histone variants and their roles in regulating chromatin structure and gene expression will become clearer. As one example, non-tail globular histone marks, such as H3K36 and H3K122 acetylation marks found in active gene promoters and a subset of enhancers, can contribute to the histone code and expand the possibilities for combinatorial histone PTMs that provide position-specific information to readers (Pradeepa et al., 2016). Non-enzymatic histone modifications, such as glycation, acylation and lipidation,

generated by spontaneous chemical reactions also have the potential to alter chromatin structure and regulate genetic processes (Maksimovic and David, 2021). The non-enzymatic modifications, like the histone marks described in this review, can be “erased” by scavenger systems (Maksimovic and David, 2021). Improved mass spectrometry and chemoproteomics will likely provide important new insights into the role of these modifications in cellular decisions including the commitment to proliferation (Maksimovic and David, 2021). As another example, additional studies are likely to reveal that changes in the specific histone variants present at different positions in the chromatin cooperate with histone PTMs to alter chromatin state and reader proteins. Some histone variants such as histone H3.1 and histone H3.3 contain different residues, such as amino acid S31 in histone H3.3 and A31 in histone H3.1 that can alter the properties of the chromatin and its accessibility to the transcription apparatus (Armache et al., 2020). Linker histone H1 variants can also affect folding of nucleosome arrays and nucleosome compaction (Fyodorov et al., 2018).

Combinations of multiple distinct genome-wide, high-throughput analyses performed in models of proliferating and quiescent cells, will also be needed to allow us to dissect the role of histone modifications and other contributors to gene expression and functional changes with quiescence. Studies in which changes in the genome-wide localization of histone marks can be correlated with chromatin accessibility using ATAC-seq, DNA methylation, and Hi-C to assess A and B compartments and topologically associating domain boundaries have the potential to yield greater insight. Combining these datasets and analyzing them with deep learning algorithms, may allow scientists to predict which combinations of marks are associated with changes in chromatin accessibility and gene expression.

## CONCLUSION

Based on the findings thus far, the specific histone marks discussed in this review, methylation of H3K4, H3K9, H3K27, H3K36, H3K79, H4K20, and acetylation of H3 and H4 have been discovered to be regulated with quiescence in different model systems. Readers, writers and erasers of these marks have been found to functionally contribute to the quiescence-proliferation transition and quiescence maintenance. The model systems employed for these studies include nutrient depletion and spore formation in yeast, cell culture models in which different anti-proliferative signals are employed, and models in which quiescent stem cells are visualized *in situ* or isolated and characterized. One of the key limitations for the field is the fact that knockout or knockdown of readers, writers and erasers can impact not just the histone marks under study, but also the PTMs of other cellular proteins as well. Also, most studies have investigated the effect of a single modification in isolation rather than the impact of several modifications together and the relationships between marks. More research with emerging technologies will be needed to determine whether there is a quiescence histone code and if

so, how changes in histones are used to create a complex and context-dependent grammar that incorporates not just levels of histone marks and their readers, but also the chromatin context (in 2D as well as in 3D). Future studies will likely address the causality of histone marks and phenotypic changes that serve as regulators of quiescence and landmarks of quiescence. These studies may define the functional consequences of these marks in terms of gene expression, chromatin conformation, and chromosomal positioning. These studies will also likely reveal the role of traditional and non-traditional histone PTMs and other changes to chromatin in the decision whether to proliferate, the mechanisms that cause cell cycle arrest, the maintenance of cells during quiescence, and the determination of quiescence depth. Altogether, these results indicate that the regulation of histone marks may help to maintain the delicate balance between quiescence, proliferation, differentiation, and cell death, with different model systems and cell types likely using both overlapping and distinct aspects of the information contained in these histone marks.

## AUTHOR CONTRIBUTIONS

MM conceived the topic and design of the review. KB and KS prepared all the figures and tables. KB, KS, MM, and HC did the literature survey. MM, HC, KB, KS, and KA wrote the manuscript. MM and HC supervised the project. All authors were involved in proof-reading.

## FUNDING

This work was supported by grants to HC NIGMS R01 GM081686, NIGMS R01 GM0866465, NIH R01 AR070245, 1 R01 CA221296-01A1, NCI RC1 CA 147961-02, National Cancer Institute P50 CA092131, the Cancer Research Institute CLIP grant, a Melanoma Research Alliance Team Science Award (<https://doi.org/10.48050/pc.gr.80537>), the Iris Cantor Women's Health Center/UCLA CTSI NIH Grant UL1TR000124, the UCLA SPORC in Prostate Cancer (P50CA092131), David Geffen School of Medicine Metabolism Theme, University of California Cancer Research Coordinating Committee, Broad Stem Cell Center Innovation Awards, and Rose Hills Foundation and Hal Gaba awards from the UCLA Broad Stem Cell Center. KA acknowledges support from 5 T32 AR 65972-5 and an MBI Whitcome Fellowship. KB acknowledges the MARC Foundation funding from NIH/NIGMS NIH MARC T34 GM008563 (PI M. M. McEvoy). HC was the Milton E. Cassel scholar of the Rita Allen Foundation (<http://www.ritaallenfoundation.org>).

## ACKNOWLEDGMENTS

We are grateful to the entire Collier laboratory for helpful conversations.

## REFERENCES

- Abbas, T., Shibata, E., Park, J., Jha, S., Karnani, N., and Dutta, A. (2010). CRL4(Cdt2) regulates cell proliferation and histone gene expression by targeting PR-Set7/Set8 for degradation. *Mol. Cell* 40, 9–21.
- Acquaviva, L., Drogat, J., Dehe, P. M., de La Roche Saint-Andre, C., and Geli, V. (2013). Spp1 at the crossroads of H3K4me3 regulation and meiotic recombination. *Epigenetics* 8, 355–360. doi: 10.4161/epi.24295
- Adikes, R. C., Kohrman, A. Q., Martinez, M. A. Q., Palmisano, N. J., Smith, J. J., Medwig-Kinney, T. N., et al. (2020). Visualizing the metazoan proliferation-quiescence decision in vivo. *Elife* 9:e63265. doi: 10.7554/eLife.63265
- Agalioti, T., Chen, G., and Thanos, D. (2002). Deciphering the transcriptional histone acetylation code for a human gene. *Cell* 111, 381–392.
- Allen, C., Büttner, S., Aragon, A. D., Thomas, J. A., Meirelles, O., Jaetao, J. E., et al. (2006). Isolation of quiescent and nonquiescent cells from yeast stationary-phase cultures. *J. Cell Biol.* 174, 89–100.
- Allfrey, V. G., Faulkner, R., and Mirsky, A. E. (1964). Acetylation and methylation of histones and their possible role in the regulation of Rna synthesis. *Proc. Natl. Acad. Sci. U.S.A.* 51, 786–794.
- Allis, C. D., and Jenuwein, T. (2016). The molecular hallmarks of epigenetic control. *Nat. Rev. Genet.* 17, 487–500.
- Armache, A., Yang, S., Martinez de Paz, A., Robbins, L. E., Durmaz, C., Cheong, J. Q., et al. (2020). Histone H3.3 phosphorylation amplifies stimulation-induced transcription. *Nature* 583, 852–857. doi: 10.1038/s41586-020-2533-0
- Atlasi, Y., Megchelenbrink, W., Peng, T., Habibi, E., Joshi, O., Wang, S. Y., et al. (2019). Epigenetic modulation of a hardwired 3D chromatin landscape in two naive states of pluripotency. *Nat. Cell Biol.* 21, 568–578.
- Bannister, A. J., and Kouzarides, T. (2011). Regulation of chromatin by histone modifications. *Cell Res.* 21, 381–395.
- Bannister, A. J., Zegerman, P., Partridge, J. F., Miska, E. A., Thomas, J. O., Allshire, R. C., et al. (2001). Selective recognition of methylated lysine 9 on histone H3 by the HP1 chromo domain. *Nature* 410, 120–124.
- Barbieri, M., Xie, S. Q., Torlai Triglia, E., Chiariello, A. M., Bianco, S., de Santiago, I., et al. (2017). Active and poised promoter states drive folding of the extended HoxB locus in mouse embryonic stem cells. *Nat. Struct. Mol. Biol.* 24, 515–524. doi: 10.1038/nsmb.3402
- Barker, N., van Es, J. H., Kuipers, J., Kujala, P., van den Born, M., Cozijnsen, M., et al. (2007). Identification of stem cells in small intestine and colon by marker gene Lgr5. *Nature* 449, 1003–1007.
- Barnes, C. E., English, D. M., and Cowley, S. M. (2019). Acetylation & Co: an expanding repertoire of histone acylations regulates chromatin and transcription. *Essays Biochem.* 63, 97–107.
- Barski, A., Cuddapah, S., Cui, K., Roh, T. Y., Schones, D. E., Wang, Z., et al. (2007). High-resolution profiling of histone methylations in the human genome. *Cell* 129, 823–837.
- Bartolomei, M. S. (2009). Genomic imprinting: employing and avoiding epigenetic processes. *Genes Dev.* 23, 2124–2133. doi: 10.1101/gad.1841409
- Basak, O., Krieger, T. G., Muraro, M. J., Wiebrands, K., Stange, D. E., Frias-Aldeguer, J., et al. (2018). Troy+ brain stem cells cycle through quiescence and regulate their number by sensing niche occupancy. *Proc. Natl. Acad. Sci. U.S.A.* 115, E610–E619. doi: 10.1073/pnas.1715911114
- Batista, P. J., and Chang, H. Y. (2013). Long noncoding RNAs: cellular address codes in development and disease. *Cell* 152, 1298–1307.
- Baxter, J., Sauer, S., Peters, A., John, R., Williams, R., Caparros, M. L., et al. (2004). Histone hypomethylation is an indicator of epigenetic plasticity in quiescent lymphocytes. *EMBO J.* 23, 4462–4472. doi: 10.1038/sj.emboj.7600414
- Beck, D. B., Oda, H., Shen, S. S., and Reinberg, D. (2012). PR-Set7 and H4K20me1: at the crossroads of genome integrity, cell cycle, chromosome condensation, and transcription. *Genes Dev.* 26, 325–337. doi: 10.1101/gad.177444.111
- Ben Hassine, S., and Arcangioli, B. (2009). Tdp1 protects against oxidative DNA damage in non-dividing fission yeast. *EMBO J.* 28, 632–640.
- Benetti, R., Gonzalo, S., Jaco, I., Schotta, G., Klatt, P., Jenuwein, T., et al. (2007). Suv4-20h deficiency results in telomere elongation and derepression of telomere recombination. *J. Cell Biol.* 178, 925–936. doi: 10.1083/jcb.200703081
- Bernhart, S. H., Kretzmer, H., Holdt, L. M., Juhling, F., Ammerpohl, O., Bergmann, A. K., et al. (2016). Changes of bivalent chromatin coincide with increased expression of developmental genes in cancer. *Sci. Rep.* 6:37393. doi: 10.1038/srep37393
- Bernstein, B. E., Mikkelsen, T. S., Xie, X., Kamal, M., Huebert, D. J., Cuff, J., et al. (2006). A bivalent chromatin structure marks key developmental genes in embryonic stem cells. *Cell* 125, 315–326.
- Bhattacharya, S., Levy, M. J., Zhang, N., Li, H., Florens, L., Washburn, M. P., et al. (2021). The methyltransferase SETD2 couples transcription and splicing by engaging mRNA processing factors through its SHI domain. *Nat. Commun.* 12:1443. doi: 10.1038/s41467-021-21663-w
- Bierhoff, H., Dammert, M. A., Brocks, D., Dambacher, S., Schotta, G., and Grummt, I. (2014). Quiescence-induced LncRNAs trigger H4K20 trimethylation and transcriptional silencing. *Mol. Cell* 54, 675–682. doi: 10.1016/j.molcel.2014.03.032
- Bierhoff, H., Schmitz, K., Maass, F., Ye, J., and Grummt, I. (2010). Noncoding transcripts in sense and antisense orientation regulate the epigenetic state of ribosomal RNA genes. *Cold Spring Harb. Symp. Quant. Biol.* 75, 357–364. doi: 10.1101/sqb.2010.75.060
- Bjornson, C. R., Cheung, T. H., Liu, L., Tripathi, P. V., Steeper, K. M., and Rando, T. A. (2012). Notch signaling is necessary to maintain quiescence in adult muscle stem cells. *Stem Cells* 30, 232–242.
- Black, J. C., Van Rechem, C., and Whetstone, J. R. (2012). Histone lysine methylation dynamics: establishment, regulation, and biological impact. *Mol. Cell* 48, 491–507.
- Blackledge, N. P., Farcas, A. M., Kondo, T., King, H. W., McGouran, J. F., Hanssen, L. L. P., et al. (2014). Variant PRC1 complex-dependent H2A ubiquitylation drives PRC2 recruitment and polycomb domain formation. *Cell* 157, 1445–1459. doi: 10.1016/j.cell.2014.05.004
- Boonsanay, V., Zhang, T., Georgieva, A., Kostin, S., Qi, H., Yuan, X., et al. (2016). Regulation of skeletal muscle stem cell quiescence by Suv4-20h1-dependent facultative heterochromatin formation. *Cell Stem Cell* 18, 229–242. doi: 10.1016/j.stem.2015.11.002
- Boroviak, T., Loos, R., Bertone, P., Smith, A., and Nichols, J. (2014). The ability of inner-cell-mass cells to self-renew as embryonic stem cells is acquired following epiblast specification. *Nat. Cell Biol.* 16, 516–528. doi: 10.1038/ncb2965
- Bousard, A., Raposo, A. C., Zylicz, J. J., Picard, C., Pires, V. B., Qi, Y., et al. (2019). The role of Xist-mediated Polycomb recruitment in the initiation of X-chromosome inactivation. *EMBO Rep.* 20:e48019. doi: 10.15252/embr.201948019
- Bridger, J. M., Boyle, S., Kill, I. R., and Bickmore, W. A. (2000). Remodelling of nuclear architecture in quiescent and senescent human fibroblasts. *Curr. Biol.* 10, 149–152. doi: 10.1016/s0960-9822(00)00312-2
- Cai, L., Sutter, B. M., Li, B., and Tu, B. P. (2011). Acetyl-CoA induces cell growth and proliferation by promoting the acetylation of histones at growth genes. *Mol. Cell* 42, 426–437. doi: 10.1016/j.molcel.2011.05.004
- Carvalho, S., Raposo, A. C., Martins, F. B., Grosso, A. R., Sridhara, S. C., Rino, J., et al. (2013). Histone methyltransferase SETD2 coordinates FACT recruitment with nucleosome dynamics during transcription. *Nucleic Acids Res.* 41, 2881–2893. doi: 10.1093/nar/gks1472
- Centore, R. C., Havens, C. G., Manning, A. L., Li, J. M., Flynn, R. L., Tse, A., et al. (2010). CRL4(Cdt2)-mediated destruction of the histone methyltransferase Set8 prevents premature chromatin compaction in S phase. *Mol. Cell* 40, 22–33. doi: 10.1016/j.molcel.2010.09.015
- Champagne, K. S., and Kutateladze, T. G. (2009). Structural insight into histone recognition by the ING PHD fingers. *Curr. Drug Targets* 10, 432–441. doi: 10.2174/138945009788185040
- Chang, H. Y., Chi, J. T., Dudoit, S., Bonadre, C., van de Rijn, M., Botstein, D., et al. (2002). Diversity, topographic differentiation, and positional memory in human fibroblasts. *Proc. Natl. Acad. Sci. U.S.A.* 99, 12877–12882.
- Cheedipudi, S., Puri, D., Saleh, A., Gala, H. P., Rumman, M., Pillai, M. S., et al. (2015). A fine balance: epigenetic control of cellular quiescence by the tumor suppressor PRDM2/RIZ at a bivalent domain in the cyclin a gene. *Nucleic Acids Res.* 43, 6236–6256. doi: 10.1093/nar/gkv567
- Cheung, T. H., and Rando, T. A. (2013). Molecular regulation of stem cell quiescence. *Nat. Rev. Mol. Cell Biol.* 14, 329–340.



- Cheung, T. H., Quach, N. L., Charville, G. W., Liu, L., Park, L., Edalati, A., et al. (2012). Maintenance of muscle stem-cell quiescence by microRNA-489. *Nature* 482, 524–528. doi: 10.1038/nature10834
- Chi, P., Allis, C. D., and Wang, G. G. (2010). Covalent histone modifications—miswritten, misinterpreted and mis-erased in human cancers. *Nat. Rev. Cancer* 10, 457–469. doi: 10.1038/nrc2876
- Chiu, N., and Baserga, R. (1975). Changes in template activity and structure of nuclei from WI-38 cells in the prereplicative phase. *Biochemistry* 14, 3126–3132. doi: 10.1021/bi00685a014
- Chu, D., and Barnes, D. J. (2016). The lag-phase during diauxic growth is a trade-off between fast adaptation and high growth rate. *Sci. Rep.* 6:25191. doi: 10.1038/srep25191
- Coller, H. A. (2019a). Regulation of cell cycle entry and exit: a single cell perspective. *Compr. Physiol.* 10, 317–344. doi: 10.1002/cphy.c190014
- Coller, H. A. (2019b). The paradox of metabolism in quiescent stem cells. *FEBS Lett.* 593, 2817–2839.
- Coller, H. A., Sang, L., and Roberts, J. M. (2006). A new description of cellular quiescence. *PLoS Biol.* 4:e83. doi: 10.1371/journal.pbio.0040083
- Cooper, S., Dienstbier, M., Hassan, R., Schermelleh, L., Sharif, J., Blackledge, N. P., et al. (2014). Targeting polycomb to pericentric heterochromatin in embryonic stem cells reveals a role for H2AK119u1 in PRC2 recruitment. *Cell Rep.* 7, 1456–1470. doi: 10.1016/j.celrep.2014.04.012
- Coppock, D. L., Kopman, C., Scandalis, S., and Gilleran, S. (1993). Preferential gene expression in quiescent human lung fibroblasts. *Cell Growth Differ.* 4, 483–493.
- Cornett, E. M., Ferry, L., Defossez, P. A., and Rothbart, S. B. (2019). Lysine methylation regulators moonlighting outside the epigenome. *Mol. Cell* 75, 1092–1101. doi: 10.1016/j.molcel.2019.08.026
- Cortini, R. (2016). The physics of epigenetics. *Rev. Modern Phys.* 88:025002.
- Corvalan, A. Z., and Coller, H. A. (2021). Methylation of histone 4's lysine 20: a critical analysis of the state of the field. *Physiol. Genomics* 53, 22–32. doi: 10.1152/physiolgenomics.00128.2020
- Cosgrove, M. S. (2012). Writers and readers: deconvoluting the harmonic complexity of the histone code. *Nat. Struct. Mol. Biol.* 19, 739–740. doi: 10.1038/nsmb.2350
- Cosgrove, M. S., Boeke, J. D., and Wolberger, C. (2004). Regulated nucleosome mobility and the histone code. *Nat. Struct. Mol. Biol.* 11, 1037–1043. doi: 10.1038/nsmb851
- Criscione, S. W., De Cecco, M., Siranosian, B., Zhang, Y., Kreiling, J. A., Sedivy, J. M., et al. (2016). Reorganization of chromosome architecture in replicative cellular senescence. *Sci. Adv.* 2:e1500882.
- Crump, N. T., Hazzalin, C. A., Bowers, E. M., Alani, R. M., Cole, P. A., and Mahadevan, L. C. (2011). Dynamic acetylation of all lysine-4 trimethylated histone H3 is evolutionarily conserved and mediated by p300/CBP. *Proc. Natl. Acad. Sci. U.S.A.* 108, 7814–7819. doi: 10.1073/pnas.1100991108
- Cui, K., Zang, C., Roh, T. Y., Schones, D. E., Childs, R. W., Peng, W., et al. (2009). Chromatin signatures in multipotent human hematopoietic stem cells indicate the fate of bivalent genes during differentiation. *Cell Stem Cell* 4, 80–93. doi: 10.1016/j.stem.2008.11.011
- Cutter, A. R., and Hayes, J. J. (2015). A brief review of nucleosome structure. *FEBS Lett.* 589, 2914–2922.
- Dai, J., Itahana, K., and Baskar, R. (2015). Quiescence does not affect p53 and stress response by irradiation in human lung fibroblasts. *Biochem. Biophys. Res. Commun.* 458, 104–109.
- Daniel, J. A., and Nussenzweig, A. (2012). Roles for histone H3K4 methyltransferase activities during immunoglobulin class-switch recombination. *Biochim. Biophys. Acta* 1819, 733–738.
- Dardick, I., Sinnott, N. M., Hall, R., Bajenko-Carr, T. A., and Setterfield, G. (1983). Nuclear morphology and morphometry of B-lymphocyte transformation. Implications for follicular center cell lymphomas. *Am. J. Pathol.* 111, 35–49.
- De Virgilio, C. (2012). The essence of yeast quiescence. *FEMS Microbiol. Rev.* 36, 306–339.
- DeChiara, T. M., Robertson, E. J., and Efstratiadis, A. (1991). Parental imprinting of the mouse insulin-like growth factor II gene. *Cell* 64, 849–859.
- Deng, Z., Norseen, J., Wiedmer, A., Riethman, H., and Lieberman, P. M. (2009). TERRA RNA binding to TRF2 facilitates heterochromatin formation and ORC recruitment at telomeres. *Mol. Cell* 35, 403–413. doi: 10.1016/j.molcel.2009.06.025
- DesJarlais, R., and Tummino, P. J. (2016). Role of histone-modifying enzymes and their complexes in regulation of chromatin biology. *Biochemistry* 55, 1584–1599.
- Dhawan, J., and Laxman, S. (2015). Decoding the stem cell quiescence cycle—lessons from yeast for regenerative biology. *J. Cell Sci.* 128, 4467–4474. doi: 10.1242/jcs.177758
- Dixon, J. R., Selvaraj, S., Yue, F., Kim, A., Li, Y., Shen, Y., et al. (2012). Topological domains in mammalian genomes identified by analysis of chromatin interactions. *Nature* 485, 376–380.
- Doil, C., Mailand, N., Bekker-Jensen, S., Menard, P., Larsen, D. H., Pepperkok, R., et al. (2009). RNF168 binds and amplifies ubiquitin conjugates on damaged chromosomes to allow accumulation of repair proteins. *Cell* 136, 435–446. doi: 10.1016/j.cell.2008.12.041
- Duina, A. A., Miller, M. E., and Keeney, J. B. (2014). Budding yeast for budding geneticists: a primer on the *Saccharomyces cerevisiae* model system. *Genetics* 197, 33–48.
- Dumont, N. A., Wang, Y. X., and Rudnicki, M. A. (2015). Intrinsic and extrinsic mechanisms regulating satellite cell function. *Development* 142, 1572–1581.
- Dykstra, B., Kent, D., Bowie, M., McCaffrey, L., Hamilton, M., Lyons, K., et al. (2007). Long-term propagation of distinct hematopoietic differentiation programs in vivo. *Cell Stem Cell* 1, 218–229. doi: 10.1016/j.stem.2007.05.015
- Edwards, C. R., Dang, W., and Berger, S. L. (2011). Histone H4 lysine 20 of *Saccharomyces cerevisiae* is monomethylated and functions in subtelomeric silencing. *Biochemistry* 50, 10473–10483. doi: 10.1021/bi201120q
- Egelhofer, T. A., Minoda, A., Klugman, S., Lee, K., Kolasinska-Zwier, P., Alekseyenko, A. A., et al. (2011). An assessment of histone-modification antibody quality. *Nat. Struct. Mol. Biol.* 18, 91–93.
- Eriksson, P. R., Ganguli, D., Nagarajavel, V., and Clark, D. J. (2012). Regulation of histone gene expression in budding yeast. *Genetics* 191, 7–20.
- Ernst, J., and Kellis, M. (2010). Discovery and characterization of chromatin states for systematic annotation of the human genome. *Nat. Biotechnol.* 28, 817–825.
- Everts, A. G., Manning, A. L., Wang, X., Dyson, N. J., Garcia, B. A., and Coller, H. A. (2013a). H4K20 methylation regulates quiescence and chromatin compaction. *Mol. Biol. Cell* 24, 3025–3037.
- Everts, A. G., Zee, B. M., Dimaggio, P. A., Gonzales-Cope, M., Coller, H. A., and Garcia, B. A. (2013b). Quantitative dynamics of the link between cellular metabolism and histone acetylation. *J. Biol. Chem.* 288, 12142–12151.
- Faghihi, M. A., and Wahlestedt, C. (2009). Regulatory roles of natural antisense transcripts. *Nat. Rev. Mol. Cell Biol.* 10, 637–643.
- Fang, J., Feng, Q., Ketel, C. S., Wang, H., Cao, R., Xia, L., et al. (2002). Purification and functional characterization of SET8, a nucleosomal histone H4-lysine 20-specific methyltransferase. *Curr. Biol.* 12, 1086–1099. doi: 10.1016/s0960-9822(02)00924-7
- Farooq, Z., Banday, S., Pandita, T. K., and Altaf, M. (2016). The many faces of histone H3K79 methylation. *Mutat. Res. Rev. Mutat. Res.* 768, 46–52. doi: 10.1016/j.mrrev.2016.03.005
- Farrelly, L. A., and Maze, I. (2019). An emerging perspective on 'histone code' mediated regulation of neural plasticity and disease. *Curr. Opin. Neurobiol.* 59, 157–163. doi: 10.1016/j.conb.2019.07.001
- Farrelly, L. A., Thompson, R. E., Zhao, S., Lepack, A. E., Lyu, Y., Bhanu, N. V., et al. (2019). Histone serotonylation is a permissive modification that enhances TFIID binding to H3K4me3. *Nature* 567, 535–539. doi: 10.1038/s41586-019-1024-7
- Finley, L. W. S., Vardhana, S. A., Carey, B. W., Alonso-Curbelo, D., Koche, R., Chen, Y., et al. (2018). Pluripotency transcription factors and Tet1/2 maintain Brd4-independent stem cell identity. *Nat. Cell Biol.* 20, 565–574. doi: 10.1038/s41556-018-0086-3
- Foudi, A., Hochedlinger, K., Van Buren, D., Schindler, J. W., Jaenisch, R., Carey, V., et al. (2009). Analysis of histone 2B-GFP retention reveals slowly cycling hematopoietic stem cells. *Nat. Biotechnol.* 27, 84–90. doi: 10.1038/nbt.1517
- Frauwirth, K. A., and Thompson, C. B. (2004). Regulation of T lymphocyte metabolism. *J. Immunol.* 172, 4661–4665.
- Frederiks, F., Tzouros, M., Oudgenoeg, G., van Welsem, T., Fornerod, M., Krijgsvel, J., et al. (2008). Nonprocessive methylation by Dot1 leads to



- functional redundancy of histone H3K79 methylation states. *Nat. Struct. Mol. Biol.* 15, 550–557. doi: 10.1038/nsmb.1432
- Freese, E. B., Chu, M. I., and Freese, E. (1982). Initiation of yeast sporulation of partial carbon, nitrogen, or phosphate deprivation. *J. Bacteriol.* 149, 840–851.
- Fu, Y., Zhu, Z., Meng, G., Zhang, R., and Zhang, Y. (2021). A CRISPR-Cas9 based shuffle system for endogenous histone H3 and H4 combinatorial mutagenesis. *Sci. Rep.* 11:3298. doi: 10.1038/s41598-021-82774-4
- Fuchs, S. M., Krajewski, K., Baker, R. W., Miller, V. L., and Strahl, B. D. (2011). Influence of combinatorial histone modifications on antibody and effector protein recognition. *Curr. Biol.* 21, 53–58. doi: 10.1016/j.cub.2010.11.058
- Fukada, S., Uezumi, A., Ikemoto, M., Masuda, S., Segawa, M., Tanimura, N., et al. (2007). Molecular signature of quiescent satellite cells in adult skeletal muscle. *Stem Cells* 25, 2448–2459.
- Fyodorov, D. V., Zhou, B. R., Skoultschi, A. I., and Bai, Y. (2018). Emerging roles of linker histones in regulating chromatin structure and function. *Nat. Rev. Mol. Cell Biol.* 19, 192–206.
- Gaertner, B., Johnston, J., Chen, K., Wallaschek, N., Paulson, A., Garruss, A. S., et al. (2012). Poised RNA polymerase II changes over developmental time and prepares genes for future expression. *Cell Rep.* 2, 1670–1683. doi: 10.1016/j.celrep.2012.11.024
- Galdieri, L., Mehrotra, S., Yu, S., and Vancura, A. (2010). Transcriptional regulation in yeast during diauxic shift and stationary phase. *OMICS* 14, 629–638.
- Gangloff, S., Achaz, G., Francesconi, S., Villain, A., Miled, S., Denis, C., et al. (2017). Quiescence unveils a novel mutational force in fission yeast. *Elife* 6:e27469. doi: 10.7554/eLife.27469
- Gangloff, S., and Arcangioli, B. (2017). DNA repair and mutations during quiescence in yeast. *FEMS Yeast Res.* 17:fox002.
- Garza, L. A., Yang, C. C., Zhao, T., Blatt, H. B., Lee, M., He, H., et al. (2011). Bald scalp in men with androgenetic alopecia retains hair follicle stem cells but lacks CD200-rich and CD34-positive hair follicle progenitor cells. *J. Clin. Invest.* 121, 613–622. doi: 10.1172/JCI44478
- Ghoneim, M., Fuchs, H. A., and Musselman, C. A. (2021). Histone tail conformations: a fuzzy affair with DNA. *Trends Biochem. Sci.* 46, 564–578. doi: 10.1016/j.tibs.2020.12.012
- Godfrey, L., Crump, N. T., Thorne, R., Lau, I. J., Repapi, E., Dimou, D., et al. (2019). DOT1L inhibition reveals a distinct subset of enhancers dependent on H3K79 methylation. *Nat. Commun.* 10:2803. doi: 10.1038/s41467-019-10844-3
- Godley, L. A., and Le Beau, M. M. (2012). The histone code and treatments for acute myeloid leukemia. *N. Engl. J. Med.* 366, 960–961.
- Gray, J. V., Petsko, G. A., Johnston, G. C., Ringe, D., Singer, R. A., and Werner-Washburne, M. (2004). "Sleeping beauty": quiescence in *Saccharomyces cerevisiae*. *Microbiol. Mol. Biol. Rev.* 68, 187–206.
- Greer, E. L., and Shi, Y. (2012). Histone methylation: a dynamic mark in health, disease and inheritance. *Nat. Rev. Genet.* 13, 343–357. doi: 10.1038/nrg3173
- Greig, D. (2009). Reproductive isolation in *Saccharomyces*. *Heredity (Edinb)* 102, 39–44.
- Grigoryev, S. A., Nikitina, T., Pehrson, J. R., Singh, P. B., and Woodcock, C. L. (2004). Dynamic relocation of epigenetic chromatin markers reveals an active role of constitutive heterochromatin in the transition from proliferation to quiescence. *J. Cell Sci.* 117(Pt 25), 6153–6162. doi: 10.1242/cs.01537
- Guan, X., Rastogi, N., Parthun, M. R., and Freitas, M. A. (2013). Discovery of histone modification crosstalk networks by stable isotope labeling of amino acids in cell culture mass spectrometry (SILAC MS). *Mol. Cell. Proteomics* 12, 2048–2059. doi: 10.1074/mcp.M112.026716
- Guidi, M., Ruault, M., Marbouty, M., Loidice, I., Cournac, A., Billaudeau, C., et al. (2015). Spatial reorganization of telomeres in long-lived quiescent cells. *Genome Biol.* 16:206. doi: 10.1186/s13059-015-0766-2
- Guttman, M., Donaghey, J., Carey, B. W., Garber, M., Grenier, J. K., Munson, G., et al. (2011). lincRNAs act in the circuitry controlling pluripotency and differentiation. *Nature* 477, 295–300.
- Hahn, M., Dambacher, S., Dulev, S., Kuznetsova, A. Y., Eck, S., Wörz, S., et al. (2013). Suv4-20h2 mediates chromatin compaction and is important for cohesin recruitment to heterochromatin. *Genes Dev.* 27, 859–872. doi: 10.1101/gad.210377.112
- Hainer, S. J., and Fazio, T. G. (2019). High-Resolution chromatin profiling using CUT&RUN. *Curr. Protoc. Mol. Biol.* 126:e85.
- Hanly, D. J., Esteller, M., and Berdasco, M. (2018). Interplay between long non-coding RNAs and epigenetic machinery: emerging targets in cancer? *Philos. Trans. R. Soc. Lond. B Biol. Sci.* 373:20170074. doi: 10.1098/rstb.2017.0074
- Hansen, K. H., Bracken, A. P., Pasini, D., Dietrich, N., Gehani, S. S., Monrad, A., et al. (2008). A model for transmission of the H3K27me3 epigenetic mark. *Nat. Cell Biol.* 10, 1291–1300. doi: 10.1038/ncb1787
- Hayashi, T., Teruya, T., Chaleckis, R., Morigasaki, S., and Yanagida, M. (2018). S-Adenosylmethionine synthetase is required for cell growth, maintenance of G0 phase, and termination of quiescence in fission yeast. *iScience* 5, 38–51. doi: 10.1016/j.isci.2018.06.011
- Hayashi-Takanaka, Y., Kina, Y., Nakamura, F., Becking, L. E., Nakao, Y., Nagase, T., et al. (2020). Histone modification dynamics as revealed by multicolor immunofluorescence-based single-cell analysis. *J. Cell Sci.* 133, doi: 10.1242/jcs.243444
- Henikoff, S., and Shilatifard, A. (2011). Histone modification: cause or cog? *Trends Genet.* 27, 389–396.
- Higuchi-Sanabria, R., Pernice, W. M., Vevea, J. D., Alessi Wolken, D. M., Boldogh, I. R., and Pon, L. A. (2014). Role of asymmetric cell division in lifespan control in *Saccharomyces cerevisiae*. *FEMS Yeast Res.* 14, 1133–1146.
- Ho, C. H., Takizawa, Y., Kobayashi, W., Arimura, Y., Kimura, H., and Kurumizaka, H. (2021). Structural basis of nucleosomal histone H4 lysine 20 methylation by SET8 methyltransferase. *Life Sci. Alliance* 4:e202000919.
- Ho, J. W., Jung, Y. L., Liu, T., Alver, B. H., Lee, S., Ikegami, K., et al. (2014). Comparative analysis of metazoan chromatin organization. *Nature* 512, 449–452.
- Hornbeck, P. V., Zhang, B., Murray, B., Kornhauser, J. M., Latham, V., and Skrzypek, E. (2015). PhosphoSitePlus, 2014: mutations, PTMs and recalibrations. *Nucleic Acids Res.* 43, D512–D520. doi: 10.1093/nar/gku1267
- Huang, J., Gujar, M. R., Deng, Q., Sook, Y. C., Li, S., Tan, P., et al. (2021). Histone lysine methyltransferase Pr-set7/SETD8 promotes neural stem cell reactivation. *EMBO Rep.* 2021:e50994. doi: 10.15252/embr.202050994
- Huen, M. S., Grant, R., Manke, I., Minn, K., Yu, X., Yaffe, M. B., et al. (2007). RNF8 transduces the DNA-damage signal via histone ubiquitylation and checkpoint protein assembly. *Cell* 131, 901–914. doi: 10.1016/j.cell.2007.09.041
- Husmann, D., and Gozani, O. (2019). Histone lysine methyltransferases in biology and disease. *Nat. Struct. Mol. Biol.* 26, 880–889.
- Hyun, K., Jeon, J., Park, K., and Kim, J. (2017). Writing, erasing and reading histone lysine methylations. *Exp. Mol. Med.* 49:e324.
- Jambhekar, A., Dhall, A., and Shi, Y. (2019). Roles and regulation of histone methylation in animal development. *Nat. Rev. Mol. Cell Biol.* 20, 625–641.
- Jamieson, K., Rountree, M. R., Lewis, Z. A., Stajich, J. E., and Selker, E. U. (2013). Regional control of histone H3 lysine 27 methylation in *Neurospora*. *Proc. Natl. Acad. Sci. U.S.A.* 110, 6027–6032.
- Jenuwein, T., and Allis, C. D. (2001). Translating the histone code. *Science* 293, 1074–1080.
- Joh, R. I., Khanduja, J. S., Calvo, I. A., Mistry, M., Palmieri, C. M., Savol, A. J., et al. (2016). Survival in quiescence requires the euchromatic deployment of Clr4/SUV39H by argonaute-associated small RNAs. *Mol. Cell* 64, 1088–1101. doi: 10.1016/j.molcel.2016.11.020
- Johnson, E. L., Robinson, D. G., and Collier, H. A. (2017). Widespread changes in mRNA stability contribute to quiescence-specific gene expression patterns in a fibroblast model of quiescence. *BMC Genomics* 18:123. doi: 10.1186/s12864-017-3521-0
- Jorgensen, S., Elvers, I., Trelle, M. B., Menzel, T., Eskildsen, M., Jensen, O. N., et al. (2007). The histone methyltransferase SET8 is required for S-phase progression. *J. Cell Biol.* 179, 1337–1345. doi: 10.1083/jcb.200706150
- Jorgensen, S., Schotta, G., and Sorensen, C. S. (2013). Histone H4 lysine 20 methylation: key player in epigenetic regulation of genomic integrity. *Nucleic Acids Res.* 41, 2797–2806. doi: 10.1093/nar/gkt012
- Julien, E., and Herr, W. (2004). A switch in mitotic histone H4 lysine 20 methylation status is linked to M phase defects upon loss of HCF-1. *Mol. Cell* 14, 713–725. doi: 10.1016/j.molcel.2004.06.008
- Kaelin, W. G. Jr., and McKnight, S. L. (2013). Influence of metabolism on epigenetics and disease. *Cell* 153, 56–69.

- Kalakonda, N., Fischle, W., Bocconi, P., Gurvich, N., Hoya-Arias, R., Zhao, X., et al. (2008). Histone H4 lysine 20 monomethylation promotes transcriptional repression by L3MBTL1. *Oncogene* 27, 4293–4304. doi: 10.1038/nc.2008.67
- Kalamakis, G., Brune, D., Ravichandran, S., Bolz, J., Fan, W., Ziebell, F., et al. (2019). Quiescence modulates stem cell maintenance and regenerative capacity in the aging brain. *Cell* 176, 1407–19.e14. doi: 10.1016/j.cell.2019.01.040
- Kalb, R., Latwiel, S., Baymaz, H. I., Jansen, P. W., Muller, C. W., Vermeulen, M., et al. (2014). Histone H2A monoubiquitination promotes histone H3 methylation in Polycomb repression. *Nat. Struct. Mol. Biol.* 21, 569–571.
- Kallingappa, P. K., Turner, P. M., Eichenlaub, M. P., Green, A. L., Oback, F. C., Chibnall, A. M., et al. (2016). Quiescence loosens epigenetic constraints in bovine somatic cells and improves their reprogramming into totipotency. *Biol. Reprod.* 95:16. doi: 10.1095/biolreprod.115.137109
- Kang, S., Long, K., Wang, S., Sada, A., and Tumber, T. (2020). Histone H3 K4/9/27 trimethylation levels affect wound healing and stem cell dynamics in adult skin. *Stem Cell Rep.* 14, 34–48. doi: 10.1016/j.stemcr.2019.11.007
- Kantidakis, T., Saponaro, M., Mitter, R., Horswell, S., Kranz, A., Boeing, S., et al. (2016). Mutation of cancer driver MLL2 results in transcription stress and genome instability. *Genes Dev.* 30, 408–420. doi: 10.1101/gad.275453.115
- Kaya-Okur, H. S., Wu, S. J., Codomo, C. A., Pledger, E. S., Bryson, T. D., Henikoff, J. G., et al. (2019). CUT&Tag for efficient epigenomic profiling of small samples and single cells. *Nat. Commun.* 10:1930.
- Kent, D., Dykstra, B., and Eaves, C. (2007). Isolation and assessment of long-term reconstituting hematopoietic stem cells from adult mouse bone marrow. *Curr. Protoc. Stem Cell Biol.* Chapter 2:Unit 2A.4.
- Kharchenko, P. V., Alekseyenko, A. A., Schwartz, Y. B., Minoda, A., Riddle, N. C., Ernst, J., et al. (2011). Comprehensive analysis of the chromatin landscape in *Drosophila melanogaster*. *Nature* 471, 480–485.
- Khoa, L. T. P., Tsan, Y. C., Mao, F., Kremer, D. M., Sajjakulnukit, P., Zhang, L., et al. (2020). Histone acetyltransferase MOF blocks acquisition of quiescence in ground-state ESCs through activating fatty acid oxidation. *Cell Stem Cell* 27, 441–458.e10. doi: 10.1016/j.stem.2020.06.005
- Kim, S. K., Jung, I., Lee, H., Kang, K., Kim, M., Jeong, K., et al. (2012). Human histone H3K79 methyltransferase DOT1L protein [corrected] binds actively transcribing RNA polymerase II to regulate gene expression. *J. Biol. Chem.* 287, 39698–39709. doi: 10.1074/jbc.M112.384057
- Kim, T. D., Shin, S., Berry, W. L., Oh, S., and Janknecht, R. (2012). The JMJD2A demethylase regulates apoptosis and proliferation in colon cancer cells. *J. Cell. Biochem.* 113, 1368–1376. doi: 10.1002/jcb.24009
- Klose, R. J., Yan, Q., Tothova, Z., Yamane, K., Erdjument-Bromage, H., Tempst, P., et al. (2007). The retinoblastoma binding protein RBP2 is an H3K4 demethylase. *Cell* 128, 889–900.
- Knosp, O., Talasz, H., and Puschendorf, B. (1991). Histone acetylation and histone synthesis in mouse fibroblasts during quiescence and restimulation into S-phase. *Mol. Cell. Biochem.* 101, 51–58. doi: 10.1007/BF00238437
- Kohlmaier, A., Savarese, F., Lachner, M., Martens, J., Jenuwein, T., and Wutz, A. (2004). A chromosomal memory triggered by Xist regulates histone methylation in X inactivation. *PLoS Biol.* 2:E171. doi: 10.1371/journal.pbio.0020171
- Kolas, N. K., Chapman, J. R., Nakada, S., Ylanko, J., Chahwan, R., Sweeney, F. D., et al. (2007). Orchestration of the DNA-damage response by the RNF8 ubiquitin ligase. *Science* 318, 1637–1640.
- Kornberg, R. D., and Lorch, Y. (2020). Primary role of the nucleosome. *Mol. Cell* 79, 371–375.
- Kourmouli, N., Jeppesen, P., Mahadevaiah, S., Burgoyne, P., Wu, R., Gilbert, D. M., et al. (2004). Heterochromatin and tri-methylated lysine 20 of histone H4 in animals. *J. Cell Sci.* 117(Pt 12), 2491–2501.
- Kurumizaka, H., Kujirai, T., and Takizawa, Y. (2021). Contributions of histone variants in nucleosome structure and function. *J. Mol. Biol.* 433:166678.
- Kwon, J. S., Everetts, N. J., Wang, X., Wang, W., Della Croce, K., Xing, J., et al. (2017). Controlling depth of cellular quiescence by an Rb-E2F network switch. *Cell Rep.* 20, 3223–3235. doi: 10.1016/j.celrep.2017.09.007
- Lachner, M., O'Carroll, D., Rea, S., Mechtler, K., and Jenuwein, T. (2001). Methylation of histone H3 lysine 9 creates a binding site for HP1 proteins. *Nature* 410, 116–120.
- Lacoste, N., Utley, R. T., Hunter, J. M., Poirier, G. G., and Cote, J. (2002). Disruptor of telomeric silencing-1 is a chromatin-specific histone H3 methyltransferase. *J. Biol. Chem.* 277, 30421–30424. doi: 10.1074/jbc.C200366200
- Laporte, D., Courtout, F., Tollis, S., and Sagot, I. (2016). Quiescent *Saccharomyces cerevisiae* forms telomere hyperclusters at the nuclear membrane vicinity through a multifaceted mechanism involving Esc1, the Sir complex, and chromatin condensation. *Mol. Biol. Cell* 27, 1875–1884. doi: 10.1091/mbc.E16-01-0069
- Laporte, D., Lebaudy, A., Sahin, A., Pinson, B., Ceschin, J., Daignan-Fornier, B., et al. (2011). Metabolic status rather than cell cycle signals control quiescence entry and exit. *J. Cell Biol.* 192, 949–957. doi: 10.1083/jcb.201009028
- Lauberth, S. M., Nakayama, T., Wu, X., Ferris, A. L., Tang, Z., Hughes, S. H., et al. (2013). H3K4me3 interactions with TAF3 regulate preinitiation complex assembly and selective gene activation. *Cell* 152, 1021–1036. doi: 10.1016/j.cell.2013.01.052
- Lavarone, E., Barbieri, C. M., and Pasini, D. (2019). Dissecting the role of H3K27 acetylation and methylation in PRC2 mediated control of cellular identity. *Nat. Commun.* 10:1679. doi: 10.1038/s41467-019-09624-w
- Lee, H. N., Mitra, M., Bosompra, O., Corney, D. C., Johnson, E. L., Rashed, N., et al. (2018). RECK isoforms have opposing effects on cell migration. *Mol. Biol. Cell* 29, 1825–1838.
- Lee, J., Kang, S., Lilja, K. C., Colletier, K. J., Scheitz, C. J., Zhang, Y. V., et al. (2016). Signalling couples hair follicle stem cell quiescence with reduced histone H3 K4/K9/K27me3 for proper tissue homeostasis. *Nat. Commun.* 7:11278. doi: 10.1038/ncomms11278
- Lee, S., Oh, S., Jeong, K., Jo, H., Choi, Y., Seo, H. D., et al. (2018). Dot1 regulates nucleosome dynamics by its inherent histone chaperone activity in yeast. *Nat. Commun.* 9:240. doi: 10.1038/s41467-017-02759-8
- Legesse-Miller, A., Raitman, I., Haley, E. M., Liao, A., Sun, L. L., Wang, D. J., et al. (2012). Quiescent fibroblasts are protected from proteasome inhibition-mediated toxicity. *Mol. Biol. Cell* 23, 3566–3581. doi: 10.1091/mbc.E12-03-0192
- Lemons, J. M., Feng, X. J., Bennett, B. D., Legesse-Miller, A., Johnson, E. L., Raitman, I., et al. (2010). Quiescent fibroblasts exhibit high metabolic activity. *PLoS Biol.* 8:e1000514. doi: 10.1371/journal.pbio.1000514
- Lesch, B. J., Dokshin, G. A., Young, R. A., McCarrey, J. R., and Page, D. C. (2013). A set of genes critical to development is epigenetically poised in mouse germ cells from fetal stages through completion of meiosis. *Proc. Natl. Acad. Sci. U.S.A.* 110, 16061–16066. doi: 10.1073/pnas.1315204110
- Li, J., Mahata, B., Escobar, M., Goell, J., Wang, K., Khemka, P., et al. (2021). Programmable human histone phosphorylation and gene activation using a CRISPR/Cas9-based chromatin kinase. *Nat. Commun.* 12:896. doi: 10.1038/s41467-021-21188-2
- Li, L., and Bhatia, R. (2011). Stem cell quiescence. *Clin. Cancer Res.* 17, 4936–4941.
- Li, L., and Clevers, H. (2010). Coexistence of quiescent and active adult stem cells in mammals. *Science* 327, 542–545.
- Lieberman-Aiden, E., van Berkum, N. L., Williams, L., Imakaev, M., Ragoczy, T., Telling, A., et al. (2009). Comprehensive mapping of long-range interactions reveals folding principles of the human genome. *Science* 326, 289–293. doi: 10.1126/science.1181369
- Lien, W. H., Guo, X., Polak, L., Lawton, L. N., Young, R. A., Zheng, D., et al. (2011). Genome-wide maps of histone modifications unwind in vivo chromatin states of the hair follicle lineage. *Cell Stem Cell* 9, 219–232. doi: 10.1016/j.stem.2011.07.015
- Liokatis, S., Stutzer, A., Elsasser, S. J., Theillet, F. X., Klingberg, R., van Rossum, B., et al. (2012). Phosphorylation of histone H3 Ser10 establishes a hierarchy for subsequent intramolecular modification events. *Nat. Struct. Mol. Biol.* 19, 819–823. doi: 10.1038/nsmb.2310
- Liu, L., Cheung, T. H., Charville, G. W., Hurgu, B. M., Leavitt, T., Shih, J., et al. (2013). Chromatin modifications as determinants of muscle stem cell quiescence and chronological aging. *Cell Rep.* 4, 189–204. doi: 10.1016/j.celrep.2013.05.043
- Liu, Y., Chen, S., Wang, S., Soares, F., Fischer, M., Meng, F., et al. (2017). Transcriptional landscape of the human cell cycle. *Proc. Natl. Acad. Sci. U.S.A.* 114, 3473–3478.

- Lomberg, G., Bensi, D., Fernandez-Zapico, M. E., and Urrutia, R. (2006). Evidence for the existence of an HP1-mediated subcode within the histone code. *Nat. Cell Biol.* 8, 407–415. doi: 10.1038/ncb1383
- Lu, X., Simon, M. D., Chodaparambil, J. V., Hansen, J. C., Shokat, K. M., and Luger, K. (2008). The effect of H3K79 dimethylation and H4K20 trimethylation on nucleosome and chromatin structure. *Nat. Struct. Mol. Biol.* 15, 1122–1124. doi: 10.1038/nsmb.1489
- Luo, M., Jeong, M., Sun, D., Park, H. J., Rodriguez, B. A., Xia, Z., et al. (2015). Long non-coding RNAs control hematopoietic stem cell function. *Cell Stem Cell* 16, 426–438.
- Lynch, M. D., and Watt, F. M. (2018). Fibroblast heterogeneity: implications for human disease. *J. Clin. Invest.* 128, 26–35.
- Ma, D. K., Bonaguidi, M. A., Ming, G. L., and Song, H. (2009). Adult neural stem cells in the mammalian central nervous system. *Cell Res.* 19, 672–682.
- Machida, S., Takizawa, Y., Ishimaru, M., Sugita, Y., Sekine, S., Nakayama, J. I., et al. (2018). Structural basis of heterochromatin formation by human HP1. *Mol. Cell* 69, 385–397.e8.
- Mailand, N., Bekker-Jensen, S., Fastrup, H., Melander, F., Bartek, J., Lukas, C., et al. (2007). RNF8 ubiquitylates histones at DNA double-strand breaks and promotes assembly of repair proteins. *Cell* 131, 887–900.
- Maki, K., Nava, M. M., Villeneuve, C., Chang, M., Furukawa, K. S., Ushida, T., et al. (2021). Hydrostatic pressure prevents chondrocyte differentiation through heterochromatin remodeling. *J. Cell Sci.* 134:jcs247643.
- Maksimovic, I., and David, Y. (2021). Non-enzymatic covalent modifications as a new chapter in the histone code. *Trends Biochem. Sci.* 46, 718–730.
- Marescal, O., and Cheeseman, I. M. (2020). Cellular mechanisms and regulation of quiescence. *Dev. Cell* 55, 259–271.
- Margaritis, T., and Holstege, F. C. (2008). Poised RNA polymerase II gives pause for thought. *Cell* 133, 581–584. doi: 10.1016/j.cell.2008.04.027
- Marguerat, S., Schmidt, A., Codlin, S., Chen, W., Aebersold, R., and Bahler, J. (2012). Quantitative analysis of fission yeast transcriptomes and proteomes in proliferating and quiescent cells. *Cell* 151, 671–683. doi: 10.1016/j.cell.2012.09.019
- Margueron, R., and Reinberg, D. (2011). The Polycomb complex PRC2 and its mark in life. *Nature* 469, 343–349.
- Margueron, R., Justin, N., Ohno, K., Sharpe, M. L., Son, J., Drury, W. J. III, et al. (2009). Role of the polycomb protein EED in the propagation of repressive histone marks. *Nature* 461, 762–767. doi: 10.1038/nature08398
- Margueron, R., Li, G., Sarma, K., Blais, A., Zavadil, J., Woodcock, C. L., et al. (2008). Ezh1 and Ezh2 maintain repressive chromatin through different mechanisms. *Mol. Cell* 32, 503–518.
- Marion, R. M., Schotta, G., Ortega, S., and Blasco, M. A. (2011). Suv4-20h abrogation enhances telomere elongation during reprogramming and confers a higher tumorigenic potential to iPS cells. *PLoS One* 6:e25680. doi: 10.1371/journal.pone.0025680
- Martens, J. H., O'Sullivan, R. J., Braunschweig, U., Opravil, S., Radolf, M., Steinlein, P., et al. (2005). The profile of repeat-associated histone lysine methylation states in the mouse epigenome. *EMBO J.* 24, 800–812. doi: 10.1038/sj.emboj.7600545
- Martinez, M. J., Roy, S., Archuletta, A. B., Wentzell, P. D., Anna-Arriola, S. S., Rodriguez, A. L., et al. (2004). Genomic analysis of stationary-phase and exit in *Saccharomyces cerevisiae*: gene expression and identification of novel essential genes. *Mol. Biol. Cell* 15, 5295–5305. doi: 10.1091/mbc.e03-11-0856
- Martinez-Reyes, I., and Chandel, N. S. (2020). Mitochondrial TCA cycle metabolites control physiology and disease. *Nat. Commun.* 11:102.
- Martynoga, B., Mateo, J. L., Zhou, B., Andersen, J., Achimastou, A., Urban, N., et al. (2013). Epigenomic enhancer annotation reveals a key role for NF1X in neural stem cell quiescence. *Genes Dev.* 27, 1769–1786. doi: 10.1101/gad.216804.113
- Maurer-Stroh, S., Dickens, N. J., Hughes-Davies, L., Kouzarides, T., Eisenhaber, F., and Ponting, C. P. (2003). The Tudor domain 'royal family': Tudor, plant Agetet, chromo, PWWP and MBT domains. *Trends Biochem. Sci.* 28, 69–74. doi: 10.1016/S0968-0004(03)00004-5
- Maya-Miles, D., Andujar, E., Perez-Alegre, M., Murillo-Pineda, M., Barrientos-Moreno, M., Cabello-Lobato, M. J., et al. (2019). Crosstalk between chromatin structure, cohesin activity and transcription. *Epigenet. Chromatin* 12, 47. doi: 10.1186/s13072-019-0293-6
- McKnight, J. N., Boerma, J. W., Breeden, L. L., and Tsukiyama, T. (2015). Global promoter targeting of a conserved lysine deacetylase for transcriptional shutoff during quiescence entry. *Mol. Cell* 59, 732–743. doi: 10.1016/j.molcel.2015.07.014
- McMahon, S. B., Wood, M. A., and Cole, M. D. (2000). The essential cofactor TRRAP recruits the histone acetyltransferase hGCN5 to c-Myc. *Mol. Cell Biol.* 20, 556–562. doi: 10.1128/MCB.20.2.556-562.2000
- Mehta, I. S., Amira, M., Harvey, A. J., and Bridger, J. M. (2010). Rapid chromosome territory relocation by nuclear motor activity in response to serum removal in primary human fibroblasts. *Genome Biol.* 11:R5. doi: 10.1186/gb-2010-11-1-r5
- Meng, F., Stamms, K., Bennewitz, R., Green, A., Obach, F., Turner, P., et al. (2020). Targeted histone demethylation improves somatic cell reprogramming into cloned blastocysts but not postimplantation bovine concepti. *Biol. Reprod.* 103, 114–125. doi: 10.1093/biolre/iaaa053
- Mews, P., Zee, B. M., Liu, S., Donahue, G., Garcia, B. A., and Berger, S. L. (2014). Histone methylation has dynamics distinct from those of histone acetylation in cell cycle reentry from quiescence. *Mol. Cell Biol.* 34, 3968–3980. doi: 10.1128/MCB.00763-14
- Michan, S., and Sinclair, D. (2007). Sirtuins in mammals: insights into their biological function. *Biochem. J.* 404, 1–13.
- Mikkelsen, T. S., Ku, M., Jaffe, D. B., Issac, B., Lieberman, E., Giannoukos, G., et al. (2007). Genome-wide maps of chromatin state in pluripotent and lineage-committed cells. *Nature* 448, 553–560. doi: 10.1038/nature06008
- Miles, S., Bradley, G. T., and Breeden, L. L. (2021). The budding yeast transition to quiescence. *Yeast* 38, 30–38.
- Miles, S., Li, L. H., Melville, Z., and Breeden, L. L. (2019). Ssd1 and the cell wall integrity pathway promote entry, maintenance, and recovery from quiescence in budding yeast. *Mol. Biol. Cell* 30, 2205–2217. doi: 10.1091/mbc.E19-04-0190
- Milne, T. A., Zhao, K., and Hess, J. L. (2009). Chromatin immunoprecipitation (ChIP) for analysis of histone modifications and chromatin-associated proteins. *Methods Mol. Biol.* 538, 409–423.
- Mitra, M., Ho, L. D., and Collier, H. A. (2018a). An in vitro model of cellular quiescence in primary human dermal fibroblasts. *Methods Mol. Biol.* 1686, 27–47. doi: 10.1007/978-1-4939-7371-2\_2
- Mitra, M., Johnson, E. L., Swamy, V. S., Nersesian, L. E., Corney, D. C., Robinson, D. G., et al. (2018b). Alternative polyadenylation factors link cell cycle to migration. *Genome Biol.* 19:176. doi: 10.1186/s13059-018-1551-9
- Mochida, S., and Yanagida, M. (2006). Distinct modes of DNA damage response in *S. pombe* G0 and vegetative cells. *Genes Cells* 11, 13–27. doi: 10.1111/j.1365-2443.2005.00917.x
- Montoya-Durango, D. E., Liu, Y., Teneng, I., Kalbfleisch, T., Lacy, M. E., Steffen, M. C., et al. (2009). Epigenetic control of mammalian LINE-1 retrotransposon by retinoblastoma proteins. *Mutat. Res.* 665, 20–28. doi: 10.1016/j.mrfmmm.2009.02.011
- Morgan, M. A. J., and Shilatifard, A. (2020). Reevaluating the roles of histone-modifying enzymes and their associated chromatin modifications in transcriptional regulation. *Nat. Genet.* 52, 1271–1281. doi: 10.1038/s41588-020-00736-4
- Morris, S. A., Shibata, Y., Noma, K., Tsukamoto, Y., Warren, E., Temple, B., et al. (2005). Histone H3 K36 methylation is associated with transcription elongation in *Schizosaccharomyces pombe*. *Eukaryot. Cell* 4, 1446–1454. doi: 10.1128/EC.4.8.1446-1454.2005
- Morrish, F., Noonan, J., Perez-Olsen, C., Gafken, P. R., Fitzgibbon, M., Kelleher, J., et al. (2010). Myc-dependent mitochondrial generation of acetyl-CoA contributes to fatty acid biosynthesis and histone acetylation during cell cycle entry. *J. Biol. Chem.* 285, 36267–36274. doi: 10.1074/jbc.M110.141606
- Mueller, D., Bach, C., Zeisig, D., Garcia-Cuellar, M. P., Monroe, S., Sreekumar, A., et al. (2007). A role for the MLL fusion partner ENL in transcriptional elongation and chromatin modification. *Blood* 110, 4445–4454.
- Muhl, L., Genove, G., Leptidis, S., Liu, J., He, L., Mocci, G., et al. (2020). Single-cell analysis uncovers fibroblast heterogeneity and criteria for fibroblast and mural cell identification and discrimination. *Nat. Commun.* 11:3953.
- Murton, B. L., Chin, W. L., Ponting, C. P., and Itzhaki, L. S. (2010). Characterising the binding specificities of the subunits associated with the KMT2/Set1 histone lysine methyltransferase. *J. Mol. Biol.* 398, 481–488. doi: 10.1016/j.jmb.2010.03.036



- Nakamura, T., Pluskal, T., Nakaseko, Y., and Yanagida, M. (2012). Impaired coenzyme A synthesis in fission yeast causes defective mitosis, quiescence-exit failure, histone hypoacetylation and fragile DNA. *Open Biol.* 2:120117. doi: 10.1098/rsob.120117
- Nakamura-Ishizu, A., Takizawa, H., and Suda, T. (2014). The analysis, roles and regulation of quiescence in hematopoietic stem cells. *Development* 141, 4656–4666.
- Nasmyth, K. (2011). Cohesin: a catenase with separate entry and exit gates? *Nat. Cell Biol.* 13, 1170–1177. doi: 10.1038/ncb2349
- Neiman, A. M. (2011). Sporulation in the budding yeast *Saccharomyces cerevisiae*. *Genetics* 189, 737–765.
- Nelson, D. M., Jaber-Hijazi, F., Cole, J. J., Robertson, N. A., Pawlikowski, J. S., Norris, K. T., et al. (2016). Mapping H4K20me3 onto the chromatin landscape of senescent cells indicates a function in control of cell senescence and tumor suppression through preservation of genetic and epigenetic stability. *Genome Biol.* 17:158. doi: 10.1186/s13059-016-1017-x
- Ngubo, M., Kemp, G., and Patterson, H. G. (2011). Nano-electrospray tandem mass spectrometric analysis of the acetylation state of histones H3 and H4 in stationary phase in *Saccharomyces cerevisiae*. *BMC Biochem.* 12:34. doi: 10.1186/1471-2091-12-34
- Nguyen, A. T., and Zhang, Y. (2011). The diverse functions of Dot1 and H3K79 methylation. *Genes Dev.* 25, 1345–1358.
- Ninova, M., Fejes Toth, K., and Aravin, A. A. (2019). The control of gene expression and cell identity by H3K9 trimethylation. *Development* 146:dev181180.
- Nishioka, K., Rice, J. C., Sarma, K., Erdjument-Bromage, H., Werner, J., Wang, Y., et al. (2002b). PR-Set7 is a nucleosome-specific methyltransferase that modifies lysine 20 of histone H4 and is associated with silent chromatin. *Mol. Cell* 9, 1201–1213. doi: 10.1016/s1097-2765(02)00548-8
- Nishioka, K., Chuikov, S., Sarma, K., Erdjument-Bromage, H., Allis, C. D., Tempst, P., et al. (2002a). Set9, a novel histone H3 methyltransferase that facilitates transcription by precluding histone tail modifications required for heterochromatin formation. *Genes Dev.* 16, 479–489. doi: 10.1101/gad.967202
- Norton, V. G., Imai, B. S., Yau, P., and Bradbury, E. M. (1989). Histone acetylation reduces nucleosome core particle linking number change. *Cell* 57, 449–457.
- Nowak, J. A., Polak, L., Pasolli, H. A., and Fuchs, E. (2008). Hair follicle stem cells are specified and function in early skin morphogenesis. *Cell Stem Cell* 3, 33–43. doi: 10.1016/j.stem.2008.05.009
- Nurse, P., and Bissett, Y. (1981). Gene required in G1 for commitment to cell cycle and in G2 for control of mitosis in fission yeast. *Nature* 292, 558–560.
- Obernier, K., Cebrian-Silla, A., Thomson, M., Parraguez, J. I., Anderson, R., Guinto, C., et al. (2018). Adult neurogenesis is sustained by symmetric self-renewal and differentiation. *Cell Stem Cell* 22, 221–234.e8.
- Oda, H., Okamoto, I., Murphy, N., Chu, J., Price, S. M., Shen, M. M., et al. (2009). Monomethylation of histone H4-lysine 20 is involved in chromosome structure and stability and is essential for mouse development. *Mol. Cell Biol.* 29, 2278–2295. doi: 10.1128/MCB.01768-08
- O'Geen, H., Echipare, L., and Farnham, P. J. (2011). Using ChIP-seq technology to generate high-resolution profiles of histone modifications. *Methods Mol. Biol.* 791, 265–286.
- Oya, E., Durand-Dubief, M., Cohen, A., Maksimov, V., Schurra, C., Nakayama, J. I., et al. (2019). Leol1 is essential for the dynamic regulation of heterochromatin and gene expression during cellular quiescence. *Epigenet. Chromatin* 12:45. doi: 10.1186/s13072-019-0292-7
- Park, S. Y., and Kim, J. S. (2020). A short guide to histone deacetylases including recent progress on class II enzymes. *Exp. Mol. Med.* 52, 204–212. doi: 10.1038/s12276-020-0382-4
- Pesavento, J. J., Yang, H., Kelleher, N. L., and Mizzen, C. A. (2008). Certain and progressive methylation of histone H4 at lysine 20 during the cell cycle. *Mol. Cell Biol.* 28, 468–486. doi: 10.1128/MCB.01517-07
- Pradeepa, M. M., Grimes, G. R., Kumar, Y., Olley, G., Taylor, G. C., Schneider, R., et al. (2016). Histone H3 globular domain acetylation identifies a new class of enhancers. *Nat. Genet.* 48, 681–686. doi: 10.1038/ng.3550
- Prakash, K., and Fournier, D. (2018). Evidence for the implication of the histone code in building the genome structure. *Biosystems* 164, 49–59. doi: 10.1016/j.biosystems.2017.11.005
- Radonjic, M., Andrau, J. C., Lijnzaad, P., Kemmeren, P., Kockelkorn, T. T., van Leenen, D., et al. (2005). Genome-wide analyses reveal RNA polymerase II located upstream of genes poised for rapid response upon *S. cerevisiae* stationary phase exit. *Mol. Cell* 18, 171–183. doi: 10.1016/j.molcel.2005.03.010
- Rando, O. J. (2012). Combinatorial complexity in chromatin structure and function: revisiting the histone code. *Curr. Opin. Genet. Dev.* 22, 148–155. doi: 10.1016/j.gde.2012.02.013
- Rao, S. S., Huntley, M. H., Durand, N. C., Stamenova, E. K., Bochkov, I. D., Robinson, J. T., et al. (2014). A 3D map of the human genome at kilobase resolution reveals principles of chromatin looping. *Cell* 159, 1665–1680.
- Rawlings, J. S., Gatzka, M., Thomas, P. G., and Ihle, J. N. (2011). Chromatin condensation via the condensin II complex is required for peripheral T-cell quiescence. *EMBO J.* 30, 263–276. doi: 10.1038/emboj.2010.314
- Rhodes, C. T., Sandstrom, R. S., Huang, S. A., Wang, Y., Schotta, G., Berger, M. S., et al. (2016). Cross-species analyses unravel the complexity of H3K27me3 and H4K20me3 in the context of neural stem progenitor cells. *Neuroepigenetics* 6, 10–25. doi: 10.1016/j.nepig.2016.04.001
- Rice, J. C., Nishioka, K., Sarma, K., Steward, R., Reinberg, D., and Allis, C. D. (2002). Mitotic-specific methylation of histone H4 Lys 20 follows increased PR-Set7 expression and its localization to mitotic chromosomes. *Genes Dev.* 16, 2225–2230. doi: 10.1101/gad.1014902
- Rickels, R., Herz, H. M., Sze, C. C., Cao, K., Morgan, M. A., Collings, C. K., et al. (2017). Histone H3K4 monomethylation catalyzed by Trr and mammalian COMPASS-like proteins at enhancers is dispensable for development and viability. *Nat. Genet.* 49, 1647–1653. doi: 10.1038/ng.3965
- Riddle, N. C., Minoda, A., Kharchenko, P. V., Alekseyenko, A. A., Schwartz, Y. B., Tolstorukov, M. Y., et al. (2011). Plasticity in patterns of histone modifications and chromosomal proteins in *Drosophila* heterochromatin. *Genome Res.* 21, 147–163. doi: 10.1101/gr.110098.110
- Rinn, J. L., Kertesz, M., Wang, J. K., Squazzo, S. L., Xu, X., Bruggmann, S. A., et al. (2007). Functional demarcation of active and silent chromatin domains in human HOX loci by noncoding RNAs. *Cell* 129, 1311–1323. doi: 10.1016/j.cell.2007.05.022
- Rittershaus, E. S., Baek, S. H., and Sassetti, C. M. (2013). The normalcy of dormancy: common themes in microbial quiescence. *Cell Host Microbe* 13, 643–651. doi: 10.1016/j.chom.2013.05.012
- Rodgers, J. T., King, K. Y., Brett, J. O., Cromie, M. J., Charville, G. W., Maguire, K. K., et al. (2014). mTORC1 controls the adaptive transition of quiescent stem cells from G0 to G(Alert). *Nature* 510, 393–396. doi: 10.1038/nature13255
- Rodriguez, C. N., and Nguyen, H. (2018). Identifying quiescent stem cells in hair follicles. *Methods Mol. Biol.* 1686, 137–147.
- Rogakou, E. P., Pilch, D. R., Orr, A. H., Ivanova, V. S., and Bonner, W. M. (1998). DNA double-strand breaks induce histone H2AX phosphorylation on serine 139. *J. Biol. Chem.* 273, 5858–5868.
- Roudier, F., Ahmed, I., Berard, C., Sarazin, A., Mary-Huard, T., Cortijo, S., et al. (2011). Integrative epigenomic mapping defines four main chromatin states in *Arabidopsis*. *EMBO J.* 30, 1928–1938. doi: 10.1038/emboj.2011.103
- Ruthenburg, A. J., Li, H., Milne, T. A., Dewell, S., McGinty, R. K., Yuen, M., et al. (2011). Recognition of a mononucleosomal histone modification pattern by BPTF via multivalent interactions. *Cell* 145, 692–706. doi: 10.1016/j.cell.2011.03.053
- Rutledge, M. T., Russo, M., Belton, J. M., Dekker, J., and Broach, J. R. (2015). The yeast genome undergoes significant topological reorganization in quiescence. *Nucleic Acids Res.* 43, 8299–8313. doi: 10.1093/nar/gkv723
- Ryall, J. G., Dell'Orso, S., Derfoul, A., Juan, A., Zare, H., Feng, X., et al. (2015). The NAD(+)-dependent SIRT1 deacetylase translates a metabolic switch into regulatory epigenetics in skeletal muscle stem cells. *Cell Stem Cell* 16, 171–183. doi: 10.1016/j.stem.2014.12.004
- Sagot, I., and Laporte, D. (2019a). Quiescence, an individual journey. *Curr. Genet.* 65, 695–699.
- Sagot, I., and Laporte, D. (2019b). The cell biology of quiescent yeast - a diversity of individual scenarios. *J. Cell Sci.* 132:jcs213025. doi: 10.1242/jcs.213025
- Sajiki, K., Hatanaka, M., Nakamura, T., Takeda, K., Shimanuki, M., Yoshida, T., et al. (2009). Genetic control of cellular quiescence in *S. pombe*. *J. Cell Sci.* 122(Pt 9), 1418–1429. doi: 10.1242/jcs.046466
- Saksouk, N., Simboeck, E., and DeJardin, J. (2015). Constitutive heterochromatin formation and transcription in mammals. *Epigenet. Chromatin* 8:3.



- Sandmeier, J. J., French, S., Osheim, Y., Cheung, W. L., Gallo, C. M., Beyer, A. L., et al. (2002). RPD3 is required for the inactivation of yeast ribosomal DNA genes in stationary phase. *EMBO J.* 21, 4959–4968. doi: 10.1093/emboj/cdf498
- Sang, L., and Collier, H. A. (2009). Fear of commitment: Hes1 protects quiescent fibroblasts from irreversible cellular fates. *Cell Cycle* 8, 2161–2167. doi: 10.4161/cc.8.14.9104
- Sang, L., Roberts, J. M., and Collier, H. A. (2010). Hijacking HES1: how tumors co-opt the anti-differentiation strategies of quiescent cells. *Trends Mol. Med.* 16, 17–26. doi: 10.1016/j.molmed.2009.11.001
- Schafer, G., McEvoy, C. R., and Patterson, H. G. (2008). The *Saccharomyces cerevisiae* linker histone Hho1p is essential for chromatin compaction in stationary phase and is displaced by transcription. *Proc. Natl. Acad. Sci. U.S.A.* 105, 14838–14843. doi: 10.1073/pnas.0806337105
- Schmitges, F. W., Prusty, A. B., Faty, M., Stutzer, A., Lingaraju, G. M., Aiwazian, J., et al. (2011). Histone methylation by PRC2 is inhibited by active chromatin marks. *Mol. Cell* 42, 330–341.
- Schneider, C., King, R. M., and Philipson, L. (1988). Genes specifically expressed at growth arrest of mammalian cells. *Cell* 54, 787–793.
- Schotta, G., Lachner, M., Sarma, K., Ebert, A., Sengupta, R., Reuter, G., et al. (2004). A silencing pathway to induce H3-K9 and H4-K20 trimethylation at constitutive heterochromatin. *Genes Dev.* 18, 1251–1262. doi: 10.1101/gad.300704
- Schotta, G., Sengupta, R., Kubicek, S., Malin, S., Kauer, M., Callen, E., et al. (2008). A chromatin-wide transition to H4K20 monomethylation impairs genome integrity and programmed DNA rearrangements in the mouse. *Genes Dev.* 22, 2048–2061. doi: 10.1101/gad.476008
- Setterfield, G., Hall, R., Bladon, T., Little, J., and Kaplan, J. G. (1983). Changes in structure and composition of lymphocyte nuclei during mitogenic stimulation. *J. Ultrastruct. Res.* 82, 264–282.
- Shi, X., Kachirskaia, I., Walter, K. L., Kuo, J. H., Lake, A., Davrazou, F., et al. (2007). Proteome-wide analysis in *Saccharomyces cerevisiae* identifies several PHD fingers as novel direct and selective binding modules of histone H3 methylated at either lysine 4 or lysine 36. *J. Biol. Chem.* 282, 2450–2455.
- Shimada, M., Niida, H., Zineldeen, D. H., Tagami, H., Tanaka, M., Saito, H., et al. (2008). Chk1 is a histone H3 threonine 11 kinase that regulates DNA damage-induced transcriptional repression. *Cell* 132, 221–232.
- Shogren-Knaak, M., Ishii, H., Sun, J. M., Pazin, M. J., Davie, J. R., and Peterson, C. L. (2006). Histone H4-K16 acetylation controls chromatin structure and protein interactions. *Science* 311, 844–847. doi: 10.1126/science.1124000
- Sieburg, H. B., Cho, R. H., Dykstra, B., Uchida, N., Eaves, C. J., and Muller-Sieburg, C. E. (2006). The hematopoietic stem compartment consists of a limited number of discrete stem cell subsets. *Blood* 107, 2311–2316. doi: 10.1182/blood-2005-07-2970
- Sims, J. K., Houston, S. I., Magazinnik, T., and Rice, J. C. (2006). A trans-tail histone code defined by monomethylated H4 Lys-20 and H3 Lys-9 demarcates distinct regions of silent chromatin. *J. Biol. Chem.* 281, 12760–12766. doi: 10.1074/jbc.M513462200
- Singer, M. S., Kahana, A., Wolf, A. J., Meisinger, L. L., Peterson, S. E., Goggin, C., et al. (1998). Identification of high-copy disruptors of telomeric silencing in *Saccharomyces cerevisiae*. *Genetics* 150, 613–632. doi: 10.1093/genetics/150.2.613
- Smeenk, G., and Mailand, N. (2016). Writers, readers, and erasers of histone ubiquitylation in DNA double-strand break repair. *Front. Genet.* 7:122. doi: 10.3389/fgene.2016.00122
- So, W. K., and Cheung, T. H. (2018). Molecular regulation of cellular quiescence: a perspective from adult stem cells and its niches. *Methods Mol. Biol.* 1686, 1–25. doi: 10.1007/978-1-4939-7371-2\_1
- Sorrell, J. M., and Caplan, A. I. (2004). Fibroblast heterogeneity: more than skin deep. *J. Cell Sci.* 117(Pt 5), 667–675.
- Soshnev, A. A., Josefowicz, S. Z., and Allis, C. D. (2016). Greater than the sum of parts: complexity of the dynamic epigenome. *Mol. Cell* 62, 681–694.
- Spain, M. M., Swygert, S. G., and Tsukiyama, T. (2018). Preparation and analysis of *Saccharomyces cerevisiae* quiescent cells. *Methods Mol. Biol.* 1686, 125–135.
- Spencer, S. L., Cappell, S. D., Tsai, F. C., Overton, K. W., Wang, C. L., and Meyer, T. (2013). The proliferation-quiescence decision is controlled by a bifurcation in CDK2 activity at mitotic exit. *Cell* 155, 369–383. doi: 10.1016/j.cell.2013.08.062
- Srivastava, S., Gala, H. P., Mishra, R. K., and Dhawan, J. (2018). Distinguishing states of arrest: genome-wide descriptions of cellular quiescence using ChIP-Seq and RNA-Seq analysis. *Methods Mol. Biol.* 1686, 215–239. doi: 10.1007/978-1-4939-7371-2\_16
- Steele-Perkins, G., Fang, W., Yang, X. H., Van Gele, M., Carling, T., Gu, J., et al. (2001). Tumor formation and inactivation of RIZ1, an Rb-binding member of a nuclear protein-methyltransferase superfamily. *Genes Dev.* 15, 2250–2262. doi: 10.1101/gad.870101
- Stender, J. D., Pascual, G., Liu, W., Kaikkonen, M. U., Do, K., Spann, N. J., et al. (2012). Control of proinflammatory gene programs by regulated trimethylation and demethylation of histone H4K20. *Mol. Cell* 48, 28–38. doi: 10.1016/j.molcel.2012.07.020
- Strahl, B. D., and Allis, C. D. (2000). The language of covalent histone modifications. *Nature* 403, 41–45.
- Stucki, M., Clapperton, J. A., Mohammad, D., Yaffe, M. B., Smerdon, S. J., and Jackson, S. P. (2005). MDC1 directly binds phosphorylated histone H2AX to regulate cellular responses to DNA double-strand breaks. *Cell* 123, 1213–1226.
- Su, S. S., Tanaka, Y., Samejima, I., Tanaka, K., and Yanagida, M. (1996). A nitrogen starvation-induced dormant G0 state in fission yeast: the establishment from uncommitted G1 state and its delay for return to proliferation. *J. Cell Sci.* 109(Pt 6), 1347–1357.
- Suh, E. J., Remillard, M. Y., Legesse-Miller, A., Johnson, E. L., Lemons, J. M., Chapman, T. R., et al. (2012). A microRNA network regulates proliferative timing and extracellular matrix synthesis during cellular quiescence in fibroblasts. *Genome Biol.* 13:R121. doi: 10.1186/gb-2012-13-12-r121
- Sun, D., and Butti, L. (2017). States of G(0) and the proliferation-quiescence decision in cells, tissues and during development. *Int. J. Dev. Biol.* 61, 357–366. doi: 10.1387/ijdb.160343LB
- Svensson, V., Vento-Tormo, R., and Teichmann, S. A. (2018). Exponential scaling of single-cell RNA-seq in the past decade. *Nat. Protoc.* 13, 599–604. doi: 10.1038/nprot.2017.149
- Swygert, S. G., Kim, S., Wu, X., Fu, T., Hsieh, T. H., Rando, O. J., et al. (2019). Condensin-Dependent chromatin compaction represses transcription globally during quiescence. *Mol. Cell* 73, 533–546.e4.
- Swygert, S. G., Lin, D., Portillo-Ledesma, S., Lin, P.-Y., Hunt, D. R., Kao, C.-F., et al. (2021). Chromatin fiber folding represses transcription and loop extrusion in quiescent cells. *bioRxiv* [preprint] doi: 10.1101/2020.11.24.396713
- Takeda, K., and Yanagida, M. (2010). In quiescence of fission yeast, autophagy and the proteasome collaborate for mitochondrial maintenance and longevity. *Autophagy* 6, 564–565.
- Takei, Y., Yun, J., Zheng, S., Ollikainen, N., Pierson, N., White, J., et al. (2021). Integrated spatial genomics reveals global architecture of single nuclei. *Nature* 590, 344–350. doi: 10.1038/s41586-020-03126-2
- Tang, G. B., Zeng, Y. Q., Liu, P. P., Mi, T. W., Zhang, S. F., Dai, S. K., et al. (2017). The histone H3K27 demethylase UTX regulates synaptic plasticity and cognitive behaviors in mice. *Front. Mol. Neurosci.* 10:267. doi: 10.3389/fnmol.2017.00267
- Tardat, M., Brustel, J., Kirsh, O., Lefevbre, C., Callanan, M., Sardet, C., et al. (2010). The histone H4 Lys 20 methyltransferase PR-Set7 regulates replication origins in mammalian cells. *Nat. Cell Biol.* 12, 1086–1093. doi: 10.1038/ncb2113
- Terzi, M. Y., Izmirli, M., and Gogebakan, B. (2016). The cell fate: senescence or quiescence. *Mol. Biol. Rep.* 43, 1213–1220.
- Tesio, M., Tang, Y., Mudder, K., Saini, M., von Paleske, L., Macintyre, E., et al. (2015). Hematopoietic stem cell quiescence and function are controlled by the CYLD-TRAF2-p38MAPK pathway. *J. Exp. Med.* 212, 525–538. doi: 10.1084/jem.20141438
- Tessarz, P., and Kouzarides, T. (2014). Histone core modifications regulating nucleosome structure and dynamics. *Nat. Rev. Mol. Cell Biol.* 15, 703–708.
- Tie, G., Yan, J., Khair, L., Tutto, A., and Messina, L. M. (2020). Hypercholesterolemia accelerates the aging phenotypes of hematopoietic stem cells by a Tet1-dependent pathway. *Sci. Rep.* 10:3567. doi: 10.1038/s41598-020-60403-w
- Tokuyasu, K., Madden, S. C., and Zeldis, L. J. (1968). Fine structural alterations of interphase nuclei of lymphocytes stimulated to growth activity in vitro. *J. Cell Biol.* 39, 630–660. doi: 10.1083/jcb.39.3.630
- Torres, I. O., Kuchenbecker, K. M., Nnadi, C. I., Fletterick, R. J., Kelly, M. J., and Fujimori, D. G. (2015). Histone demethylase KDM5A is regulated by its

- reader domain through a positive-feedback mechanism. *Nat. Commun.* 6:6204. doi: 10.1038/ncomms7204
- Tripputi, P., Emanuel, B. S., Croce, C. M., Green, L. G., Stein, G. S., and Stein, J. L. (1986). Human histone genes map to multiple chromosomes. *Proc. Natl. Acad. Sci. U.S.A.* 83, 3185–3188.
- Trojer, P., and Reinberg, D. (2007). Facultative heterochromatin: is there a distinctive molecular signature? *Mol. Cell* 28, 1–13. doi: 10.1016/j.molcel.2007.09.011
- Trojer, P., Li, G., Sims, R. J. III, Vaquero, A., Kalakonda, N., Bocconi, P., et al. (2007). L3MBTL1, a histone-methylation-dependent chromatin lock. *Cell* 129, 915–928. doi: 10.1016/j.cell.2007.03.048
- Tsai, W. W., Wang, Z., Yiu, T. T., Akdemir, K. C., Xia, W., Winter, S., et al. (2010). TRIM24 links a non-canonical histone signature to breast cancer. *Nature* 468, 927–932. doi: 10.1038/nature09542
- Tumpel, S., and Rudolph, K. L. (2019). Quiescence: good and bad of stem cell aging. *Trends Cell Biol.* 29, 672–685. doi: 10.1016/j.tcb.2019.05.002
- Turner, B. M. (2002). Cellular memory and the histone code. *Cell* 111, 285–291.
- Urbán, N., and Cheung, T. H. (2021). Stem cell quiescence: the challenging path to activation. *Development* 148, doi: 10.1242/dev.165084
- Vakoc, C. R., Mandat, S. A., Olenchok, B. A., and Blobel, G. A. (2005). Histone H3 lysine 9 methylation and HP1gamma are associated with transcription elongation through mammalian chromatin. *Mol. Cell* 19, 381–391.
- Valcourt, J. R., Lemons, J. M., Haley, E. M., Kojima, M., Demuren, O. O., and Collier, H. A. (2012). Staying alive: metabolic adaptations to quiescence. *Cell Cycle* 11, 1680–1696. doi: 10.4161/cc.19879
- van Leeuwen, F., Gafken, P. R., and Gottschling, D. E. (2002). Dot1p modulates silencing in yeast by methylation of the nucleosome core. *Cell* 109, 745–756. doi: 10.1016/s0092-8674(02)00759-6
- van Velthoven, C. T. J., de Morree, A., Egner, I. M., Brett, J. O., and Rando, T. A. (2017). Transcriptional profiling of quiescent muscle stem cells in vivo. *Cell Rep.* 21, 1994–2004.
- Vander Heiden, M. G., Cantley, L. C., and Thompson, C. B. (2009). Understanding the Warburg effect: the metabolic requirements of cell proliferation. *Science* 324, 1029–1033.
- Vasquez, J. J., Wedel, C., Cosentino, R. O., and Siegel, T. N. (2018). Exploiting CRISPR-Cas9 technology to investigate individual histone modifications. *Nucleic Acids Res.* 46:e106. doi: 10.1093/nar/gky517
- Venezia, T. A., Merchant, A. A., Ramos, C. A., Whitehouse, N. L., Young, A. S., Shaw, C. A., et al. (2004). Molecular signatures of proliferation and quiescence in hematopoietic stem cells. *PLoS Biol.* 2:e301. doi: 10.1371/journal.pbio.0020301
- Venkatraman, A., He, X. C., Thorvaldsen, J. L., Sugimura, R., Perry, J. M., Tao, F., et al. (2013). Maternal imprinting at the H19-Igf2 locus maintains adult haematopoietic stem cell quiescence. *Nature* 500, 345–349. doi: 10.1038/nature12303
- Vizán, P., Gutiérrez, A., Espejo, I., García-Montolio, M., Lange, M., Carretero, A., et al. (2020). The Polycomb-associated factor PHF19 controls hematopoietic stem cell state and differentiation. *Sci. Adv.* 6:eabb2745. doi: 10.1126/sciadv.abb2745
- Voigt, P., Tee, W. W., and Reinberg, D. (2013). A double take on bivalent promoters. *Genes Dev.* 27, 1318–1338. doi: 10.1101/gad.219626.113
- Volker-Albert, M. C., Schmidt, A., Forne, I., and Imhof, A. (2018). Analysis of histone modifications by mass spectrometry. *Curr. Protoc. Protein Sci.* 92:e54.
- Wagner, E. J., and Carpenter, P. B. (2012). Understanding the language of Lys36 methylation at histone H3. *Nat. Rev. Mol. Cell Biol.* 13, 115–126. doi: 10.1038/nrm3274
- Walter, D., Matter, A., and Fahrenkrog, B. (2014). Loss of histone H3 methylation at lysine 4 triggers apoptosis in *Saccharomyces cerevisiae*. *PLoS Genet.* 10:e1004095. doi: 10.1371/journal.pgen.1004095
- Wang, D., Mansidior, A., Prabhakar, G., and Hochwagen, A. (2016). Condensin and Hmo1 mediate a starvation-induced transcriptional position effect within the ribosomal DNA array. *Cell Rep.* 17:624.
- Wang, G. G., and Allis, C. D. (2009). "Misinterpretation" of a histone mark is linked to aberrant stem cells and cancer development. *Cell Cycle* 8, 1982–1983.
- Wang, Z., Gerstein, M., and Snyder, M. (2009). RNA-Seq: a revolutionary tool for transcriptomics. *Nat. Rev. Genet.* 10, 57–63.
- Wang, Z., Zang, C., Rosenfeld, J. A., Schones, D. E., Barski, A., Cuddapah, S., et al. (2008). Combinatorial patterns of histone acetylations and methylations in the human genome. *Nat. Genet.* 40, 897–903.
- Watanabe, S., Mishima, Y., Shimizu, M., Suetake, I., and Takada, S. (2018). Interactions of HP1 bound to H3K9me3 dinucleosome by molecular simulations and biochemical assays. *Biophys. J.* 114, 2336–2351. doi: 10.1016/j.bpj.2018.03.025
- Wei, Y., Yu, L., Bowen, J., Gorovsky, M. A., and Allis, C. D. (1999). Phosphorylation of histone H3 is required for proper chromosome condensation and segregation. *Cell* 97, 99–109.
- Werner-Washburne, M., Braun, E. L., Crawford, M. E., and Peck, V. M. (1996). Stationary phase in *Saccharomyces cerevisiae*. *Mol. Microbiol.* 19, 1159–1166.
- Wiles, E. T., and Selker, E. U. (2017). H3K27 methylation: a promiscuous repressive chromatin mark. *Curr. Opin. Genet. Dev.* 43, 31–37. doi: 10.1016/j.gde.2016.11.001
- Wilson, A., Laurenti, E., Oser, G., van der Wath, R. C., Blanco-Bose, W., Jaworski, M., et al. (2008). Hematopoietic stem cells reversibly switch from dormancy to self-renewal during homeostasis and repair. *Cell* 135, 1118–1129. doi: 10.1016/j.cell.2008.10.048
- Winter, S., Simboeck, E., Fischle, W., Zupkovitz, G., Dohnal, I., Mechtler, K., et al. (2008). 14-3-3 proteins recognize a histone code at histone H3 and are required for transcriptional activation. *EMBO J.* 27, 88–99. doi: 10.1038/sj.emboj.7601954
- Wu, S., Wang, W., Kong, X., Congdon, L. M., Yokomori, K., Kirschner, M. W., et al. (2010). Dynamic regulation of the PR-Set7 histone methyltransferase is required for normal cell cycle progression. *Genes Dev.* 24, 2531–2542. doi: 10.1101/gad.1984210
- Wu, T., Yoon, H., Xiong, Y., Dixon-Clarke, S. E., Nowak, R. P., and Fischer, E. S. (2020). Targeted protein degradation as a powerful research tool in basic biology and drug target discovery. *Nat. Struct. Mol. Biol.* 27, 605–614.
- Xu, J., and Kidder, B. L. (2018). H4K20me3 co-localizes with activating histone modifications at transcriptionally dynamic regions in embryonic stem cells. *BMC Genomics* 19:514. doi: 10.1186/s12864-018-4886-4
- Xu, J., Ma, H., Jin, J., Uttam, S., Fu, R., Huang, Y., et al. (2018). Super-Resolution imaging of higher-order chromatin structures at different epigenomic states in single mammalian cells. *Cell Rep.* 24, 873–882.
- Xu, M., Solovychik, M., Ranger, M., Schertzberg, M., Shah, Z., Raisner, R., et al. (2012). Timing of transcriptional quiescence during gametogenesis is controlled by global histone H3K4 demethylation. *Dev. Cell* 23, 1059–1071. doi: 10.1016/j.devcel.2012.10.005
- Yan, H., Evans, J., Kalmbach, M., Moore, R., Middha, S., Luban, S., et al. (2014). HiChIP: a high-throughput pipeline for integrative analysis of ChIP-Seq data. *BMC Bioinformatics* 15:280. doi: 10.1186/1471-2105-15-280
- Yang, K., and Chi, H. (2018). Investigating cellular quiescence of T lymphocytes and antigen-induced exit from quiescence. *Methods Mol. Biol.* 1686, 161–172. doi: 10.1007/978-1-4939-7371-2\_12
- Yildirim, E., Kirby, J. E., Brown, D. E., Mercier, F. E., Sadreyev, R. I., Scadden, D. T., et al. (2013). Xist RNA is a potent suppressor of hematologic cancer in mice. *Cell* 152, 727–742. doi: 10.1016/j.cell.2013.01.034
- Yin, H., Price, F., and Rudnicki, M. A. (2013). Satellite cells and the muscle stem cell niche. *Physiol. Rev.* 93, 23–67.
- Young, C. P., Hillyer, C., Hokamp, K., Fitzpatrick, D. J., Konstantinov, N. K., Welty, J. S., et al. (2017). Distinct histone methylation and transcription profiles are established during the development of cellular quiescence in yeast. *BMC Genomics* 18:107. doi: 10.1186/s12864-017-3509-9
- Yuan, W., Xu, M., Huang, C., Liu, N., Chen, S., and Zhu, B. (2011). H3K36 methylation antagonizes PRC2-mediated H3K27 methylation. *J. Biol. Chem.* 286, 7983–7989.
- Zahedi, Y., Durand-Dubief, M., and Ekwall, K. (2020). High-Throughput flow cytometry combined with genetic analysis brings new insights into the understanding of chromatin regulation of cellular quiescence. *Int J Mol Sci.* 21:9022. doi: 10.3390/ijms21239022

- Zhang, T., Cooper, S., and Brockdorff, N. (2015). The interplay of histone modifications - writers that read. *EMBO Rep.* 16, 1467–1481.
- Zhou, K., Gaullier, G., and Luger, K. (2019). Nucleosome structure and dynamics are coming of age. *Nat. Struct. Mol. Biol.* 26, 3–13.
- Zhou, Y., Yan, X., Feng, X., Bu, J., Dong, Y., Lin, P., et al. (2018). Setd2 regulates quiescence and differentiation of adult hematopoietic stem cells by restricting RNA polymerase II elongation. *Haematologica* 103, 1110–1123. doi: 10.3324/haematol.2018.187708
- Zhu, C., Zhang, Y., Li, Y. E., Lucero, J., Behrens, M. M., and Ren, B. (2021). Joint profiling of histone modifications and transcriptome in single cells from mouse brain. *Nat. Methods* 18, 283–292. doi: 10.1038/s41592-021-01060-3
- Zippo, A., Serafini, R., Rocchigiani, M., Pennacchini, S., Krepelova, A., and Oliviero, S. (2009). Histone crosstalk between H3S10ph and H4K16ac generates a histone code that mediates transcription elongation. *Cell* 138, 1122–1136. doi: 10.1016/j.cell.2009.07.031

**Conflict of Interest:** The authors declare that the research was conducted in the absence of any commercial or financial relationships that could be construed as a potential conflict of interest.

**Publisher's Note:** All claims expressed in this article are solely those of the authors and do not necessarily represent those of their affiliated organizations, or those of the publisher, the editors and the reviewers. Any product that may be evaluated in this article, or claim that may be made by its manufacturer, is not guaranteed or endorsed by the publisher.

Copyright © 2021 Bonitto, Sarathy, Atai, Mitra and Collier. This is an open-access article distributed under the terms of the Creative Commons Attribution License (CC BY). The use, distribution or reproduction in other forums is permitted, provided the original author(s) and the copyright owner(s) are credited and that the original publication in this journal is cited, in accordance with accepted academic practice. No use, distribution or reproduction is permitted which does not comply with these terms.



# Monitoring Spontaneous Quiescence and Asynchronous Proliferation-Quiescence Decisions in Prostate Cancer Cells

Ajai J. Pulianmackal<sup>1</sup>, Dan Sun<sup>1</sup>, Kenji Yumoto<sup>2</sup>, Zhengda Li<sup>3</sup>, Yu-Chih Chen<sup>4,5</sup>, Meha V. Patel<sup>1</sup>, Yu Wang<sup>2</sup>, Euisik Yoon<sup>4,6,7</sup>, Alexander Pearson<sup>8</sup>, Qiong Yang<sup>3</sup>, Russell Taichman<sup>2,9</sup>, Frank C. Cackowski<sup>2,10\*</sup> and Laura A. Buttitta<sup>1\*</sup>

## OPEN ACCESS

### Edited by:

Guang Yao,  
University of Arizona, United States

### Reviewed by:

Nadine Wiper-Bergeron,  
University of Ottawa, Canada  
Hadrien De Blander,  
VIB KU Leuven Center for Cancer  
Biology, Belgium

### \*Correspondence:

Frank C. Cackowski  
cackowskif@karmanos.org  
Laura A. Buttitta  
buttitta@umich.edu

### Specialty section:

This article was submitted to  
Cell Growth and Division,  
a section of the journal  
Frontiers in Cell and Developmental  
Biology

**Received:** 21 June 2021

**Accepted:** 19 November 2021

**Published:** 10 December 2021

### Citation:

Pulianmackal AJ, Sun D, Yumoto K,  
Li Z, Chen Y-C, Patel MV, Wang Y,  
Yoon E, Pearson A, Yang Q,  
Taichman R, Cackowski FC and  
Buttitta LA (2021) Monitoring  
Spontaneous Quiescence and  
Asynchronous Proliferation-  
Quiescence Decisions in Prostate  
Cancer Cells.  
Front. Cell Dev. Biol. 9:728663.  
doi: 10.3389/fcell.2021.728663

<sup>1</sup>Molecular, Cellular and Developmental Biology, University of Michigan, Ann Arbor, MI, United States, <sup>2</sup>School of Dentistry, University of Michigan, Ann Arbor, MI, United States, <sup>3</sup>Department of Biophysics, University of Michigan, Ann Arbor, MI, United States, <sup>4</sup>Department of Electrical Engineering and Computer Science, University of Michigan, Ann Arbor, MI, United States, <sup>5</sup>Department of Computational and Systems Biology, Hillman Cancer Center, University of Pittsburgh School of Medicine, Pittsburgh, PA, United States, <sup>6</sup>Department of Biomedical Engineering, University of Michigan, Ann Arbor, MI, United States, <sup>7</sup>Center for Nanomedicine, Institute for Basic Science (IBS) and Graduate Program of Nano Biomedical Engineering (Nano BME), Advanced Science Institute, Yonsei University, Seoul, Korea, South Korea, <sup>8</sup>Department of Medicine, Section of Hematology/Oncology, University of Chicago Medical Center, Chicago, IL, United States, <sup>9</sup>Department of Periodontology, School of Dentistry, University of Alabama at Birmingham, Birmingham, AL, United States, <sup>10</sup>Department of Oncology, Karmanos Cancer Institute and Wayne State University, Detroit, MI, United States

The proliferation-quiescence decision is a dynamic process that remains incompletely understood. Live-cell imaging with fluorescent cell cycle sensors now allows us to visualize the dynamics of cell cycle transitions and has revealed that proliferation-quiescence decisions can be highly heterogeneous, even among clonal cell lines in culture. Under normal culture conditions, cells often spontaneously enter non-cycling G0 states of varying duration and depth. This also occurs in cancer cells and G0 entry in tumors may underlie tumor dormancy and issues with cancer recurrence. Here we show that a cell cycle indicator previously shown to indicate G0 upon serum starvation, mVenus-p27K-, can also be used to monitor spontaneous quiescence in untransformed and cancer cell lines. We find that the duration of spontaneous quiescence in untransformed and cancer cells is heterogeneous and that a portion of this heterogeneity results from asynchronous proliferation-quiescence decisions in pairs of daughters after mitosis, where one daughter cell enters or remains in temporary quiescence while the other does not. We find that cancer dormancy signals influence both entry into quiescence and asynchronous proliferation-quiescence decisions after mitosis. Finally, we show that spontaneously quiescent prostate cancer cells exhibit altered expression of components of the Hippo pathway and are enriched for the stem cell markers CD133 and CD44. This suggests a hypothesis that dormancy signals could promote cancer recurrence by increasing the proportion of quiescent tumor cells poised for cell cycle re-entry with stem cell characteristics in cancer.

**Keywords:** quiescence, dormancy, prostate cancer, cell cycle, live imaging



## INTRODUCTION

Cycling cells tend to enter quiescence, a reversible, non-cycling state in response to contact inhibition, reduced levels of mitogens, or under various stress conditions. Quiescent cells retain the ability to re-enter the cycle upon the addition of serum or under favorable conditions (Coller et al., 2006; Yao, 2014). However, studies of mammalian cells in the past few years have found that many cells enter a spontaneous reversible G0-like state in cell culture even in the presence of mitogens and abundant nutrients (Spencer et al., 2013; Overton et al., 2014; Min and Spencer, 2019). This suggests that the proliferation-quiescence decision is constantly regulated—even under optimal growth conditions.

The relative percentage of cells that enter a temporary G0-like state after mitosis varies with cell type and culture conditions, suggesting many signaling inputs influence the proliferation-quiescence decision (Spencer et al., 2013). This is also consistent with findings in several cancer cell lines, where some cells enter a temporary quiescent state while others do not (Dey-Guha et al., 2011). This leads to heterogeneity in cell culture, with a subpopulation of cells entering and leaving temporary quiescent states (Overton et al., 2014). This proliferative heterogeneity may underlie states of dormancy in cancer and has been shown to be related to cancer therapeutic resistance (Recasens and Munoz, 2019; Risson et al., 2020; Nik Nabil et al., 2021). This is particularly relevant in prostate cancer, where it is thought that early spreading of tumor cells to the bone marrow and other tissues may provide signals leading to quiescence and tumor dormancy (Chen et al., 2021). Prostate cancer dormancy in tissues such as the bone are problematic as a percentage of patients will later develop recurrent cancer with significant metastases from these cells, which are often also resistant to treatment (Lam et al., 2014). Understanding how and why quiescent cancer cells reside in environments such as the bone marrow for long periods of time, and finding ways to eliminate them, is an important ongoing challenge in prostate cancer research and treatment.

The difficulties in monitoring the proliferation-quiescence decision and distinguishing different states and lengths of G0 has limited our ability to understand how signals impact the heterogeneity of quiescence in cell populations. Most assays for cell cycling status use immunostaining of cell cycle phase markers or nucleotide analogue incorporation, both of which assess static conditions in fixed samples (Matson and Cook, 2017). Cell cycle reporters such as the FUCCI system (Fluorescent Ubiquitination-based Cell Cycle Indicator), have become widely used to track cell cycle dynamics live in individual cells (Sakaue-Sawano et al., 2008). The FUCCI system and related systems such as CycleTrak and others including a constitutive nuclear marker are able to differentially label cells in G1, S and G2/M phases, allowing us to visualize the G1-M transition, however G0 cannot be distinguished from G1 in these approaches (Ridenour et al., 2012; Chittajallu et al., 2015).

Recent methods to monitor quiescence heterogeneity have used live cell imaging with sensors for Cdk2 activity, Ki-67 expression, and expression of Cdk inhibitors such as p21 and p27 (Spencer et al., 2013; Overton et al., 2014; Stewart-Ornstein

and Lahav, 2016; Miller et al., 2018; Zamboni et al., 2020). Here we take advantage of the cell cycle indicator, mVenus-p27K<sup>-</sup>, which was generated to work in combination with the G0/G1 FUCCI reporter mCherry-hCdt1 (30/120), to specifically label quiescent cells (Oki et al., 2014). This probe is a fusion protein consisting of a fluorescent protein mVenus and a Cdk binding defective mutant of p27 (p27K<sup>-</sup>). p27 accumulates during quiescence and is degraded by two ubiquitin ligases: the Kip1 ubiquitination-promoting complex (KPC) at the G0-G1 transition, and the SCF<sup>Skp2</sup> complex at S/G2/M phases (Kamura et al., 2004). When used in combination with the G0/G1 FUCCI reporter, cells can be tracked from a few hours after mitosis until early S phase with distinct colors. This allows us to examine the dynamics of the proliferation-quiescence transition after mitosis on a single-cell level without artificial synchronization.

Prior work with a Cdk2 sensor and monitoring p21 levels revealed that both non-transformed and cancer cells in culture can enter “spontaneously” quiescent states of variable length, even under optimal growth conditions (Spencer et al., 2013; Overton et al., 2014; Yang et al., 2017; Min and Spencer, 2019). The proportion of spontaneously quiescent cells in a population and their variability in the length of quiescence leads to cell cycle heterogeneity (Overton et al., 2014), which may in part also underlie cell cycle heterogeneity within clonal tumors (Dey-Guha et al., 2011; Dey-Guha et al., 2015). This led us to examine whether we could monitor spontaneous quiescence using the mVenus-p27K<sup>-</sup> G0 reporter. Here we show that by tracking the trajectory of this reporter activity, we can monitor spontaneous quiescence in non-transformed mouse fibroblasts and prostate cancer cells. While measuring the heterogeneity of spontaneous quiescence, we also observed that a pair of daughter cells resulting from a single mitosis can make asynchronous proliferation-quiescence decisions. In this type of asynchronous decision, one daughter from a mitosis enters G0, while the other enters G1, further increasing cell cycle heterogeneity within a clonal population (Dey-Guha et al., 2011). We find that signals associated with promoting or releasing tumor dormancy can influence quiescence and asynchronous proliferation-quiescence decisions in prostate cancer cells. Using the mVenus-p27K<sup>-</sup> G0 reporter, we isolate populations containing quiescent cancer cells and find they are enriched for a subpopulation expressing stem cell markers and express high levels of Hippo pathway signaling components, but with inactivated YAP, which may indicate a state poised for cell cycle re-entry. Finally, we provide evidence that the expression of immune recognition signals may be decreased in populations containing quiescent cancer cells, suggesting a hypothesis for how these cancer cells may preferentially evade the immune system.

## RESULTS

### mVenus-p27K<sup>-</sup> Based G0/G1 Cell Cycle Indicators Track Spontaneous Quiescence

To characterize the proliferation-quiescence transition at single-cell resolution in mouse 3T3 cells under full serum conditions without synchronization, we used the G0 cell cycle indicator

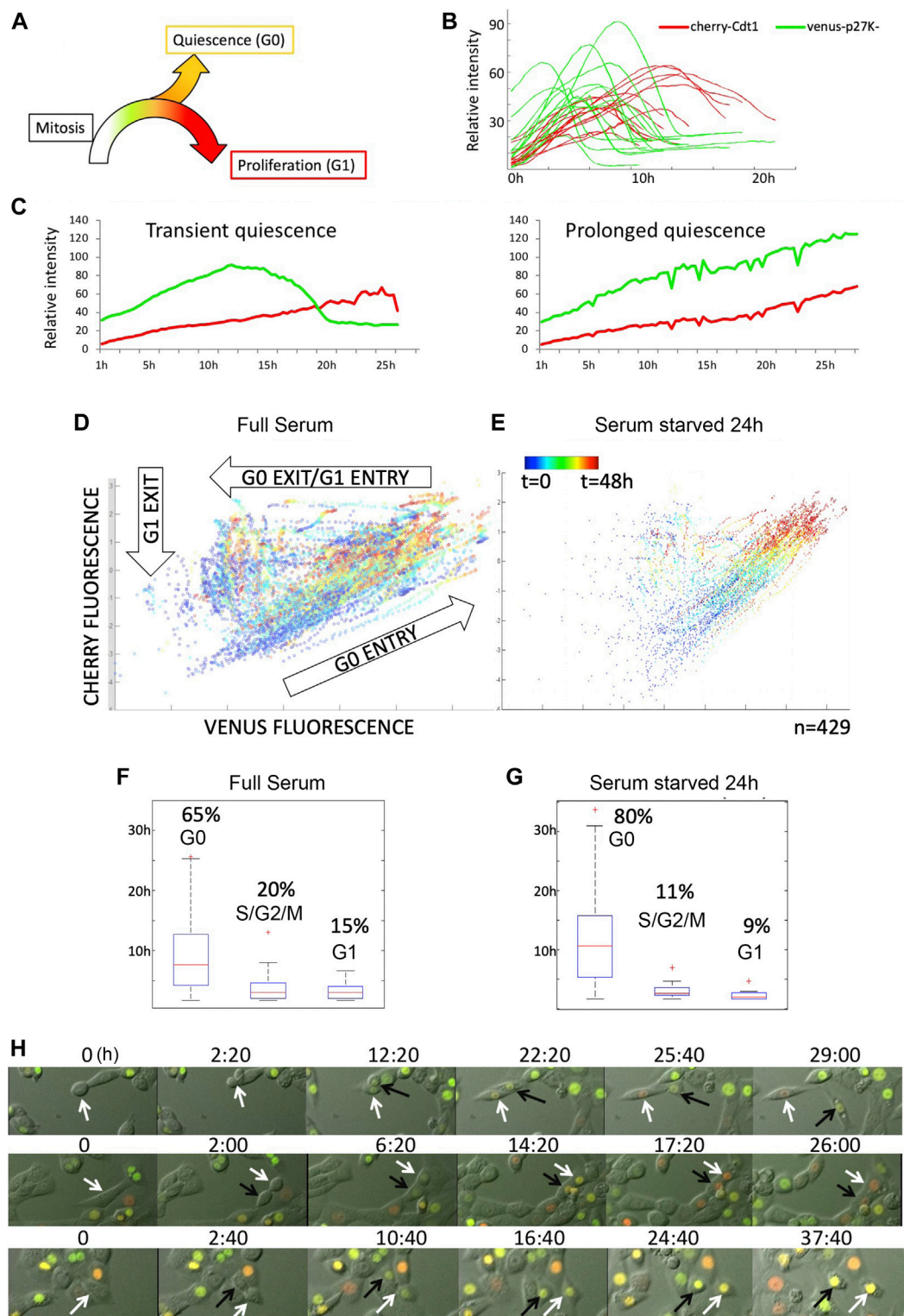


**FIGURE 1 |** The G0 sensor, mVenus-p27K-, can be used to monitor spontaneous quiescence and asynchronous proliferation-quiescence decisions in untransformed cells. **(A)** The proliferation-quiescence decision as monitored with the G0 sensor, mVenus-p27K- (G0-Venus) and G1 sensor hCdt1<sub>(30-120)</sub>-Cherry (G1-Cherry). For NIH/3T3 cells, on average, 2–4 h after cytokinesis, G0-Venus expression begins increasing, followed approximately 3–4 h later by G1-Cherry expression. For cells entering G1, the Venus/Cherry double-positive phase lasts 5–10 h. For quantification purposes we define a Venus/Cherry double-positive phase prolonged beyond 14 h as spontaneous G0. **(B)** Example traces of G0-Venus/G1-Cherry reporter dynamics in cells entering the cell cycle. 0 h is relative time, aligned to (Continued)

**FIGURE 1** | the start of G0-Venus reporter increase. **(C)** Example traces of G0-Venus/G1-Cherry reporter dynamics in cells under full serum conditions. Left shows a transient spontaneous G0 state of less than 15 h, while right shows an example of prolonged, spontaneous quiescence lasting over 24 h. **(D)** Cell trajectories followed over time from several movies show reporter behaviors consistent with G0 entry, G0 exit and G1 entry, and exit from G1 and early S-phase under full serum conditions. **(E)** Under serum starvation for 24 h, multiple trajectories collapse into G0 entry. **(F)** Under full serum conditions, time spent in G0 is highly variable. **(G)** Under serum starvation for 24 h G0 is prolonged. **(H)** Frames from movies showing examples of mitoses followed by an asynchronous G0/G1 decision (**top**), synchronous G1 decision (**middle**) and synchronous G0 decision (**bottom**).

mVenus-p27K<sup>-</sup> combined with the G0/G1 reporter from the FUCCI cell cycle system, mCherry-hCdt1 (30/120) to distinguish G0 cells from G1 cells as previously described (Oki et al., 2014). We first manually examined movies of asynchronously proliferating 3T3 cells stably expressing these reporters to monitor reporter dynamics (**Supplementary Movie S1, S2**). With this combination of cell cycle reporters, mVenus-p27K<sup>-</sup> expression begins approximately 2–6 h after cytokinesis is complete, followed by mCherry-hCdt1 expression approximately 2–6 h later. Most cells then exhibit a rapid reduction in mVenus-p27K<sup>-</sup> within approximately 3 h, signaling G1 entry followed by mCherry-hCdt1 degradation at G1 exit (**Figures 1A,B**). However, for a fraction of cells (ranging between 20–65% in different movies) we observed both mVenus-p27K<sup>-</sup> and mCherry-hCdt1 to both continue to accumulate for up to 14 h and beyond, without division or evidence of S/G2/M entry for 20 h or more, signaling spontaneous G0 entry (**Figure 1C**). This progression of reporter expression in order from mVenus-p27K<sup>-</sup> positive to mVenus-p27K<sup>-</sup> and mCherry-hCdt1 double positive to mCherry-hCdt1 was invariant in the movies, although we did observe some cell to cell variation in reporter expression intensity, despite using a clonal cell line.

To monitor and quantitatively measure the dynamic transitions of cell cycle states—from cytokinesis to S phase entry, we developed an Automated temporal Tracking of Cellular Quiescence (ATCQ) analysis platform. This platform includes a computational framework for automated cell segmentation (identification of individual cells in an image), tracking, cell cycle state identification, and quantification from movies (**Supplementary Figure S1**). The cell segmentation and tracking allows us to record the fluorescent reporter intensity changes within individual cells in real-time imaging, without the aid of a constitutive nuclear marker. The single-cell fluorescence changes over time, in turn, are used to obtain cell cycle state identification (G0, G1, or early S phase) and quantification, which allows us to examine the kinetics of the proliferation-quiescence transition. The single-cell traces of fluorescent reporters, mVenus-p27K<sup>-</sup> and mCherry-hCdt1, graphed by ATCQ is consistent with trajectories of G0 entry (increasing Venus and Cherry), G0 exit/G1 entry (degradation of Venus, increasing Cherry), and G1 exit/S-phase progression (degradation of Cherry) we manually observed in movies (**Figure 1D**).

To confirm that the Venus/Cherry-double positive population represents G0 phase, we performed a short-term (24 h, 1%FBS) serum starvation treatment followed by 48 h of live imaging. As expected in low serum, the reporter trajectories collapsed into predominantly G0 entry (**Figure 1E**). When we measure the

timing of the reporter trajectories we find that the timing of G0 is heterogeneous compared to G1 entry and G1 exit and becomes further prolonged under low serum (**Figures 1F,G**).

We next examined whether the mVenus-p27K<sup>-</sup>/mCherry-hCdt1 double positive population under full serum conditions exhibits molecular markers of G0. To do this, we sorted cells into Venus/Cherry double-positive, Cherry single-positive, and Venus/Cherry double-negative populations and performed western blots for markers of G0 vs G1 phase. As a positive control for G0, cells cultured under serum deprivation were sorted in a similar manner (**Supplementary Figure S2**). We found that Venus/Cherry double-positive cells under full serum conditions exhibited hypo-phosphorylated pocket proteins RB and p130, increased endogenous p27, and reduced phosphorylation of Cdk2 on the activating T-Loop (Jeffrey et al., 1995; Sherr and Roberts, 1999; Tedesco et al., 2002). We also confirmed reduced expression of cell cycle genes, and upregulated expression of genes associated with G0 in the double positive cells in full serum by qRT-PCR on sorted cells (**Supplementary Figure S2**) (Oki et al., 2014). Taken together, our tracking and molecular data suggests that many of the Venus/Cherry double-positive cells under full serum conditions enter a temporary G0 of variable length. We therefore conclude that this reporter combination also captures temporary, spontaneous quiescence in a fraction of asynchronously proliferating cells.

## Asynchrony in the Proliferation-Quiescence Decision

In the manual tracking of dividing cells, we noticed several instances where pairs of daughters, born of a single mitosis, make different proliferation-quiescence decisions. In this situation, one daughter will remain G0, while the other daughter born at the same time will degrade the mVenus-p27K<sup>-</sup> reporter and enter G1, followed by S/G2 and mitosis (**Figure 1H**). Under normal culture conditions we observe this in 20–40% of 3T3 cells entering G0, with the differences in the timing of G1 entry between asynchronous daughters varying from 1–15 h. We also find that daughters can exhibit varying lengths of the Venus/Cherry double-positive state (from 5–24 h) before one from the pair enters G1. We next examined whether such asynchrony in the cell cycle progression of two daughters born of the same mitosis could be observed in other cell types. We manually examined movies of published live cell imaging and observed instances of cell cycle asynchrony in pairs of daughters in BT549 and MCF10A cells (**Supplementary Table S1**). Cell cycle asynchrony in daughters born of the same mitosis has also been reported in MCF7 and HCT116 cells and referred to as “asymmetric” cell divisions, accompanied by differences in AKT



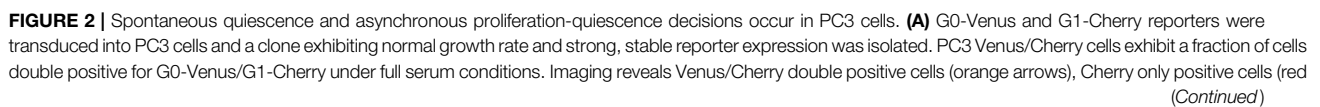




**FIGURE 2** | (arrows) and double negative cells (not indicated). **(B)** PC3 cells double positive for G0-Venus/G1-Cherry are Ki-67 negative, **(C)** EdU negative, **(D)** and cells in mitosis are negative for both reporters. **(E)** G0-Venus and G1-Cherry reporters in PC3 cells respond to serum starvation and re-stimulation as expected. G1 (Cherry-only) cells were isolated by FACS and cultured in serum free media for 3 days. By 3 days, 90% of cells become Venus/Cherry double positive demonstrating that nearly all cells retain the dual reporters. In parallel, double negative late S, G2/M cells were isolated by FACS and cultured in serum free media. By 3 days, 85% of cells become Venus/Cherry double positive, demonstrating that actively proliferating cells retain the dual reporters. Serum was then added back to G0 arrested cells, and within 2–3 days (days 5 and 7 of the entire timecourse) the distribution of G0, G1, S, G2/M cells returns to normal. **(F)** PC3 Venus/Cherry cells were cultured in a microfluidics chamber termed the “cell hotel” for single cell tracking and imaging of daughters. Examples of asynchronous G0/G1 decisions, as well as synchronous spontaneous G0 and synchronous G1 entry are observed in PC3 cells under full serum conditions. Orange arrows indicate cells entering G0 (G0-Venus, G1-Cherry double positive), red arrows indicate cells entering G1 (G1-Cherry only). **(G)** To measure heterogeneity of G0 in PC3 cells under full serum conditions, we quantified time spent in a double-positive Venus/Cherry state for 90 cells. We found G0 length to be highly heterogeneous, compared to the rest of the cell cycle timing for G1, S and G2/M. **(H)** We measured the length of the double Venus/Cherry positive G0 state for ~50 PC3 and 3T3 cells under full serum conditions in the cell hotel. For PC3, we found that most cells transitioned to G1 by 14 h after the initial rise in G0-Venus fluorescence, with a small number of cells (27.5%) exhibiting longer G0-Venus fluorescence consistent with spontaneous quiescence. By contrast, for 3T3 cells we observed 64.4% of cells to exhibit spontaneous quiescence, a double-positive state lasting more than 14 h (dotted line). ( $p = 0.0005$  by Mann-Whitney test.) **(I)** We also compared the frequency of asynchronous proliferation-quiescence decisions in PC3 vs 3T3 cells ( $p < 0.0001$  by Mann-Whitney test) and **(G)** the length of the time difference until G1 entry between asynchronous daughters in PC3 and 3T3 cells. Lines show the mean and error bars are  $\pm$ SEM from at least three independent experiments.

signaling between daughters after telophase (Dey-Guha et al., 2011; Dey-Guha et al., 2015). We suggest that both spontaneous G0 and asynchronous proliferation-quiescence decisions in pairs of daughters after mitosis both contribute to cell cycle heterogeneity in clonal cell populations.

### PC3 Prostate Cancer Cells Exhibit Spontaneous Quiescence and Asynchrony in the Proliferation-Quiescence Decision

Cellular quiescence in prostate cancer is thought to contribute to tumor dormancy and issues with metastatic cancer recurrence. However, it is not well understood how and why prostate cancer cells enter and exit quiescence. We wondered whether spontaneous quiescence and asynchronous proliferation-quiescence decisions may, in part, underlie cell cycle heterogeneity in prostate cancer cells. To examine this, we transduced the mVenus-p27K<sup>-</sup> G0 and mCherry-hCdt1 G1 reporters into PC3 cells. We initially selected pools of transduced cells expressing both reporters under reduced serum conditions by FACS. We found that sorted, pooled cells quickly lost expression of one or the other reporter after a limited number of passages. We therefore isolated clones and selected a clonal PC3 Venus-Cherry cell line, stably expressing both reporters at visible levels with normal cell cycle dynamics (i.e. a cell doubling time similar to parental PC3). In this line, we readily observe double positive Venus/Cherry cells under normal full-serum culture conditions (**Figure 2A**) that are negative for EdU incorporation, negative for Ki-67 and both reporters are silent in cells that progress through the cell cycle into mitosis (**Figures 2B–D**). We also confirmed that the reporters exhibited the expected G0/G1 dynamics during serum withdrawal and serum re-addition in PC3 cells (**Figure 2E**).

We next attempted to track the reporter dynamics in PC3 cells with live cell imaging and found that these cancer cells were too motile to be tracked accurately for more than a few hours. We therefore used a microfluidic device we term the “cell hotel,” to capture one or a few cells and trap them in a chamber, to allow for manual tracking of individual cells and their daughters (Cheng et al., 2016). Each cell hotel slide allows simultaneous recording of up to 27 chambers under  $\times 10$  magnification. We confirmed that

the PC3 Venus-Cherry cells in the cell hotel exhibited similar growth and cell doubling times as previously reported for PC3 cells in bulk cell culture. In addition we repeated measurements of 3T3 Venus/Cherry cells in the cell hotel for all comparisons to PC3 (**Figures 2F–J**).

Similar to the 3T3 cells, we observed a nearly invariant reporter progression of mVenus-p27K<sup>-</sup> expression  $\sim 2$  h after cytokinesis, followed by mCherry-hCdt1 expression approximately 2 h later. Cells that enter the cell cycle, degrade mVenus-p27K<sup>-</sup> within approximately 4 h, followed by mCherry-hCdt1 degradation and ultimately cell division (**Figure 2F**). As in 3T3 cells, we observed 20% of cells with stabilized mVenus-p27K<sup>-</sup> and mCherry-hCdt1 for 14 h and beyond, without division or evidence of S/G2/M entry for 20 h or more, suggestive of spontaneous G0 entry in PC3 cells (**Figures 2G,H**). Notably, spontaneous quiescence in PC3 cells tends to be more rare and shorter than in 3T3 cells (**Figure 2H**). This could reflect the important role for p53 signaling in spontaneous quiescence (Arora et al., 2017; Yang et al., 2017), as PC3 cells lack functional p53 (Carroll et al., 1993). We also observed evidence of asynchronous proliferation-quiescence decisions, with 30% of daughters making asynchronous G0/G1 decisions within 1–6 h of each other (**Figures 2I,J**). Interestingly, the asynchronous proliferation-quiescence decisions were also rarer and the difference in timing between asynchronous daughters was less dramatic in PC3 cells (**Figure 2J**).

### Tumor Dormancy Signals can Influence Quiescence and Asynchronous Proliferation-Quiescence Decisions

Bone is a common site for prostate cancer metastasis and work from our group and others have shown that signals from osteoblasts can influence prostate cancer dormancy and PC3 cell cycle dynamics (Jung et al., 2016; Lee et al., 2016; Yumoto et al., 2016). Our previous work on PC3 cell cycle dynamics used the Fucci cell cycle reporters, which could not distinguish between G0 and G1 arrest (Jung et al., 2016). We therefore examined whether PC3 Venus-Cherry cells co-cultured with osteoblasts increased entry into G0 quiescence. We found that

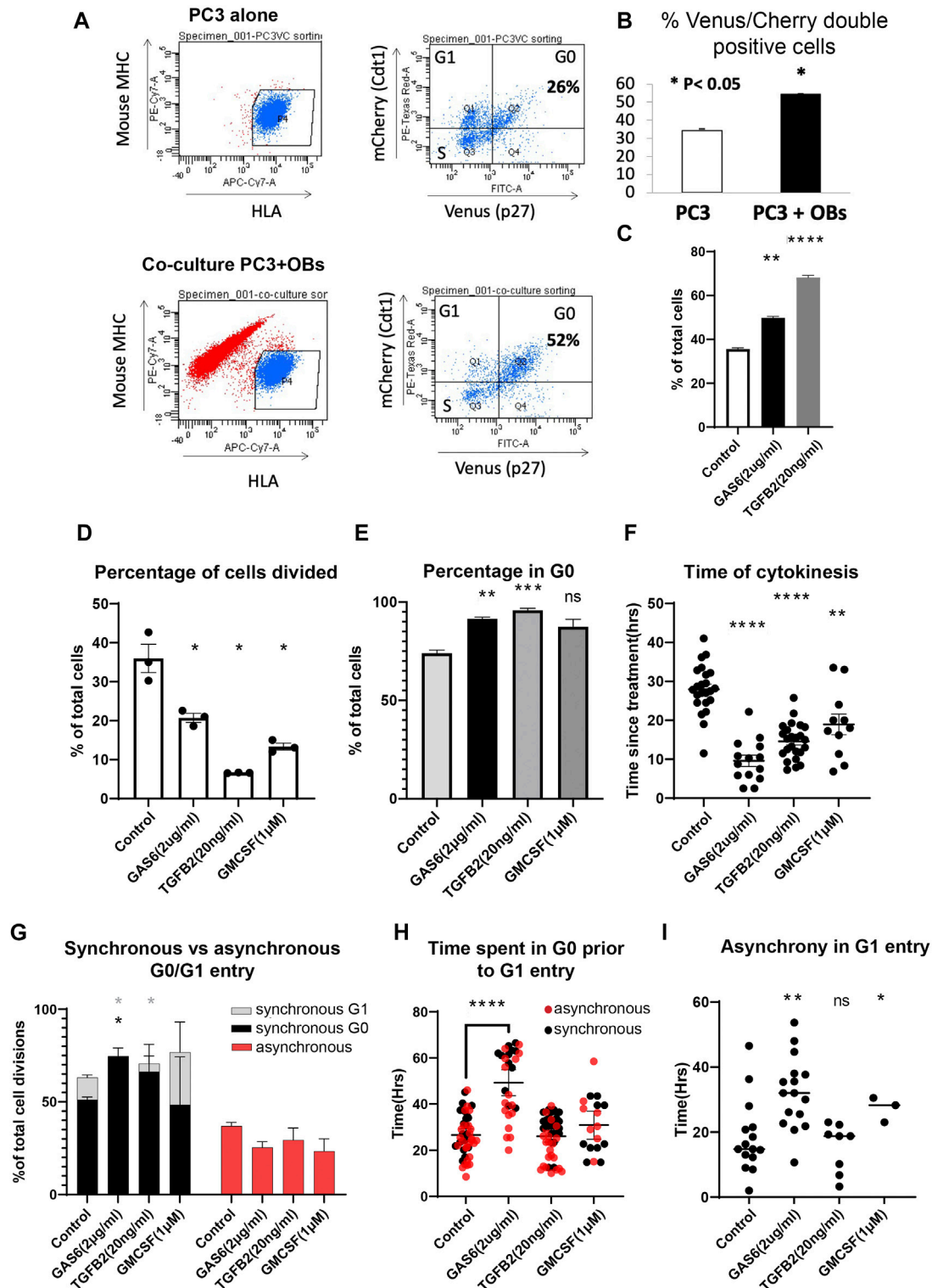


**FIGURE 3 |** Tumor dormancy signals influence quiescence and asynchronous proliferation-quiescence decisions. **(A)** PC3 Venus/Cherry cells were either cultured alone or co-cultured with mouse osteoblasts, which were excluded from cell cycle analysis by negative human HLA staining and positive anti-mouse MHC staining. **(B)** PC3 co-culture with osteoblasts induced a significant increase in G0 cells under full serum conditions. **(C)** PC3 cells treated with Gas6 or TGFβ2 also exhibit a significant increase in G0 cells, measured by flow cytometry. **(D)** G0-Venus reporter dynamics were tracked using the cell hotel for cells exposed to Gas 6 ( $n = 583$ ), TGFβ2 ( $n = 1,576$ ) or GM-CSF ( $n = 330$ ) or vehicle only controls ( $n = 336$ ). Experiments were performed at least in triplicate. Gas6, TGFβ2 and GM-CSF significantly decreased the (Continued)

**FIGURE 3** | percentage of cells that divide. **(E)** We quantified the percent of cells for each treatment that exhibited G0, defined as a Venus/Cherry double positive state for >14 h. **(F)** We tracked the timing of asynchronous cell divisions with Gas6, TGFβ2 and GM-CSF treatment, and most divisions occurred significantly earlier followed by entry into quiescence. **(G)** Synchronous G0 entry, synchronous G1 entry and asynchronous G0/G1 entry was tracked for cell divisions in Gas 6 ( $n = 121$ ), TGFβ2 ( $n = 104$ ), GM-CSF ( $n = 44$ ) or vehicle only controls ( $n = 120$ ). For Gas 6 and TGFβ2 we observe a significant increase in synchronous G0 entry, while treatment with GM-CSF increased synchronous entry into G1. **(H)** To measure transient G0, we identified cells that spent more than 4 h in G0 prior to G1 entry and measured the length of their G0. Treatment with Gas6 significantly prolonged G0, even in cells that enter transient G0. Cells that enter G1 synchronously are in black, while asynchronous cells are in red. **(I)** For pairs of daughters that enter G1 asynchronously, we measured the difference in time for G1 entry. Gas6 significantly increased the time difference for asynchronous G1 entry. Lines or bars show the mean and error bars are  $\pm$ SEM. All experiments were performed at least in triplicate and compared to controls with an unpaired  $t$ -test, \* indicates  $p < 0.05$ , \*\* indicates  $p < 0.01$ , \*\*\*\* indicates  $p < 0.001$ .

co-culture with mouse MC3T3-E1 pre-osteoblasts under full serum conditions significantly increased the fraction of double positive PC3 Venus-Cherry cells consistent with increased entry into G0 (**Figures 3A,B**). We next examined whether Gas6 and TGFβ2, signals from osteoblasts we have previously shown to induce a G0/G1 cell cycle arrest (Jung et al., 2016; Lee et al., 2016; Yumoto et al., 2016), induced entry into G0. Indeed, exposure to Gas6 or TGFβ2 significantly increased the fraction of double positive PC3 Venus-Cherry cells after 48 h, suggesting the G0/G1 arrest we previously observed was indeed arrest in G0 (**Figure 3C**).

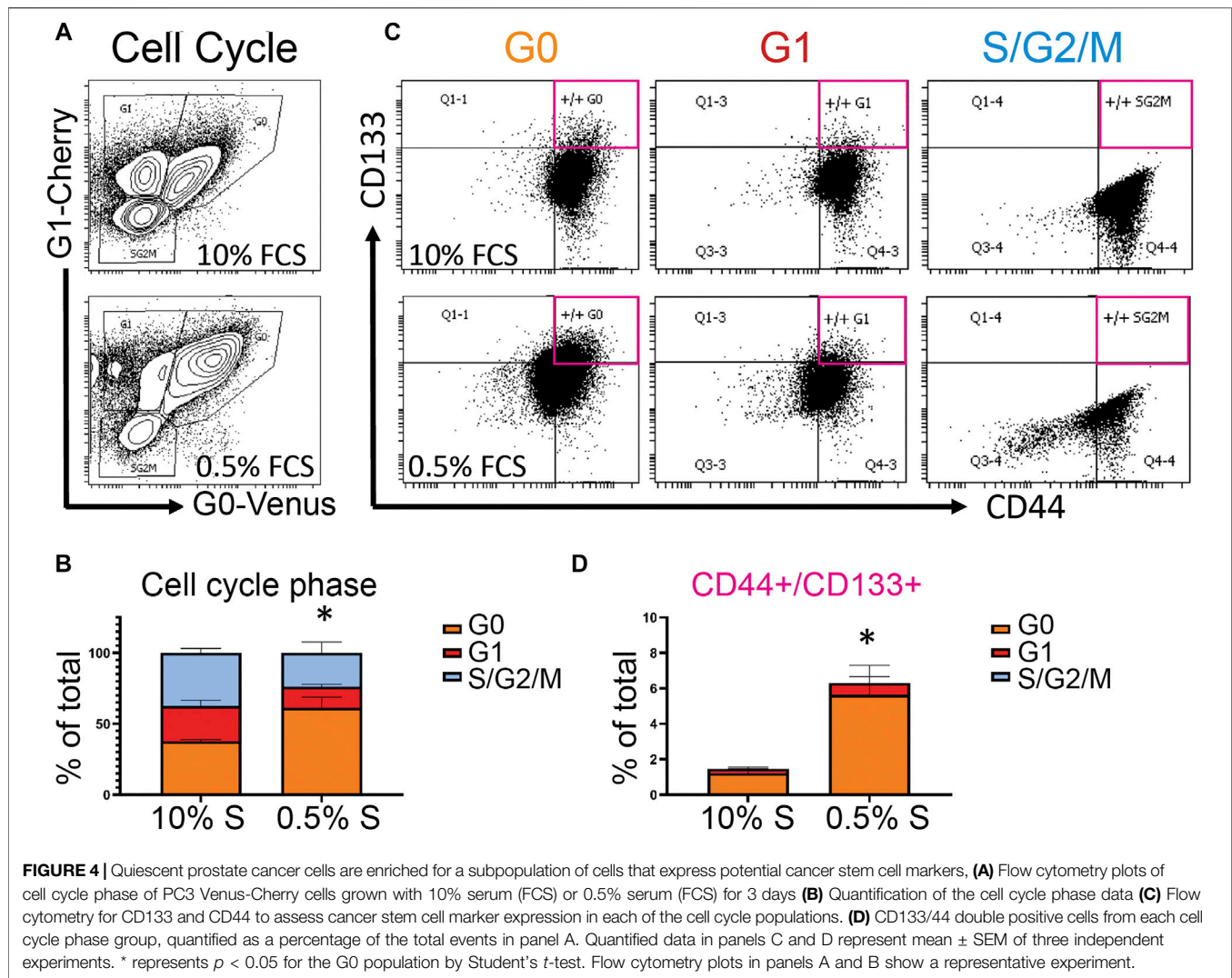
In the bone marrow, Gas6 and TGFβ2 are thought to promote prostate cancer dormancy (Jung et al., 2012; Taichman et al., 2013; Ruppender et al., 2015; Yumoto et al., 2016) while GM-CSF promotes stem cell release from the bone marrow, which may provide cues for metastatic cancer cells in the bone marrow to exit from dormancy and proliferate (Dai et al., 2010). While some of the role for GM-CSF is thought to be due to indirect effects on the bone marrow stem cell niche, studies of GM-CSF directly added to cultured PC3 cells also show increased S-phase entry, proliferation and clonogenic growth consistent with exit from dormancy (Lang et al., 1994; Savarese et al., 1998). We therefore wanted to test whether GM-CSF impacted the proliferation-quiescence decision in PC3 cells and compare this to the effects of the dormancy associated signals Gas6 and TGFβ2 on G0. We used the cell hotel to track cell cycle and mVenus-p27K<sup>+</sup> and mCherry-hCdt1 dynamics in PC3 cells 2 h after the addition of Gas 6, TGFβ2 or GM-CSF. In response to Gas6 and TGFβ2 we observed a significant decrease in the number of cells undergoing divisions during the 72 h live imaging period, consistent with an increase in G0 entry (**Figures 3D,E**). Unexpectedly, we also observed a similar decrease in cell divisions for cells treated with GM-CSF, and an increase in Venus-Cherry double positive cells, suggesting GM-CSF also promotes G0 entry. For the fraction of cells undergoing divisions during the live imaging, we tracked when these cell divisions occur. We found that control cells asynchronously proliferate throughout the live imaging time course, while most cells treated with Gas6, TGFβ2 or GM-CSF divide within the first 24 h of imaging (**Figure 3F**). These data suggest that cells uncommitted to the cell cycle either enter or remain in quiescence in response to Gas6, TGFβ2 or GM-CSF. Cells that are past the restriction point when the treatment begins, and therefore committed to cycle, must make a subsequent proliferation-quiescence decision after mitosis that may be tipped toward quiescence. To confirm this, we examined the proliferation-quiescence choices made by pairs of daughters that divide under each treatment, broken down into: synchronous

entry into G0, synchronous entry into G1 or asynchronous entry with one daughter entering G1 while the other remains in G0. For Gas6 and TGFβ2 treated cells, we observed a significant increase in synchronous entry into G0 at the expense of synchronous entry into G1, with little impact on the proportion of cells that exhibit asynchronous proliferation-quiescence decisions (**Figure 3G**). This suggests that Gas6 and TGFβ2 continue to promote quiescence in cells that are already committed to cycle after treatment addition. By contrast, GM-CSF treatment increased the proportion of divisions resulting in synchronous entry into G1, suggesting prolonged GM-CSF exposure may eventually promote cell cycle entry in a subset of the population (**Figure 3G**). Of note the pro-proliferative effects previously reported were seen in experiments performed on much longer timescales of at least 3–4 days (Lang et al., 1994; Savarese et al., 1998), suggesting the response to GM-CSF may be complex. Our data suggests GM-CSF treatment initially promotes quiescence entry in cells that are prior to the restriction point, but for a subset of cells past the restriction point it promotes their daughters to preferentially enter G1.

We next tracked pairs of daughters from the dividing cells under treatment and measured how long they spent in a Venus/Cherry double positive G0 state after mitosis prior to entering a Cherry-only G1 state. The goal was to determine whether each treatment also impacted the heterogeneity of transient quiescence, a feature that may initially promote tumor dormancy, but also lead to later recurrence. We found that only treatment with Gas6 impacted cells that entered transient quiescence, by significantly prolonging the time spent in G0 prior to the next G0-G1 transition (**Figure 3H**). This prolonged G0 occurred whether the pairs of daughters entered into G1 synchronously or asynchronously, and increased the differences in timing of G1 entry between pairs of asynchronous daughters (**Figure 3I**). This suggests that Gas6 promotes quiescence, but also promotes quiescence heterogeneity in cells that retain the ability to re-enter the cell cycle.

## Quiescent Cancer Cells are Enriched for Stem Cell Markers and Express High Levels of Hippo Pathway Signaling Components

Identifying molecular markers of quiescent cancer cells that could be assayed in patient samples is an attractive approach to identify those at risk for metastasis and recurrence. Toward this goal, we used the PC3 Venus-Cherry cells to isolate populations enriched for quiescent cancer cells by FACS, to examine their cell surface markers and gene expression changes. (**Figures 4,5**). We first

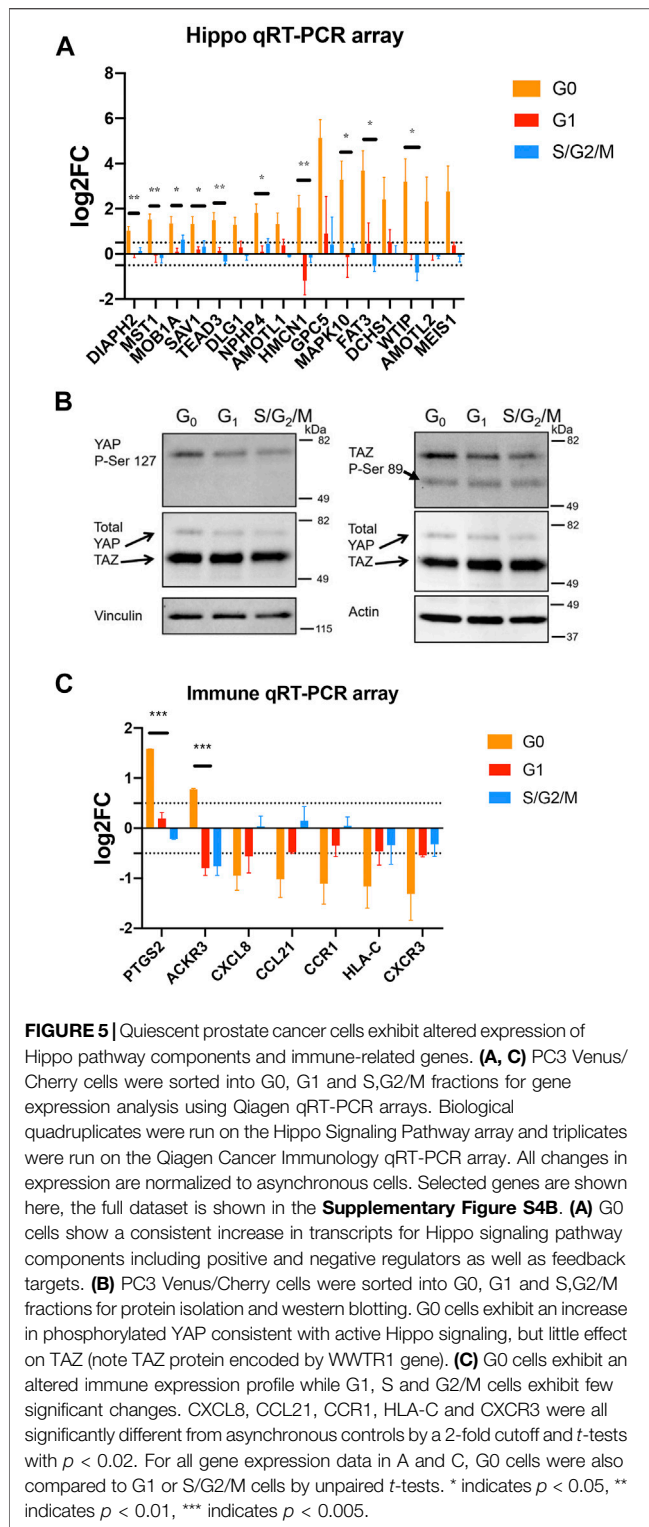


assayed the prostate cancer stem cell markers CD133 and CD44 to determine whether increasing cellular quiescence could increase the fraction of CD133/CD44 double positive potential cancer stem cells (Jung et al., 2016). We cultured PC3 Venus/Cherry cells under normal 10% serum conditions, or reduced 0.5% serum conditions for 72 h. We confirmed an increase in the G0 population under reduced serum (**Figure 4A, B**) and compared the fraction of CD133/CD44 double positive cells in the G0, G1 and S/G2/M populations (**Figure 4C**). We observed the majority of the CD133/CD44 double positive cells to be in the G0 population, with a much smaller fraction in G1 and almost none in the S/G2/M population (**Figures 4C,D**). This suggests that signals in the tumor environment that increase the quiescent population in prostate cancer may also increase the number of potential cancer stem cells that could underlie recurrence.

We previously established a mouse xenograft model of prostate cancer bone metastasis using Du-145 cells, that recapitulates aspects of dormancy and recurrence (Cackowski et al., 2017). We attempted to use the PC3 Venus/Cherry cells in a

similar xenograft model, but found that the cells quickly silenced the cell cycle reporters *in vivo*. We therefore used the xenograft model with Du-145 cells as a tool to compare gene expression profiles for cells in actively growing bone metastases as assessed by bioluminescence imaging (“involved”) vs bones without imaging detected metastases, but which still contained cancer cells that were fewer in number and presumably more slowly growing (“uninvolved”). Use of this approach of comparing cancer cells from high burden/involved vs low burden/uninvolved sites was previously used in a breast cancer model and showed that cancer cells from the uninvolved sites had more stem-like properties (Lawson et al., 2015). We isolated cells from mouse marrow under both conditions and performed bulk RNA-seq to compare global gene expression changes in the growing vs dormant state. Due to the small number of human cells recovered from uninvolved bones, we were only able to accurately assign differences in expression for 117 genes (**Supplementary Figure S3**). Nonetheless using DAVID and the KEGG database to perform pathway analysis of differentially expressed genes, we found an enrichment of genes involved in extracellular matrix





interactions and the TGF-beta signaling pathway, factors known to impact prostate cancer dormancy and dormancy escape (White et al., 2006; Bragado et al., 2013; Ruppender et al., 2015). We noted that several of the genes falling into these enriched categories also interface with Hippo signaling,

which is a key regulator of cell cycle exit (Zheng and Pan, 2019). We therefore decided to examine whether components of Hippo signaling may be altered in quiescent prostate cancer cells.

To examine differences in gene expression between G0, G1, and S/G2/M populations, we sorted populations and examined gene expression differences using a Hippo signaling Pathway qRT-PCR array (**Figure 5A**). In G0 cells, we noted a widespread increase in transcripts for Hippo signaling pathway components (e.g., DCHS1, FAT3, MST1, MOB1A, SAV1), transcriptional regulators (TEAD3, MEIS1) as well as targets (AMOTL1, AMOTL2) (Wang et al., 2018). The increased expression of some transcriptional targets of Hippo signaling is surprising, since these cells are in G0 and therefore would be expected to have Hippo signaling on. Hippo signaling acts via phosphorylation to suppress the activity of the downstream transcriptional effectors YAP1 and TAZ (encoded by the WWTR1 gene in humans) (Zheng and Pan, 2019). We therefore examined whether YAP and TAZ are suppressed via phosphorylation in G0 cells through active Hippo signaling. We performed westerns for the inactivating phosphorylations on YAP1 and TAZ in G0, G1 and S/G2/M sorted cells (**Figure 5B**) and found a small increase in phosphorylated YAP, but no effect on TAZ. We hypothesize the increased expression of Hippo pathway components may poise quiescent cells to re-enter the cell cycle upon receipt of a dormancy escape signal, but that during G0, active Hippo signaling restrains YAP transcriptional activity through inhibitory phosphorylation. (**Figure 5** and **Supplementary Figure S4**).

Hippo signaling in cancer has been associated with restraining proliferation (Zheng and Pan, 2019), but also has been shown to alter immune response, with active Hippo signaling suppressing tumor immunogenicity (Moroishi et al., 2016; Yamauchi and Moroishi, 2019). We therefore next examined whether G0 cells exhibited alterations in expression of immune response-associated signals. Using the Qiagen Cancer Immunology array on sorted G0, G1 and S/G2/M PC3 cells vs the mixed population as a reference, we observed a moderate but widespread decrease in the expression of immune-related genes including signals known to target cancer cells for host immune destruction, such as CXCR3, CXCL8, and HLA-C (**Figure 5C**) in G0 cells. This suggests that spontaneously quiescent cancer cells may exhibit altered immunoreactivity. Interestingly, one pro-inflammatory gene, PTGS2 (Cox-2), was strongly upregulated in G0 cells (**Figure 5C**), consistent with the previous work showing this target to be de-repressed when upstream Hippo signaling is active and YAP/TAZ are suppressed by phosphorylation (Zhang et al., 2018). Taken together, our results suggest the inherent cell cycle heterogeneity of metastatic prostate cancer includes a fraction of spontaneously quiescent cells that are enriched for cells expressing cancer stem cell markers and exhibit gene expression changes consistent with a state poised to re-enter the cell cycle, but potentially less visible to the host immune system.

## DISCUSSION

Several cancers contain heterogeneous populations with varying levels of proliferation (Davis et al., 2019). Some studies suggest

that quiescent tumor cells contribute to drug-resistance, by providing a population of non-cycling cells that survive cytotoxic chemotherapy (De Angelis et al., 2019; Talukdar et al., 2019; Hen and Barkan, 2020). Understanding the molecular basis of proliferative heterogeneity therefore may assist in developing better therapeutic approaches for cancer. Here, we show that untransformed 3T3 cells and PC3 prostate cancer cells show spontaneous quiescence and heterogeneous G0 lengths under pro-proliferative culture conditions. We propose that spontaneous quiescence may be related to quiescence in cancer, since quiescent cancer cells must leave the cell cycle in the presence of pro-proliferative growth factor and oncogenic signaling.

Spontaneous quiescence has been shown to underlie clonal cell cycle heterogeneity (Overton et al., 2014) and may in part underlie cell cycle heterogeneity in tumors. Here we show an additional mechanism to create heterogeneity, asynchronous G0/G1 decisions, where one daughter from a mitotic event remains in G0, while the other enters G1. These asynchronous decisions are somewhat surprising, since recent work has suggested the signals that influence the proliferation-quiescence decision are integrated over the previous cell cycle phases prior to mitosis and therefore would be expected to be inherited equally in daughters after mitosis (Yang et al., 2017; Min et al., 2020). The asynchrony in asynchronous PC3 cell divisions is often only a few hours but can extend to over 20 h or more in the presence of the dormancy inducing factor, Gas6 (**Figure 3I**). Small differences in asynchronous pairs of daughters may possibly be explained by fluctuations resulting in unequal protein and transcript inheritance at mitosis. However, this is a less satisfying hypothesis for differences in G0 exit between asynchronous daughters longer than 10 h. Previous work in MCF7 breast and HCT116 colon cancer cells has shown a population of dormant cells resulting from asymmetric Akt signaling after cell divisions (Dey-Guha et al., 2011). In this example, about 1% of cell divisions exhibit asymmetry, resulting in a daughter with low Akt signaling. Importantly, elimination of Akt prevented proliferative heterogeneity in these lines in cell culture (Dey-Guha et al., 2015), and inhibition of asymmetric Akt signaling reduced tumor recurrence after treatment in a xenograft model (Alves et al., 2018). It is worth noting that PC3 cells lack functional PTEN (Huang et al., 2001; Dubrovskaya et al., 2009) and therefore would be expected to have higher endogenous Akt signaling that suppresses some degree of asymmetry. In addition, Gas6 and other TYRO3/AXL/MERTK ligands signal in part through Akt, and therefore may also impact Akt asymmetry (Cosemans et al., 2010; Kasikara et al., 2017). Inhibition of Akt signaling can lead to up regulation of p27 in PC3 cells (Van Duijn and Trapman, 2006), while over expression of p27 can also inhibit Akt signaling (Chen et al., 2009). Further work will be needed to determine if asymmetric Akt signaling may be a cause or consequence of asynchronous proliferation-quiescence decisions in prostate cancer.

The relationship of dormancy and cellular quiescence remains unclear. Here we show that dormancy-associated signals in prostate cancer, Gas6 and TGF $\beta$ 2, rapidly within a few hours, induce quiescence entry in prostate cancer cells after mitosis. This

is in part because these signals tip the balance of proliferation-quiescence decisions in favor of synchronous G0 entry. By contrast, a presumed pro-proliferative signal for PC3 cells, GM-CSF tips the balance in favor of synchronous divisions into G1 for the cells that divide after initial exposure. Thus, although GM-CSF promotes G0 entry initially, sustained signaling may promote cell cycle re-entry in the longer term. Gas6 also has a complex effect on the proliferation-quiescence decision. In addition to promoting G0 in cells that are uncommitted to the cell cycle, Gas6 also prolongs G0 in cells that retain the ability to eventually re-enter the cell cycle. This suggests that the quiescence response to Gas 6 is not an all or nothing response and it can be graded, resulting in varying lengths of G0 to promote quiescence heterogeneity. While none of the signals we tested significantly altered the frequency of asynchronous cell cycle entry in pairs of daughters after mitosis, Gas6 significantly increased the asynchrony in G0 exit and G1 entry. We suggest this could be another source of quiescence heterogeneity in cancer.

Understanding the gene expression changes in dormant cancer cells will be essential to understanding their biology, but will also be useful tools as molecular markers for identifying them in patient samples. Here we show that quiescent PC3 cells are enriched for prostate cancer stem cell markers CD133 and 44 and that driving quiescence entry through serum starvation significantly increases the population of CD133/44 double positive cells in the population. Quiescent prostate cancer cells also exhibit increased expression of some Hippo pathway components, while the Hippo pathway remains on to restrain cell cycle entry. This finding in cell culture was also supported by our gene expression analysis in an *in vivo* xenograft model for prostate cancer tumor dormancy (**Supplementary Figure S3**). Interestingly, this is correlated with suppressed levels of mRNA for immune targeting factors, and may suggest a mechanism by which quiescent cancer cells evade host immune attack. Whether there is a direct or indirect relationship between the Hippo signaling status and expression of immune targets in quiescent cells remains to be examined.

## MATERIALS AND METHODS

### Cells and Cell Culture

The mouse embryonic fibroblast 3T3 cell line containing the G0 and G1 cell cycle reporters were kindly provided by Dr. Toshihiko Oki (University of Tokyo). These cells were grown in Dulbecco's modified Eagle's medium (DMEM; Gibco) supplemented with 10% fetal bovine serum (FBS) and 1% penicillin-streptomycin. Serum levels were reduced as indicated in the figures and text for serum starvation experiments. PC3 prostate cancer cells were cultured in RPMI medium with 10% serum and 1% penicillin-streptomycin and transduced with the G0 and G1 cell cycle reporters as previously described (Takahashi et al., 2019).

### Live Cell Imaging

NIH/3T3 cells were cultured at low density (to avoid contact inhibition) on 12-well plates in phenol red-free DMEM/10%FBS

or 1%DMEM. Experiments in **Figure 1** (and **Supplementary Figure S1**) were performed using an EVOS FL cell imaging system with a  $\times 20$  objective lens or an IncuCyte Zoom at 37°C, 5% CO<sub>2</sub>. The imaging intervals were 20–30 min.

For experiments using the “Cell Hotel” (**Figures 2, 3**), 10,000 PC3 cells in RPMI medium with 10% serum were loaded into the inlet of the microfluidic chamber. The chamber loading was monitored until most of the chambers were occupied with single cells (~5 mins). Remaining cells were then removed from the inlet and the outlet and replenished with fresh media. Imaging was performed using a Leica DMI 6000 with a Tokai Hit stage-top environmental chamber at 37°C, 5% CO<sub>2</sub>. TGF $\beta$ 2, Gas6 and GM-CSF (R&D systems) were reconstituted according to the manufacturer’s guidelines (R&D systems). For Gas6, TGF $\beta$ 2 and GM-CSF treatments, 10,000 PC3 cells were mixed with media containing the ligand (2  $\mu$ g/ml for Gas6, 20 ng/ml for TGF $\beta$ 2 and 1  $\mu$ M for GM-CSF) and introduced into the chamber. Cells were then incubated in media with the indicated ligand for 2 h of pre-equilibration prior to imaging every 30 min.

## Fabrication of the Microfluidic Device for Single-Cell Tracking

The microfluidic device used for single-cell tracking was developed in our previous work (Cheng et al., 2016). The device was built by bonding a PDMS (Polydimethylsiloxane, Sylgard 184, Dow Corning) layer with microfluidic patterns to a glass slide. The PDMS layer was formed by standard soft lithography. The SU-8 mold used for soft-lithography was created by a 3-layer photolithography process with 10  $\mu$ m, 40  $\mu$ m, and 100  $\mu$ m thick SU-8 (Microchem) following the manufacturer’s protocol. PDMS was prepared by mixing with 10 (elastomer): 1 (curing agent) (w/w) ratio, poured on SU-8 molds, and cured at 100°C overnight. Inlet and outlet holes are created by biopsy punch cutting. The PDMS with microfluidic channel structures and the glass slide were treated using oxygen plasma (80 W for 60 s) and bonded. The devices after bonding were heated at 80°C for an hour to ensure bonding quality. The microfluidic chips were sanitized using UV radiation and primed using a either a Collagen solution (1.45 ml Collagen (Collagen Type 1, 354,236, BD Biosciences) or Fibronectin solution, 0.1 ml acetic acid in 50 ml DI Water) overnight before use.

## Flow Cytometry Analysis and FACS

For cell sorting and flow cytometry assays in **Figures 2–5**, cells were cultured in RPMI supplemented with either 10% FBS or 1% as indicated and subpopulations were sorted according to the intensity of their fluorescent reporters, using a BD FACS Aria II system. Cells were sorted into SDS-PAGE loading buffer or RLT (Qiagen) for immediate protein extraction or RNA isolation. A minimum of  $\sim 10^5$  cells were collected for each experiment. Antibodies used for PC3 isolation from osteoblasts co-culture in **Figure 2** were APC/Cy7 anti-human HLA A,B,C antibody (Biolegend #311426).

For **Figure 4**, we assessed PC3 cells for dual positivity for CD44 and CD133 as we previously described (Shiozawa et al.,

2016). PC3 cells were seeded at  $10^5$  cells per well of six well plates in RPMI with 1% penicillin/streptomycin and either 10% or 0.5% serum, then cultured for 3 days. Both adherent and floating cells were analyzed for flow cytometry using a four laser BD LSR II instrument and FACSDiva™ software. We plotted G0-Venus vs G1-Cherry from the single, viable (DAPI negative) population and drilled down from each cell cycle phase group (G0, G1, or S/G/M) to analyze the percent CD133+/CD44 + cells from each population. Antibodies were PE-vio770 conjugated CD133/1, clone AC133 (Miltenyi Biotech #130–113–672) diluted 1:50 and APC conjugated CD44 (BD #559942) diluted 1:5.

## Western Blotting

Cleared cell lysates in SDS loading buffers were separated on 4–20% SDS PAGE gels under reducing conditions and transferred to PVDF membranes. Membranes were blocked with 5% milk in TBST and probed with primary antibodies diluted 1:1,000 in 5% BSA TBST; YAP1 phospho-serine 127 (Cell Signaling Technology #4911) and TAZ phospho-serine 89 (Cell Signaling Technology #59971). The secondary antibody was Cell Signaling #7074 diluted 1:1,000 in 1% milk TBST. Blots were developed in Pierce Supersignal Pico ECL substrate and visualized with a Biorad Image Doc Touch system. The membranes were subsequently stripped and reprobed for total YAP1 (CST #14074), total TAZ (CST #83669), beta actin (CST #4970), or vinculin (CST #13901) as indicated.

## qRT-PCR Arrays

PC3 Venus/Cherry cells were seeded at  $10^5$  cells per dish in 10 cm dishes and cultured for 3 days in RPMI media with 1% FCS. Cells were seeded on different days for biologic triplicate or quadruplicate samples. After 3 days of culture, cells were released by trypsinization, stained with DAPI for viability and sorted by FACS into either the total (mixed) viable cell population, G0, G1, or S/G2/M phases using the Venus/Cherry markers.  $10^5$  viable cell events for each population were collected directly into Qiagen RLT buffer containing  $\beta$ -mercaptoethanol. Total RNA was isolated with Qiagen RNeasy kits. The samples were analyzed with the Human Hippo Signaling RT2 Profiler PCR array (Qiagen #PAHS-172ZA) or Human Cancer Inflammation and Immunity Crosstalk array (Qiagen #PAHS-181ZA) using the recommended cDNA synthesis and PCR reagents. Data are presented as biologic quadruplicate or triplicate samples of expression relative to the total viable population sample. Visualization and hierarchical clustering was prepared with Morpheus software (Broad Institute).

Additional Methods and details for ATCQ and Supplemental Figures are included in the Supplemental Data file.

## DATA AVAILABILITY STATEMENT

The original contributions presented in the study are included in the article/**Supplementary Material**, further inquiries can be directed to the corresponding authors.

## ETHICS STATEMENT

The animal study was reviewed and approved by University of Michigan Committee for the Use and Care of Animals.

## AUTHOR CONTRIBUTIONS

All authors listed have made a substantial, direct, and intellectual contribution to the work and approved it for publication.

## FUNDING

This work in the Buttitta Lab was supported by funding from the American Cancer Society (RSG-15-161-01-DDC), and the Dept. of Defense (W81XWH1510413). Work in the Yang Lab is supported by the National Science Foundation (Early CAREER Grant #1553031 and MCB#1817909) and the National Institutes of Health (MIRA GM119688). Work in the Pearson lab is supported by the National Institutes of Health (K08-DE026500

and U01-CA243075). Work in the Yoon Lab was in part supported by the National Institute of Health (R01-CA203810). Work in the Cackowski Lab is supported by a Prostate Cancer Foundation Challenge award, University of Michigan Prostate Cancer S.P.O.R.E. NIH/NCI 5 P50CA18678605, Career Enhancement sub-award to F.C.C. F048931, Prostate Cancer Foundation Young Investigator Award 18YOUN04, Department of Defense Prostate Cancer Research Program Physician Research Award W81XWH2010394, and start-up funds from The University of Michigan and Karmanos Cancer Institute. Work in the Taichman lab was supported by National Institutes of Health (3P01CA093900-06) and the Prostate Cancer Foundation (16CHAL05).

## SUPPLEMENTARY MATERIAL

The Supplementary Material for this article can be found online at: <https://www.frontiersin.org/articles/10.3389/fcell.2021.728663/full#supplementary-material>

## REFERENCES

- Alves, C. P., Dey-Guha, I., Kabraji, S., Yeh, A. C., Talele, N. P., Solé, X., et al. (2018). AKT1low Quiescent Cancer Cells Promote Solid Tumor Growth. *Mol. Cancer Ther.* 17, 254–263. doi:10.1158/1535-7163.mct-16-0868
- Arora, M., Moser, J., Phadke, H., Basha, A. A., and Spencer, S. L. (2017). Endogenous Replication Stress in Mother Cells Leads to Quiescence of Daughter Cells. *Cel Rep.* 19, 1351–1364. doi:10.1016/j.celrep.2017.04.055
- Bragado, P., Estrada, Y., Parikh, F., Krause, S., Capobianco, C., Farina, H. G., et al. (2013). TGF- $\beta$ 2 Dictates Disseminated Tumour Cell Fate in Target Organs Through TGF- $\beta$ -RIII and P38 $\alpha$ / $\beta$  Signalling. *Nat. Cel Biol.* 15, 1351–1361. doi:10.1038/ncb2861
- Cackowski, F. C., Eber, M. R., Rhee, J., Decker, A. M., Yumoto, K., Berry, J. E., et al. (2017). Mer Tyrosine Kinase Regulates Disseminated Prostate Cancer Cellular Dormancy. *J. Cel Biochem.* 118, 891–902. doi:10.1002/jcb.25768
- Carroll, A. G., Voeller, H. J., Sugars, L., and Gelmann, E. P. (1993). p53 Oncogene Mutations in Three Human Prostate Cancer Cell Lines. *Prostate.* 23, 123–134. doi:10.1002/pros.2990230206
- Chen, F., Han, Y., and Kang, Y. (2021). Bone Marrow Niches in the Regulation of Bone Metastasis. *Br. J. Cancer.* 124, 1912–1920. doi:10.1038/s41416-021-01329-6
- Chen, J., Xia, D., Luo, J.-D., and Wang, P. (2009). Exogenous p27KIP1 Expression Induces Anti-Tumour Effects and Inhibits the EGFR/PI3K/Akt Signalling Pathway in PC3 Cells. *Asian J. Androl.* 11, 669–677. doi:10.1038/aja.2009.51
- Cheng, Y.-H., Chen, Y.-C., Brien, R., and Yoon, E. (2016). Scaling and Automation of a High-Throughput Single-Cell-Derived Tumor Sphere Assay Chip. *Lab. Chip.* 16, 3708–3717. doi:10.1039/c6lc00778c
- Chittajallu, D. R., Florian, S., Kohler, R. H., Iwamoto, Y., Orth, J. D., Weissleder, R., et al. (2015). In Vivo Cell-Cycle Profiling in Xenograft Tumors by Quantitative Intravital Microscopy. *Nat. Methods.* 12, 577–585. doi:10.1038/nmeth.3363
- Coller, H. A., Sang, L., and Roberts, J. M. (2006). A New Description of Cellular Quiescence. *Plos Biol.* 4, e83. doi:10.1371/journal.pbio.0040083
- Cosemans, J. M. E. M., Van Kruchten, R., Olieslagers, S., Schurgers, L. J., Verheyen, F. K., Munnix, I. C. A., et al. (2010). Potentiating Role of Gas6 and Tyro3, Axl and Mer (TAM) Receptors in Human and Murine Platelet Activation and Thrombus Stabilization. *J. Thromb. Haemost.* 8, 1797–1808. doi:10.1111/j.1538-7836.2010.03935.x
- Dai, J., Lu, Y., Yu, C., Keller, J. M., Mizokami, A., Zhang, J., et al. (2010). Reversal of Chemotherapy-Induced Leukopenia Using Granulocyte Macrophage Colony-Stimulating Factor Promotes Bone Metastasis that Can Be Blocked With Osteoclast Inhibitors. *Cancer Res.* 70, 5014–5023. doi:10.1158/0008-5472.can-10-0100
- Davis, J. E., Jr., Kirk, J., Ji, Y., and Tang, D. G. (2019). Tumor Dormancy and Slow-Cycling Cancer Cells. *Adv. Exp. Med. Biol.* 1164, 199–206. doi:10.1007/978-3-030-22254-3\_15
- De Angelis, M. L., Francescangeli, F., La Torre, F., and Zeuner, A. (2019). Stem Cell Plasticity and Dormancy in the Development of Cancer Therapy Resistance. *Front. Oncol.* 9, 626. doi:10.3389/fonc.2019.00626
- Dey-Guha, I., Alves, C. P., Yeh, A. C., SalonySole, X., Sole, X., Darp, R., et al. (2015). A Mechanism for Asymmetric Cell Division Resulting in Proliferative Asynchronicity. *Mol. Cancer Res.* 13, 223–230. doi:10.1158/1541-7786.mcr-14-0474
- Dey-Guha, I., Wolfer, A., Yeh, A. C., G. Albeck, J., Darp, R., Leon, E., et al. (2011). Asymmetric Cancer Cell Division Regulated by AKT. *Proc. Natl. Acad. Sci.* 108, 12845–12850. doi:10.1073/pnas.1109632108
- Dubrovskaya, A., Kim, S., Salamone, R. J., Walker, J. R., Maira, S.-M., Garcia-Echeverria, C., et al. (2009). The Role of PTEN/Akt/PI3K Signaling in the Maintenance and Viability of Prostate Cancer Stem-Like Cell Populations. *Proc. Natl. Acad. Sci.* 106, 268–273. doi:10.1073/pnas.0810956106
- Hen, O., and Barkan, D. (2020). Dormant Disseminated Tumor Cells and Cancer Stem/Progenitor-like Cells: Similarities and Opportunities. *Semin. Cancer Biol.* 60, 157–165. doi:10.1016/j.semcancer.2019.09.002
- Huang, H., Cheville, J. C., Pan, Y., Roche, P. C., Schmidt, L. J., and Tindall, D. J. (2001). PTEN Induces Chemosensitivity in PTEN-Mutated Prostate Cancer Cells by Suppression of Bcl-2 Expression. *J. Biol. Chem.* 276, 38830–38836. doi:10.1074/jbc.m103632200
- Jeffrey, P. D., Russo, A. A., Polyak, K., Gibbs, E., Hurwitz, J., Massagué, J., et al. (1995). Mechanism of CDK Activation Revealed by the Structure of a cyclin-A-CDK2 Complex. *Nature.* 376, 313–320. doi:10.1038/376313a0
- Jung, Y., Decker, A. M., Wang, J., Lee, E., Kana, L. A., Yumoto, K., et al. (2016). Endogenous GAS6 and Mer Receptor Signaling Regulate Prostate Cancer Stem Cells in Bone Marrow. *Oncotarget.* 7, 25698–25711. doi:10.18632/oncotarget.8365
- Jung, Y., Shiozawa, Y., Wang, J., McGregor, N., Dai, J., Park, S. I., et al. (2012). Prevalence of Prostate Cancer Metastases After Intravenous Inoculation Provides Clues into the Molecular Basis of Dormancy in the Bone Marrow Microenvironment. *Neoplasia.* 14, 429–439. doi:10.1596/neo.111740
- Kamura, T., Hara, T., Matsumoto, M., Ishida, N., Okumura, F., Hatakeyama, S., et al. (2004). Cytoplasmic Ubiquitin Ligase KPC Regulates Proteolysis of p27Kip1 at G1 Phase. *Nat. Cel Biol.* 6, 1229–1235. doi:10.1038/ncb1194



- Kasikara, C., Kumar, S., Kimani, S., Tsou, W.-I., Geng, K., Davra, V., et al. (2017). Phosphatidylinositol Sensing by TAM Receptors Regulates AKT-Dependent Chemoresistance and PD-L1 Expression. *Mol. Cancer Res.* 15, 753–764. doi:10.1158/1541-7786.mcr-16-0350
- Lam, H.-M., Vessella, R. L., and Morrissey, C. (2014). The Role of the Microenvironment-Dormant Prostate Disseminated Tumor Cells in the Bone Marrow. *Drug Discov. Today Tech.* 11, 41–47. doi:10.1016/j.ddtec.2014.02.002
- Lang, S. H., Miller, W. R., Duncan, W., and Habib, F. K. (1994). Production and Response of Human Prostate Cancer Cell Lines to Granulocyte Macrophage-Colony Stimulating Factor. *Int. J. Cancer.* 59, 235–241. doi:10.1002/ijc.2910590216
- Lawson, D. A., Bhakta, N. R., Kessenbrock, K., Prummel, K. D., Yu, Y., Takai, K., et al. (2015). Single-cell Analysis Reveals a Stem-Cell Program in Human Metastatic Breast Cancer Cells. *Nature.* 526, 131–135. doi:10.1038/nature15260
- Lee, E., Decker, A. M., Cackowski, F. C., Kana, L. A., Yumoto, K., Jung, Y., et al. (2016). Growth Arrest-Specific 6 (GAS6) Promotes Prostate Cancer Survival by G Arrest/S Phase Delay and Inhibition of Apoptotic Pathway During Chemotherapy in Bone Marrow. *J. Cell Biochem.* 117, 2815–2824.
- Matson, J. P., and Cook, J. G. (2017). Cell Cycle Proliferation Decisions: the Impact of Single Cell Analyses. *FEBS J.* 284, 362–375. doi:10.1111/febs.13898
- Miller, I., Min, M., Yang, C., Tian, C., Gookin, S., Carter, D., et al. (2018). Ki67 Is a Graded Rather Than a Binary Marker of Proliferation versus Quiescence. *Cel Rep.* 24, 1105–1112. doi:10.1016/j.celrep.2018.06.110
- Min, M., Rong, Y., Tian, C., and Spencer, S. L. (2020). Temporal Integration of Mitogen History in Mother Cells Controls Proliferation of Daughter Cells. *Science.* 368, 1261–1265. doi:10.1126/science.ayy8241
- Min, M., and Spencer, S. L. (2019). Spontaneously Slow-Cycling Subpopulations of Human Cells Originate From Activation of Stress-Response Pathways. *Plos Biol.* 17, e3000178. doi:10.1371/journal.pbio.3000178
- Moroishi, T., Hayashi, T., Pan, W.-W., Fujita, Y., Holt, M. V., Qin, J., et al. (2016). The Hippo Pathway Kinases LATS1/2 Suppress Cancer Immunity. *Cell.* 167, 1525–1539. e1517. doi:10.1016/j.cell.2016.11.005
- Nik Nabil, W. N., Xi, Z., Song, Z., Jin, L., Zhang, X. D., Zhou, H., et al. (2021). Towards a Framework for Better Understanding of Quiescent Cancer Cells. *Cells.* 10, 562. doi:10.3390/cells10030562
- Oki, T., Nishimura, K., Kitaura, J., Togami, K., Maehara, A., Izawa, K., et al. (2014). A Novel Cell-Cycle-Indicator, mVenus-p27K-, Identifies Quiescent Cells and Visualizes G0-G1 Transition. *Sci Rep.* 4, 4012. doi:10.1038/srep04012
- Overton, K. W., Spencer, S. L., Noderer, W. L., Meyer, T., and Wang, C. L. (2014). Basal P21 Controls Population Heterogeneity in Cycling and Quiescent Cell Cycle States. *Proc. Natl. Acad. Sci.* 111, E4386–E4393. doi:10.1073/pnas.1409797111
- Recasens, A., and Munoz, L. (2019). Targeting Cancer Cell Dormancy. *Trends Pharmacol. Sci.* 40, 128–141. doi:10.1016/j.tips.2018.12.004
- Ridenour, D. A., McKinney, M. C., Bailey, C. M., and Kulesa, P. M. (2012). CycleTrak: a Novel System for the Semi-Automated Analysis of Cell Cycle Dynamics. *Developmental Biol.* 365, 189–195. doi:10.1016/j.ydbio.2012.02.026
- Risson, E., Nobre, A. R., Maguer-Satta, V., and Aguirre-Ghiso, J. A. (2020). The Current Paradigm and Challenges Ahead for the Dormancy of Disseminated Tumor Cells. *Nat. Cancer.* 1, 672–680. doi:10.1038/s43018-020-0088-5
- Ruppender, N., Larson, S., Lakely, B., Kollath, L., Brown, L., Coleman, I., et al. (2015). Cellular Adhesion Promotes Prostate Cancer Cells Escape from Dormancy. *PLoS One.* 10, e0130565. doi:10.1371/journal.pone.0130565
- Sakaue-Sawano, A., Kurokawa, H., Morimura, T., Hanyu, A., Hama, H., Osawa, H., et al. (2008). Visualizing Spatiotemporal Dynamics of Multicellular Cell-Cycle Progression. *Cell.* 132, 487–498. doi:10.1016/j.cell.2007.12.033
- Savarese, D. M. F., Valinski, H., Quesenberry, P., and Savarese, T. (1998). Expression and Function of Colony-Stimulating Factors and Their Receptors in Human Prostate Carcinoma Cell Lines. *Prostate.* 34, 80–91. doi:10.1002/(sici)1097-0045(19980201)34:2<80::aid-pros2>3.0.co;2-n
- Sherr, C. J., and Roberts, J. M. (1999). CDK Inhibitors: Positive and Negative Regulators of G1-phase Progression. *Genes Development.* 13, 1501–1512. doi:10.1101/gad.13.12.1501
- Shiozawa, Y., Berry, J. E., Eber, M. R., Jung, Y., Yumoto, K., Cackowski, F. C., et al. (2016). The Marrow Niche Controls the Cancer Stem Cell Phenotype of Disseminated Prostate Cancer. *Oncotarget* 7, 41217–41232. doi:10.18632/oncotarget.9251
- Spencer, S. L., Cappell, S. D., Tsai, F.-C., Overton, K. W., Wang, C. L., and Meyer, T. (2013). The Proliferation-Quiescence Decision Is Controlled by a Bifurcation in CDK2 Activity at Mitotic Exit. *Cell.* 155, 369–383. doi:10.1016/j.cell.2013.08.062
- Stewart-Ornstein, J., and Lahav, G. (2016). Dynamics of CDKN1A in Single Cells Defined by an Endogenous Fluorescent Tagging Toolkit. *Cel Rep.* 14, 1800–1811. doi:10.1016/j.celrep.2016.01.045
- Taichman, R. S., Patel, L. R., Bedenis, R., Wang, J., Weidner, S., Schumann, T., et al. (2013). GAS6 Receptor Status Is Associated with Dormancy and Bone Metastatic Tumor Formation. *PLoS One.* 8, e61873. doi:10.1371/journal.pone.0061873
- Takahashi, H., Yumoto, K., Yasuhara, K., Nadres, E. T., Kikuchi, Y., Buttitta, L., et al. (2019). Anticancer Polymers Designed for Killing Dormant Prostate Cancer Cells. *Sci. Rep.* 9, 1096. doi:10.1038/s41598-018-36608-5
- Talukdar, S., Bhooopathi, P., Emdad, L., Das, S., Sarkar, D., and Fisher, P. B. (2019). Dormancy and Cancer Stem Cells: An Enigma for Cancer Therapeutic Targeting. *Adv. Cancer Res.* 141, 43–84. doi:10.1016/bs.acr.2018.12.002
- Tedesco, D., Lukas, J., and Reed, S. I. (2002). The pRb-Related Protein P130 Is Regulated by Phosphorylation-Dependent Proteolysis via the Protein-Ubiquitin Ligase SCFSkp2. *Genes Dev.* 16, 2946–2957. doi:10.1101/gad.1011202
- Van Duijn, P. W., and Trapman, J. (2006). PI3K/Akt Signaling Regulates P27kip1 Expression via Skp2 in PC3 and DU145 Prostate Cancer Cells, but Is Not a Major Factor in P27kip1 Regulation in LNCaP and PC346 Cells. *Prostate.* 66, 749–760. doi:10.1002/pros.20398
- Wang, Y., Xu, X., Maglic, D., Dill, M. T., Mojumdar, K., Ng, P. K., et al. (2018). Comprehensive Molecular Characterization of the Hippo Signaling Pathway in Cancer. *Cel Rep.* 25, 1304–e5. doi:10.1016/j.celrep.2018.10.001
- White, D. E., Rayment, J. H., and Muller, W. J. (2006). Addressing the Role of Cell Adhesion in Tumor Cell Dormancy. *Cell Cycle.* 5, 1756–1759. doi:10.4161/cc.5.16.2993
- Yamauchi, T., and Moroishi, T. (2019). Hippo Pathway in Mammalian Adaptive Immune System. *Cells.* 8, 398. doi:10.3390/cells8050398
- Yang, H. W., Chung, M., Kudo, T., and Meyer, T. (2017). Competing Memories of Mitogen and P53 Signalling Control Cell-Cycle Entry. *Nature.* 549, 404–408. doi:10.1038/nature23880
- Yao, G. (2014). Modelling Mammalian Cellular Quiescence. *Interf. Focus.* 4, 20130074. doi:10.1098/rsfs.2013.0074
- Yumoto, K., Eber, M. R., Wang, J., Cackowski, F. C., Decker, A. M., Lee, E., et al. (2016). Axl Is Required for TGF- $\beta$ 2-Induced Dormancy of Prostate Cancer Cells in the Bone Marrow. *Sci. Rep.* 6, 36520. doi:10.1038/srep36520
- Zamboni, A. C., Hsu, T., Kim, S. E., Klinck, M., Stowe, J., Henderson, L. M., et al. (2020). Methods and Sensors for Functional Genomic Studies of Cell-Cycle Transitions in Single Cells. *Physiol. Genomics.* 52, 468–477. doi:10.1152/physiolgenomics.00065.2020
- Zhang, Q., Han, X., Chen, J., Xie, X., Xu, J., Zhao, Y., et al. (2018). Yes-Associated Protein (YAP) and Transcriptional Coactivator With PDZ-Binding Motif (TAZ) Mediate Cell Density-Dependent Proinflammatory Responses. *J. Biol. Chem.* 293, 18071–18085. doi:10.1074/jbc.ra118.004251
- Zheng, Y., and Pan, D. (2019). The Hippo Signaling Pathway in Development and Disease. *Developmental Cell.* 50, 264–282. doi:10.1016/j.devcel.2019.06.003

**Conflict of Interest:** The authors declare that the research was conducted in the absence of any commercial or financial relationships that could be construed as a potential conflict of interest.

**Publisher's Note:** All claims expressed in this article are solely those of the authors and do not necessarily represent those of their affiliated organizations, or those of the publisher, the editors and the reviewers. Any product that may be evaluated in this article, or claim that may be made by its manufacturer, is not guaranteed or endorsed by the publisher.

Copyright © 2021 Pulianmackal, Sun, Yumoto, Li, Chen, Patel, Wang, Yoon, Pearson, Yang, Taichman, Cackowski and Buttitta. This is an open-access article distributed under the terms of the Creative Commons Attribution License (CC BY). The use, distribution or reproduction in other forums is permitted, provided the original author(s) and the copyright owner(s) are credited and that the original publication in this journal is cited, in accordance with accepted academic practice. No use, distribution or reproduction is permitted which does not comply with these terms.



# Why Senescent Cells Are Resistant to Apoptosis: An Insight for Senolytic Development

Li Hu<sup>1,2,3†</sup>, Huiqin Li<sup>2†</sup>, Meiting Zi<sup>2</sup>, Wen Li<sup>4</sup>, Jing Liu<sup>5</sup>, Yang Yang<sup>6</sup>, Daohong Zhou<sup>6</sup>, Qing-Peng Kong<sup>2</sup>, Yunxia Zhang<sup>1,3\*</sup> and Yonghan He<sup>2\*</sup>

<sup>1</sup>Department of Geriatrics, The Second Affiliated Hospital of Hainan Medical University, Haikou, China, <sup>2</sup>State Key Laboratory of Genetic Resources and Evolution, Kunming Institute of Zoology, Chinese Academy of Sciences, Kunming, China, <sup>3</sup>College of Basic Medicine and Life Sciences, Hainan Medical University, Haikou, China, <sup>4</sup>Department of Endocrinology, The Third People's Hospital of Yunnan Province, Kunming, China, <sup>5</sup>Lab of Molecular Genetics of Aging and Tumor, Medical School, Kunming University of Science and Technology, Kunming, China, <sup>6</sup>Department of Pharmacodynamics, College of Pharmacy, University of Florida, Gainesville, FL, United States

## OPEN ACCESS

### Edited by:

Guang Yao,  
University of Arizona, United States

### Reviewed by:

Joseph William Landry,  
Virginia Commonwealth University,  
United States  
Oliver Bischof,  
Délégation Ile-de-France Ouest et  
Nord (CNRS), France

### \*Correspondence:

Yonghan He  
heyonghan@mail.kiz.ac.cn  
Yunxia Zhang  
zhangyunxia@hainmc.edu.cn

<sup>†</sup>These authors have contributed  
equally to this work

### Specialty section:

This article was submitted to  
Cell Growth and Division,  
a section of the journal  
Frontiers in Cell and Developmental  
Biology

**Received:** 26 November 2021

**Accepted:** 26 January 2022

**Published:** 16 February 2022

### Citation:

Hu L, Li H, Zi M, Li W, Liu J, Yang Y,  
Zhou D, Kong Q-P, Zhang Y and He Y  
(2022) Why Senescent Cells Are  
Resistant to Apoptosis: An Insight for  
Senolytic Development.  
Front. Cell Dev. Biol. 10:822816.  
doi: 10.3389/fcell.2022.822816

Cellular senescence is a process that leads to a state of irreversible cell growth arrest induced by a variety of intrinsic and extrinsic stresses. Senescent cells (SnCs) accumulate with age and have been implicated in various age-related diseases in part via expressing the senescence-associated secretory phenotype. Elimination of SnCs has the potential to delay aging, treat age-related diseases and extend healthspan. However, once cells becoming senescent, they are more resistant to apoptotic stimuli. Senolytics can selectively eliminate SnCs by targeting the SnC anti-apoptotic pathways (SCAPs). They have been developed as a novel pharmacological strategy to treat various age-related diseases. However, the heterogeneity of the SnCs indicates that SnCs depend on different proteins or pathways for their survival. Thus, a better understanding of the underlying mechanisms for apoptotic resistance of SnCs will provide new molecular targets for the development of cell-specific or broad-spectrum therapeutics to clear SnCs. In this review, we discussed the latest research progresses and challenge in senolytic development, described the significance of regulation of senescence and apoptosis in aging, and systematically summarized the SCAPs involved in the apoptotic resistance in SnCs.

**Keywords:** aging, apoptosis, resistance, senescent cell, senolytic

## INTRODUCTION

Aging is a time-dependent functional decline that affects most living organisms. It is characterized by a progressive loss of physiological integrity, causing impaired function and increased vulnerability to death (López-Otín et al., 2013). Aging results from the time-dependent accumulation of a wide range of molecular and cellular damage over time. In humans, aging increases the risk of various age-related diseases. In 2013, López-Otín et al. identified and categorized the cellular and molecular hallmarks of aging, including genomic instability, telomere attrition, epigenetic alterations, loss of proteostasis, deregulated nutrient sensing, mitochondrial dysfunction, cellular senescence, stem cell exhaustion and altered intercellular communication (López-Otín et al., 2013). All of these hallmarks occur during aging and are interconnected. Among them, cellular senescence can link to almost all of other aging hallmarks, representing a good example to study healthy aging from basic research to therapeutics (Campisi et al., 2019; Di Micco et al., 2021).

Cellular senescence is a process that leads to a state of irreversible growth arrest in response to a variety of intrinsic and extrinsic stresses (Hernandez-Segura et al., 2017). Initially, the phenomenon was found when cultured cells were shown to undergo a limited number of cell divisions *in vitro* (Hayflick and Moorhead, 1961; Hayflick, 1965). Cellular senescence is different from cell quiescence which represents a transient and reversible cell cycle arrest. Cellular senescence can be a physiologically or pathologically relevant program depending on the specific situation (Burton and Krizhanovsky, 2014; Herranz and Gil, 2018). It normally functions as a vital tumor suppressive mechanism and also plays an important role in tissue damage repair (Demaria et al., 2014; Gorgoulis et al., 2019; Moiseeva et al., 2020). However, senescent cells (SnCs) have been implicated in various age-related diseases (Palmer et al., 2015; Ogrodnik et al., 2017; Aguayo-Mazzucato et al., 2019; Zhang et al., 2019). Accordingly, selective elimination of SnCs has been exploited as a novel strategy to treat the diseases. In addition, SnCs have also been implicated in infectious diseases. For example, virus infection can induce cellular senescence, which was found to be a pathogenic trigger of cytokine escalation and organ damage, and recently found to be associated with the COVID-19 severity in the elderly (Nehme et al., 2020; Gerdes et al., 2021; Lee et al., 2021; Mohiuddin and Kasahara, 2021). Clearance of virus-induced SnCs was considered as a novel treatment option against severe acute respiratory syndrome coronavirus 2 (SARS-CoV-2) (Lee et al., 2021) and perhaps other viral infections (Camell et al., 2021).

One of the characteristics of SnCs is their ability to resist apoptosis. Until now, small molecules that can selectively kill SnCs, termed senolytics, were developed to target the proteins in the SnC anti-apoptotic pathways (SCAPs) (Childs et al., 2017; Kirkland and Tchkonja, 2017; Niedernhofer and Robbins, 2018). However, due to the high heterogeneity in gene expression and their diverse origins, SnCs may use different SCAPs to maintain their survival, making it difficult to use a single senolytic to kill all types of SnCs. Although significant progresses on the development of senolytics have been made, some proteins involved in the SCAPs have been overlooked, neither their potential of being senolytic targets have been investigated. Therefore, gaining more insights into the apoptosis-resistant mechanism of SnCs may greatly help to design or screen more effective senolytics that can be used to treat SnC-associated disorders. In this review, we systematically summarized the proteins or pathways involved in SnC apoptotic resistance documented in the publications since 1995 (Wang, 1995), when the first result of SnC resistance to apoptosis was reported.

## SNCS ARE NOVEL THERAPEUTIC TARGETS FOR AGING AND AGE-RELATED DISEASES

Cellular senescence is the irreversible growth arrest of individual mitotic cells. It was first described by Leonard Hayflick and Paul Moorhead (Hayflick and Moorhead, 1961). In their work they found that the cultured human

fibroblasts lost the ability to proliferate, reaching permanent arrest after about 50 population doublings (Hayflick and Moorhead, 1961; Hayflick, 1965). This type of cellular senescence is referred to as replicative senescence, which is caused by telomere shortening after extensive cell proliferations. Another major type of cellular senescence is stress-induced premature cellular senescence, which is resulted from exposure to various genotoxic stressors, such as oxidative stress, and chemotherapy. In addition, the activation of various oncogenes can also induce senescence termed as oncogene-induced senescence, which is caused by DNA replicative stress (Di Micco et al., 2006). After being senescent, cells display a series of cellular and molecular changes, such as enlarged cell size, irregularly shaped cell body, increased lysosomal content, accumulation of mitochondria, enlarged nuclear size and increased DNA damage (Hernandez-Segura et al., 2018). The hallmarks of cellular senescence were well summarized elsewhere (Hernandez-Segura et al., 2018). Some of them, such as increased p16 and beta-galactosidase activity, are widely used for identifying SnCs *in vitro* and *in vivo* (Childs et al., 2017).

Cellular senescence is a key mechanism for the body to prevent the propagation of damaged cells (Herranz and Gil, 2018; Gorgoulis et al., 2019). In this regards, cellular senescence acts as a tumor suppressor mechanism (Sarkisian et al., 2007; Burton and Krizhanovsky, 2014), and it also shows beneficial effects in development (Muñoz-Espín et al., 2013) and tissue repair (Demaria et al., 2014). However, SnCs can accumulate when their production persists beyond the immune clearance capacity or the immune system is compromised. Under such circumstances, SnCs may play a causative role in aging and age-related diseases by inducing reactive oxygen species (ROS) and secreting a plethora of inflammatory mediators (e.g., cytokines and chemokines), growth factors, and extracellular proteases—termed as the senescence-associated secretory phenotype (SASP) (Demaria et al., 2017; Alimirah et al., 2020). Therefore, cellular senescence is both a physiologically and pathologically relevant program depending on the specific situation.

In 2011 and 2016, Baker et al. reported that elimination of SnCs by a transgenic approach delayed the onset of several age-related diseases and prolonged lifespan in progeroid and naturally aged mice, respectively (Baker et al., 2011, 2016). They provided solid evidence for that SnCs are causally implicated in generating age-related phenotypes and that clearance of SnCs can prevent or delay tissue dysfunction and extend healthspan. Later on, accumulating data demonstrate the involvement of SnCs in various age-related diseases and disorders (Childs et al., 2015, 2017; Kirkland and Tchkonja, 2017; Niedernhofer and Robbins, 2018), such as neurodegenerative diseases (Chinta et al., 2018; Zhang et al., 2019), diabetes (Aguayo-Mazzucato et al., 2019), atherosclerosis (Childs et al., 2016), osteoarthritis (Jeon et al., 2017), and tumors (Demaria et al., 2017; Takasugi et al., 2017). In sum, these findings suggest that SnCs are an emerging therapeutic target of aging and age-related diseases.

**TABLE 1 |** Senolytic targets and agents.

Senolytic targets	Senolytic agents	References
BCL-XL/BCL-W	Navitoclax, PZ15227, A1331852, A1155463	(Zhu et al., 2015, 2017; Chang et al., 2016; Yosef et al., 2016; He et al., 2020b)
HSP90	17-DMAG	Fuhrmann-Stroissnigg et al. (2017)
MDM2	UBX0101	Jeon et al. (2017)
USP7	P5091	He et al. (2020a)
FOXO4	FOXO4-p53 interfering peptide	Baar et al. (2017)
OXR1	Piperlongumine	Zhang et al. (2018)
RTK	Dasatinib	Zhu et al. (2015)
Na <sup>+</sup> /K <sup>+</sup> ATPase	Ouabain, Digoxin	(Guerrero et al., 2019; Triana-Martínez et al., 2019)
BRD4	JQ1, ARV825	Wakita et al. (2020)
GLS1	BPTEs	Johmura et al. (2021)
FAK	R406	Cho et al. (2020)
TPP	Alkyl-di-quaternary Alkyl-monoquaternary	Jana et al. (2021)
LC3-II/LC3	Azithromycin, Roxithromycin GL-V9	(Ozsvari et al., 2018; Yang et al., 2021)
C-IAP1/C-IAP2/BCL-2	Temozolomide	Schwarzenbach et al. (2021)
HDAC	Hinokitiol, Preussomerin C Tanshinone I	Barrera-Vázquez et al. (2021)
PPAR $\alpha$	Fenofibrate	Nogueira-Recalde et al. (2019)

## TARGETING SENESCENT CELLS WITH SENOLYTICS AND NEW STRATEGIES

The evidence that elimination of SnCs by genetic strategy can extend the healthspan in mice prompts a gold rush in the development of pharmaceutical small molecules that can selectively kill SnCs to combat aging and age-related conditions. As these molecules are called ‘senolytics’, whereas those that can suppress SASP production, named senomorphics. Both senolytics and senomorphics have the potential to prevent or treat age-related diseases and to extend healthspan. However, more efforts were made on developing senolytics compared to senomorphics considering that senolytics have more favorable drug exposure, toxicity and durable effects (He et al., 2020c).

Until now, several classes of senolytics have been developed, including naturally occurring compounds and their derivatives [e.g., quercetin (Zhu et al., 2015), fisetin (Yousefzadeh et al., 2018), piperlongumine (Wang et al., 2016), EF24 (Li et al., 2019a)], cardiac glycosides [e.g., ouabain (Guerrero et al., 2019), digoxin (Triana-Martínez et al., 2019)], and targeted therapeutics [dasatinib (Zhu et al., 2015), ABT263 (Chang et al., 2016), HSP90 inhibitor (Fuhrmann-Stroissnigg et al., 2017), and FOXO4-p53 interfering peptide (Baar et al., 2017)] (Table 1). We have previously reviewed the progresses on naturally occurring and targeted senolytics (Li et al., 2019b; Ge et al., 2021). It is very encouraging that several senolytics have been approved to enter clinical trials and shown benefits as therapeutics for aging or age-related diseases (Childs et al., 2017; Kirkland and Tchkonja, 2017, 2020; Campisi et al., 2019; Thoppil and Riabowol, 2019; Di Micco et al., 2021). Even though, current senolytics still have some limitations in terms of potency, safety, specificity, broad-spectrum activity, pharmacodynamics and pharmacokinetics. For example, one of the most widely used senolytics, i.e. the combination of dasatinib and quercetin (D + Q), was well tolerated and could

reduce SnC burden in patients (Thoppil and Riabowol, 2019; Kirkland and Tchkonja, 2020). However, quercetin is a polypharmacologic agent and its mechanisms of action have not been well defined. ABT263, a Bcl-2 and Bcl-xL dual inhibitor, has been extensively used as a potent and broad-spectrum senolytic agent (Chang et al., 2016). Its on-target toxicity of thrombocytopenia induced by Bcl-xL inhibition prevents its use in clinic even for tumor patients (Gandhi et al., 2011; Souers et al., 2013; Levenson et al., 2015; Ashkenazi et al., 2017). To overcome these challenges, some novel strategies, such as proteolysis-targeting chimera (PROTAC) technology (He et al., 2020b), chimeric antigen receptor (CAR) T cells (Amor et al., 2020), and  $\beta$ -galactosidase-modified prodrugs (Cai et al., 2020; Guerrero et al., 2020), have been developed to eliminate SnCs and shown promising therapeutic potential in the treatment of age-related diseases (Ge et al., 2021).

One major characteristic of SnCs is that they are resistant to apoptosis. This is attributable to the upregulation of certain proteins in the SCAPs, which enables SnCs to accumulate during aging. Most of the abovementioned senolytics were developed to selectively kill SnCs by targeting the known SCAPs. However, the transcriptional heterogeneity (Hernandez-Segura et al., 2017) and the diverse tissue origins of SnCs, render SnCs depend on different SCAPs to maintain their survival, which makes it a challenge to develop certain senolytics to eliminate SnCs in various cell types. For example, we found that ABT263 is very potent to selectively kill senescent human lung diploid fibroblasts (HDF) (Chang et al., 2016; He et al., 2020b), but it does not work in senescent HDF isolated from human foreskins (Cho et al., 2020), suggesting that HDF from different tissue origins may have different apoptotic resistance mechanisms. Therefore, gaining deep insights into the apoptosis-resistant proteins or pathways of SnCs may help to develop cell-specific or broad-spectrum senolytics to clear SnCs. In the following sections, we will focus on reviewing cell apoptosis and its significance in aging and



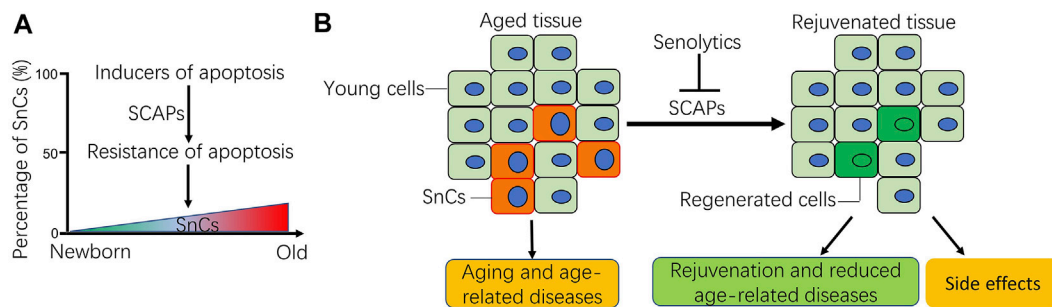


**FIGURE 1 |** Schematic of apoptotic resistance of senescent cells (SnCs) in aging and age-related diseases. **(A)** During the aging process, aging-related disruptions in systemic and inter-cell signaling, together with cell-autonomous damage and mitochondrial malfunction result in either increased or decreased cell apoptosis depending on cellular context (Tower, 2015). As for SnCs, their percentage usually increases in tissues with age as they acquire resistance to apoptotic stimuli via the SnC anti-apoptotic pathways (SCAPs). **(B)** Accumulation of SnCs in tissues contributes to aging and the occurrence of age-related diseases. Senolytics can selectively clear the SnCs by targeting the SCAPs, which promote the regeneration of young cells, rejuvenate aged tissues and reduce age-related diseases. Sometimes, senolytics can also cause side effects, more caution should be exercised for the systemic use of senolytics for health benefits. Note: **B** was modified from our previous publication (Li et al., 2019a; Li et al., 2019b).

age-related diseases, as well as summarizing the emerging proteins or pathways involved in apoptotic resistance of SnCs.

## THE SIGNIFICANCE OF APOPTOSIS IN AGING AND AGE-RELATED DISEASES

Apoptosis is defined as a programmed cell death, which has received a lot of attention because of its importance during tissue development (Wanner et al., 2020), and maintenance of tissue homeostasis (Elmore, 2007; Günther et al., 2013; Kile, 2014; Singh et al., 2019). Apoptosis occurs when cells undergo exogenous stimuli or intrinsic signals and is required to maintain the integrity and homeostasis of tissues, and dysregulation of which is implicated in the development of various diseases (Singh et al., 2019). For example, increased cellular apoptosis is known to contribute to age-related diseases in the brain (Mattson et al., 2001). Unlike cellular necrosis, a way of cell death resulting from acute cellular injury, apoptosis does not induce an inflammation response to cause a bystander effect.

Aging has been associated with decreased apoptosis in some cell types (Figure 1A), such as adipose mesenchymal stem cells (Alt et al., 2012), and bone marrow mesenchymal stem cells (Wilson et al., 2010). *In vivo*, it has been reported that apoptotic potential was dramatically reduced in the liver of aged rats challenged with a DNA-damaging agent (Suh et al., 2002). Similarly, apoptosis induced by radiation was significantly reduced in peripheral blood lymphocytes isolated from aged mice (Polyak et al., 1997). In humans, the peripheral blood mononuclear cells (PBMCs) from old people and centenarians showed an increased resistance to apoptosis induced by 2-deoxy-D-ribose (dRib), which may contribute to immunosenescence (Monti et al., 2000). Consistently, there is a reduction in the markers of apoptosis in human serum during aging (Kavathia et al., 2009). In a few cases, the apoptosis is increased in some cell types during aging. For example, there is a significant loss of cells in the thymus and bone marrow, associated with an increase in the number of apoptotic lymphocytes during the aging process

(Sainz et al., 2003). The discrepancy of apoptosis in different cell types during aging is likely due to the age-related disruptions in systemic and intracellular signaling combined with cell-autonomous effects (Tower, 2015). Because apoptosis is required for normal cell turnover and tissue homeostasis, dysregulation of apoptosis at old age is increasingly implicated in various age-related diseases, such as tumor (DePinho, 2000), and neurodegenerative diseases (Erekat, 2021). However, SnCs are highly resistant to apoptosis (Wang, 1995), likely enabling them accumulate during aging (Salminen et al., 2011), and age-related diseases (Kirkland and Tchkonja, 2017; Niedernhofer and Robbins, 2018; Thoppil and Riabowol, 2019; Di Micco et al., 2021; Ge et al., 2021). Thus, it is imperative to understand why SnCs are resistant to apoptosis. A better understanding of the underlying mechanisms for apoptotic resistance of SnCs is likely to provide novel molecular targets for the development of therapeutic senolytics to combat aging and age-related diseases (Figure 1B).

## APOPTOTIC RESISTANCE AND THE UNDERLYING MECHANISM IN SnCs

Since the first observation of apoptotic resistance in SnC human fibroblasts was reported in 1995 (Wang, 1995), the phenomenon was later found in a variety of cell types when they became senescent, including senescent immune cells (Spaulding et al., 1999), keratinocytes (KCs) (Chaturvedi et al., 2004), human endometrium-derived mesenchymal stem cells (MESC) (Burova et al., 2013) and hepatic stellate cells (HSC) (Kawada, 2006). There are various mechanisms that promote the survival of SnCs *in vitro* and *in vivo*, such as metabolic reprogramming, activation of unfolded protein response, and immune evasion (Soto-Gamez et al., 2019). In this review, we focus on the SCAPs, as most of the known senolytics were developed by targeting individual SCAPs (Figure 1B). Emerging SCAPs are reported along with the findings of SnC resistance to apoptosis in different cell types, providing new target candidates for developing either

**TABLE 2 |** Proteins implicated in the apoptotic resistance of senescent cells (SnCs).

Proteins	Cell type	Apoptotic stimuli	Type of Senescence	References
Bcl-2 family	Human lung fibroblast WI-38	Serum deprivation	Replicative senescence	Wang, (1995)
	Human diploid fibroblast from foreskin	H <sub>2</sub> O <sub>2</sub> , staurosporine, thapsigargin	Replicative senescence	Ryu et al. (2007)
	Human CD8 <sup>+</sup> T cells	Anti-CD3 mAb, anti-Fas mAb, IL-2 withdrawal, staurosporine, galectin-1, dexamethasone, mild heat shock	Replicative senescence	Spaulding et al. (1999)
	Human diploid fibroblast IMR-90	H <sub>2</sub> O <sub>2</sub>	Replicative senescence	Sanders et al. (2013)
	Human fibroblast WI-38, IMR-90 and human renal epithelial cells IMR-90, MEF	ABT263	IR induced senescence	Chang et al. (2016)
P53		TNF $\alpha$ +cycloheximide, UV	Etoposide induced senescence; Replicative senescence; Oncogene-induced senescence	Yosef et al. (2016)
	Cholangiocyte	TRAIL	LPS induced senescence	O'Hara et al. (2019)
	Human lung fibroblast WI-38	Actinomycin D, UV, etoposide, cisplatin	Replicative senescence	Seluanov et al. (2001)
	Foreskin derived fibroblast HCA2 and IMR-90	NA	Replicative senescence	Jackson and Pereira-Smith, (2006)
	Human skin fibroblast	UV	UV induced senescence	Chen et al. (2008)
Heat shock protein	Keratinocyte isolated from neonatal foreskin	UV	IFN plus TPA induced senescence	Chaturvedi et al. (2004)
	MEF	NA	Primary MEFs from <i>Ercc1</i> <sup>-/-</sup> mice	Fuhrmann-Stroissnigg et al. (2017)
	Keratinocyte isolated from neonatal foreskin	UV	Replicative senescence	Chaturvedi et al. (1999)
	Human primary foreskin fibroblast	UV	Replicative senescence; H <sub>2</sub> O <sub>2</sub> induced senescence	Yeo et al. (2000)
	Human diploid fibroblast from foreskin	H <sub>2</sub> O <sub>2</sub> , staurosporine, thapsigargin	Replicative senescence	Kim et al. (2011)
Insulin/IGF axis	Human diploid fibroblast from foreskin	Serum deprivation	Replicative senescence	Hampel et al. (2005)
	Human lung fibroblast WI-38	UV, staurosporine	Replicative senescence	Marcotte et al. (2004)
	Normal human skin fibroblast (HFSN1) and mouse embryonic fibroblast (MEF)	$\gamma$ -ray, Cisplatin, H <sub>2</sub> O <sub>2</sub> , UV	Replicative senescence	Al-Khalaf and Aboussekhra, (2013)
	HeLa and HCT116	Doxorubicin	Doxorubicin induced senescence	Ma et al. (2016)
	Gelsolin, FAK and MVP			
Gelsolin	Human diploid fibroblast from foreskin	Menadione	Replicative senescence	(Ahn et al., 2003a; 2003b)
	FAK	H <sub>2</sub> O <sub>2</sub> , staurosporine	Replicative senescence	Ryu et al. (2006)
	MVP	H <sub>2</sub> O <sub>2</sub> , staurosporine, thapsigargin	Replicative senescence	(Ryu et al., 2008; Ryu and Park, 2009)
Others	DcR2	Human diploid fibroblast IMR-90 and primary human hepatic myofibroblasts (activated HSCs)	Etoposide	Sagiv et al. (2013)
	GLS1	hHCA2, hIMR-90, hRPE-1, and mouse embryo fibroblast (MEF)	Nutlin3a, Doxorubicin, tert-butyl hydroperoxide, Replicative senescence	Johmura et al. (2021)
	SENEX	The human DLBCL (Diffuse large B-cell lymphoma) cell line OCI-LY8	Doxorubicin induced senescence	Wang et al. (2020)
	NA	Primary foreskin fibroblast	Replicative senescence	Hampel et al. (2004)
	NA	Human mesenchymal stem cells (hMESC)	H <sub>2</sub> O <sub>2</sub> induced senescence	Burova et al. (2013)
NA	Cells in aged liver	Methyl methanesulfonate	Naturally aged rats	Suh et al. (2002)

NA, not available.

cell-specific or broad-spectrum senolytics. In this section, we review the findings of SnC apoptotic resistance reported since 1995 and tempt to broaden the knowledge of SCAPs for the development of senolytics. The known proteins or pathways responsible for apoptotic resistance in SnCs are listed in **Table 2**.

## The Bcl-2 Family Members

The Bcl-2 family proteins, consisting of antiapoptotic and proapoptotic proteins, play critical roles in the regulation of apoptosis (Youle and Strasser, 2008). The Bcl-2 antiapoptotic proteins are multi-BH-domain proteins including Bcl-2, Bcl-xL,

Mcl-1, Bcl-w and Bfl1. They can inhibit apoptosis by binding to the multi-BH-domain and BH3-only proapoptotic proteins. Wang et al. first observed that aged human WI-38 cells were resistant to programmed cell death induced by serum deprivation. They found that the levels of Bcl-2 was undetectable in young WI-38 cells, but remained unchanged in senescent WI-38 cells after serum deprivation (Wang, 1995). This finding suggests that Bcl-2 might be primarily responsible for the resistance of cell death in senescent WI-38 cells. In HDF, several apoptotic stimuli such as  $H_2O_2$ , staurosporine and thapsigargin, can induce the downregulation of Bcl-2 and apoptosis in young cells but not in SnCs (Ryu et al., 2007). Spaulding et al. reported that replicative senescence in  $CD8^+$  T cells was associated with a significant increase in resistance to apoptosis, which was also associated with increased Bcl-2 expression (Spaulding et al., 1999). On the contrary, Bcl-2 was reduced in senescent HSC that were sensitive to TNF- $\alpha$ -induced cell death (Novo et al., 2006). Mechanistically, global and locus-specific histone modifications of chromatin regulate the gene expression of *Bcl-2* and *Bax* in senescent fibroblasts, which in turn may mediate the resistance of apoptosis in SnCs (Sanders et al., 2013).

In contrast, Sasaki et al. observed the apoptotic resistance in several cell lines (human foreskin fibroblast strain HCA2, human fetal lung fibroblast strains TIG-1, TIG-3 and WI-38) when they became senescent (Sasaki et al., 2001). However, in these SnCs the Bcl-2 family members were not responsible for the resistance to apoptosis. Instead, they attributed the resistance to cell cycle arrest (Sasaki et al., 2001). Different from above findings, we and others demonstrated that Bcl-xL is primarily responsible for SnC resistance to apoptosis as inhibition of Bcl-xL with a Bcl-xL specific inhibitor (such as A-1331852 and A1155463) (Zhu et al., 2017) or a Bcl-2 and Bcl-xL dual inhibitor (such as ABT263 and ABT737) can effectively induce apoptosis in a variety of SnCs (Rochette and Brash, 2008; Chang et al., 2016; Yosef et al., 2016; Zhu et al., 2016; Baar et al., 2017; Zhu et al., 2017; He et al., 2020b), whereas inhibition of Bcl-2 alone with its specific inhibitor has no or weak effect on SnC survival (Chang et al., 2016; Yosef et al., 2016; He et al., 2020b). The induction of Bcl-xL in SnC and its role in mediating apoptotic resistance is likely regulated by the transcription factor ETS protooncogene 1 (ETS1) (O'Hara et al., 2019). Although ABT263 is one of the most potent and broad-spectrum senolytics identified to date (Zhu et al., 2015, 2017; Chang et al., 2016), Bcl-xL inhibition with ABT263 or other small molecular inhibitors induces platelet apoptosis and results in severe thrombocytopenia, which prevents their use in the clinic—even for tumor patients (Gandhi et al., 2011; Souers et al., 2013; Levenson et al., 2015; Ashkenazi et al., 2017). We have successfully used the PROTAC technology to overcome the on-target drug toxicity, and improved the senolytic activity of ABT263 (He et al., 2020b). As one of the most important Bcl-2 family members, Mcl-1 plays critical roles in suppressing apoptosis in tumor cells (Ramsey et al., 2018; Mukherjee et al., 2020; Seiller et al., 2020), which however may not affect the survival of SnCs, as inhibition of Mcl-1 with its specific inhibitor did not cause cell death in SnCs (Chang et al., 2016; He et al., 2020b). Of note is that Mcl-1 expression varies in SnCs induced

by different stress-stimulus (Yosef et al., 2016), and it is a highly regulated protein with a short half life (Michels et al., 2005), implying that Mcl-1 may circumvent the inhibition of Bcl-2 or Bcl-xL and help SnCs to acquire apoptotic resistance. In sum, Bcl-2 family members are implicated in the apoptotic resistance of SnCs, but their expression levels and roles differ depending on cell types and senescence inducers.

## The p53 Pathway

p53 is a well-known tumor suppressor that acts as a double-edged sword in the regulation of cellular senescence, aging, and tumor (Johmura and Nakanishi, 2016; Wu and Prives, 2018). The host defense function of p53 in protecting tissues against tumor growth via induction of apoptosis and cellular senescence has been widely studied in tumors. The p53 levels and activities increase when cells enter a presenescent state upon activation of the DNA damage response (DDR), triggering the initiation of cellular senescence (Hernandez-Segura et al., 2018). p53 can promote apoptosis through transcription-dependent and -independent mechanisms (Fridman and Lowe, 2003). The transcriptional pathway involves the induction of pro-apoptotic Bcl-2 family members (i.e., Bax, Bid, Noxa, and Puma), and repression of anti-apoptotic proteins (i.e., Bcl-2, Bcl-xL, and survivin). The non-transcriptional regulation of apoptosis by p53 includes its direct interaction with members of the Bcl-2 family anti-apoptotic proteins to control mitochondrial outer membrane permeabilization (MOMP) (Fridman and Lowe, 2003).

The role of p53 in regulating apoptotic resistance in SnCs has been reported in multiple cell types. Seluanov et al. studied the responses of cultured young and old WI-38 to a variety of genotoxic stresses and found that young cells were able to undergo p53-dependent and p53-independent apoptosis. In contrast, senescent fibroblasts were unable to undergo p53-dependent apoptosis. They concluded that stabilization of p53 in response to DNA damage is impaired in old fibroblasts, resulting in the resistance to apoptotic stimuli (Seluanov et al., 2001). Gansauge et al. also observed the same phenomenon in the same cell line (Gansauge et al., 1997). Similar findings were reported in senescent KCs (Chaturvedi et al., 2004), human skin fibroblasts (Chen et al., 2008) and HCA2 cells (Jackson and Pereira-Smith, 2006). The cellular levels of p53 usually increase in response to DNA damage stimuli. However, the increased levels of p53 subside when cells become fully senescent. This phenomenon was observed in senescent KCs (Kim et al., 2015), human fibroblast cell lines (Sisoula et al., 2011; Johmura and Nakanishi, 2016), human prostate epithelial and uroepithelial cells (Schwarze et al., 2001). The downregulation of p53 levels in SnCs may be attributable to the upregulation of C-terminus of Hsp70-interacting protein (CHIP) (Sisoula et al., 2011) and SCFFbxo22 (Johmura et al., 2016) E3 ligases, which promote p53 degradation through the ubiquitination-proteasome system. The reduction of p53 in SnCs may protect them from apoptosis and cause the accumulation of SnCs and higher prevalence of tumor during aging, which agrees with the finding that p53 activity was reduced along with accumulation of SnCs in aged

tissues (Feng et al., 2007; Baker et al., 2016). Therefore, restoration of p53 activity has the potential to eliminate SnCs by inducing apoptosis. Baar et al. designed a peptide (termed as proxofim peptide) comprising part of the p53-interaction domain in FOXO4, which selectively induced p53 nuclear exclusion and cell-intrinsic apoptosis in SnCs (Baar et al., 2017; Zhang et al., 2020). However, there remain challenges using a peptide as a therapeutic. Inhibiting the interaction between MDM2 and p53 can also increase p53 stability and activity (Moll and Petrenko, 2003). UBX0101, an inhibitor of MDM2, has been shown to selectively kill SnCs in culture and treat post-traumatic osteoarthritis *in vivo* (Jeon et al., 2017). Nevertheless, UBX0101 was failed for the treatment of osteoarthritis in patients in a phase II clinical trial (Lane et al., 2021). We have previously reported that the ubiquitin-specific peptidase 7 (USP7) may be a novel target for senolysis as inhibition of USP7 can selectively induce apoptosis of SnCs by increasing the level of p53 (He et al., 2020a). However, USP7 is widely expressed in many tissues and has multiple substrates with different physiological functions (Zhou et al., 2018; Pozhidaeva and Bezsonova, 2019). It has yet to be determined whether USP7 can be safely used to clear SnCs without causing significant side effects.

## Heat Shock Proteins

Heat shock proteins (HSPs) are evolutionarily conserved proteins whose expression is induced by different kinds of stresses (Jäättelä, 1999; Jegu et al., 2013). They are involved in protein folding and maturation of various proteins and play an important role in regulation of cellular response to homeostatic challenges (Chatterjee and Burns, 2017). HSPs regulate protein assembly, secretion, transportation, translocation, and protein degradation. According to their molecular sizes, HSPs are grouped into six families, including HSP27, HSP40, HSP60, HSP70, HSP90 families, and the family of large HSPs (HSP110 and glucose-regulated protein 170, GRP170) (Chatterjee and Burns, 2017). When cells are subjected to stress, they can undergo either senescence or cell death and HSPs are involved in both two responses (Takayama et al., 2003; He et al., 2019; Srivastava et al., 2019; Kanugovi et al., 2020; Omer et al., 2020; Kanugovi Vijayavittal and Amere Subbarao, 2021). The role of HSPs in regulating cell apoptosis has been well reviewed elsewhere (Takayama et al., 2003; Lanneau et al., 2008). As the expression/activity of HSPs is significantly higher in tumors and responsive to different death stimuli (Jegu et al., 2013), inhibition of HSPs has emerged as a novel therapeutic strategy for tumor therapy (Chatterjee and Burns, 2017).

Among the HSP families, HSP90 has been implicated as an anti-apoptotic and pro-survival factor in SnCs, and the inhibitor of HSP90 was identified as a new class of senolytic (Fuhrmann-Stroissnigg et al., 2017, 2018). Inhibition of HSP90 by its inhibitors, such as 17-DMAG, can sufficiently reduce the level of phosphorylated AKT and selectively induce apoptosis in SnCs (Fuhrmann-Stroissnigg et al., 2017, 2018). However, most of the known HSP90 inhibitors may have limited usage as senolytics because they can cause some dose-limiting toxicities and have

poor pharmacokinetic profiles (Sanchez et al., 2020). These limitations may preclude their clinical use as an anti-aging agent as older people are more susceptible to adverse drug effects than younger individuals (He et al., 2020c).

## The Autophagy-Lysosomal Pathway

Autophagy is an evolutionarily conserved process in eukaryotic cells, which is involved in scavenging and recycling senescent or damaged organelles and biological macromolecules by lysosomal degradation to maintain cellular homeostasis. Autophagy can be a physiologically or pathologically relevant program depending on the specific situation. In normal situations, autophagy can be induced by physiological signals such as starvation, to facilitate cell survival (Giampieri et al., 2019). Caloric restriction (CR) is one of the most important inducers of autophagy, leading to an increase of lifespan and delaying the onset of age-related diseases (Bergamini et al., 2007). Nevertheless, excessive autophagy is detrimental and results in “autophagic cell death” that describes a form of programmed cell death morphologically distinct from apoptosis. In autophagic programmed cell death, there is early degradation of organelles but preservation of cytoskeletal elements until late stages (Levine and Yuan, 2005). Different from necrosis, both apoptotic and autophagic cell death are characterized by the lack of a tissue inflammatory response. Autophagy have been linked to aging and various pathological conditions (Green et al., 2011; Giampieri et al., 2019), and thus it has become a major target for drug discovery and development (Kroemer, 2015; Leidal et al., 2018). However, as autophagy can act as both a cell survival and death mechanism, it is challenging to selectively turn on or turn off autophagic survival and death pathways in the treatment of autophagy-related diseases (Levine and Yuan, 2005). Beyond the abovementioned roles, autophagy has been shown to influence cellular immune responses (Ma et al., 2013). Particularly, autophagy can influence the antigenic profile of antigen-donor cells (ADCs) and their ability to release immunogenic signals (Michaud et al., 2011), as well as the survival, differentiation, and function of antigen-presenting cells (APCs) and T lymphocytes (Pua et al., 2007; Jia and He, 2011; Wildenberg et al., 2012; Fiegl et al., 2013). Autophagic responses in ADCs can enhance the release of “find-me” and “eat me” signals, which attract APC progenitors and facilitate antigen uptake, respectively (Ma et al., 2013). Theoretically, the autophagy-enhanced cellular immune responses may facilitate the immune system to recognize and eliminate SnCs, which has yet to be validated. The relationship between autophagy and cellular senescence is inconclusive (Gewirtz, 2013). Some studies suggest that autophagy is activated during senescence and inhibition of autophagy delays the senescence phenotype (Young et al., 2009; Gewirtz, 2013; Zhang et al., 2017), whereas increasing evidence reveals a negative correlation between them (Kang et al., 2011; Tai et al., 2017). For example, rapamycin, a mammalian target of rapamycin complex 1 (mTOR1) inhibitor and an autophagy activator, can efficiently suppress cellular senescence (Demidenko et al., 2009; Tai et al., 2017), and extend the life span of mice (Harrison et al., 2009). Fenofibrate (FN), a PPAR $\alpha$  agonist used for dyslipidemia in humans, was reported to protect against cartilage degradation



by reducing the number of senescent chondrocytes via inducing apoptosis in combination with increasing autophagic flux (Nogueira-Recalde et al., 2019). In addition, a BET family protein degrader was shown to provoke senolysis by targeting the attenuation of nonhomologous end joining (NHEJ) and autophagy in SnCs (Wakita et al., 2020). Lysosomes are degradative organelles essential for cell homeostasis that regulate various biological processes (Gómez-Sintes et al., 2016). Senescence-associated beta-galactosidase (SA-beta-gal) is the most common marker of lysosomal activity and one of the first tests used to determine senescence (Lee et al., 2006). Enhanced lysosomal activity can protect cells from oxidative stresses (Chakraborty et al., 2019; Nagakannan et al., 2020; Li et al., 2021), likely contributing to the resistance of apoptosis in SnCs. However, different forms of stress can induce lysosomal membrane permeabilization (LMP), leading to the translocation to the cytoplasm of intralysosomal components, such as cathepsins, inducing lysosomal-dependent cell death (LDCD) (Wang et al., 2018). Accumulating evidence indicate that aging significantly influences lysosomal activity by altering the physical and chemical properties of lysosomes (Gómez-Sintes et al., 2016). Most cells display an age-associated increase in lysosome number and size. The intracellular pH in SnCs was lowered by lysosomal membrane damage, but SnCs can resist the lowered pH by producing ammonia *via* glutaminolysis, which can neutralize the lower pH (Johmura et al., 2021). On the contrary, it was reported that lysosomes exhibited higher pH in aged animals than young mice (Liu et al., 2008). Lysosomal reacidification by inhibiting the ataxia telangiectasia mutated (ATM) induced functional recovery of the lysosome, which led to alleviated cellular senescence by accelerating the removal of dysfunctional mitochondria and recovering the mitochondrial function (Kang et al., 2017). Taken together, the autophagy-lysosomal pathway plays critical roles in maintaining cellular homeostasis, targeting the proteins in the pathway have become an attractive anti-aging strategy by either suppressing senescence or inducing apoptosis of SnCs.

## Epigenetic Regulation

Alterations in the methylation of DNA or post-translational modification of histones, and other chromatin-associated proteins, can induce epigenetic changes that contribute to the aging process (López-Otín et al., 2013). We and others have previously reviewed the effects of DNA methylation on aging and longevity (Xiao et al., 2016; Sidler et al., 2017; Kane and Sinclair, 2019; Morris et al., 2019). Likewise, epigenetic changes have significant impact on the senescence phenotypes, notably the proliferative arrest and SASP (Nacarelli et al., 2017). For example, the INK4-ARF locus encodes proteins that drive cell growth arrest, and the polycomb group (PcG) proteins can epigenetically regulate the INK4-ARF locus, as well as catalyze histone modifications that promote changes in chromatin structure, leading to transcriptional repression (Simboeck et al., 2011). SIRT1, an NAD<sup>+</sup>-dependent protein deacetylase, suppresses the SASP through epigenetic gene regulation (Hayakawa et al., 2015; Hekmatimoghaddam et al., 2017). Besides the impacts on cellular senescence and SASP, epigenetic mechanisms are

involved in the apoptotic resistance in SnCs. CpG nucleotide-rich regions in mammalian genomes are called CpG islands, which reside in very close proximity to gene promoters (Fatemi et al., 2005). In tumor cells, CpG islands at proapoptotic gene promoters are mostly hypermethylated due to methyltransferase (DNMT) overexpression (Roll et al., 2008). Hypermethylation blocks both intrinsic and extrinsic apoptosis by modulating the expression of major players of cell death cascade, as previously reviewed elsewhere (Elmallah and Micheau, 2019; Ozyerli-Goknar and Bagci-Onder, 2021). However, the expression of DNMT was found to be downregulated in SnCs although they harbour some features of the tumor epigenome (Cruickshanks et al., 2013). Thus, whether DNA methylation contributes to the apoptotic resistance in SnCs has yet to be investigated. In contrast, there is evidence showing that histone modification may affect the sensitivity of SnCs to cell death stimuli. Sanders et al. revealed that both global and locus-specific histone modifications of chromatin regulated altered Bcl-2:Bax gene expression in senescent fibroblasts, contributing to its apoptosis-resistant phenotype (Sanders et al., 2013). The heterochromatinization that surrounds and borders double-strand breaks (DSBs) enhances the pro-survival responses in SnCs, as evidenced by that HDAC inhibition triggered apoptosis (Di Micco et al., 2006; Paluvai et al., 2020). Panobinostat, an FDA-approved histone deacetylase inhibitor, was found to be a post-chemotherapy senolytic agent with the potential to kill persistent SnCs in non-small cell lung cancer (NSCLC) and head and neck squamous cell carcinoma (HNSCC) (Samaraweera et al., 2017). However, our preliminary data show that panobinostat was toxic to normal cells (data now shown). Therefore, whether the histone deacetylase inhibitors can be anti-aging senolytic targets has yet to be investigated.

## The MAPK-NF-κB Axis

The nuclear factor κB (NF-κB) is a transcription factor complex consisting of homo- and heterodimers of five members of the Rel family including RelA (p65), RelB, c-Rel, NF-κB1 (p50/p105), and NF-κB2 (p52/p100). The NF-κB pathway transcriptionally controls a large set of target genes that play important roles in cell survival, inflammation, and immune responses (Hayden and Ghosh, 2008). Previous studies have correlated NF-κB signaling with cellular senescence. For example, indoxyl sulfate can induce cellular senescence via activation of the ROS-NF-κB-p53 pathway in proximal tubular cells (Shimizu et al., 2011). It has been well known that various DNA damage stimuli can activate NF-κB signaling, which stimulates the production of SASP in SnCs (Salminen et al., 2012), and regulates expression of genes that regulate apoptosis, cell cycle progression, and inflammation. Recently, we reported that SnCs not only expressed higher basal levels of various inflammatory cytokines and chemokines as a manifestation of the SASP, but also exhibited hyper-activation for the induction of a variety of inflammatory mediators in response to LPS, IL1β and TNFα stimulation (Budamagunta et al., 2021). This senescence-associated hyper-activation is mediated in part via the NF-κB pathway (Budamagunta et al., 2021). More importantly, NF-κB plays a crucial role in the induction of tumor resistance to

apoptosis (Mortezaee et al., 2019). We previously reported that the curcumin analog EF24, a new senolytic which can downregulate anti-apoptotic family proteins, likely via the proteasome degradation of the Bcl-2 as the proteasome inhibitor MG132 partially prevented the degradation effect of EF24 (Li et al., 2019a). EF24 is also an anti-tumor agent that can kill melanoma cells effectively via downregulating the expression of Bcl-2 and IAP by inhibiting the NF- $\kappa$ B signaling (He et al., 2021). In an early study, senescent KCs were found to be resistant to apoptosis, which was associated with the anti-apoptotic role of NF- $\kappa$ B (Chaturvedi et al., 1999). NF- $\kappa$ B is upregulated in a variety of tissues with aging, and the inhibition of NF- $\kappa$ B has been shown to delay the onset of aging-related symptoms and pathologies such as diabetes, atherosclerosis, and tumor (Kanigur Sultuybek et al., 2019). Metformin is an anti-diabetic medication in type 2 diabetes (T2DM) (Dunn and Peters, 1995), and it has become a therapeutic candidate in the improvement of ageing and aging-related diseases (Hu et al., 2021). One of the major roles of metformin is to inhibit the NF- $\kappa$ B pathway, by which it reduce the susceptibility to age-related diseases (Kanigur Sultuybek et al., 2019). Many naturally-occurring compounds were reported to have anti-aging effects, either via triggering the apoptosis of SnCs (such as quercetin, fisetin, piperlongumine) (Li et al., 2019b), or inhibiting production of SASP via suppressing the NF- $\kappa$ B pathway (such as apigenin) (Lim et al., 2015; Perrott et al., 2017). In addition, some small chemical inhibitors of NF- $\kappa$ B, such as BAY 11-7082 (Pierce et al., 1997), also show good activity in reducing the expression of inflammatory cytokines (Lappas et al., 2005; Juliana et al., 2010; Zang et al., 2017), and protecting organs from oxidative injury (Kim et al., 2010; Kolati et al., 2015). However, more deep studies are needed to test whether NF- $\kappa$ B inhibitors could be safe anti-aging agents in the future.

The mitogen-activated protein kinase (MAPK) family can act as an upstream of the NF- $\kappa$ B pathway. MAP kinases are grouped into three families: stress-activated protein kinases (p38/SAPKs), Jun amino-terminal kinases (JNKs), and extracellular-signal-regulated kinases (ERKs). In cellular senescence, p38 induces the expression of the SASP largely by increasing NF- $\kappa$ B transcriptional activity (Freund et al., 2011; Budamagunta et al., 2021). JNKs play important roles in acquiring the resistance of senescent human fibroblasts to UV-induced DNA fragmentation (Yeo et al., 2000). In addition, ERK and p38 are also involved in the apoptotic resistance in SnCs (Kim et al., 2011). Kim et al. revealed that the nuclear translocation of activated ERK or p38 was implicated in the transduction of death signals, and that a decrease in nucleocytoplasmic trafficking of these proteins in SnCs caused the senescence-associated resistance to apoptosis (Kim et al., 2011). In conclusion, the MAPK-NF- $\kappa$ B axis plays important roles in mediating apoptotic resistance as well as modulating the production of various inflammatory cytokines in SnCs.

## The Insulin/IGF Axis

The insulin/IGF signaling pathway plays a major role in determining the rate of aging in many species (Gems and Partridge, 2001; Cheng et al., 2005), which is an evolutionarily conserved mechanism from yeast to humans

(Barbieri et al., 2003). In higher eukaryotes, signal transduction through the IGF pathway is modulated by IGF-binding protein (IGFBPs) family, among which IGFBP-3 regulates proliferation and survival in many mammalian cell types (Firth and Baxter, 2002). Moreover, another IGF protein IGFBP-7 can also induce cellular senescence and apoptosis through autocrine/paracrine pathways in melanocytes (Wajapeyee et al., 2008). However, why SnCs secrete IGF proteins but can resist their pro-apoptotic effect is not known at the present. Hampel et al. found that IGFBP-3 accumulated in conditioned medium of senescent human fibroblasts, which may contribute to growth arrest of these cells. As IGFBP-3 can enhance apoptosis by activating intracellular regulators of apoptosis, whereas IGFBP-3 cannot be endocytosed by SnCs, which may contribute to the well-established apoptotic resistance of senescent human fibroblasts (Hampel et al., 2005). Further we also have previously reported that IGFBP-3 gene polymorphism rs11977526 with longevity in Chinese (He et al., 2014). These findings suggest that the insulin/IGF axis is an important determinant of aging, and acts as a mechanism by which SnCs acquire resistance to apoptosis.

## Caspase-3

Caspases are a family of endoproteases that provide critical links in cell regulatory networks controlling inflammation and cell death. They are inactive until being cleaved at specific aspartate residues (McIlwain et al., 2013). Wang's group reported the first observation of apoptotic resistance in senescent fibroblasts in 1995 (Wang, 1995). A few years later, they found that caspase-3 gene expression level was decreased in human senescent fibroblasts (WI-38) and could not be activated by UV or staurosporine treatment. They concluded that the resistance to apoptotic death seen in senescent fibroblasts was not simply due to increased Bcl-2 levels, but also attributable to a lack of caspase activity (Marcotte et al., 2004). However, in some cell types, cell death seems to be independent of caspase activity, such as in HDF isolated from skin, given that the treatment of HDF did not trigger the cleavage of caspase-3 or poly (ADP-ribose) polymerase (PARP) (Ryu et al., 2006).

## Survivin

Survivin is an important anti-apoptotic protein. It is highly expressed in most tumors, which is also generally arised in cells of older individuals (Unruhe et al., 2016). Al-Khalaf et al. found that survivin and phospho-survivin were accumulated in aged normal human skin fibroblasts and mice organs, which may be attributable to HSP90-mediated stabilization of survivin. Inhibition of survivin by flavopiridol or shRNAs increased the apoptotic response of old fibroblasts to various genotoxic agents by restoring the pro-apoptotic Bax/Bcl-2 ratio and increasing the levels of cleaved caspase-3 and PARP (Al-Khalaf and Aboussekhra, 2013). Another study indicated that nuclear accumulation of Yes-associated protein (YAP) could promote the survival of senescent tumor cells by increasing the expression of survivin (Ma et al., 2016).

Whether survivin can be a significant senolytic target has yet to be determined.

## Gelsolin, FAK and MVP

Park's group showed that the protein and mRNA levels of gelsolin, a  $\text{Ca}^{2+}$ -dependent actin regulatory protein, were increased in senescent HDF. Downregulation of gelsolin in senescent HDF resulted in increased sensitivity to menadione-induced apoptotic cell death (Ahn et al., 2003b; 2003a). The effect of gelsolin in mediating apoptotic resistance of SnCs was independent of Bcl-2 (Ahn et al., 2003a). Later, they reported that the focal adhesion kinase (FAK) might differently regulate apoptosis and focal adhesion formation in SnCs (Ryu et al., 2006). Furthermore, they identified a novel senolytic drug R406 that showed selective toxicity in HDF by inhibiting FAK and p38MAPK activity (Cho et al., 2020). They also found that the major vault protein (MVP) was markedly increased in senescent HDF as well as in aged organs, downregulation of MVP increased the sensitivity of senescent HDF to apoptosis by modulation of Bcl-2 expression (Ryu et al., 2008). MVP was a transcriptional target of p53 (An et al., 2009), being a potential therapeutic target for modulation of resistance to apoptosis (Ryu and Park, 2009). These new proteins involved in resistance to apoptosis expanded the scope of existed SCAPs, which have great potential to be senolytic targets.

## The Extrinsic Apoptosis Pathway

The extrinsic apoptosis pathway is triggered by the binding of death ligands to their appropriate death receptors (DRs) on the cell surface (Sayers, 2011). The best-described death ligands belong to the TNF family of proteins, comprising TNF, FasL, and TRAIL, which are predominantly produced by immune cells such as T cells, NK cells, NKT cells, macrophages, and dendritic cells. The DRs include TNF receptor 1 (TNFR1), CD95 (Fas), and TNF-related apoptosis inducing ligand-receptor (Ashkenazi, 2008; Sayers, 2011; Nair et al., 2014). Upon ligand binding, DRs trimerizes and recruits specialized adaptor proteins via their death domain (DD), such as Fas-associated death domain (FADD), which transmits the death signal from the cell surface to the intracellular signaling pathways. In turn, DD can recruit pro-caspase-8 and form a death-inducing signaling complex (DISC) capable of activating inducer caspases-8, which are then processed into its mature form. The mature caspases-8 subsequently activates downstream effector caspases such as caspase-3, and trigger apoptosis. DRs-mediated apoptosis can be inhibited by a protein called c-FLIP which can bind to DD and caspase-8, rendering them ineffective (French and Tschopp, 1999). In addition, decoy receptors (DcRs) have similar extracellular structure to DRs but lack an intracellular death domain, which can bind the ligand but cannot transmit death signals (Ashkenazi, 2002). Therefore, both c-FLIP and DcRs act as inhibitory mechanisms of extrinsic apoptosis. The expression of c-FLIP was reported to decline with age in normal thymus, and negatively associated with the levels of senescence markers in primary thymic epithelial cells, suggesting that cFLIP may not play a role in the apoptotic resistance of SnCs (Belharazem et al., 2017). Nevertheless, the expression of cFLIP was downregulated by senescence-secreted SASP via an activation of the Myc oncogene,

which can sensitize pretransformed cells to TRAIL-induced apoptosis (Vjetrovic et al., 2014). These findings suggest that SnCs may not depend on cFLIP for survival, instead they may regulate cFLIP to prime pretransformed cells to undergo apoptosis. DcR2 (TNFRSF10D) have been shown to be upregulated in SnCs (Sagiv et al., 2013), which represents as a marker of cellular senescence (Chen et al., 2017). DcR2 may in part account for the resistance of SnCs to apoptosis, as suggested by that TRAIL induced twofold more killing in senescent IMR-90 cells with DcR2 silencing compared with the control (Sagiv et al., 2013). Similarly, DcR1 (TNFRSF10C) was also observed to be upregulated in SnCs and was viewed as a senescence marker (Shah et al., 2013; Wiley et al., 2017). As DcRs act as competitive inhibitors of death receptor signaling by death ligands (such as Fas or TRAIL), it is feasible to use the specific antibody of DcRs to enhance the killing effect of immune cells (such as NK cells) on SnCs. In addition, we can take advantage of the CAR-T strategy (Amor et al., 2020) to establish DcR-sepecific CAR T cells to kill SnCs as will be discussed later.

## Surface Molecules and Immunosurveillance for Senolysis

Emerging molecules or proteins specifically present on the surface of SnCs have been discovered, which may play roles in the maintenance and survival of SnCs, targeting of which have been a novel senolytic strategy recently (Rossi and Abdelmohsen, 2021). The surface molecules have been shown to have a major role in the recognition and clearance of SnCs by the immune system. For example, SnCs express ligands for the NKG2D receptor of NK cells including MICA/B and ULBP2, which may drive the recognition and elimination of SnCs by NK-mediated cytotoxicity (Sagiv et al., 2016; Muñoz et al., 2019). SnCs express non-classical MHC molecule HLA-E, which interacts with the inhibitory receptor NKG2A of NK cells and highly differentiated  $\text{CD8}^+$  T cells to inhibit immune responses against SnCs. Accordingly, blocking the interaction between HLA-E and NKG2A boosts immune responses against SnCs (Pereira et al., 2019). Proteomics analysis identified dipeptidyl peptidase 4 (DPP4) as a novel protein marker on the surface of SnCs, targeting of which sensitized SnCs, but not dividing fibroblasts to cytotoxicity by natural killer cells (Kim et al., 2017). Amor et al. identified the urokinase-type plasminogen activator receptor (uPAR) as a cell-surface protein that is upregulated in SnCs *in vitro* and *in vivo* (Amor et al., 2020). They established uPAR-specific chimeric antigen receptor (CAR) T cells (CAR-T) to selectively clear SnCs, which extended the survival of mice with lung adenocarcinoma that were treated with MEK and CDK4/6 inhibitors to induce senescence, ameliorated liver fibrosis and improved liver function by clearing senescent hepatic stellate cells (Amor et al., 2020). In addition, Althubiti et al. have screened a series of the plasma membrane-associated proteins preferentially expressed on the surface of SnCs (Althubiti et al., 2014). The surface molecules and their implications in senolysis have been systematically summarized and reviewed (Rossi and Abdelmohsen, 2021). However, there are still some safety concerns on the use of immune system to eliminate SnCs.

Although the surface molecules are highly expressed in SnCs, they can be expressed in proliferating cells, albeit at low levels, leading to side effects (Ravichandra et al., 2021). More researches are needed to verify the senolytic effect and evaluate the safety of immune clearance of SnCs.

## CONCLUSIONS AND PERSPECTIVES

Aging represents a progressive decline in the physiological properties of tissues/organs and the overall fitness of the organism. SnCs accumulate with age and play a casual role in aging as well as age-related pathologies. One major characteristic of SnCs is their ability to resist apoptosis induced by different stimuli. For normal cells, increased resistance is an important safety mechanism against acute stress to maintain homeostasis. However, for SnCs, apoptotic resistance can lead to abnormal accumulation, which is detrimental to the organism. Senolytics and other novel strategies (PROTAC,  $\beta$ -galactosidase-modified prodrugs and CAR-T cells) were developed to selectively target SnCs and have shown great potential to delay aging and to treat age-related diseases. It is encouraging to know that several senolytics have been approved for clinical trial and have shown beneficial effects (Niedernhofer and Robbins, 2018; Thoppil and Riabowol, 2019; Kirkland and Tchkonja, 2020). The latest findings that senolytics can be used to prevent or treat virus infection-associated diseases, such as COVID-19 infection, expanding the applications of senolytics in clinic. Most of the current senolytics are discovered by targeting the SCAPs. However, the major challenge in developing senolytics is the high heterogeneity of SnCs, and their diverse origins. SnCs can resist apoptosis via different mechanisms depending on cell type and apoptotic stimuli. In this review, we systematically summarized the proteins or pathways involved in the apoptotic resistance of SnCs, which are not independent but rather interconnected. Inhibitors targeting some of the proteins or pathways have been developed as novel senolytics. However, whether the rest ones are senolytic targets has yet to be investigated. We believe that understanding of the

underlying mechanisms for apoptotic resistance of SnCs can help to identify more targets that can be used to develop cell-specific or broad-spectrum therapeutic senolytics to clear SnCs. It should be noted that clearance of SnCs can cause undesirable side effects. For example, continuous or acute elimination of SnCs disrupted blood-tissue barriers with subsequent liver and perivascular tissue fibrosis and health deterioration (Grosse et al., 2020). More caution should be exercised for the systemic use of senolytics for health benefits (Figure 1B). We expect to witness more discoveries in novel and safe senolytics for the use as an intervention to treat SnC-related diseases in the near future.

## AUTHOR CONTRIBUTIONS

Conceptualization: YH and YZ; Writing-Original Draft Preparation: YH, LH, and HL; Writing-Review and Editing: YH, WL, JL, YY, DZ, and Q-PK; Literature collection: YH, HL, and LH.

## FUNDING

This study was supported jointly and equally by grants from the National Key R&D Program of China (2018YFC2000400, 2018YFE0203700). Additional support was received from the Key Research Program (KFZD-SW-221), Key Research Program of Frontiers Science (QYZDB-SSW-SMC020), and Strategic Priority Research Program (XDPB17) of the Chinese Academy of Sciences, the National Natural Science Foundation of China (82171558, 31760310), the Basic Research Projects of Yunnan Province (202101AS070137, 202101BA070001-110), and the Key Research and Development Project of Hainan Province (ZDYF2021SHFZ227).

## ACKNOWLEDGMENTS

The authors would like to thank the members of the He laboratory for their thoughtful discussion and assistance and Zia Ur Rahman from Kong laboratory for editorial assistance.

## REFERENCES

- Aguayo-Mazzucato, C., Andle, J., Lee, T. B., Midha, A., Talemal, L., Chipashvili, V., et al. (2019). Acceleration of  $\beta$  Cell Aging Determines Diabetes and Senolysis Improves Disease Outcomes. *Cel Metab.* 30, 129–142. doi:10.1016/j.cmet.2019.05.006
- Ahn, J. S., Jang, I.-S., Kim, D.-I., Cho, K. A., Park, Y. H., Kim, K., et al. (2003a). Aging-associated Increase of Gelsolin for Apoptosis Resistance. *Biochem. Biophysical Res. Commun.* 312, 1335–1341. doi:10.1016/j.bbrc.2003.11.061
- Ahn, J. S., Jang, I.-S., Rhim, J. H., Kim, K., Yeo, E.-J., and Park, S. C. (2003b). Gelsolin for Senescence-Associated Resistance to Apoptosis. *Ann. N. Y. Acad. Sci.* 1010, 493–495. doi:10.1196/annals.1299.090
- Al-Khalaf, H. H., and Aboussekhr, A. (2013). Survivin Expression Increases during Aging and Enhances the Resistance of Aged Human Fibroblasts to Genotoxic Stress. *Age* 35, 549–562. doi:10.1007/s11357-011-9378-2
- Alimirah, F., Pulido, T., Valdovinos, A., Alptekin, S., Chang, E., Jones, E., et al. (2020). Cellular Senescence Promotes Skin Carcinogenesis through p38MAPK and p44/42MAPK Signaling. *Cancer Res.* 80, 3606–3619. doi:10.1158/0008-5472.CAN-20-0108
- Alt, E. U., Senst, C., Murthy, S. N., Slakey, D. P., Dupin, C. L., Chaffin, A. E., et al. (2012). Aging Alters Tissue Resident Mesenchymal Stem Cell Properties. *Stem Cell Res.* 8, 215–225. doi:10.1016/j.scr.2011.11.002
- Althubiti, M., Lezina, L., Carrera, S., Jukes-Jones, R., Giblett, S. M., Antonov, A., et al. (2014). Characterization of Novel Markers of Senescence and Their Prognostic Potential in Cancer. *Cell Death Dis* 5, e1528. doi:10.1038/cddis.2014.489
- Amor, C., Feucht, J., Leibold, J., Ho, Y.-J., Zhu, C., Alonso-Curbelo, D., et al. (2020). Senolytic CAR T Cells Reverse Senescence-Associated Pathologies. *Nature* 583, 127–132. doi:10.1038/s41586-020-2403-9
- An, H.-J., Ryu, S.-J., Kim, S.-Y., Choi, H.-R., Chung, J.-H., and Park, S.-C. (2009). Age Associated High Level of Major Vault Protein Is P53 Dependent. *Cell Biochem. Funct.* 27, 289–295. doi:10.1002/cbf.1571
- Ashkenazi, A., Fairbrother, W. J., Levenson, J. D., and Souers, A. J. (2017). From Basic Apoptosis Discoveries to Advanced Selective BCL-2 Family Inhibitors. *Nat. Rev. Drug Discov.* 16, 273–284. doi:10.1038/nrd.2016.253
- Ashkenazi, A. (2002). Targeting Death and Decoy Receptors of the Tumour-Necrosis Factor Superfamily. *Nat. Rev. Cancer* 2, 420–430. doi:10.1038/nrc821



- Ashkenazi, A. (2008). Targeting the Extrinsic Apoptosis Pathway in Cancer. *Cytokine Growth Factor Rev.* 19, 325–331. doi:10.1016/j.cytogfr.2008.04.001
- Baar, M. P., Brandt, R. M. C., Putavet, D. A., Klein, J. D. D., Derks, K. W. J., Bourgeois, B. R. M., et al. (2017). Targeted Apoptosis of Senescent Cells Restores Tissue Homeostasis in Response to Chemotoxicity and Aging. *Cell* 169, 132–147. doi:10.1016/j.cell.2017.02.031
- Baker, D. J., Childs, B. G., Durik, M., Wijers, M. E., Sieben, C. J., Zhong, J., et al. (2016). Naturally Occurring p16Ink4a-Positive Cells Shorten Healthy Lifespan. *Nature* 530, 184–189. doi:10.1038/nature16932
- Baker, D. J., Wijshake, T., Tchkonja, T., LeBrasseur, N. K., Childs, B. G., van de Sluis, B., et al. (2011). Clearance of p16Ink4a-Positive Senescent Cells Delays Ageing-Associated Disorders. *Nature* 479, 232–236. doi:10.1038/nature10600
- Barbieri, M., Bonafè, M., Franceschi, C., and Paolisso, G. (2003). Insulin/IGF-I-signaling Pathway: an Evolutionarily Conserved Mechanism of Longevity from Yeast to Humans. *Am. J. Physiology-Endocrinology Metab.* 285, E1064–E1071. doi:10.1152/ajpendo.00296.2003
- Barrera-Vázquez, O. S., Gómez-Verjan, J. C., and Magos-Guerrero, G. A. (2021). Chemoinformatic Screening for the Selection of Potential Senolytic Compounds from Natural Products. *Biomolecules* 11, 467. doi:10.3390/biom11030467
- Belharazem, D., Grass, A., Paul, C., Vitacolonna, M., Schalke, B., Rieker, R. J., et al. (2017). Increased cFLIP Expression in Thymic Epithelial Tumors Blocks Autophagy via NF-Kb Signalling. *Oncotarget* 8, 89580–89594. doi:10.18632/oncotarget.15929
- Bergamini, E., Cavallini, G., Donati, A., and Gori, Z. (2007). The Role of Autophagy in Aging: its Essential Part in the Anti-aging Mechanism of Caloric Restriction. *Ann. New York Acad. Sci.* 1114, 69–78. doi:10.1196/annals.1396.020
- Budamagunta, V., Manohar-Sindhu, S., Yang, Y., He, Y., Traktuev, D. O., Foster, T. C., et al. (2021). Senescence-associated Hyper-Activation to Inflammatory Stimuli *In Vitro*. *Aging* 13, 19088–19107. doi:10.18632/aging.203396
- Burova, E., Borodkina, A., Shatrova, A., and Nikolsky, N. (2013). Sublethal Oxidative Stress Induces the Premature Senescence of Human Mesenchymal Stem Cells Derived from Endometrium. *Oxidative Med. Cell Longevity* 2013, 1–12. doi:10.1155/2013/474931
- Burton, D. G. A., and Krizhanovsky, V. (2014). Physiological and Pathological Consequences of Cellular Senescence. *Cell. Mol. Life Sci.* 71, 4373–4386. doi:10.1007/s00181-014-1691-3
- Cai, Y., Zhou, H., Zhu, Y., Sun, Q., Ji, Y., Xue, A., et al. (2020). Elimination of Senescent Cells by  $\beta$ -galactosidase-targeted Prodrug Attenuates Inflammation and Restores Physical Function in Aged Mice. *Cell Res* 30, 574–589. doi:10.1038/s41422-020-0314-9
- Camell, C. D., Yousefzadeh, M. J., Zhu, Y., Prata, L. G. P. L., Huggins, M. A., Pierson, M., et al. (2021). Senolytics Reduce Coronavirus-Related Mortality in Old Mice. *Science* 373, eabe4832. doi:10.1126/science.abe4832
- Campisi, J., Kapahi, P., Lithgow, G. J., Melov, S., Newman, J. C., and Verdin, E. (2019). From Discoveries in Ageing Research to Therapeutics for Healthy Ageing. *Nature* 571, 183–192. doi:10.1038/s41586-019-1365-2
- Chakraborty, D., Felzen, V., Hiebel, C., Stürner, E., Perumal, N., Manicam, C., et al. (2019). Enhanced Autophagic-Lysosomal Activity and Increased BAG3-Mediated Selective Macroautophagy as Adaptive Response of Neuronal Cells to Chronic Oxidative Stress. *Redox Biol.* 24, 101181. doi:10.1016/j.redox.2019.101181
- Chang, J., Wang, Y., Shao, L., Laberge, R.-M., Demaria, M., Campisi, J., et al. (2016). Clearance of Senescent Cells by ABT263 Rejuvenates Aged Hematopoietic Stem Cells in Mice. *Nat. Med.* 22, 78–83. doi:10.1038/nm.4010
- Chatterjee, S., and Burns, T. (2017). Targeting Heat Shock Proteins in Cancer: A Promising Therapeutic Approach. *Ijms* 18, 1978. doi:10.3390/ijms18091978
- Chaturvedi, V., Qin, J.-Z., Denning, M. F., Choubey, D., Diaz, M. O., and Nickoloff, B. J. (1999). Apoptosis in Proliferating, Senescent, and Immortalized Keratinocytes. *J. Biol. Chem.* 274, 23358–23367. doi:10.1074/jbc.274.33.23358
- Chaturvedi, V., Qin, J.-Z., Stennett, L., Choubey, D., and Nickoloff, B. J. (2004). Resistance to UV-Induced Apoptosis in Human Keratinocytes during Accelerated Senescence Is Associated with Functional Inactivation of P53. *J. Cell. Physiol.* 198, 100–109. doi:10.1002/jcp.10392
- Chen, J., Chen, K.-H., Fu, B.-Q., Zhang, W., Dai, H., Lin, L.-R., et al. (2017). Isolation and Identification of Senescent Renal Tubular Epithelial Cells Using Immunomagnetic Beads Based on DcR2. *Exp. Gerontol.* 95, 116–127. doi:10.1016/j.exger.2017.04.008
- Chen, W., Kang, J., Xia, J., Li, Y., Yang, B., Chen, B., et al. (2008). p53-related Apoptosis Resistance and Tumor Suppression Activity in UVB-Induced Premature Senescent Human Skin Fibroblasts. *Int. J. Mol. Med.* 21, 645–653. doi:10.3892/ijmm.21.5.645
- Cheng, C.-L., Gao, T.-Q., Wang, Z., and Li, D.-D. (2005). Role of Insulin/insulin-like Growth Factor 1 Signaling Pathway in Longevity. *Wjg* 11, 1891–1895. doi:10.3748/wjg.v11.i13.1891
- Childs, B. G., Baker, D. J., Wijshake, T., Conover, C. A., Campisi, J., and van Deursen, J. M. (2016). Senescent Intimal Foam Cells Are Deleterious at All Stages of Atherosclerosis. *Science* 354, 472–477. doi:10.1126/science.aaf6659
- Childs, B. G., Durik, M., Baker, D. J., and van Deursen, J. M. (2015). Cellular Senescence in Aging and Age-Related Disease: from Mechanisms to Therapy. *Nat. Med.* 21, 1424–1435. doi:10.1038/nm.4000
- Childs, B. G., Gluscevic, M., Baker, D. J., Laberge, R.-M., Marquess, D., Dananberg, J., et al. (2017). Senescent Cells: an Emerging Target for Diseases of Ageing. *Nat. Rev. Drug Discov.* 16, 718–735. doi:10.1038/nrd.2017.116
- Chinta, S. J., Woods, G., Demaria, M., Rane, A., Zou, Y., McQuade, A., et al. (2018). Cellular Senescence Is Induced by the Environmental Neurotoxin Paraquat and Contributes to Neuropathology Linked to Parkinson's Disease. *Cel Rep.* 22, 930–940. doi:10.1016/j.celrep.2017.12.092
- Cho, H.-J., Yang, E. J., Park, J. T., Kim, J.-R., Kim, E.-C., Jung, K.-J., et al. (2020). Identification of SYK Inhibitor, R406 as a Novel Senolytic Agent. *Aging* 12, 8221–8240. doi:10.18632/aging.103135
- Cruikshanks, H. A., McBryan, T., Nelson, D. M., Vanderkraats, N. D., Shah, P. P., van Tuyn, J., et al. (2013). Senescent Cells Harbour Features of the Cancer Epigenome. *Nat. Cell Biol.* 15, 1495–1506. doi:10.1038/ncb2879
- Demaria, M., O'Leary, M. N., Chang, J., Shao, L., Liu, S., Alimirah, F., et al. (2017). Cellular Senescence Promotes Adverse Effects of Chemotherapy and Cancer Relapse. *Cancer Discov.* 7, 165–176. doi:10.1158/2159-8290.CD-16-0241
- Demaria, M., Ohtani, N., Youssef, S. A., Rodier, F., Toussaint, W., Mitchell, J. R., et al. (2014). An Essential Role for Senescent Cells in Optimal Wound Healing through Secretion of PDGF-AA. *Developmental Cell* 31, 722–733. doi:10.1016/j.devcel.2014.11.012
- Demidenko, Z. N., Zubova, S. G., Bukreeva, E. I., Pospelov, V. A., Pospelova, T. V., and Blagosklonny, M. V. (2009). Rapamycin Decelerates Cellular Senescence. *Cell Cycle* 8, 1888–1895. doi:10.4161/cc.8.12.8606
- DePinto, R. A. (2000). The Age of Cancer. *Nature* 408, 248–254. doi:10.1038/35041694
- Di Micco, R., Fumagalli, M., Cicalese, A., Piccinin, S., Gasparini, P., Luise, C., et al. (2006). Oncogene-induced Senescence Is a DNA Damage Response Triggered by DNA Hyper-Replication. *Nature* 444, 638–642. doi:10.1038/nature05327
- Di Micco, R., Krizhanovsky, V., Baker, D., and d'Adda di Fagnola, F. (2021). Cellular Senescence in Ageing: from Mechanisms to Therapeutic Opportunities. *Nat. Rev. Mol. Cell Biol.* 22, 75–95. doi:10.1038/s41580-020-00314-w
- Dunn, C. J., and Peters, D. H. (1995). Metformin. *Drugs* 49, 721–749. doi:10.2165/00003495-199549050-00007
- Elmallah, M. I. Y., and Micheau, O. (2019). Epigenetic Regulation of TRAIL Signaling: Implication for Cancer Therapy. *Cancers* 11, 850. doi:10.3390/cancers11060850
- Elmore, S. (2007). Apoptosis: a Review of Programmed Cell Death. *Toxicol. Pathol.* 35, 495–516. doi:10.1080/01926230701320337
- Erekat, N. S. (2021). Apoptosis and its Therapeutic Implications in Neurodegenerative Diseases. *Clin. Anat.* 35, 65–78. doi:10.1002/ca.23792
- Fatemi, M., Pao, M. M., Jeong, S., Gal-Yam, E. N., Egger, G., Weisenberger, D. J., et al. (2005). Footprinting of Mammalian Promoters: Use of a CpG DNA Methyltransferase Revealing Nucleosome Positions at a Single Molecule Level. *Nucleic Acids Res.* 33, e176. doi:10.1093/nar/gni180
- Feng, Z., Hu, W., Teresky, A. K., Hernando, E., Cordon-Cardo, C., and Levine, A. J. (2007). Declining P53 Function in the Aging Process: a Possible Mechanism for the Increased Tumor Incidence in Older Populations. *Proc. Natl. Acad. Sci.* 104, 16633–16638. doi:10.1073/pnas.0708043104
- Fiegl, D., Kägebein, D., Liebler-Tenorio, E. M., Weisser, T., Sens, M., Gutjahr, M., et al. (2013). Amphisomal Route of MHC Class I Cross-Presentation in Bacteria-Infected Dendritic Cells. *J. I.* 190, 2791–2806. doi:10.4049/jimmunol.1202741
- Firth, S. M., and Baxter, R. C. (2002). Cellular Actions of the Insulin-like Growth Factor Binding Proteins. *Endocr. Rev.* 23, 824–854. doi:10.1210/er.2001-0033

- French, L. E., and Tschopp, J. (1999). Inhibition of Death Receptor Signaling by FLICE-Inhibitory Protein as a Mechanism for Immune Escape of Tumors. *J. Exp. Med.* 190, 891–894. doi:10.1084/jem.190.7.891
- Freund, A., Patil, C. K., and Campisi, J. (2011). p38MAPK Is a Novel DNA Damage Response-independent Regulator of the Senescence-Associated Secretory Phenotype. *EMBO J.* 30, 1536–1548. doi:10.1038/emboj.2011.69
- Fridman, J. S., and Lowe, S. W. (2003). Control of Apoptosis by P53. *Oncogene* 22, 9030–9040. doi:10.1038/sj.onc.1207116
- Fuhrmann-Stroissnigg, H., Ling, Y. Y., Zhao, J., McGowan, S. J., Zhu, Y., Brooks, R. W., et al. (2017). Identification of HSP90 Inhibitors as a Novel Class of Senolytics. *Nat. Commun.* 8, 422. doi:10.1038/s41467-017-00314-z
- Fuhrmann-Stroissnigg, H., Niedernhofer, L. J., and Robbins, P. D. (2018). Hsp90 Inhibitors as Senolytic Drugs to Extend Healthy Aging. *Cell Cycle* 17, 1048–1055. doi:10.1080/15384101.2018.1475828
- Gandhi, L., Camidge, D. R., Ribeiro de Oliveira, M., Bonomi, P., Gandara, D., Khaira, D., et al. (2011). Phase I Study of Navitoclax (ABT-263), a Novel Bcl-2 Family Inhibitor, in Patients with Small-Cell Lung Cancer and Other Solid Tumors. *Jco* 29, 909–916. doi:10.1200/JCO.2010.31.6208
- Gansauge, S., Gansauge, F., Gause, H., Poch, B., Schoenberg, M. H., and Beger, H. G. (1997). The Induction of Apoptosis in Proliferating Human Fibroblasts by Oxygen Radicals Is Associated with a P53- and p21WAF1/CIP1 Induction. *FEBS Lett.* 404, 6–10. doi:10.1016/S0014-5793(97)00059-8
- Ge, M., Hu, L., Ao, H., Zi, M., Kong, Q., and He, Y. (2021). Senolytic Targets and New Strategies for Clearing Senescent Cells. *Mech. Ageing Development* 195, 111468. doi:10.1016/j.mad.2021.111468
- Gems, D., and Partridge, L. (2001). Insulin/IGF Signalling and Ageing: Seeing the Bigger Picture. *Curr. Opin. Genet. Dev.* 11, 287–292. doi:10.1016/S0959-437X(00)00192-1
- Gewirtz, D. A. (2013). Autophagy and Senescence. *Autophagy* 9, 808–812. doi:10.4161/auto.23922
- Giampieri, F., Afrin, S., Forbes-Hernandez, T. Y., Gasparrini, M., Cianciosi, D., Reboledo-Rodriguez, P., et al. (2019). Autophagy in Human Health and Disease: Novel Therapeutic Opportunities. *Antioxid. Redox Signaling* 30, 577–634. doi:10.1089/ars.2017.7234
- Gómez-Sintes, R., Ledesma, M. D., and Boya, P. (2016). Lysosomal Cell Death Mechanisms in Aging. *Ageing Res. Rev.* 32, 150–168. doi:10.1016/j.arr.2016.02.009
- Gorgoulis, V., Adams, P. D., Alimonti, A., Bennett, D. C., Bischof, O., Bishop, C., et al. (2019). Cellular Senescence: Defining a Path Forward. *Cell* 179, 813–827. doi:10.1016/j.cell.2019.10.005
- Green, D. R., Galluzzi, L., and Kroemer, G. (2011). Mitochondria and the Autophagy-Inflammation-Cell Death axis in Organismal Aging. *Science* 333, 1109–1112. doi:10.1126/science.1201940
- Grosse, L., Wagner, N., Emelyanov, A., Molina, C., Lacas-Gervais, S., Wagner, K.-D., et al. (2020). Defined p16High Senescent Cell Types are Indispensable for Mouse Healthspan. *Cel. Metab.* 32, 87–99. doi:10.1016/j.cmet.2020.05.002
- Guerrero, A., Guiho, R., Herranz, N., Uren, A., Withers, D. J., Martínez-Barbera, J. P., et al. (2020). Galactose-modified Duocarmycin Prodrugs as Senolytics. *Ageing Cell* 19, e13133. doi:10.1111/accel.13133
- Guerrero, A., Herranz, N., Sun, B., Wagner, V., Gallage, S., Guiho, R., et al. (2019). Cardiac Glycosides Are Broad-Spectrum Senolytics. *Nat. Metab.* 1, 1074–1088. doi:10.1038/s42255-019-0122-z
- Günther, C., Neumann, H., Neurath, M. F., and Becker, C. (2013). Apoptosis, Necrosis and Necroptosis: Cell Death Regulation in the Intestinal Epithelium. *Gut* 62, 1062–1071. doi:10.1136/gutjnl-2011-301364
- Hampel, B., Malisan, F., Niederegger, H., Testi, R., and Jansen-Dürr, P. (2004). Differential Regulation of Apoptotic Cell Death in Senescent Human Cells. *Exp. Gerontol.* 39, 1713–1721. doi:10.1016/j.exger.2004.05.010
- Hampel, B., Wagner, M., Teis, D., Zwierschke, W., Huber, L. A., and Jansen-Dürr, P. (2005). Apoptosis Resistance of Senescent Human Fibroblasts Is Correlated with the Absence of Nuclear IGFBP-3. *Ageing Cell* 4, 325–330. doi:10.1111/j.1474-9726.2005.00180.x
- Harrison, D. E., Strong, R., Sharp, Z. D., Nelson, J. F., Astle, C. M., Flurkey, K., et al. (2009). Rapamycin Fed Late in Life Extends Lifespan in Genetically Heterogeneous Mice. *Nature* 460, 392–395. doi:10.1038/nature08221
- Hayakawa, T., Iwai, M., Aoki, S., Takimoto, K., Maruyama, M., Maruyama, W., et al. (2015). SIRT1 Suppresses the Senescence-Associated Secretory Phenotype through Epigenetic Gene Regulation. *PLoS One* 10, e0116480. doi:10.1371/journal.pone.0116480
- Hayden, M. S., and Ghosh, S. (2008). Shared Principles in NF- $\kappa$ B Signaling. *Cell* 132, 344–362. doi:10.1016/j.cell.2008.01.020
- Hayflick, L., and Moorhead, P. S. (1961). The Serial Cultivation of Human Diploid Cell Strains. *Exp. Cell Res.* 25, 585–621. doi:10.1016/0014-4827(61)90192-6
- Hayflick, L. (1965). The Limited *In Vitro* Lifetime of Human Diploid Cell Strains. *Exp. Cell Res.* 37, 614–636. doi:10.1016/0014-4827(65)90211-9
- He, M. Y., Xu, S. B., Qu, Z. H., Guo, Y. M., Liu, X. C., Cong, X. X., et al. (2019). Hsp90 $\beta$  Interacts with MDM2 to Suppress P53-dependent Senescence during Skeletal Muscle Regeneration. *Ageing Cell* 18, e13003. doi:10.1111/accel.13003
- He, Y.-H., Lu, X., Yang, L.-Q., Xu, L.-Y., and Kong, Q.-P. (2014). Association of the Insulin-like Growth Factor Binding Protein 3 (IGFBP-3) Polymorphism with Longevity in Chinese Nonagenarians and Centenarians. *Ageing* 6, 944–951. doi:10.18632/aging.100703
- He, Y., Li, W., Lv, D., Zhang, X., Zhang, X., Ortiz, Y. T., et al. (2020a). Inhibition of USP7 Activity Selectively Eliminates Senescent Cells in Part via Restoration of P53 Activity. *Ageing Cell* 19, e13117. doi:10.1111/accel.13117
- He, Y., Li, W., Zhang, J., Yang, Y., Qian, Y., and Zhou, D. (2021). The Curcumin Analog EF24 Is Highly Active against Chemotherapy-Resistant Melanoma Cells. *Cdts* 21, 608–618. doi:10.2174/1568009621666210303092921
- He, Y., Zhang, X., Chang, J., Kim, H.-N., Zhang, P., Wang, Y., et al. (2020b). Using Proteolysis-Targeting Chimera Technology to Reduce Navitoclax Platelet Toxicity and Improve its Senolytic Activity. *Nat. Commun.* 11, 1996. doi:10.1038/s41467-020-15838-0
- He, Y., Zheng, G., and Zhou, D. (2020c). “Senolytic Drug Development,” in “*Senolytic Drug Development*,” in *Senolytics In Disease, Ageing And Longevity*. Editors D. Muñoz-Espin and M. Demaria (Cham: Springer International Publishing), 3–20. doi:10.1007/978-3-030-44903-2\_1
- Hekmatimoghaddam, S., Dehghani Firoozabadi, A., Zare-Khormizi, M. R., and Pourrajab, F. (2017). Sirt1 and Parp1 as Epigenome Safeguards and microRNAs as SASP-Associated Signals, in Cellular Senescence and Aging. *Ageing Res. Rev.* 40, 120–141. doi:10.1016/j.arr.2017.10.001
- Hernandez-Segura, A., de Jong, T. V., Melov, S., Guryev, V., Campisi, J., and Demaria, M. (2017). Unmasking Transcriptional Heterogeneity in Senescent Cells. *Curr. Biol.* 27, 2652–2660. doi:10.1016/j.cub.2017.07.033
- Hernandez-Segura, A., Nehme, J., and Demaria, M. (2018). Hallmarks of Cellular Senescence. *Trends Cel Biol.* 28, 436–453. doi:10.1016/j.tcb.2018.02.001
- Herranz, N., and Gil, J. (2018). Mechanisms and Functions of Cellular Senescence. *J. Clin. Invest.* 128, 1238–1246. doi:10.1172/JCI95148
- Hu, D., Xie, F., Xiao, Y., Lu, C., Zhong, J., Huang, D., et al. (2021). Metformin: A Potential Candidate for Targeting Aging Mechanisms. *Ageing Dis.* 12, 480–493. doi:10.14336/AD.2020.0702
- Jäättelä, M. (1999). Heat Shock Proteins as Cellular Lifeguards. *Ann. Med.* 31, 261–271. doi:10.3109/0785389990895889
- Jackson, J. G., and Pereira-Smith, O. M. (2006). p53 Is Preferentially Recruited to the Promoters of Growth Arrest Genes P21 and GADD45 during Replicative Senescence of normal Human Fibroblasts. *Cancer Res.* 66, 8356–8360. doi:10.1158/0008-5472.CAN-06-1752
- Jana, B., Kim, S., Chae, J. B., Chung, H., Kim, C., and Ryu, J. H. (2021). Mitochondrial Membrane Disrupting Molecules for Selective Killing of Senescent Cells. *Chembiochem* 22, 3391–3397. doi:10.1002/cbic.202100412
- Jego, G., Hazoumé, A., Seigneure, R., and Garrido, C. (2013). Targeting Heat Shock Proteins in Cancer. *Cancer Lett.* 332, 275–285. doi:10.1016/j.canlet.2010.10.014
- Jeon, O. H., Kim, C., Laberge, R.-M., Demaria, M., Rathod, S., Vasserot, A. P., et al. (2017). Local Clearance of Senescent Cells Attenuates the Development of post-traumatic Osteoarthritis and Creates a Pro-regenerative Environment. *Nat. Med.* 23, 775–781. doi:10.1038/nm.4324
- Jia, W., and He, Y.-W. (2011). Temporal Regulation of Intracellular Organelle Homeostasis in T Lymphocytes by Autophagy. *J.I.* 186, 5313–5322. doi:10.4049/jimmunol.1002404
- Johmura, Y., and Nakanishi, M. (2016). Multiple Facets of P53 in Senescence Induction and Maintenance. *Cancer Sci.* 107, 1550–1555. doi:10.1111/cas.13060

- Johmura, Y., Sun, J., Kitagawa, K., Nakanishi, K., Kuno, T., Naiki-Ito, A., et al. (2016). SCFFbxo22-KDM4A Targets Methylated P53 for Degradation and Regulates Senescence. *Nat. Commun.* 7, 10574. doi:10.1038/ncomms10574
- Johmura, Y., Yamanaka, T., Omori, S., Wang, T.-W., Sugiyama, Y., Matsumoto, M., et al. (2021). Senolysis by Glutaminolysis Inhibition Ameliorates Various Age-Associated Disorders. *Science* 371, 265–270. doi:10.1126/science.abb5916
- Juliana, C., Fernandes-Alnemri, T., Wu, J., Datta, P., Solorzano, L., Yu, J.-W., et al. (2010). Anti-inflammatory Compounds Parthenolide and Bay 11-7082 Are Direct Inhibitors of the Inflammasome. *J. Biol. Chem.* 285, 9792–9802. doi:10.1074/jbc.M109.082305
- Kane, A. E., and Sinclair, D. A. (2019). Epigenetic Changes during Aging and Their Reprogramming Potential. *Crit. Rev. Biochem. Mol. Biol.* 54, 61–83. doi:10.1080/10409238.2019.1570075
- Kang, H. T., Lee, K. B., Kim, S. Y., Choi, H. R., and Park, S. C. (2011). Autophagy Impairment Induces Premature Senescence in Primary Human Fibroblasts. *PLoS One* 6, e23367. doi:10.1371/journal.pone.0023367
- Kang, H. T., Park, J. T., Choi, K., Kim, Y., Choi, H. J. C., Jung, C. W., et al. (2017). Chemical Screening Identifies ATM as a Target for Alleviating Senescence. *Nat. Chem. Biol.* 13, 616–623. doi:10.1038/nchembio.2342
- Kanigur Sultuybek, G., Soydas, T., and Yenmis, G. (2019). NF- $\kappa$ B as the Mediator of Metformin's Effect on Ageing and Ageing-related Diseases. *Clin. Exp. Pharmacol. Physiol.* 46, 413–422. doi:10.1111/1440-1681.13073
- Kanugovi, A. V., Joseph, C., Siripini, S., Paithankar, K., and Amere, S. S. (2020). Compromising the Constitutive P16 INK4a Expression Sensitizes Human Neuroblastoma Cells to Hsp90 Inhibition and Promotes Premature Senescence. *J. Cel Biochem* 121, 2770–2781. doi:10.1002/jcb.29493
- Kanugovi Vijayavittal, A., and Amere Subbarao, S. (2021). The Conformation-specific Hsp90 Inhibition Interferes with the Oncogenic RAF Kinase Adaptation and Triggers Premature Cellular Senescence, Hence, Acts as a Tumor Suppressor Mechanism. *Biochim. Biophys. Acta (Bba) - Mol. Cel Res.* 1868, 118943. doi:10.1016/j.bbmr.2020.118943
- Kavathia, N., Jain, A., Walston, J., Beamer, B. A., and Fedarko, N. S. (2009). Serum Markers of Apoptosis Decrease with Age and Cancer Stage. *Aging* 1, 652–663. doi:10.18632/aging.100069
- Kawada, N. (2006). Human Hepatic Stellate Cells Are Resistant to Apoptosis: Implications for Human Fibrogenic Liver Disease. *Gut* 55, 1073–1074. doi:10.1136/gut.2005.090449
- Kile, B. T. (2014). The Role of Apoptosis in Megakaryocytes and Platelets. *Br. J. Haematol.* 165, 217–226. doi:10.1111/bjh.12757
- Kim, K. M., Noh, J. H., Bodogai, M., Martindale, J. L., Yang, X., Indig, F. E., et al. (2017). Identification of Senescent Cell Surface Targetable Protein DPP4. *Genes Dev.* 31, 1529–1534. doi:10.1101/gad.302570.117
- Kim, R. H., Kang, M. K., Kim, T., Yang, P., Bae, S., Williams, D. W., et al. (2015). Regulation of P53 during Senescence in normal Human Keratinocytes. *Aging Cell* 14, 838–846. doi:10.1111/acel.12364
- Kim, S. Y., Ryu, S. J., Kang, H. T., Choi, H. R., and Park, S. C. (2011). Defective Nuclear Translocation of Stress-Activated Signaling in Senescent Diploid Human Fibroblasts: a Possible Explanation for Aging-Associated Apoptosis Resistance. *Apoptosis* 16, 795–807. doi:10.1007/s10495-011-0612-2
- Kim, Y. S., Kim, J. S., Kwon, J. S., Jeong, M. H., Cho, J. G., Park, J. C., et al. (2010). BAY 11-7082, a Nuclear Factor- $\kappa$ B Inhibitor, Reduces Inflammation and Apoptosis in a Rat Cardiac Ischemia-Reperfusion Injury Model. *Int. Heart J.* 51, 348–353. doi:10.1536/ihj.51.348
- Kirkland, J. L., and Tchkonja, T. (2017). Cellular Senescence: A Translational Perspective. *EBioMedicine* 21, 21–28. doi:10.1016/j.ebiom.2017.04.013
- Kirkland, J. L., and Tchkonja, T. (2020). Senolytic Drugs: from Discovery to Translation. *J. Intern. Med.* 288, 518–536. doi:10.1111/joim.13141
- Kolati, S. R., Kasala, E. R., Bodduluru, L. N., Mahareddy, J. R., Uppulapu, S. K., Gogoi, R., et al. (2015). BAY 11-7082 Ameliorates Diabetic Nephropathy by Attenuating Hyperglycemia-Mediated Oxidative Stress and Renal Inflammation via NF- $\kappa$ B Pathway. *Environ. Toxicol. Pharmacol.* 39, 690–699. doi:10.1016/j.etap.2015.01.019
- Kroemer, G. (2015). Autophagy: a Druggable Process that Is Deregulated in Aging and Human Disease. *J. Clin. Invest.* 125, 1–4. doi:10.1172/JCI78652
- Lane, N., Hsu, B., Visich, J., Xie, B., Khan, A., and Dananberg, J. (2021). A Phase 2, Randomized, Double-Blind, Placebo-Controlled Study of Senolytic Molecule UBX0101 in the Treatment of Painful Knee Osteoarthritis. *Osteoarthritis and Cartilage* 29, S52–S53. doi:10.1016/j.joca.2021.02.077
- Lanneau, D., Brunet, M., Frisan, E., Solary, E., Fontenay, M., and Garrido, C. (2008). Heat Shock Proteins: Essential Proteins for Apoptosis Regulation. *J. Cell. Mol. Med.* 12, 743–761. doi:10.1111/j.1582-4934.2008.00273.x
- Lappas, M., Yee, K., Permezel, M., and Rice, G. E. (2005). Sulfasalazine and BAY 11-7082 Interfere with the Nuclear Factor- $\kappa$ B and I $\kappa$ B Kinase Pathway to Regulate the Release of Proinflammatory Cytokines from Human Adipose Tissue and Skeletal Muscle *In Vitro*. *Endocrinology* 146, 1491–1497. doi:10.1210/en.2004-0809
- Lee, B. Y., Han, J. A., Im, J. S., Morrone, A., Johung, K., Goodwin, E. C., et al. (2006). Senescence-associated  $\beta$ -galactosidase Is Lysosomal  $\beta$ -galactosidase. *Aging Cell* 5, 187–195. doi:10.1111/j.1474-9726.2006.00199.x
- Lee, S., Yu, Y., Trimpert, J., Benthani, F., Mairhofer, M., Richter-Pechanska, P., et al. (2021). Virus-induced Senescence Is a Driver and Therapeutic Target in COVID-19. *Nature* 599, 283–289. doi:10.1038/s41586-021-03995-1
- Leidal, A. M., Levine, B., and Debnath, J. (2018). Autophagy and the Cell Biology of Age-Related Disease. *Nat. Cel Biol* 20, 1338–1348. doi:10.1038/s41556-018-0235-8
- Leverson, J. D., Phillips, D. C., Mitten, M. J., Boghaert, E. R., Diaz, D., Tahir, S. K., et al. (2015). Exploiting Selective BCL-2 Family Inhibitors to Dissect Cell Survival Dependencies and Define Improved Strategies for Cancer Therapy. *Sci. Transl. Med.* 7, 279ra40. doi:10.1126/scitranslmed.aaa4642
- Levine, B., and Yuan, J. (2005). Autophagy in Cell Death: an Innocent Convict? *J. Clin. Invest.* 115, 2679–2688. doi:10.1172/JCI26390
- Li, W., He, Y., Zhang, R., Zheng, G., and Zhou, D. (2019a). The Curcumin Analog EF24 Is a Novel Senolytic Agent. *Aging* 11, 771–782. doi:10.18632/aging.101787
- Li, W., Qin, L., Feng, R., Hu, G., Sun, H., He, Y., et al. (2019b). Emerging Senolytic Agents Derived from Natural Products. *Mech. Ageing Development* 181, 1–6. doi:10.1016/j.mad.2019.05.001
- Li, Z., Zhu, Y.-T., Xiang, M., Qiu, J.-L., Luo, S.-Q., and Lin, F. (2021). Enhanced Lysosomal Function Is Critical for Paclitaxel Resistance in Cancer Cells: Reversed by Artesunate. *Acta Pharmacol. Sin* 42, 624–632. doi:10.1038/s41401-020-0445-z
- Lim, H., Park, H., and Kim, H. P. (2015). Effects of Flavonoids on Senescence-Associated Secretory Phenotype Formation from Bleomycin-Induced Senescence in BJ Fibroblasts. *Biochem. Pharmacol.* 96, 337–348. doi:10.1016/j.bcp.2015.06.013
- Liu, J., Lu, W., Reigada, D., Nguyen, J., Laties, A. M., and Mitchell, C. H. (2008). Restoration of Lysosomal pH in RPE Cells from Cultured Human and ABCA4 $^{-/-}$  Mice: Pharmacologic Approaches and Functional Recovery. *Invest. Ophthalmol. Vis. Sci.* 49, 772–780. doi:10.1167/iiov.07-0675
- López-Otín, C., Blasco, M. A., Partridge, L., Serrano, M., and Kroemer, G. (2013). The Hallmarks of Aging. *Cell* 153, 1194–1217. doi:10.1016/j.cell.2013.05.039
- Ma, K., Xu, Q., Wang, S., Zhang, W., Liu, M., Liang, S., et al. (2016). Nuclear Accumulation of Yes-Associated Protein (YAP) Maintains the Survival of Doxorubicin-Induced Senescent Cells by Promoting Survivin Expression. *Cancer Lett.* 375, 84–91. doi:10.1016/j.canlet.2016.02.045
- Ma, Y., Galluzzi, L., Zitvogel, L., and Kroemer, G. (2013). Autophagy and Cellular Immune Responses. *Immunity* 39, 211–227. doi:10.1016/j.immuni.2013.07.017
- Marcotte, R., Lacelle, C., and Wang, E. (2004). Senescent Fibroblasts Resist Apoptosis by Downregulating Caspase-3. *Mech. Ageing Development* 125, 777–783. doi:10.1016/j.mad.2004.07.007
- Mattson, M. P., Duan, W., Pedersen, W. A., and Culmsee, C. (2001). Neurodegenerative Disorders and Ischemic Brain Diseases. *Apoptosis* 6, 69–81. doi:10.1023/a:1009676112184
- McIlwain, D. R., Berger, T., and Mak, T. W. (2013). Caspase Functions in Cell Death and Disease. *Cold Spring Harbor Perspect. Biol.* 5, a008656. doi:10.1101/cshperspect.a008656
- Michaud, M., Martins, I., Sukkurwala, A. Q., Adjemian, S., Ma, Y., Pellegatti, P., et al. (2011). Autophagy-dependent Anticancer Immune Responses Induced by Chemotherapeutic Agents in Mice. *Science* 334, 1573–1577. doi:10.1126/science.1208347
- Michels, J., Johnson, P. W. M., and Packham, G. (2005). Mcl-1. *Int. J. Biochem. Cel Biol.* 37, 267–271. doi:10.1016/j.biocel.2004.04.007



- Mohiuddin, M., and Kasahara, K. (2021). The Emerging Role of Cellular Senescence in Complications of COVID-19. *Cancer Treat. Res. Commun.* 28, 100399. doi:10.1016/j.ctarc.2021.100399
- Moiseeva, O., Guillon, J., and Ferbeyre, G. (2020). Senescence: A Program in the Road to Cell Elimination and Cancer. *Semin. Cancer Biol.* S1044-579X (20), 30277-7. doi:10.1016/j.semcancer.2020.12.017
- Moll, U. M., and Petrenko, O. (2003). The MDM2-P53 Interaction. *Mol. Cancer Res.* 1, 1001-1008.
- Monti, D., Salvioli, S., Capri, M., Malorni, W., Straface, E., Cossarizza, A., et al. (2000). Decreased Susceptibility to Oxidative Stress-Induced Apoptosis of Peripheral Blood Mononuclear Cells from Healthy Elderly and Centenarians. *Mech. Ageing Dev.* 121, 239-250. doi:10.1016/s0047-6374(00)00220-7
- Morris, B. J., Willcox, B. J., and Donlon, T. A. (2019). Genetic and Epigenetic Regulation of Human Aging and Longevity. *Biochim. Biophys. Acta (Bba) - Mol. Basis Dis.* 1865, 1718-1744. doi:10.1016/j.bbdis.2018.08.039
- Mortezaee, K., Najafi, M., Farhood, B., Ahmadi, A., Shabeeb, D., and Musa, A. E. (2019). NF- $\kappa$ B Targeting for Overcoming Tumor Resistance and normal Tissues Toxicity. *J. Cel Physiol* 234, 17187-17204. doi:10.1002/jcp.28504
- Mukherjee, N., Amato, C. M., Skees, J., Todd, K. J., Lambert, K. A., Robinson, W. A., et al. (2020). Simultaneously Inhibiting BCL2 and MCL1 Is a Therapeutic Option for Patients with Advanced Melanoma. *Cancers* 12, 2182. doi:10.3390/cancers12082182
- Muñoz, D. P., Yannone, S. M., Daemen, A., Sun, Y., Vakar-Lopez, F., Kawahara, M., et al. (2019). Targetable Mechanisms Driving Immuno-evasion of Persistent Senescent Cells Link Chemotherapy-Resistant Cancer to Aging. *JCI Insight* 4, 124716. doi:10.1172/jci.insight.124716
- Muñoz-Espín, D., Cañamero, M., Maraver, A., Gómez-López, G., Contreras, J., Murillo-Cuesta, S., et al. (2013). Programmed Cell Senescence during Mammalian Embryonic Development. *Cell* 155, 1104-1118. doi:10.1016/j.cell.2013.10.019
- Nacarelli, T., Liu, P., and Zhang, R. (2017). Epigenetic Basis of Cellular Senescence and its Implications in Aging. *Genes* 8, 343. doi:10.3390/genes8120343
- Nagakannan, P., Tabeshmehr, P., and Eftekharpour, E. (2020). Oxidative Damage of Lysosomes in Regulated Cell Death Systems: Pathophysiology and Pharmacologic Interventions. *Free Radic. Biol. Med.* 157, 94-127. doi:10.1016/j.freeradbiomed.2020.04.001
- Nair, P., Lu, M., Petersen, S., and Ashkenazi, A. (2014). Apoptosis Initiation through the Cell-Extrinsic Pathway. *Methods Enzymol.* 544, 99-128. doi:10.1016/B978-0-12-417158-9.00005-4
- Nehme, J., Borghesan, M., Mackedenski, S., Bird, T. G., and Demaria, M. (2020). Cellular Senescence as a Potential Mediator of COVID-19 Severity in the Elderly. *Aging Cell* 19, e13237. doi:10.1111/acer.13237
- Niedernhofer, L. J., and Robbins, P. D. (2018). Senotherapeutics for Healthy Ageing. *Nat. Rev. Drug Discov.* 17, 377. doi:10.1038/nrd.2018.44
- Nogueira-Recalde, U., Lorenzo-Gómez, I., Blanco, F. J., Loza, M. I., Grassi, D., Shirinsky, V., et al. (2019). Fibrates as Drugs with Senolytic and Autophagic Activity for Osteoarthritis Therapy. *EBioMedicine* 45, 588-605. doi:10.1016/j.ebiom.2019.06.049
- Novo, E., Marra, F., Zamara, E., Valfrè di Bonzo, L., Monitillo, L., Cannito, S., et al. (2006). Overexpression of Bcl-2 by Activated Human Hepatic Stellate Cells: Resistance to Apoptosis as a Mechanism of Progressive Hepatic Fibrogenesis in Humans. *Gut* 55, 1174-1182. doi:10.1136/gut.2005.082701
- O'Hara, S. P., Splinter, P. L., Trussoni, C. E., Guicciardi, M. E., Splinter, N. P., Al Suraih, M. S., et al. (2019). The Transcription Factor ETS1 Promotes Apoptosis Resistance of Senescent Cholangiocytes by Epigenetically Up-Regulating the Apoptosis Suppressor BCL2L1. *J. Biol. Chem.* 294, 18698-18713. doi:10.1074/jbc.RA119.010176
- Ogrodnik, M., Miwa, S., Tchkonja, T., Tiniakos, D., Wilson, C. L., Lahat, A., et al. (2017). Cellular Senescence Drives Age-dependent Hepatic Steatosis. *Nat. Commun.* 8, 15691. doi:10.1038/ncomms15691
- Omer, A., Patel, D., Moran, J. L., Lian, X. J., Di Marco, S., and Gallouzi, I.-E. (2020). Autophagy and Heat-Shock Response Impair Stress Granule Assembly during Cellular Senescence. *Mech. Ageing Development* 192, 111382. doi:10.1016/j.mad.2020.111382
- Ozsvari, B., Nuttall, J. R., Sotgia, F., and Lisanti, M. P. (2018). Azithromycin and Roxithromycin Define a New Family of "Senolytic" Drugs that Target Senescent Human Fibroblasts. *Aging* 10, 3294-3307. doi:10.18632/aging.101633
- Ozyerli-Goknar, E., and Bagci-Onder, T. (2021). Epigenetic Dysregulation of Apoptosis in Cancers. *Cancers* 13, 3210. doi:10.3390/cancers13133210
- Palmer, A. K., Tchkonja, T., LeBrasseur, N. K., Chini, E. N., Xu, M., and Kirkland, J. L. (2015). Cellular Senescence in Type 2 Diabetes: A Therapeutic Opportunity. *Diabetes* 64, 2289-2298. doi:10.2337/db14-1820
- Paluvai, H., Di Giorgio, E., and Brancolini, C. (2020). The Histone Code of Senescence. *Cells* 9, 466. doi:10.3390/cells9020466
- Pereira, B. I., Devine, O. P., Vukmanovic-Stejić, M., Chambers, E. S., Subramanian, P., Patel, N., et al. (2019). Senescent Cells Evade Immune Clearance via HLA-E-Mediated NK and CD8<sup>+</sup> T Cell Inhibition. *Nat. Commun.* 10, 2387. doi:10.1038/s41467-019-10335-5
- Perrott, K. M., Wiley, C. D., Desprez, P.-Y., and Campisi, J. (2017). Apigenin Suppresses the Senescence-Associated Secretory Phenotype and Paracrine Effects on Breast Cancer Cells. *Geroscience* 39, 161-173. doi:10.1007/s11357-017-9970-1
- Pierce, J. W., Schoenleber, R., Jesmok, G., Best, J., Moore, S. A., Collins, T., et al. (1997). Novel Inhibitors of Cytokine-Induced I $\kappa$ B $\alpha$  Phosphorylation and Endothelial Cell Adhesion Molecule Expression Show Anti-inflammatory Effects In Vivo. *J. Biol. Chem.* 272, 21096-21103. doi:10.1074/jbc.272.34.21096
- Polyak, K., Wu, T.-T., Hamilton, S. R., Kinzler, K. W., and Vogelstein, B. (1997). Less Death in the Dying. *Cell Death Differ* 4, 242-246. doi:10.1038/sj.cdd.4400226
- Pozhidaeva, A., and Bezsonova, I. (2019). USP7: Structure, Substrate Specificity, and Inhibition. *DNA Repair* 76, 30-39. doi:10.1016/j.dnarep.2019.02.005
- Pua, H. H., Dzhalagov, I., Chuck, M., Mizushima, N., and He, Y.-W. (2007). A Critical Role for the Autophagy Gene Atg5 in T Cell Survival and Proliferation. *J. Exp. Med.* 204, 25-31. doi:10.1084/jem.20061303
- Ramsey, H. E., Fischer, M. A., Lee, T., Gorska, A. E., Arrate, M. P., Fuller, L., et al. (2018). A Novel MCL1 Inhibitor Combined with Venetoclax Rescues Venetoclax-Resistant Acute Myelogenous Leukemia. *Cancer Discov.* 8, 1566-1581. doi:10.1158/2159-8290.CD-18-0140
- Ravichandra, A., Filliol, A., and Schwabe, R. F. (2021). Chimeric Antigen Receptor T Cells as Senolytic and Antifibrotic Therapy. *Hepatology* 73, 1227-1229. doi:10.1002/hep.31596
- Rochette, P. J., and Brash, D. E. (2008). Progressive Apoptosis Resistance Prior to Senescence and Control by the Anti-apoptotic Protein BCL-xL. *Mech. Ageing Development* 129, 207-214. doi:10.1016/j.mad.2007.12.007
- Roll, J. D., Rivenbark, A. G., Jones, W. D., and Coleman, W. B. (2008). DNMT3b Overexpression Contributes to a Hypermethylator Phenotype in Human Breast Cancer Cell Lines. *Mol. Cancer* 7, 15. doi:10.1186/1476-4598-7-15
- Rossi, M., and Abdelmohsen, K. (2021). The Emergence of Senescent Surface Biomarkers as Senotherapeutic Targets. *Cells* 10, 1740. doi:10.3390/cells10071740
- Ryu, S. J., An, H. J., Oh, Y. S., Choi, H. R., Ha, M. K., and Park, S. C. (2008). On the Role of Major Vault Protein in the Resistance of Senescent Human Diploid Fibroblasts to Apoptosis. *Cell Death Differ* 15, 1673-1680. doi:10.1038/cdd.2008.96
- Ryu, S. J., Cho, K. A., Oh, Y. S., and Park, S. C. (2006). Role of Src-specific Phosphorylation Site on Focal Adhesion Kinase for Senescence-Associated Apoptosis Resistance. *Apoptosis* 11, 303-313. doi:10.1007/s10495-006-3978-9
- Ryu, S. J., Oh, Y. S., and Park, S. C. (2007). Failure of Stress-Induced Downregulation of Bcl-2 Contributes to Apoptosis Resistance in Senescent Human Diploid Fibroblasts. *Cell Death Differ* 14, 1020-1028. doi:10.1038/sj.cdd.4402091
- Ryu, S. J., and Park, S. C. (2009). Targeting Major Vault Protein in Senescence-Associated Apoptosis Resistance. *Expert Opin. Ther. Targets* 13, 479-484. doi:10.1517/14728220902832705
- Sagiv, A., Biran, A., Yon, M., Simon, J., Lowe, S. W., and Krizhanovsky, V. (2013). Granule Exocytosis Mediates Immune Surveillance of Senescent Cells. *Oncogene* 32, 1971-1977. doi:10.1038/onc.2012.206
- Sagiv, A., Burton, D. G. A., Moshayev, Z., Vadai, E., Wensveen, F., Ben-Dor, S., et al. (2016). NKG2D Ligands Mediate Immunosurveillance of Senescent Cells. *Aging* 8, 328-344. doi:10.18632/aging.100897
- Sainz, R. M., Mayo, J. C., Reiter, R. J., Tan, D. X., and Rodriguez, C. (2003). Apoptosis in Primary Lymphoid Organs with Aging. *Microsc. Res. Tech.* 62, 524-539. doi:10.1002/jemt.10414



- Salminen, A., Kauppinen, A., and Kaarniranta, K. (2012). Emerging Role of NF-KB Signaling in the Induction of Senescence-Associated Secretory Phenotype (SASP). *Cell Signal.* 24, 835–845. doi:10.1016/j.cellsig.2011.12.006
- Salminen, A., Ojala, J., and Kaarniranta, K. (2011). Apoptosis and Aging: Increased Resistance to Apoptosis Enhances the Aging Process. *Cel. Mol. Life Sci.* 68, 1021–1031. doi:10.1007/s00018-010-0597-y
- Samaraweera, L., Adomako, A., Rodriguez-Gabin, A., and McDaid, H. M. (2017). A Novel Indication for Panobinostat as a Senolytic Drug in NSCLC and HNSCC. *Sci. Rep.* 7, 1900. doi:10.1038/s41598-017-01964-1
- Sanchez, J., Carter, T. R., Cohen, M. S., and Blagg, B. S. J. (2020). Old and New Approaches to Target the Hsp90 Chaperone. *Ccvt* 20, 253–270. doi:10.2174/1568009619666191202101330
- Sanders, Y. Y., Liu, H., Zhang, X., Hecker, L., Bernard, K., Desai, L., et al. (2013). Histone Modifications in Senescence-Associated Resistance to Apoptosis by Oxidative Stress. *Redox Biol.* 1, 8–16. doi:10.1016/j.redox.2012.11.004
- Sarkisian, C. J., Keister, B. A., Stairs, D. B., Boxer, R. B., Moody, S. E., and Chodosh, L. A. (2007). Dose-dependent Oncogene-Induced Senescence *In Vivo* and its Evasion during Mammary Tumorigenesis. *Nat. Cel Biol* 9, 493–505. doi:10.1038/ncb1567
- Sasaki, M., Kumazaki, T., Takano, H., Nishiyama, M., and Mitsui, Y. (2001). Senescent Cells Are Resistant to Death Despite Low Bcl-2 Level. *Mech. Ageing Development* 122, 1695–1706. doi:10.1016/s0047-6374(01)00281-0
- Sayers, T. J. (2011). Targeting the Extrinsic Apoptosis Signaling Pathway for Cancer Therapy. *Cancer Immunol. Immunother.* 60, 1173–1180. doi:10.1007/s00262-011-1008-4
- Schwarze, S. R., Shi, Y., Fu, V. X., Watson, P. A., and Jarrard, D. F. (2001). Role of Cyclin-dependent Kinase Inhibitors in the Growth Arrest at Senescence in Human Prostate Epithelial and Uroepithelial Cells. *Oncogene* 20, 8184–8192. doi:10.1038/sj.onc.1205049
- Schwarzenbach, C., Tatsch, L., Brandstetter Vilar, J., Rasenberger, B., Beltzig, L., Kaina, B., et al. (2021). Targeting C-IAP1, C-IAP2, and Bcl-2 Eliminates Senescent Glioblastoma Cells Following Temozolomide Treatment. *Cancers* 13, 3585. doi:10.3390/cancers13143585
- Seiller, C., Maiga, S., Touzeau, C., Bellanger, C., Kervoëlen, C., Descamps, G., et al. (2020). Dual Targeting of BCL2 and MCL1 Rescues Myeloma Cells Resistant to BCL2 and MCL1 Inhibitors Associated with the Formation of BAX/BAK Hetero-Complexes. *Cel Death Dis* 11, 316. doi:10.1038/s41419-020-2505-1
- Seluanov, A., Gorbunova, V., Falcovitz, A., Sigal, A., Milyavsky, M., Zurer, I., et al. (2001). Change of the Death Pathway in Senescent Human Fibroblasts in Response to DNA Damage Is Caused by an Inability to Stabilize P53. *Mol. Cel Biol* 21, 1552–1564. doi:10.1128/MCB.21.5.1552-1564.2001
- Shah, P. P., Donahue, G., Otte, G. L., Capell, B. C., Nelson, D. M., Cao, K., et al. (2013). Lamin B1 Depletion in Senescent Cells Triggers Large-Scale Changes in Gene Expression and the Chromatin Landscape. *Genes Dev.* 27, 1787–1799. doi:10.1101/gad.223834.113
- Shimizu, H., Bolati, D., Adijiang, A., Muteliefu, G., Enomoto, A., Nishijima, F., et al. (2011). NF- $\kappa$ B Plays an Important Role in Indoxyl Sulfate-Induced Cellular Senescence, Fibrotic Gene Expression, and Inhibition of Proliferation in Proximal Tubular Cells. *Am. J. Physiology-Cell Physiol.* 301, C1201–C1212. doi:10.1152/ajpcell.00471.2010
- Sidler, C., Kovalchuk, O., and Kovalchuk, I. (2017). Epigenetic Regulation of Cellular Senescence and Aging. *Front. Genet.* 8, 138. doi:10.3389/fgene.2017.00138
- Simboeck, E., Ribeiro, J. D., Teichmann, S., and Di Croce, L. (2011). Epigenetics and Senescence: Learning from the INK4-ARF Locus. *Biochem. Pharmacol.* 82, 1361–1370. doi:10.1016/j.bcp.2011.07.084
- Singh, R., Letai, A., and Sarosiek, K. (2019). Regulation of Apoptosis in Health and Disease: the Balancing Act of BCL-2 Family Proteins. *Nat. Rev. Mol. Cel Biol* 20, 175–193. doi:10.1038/s41580-018-0089-8
- Sisoula, C., Trachana, V., Patterson, C., and Gonos, E. S. (2011). CHIP-dependent P53 Regulation Occurs Specifically during Cellular Senescence. *Free Radic. Biol. Med.* 50, 157–165. doi:10.1016/j.freeradbiomed.2010.10.701
- Soto-Gamez, A., Quax, W. J., and Demaria, M. (2019). Regulation of Survival Networks in Senescent Cells: From Mechanisms to Interventions. *J. Mol. Biol.* 431, 2629–2643. doi:10.1016/j.jmb.2019.05.036
- Souers, A. J., Levenson, J. D., Boghaert, E. R., Ackler, S. L., Catron, N. D., Chen, J., et al. (2013). ABT-199, a Potent and Selective BCL-2 Inhibitor, Achieves Antitumor Activity while Sparing Platelets. *Nat. Med.* 19, 202–208. doi:10.1038/nm.3048
- Spaulding, C., Guo, W., and Effros, R. B. (1999). Resistance to Apoptosis in Human CD8+ T Cells that Reach Replicative Senescence after Multiple Rounds of Antigen-specific Proliferation. *Exp. Gerontol.* 34, 633–644. doi:10.1016/s0531-5565(99)00033-9
- Srivastava, S., Vishwanathan, V., Birje, A., Sinha, D., and D'Silva, P. (2019). Evolving Paradigms on the Interplay of Mitochondrial Hsp70 Chaperone System in Cell Survival and Senescence. *Crit. Rev. Biochem. Mol. Biol.* 54, 517–536. doi:10.1080/10409238.2020.1718062
- Suh, Y., Lee, K.-A., Kim, W.-H., Han, B.-G., Vijg, J., and Park, S. C. (2002). Aging Alters the Apoptotic Response to Genotoxic Stress. *Nat. Med.* 8, 3–4. doi:10.1038/nm0102-3
- Tai, H., Wang, Z., Gong, H., Han, X., Zhou, J., Wang, X., et al. (2017). Autophagy Impairment with Lysosomal and Mitochondrial Dysfunction Is an Important Characteristic of Oxidative Stress-Induced Senescence. *Autophagy* 13, 99–113. doi:10.1080/15548627.2016.1247143
- Takasugi, M., Okada, R., Takahashi, A., Virya Chen, D., Watanabe, S., and Hara, E. (2017). Small Extracellular Vesicles Secreted from Senescent Cells Promote Cancer Cell Proliferation through EphA2. *Nat. Commun.* 8, 15729. doi:10.1038/ncomms15728
- Takayama, S., Reed, J. C., and Homma, S. (2003). Heat-shock Proteins as Regulators of Apoptosis. *Oncogene* 22, 9041–9047. doi:10.1038/sj.onc.1207114
- Thoppil, H., and Riabowol, K. (2019). Senolytics: A Translational Bridge between Cellular Senescence and Organismal Aging. *Front. Cel Dev. Biol.* 7, 367. doi:10.3389/fcell.2019.00367
- Tower, J. (2015). Programmed Cell Death in Aging. *Ageing Res. Rev.* 23, 90–100. doi:10.1016/j.arr.2015.04.002
- Triana-Martínez, F., Picallós-Rabina, P., Da Silva-Álvarez, S., Pietrocola, F., Llanos, S., Rodilla, V., et al. (2019). Identification and Characterization of Cardiac Glycosides as Senolytic Compounds. *Nat. Commun.* 10, 4731. doi:10.1038/s41467-019-12888-x
- Unruhe, B., Schröder, E., Wünsch, D., and Knauer, S. K. (2016). An Old Flame Never Dies: Survivin in Cancer and Cellular Senescence. *Gerontology* 62, 173–181. doi:10.1159/000432398
- Vjetrovic, J., Shankaranarayanan, P., Mendoza-Parra, M. A., and Gronemeyer, H. (2014). Senescence-secreted Factors Activate M Yc and Sensitize Pretransformed Cells to TRAIL-induced Apoptosis. *Ageing Cell* 13, 487–496. doi:10.1111/ace.12197
- Wajapeyee, N., Serra, R. W., Zhu, X., Mahalingam, M., and Green, M. R. (2008). Oncogenic BRAF Induces Senescence and Apoptosis through Pathways Mediated by the Secreted Protein IGFBP7. *Cell* 132, 363–374. doi:10.1016/j.cell.2007.12.032
- Wakita, M., Takahashi, A., Sano, O., Loo, T. M., Imai, Y., Narukawa, M., et al. (2020). A BET Family Protein Degradator Provokes Senolysis by Targeting NHEJ and Autophagy in Senescent Cells. *Nat. Commun.* 11, 1935. doi:10.1038/s41467-020-15719-6
- Wang, E. (1995). Senescent Human Fibroblasts Resist Programmed Cell Death, and Failure to Suppress Bcl2 Is Involved. *Cancer Res.* 55, 2284–2292.
- Wang, F., Gómez-Sintes, R., and Boya, P. (2018). Lysosomal Membrane Permeabilization and Cell Death. *Traffic* 19, 918–931. doi:10.1111/tra.12613
- Wang, J., Tao, Q., Pan, Y., Wanyan, Z., Zhu, F., Xu, X., et al. (2020). Stress-induced Premature Senescence Activated by the SENEX Gene Mediates Apoptosis Resistance of Diffuse Large B-cell Lymphoma via Promoting Immunosuppressive Cells and Cytokines. *Immun. Inflamm. Dis.* 8, 672–683. doi:10.1002/iid3.356
- Wang, Y., Chang, J., Liu, X., Zhang, X., Zhang, S., Zhang, X., et al. (2016). Discovery of Piperlongumine as a Potential Novel lead for the Development of Senolytic Agents. *Ageing* 8, 2915–2926. doi:10.18632/aging.101100
- Wanner, E., Thoppil, H., and Riabowol, K. (2020). Senescence and Apoptosis: Architects of Mammalian Development. *Front. Cel Dev. Biol.* 8, 620089. doi:10.3389/fcell.2020.620089
- Wildenberg, M. E., Vos, A. C. W., Wolfkamp, S. C. S., Duijvestein, M., Verhaar, A. P., Te Velde, A. A., et al. (2012). Autophagy Attenuates the Adaptive Immune Response by Destabilizing the Immunologic Synapse. *Gastroenterology* 142, 1493–1503. doi:10.1053/j.gastro.2012.02.034

- Wiley, C. D., Flynn, J. M., Morrissey, C., Lebofsky, R., Shuga, J., Dong, X., et al. (2017). Analysis of Individual Cells Identifies Cell-To-Cell Variability Following Induction of Cellular Senescence. *Aging Cell* 16, 1043–1050. doi:10.1111/accel.12632
- Wilson, A., Shehadeh, L. A., Yu, H., and Webster, K. A. (2010). Age-related Molecular Genetic Changes of Murine Bone Marrow Mesenchymal Stem Cells. *BMC Genomics* 11, 229. doi:10.1186/1471-2164-11-229
- Wissler Gerdes, E. O., Vanichkachorn, G., Verdoorn, B. P., Hanson, G. J., Joshi, A. Y., Murad, M. H., et al. (2021). Role of Senescence in the Chronic Health Consequences of COVID-19. *Translational Res.* S1931-5244 (21), 00259. doi:10.1016/j.trsl.2021.10.003
- Wu, D., and Prives, C. (2018). Relevance of the P53-MDM2 axis to Aging. *Cel Death Differ* 25, 169–179. doi:10.1038/cdd.2017.187
- Xiao, F.-H., Kong, Q.-P., Perry, B., and He, Y.-H. (2016). Progress on the Role of DNA Methylation in Aging and Longevity. *Brief. Funct. Genomics* 15, elw009–459. doi:10.1093/bfpg/elw009
- Yang, D., Tian, X., Ye, Y., Liang, Y., Zhao, J., Wu, T., et al. (2021). Identification of GL-V9 as a Novel Senolytic Agent against Senescent Breast Cancer Cells. *Life Sci.* 272, 119196. doi:10.1016/j.lfs.2021.119196
- Yeo, E. J., Hwang, Y. C., Kang, C. M., Choy, H. E., and Park, S. C. (2000). Reduction of UV-Induced Cell Death in the Human Senescent Fibroblasts. *Mol. Cell* 10, 415–422.
- Yosef, R., Pilpel, N., Tokarsky-Amiel, R., Biran, A., Ovadya, Y., Cohen, S., et al. (2016). Directed Elimination of Senescent Cells by Inhibition of BCL-W and BCL-XL. *Nat. Commun.* 7, 11190. doi:10.1038/ncomms11190
- Youle, R. J., and Strasser, A. (2008). The BCL-2 Protein Family: Opposing Activities that Mediate Cell Death. *Nat. Rev. Mol. Cel Biol* 9, 47–59. doi:10.1038/nrm2308
- Young, A. R. J., Narita, M., Ferreira, M., Kirschner, K., Sadaie, M., Darot, J. F. J., et al. (2009). Autophagy Mediates the Mitotic Senescence Transition. *Genes Dev.* 23, 798–803. doi:10.1101/gad.519709
- Yousefzadeh, M. J., Zhu, Y., McGowan, S. J., Angelini, L., Fuhrmann-Stroissnigg, H., Xu, M., et al. (2018). Fisetin Is a Senotherapeutic that Extends Health and Lifespan. *EBioMedicine* 36, 18–28. doi:10.1016/j.ebiom.2018.09.015
- Zang, J., Sha, M., Zhang, C., Ye, J., Zhang, K., and Gao, J. (2017). Senescent Hepatocyte Secretion of Matrix Metalloproteinases Is Regulated by Nuclear Factor-Kb Signaling. *Life Sci.* 191, 205–210. doi:10.1016/j.lfs.2017.10.023
- Zhang, C., Xie, Y., Chen, H., Lv, L., Yao, J., Zhang, M., et al. (2020). FOXO4-DRI Alleviates Age-Related Testosterone Secretion Insufficiency by Targeting Senescent Leydig Cells in Aged Mice. *Aging* 12, 1272–1284. doi:10.18632/aging.102682
- Zhang, P., Kishimoto, Y., Grammatikakis, I., Gottimukkala, K., Cutler, R. G., Zhang, S., et al. (2019). Senolytic Therapy Alleviates A $\beta$ -Associated Oligodendrocyte Progenitor Cell Senescence and Cognitive Deficits in an Alzheimer's Disease Model. *Nat. Neurosci.* 22, 719–728. doi:10.1038/s41593-019-0372-9
- Zhang, X., Zhang, S., Liu, X., Wang, Y., Chang, J., Zhang, X., et al. (2018). Oxidation Resistance 1 Is a Novel Senolytic Target. *Aging Cell* 17, e12780. doi:10.1111/accel.12780
- Zhang, Z., Yao, Z., Zhao, S., Shao, J., Chen, A., Zhang, F., et al. (2017). Interaction between Autophagy and Senescence Is Required for Dihydroartemisinin to Alleviate Liver Fibrosis. *Cel Death Dis* 8, e2886. doi:10.1038/cddis.2017.255
- Zhou, J., Wang, J., Chen, C., Yuan, H., Wen, X., and Sun, H. (2018). USP7: Target Validation and Drug Discovery for Cancer Therapy. *Mc* 14, 3–18. doi:10.2174/1573406413666171020115539
- Zhu, Y., Dornnebal, E. J., Pirtskhalava, T., Giorgadze, N., Wentworth, M., Fuhrmann-Stroissnigg, H., et al. (2017). New Agents that Target Senescent Cells: the Flavone, Fisetin, and the BCL-XL Inhibitors, A1331852 and A1155463. *Aging* 9, 955–963. doi:10.18632/aging.101202
- Zhu, Y., Tchkonja, T., Fuhrmann-Stroissnigg, H., Dai, H. M., Ling, Y. Y., Stout, M. B., et al. (2016). Identification of a Novel Senolytic Agent, Navitoclax, Targeting the Bcl-2 Family of Anti-apoptotic Factors. *Aging Cell* 15, 428–435. doi:10.1111/accel.12445
- Zhu, Y., Tchkonja, T., Pirtskhalava, T., Gower, A. C., Ding, H., Giorgadze, N., et al. (2015). The Achilles' Heel of Senescent Cells: from Transcriptome to Senolytic Drugs. *Aging Cell* 14, 644–658. doi:10.1111/accel.12344

**Conflict of Interest:** DZ is a co-founder and a stockholder of Unity Biotechnology that develops senolytics as therapeutics for various age-related diseases. DZ and YH are inventors on several patent applications for the use of Bcl-xL and Bcl-2 inhibitors and PROTACs to clear SnCs.

The remaining authors declare that the research was conducted in the absence of any commercial or financial relationships that could be construed as a potential conflict of interest.

**Publisher's Note:** All claims expressed in this article are solely those of the authors and do not necessarily represent those of their affiliated organizations, or those of the publisher, the editors and the reviewers. Any product that may be evaluated in this article, or claim that may be made by its manufacturer, is not guaranteed or endorsed by the publisher.

Copyright © 2022 Hu, Li, Zi, Li, Liu, Yang, Zhou, Kong, Zhang and He. This is an open-access article distributed under the terms of the Creative Commons Attribution License (CC BY). The use, distribution or reproduction in other forums is permitted, provided the original author(s) and the copyright owner(s) are credited and that the original publication in this journal is cited, in accordance with accepted academic practice. No use, distribution or reproduction is permitted which does not comply with these terms.



# Extracellular Fluid Flow Induces Shallow Quiescence Through Physical and Biochemical Cues

Bi Liu<sup>1,2†</sup>, Xia Wang<sup>2,3†</sup>, Linan Jiang<sup>4\*</sup>, Jianhua Xu<sup>1</sup>, Yitshak Zohar<sup>4</sup> and Guang Yao<sup>2\*</sup>

<sup>1</sup>School of Pharmacy, Fujian Provincial Key Laboratory of Natural Medicine Pharmacology, Fujian Medical University, Fuzhou, China, <sup>2</sup>Department of Molecular and Cellular Biology, University of Arizona, Tucson, AZ, United States, <sup>3</sup>College of Animal Science and Technology, Northwest A&F University, Yangling, China, <sup>4</sup>Aerospace and Mechanical Engineering, University of Arizona, Tucson, AZ, United States

## OPEN ACCESS

### Edited by:

Weimin Li,  
Washington State University,  
United States

### Reviewed by:

Diane Alicia de Zélicourt,  
University of Zurich, Switzerland  
Taeko Kobayashi,  
Kyoto University, Japan

### \*Correspondence:

Linan Jiang  
jiangl@arizona.edu  
Guang Yao  
guangyao@arizona.edu

<sup>†</sup>These authors have contributed  
equally to this work

### Specialty section:

This article was submitted to  
Cell Growth and Division,  
a section of the journal  
Frontiers in Cell and Developmental  
Biology

**Received:** 11 October 2021

**Accepted:** 08 February 2022

**Published:** 24 February 2022

### Citation:

Liu B, Wang X, Jiang L, Xu J, Zohar Y  
and Yao G (2022) Extracellular Fluid  
Flow Induces Shallow Quiescence  
Through Physical and  
Biochemical Cues.  
Front. Cell Dev. Biol. 10:792719.  
doi: 10.3389/fcell.2022.792719

The balance between cell quiescence and proliferation is fundamental to tissue physiology and homeostasis. Recent studies have shown that quiescence is not a passive and homogeneous state but actively maintained and heterogeneous. These cellular characteristics associated with quiescence were observed primarily in cultured cells under a static medium. However, cells *in vivo* face different microenvironmental conditions, particularly, under interstitial fluid flows distributed through extracellular matrices. Interstitial fluid flow exerts shear stress on cells and matrix strain, and results in continuous replacement of extracellular factors. In this study, we analyzed individual cells under varying fluid flow rates in microfluidic devices. We found quiescence characteristics previously identified under conventional static medium, including serum signal-dependant quiescence entry and exit and time-dependant quiescence deepening, are also present under continuous fluid flow. Furthermore, increasing the flow rate drives cells to shallower quiescence and become more likely to reenter the cell cycle upon growth stimulation. This effect is due to flow-induced physical and biochemical cues. Specifically, increasing shear stress or extracellular factor replacement individually, without altering other parameters, results in shallow quiescence. We show our experimental results can be quantitatively explained by a mathematical model connecting extracellular fluid flow to an Rb-E2f bistable switch that regulates the quiescence-to-proliferation transition. Our findings uncover a previously unappreciated mechanism that likely underlies the heterogeneous responses of quiescent cells for tissue repair and regeneration in different physiological tissue microenvironments.

**Keywords:** cellular quiescence, quiescence depth, extracellular fluid flow, flow shear stress, extracellular factors, microenvironment, microfluidics, mathematical model

## INTRODUCTION

Quiescence is a dormant, non-proliferative cellular state. Quiescent cells, however, still maintain the potential to proliferate upon physiological signals, making them distinct from other dormant cells that are irreversibly arrested, such as those in senescence or terminal differentiation. Activating quiescent cells (e.g., adult stem and progenitor cells) to proliferate is fundamental to tissue homeostasis and repair (Coller et al., 2006; Wilson et al., 2008; Li and Clevers, 2010; Cheung and Rando, 2013). Quiescence has long been viewed as a passive cellular state lacking cell cycle

activity. Recent studies, however, have revealed that quiescence is rather actively maintained and highly heterogeneous (Coller et al., 2006; Sang et al., 2008; Cheung and Rando, 2013; Spencer et al., 2013; Wang et al., 2017).

The heterogeneity of quiescent cells in their proliferation potential can be described as a graded depth. Cells in deeper quiescence require stronger growth stimulation and take longer to exit quiescence and reenter the cell cycle than in shallower quiescence (Augenlicht and Baserga, 1974; Kwon et al., 2017; Fujimaki et al., 2019). Hepatocytes in older rats are an example of deeper quiescent cells, displaying a longer delay before reentering the cell cycle and reinitiating DNA replication following partial hepatectomy, as compared to those in younger rats (Bucher, 1963). Certain muscle and neural stem cells after tissue injury are examples of shallow quiescent cells, primed to reenter the cell cycle faster upon the next damage (Rodgers et al., 2014; Llorens-Bobadilla et al., 2015). The dysregulation of cellular quiescence depth can lead to disrupted tissue homeostasis, exhibiting either an insufficient number of growing cells due to an abnormally deep quiescence, or a depleted pool of quiescent stem and progenitor cells due to an abnormally shallow quiescence (Orford and Scadden, 2008; Cheung and Rando, 2013; Fujimaki and Yao, 2020).

Although dormant and non-proliferative, quiescent cells reside in and interact with dynamic microenvironments. A particular microenvironmental factor is the interstitial fluid flowing over tissue cells, which transports nutrients and other dissolved molecules that influence cellular activities (Jain, 1987; Swartz and Fleury, 2007; Freund et al., 2012; Yao et al., 2013). Interstitial flow also generates mechanical shear stress on cells, which affects cell morphology, migration, growth, and differentiation (Jain, 1987; Ng and Swartz, 2003; Tarbell et al., 2005; Swartz and Fleury, 2007; Polacheck et al., 2011; Shirure et al., 2017; Chen et al., 2019). To date, though, cellular quiescence has been mostly studied in cell cultures under static medium or in animal models without examining the effects of interstitial fluid flow. Whether and how extracellular fluid flow affects cellular quiescence remain largely unknown.

In this study, we examined the effects of extracellular fluid flow on cellular quiescence depth using a microfluidic system with a controllable medium flow rate. First, we found many quiescence characteristics previously observed in cell cultures under a static medium were also present in the microfluidic system under continuous medium flow. Furthermore, the medium flow affected cellular quiescence depth, and thus, the likelihood of cell cycle reentry upon growth stimulation. This result was further explained by the combined effect of flow-induced hydrodynamic shear stress and extracellular substance replacement. Lastly, the experimental results were integrated into a mathematic model that helps understand and predict how extracellular fluid flow modulates quiescence depth. To the best of our knowledge, this study is the first to characterize the effects of extracellular fluid flow on cellular quiescence, which could help better understand the heterogeneous response of quiescent cells for

tissue repair and regeneration in different physiological contexts of living tissues.

## MATERIAL AND METHODS

### Microfluidic Device Design and Fabrication

A microfluidic system was developed to study cellular quiescence under medium flow. To obtain sufficient numbers of cells for flow cytometry analyses, a microfluidic device was designed featuring a straight channel 420  $\mu\text{m}$  in height, 4 mm in width, and 4 cm in length. The microdevices, made of optically transparent polydimethylsiloxane (PDMS, Sylgard 184, Dow Corning Corporation, 3097358-1004), also allow real-time imaging of cells during experimentation.

The device fabrication process, illustrated in **Figure 1**, started with the fabrication of a master mold. The mold with features of microchannel patterns was made in an aluminum block using a computer numerical control (CNC) machine based on a 3D Computer-Aided Design (CAD). PDMS mixture, consisting of 10:1 base and curing agent, was poured onto the mold. After air bubble removal from the mixture under vacuum, the PDMS was cured at 55°C for 3 h. The cured PDMS substrate was then peeled off the mold with formed microchannel grooves (**Figure 1A**). After punching inlet and outlet holes at the two ends of a channel, the PDMS microchannel was bonded with a glass slide following oxygen plasma treatment of the bonding surfaces (**Figure 1B**). Next, a pair of inlet and outlet tubing adapters was assembled for each device to connect the microchannel to the external flow control system. The device fabrication and packaging were completed with incubation at 55°C for an hour to enhance the bonding strength (**Figure 1C**). Prior to experiments, the microfluidic devices were sterilized by flowing ethanol through the microchannels, followed by UV irradiation for 1 h inside a biosafety hood. The inner surfaces of the microchannel were coated with 2% (w/w) fibronectin to enhance the adhesion of cells to the bottom surface.

### Flow Rate and Flow-Induced Shear Stress

The total volume of medium in a microdevice (including tubing at the inlet/outlet of the channel but not connectors, **Figure 1C**) is approximately 140  $\mu\text{L}$ , and the medium volume in the microfluidic channel alone is about 67  $\mu\text{L}$ . In this study, a continuous medium flow with a fixed flow rate (5 or 20  $\mu\text{L}/\text{h}$ ) was fed into the channel to mimic the typical interstitial flow velocity in soft tissues (Swartz and Fleury, 2007) unless otherwise noted. Correspondingly, the flow rate, rather than the priming volume, is used to characterize the flow effect. We also consider the concentration of the bulk fluid is uniform spatially, and local diffusion and convection at the interfaces between the fluid and cells can be neglected.

Pressure-driven flow in a microchannel presents a non-uniform velocity profile, which gives rise to shear stress. The shear stress for a Newtonian fluid is directly proportional to the product of the velocity gradient and fluid viscosity. Assuming a 2-D parabolic velocity profile in a microchannel with a rectangular



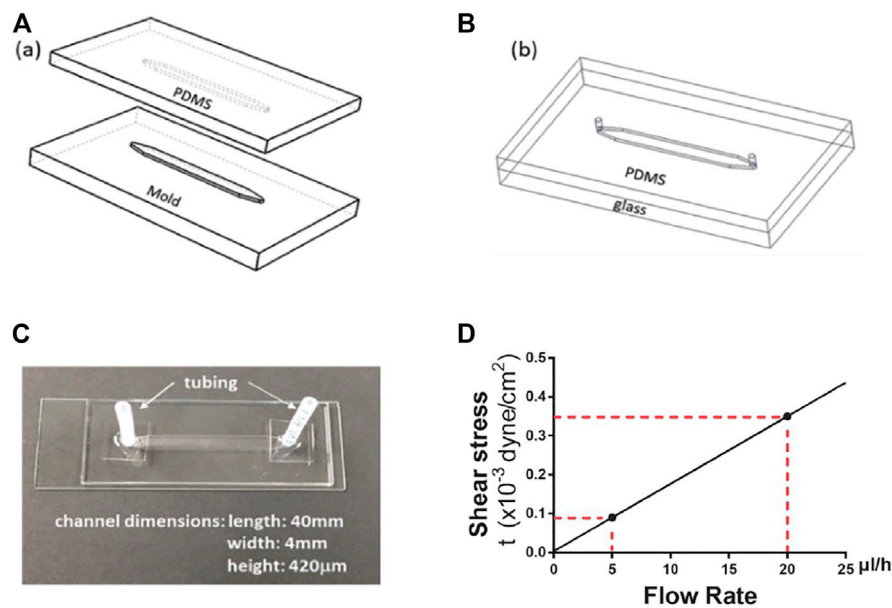


**FIGURE 1 |** Microdevice fabrication and dimensions. **(A)** aluminum mold and PDMS replicate. **(B)** PDMS microchannel bond onto a glass slide. **(C)** A microfluidic device with the microchannel dimensions. **(D)** The linear dependence of wall shear stress on fluid flow rate. The red dotted lines indicate the wall shear stress levels at the flow rates of 5 and 20 μl/h, respectively.

**TABLE 1 |** Flow-induced shear stress in medium containing varying dextran concentrations.

Dextran concentration (mg/ml)	Viscosity (cP)	Wall shear stress at 5 μl/h flow rate (10 <sup>-3</sup> dyne/cm <sup>2</sup> )	Wall shear stress at 20 μl/h flow rate (10 <sup>-3</sup> dyne/cm <sup>2</sup> )
0	0.73	0.09	0.35
25	1.95	0.23	0.93
50	4.64	0.55	2.20
100	23.78	2.82	11.28

cross-section, the wall shear stress,  $\tau_w$ , experienced by cells attached on the bottom surface of the microchannel, is given by:

$$\tau_w = \frac{6\mu Q}{WH^2} \quad (1)$$

where  $W$  and  $H$  are the microchannel width and height, respectively,  $\mu$  is the fluid viscosity, and  $Q$  is the volumetric flow rate. For a fixed medium viscosity, estimated to be  $\mu = 0.73$  cP at 37°C, and given the microchannel dimensions,  $W = 4$  mm and  $H = 420$  μm, the shear stress is linearly proportional to the fluid flow rate. Thus, the two flow rates used in this study,  $Q = 5$  and 20 μl/h, correspond to shear stress values  $\tau_w = 0.09 \times 10^{-3}$  and  $0.35 \times 10^{-3}$  dyne/cm<sup>2</sup>, respectively (Figure 1D).

In Eq. 1, for a fixed flow rate and microchannel dimensions, wall shear stress is linearly proportional to the medium viscosity. Dextran (Sigma, D5251; ~ 500,000 average molecular weight) was dissolved in the medium in various final concentrations to obtain correspondingly various medium viscosities. Table 1 summarizes the resultant dextran-containing medium concentrations,

viscosity at 37°C, and corresponding shear stress values for the two flow rates (Carrasco et al., 1989).

## Cell Culture

REF/E23 cells used in this work were derived from rat embryonic fibroblasts REF52 cells as a single-cell clone containing a stably integrated E2f1 promoter-driven destabilized GFP reporter (E2f-GFP for short), as previously described (Yao et al., 2008). Cells were maintained at 37°C with 5% CO<sub>2</sub> in the growth medium: DMEM (Coring, 15013-CV supplemented with 2x Glutamax (Gibco, 35050)) containing 10% bovine growth serum BGS (HyClone, SH30541.03).

## Quiescence Depth Measurement Under Extracellular Fluid Flow

To induce cellular quiescence, growing cells were trypsinized (Coring, 25052-CI), and 70 μl of cell suspension (0.6 million cells/ml) was seeded into a microfluidic channel; after cell

attachment on the bottom surface of the channel overnight, growth medium inside the channel was replaced by a continuous flow of serum-starvation medium (0.02% BGS in DMEM) at a designated flow rate controlled by a programmable syringe pump (Harvard PHD 2000). Cell morphologies were found comparable across the flow rate range (0–20  $\mu\text{l/h}$ ) (**Supplementary Figure S1A**). To induce quiescence exit, following serum starvation, the microdevice was disconnected from the flow-feeding setup (syringe and pump), and serum-stimulation medium (1–4% BGS in DMEM) was gently flowed into the micro-chamber using a pipette and a tip at the inlet tubing of the device. The medium change step is fast (<1 min for 140  $\mu\text{l}$  medium) and identical to all quiescent cell groups, avoiding the bias in the exposure time of cells to the stimulation medium (if otherwise using slow flows at different flow rates, 5 or 20  $\mu\text{l/h}$ ). Cells were then incubated with serum-stimulation medium at static condition (again, identical to all quiescent cell groups). After 26 h of serum stimulation, cells inside the channel were harvested, and the intensities of E2f-GFP signals from individual cells were measured using a flow cytometer (BD LSR II). Flow cytometry data were analyzed using FlowJo software (version 10.0).

The percentage of cells with the E2f at the “On” state (E2f-On %) in a cell population after serum stimulation was used as an index for quiescence depth before stimulation: the smaller the E2f-On%, the deeper the quiescence depth prior to serum stimulation (Kwon et al., 2017). Consistent with our previous studies in static-medium experiments (Kwon et al., 2017; Wang et al., 2017; Fujimaki et al., 2019), E2f-On% was found comparable to the percentage of cells with EdU incorporation (EdU+) in the microfluidic experiments under continuous flows (**Supplementary Figures S1B,C**). In the EdU incorporation assay, 1  $\mu\text{M}$  EdU was added to the serum-stimulation medium at 0 h, and the EdU signal intensity was measured 30 h after serum stimulation by the Click-iT EdU assay following the manufacturer’s protocol (ThermoFisher, C10634).

## Mathematical Modeling and Stochastic Simulations

To account for the effects of extracellular fluid flow on quiescence depth, the fluid flow-associated terms were added to the serum response terms in our previously established Rb-E2F bistable switch model (**Supplementary Table S1**) (Yao et al., 2008). Based on the resultant ordinary differential equation (ODE) framework (**Supplementary Table S1**), a Langevin-type stochastic differential equation (SDE) model was constructed as follows (Gillespie, 2000; Lee et al., 2010):

$$X_i(t + \tau) = X_i(t) + \sum_{j=1}^M v_{ji} a_j [X(t)] \tau + \theta \sum_{j=1}^M v_{ji} (a_j [X(t)] \tau)^{1/2} \gamma + \delta \omega \tau^{1/2} \quad (2)$$

where the first two terms on the right account for deterministic kinetics, and the third and fourth terms represent intrinsic and

extrinsic noise, respectively.  $X(t) = (X_1(t), \dots, X_n(t))$  is the system state at time  $t$ .  $X_i(t)$  is the molecule number of species  $i$  ( $i = 1, \dots, n$ ) at time  $t$ . The time evolution of the system is measured based on the rates  $a_j[X(t)]$  ( $j = 1, \dots, M$ ) with the corresponding change of molecule number  $j$  described in  $v_{ji}$ . Factors  $\gamma$  and  $\omega$  are two independent and uncorrelated Gaussian noises. Scaling factors  $\theta$  and  $\delta$  are implemented for the adjustment of intrinsic and extrinsic noise levels, respectively (unless otherwise noted,  $\theta = 0.4$ ,  $\delta = 40$ , as selected to be consistent with the experimental data presented in **Figure 3**). Units of model parameters and species concentrations (**Supplementary Table S2**) in the ODE model were converted to molecule numbers. The E2f-On state was defined as the E2f molecule number at the 26th h after serum stimulation reaching beyond a threshold value of 300. All SDEs were implemented and solved in Matlab.

## RESULTS

### Quiescence Induction and Deepening Over Time are Consistent With or Without Medium Flow

To test whether and how extracellular fluid flow affects cellular quiescence, we cultured REF/E23 cells in microfluidic devices under medium flow (**Figure 1**). Two flow rates ( $Q = 5$  and  $20 \mu\text{l/h}$ ) were used in this study; they generated average velocities of 0.82 and  $3.33 \mu\text{m/s}$  on the microfluidic platform, respectively, which are on the order of typical interstitial flow velocity in soft tissues (Swartz and Fleury, 2007). Cells were seeded in microfluidic devices, and cell quiescence and proliferation status were assessed using a previously established and stably integrated E2f-GFP reporter (Yao et al., 2008), which was validated by standard EdU-incorporation assay in regular cell cultures (Kwon et al., 2017; Wang et al., 2017; Fujimaki et al., 2019) as well as here on the microfluidic platform (**Supplementary Figures S1B,C**; see Methods).

To induce quiescence, cells in microfluidic devices were cultured in serum-starvation medium (0.02% serum) for 4 days under a given extracellular fluid flow (5 or  $20 \mu\text{l/h}$ ). In these conditions, about 95% of cells or more entered quiescence (**Figures 2A,B**, 0.02% serum, 4-days), as indicated by the Off-state of the E2f-GFP reporter (E2f-Off for short, the lower/left mode of the E2f-GFP histograms in **Figure 2**). Quiescent cells were subsequently stimulated to reenter the cell cycle with serum at varying concentrations (without flow, see Methods for details). Cells were harvested after 26 h of serum stimulation, and the E2f-GFP reporter activity was measured by flow cytometry. With increasing serum concentrations (0.02–4% serum, 4 days, **Figure 2**), higher percentages of cells exited quiescence and reentered the cell cycle, as indicated by the On-state of the E2f-GFP reporter (E2f-On for short, the higher/right mode of the E2f-GFP histograms in **Figure 2**). The observations that cells entered quiescence upon serum deprivation under an extracellular fluid flow and then reentered the cell cycle upon

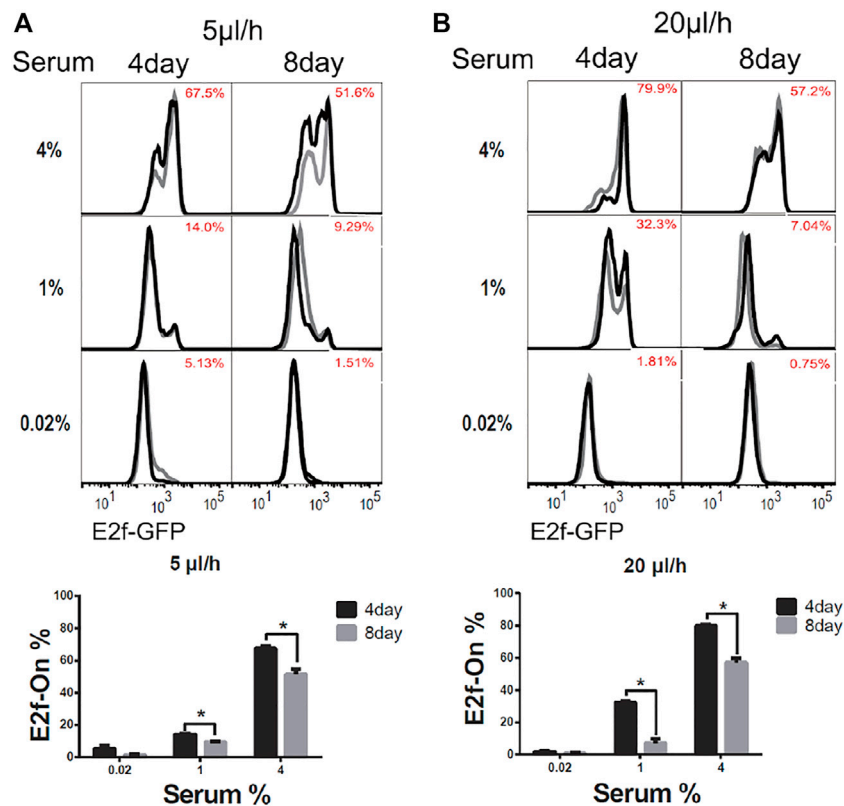


**FIGURE 2 |** Longer-term serum starvation under extracellular fluid flow leads to deeper quiescence. REF/E23 cells seeded in microfluidic devices were induced to and maintained in quiescence by culturing them in serum-starvation medium for either 4 or 8 days under the medium flow rates of 5 µl/h (A) and 20 µl/h (B). Cells were subsequently stimulated with serum at the indicated concentrations for 26 h, and the E2f-On% were assayed. (Top) E2f-GFP histograms with red numbers indicating the average E2f-On% (the areas below the right “peaks” of the bimodal histograms; same below) from duplicate samples (black and grey). (Bottom) Statistic bar chart of the E2f-On% in cell populations (from the top) as a function of serum-starvation duration and serum concentration in serum-stimulation. Error bars, SEM ( $n = 2$ ),  $*p < 0.05$ .

serum stimulation are consistent with the cell behaviors in conventional static medium (Coller et al., 2006; Yao et al., 2008).

We next compared cells induced to quiescence by 8 vs. 4 days of serum starvation in the presence of extracellular fluid flow. Previous work, including ours, showed that cells moved into deeper quiescence when they remained quiescent for longer durations in conventional static-medium cell cultures (Augenlicht and Baserga, 1974; Owen et al., 1989; Kwon et al., 2017; Fujimaki et al., 2019). One may wonder, however, whether this phenotype was caused by the gradual depletion of nutrients in the static culture medium *in vitro*, which may behave differently *in vivo* under an interstitial fluid flow replenishing nutrients. In the microfluidic platform under a constant fluid flow (either 5 or 20 µl/h) during serum starvation, we found cells that remained quiescent for a longer period of time (8 days) entered a deeper quiescent state and became less likely to exit: they had a smaller E2f-On% upon a given serum stimulation than those that remained quiescent for a shorter time (4 days, **Figure 2**). Together, these results showed that cellular behaviors in 1) serum signal-dependant quiescence entry and exit and 2) quiescence deepening over time are consistent regardless

whether cells are in microfluidic devices exposed to extracellular fluid flows or in conventional static-medium cultures.

## Fast Extracellular Fluid Flow Results in Shallow Quiescence

To examine whether and how extracellular fluid flow may affect cellular quiescence depth, we compared the cells induced to quiescence by serum starvation under different medium flow rates but otherwise in the same conditions. Specifically, cells in microfluidic devices were cultured in serum-starvation medium (0.02% serum) for 4 days under an extracellular fluid flow (0, 5, or 20 µl/h); serum-starvation medium was then replaced by serum-stimulation medium (1–4% serum) using a pipette—this medium change procedure in each microfluidic device was completed within 1 min (compared to otherwise more than 20 and 5 h under a pump-driven slow flow of 5 and 20 µl/h, respectively); cells were then cultured in static medium during serum stimulation. This identical serum-stimulation condition was applied in this study (see Methods for details), so that the subsequent cell cycle reenter

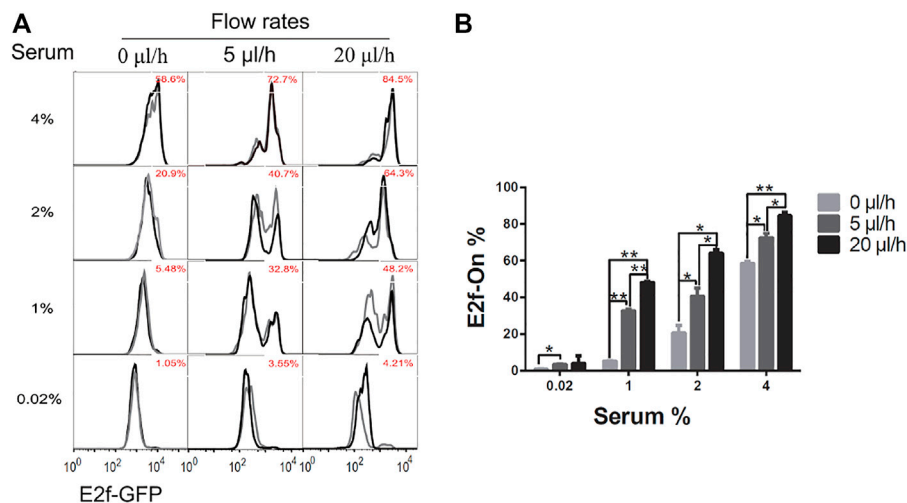


**FIGURE 3 |** Higher extracellular medium flow rates lead to shallower quiescence. REF/E23 cells seeded in microfluidic devices were induced to and maintained in quiescence by culturing them in serum-starvation medium for 4 days under various medium flow rates as indicated. Cells were then stimulated with serum at the indicated concentrations for 26 h, and the E2f-GFP signals were measured using flow cytometry. **(A)** The E2f-GFP histograms. Numbers in red indicate the average percentages of cells with E2f-GFP at the “On” state (see **Supplementary Figure S1D** for examples) based on duplicate samples (black and grey histograms). **(B)** Statistic bar chart of the E2f-On% in cell populations (from A) as a function of medium flow rate (in serum-starvation) and serum concentration (in serum-stimulation). Error bars, SEM ( $n = 2$ ), \* $p < 0.05$ , \*\* $p < 0.01$  (1-tailed t-test; the same below).

and thus the assessment of quiescence depth were not biased by different effective exposure time of cells to the serum-stimulation medium (if the medium was fed by different pump-driven flows) and thus comparable across different quiescent cell groups (which were induced by serum starvation under different medium flow rates).

Upon serum stimulation (with 1, 2, or 4% serum), the fraction of cells reentering the cell cycle from quiescence, as indicated by E2f-On% in **Figure 3**, were positively correlated with the medium flow rate applied to cells during quiescence induction (serum starvation). These results suggest that a higher extracellular fluid flow rate leads to shallower quiescence, from which cells are more likely to reenter the cell cycle upon stimulation.

## Mechanical Shear Stress Drives Shallow Quiescence

Fluid flow introduces two types of cues to cells: 1) hydrodynamic shear stress (physical cue), and 2) continuous replenishment of nutrients and other compounds dissolved in the fluid and removal of local cell-secreted substances (collectively as extracellular factor replacement; biochemical cue). To determine whether these physical and biochemical cues act agonistically or antagonistically (thereby potentiating or attenuating the combined effect) in affecting cellular quiescence depth, we next conducted experiments to delineate the effect of each of the two cues.

To isolate the effect of mechanical shear stress from that of extracellular factor replacement on cellular quiescence depth, the viscosity of the culture medium was varied while its flow rate (and thus the pace of extracellular fluid replacement) was maintained at a constant level. The flow-induced shear stress is linearly

proportional to the viscosity of working fluid (**Eq. 1**), which can be manipulated by varying the amount of high-molecular-weight dextran dissolved in the medium (**Table 1**).

Accordingly, REF/E23 cells were first induced to quiescence by culturing them in the serum-starvation medium containing 0, 25, 50, or 100 mg/ml high molecular weight ( $\sim 500,000$ ) dextran, respectively, for 4 days under 5 or 20  $\mu\text{l/h}$  flow rate. The cells were then stimulated with 2% or 4% serum for 26 h, and the fraction of cells that exited quiescence (E2f-On%) was measured. As shown in **Figures 4A,B**, E2f-On% increased with increasing dextran concentration in the serum-starvation medium under either 5 or 20  $\mu\text{l/h}$  flow rate. By contrast, cells cultured in static serum-starvation medium containing the same higher dextran concentration entered deeper rather than shallower quiescence (**Supplementary Figure S2**; see Discussion). These results suggest that the dextran-induced shallow quiescence in the presence of extracellular fluid flow was primarily due to the viscosity-dependent shear stress (instead of other dextran-associated effects such as being a metabolic source). The higher dextran concentration, thus higher viscosity, of the medium flow generates higher shear stress under a continuous flow rate (5 or 20  $\mu\text{l/h}$ , see **Table 1**; but not static 0  $\mu\text{l/h}$ ). Put together, our results showed that increasing only the fluid flow shear stress, while keeping the same flow rate and pace of extracellular factor replacement, leads to shallower quiescence.

## Extracellular Factor Replacement Drives Shallow Quiescence

The effect of continuous extracellular factor replacement on cellular quiescence depth was examined next. Some of the extracellular factors (such as nutrients) are expected to



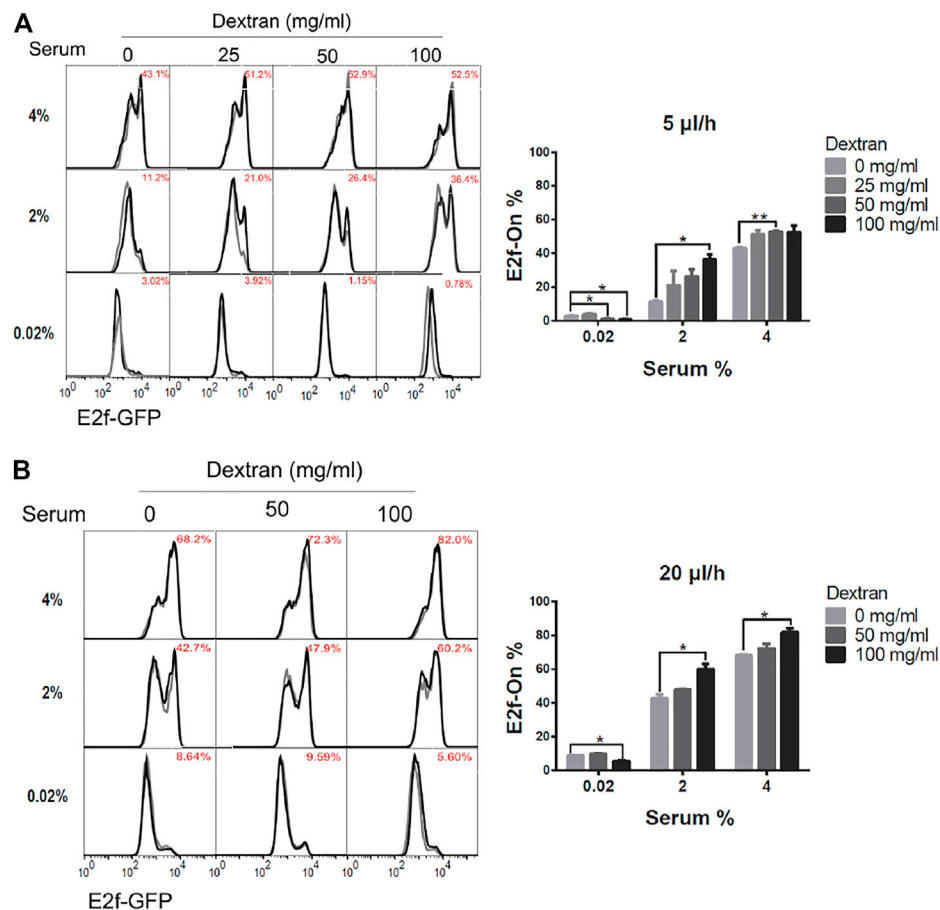


**FIGURE 4 |** Higher shear stress leads to shallower quiescence. REF/E23 cells seeded in microfluidic devices were induced to and maintained in quiescence by culturing them in serum-starvation medium for 4 days under the flow rates of 5 µl/h (A) and 20 µl/h (B). Dextran at the indicated concentrations was dissolved in the serum-starvation medium. Cells were subsequently stimulated with serum at the indicated concentrations for 26 h, and the E2f-On% were assayed. (Left) E2f-GFP histograms with red numbers indicating the average E2f-On% from duplicate samples (black and grey). (Right) Statistic bar chart of the E2f-On% in cell populations (from the left) as a function of dextran concentration (in serum-starvation) and serum concentration (in serum-stimulation). Error bars, SEM ( $n = 2$ ), \* $p < 0.05$ , \*\* $p < 0.01$ .

facilitate quiescence exit and cell cycle reentry, while others may play inhibitory roles (such as certain extracellular matrix (ECM) factors secreted by fibroblasts). To assess the net effect of extracellular factor replacement, while decoupling it from the effect of mechanical shear stress, we set up two test configurations. In the first “recycled-medium” configuration, a total fluid volume of either  $V = 120$  or  $480$  µl oscillated back-and-forth through the microchannel at a constant flow rate of either  $Q = 5$  or  $20$  µl/h, respectively. Thus, when the flow direction was switched every 24 h, the complete fluid volume  $V$  passed through the microchannel once. In the second “fresh-medium” configuration, the fluid oscillated exactly as in the first configuration, but fresh medium of volume  $V$  was supplied to replace previous medium at each flow direction switch. In both the recycled-medium and fresh-medium experiments, cells were serum-starved for 4 days at a given flow rate  $Q$  (5 or 20 µl/h) and subsequently stimulated with serum (1 and 2%, respectively) for 26 h.

The quiescence depth measurements are shown in **Figure 5**. The fractions of cells exiting quiescence and reentering cell cycle

(E2f-On%) were significantly higher in “fresh-medium” than in “recycled-medium” at a given serum stimulation condition. These results were obtained at the same flow rate (either 5 or 20 µl/h) and thus under the same mechanical shear stress. The difference that the cells experienced was medium replacement: once per 24 h during the 4-days serum-starvation in the fresh-medium configuration, whereas no medium replacement during the same period in the recycled-medium configuration. These results suggest that with the flow rate and shear stress being equal, extracellular factor replacement alone (as in “fresh-medium”) induces shallower quiescence than without such a replacement (as in “recycled-medium”).

## A Dynamic Model of Extracellular Fluid Flow Regulating Quiescence Depth

We next sought to develop a mathematical model to gain potential mechanistic insight into the effects of extracellular fluid flow on cellular quiescence depth. Previously, we have shown that the Rb-E2f pathway functions as a bistable gene-

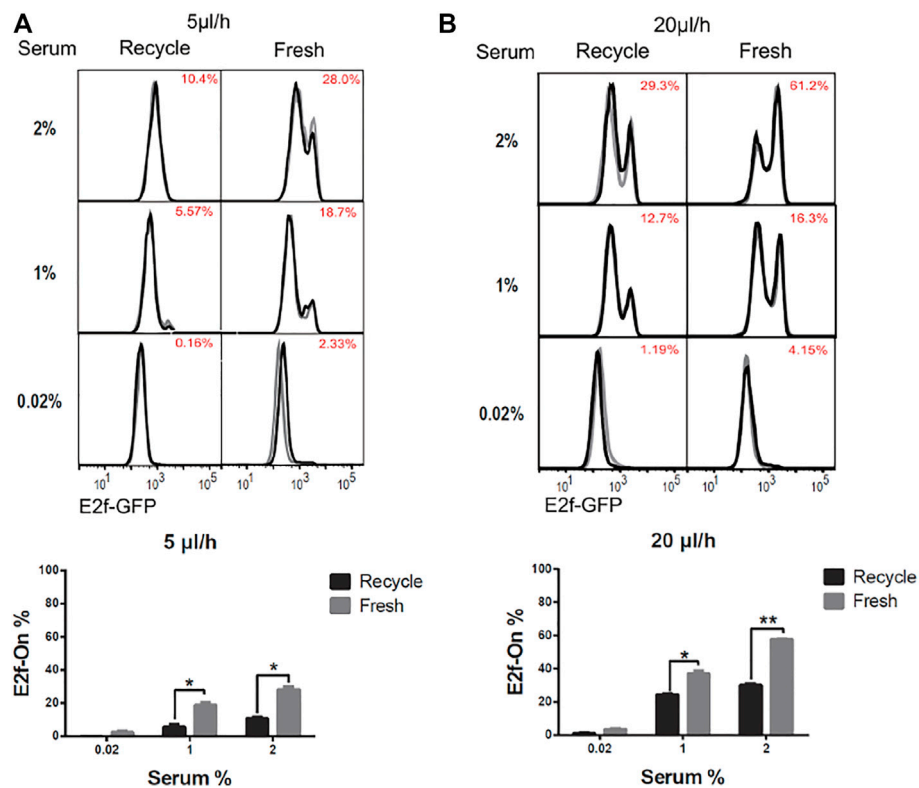


**FIGURE 5 |** Extracellular factor replacement drive cells to shallow quiescence. REF/E23 cells seeded in microfluidic devices were induced to and maintained in quiescence by culturing them in serum-starvation medium for 4 days under the flow rates of 5  $\mu\text{l/h}$  (A) and 20  $\mu\text{l/h}$  (B). During this period, the flow direction was switched every 24 h, after a complete volume of medium ( $V = 120$  and  $480 \mu\text{l}$ , respectively, for  $r = 5$  and  $20 \mu\text{l/h}$ ) passed through the microchannel; the previous medium (“recycled”) or a fresh medium (“fresh”) of volume  $V$  was used to continue the flow experiment in the microfluidic device. Cells were subsequently stimulated with serum at the indicated concentrations for 26 h, and the E2f-On% were assayed. (Top) E2f-GFP histograms with red numbers indicating the average E2f-On% from duplicate samples (black and grey). (Bottom) Statistic bar chart of the E2f-On% in cell populations (from the top) as a function of extracellular fluid replacement configuration (in serum-starvation) and serum concentration (in serum-stimulation). Error bars, SEM ( $n = 2$ ), \* $p < 0.05$ , \*\* $p < 0.01$ .

network switch that converts graded and transient serum growth signals into an all-or-none transition from quiescence to proliferation (Yao et al., 2008; Yao et al., 2011). Specifically, the minimum serum concentration required to activate this Rb-E2f bistable switch (the E2f-activation threshold for short) determines quiescence depth (Yao, 2014; Kwon et al., 2017). The experimental results in this study suggested that extracellular fluid flow generates or changes physical (mechanical shear stress) and biochemical (extracellular substances) cues that drive cells to shallow quiescence. We hypothesized that these flow-associated cues boost the cellular responses to serum growth signals and thereby reduce the serum level required to activate the Rb-E2f bistable switch, which results in shallow quiescence.

Accordingly, our previously established mathematical model of the Rb-E2f bistable switch (Yao et al., 2008) was extended, incorporating the extracellular fluid flow effects (FR) into the serum signal terms in the governing ordinary differential equations (ODEs) (Supplementary Table S1). The augmented model was utilized to simulate the responses (E2f-On or -Off) of cells to serum stimulation under the influence of extracellular fluid flow varying in rate. The simulations were carried out following the chemical Langevin formulation of the ODE

framework, which considered both intrinsic and extrinsic noise in the system (see Methods for detail), and the results are shown in Figure 6.

A direct comparison between Figure 3B and Figure 6A demonstrates that the simulation results, based on the fluid flow-incorporated Rb-E2f bistable switch model, are qualitatively and quantitatively in good agreement with the experimental measurements. This finding supports our hypothesis regarding how extracellular fluid flow may sensitize cells to serum growth signals and activate the Rb-E2f bistable switch, and thus, reduces quiescence depth. Simulation results further show that the effect of extracellular fluid flow is more pronounced than that of mechanical shear stress alone in promoting quiescence exit (E2f-On%, Figure 6B). The “delta” between the two curves (orange minus blue) presumably reflects the effect of extracellular factor replacement in reducing quiescence depth (dotted grey curve, Figure 6B); this effect also increases with a higher flow rate (thus, an increasing pace of fluid replacement). Although how shear stress and extracellular factor replacement promote quiescence exit is unknown, taking a simple assumption that shear stress and extracellular factor replacement alone effectively corresponds to a portion (0.75

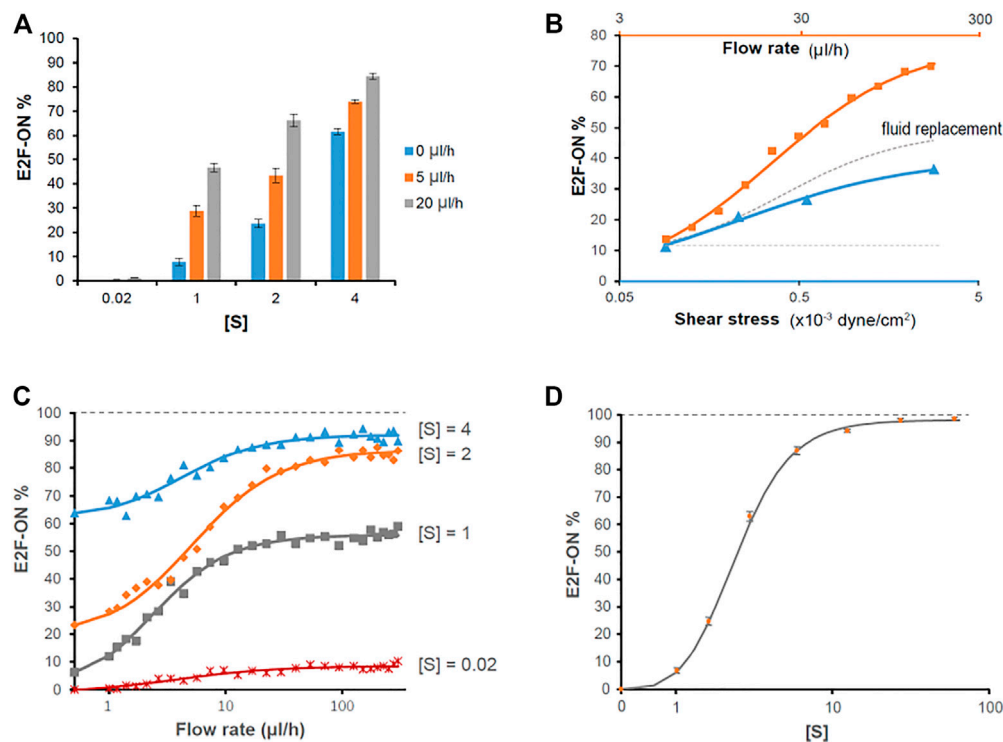


**FIGURE 6 |** Simulation results on the effects of extracellular fluid flow on quiescence depth. **(A, C, D)** Simulated cell responses to serum stimulation using the fluid flow-incorporated Rb-E2f bistable switch model. Serum starvation-induced quiescent cells, under the influence of extracellular fluid flow at the indicated rates **(A, C)** or without fluid flow **(D)**, were stimulated with serum at indicated concentrations [S]. The average E2f-On% from five sets of stochastic simulations (200 runs each) is shown for each condition. Error bars in A and D, SEM ( $n = 5$ ). **(B)** The effects of fluid flow rate (orange), mechanical shear stress (blue), and extracellular factor replacement (gray) on quiescence depth. Blue triangle, the average E2f-On% in response to 2% serum stimulation, in cells under 5 µl/h extracellular fluid flow with the indicated shear stress level during serum starvation (based on **Figure 4A** and **Table 1**). Orange square, the average E2f-On% calculated from five sets of stochastic simulations in response to 2% serum stimulation under the influence of the indicated fluid flow rate. Parameters used in this simulation ( $\theta = 0.3$ ,  $\delta = 32$ ) were determined to fit the simulated E2f-On% to the experimental results shown in **Figure 4A** (at 5 µl/h medium flow rate with 0 mg/ml dextran). The values of flow rate in the orange curve and the corresponding values of shear stress in the blue curve are related based on **Eq. 1**. The dotted gray curve represents the "delta" between the orange and blue curves; the dotted horizontal line is for the guide of eye extending from the initial data point (5 µl/h). **(B–D)** Each solid curve represents the best fit of data points to a Hill function.

and 0.85, respectively) of the extracellular fluid flow term FR in the model (**Supplementary Table S1**), the simulation results are reasonably (although not perfectly) consistent with the experimental observations (regarding the shear stress effects, **Supplementary Figure S3**). Together, our modeling and experimental results suggest that the flow-induced shear stress (physical cue) and replacement of extracellular factors (biochemical cues) contribute agnostically to the effect of extracellular fluid flow in promoting quiescence exit by lowering the activation threshold of the Rb-E2f bistable switch.

The good agreement between simulations and experiments motivated the application of the model for predicting the cell responses to higher fluid flow rates above 20 µl/h, under which cells started to partially detach from the microchannel bottom surface and hence excluded from the current experimental study. The simulation results show that the additive effect of extracellular fluid flow to a given serum signal on quiescence exit (E2f-On%) can be well fitted with a Hill function (**Figure 6C**). Namely, E2f-On% increases monotonically with increasing flow rate but is asymptotically bound by a serum concentration-

dependent level. By contrast, with sufficiently high serum concentration, the entire cell population can exit quiescence (i.e., E2f-On% approaches 100%) in our model even without extracellular fluid flow (**Figure 6D**). This latter result is consistent with what we experimentally observed previously in REF/E23 cells under static medium (Yao et al., 2008; Kwon et al., 2017; Fujimaki et al., 2019). Therefore, it appears that extracellular fluid flow facilitates quiescence exit by reducing the E2f-activation serum threshold, but unlikely to fully replace the role of serum growth factors in this process.

## DISCUSSION

Quiescence is a reversible cellular dormancy state that can persist over prolonged periods of time. The on-demand reactivation of quiescent cells to divide serves as the basis for tissue homeostasis and repair (Coller et al., 2006; Wilson et al., 2008; Cheung and Rando, 2013). Thus far, characteristics of cellular quiescence have been mostly

studied and discovered in conventional static-medium cell cultures, including the basic approaches applied to induce quiescence entry (e.g., serum deprivation, contact inhibition, and loss of adhesion) and exit (by reverting the aforementioned inducing signals). The microenvironment experienced by cultured cells under static medium, however, is different from that experienced by tissue cells *in vivo* where they are exposed to continuous interstitial fluid flows. The interstitial flow exerts hydrodynamic shear stress on cells due to fluid flow viscosity and shear strain rate; the flow also carries fresh nutrients along with dissolved compounds and removes local substances secreted by cells (Jain, 1987; Wiig, 1990; Wang and Tarbell, 1995; Ng and Swartz, 2003; Swartz and Fleury, 2007; Shi and Tarbell, 2011; Freund et al., 2012; Galie et al., 2012). As such, extracellular fluid flow is known to play a critical role in repairing and remodeling tissues, such as the vascular, lung, and bone (Hillsley and Frangos, 1994; Liu et al., 1999; Louis et al., 2006; Rensen et al., 2007), through affecting cell morphology, adhesion, motility, metabolism, and differentiation (Yamamoto et al., 2005; Lutolf et al., 2009; Toh and Voldman, 2011; Hyler et al., 2018; Chen et al., 2019). However, whether and how extracellular fluid flow affects cellular quiescence remains unclear.

In this study, a microfluidic platform is designed to mimic the physiologically relevant interstitial fluid flow with varying rates (**Figure 1**) and investigate the flow effects on cellular quiescence. Experimental parameters, including flow rate, fluid viscosity, and flow volume, were varied to test the effects of flow rate, shear stress, and extracellular factor replacement on cellular quiescence depth.

Our results show that, first, several quiescence characteristics identified previously under static medium are also present under continuous fluid flow, including the serum signal-dependant quiescence entry and exit and the time-dependant quiescence deepening (**Figure 2**). Second, extracellular fluid flow sensitizes cells to serum growth signals and thus leads to shallow quiescence. Particularly, increasing the fluid flow rate reduces the serum level needed for quiescence exit and cell cycle reentry. This result is likely due to the extracellular fluid flow lowering the activation threshold of the Rb-E2f bistable switch that controls the quiescence-to-proliferation transition (Yao et al., 2008; Kwon et al., 2017), as suggested by our model simulations (**Figure 6**). A higher fluid flow rate entails higher mechanical shear stress and a faster pace of extracellular factor replacement. These physical and biochemical cues are able to drive cells into shallow quiescence when present either together (**Figure 3**) or separately (**Figures 4, 5**). As a result, exposed to a faster extracellular fluid flow, cells become more sensitive to serum growth signals and more likely to reenter the cell cycle.

Several questions are left unanswered in our study. First, the molecular mechanisms are to be identified by which flow-induced shear stress and extracellular factor replacement lower the activation threshold of the Rb-E2f bistable switch. Interestingly, increasing medium viscosity (by a higher dextran concentration) promotes quiescence exit under a medium flow (**Figure 4**), but it inhibits quiescence exit in static medium (**Supplementary Figure S2**). This result may be associated

with medium viscosity-induced changes in certain lipoprotein synthesis (Yedgar et al., 1982), cytoskeleton and cell morphology (Khorshid, 2005), cell attachment and inflammation (Rouleau et al., 2010), or other cellular activities that inhibit quiescence exit in static medium. These changes, if also present under continuous medium flow, appear to be surpassed by the effects of shear stress that promote quiescence exit. The exact mechanism needs to be investigated in future studies. Additionally, quiescent cells cultured in the microfluidic device appear to be generally deeper in quiescence than those cultured in well plates under otherwise the same conditions (e.g., comparing the E2f-On% upon 2% serum stimulation in microdevice (**Figure 3**) and that in the comparable condition in well plate (**Supplementary Figure S2**), both being in static medium, 0  $\mu$ l/h, and without added dextran). We speculate this difference may be due to the different surfaces that cells were attached to (glass in the microchannel *versus* plastic in the well plate), or different medium height (<0.5 mm in the microchannel *versus* 3–4 mm in the well plate) that could result in different nutrient/factor availability, gas/heat exchange etc., or both. The exact mechanism needs to be further investigated. Nevertheless, the current study demonstrated, for the first time to our best knowledge, the direct effects of extracellular fluid flow and its corresponding components (shear stress and extracellular factor replacement) on cell quiescence depth.

Individual quiescent cells *in vivo*, including stem and progenitor cells in their tissue niches, experience interstitial fluid flows with varying rates and viscosities depending on local tissue structures and distances from nearby blood vessels. The flow-driven heterogeneity in cellular quiescence depth, as demonstrated in this study, may shed light on the heterogeneous responses of quiescent cells in tissue repair and regeneration in different physiological contexts of living tissues.

## DATA AVAILABILITY STATEMENT

The original contributions presented in the study are included in the article/**Supplementary Material**, further inquiries can be directed to the corresponding authors.

## AUTHOR CONTRIBUTIONS

BL, LJ, JX, YZ, and GY designed research; BL performed experiments; XW performed mathematical modeling and simulation; LJ designed, fabricated, and configured the microfluidic system; BL, LJ, and GY analyzed data; BL, YZ, LJ, and GY wrote the paper.

## FUNDING

This work was supported by grants from the NSF of USA (#2016035 and #3038431 to GY), the Startup Fund for scientific research of Fujian Medical University (#2017XQ2016 to BL), and the NSF of China (#31500676 to XW).



## ACKNOWLEDGMENTS

We thank the Foundation for Scholarly Exchange of Fujian Medical University for sponsoring BL.

## SUPPLEMENTARY MATERIAL

The Supplementary Material for this article can be found online at: <https://www.frontiersin.org/articles/10.3389/fcell.2022.792719/full#supplementary-material>

**Supplementary Figure S1** | Experimental system configuration and validation. (A) Cell morphology under varying medium flow rates. REF/E23 cells seeded in microfluidic devices were induced to and maintained in quiescence by culturing them in serum-starvation medium for 4 days under the indicated flow rates, then either remained in quiescence (0.02% serum) or stimulated with serum at the indicated concentrations (1–4%) for 26 hours. Phase-contrast images were taken with a 20x objective lens. (B, C) E2f-GFP and EdU-incorporation readouts of cellular quiescence and cell cycle reentry. REF/E23 cells were induced to quiescence as in (A) under a medium flow rate of 5  $\mu\text{L/h}$  (B) or 20  $\mu\text{L/h}$  (C), and then stimulated with serum at the indicated concentrations. Cells were harvested after 26 and 30 hours of simulation, respectively, for E2f-GFP and EdU assays. (Left) Numbers in red indicate the

average E2f-On% or EdU+% as indicated from duplicate samples (black and grey histograms). (Right) Statistic bar chart of E2f-On% and EdU+% from the left-panel histograms. Error bars, SEM ( $n = 2$ ), \*  $p < 0.05$ , \*\*  $p < 0.01$ , \*\*\*  $p < 0.001$ . (D) Dot plots of Fig 3A. Y-axis, forward-scatter; x-axis, E2f-GFP.

**Supplementary Figure S2** | The effect of varying dextran concentrations on quiescence depth in static culture. REF/E23 cells were induced to and maintained in quiescence by culturing them in static serum-starvation medium (in well plate) for 4 days with dextran at the indicated concentrations. Cells were subsequently stimulated with serum at the indicated concentrations for 26 hours, and the E2f-On% were assayed. (A) E2f-GFP histograms with red numbers indicating the average E2f-On% from duplicate samples (black and grey). (B) Statistic bar chart of the E2f-On% in cell populations (from A) as a function of dextran concentration (in serum-starvation) and serum concentration (in serum-stimulation). Bar graphs showing the E2f-On% from the left panels. Error bars, SEM ( $n = 2$ ), \*  $p < 0.05$ , \*\*  $p < 0.01$ .

**Supplementary Figure S3** | Simulation results on the effects of shear stress and extracellular factor replacement on quiescence depth. Simulations of fluid flow rate effects (orange) are the same as in **Figure 6B**. Simulations of the effects of shear stress (red) and extracellular factor replacement (purple) were performed in the same way as the simulations of fluid flow rate effects (orange), except that the FR term in **Supplementary Table S1** was multiplied by 0.75 and 0.85, respectively. Blue triangle, the average E2f-On% in response to 2% serum stimulation, in cells under 5  $\mu\text{L/h}$  extracellular fluid flow with the indicated shear stress level during serum starvation (as in **Figure 6B**, based on **Figure 4A** and **Table 1**). Each solid curve represents the best fit of simulation data points to a Hill function.

## REFERENCES

- Augenlicht, L., and Baserga, R. (1974). Changes in the G0 State of WI-38 Fibroblasts at Different Times after confluence. *Exp. Cell Res.* 89, 255–262. doi:10.1016/0014-4827(74)90789-7
- Bucher, N. L. R. (1963). “Regeneration of Mammalian Liver,” in *International Review of Cytology*. Editors G.H. Bourne and J.F. Danielli (New York: Academic Press), 245–300. doi:10.1016/s0074-7696(08)61119-5
- Carrasco, F., Chornet, E., Overend, R. P., and Costa, J. (1989). A Generalized Correlation for the Viscosity of Dextran in Aqueous Solutions as a Function of Temperature, Concentration, and Molecular Weight at Low Shear Rates. *J. Appl. Polym. Sci.* 37, 2087–2098. doi:10.1002/app.1989.070370801
- Chen, H., Yu, Z., Bai, S., Lu, H., Xu, D., Chen, C., et al. (2019). Microfluidic Models of Physiological or Pathological Flow Shear Stress for Cell Biology, Disease Modeling and Drug Development. *Trac Trends Anal. Chem.* 117, 186–199. doi:10.1016/j.trac.2019.06.023
- Cheung, T. H., and Rando, T. A. (2013). Molecular Regulation of Stem Cell Quiescence. *Nat. Rev. Mol. Cell Biol.* 14, 329–340. doi:10.1038/nrm3591
- Coller, H. A., Sang, L., and Roberts, J. M. (2006). A New Description of Cellular Quiescence. *Plos Biol.* 4, e83. doi:10.1371/journal.pbio.0040083
- Freund, J. B., Goetz, J. G., Hill, K. L., and Vermot, J. (2012). Fluid Flows and Forces in Development: Functions, Features and Biophysical Principles. *Development* 139, 1229–1245. doi:10.1242/dev.073593
- Fujimaki, K., Li, R., Chen, H., Della Croce, K., Zhang, H. H., Xing, J., et al. (2019). Graded Regulation of Cellular Quiescence Depth between Proliferation and Senescence by a Lysosomal Dimmer Switch. *Proc. Natl. Acad. Sci. USA* 116, 22624–22634. doi:10.1073/pnas.1915905116
- Fujimaki, K., and Yao, G. (2020). Cell Dormancy Plasticity: Quiescence Deepens into Senescence through a Dimmer Switch. *Physiol. Genomics* 52, 558–562. doi:10.1152/physiolgenomics.00068.2020
- Galie, P. A., Russell, M. W., Westfall, M. V., and Stegmann, J. P. (2012). Interstitial Fluid Flow and Cyclic Strain Differentially Regulate Cardiac Fibroblast Activation via AT1R and TGF- $\beta$ 1. *Exp. Cell Res.* 318, 75–84. doi:10.1016/j.yexcr.2011.10.008
- Gillespie, D. T. (2000). The Chemical Langevin Equation. *J. Chem. Phys.* 113, 297–306. doi:10.1063/1.481811
- Hillsley, M. V., and Frangos, J. A. (1994). Review: Bone Tissue Engineering: The Role of Interstitial Fluid Flow. *Biotechnol. Bioeng.* 43, 573–581. doi:10.1002/bit.260430706
- Hyler, A. R., Baudoin, N. C., Brown, M. S., Stremmer, M. A., Cimini, D., Davalos, R. V., et al. (2018). Fluid Shear Stress Impacts Ovarian Cancer Cell Viability, Subcellular Organization, and Promotes Genomic Instability. *PLoS One* 13, e0194170. doi:10.1371/journal.pone.0194170
- Jain, R. K. (1987). Transport of Molecules in the Tumor Interstitium: A Review. *Cancer Res.* 47, 3039–3051.
- Khorshid, F. A. (2005). The Effect of the Medium Viscosity on the Cells Morphology in Reaction of Cells to Topography—I. *Proc. 2nd Saudi Sci. Conf., Fac. Sci.* KAU; 15–17 March 2004, Part I, 67–98.
- Kwon, J. S., Everetts, N. J., Wang, X., Wang, W., Della Croce, K., Xing, J., et al. (2017). Controlling Depth of Cellular Quiescence by an Rb-E2f Network Switch. *Cel Rep.* 20, 3223–3235. doi:10.1016/j.celrep.2017.09.007
- Lee, T. J., Yao, G., Bennett, D. C., Nevins, J. R., and You, L. (2010). Stochastic E2F Activation and Reconciliation of Phenomenological Cell-Cycle Models. *Plos Biol.* 8, e1000488. doi:10.1371/journal.pbio.1000488
- Li, L., and Clevers, H. (2010). Coexistence of Quiescent and Active Adult Stem Cells in Mammals. *Science* 327, 542–545. doi:10.1126/science.1180794
- Liu, M., Tanswell, A. K., and Post, M. (1999). Mechanical Force-Induced Signal Transduction in Lung Cells. *Am. J. Physiology-Lung Cell Mol. Physiol.* 277, L667–L683. doi:10.1152/ajplung.1999.277.4.L667
- Llorens-Bobadilla, E., Zhao, S., Baser, A., Saiz-Castro, G., Zwadlo, K., and Martin-Villalba, A. (2015). Single-Cell Transcriptomics Reveals a Population of Dormant Neural Stem Cells that Become Activated upon Brain Injury. *Cell Stem Cell* 17, 329–340. doi:10.1016/j.stem.2015.07.002
- Louis, H., Lacolley, P., Kakou, A., Cattani, V., Daret, D., Safar, M., et al. (2006). Early Activation of Internal Medial Smooth Muscle Cells in the Rabbit Aorta after Mechanical Injury: Relationship with Intimal Thickening and Pharmacological Applications. *Clin. Exp. Pharmacol. Physiol.* 33, 131–138. doi:10.1111/j.1440-1681.2006.04339.x
- Lutolf, M. P., Gilbert, P. M., and Blau, H. M. (2009). Designing Materials to Direct Stem-Cell Fate. *Nature* 462, 433–441. doi:10.1038/nature08602
- Ng, C. P., and Swartz, M. A. (2003). Fibroblast Alignment under Interstitial Fluid Flow Using a Novel 3-D Tissue Culture Model. *Am. J. Physiology-Heart Circulatory Physiol.* 284, H1771–H1777. doi:10.1152/ajpheart.01008.2002
- Orford, K. W., and Scadden, D. T. (2008). Deconstructing Stem Cell Self-Renewal: Genetic Insights into Cell-Cycle Regulation. *Nat. Rev. Genet.* 9, 115–128. doi:10.1038/nrg2269
- Owen, T. A., Soprano, D. R., and Soprano, K. J. (1989). Analysis of the Growth Factor Requirements for Stimulation of WI-38 Cells after Extended Periods of Density-dependent Growth Arrest. *J. Cel. Physiol.* 139, 424–431. doi:10.1002/jcp.1041390227

- Polacheck, W. J., Charest, J. L., and Kamm, R. D. (2011). Interstitial Flow Influences Direction of Tumor Cell Migration through Competing Mechanisms. *Proc. Natl. Acad. Sci.* 108, 11115–11120. doi:10.1073/pnas.1103581108
- Rensen, S. S. M., Doevendans, P. A. F. M., and van Eys, G. J. J. M. (2007). Regulation and Characteristics of Vascular Smooth Muscle Cell Phenotypic Diversity. *Nhjl* 15, 100–108. doi:10.1007/BF03085963
- Rodgers, J. T., King, K. Y., Brett, J. O., Cromie, M. J., Charville, G. W., Maguire, K. K., et al. (2014). mTORC1 Controls the Adaptive Transition of Quiescent Stem Cells from G0 to GAlert. *Nature* 510, 393–396. doi:10.1038/nature13255
- Rouleau, L., Rossi, J., and Leask, R. L. (2010). Concentration and Time Effects of Dextran Exposure on Endothelial Cell Viability, Attachment, and Inflammatory Marker Expression *In Vitro*. *Ann. Biomed. Eng.* 38, 1451–1462. doi:10.1007/s10439-010-9934-4
- Sang, L., Coller, H. A., and Roberts, J. M. (2008). Control of the Reversibility of Cellular Quiescence by the Transcriptional Repressor HES1. *Science* 321, 1095–1100. doi:10.1126/science.1155998
- Shi, Z.-D., and Tarbell, J. M. (2011). Fluid Flow Mechanotransduction in Vascular Smooth Muscle Cells and Fibroblasts. *Ann. Biomed. Eng.* 39, 1608–1619. doi:10.1007/s10439-011-0309-2
- Shirure, V. S., Lezia, A., Tao, A., Alonzo, L. F., and George, S. C. (2017). Low Levels of Physiological Interstitial Flow Eliminate Morphogen Gradients and Guide Angiogenesis. *Angiogenesis* 20, 493–504. doi:10.1007/s10456-017-9559-4
- Spencer, S. L., Cappell, S. D., Tsai, F.-C., Overton, K. W., Wang, C. L., and Meyer, T. (2013). The Proliferation-Quiescence Decision Is Controlled by a Bifurcation in CDK2 Activity at Mitotic Exit. *Cell* 155, 369–383. doi:10.1016/j.cell.2013.08.062
- Swartz, M. A., and Fleury, M. E. (2007). Interstitial Flow and its Effects in Soft Tissues. *Annu. Rev. Biomed. Eng.* 9, 229–256. doi:10.1146/annurev.bioeng.9.060906.151850
- Tarbell, J. M., Weinbaum, S., and Kamm, R. D. (2005). Cellular Fluid Mechanics and Mechanotransduction. *Ann. Biomed. Eng.* 33, 1719–1723. doi:10.1007/s10439-005-8775-z
- Toh, Y. C., and Voldman, J. (2011). Fluid Shear Stress Primes Mouse Embryonic Stem Cells for Differentiation in a Self-renewing Environment via Heparan Sulfate Proteoglycans Transduction. *FASEB j.* 25, 1208–1217. doi:10.1096/fj.10-168971
- Wang, D. M., and Tarbell, J. M. (1995). Modeling Interstitial Flow in an Artery Wall Allows Estimation of Wall Shear Stress on Smooth Muscle Cells. *J. Biomechanical Eng.* 117, 358–363. doi:10.1115/1.2794192
- Wang, X., Fujimaki, K., Mitchell, G. C., Kwon, J. S., Della Croce, K., Langsdorf, C., et al. (2017). Exit from Quiescence Displays a Memory of Cell Growth and Division. *Nat. Commun.* 8, 321. doi:10.1038/s41467-017-00367-0
- Wiig, H. (1990). Evaluation of Methodologies for Measurement of Interstitial Fluid Pressure (Pi): Physiological Implications of Recent Pi Data. *Crit. Rev. Biomed. Eng.* 18, 27–54.
- Wilson, A., Laurenti, E., Oser, G., van der Wath, R. C., Blanco-Bose, W., Jaworski, M., et al. (2008). Hematopoietic Stem Cells Reversibly Switch from Dormancy to Self-Renewal during Homeostasis and Repair. *Cell* 135, 1118–1129. doi:10.1016/j.cell.2008.10.048
- Yamamoto, K., Sokabe, T., Watabe, T., Miyazono, K., Yamashita, J. K., Obi, S., et al. (2005). Fluid Shear Stress Induces Differentiation of Flk-1-Positive Embryonic Stem Cells into Vascular Endothelial Cells *In Vitro*. *Am. J. Physiology-Heart Circulatory Physiol.* 288, H1915–H1924. doi:10.1152/ajpheart.00956.2004
- Yao, G., Lee, T. J., Mori, S., Nevins, J. R., and You, L. (2008). A Bistable Rb-E2f Switch Underlies the Restriction point. *Nat. Cell Biol.* 10, 476–482. doi:10.1038/ncb1711
- Yao, G. (2014). Modelling Mammalian Cellular Quiescence. *Interf. Focus.* 4, 20130074. doi:10.1098/rsfs.2013.0074
- Yao, G., Tan, C., West, M., Nevins, J. R., and You, L. (2011). Origin of Bistability Underlying Mammalian Cell Cycle Entry. *Mol. Syst. Biol.* 7, 485. doi:10.1038/msb.2011.19
- Yao, W., Li, Y.-b., and Chen, N. (2013). Analytic Solutions of the Interstitial Fluid Flow Models. *J. Hydrodyn* 25, 683–694. doi:10.1016/s1001-6058(13)60413-8
- Yedgar, S., Weinstein, D. B., Patsch, W., Schonfeld, G., Casanada, F. E., and Steinberg, D. (1982). Viscosity of Culture Medium as a Regulator of Synthesis and Secretion of Very Low Density Lipoproteins by Cultured Hepatocytes. *J. Biol. Chem.* 257, 2188–2192. doi:10.1016/s0021-9258(18)34904-4

**Conflict of Interest:** The authors declare that the research was conducted in the absence of any commercial or financial relationships that could be construed as a potential conflict of interest.

**Publisher's Note:** All claims expressed in this article are solely those of the authors and do not necessarily represent those of their affiliated organizations, or those of the publisher, the editors and the reviewers. Any product that may be evaluated in this article, or claim that may be made by its manufacturer, is not guaranteed or endorsed by the publisher.

Copyright © 2022 Liu, Wang, Jiang, Xu, Zohar and Yao. This is an open-access article distributed under the terms of the Creative Commons Attribution License (CC BY). The use, distribution or reproduction in other forums is permitted, provided the original author(s) and the copyright owner(s) are credited and that the original publication in this journal is cited, in accordance with accepted academic practice. No use, distribution or reproduction is permitted which does not comply with these terms.

# Advantages of publishing in Frontiers



## OPEN ACCESS

Articles are free to read  
for greatest visibility  
and readership



## FAST PUBLICATION

Around 90 days  
from submission  
to decision



## HIGH QUALITY PEER-REVIEW

Rigorous, collaborative,  
and constructive  
peer-review



## TRANSPARENT PEER-REVIEW

Editors and reviewers  
acknowledged by name  
on published articles

## Frontiers

Avenue du Tribunal-Fédéral 34  
1005 Lausanne | Switzerland

Visit us: [www.frontiersin.org](http://www.frontiersin.org)

Contact us: [frontiersin.org/about/contact](http://frontiersin.org/about/contact)



## REPRODUCIBILITY OF RESEARCH

Support open data  
and methods to enhance  
research reproducibility



## DIGITAL PUBLISHING

Articles designed  
for optimal readership  
across devices



## FOLLOW US

@frontiersin



## IMPACT METRICS

Advanced article metrics  
track visibility across  
digital media



## EXTENSIVE PROMOTION

Marketing  
and promotion  
of impactful research



## LOOP RESEARCH NETWORK

Our network  
increases your  
article's readership